ANALOG METHODS

McGRAW-HILL SERIES IN ENGINEERING SCIENCES

STEPHEN H. CRANDALL AND PAUL M. NAGHDI, *Consulting Editors*

ANALOG METHODS

Computation and Simulation

Walter J. Karplus, Ph.D.

ASSOCIATE PROFESSOR OF ENGINEERING
UNIVERSITY OF CALIFORNIA, LOS ANGELES

Walter W. Soroka, Sc.D.

PROFESSOR OF MECHANICAL ENGINEERING
UNIVERSITY OF CALIFORNIA, BERKELEY

SECOND EDITION

ANALOG METHODS

PREFACE

The term analogy is defined as similarity of properties or relations without identity. When analogous systems are found to exist, measurements or other observations made on one of these systems can be used to predict the behavior of the others. The systems need not necessarily be analogous in every respect, but only in those respects of interest.

The existence of analogies, as recognized by the fact that equations of similar form are found to govern otherwise unrelated phenomena, has a twofold significance:

1. One can visualize the behavior of unfamiliar systems on the basis of a prior knowledge of the behavior of analogous familiar systems. Here, the analogy is set up intuitively and no experimental work is involved.

2. One can set up convenient and often relatively inexpensive experimental models or calculating devices, which simulate the characteristics of other systems without necessarily bearing any physical resemblance to them.

Through the years, the field of analog computation has undergone a continuous series of far-reaching evolutions and transformations. The earliest analog models to achieve a measure of importance in engineering work were the soap-film and fluid flow models, introduced around the turn of the century. These were followed by the direct electric analogs, the network analyzers, used primarily to solve electrical-power-distribution problems. The Bush mechanical differential analyzer developed in the late 1920s represented the first large-scale attempt to employ indirect analog-computation techniques. Through the 1930s, mechanical methods of solving algebraic and ordinary differential equations continued to attract wide interest. Military requirements in World War II and the development of new and improved electronic techniques and components led to the introduction of electronic differential analyzers. In the decade following World War II, truly phenomenal progress was made in this method of automatic computation, until today the term "analog computer" is virtually synonymous with "electronic differential analyzer."

The revisions of this textbook reflect these changes in the field of analog

computation. Thus, when the first edition was prepared, mechanical differential analyzers still occupied an important place while electronic techniques were just in their adolescence. Therefore, in the first edition, a separate chapter was devoted to the mechanical differential analyzer and only two chapters dealt with the indirect electrical methods. In the present revised edition, the emphasis has been shifted strongly toward electronic analog computers. The original chapter on electrical, electro-mechanical, and electronic computing elements has been expanded into three chapters, and the length of the discussion of electronic differential analyzers has been more than tripled. The chapter on network-analyzer techniques has been completely revised and augmented to reflect recent developments in that field. At the same time, the discussion of mechanical differential analyzers and other outmoded techniques has been shortened considerably. The chapter dealing with mechanical computing elements has been retained, because these devices still play an important part in special-purpose computers.

Although recognizing the current importance of electronic analog computers, the authors are of the opinion that an introductory text in analog methods should do much more than serve as an instruction manual for these devices. Accordingly, the book is organized to provide a broad and complete insight into the nature and operation of linear and nonlinear computing elements prior to discussing the interconnection of these elements to solve equations. Using this approach, the student's entrance into the laboratory to solve actual problems is slightly delayed in order to give him the background necessary to utilize computer elements in special-purpose designs as well as in general-purpose installations.

As presently constituted, the text consists of an introductory chapter and three main parts. Part One is a survey of the methods by which the mathematical operations required for indirect computations are accomplished. Chapters 2, 3, and 4 are devoted to the utilization of electrical and electronic circuits for the performance of linear operations, for multiplication and division, and for function generation, respectively. Chapter 5 covers the indirect mechanical computing elements.

Part Two, Indirect Analog Computers, includes three chapters, treating in turn the analog solution of differential equations, simultaneous linear algebraic equations, and nonlinear algebraic equations.

Part Three is devoted to direct simulators. In Chap. 9, the analogy between electrical circuits and mechanical systems is taken as the basis for representing mechanical systems in lumped form by equivalent electrical circuits with lumped parameters. In Chap. 10, ordinary and partial differential equations, of varying degrees of complexity, both linear and nonlinear, are approximated by finite-difference expressions,

and electrical networks are developed for their solution. The final chapter treats the simulation of field problems, characterized by partial differential equations, by analogs having distributed parameters, in particular by membranes and by electrically conductive sheets. Problems for classroom use and laboratory exercises are included in appendix form.

The book is intended to serve as a general introduction or survey of the entire analog field. It is hoped that the broad review and the many references made to current literature will serve to point out the usefulness of analogies and will lead individuals to more intensive studies of specialized problems of interest to them.

In an engineering curriculum, this book can serve as the text for a one-semester introductory course in analog computation, generally taught in the senior or first graduate year. The student is expected to have a background including a course in differential equations and a course in electrical circuits. Typically, the course in analog computation will emphasize the material in Chaps. 1, 2, 3, 4, and 6 and will treat the material in the other chapters more superficially. Where possible, the classroom work should be supplemented by the performance of as many of the laboratory exercises (Appendix C) as available equipment permits.

The authors are deeply indebted to Professors T. A. Rogers and G. Bekey of UCLA, Professor C. P. Atkinson of the University of California at Berkeley, Professor H. A. Rothbart of the City College of New York, and Mr. I. Pfeffer for critical reviews of the manuscript and the contribution of much useful and original material. The support given by Dean L. M. K. Boelter and by the Engineering Extension of UCLA is also gratefully acknowledged.

<div align="right">

Walter J. Karplus
Walter W. Soroka

</div>

CONTENTS

PART TWO. INDIRECT COMPUTERS

PART THREE. DIRECT COMPUTERS (SIMULATORS)

1

INTRODUCTION

Technological progress in our modern society is evidenced by the development of ever more impressive engineering systems and by the continuing efforts of man to study and understand the universe. These endeavors have been paralleled from the start by the search for tools and techniques designed to supplement man's capabilities. One large category of these auxiliary devices is employed to extend man's physical prowess, to relieve him of the burden of heavy manual efforts. In the nineteenth century the Industrial Revolution, brought about by the introduction and widespread use of such new machines, wrought fundamental changes in our way of life. More recently, a new type of engineering tool, the automatic computer, has come into its own. It is the purpose of these devices to ease the intellectual tasks of the scientist and the engineer, as well as to relieve him of lengthy and tedious routine tasks.

The development of such machines was necessitated by the fact that the solution of the new and increasingly complex problems by the conventional, analytical, pencil-and-paper techniques became more and more difficult and time-consuming, indeed sometimes impossible. Furthermore, in many modern systems elaborate computations must be performed as parts of control processes so that solutions must be made available with extreme rapidity to assure the proper functioning of the system. Modern technological advances have placed increasing requirements upon automatic computing machinery; at the same time, however, some of the very same inventions, which were facilitated by computers, led to the development of new and improved computing systems. Especially, the progress during and after World War II in the area of electronic instruments and components helped to extend greatly the capabilities of automatic computers and opened up entirely new areas of computer activities.

1.1. Types of Automatic Computers. The fields of automatic computation and simultation include all the devices which are designed to assist

the engineer and the scientist in the solution of mathematical problems and in the analysis, design, and control of physical systems by accomplishing tasks which would otherwise require difficult and time-consuming mental efforts. Clearly a tremendous variety of mechanisms, machines, and systems is included in such a broad definition. Automatic calculators range all the way from the simple slide rule and the abacus to intricate digital computer installations, occupying whole buildings and containing hundreds of thousands of components. To discuss and study profitably various topics and aspects in this field, it is useful, indeed invaluable, to organize and classify in a logical manner its many diverse members.

A basic and useful method of classification involves the manner in which the computer or simulator handles the data or other quantitative information being processed. In all computing and simulating devices, quantitative information, the given information of the problem, is applied to the machine. The computer then performs various quantitative operations on this data. In some machines, this information is expressed at all points within the computer in terms of discrete numbers having a specified number of significant figures. In the other major type of computing systems, all information is handled in a continuous fashion. The former of these devices are known as *digital* computers, while the latter are termed *analog* computers or simulators.

The use of both digital and analog computers can be traced back to antiquity. The use of the fingers of the hand to facilitate the simple arithmetic operations may be taken as one of the earliest applications of digital-computing concepts. The abacus, used in primitive forms in the Middle East as early as 2000 B.C. and still widely used today in the Far East, represents one of the next major advances in this field. The first desk calculator was invented by Pascal in 1642, and mechanical machines using toothed wheels and gears were progressively refined throughout the next 300 years. During World War II, emphasis was placed on the development of digital computers employing electrical and electronic components. The present large-scale general-purpose electronic computers, such as the IBM 709, the UNIVAC, the SWAC, and many others, represent the culmination to date of the progressive development in this area of computer technology.

Analog devices were employed in surveying and other cartographic projects by the Babylonians as early as 3800 B.C. The introduction of the slide rule in the early part of the seventeenth century and that of the planimeter, developed about 1814, represent important steps in the evolution of analog-computing instruments. Mechanical devices for solving simultaneous algebraic equations, used in harmonic analysis and subsequently for the solution of differential equations, became more and more widely used in the early part of the twentieth century. Network analyzers for the treatment of simultaneous algebraic equations were

introduced about 1925. Finally, World War II gave added impetus to the development of powerful electronic devices for general-purpose applications.

As pointed out above, the fundamental difference in analog and digital devices is that digital computers deal with discrete quantities such as beads on an abacus, notches on a toothed wheel, or electrical pulses while analog computers deal with continuous physical variables such as electrical voltages or mechanical shaft rotations. From this basic distinction follow a number of important differences between the two systems. The precision, or number of meaningful significant figures in a solution furnished by an analog computer, is determined by the precision with which the continuous variable constituting the data can be sensed and displayed. This, in turn, is related to the quality of the components used in constructing the computer, for example, the tolerance of electrical resistors or mechanical shafts, and the quality of the output equipment.

On the other hand, the precision of a digital computer is governed entirely by the number of significant figures carried in the computations. This, in turn, is primarily determined by the size of the installation. The precision of a digital computer is essentially unlimited, for in order to increase its precision, it is only necessary to enlarge the existing installation, to provide more toothed wheels or larger electronic memory units. Many digital machines carry over 20 significant figures. By contrast, it is difficult to obtain a precision in excess of 0.01 to 0.1 per cent on an analog device, since this requires electrical or mechanical components having an extremely exacting tolerance. The digital computer is, therefore, in general capable of higher precision and accuracy.

For many engineering applications, solutions having accuracies of the order of 1 per cent are adequate. Under these conditions, an analog computer is frequently preferred. First, an analog-computing facility tends to be less expensive to purchase and to operate than a corresponding digital facility. Second, in analog computers, each step or mathematical operation is performed by a separate unit, with all units operating simultaneously. The solution of the problem therefore becomes available almost immediately, and this permits the engineer to adjust or to vary any of the design parameters and to observe at once the effect of these variations upon the response of the system. In digital computers, on the other hand, the mathematical operations are performed in a predetermined sequence, and the solution time is a function of the complexity of the problem. Finally, the analog computer is more conducive to "experimental engineering." On an analog computer, each subunit or component has a direct significance in terms of the system under analysis. By programming the computer and by "playing around," for example, by varying electrical potentiometer settings, the engineer is permitted to gain an insight into the basic operation of the system.

By contrast, in the case of digital machines the mathematical operations are performed as a sequence of arithmetic operations which generally bear no direct relationship to the system under study. Furthermore, the setting up or programming of the computer is generally so specialized and difficult that the engineer with a problem to solve almost invariably turns the problem over to an experienced specialist assigned to the computer. In the process, the engineer loses all direct contact with the problem in its various states of solution.

It is apparent that both digital and analog devices have a number of inherent advantages and disadvantages and that, in many cases, the choice of one or the other is not a clear-cut one. Unfortunately, the development of new analog and digital machines has been so rapid that few engineers have become sufficiently expert in both of these areas to perform an objective analysis. Too often, a specific computer approach is selected merely because the engineer happens to be more familiar with one or the other of the available computers. The lack of the necessary and broad understanding of the entire computing art has led in some instances to an unfortunate rivalry or competition between exponents of the analog- and the digital-computer approaches. It is to be hoped that such an attitude reflects only a passing phase. As both analog and digital techniques become more systematized in their application, it is to be expected that the optimum spheres of application of both methods will be more clearly recognized and that a cursory examination of a specific problem will be sufficient to reveal whether an analog or a digital approach is more suitable. Encouraging in this respect is the recent emergence of "hybrid" systems, employing both analog and digital units to advantage in achieving an over-all objective.

1.2. Classification of Analog Methods. The various devices comprising the general area of analog computers and simulators, which constitute the subject matter of this book, are best classified according to their basic principles of operation. The systems falling into the resulting categories are subdivided, in turn, according to the type of physical variables which constitute the continuous data within the computer.

One major class of analog devices depends for its operation upon the existence of a direct physical analogy between the analog and the prototype system under study. Such an analogy is recognized by comparing the characteristic equations describing the dynamic or static behavior of the two systems. An analogy is said to exist if these characteristic equations are similar in form. Such a similarity is possible only if there is a one-to-one correspondence between elements in the analog and in the prototype system. For every element in the original system, there must be present in the analog system an element having similar properties, that is, an element having a similar excitation-response relationship; furthermore, the elements in the analog must be interconnected in

the same fashion as the elements in the original system. Members of this category of analog devices are termed *direct analogs* and are also frequently referred to as *simulators*.

Direct analogs may be of either the discrete or the continuous variety. Discrete analogs employ lumped physical elements, such as resistors and capacitors, and the behavior of the system is defined only for the junction points of the circuit. Other simulators make use of distributed elements, such as sheets or solids, made of a conductive material, so that every point in the analog corresponds to a specific point in the prototype. Networks of electrical resistors, capacitors, and sometimes inductors constitute the most important discrete simulators. On rare occasions, mechanical systems, comprised of masses, springs, and dashpots, have been used for this purpose. Among the distributed direct-analog systems, the electrical devices have played the major role. Foremost among these are the electrolytic-tank analogs, which employ a conductive liquid layer to simulate Laplacian fields, and more recently, the resistance-paper analogs. Stretched-membrane models, in which soap films or thin rubber sheets are pressed over a mechanical framework, also constitute widely used distributed mechanical simulators. Hydrodynamic models, commonly termed "fluid mappers," have also been useful on occasions. Other direct-analog simulators make use of thermal fields, electrochemical diffusion phenomena, polarized light, and electrostatic fields to simulate continuous systems.

The other major class of analog systems includes mathematical rather than physical analogs. The behavior of the system under study, or the problem to be solved, is first expressed as a set of algebraic or differential equations. An assemblage of computing units or elements, each capable of performing some specific mathematical operation, such as addition, multiplication, or integration, is provided, and these units are interconnected so as to generate solutions of the problem. The resulting computing systems are termed *indirect analogs* or *analog computers*. An important distinction between the direct and the indirect analogs involves the significance of the physical variable within the computer. In a direct analog, the analog variable has the same significance everywhere within the analog system. For example, in the electrical simulation of a mechanical system, voltage everywhere in the analog may represent velocity. The time derivative of voltage then represents acceleration everywhere in the analog system. In an indirect analog, on the other hand, a transient voltage at some point in the computer may represent acceleration; this voltage is then applied to an integrator, and the transient voltage at the output of the integrator represents velocity.

Indirect analogs are employed to solve problems involving algebraic and ordinary differential equations. To solve systems of simultaneous algebraic equations and to determine the roots of algebraic equations,

both mechanical and electrical analog computers are widely used. Computers which are designed for the solution of differential equations are termed *differential analyzers*. Mechanical differential analyzers were relatively widely used before World War II but have now been almost completely replaced by the more convenient electronic differential analyzers. So popular have these electronic devices become in recent years that the term analog computer is taken in many quarters as being synonymous with electronic differential analyzer. Most of the indirect
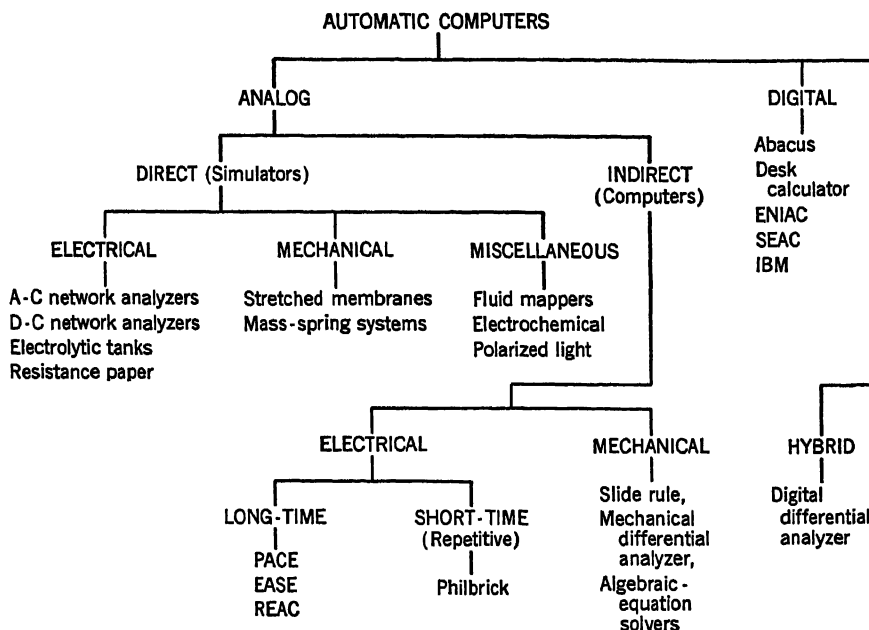
Fig. 1.1. Classification of automatic computers.

electric analog computers have solution times ranging from 10 sec to 3 min and employ graphical output equipment. Other electronic computers have solution times of the order of 5 msec and repeat this solution periodically to facilitate the display of the output curves by means of cathode-ray oscilloscopes.

The general classification of analog methods is illustrated diagrammatically in Fig. 1.1. Part One of this text represents a survey of the electrical, electronic, and mechanical computing elements and units which form the building blocks of the indirect computers. The solution of linear algebraic equations, nonlinear algebraic equations, and differential equations is considered in Part Two. Part Three is devoted to the direct simulation methods, including the discrete-element and distributed-element analog systems.

Part One

INDIRECT COMPUTING ELEMENTS

2

LINEAR ELECTRICAL
COMPUTING ELEMENTS

2.1. General Remarks. In the indirect approach to analog computation, physical units or elements are constructed to perform mathematical operations. These units are then interconnected as determined by the problem under study. In each computing element and throughout the computing system a physical quantity termed the "machine variable" represents, or is analogous to, the problem variables. Theoretically, this machine variable could belong to any one of a wide variety of physical areas such as heat transfer, fluid mechanics, magnetism, etc. In practice, however, only two types of analog variables have assumed important roles in indirect analog computation: electrical voltages and mechanical displacements.

Electrical computing elements and electrical computing systems owe their wide acceptance to the convenience, from the standpoint of construction and of operation, that attends their use. Electrical components, particularly resistors and capacitors, having an extremely wide range of magnitudes are mass-produced and are readily available with tolerances as small as 0.01 per cent. Electrical circuits can be wired and assembled by relatively untrained personnel, are light in weight and compact, and do not require expensive maintenance. The use of electronic amplifiers, semiconductors, and electromechanical devices makes electrical computing systems adaptable to a wider variety of problems than can be handled by any other analog-computing method.

The two dependent variables in electrical circuits are the *voltages* across the circuit elements or from node points to ground and the *currents* through each element. Voltages are used almost exclusively as the computing variable in electric analogs, because these can be measured and recorded at any point in the electrical circuit without circuit modification. To measure the current through an element, it is necessary to open the circuit and to introduce an ammeter in series with the element.

9

A voltmeter, on the other hand, is attached in parallel with the circuit element under study.

Both alternating- and direct-current excitations are used in electric analog computing. Alternating-current analog computers are generally less expensive to build and require less complex auxiliary devices. On the other hand, in order that such devices operate effectively, the voltages at all points in the computer must be in phase. The errors attending phase shifts tend to make this type of computer less accurate than the corresponding d-c computer. For this reason, most large-scale general-purpose installations use d-c voltages as the problem variables.

The basic operations performed in the solution of linear algebraic and differential equations with constant coefficients include multiplication by a constant, addition, subtraction, integration, and differentiation. The electrical devices for performing these operations are termed *passive* if they consist solely of fixed or variable resistors, capacitors, inductors, and transformers. If electronic amplifiers are included in the computing units, the elements are termed *active* or electronic elements. In this chapter, the performance of the basic linear operations by means of passive computing elements is first discussed. Then the use of active elements to perform these same operations is considered.

PASSIVE COMPUTING ELEMENTS

2.2. Potentiometric Multiplication by a Constant. Potentiometers are the basic components in both d-c and a-c computers for the multiplication of the variable electrical voltages by a constant. A potentiometer is a resistance element having terminal connections at each end and a sliding contact, which is capable of traversing this element over its entire length, thereby permitting a variation in the resistance between the sliding contact and one of the fixed terminals. The principal characteristics which determine the quality of such an element are the linearity and the resolution.[1] Potentiometer linearity deviation is the maximum deviation from the best straight line which can be drawn through the points of a resistance vs. rotation graph, as shown in Fig. 2.1. This deviation is generally expressed as percentage of total resistance. The resolution of a potentiometer refers to the accuracy with which any shaft setting can be obtained. Since most potentiometers are of the wire-wound type, a graph of resistance vs. rotation has the shape of a staircase rather than a continuous curve, as shown in Fig. 2.2. The number of steps, and hence the resolution of the element, is determined by the total number of turns of wire used in winding the potentiometer.

[1] Superscript numbers refer to references listed at the end of each chapter.

Precision potentiometers with linearity tolerances as close as 0.01 per cent, multiturn constructions for high resolution and an extremely low noise level are mass-produced for analog applications.

The elementary multiplication circuit is shown in Fig. 2.3. The output voltage e_o is to be the product of two other quantities present in the computing circuit. One of these variables appears as a voltage applied
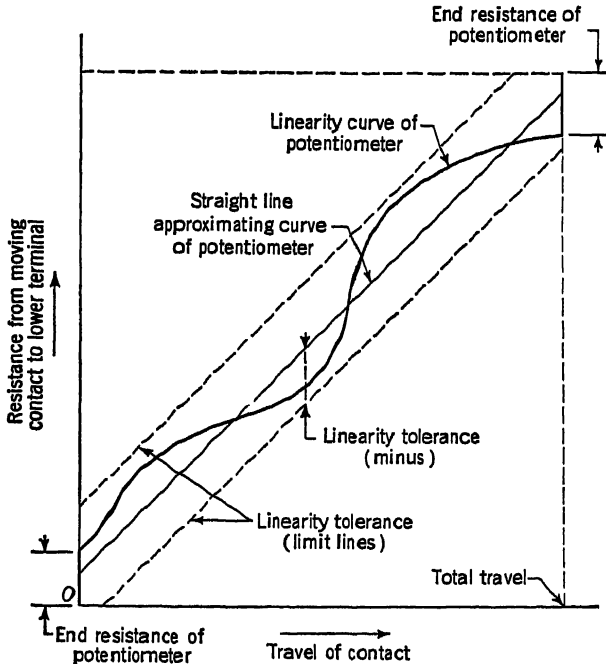
Fig. 2.1. (D. C. Duncan, "Characteristics of Precision Servo Computer Potentiometers," paper presented at AIEE Conference on Feedback Control Systems, Atlantic City, N.J., December, 1951.)

to one end of a linear potentiometer of total resistance R_T. The other appears as a shaft rotation which sets off the resistance R. In a linear potentiometer the resistance R is directly proportional to the angle of rotation of the potentiometer shaft. At the setting indicated by R, the open-circuit voltage at the potentiometer brush is

$$e_o = \frac{R}{R_T} e_i \qquad (2.1)$$

This voltage will be the output voltage as long as the measuring device or other computer element taking e_o as an input does not draw appreciable current from the potentiometer. This would be the case, for example,

if e_o were applied to the grid of a vacuum tube in a cathode-follower amplifier.

If the output voltage e_o is impressed across a load, the output voltage will deviate from strict proportionality to the shaft rotation, the amount of deviation being a function of this "loading" effect.[2]   This is illustrated
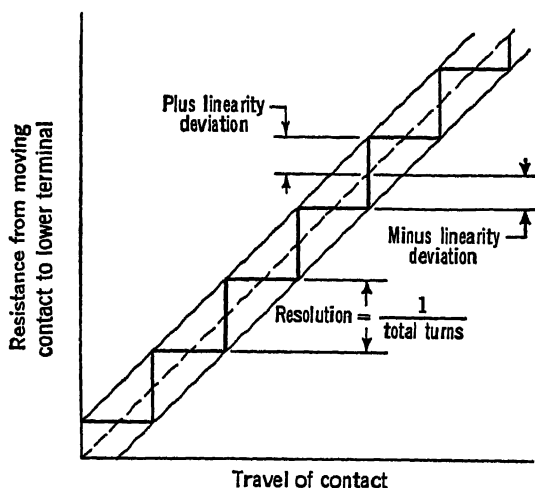
Fig. 2.2. (D. C. Duncan, "Characteristics of Precision Servo Computer Potentiometers," paper presented at AIEE Conference on Feedback Control Systems, Atlantic City, N.J., December, 1951.)
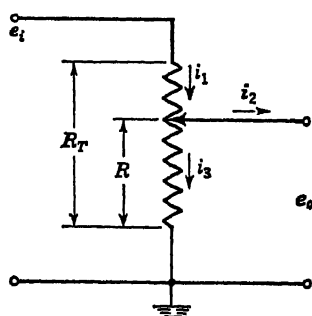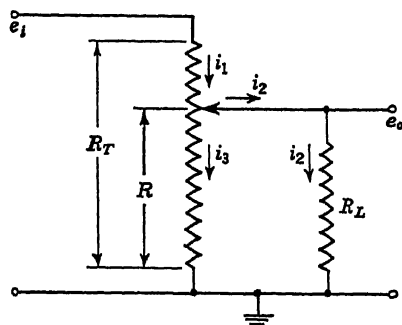
Fig. 2.3   Fig. 2.4

in Fig. 2.4 where the potentiometer is loaded by a resistance R_L.   The voltage across R_L is the potentiometer output.

Kirchhoff's current law at the potentiometer brush specifies that

$$i_1 - i_2 - i_3 = 0 \qquad (2.2)$$

From Ohm's law

$$i_1 = \frac{e_i - e_o}{R_T - R} \qquad i_3 = \frac{e_o}{R} \qquad (2.3)$$

therefore
$$e_o = \frac{R}{R_T} e_i - i_2 \left(1 - \frac{R}{R_T}\right) R \tag{2.4}$$

The current i_2 has been purposely left in Eq. (2.4) in order to show how the loading effect of the output circuit influences the voltage e_o. The nature of the output circuit (indicated by R_L in Fig. 2.4) does not appear at all in Eq. (2.4). This loading might be produced by a much more complicated circuit than an ordinary resistor. The important point is that whatever the load might be, it does draw the current i_2 from the potentiometer. As a result, the output voltage is not proportional to shaft rotation but is less than this value by an amount which depends on the current drain as well as on the setting of the potentiometer and its total resistance. Advantage is sometimes taken of this loading effect on the potentiometer to obtain a nonlinear dependence between output voltage and shaft rotation while using a linear potentiometer.

Where a resistance R_L is the load, the current i_2 is e_0/R_L, whereupon the output voltage is
$$e_o = \frac{(R/R_T)e_i}{1 + (1 - R/R_T)R/R_L} \tag{2.5}$$

Except for values of $R = 0$ or $R = R_T$, the factor in the denominator is greater than unity, again indicating a lowering of the potentiometer-brush voltage due to current drain into R_L. For $R = 0$ and $R = R_T$, the denominator is unity. The deviation from unity thus rises from zero, reaches a maximum, and then returns to zero again as the potentiometer setting is varied between zero and maximum. The deviation of e_o from the geometrical setting $e_i(R/R_T)$ is
$$\Delta = \frac{R}{R_T} e_i \left[1 - \frac{1}{1 + (1 - R/R_T)R/R_L} \right] \tag{2.6}$$
In terms of the geometrical setting, the deviation is
$$\frac{\Delta}{(R/R_T)e_i} = 1 - \frac{1}{1 + R/R_L(1 - R/R_T)}$$
$$= 1 - \frac{1}{1 + (R_T/R_L)(1 - R/R_T)(R/R_T)} \tag{2.7}$$

The deviation from geometrical setting is shown in Fig. 2.5 in a family of curves plotted against geometrical setting R/R_T, with the load-resistance ratio R_L/R_T as parameter. The curves show the maximum error to occur at the mid-point setting of the potentiometer. This can be determined directly by differentiating Eq. (2.7) with respect to R/R_T.
$$\frac{d}{d(R/R_T)} \left[\frac{\Delta}{(R/R_T)e_i} \right] = 0 = 1 - 2\frac{R}{R_T}$$
$$\frac{R}{R_T} = \frac{1}{2} \tag{2.8}$$

Substituting from Eq. (2.8) into Eq. (2.7) gives the maximum error in the output voltage due to loading as

$$\frac{\Delta}{(R/R_T)e_i} = \frac{0.25r}{1 + 0.25r} \tag{2.9}$$

where $r = R_T/R_L$.

With the load resistance equal to the potentiometer resistance, a maximum error of 20 per cent can be expected in the output voltage as compared with the potentiometer geometrical setting. If the load resistor is ten times the resistance of the potentiometer ($r = 0.1$), the maximum error becomes slightly less than 2.5 per cent. The maximum error as a function of resistance ratio, $R_L/R_T = 1/r$, is shown in Fig. 2.6.
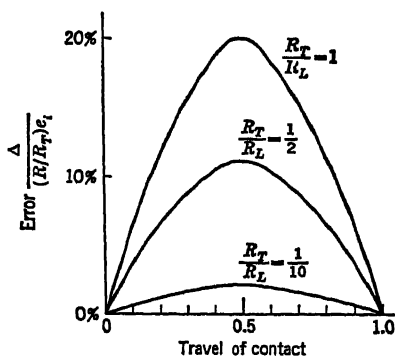
Fig. 2.5
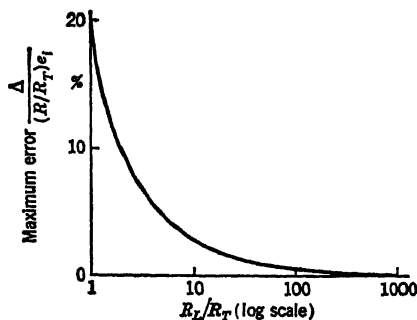
Fig. 2.6

If one is interested in the actual magnitude of the error rather than in the ratio of the error to the correct value,

$$\epsilon = \frac{R}{R_T} - \frac{e_o}{e_i}$$

inserting Eq. (2.5) and rearranging

$$\epsilon = \frac{R^2(1 - R/R_T)}{R_L R_T + R R_T - R^2} \tag{2.10}$$

Provided R_L is large compared with R_T, this reduces to

$$\frac{R_L}{R_T} \epsilon = \left(\frac{R}{R_T}\right)^2 \left(1 - \frac{R}{R_T}\right) \tag{2.11}$$

Differentiating to determine the location of the maximum error,

$$\frac{d}{d(R/R_T)} \frac{R_L}{R_T} \epsilon = \frac{R}{R_T}\left(2 - \frac{3R}{R_T}\right) = 0 \tag{2.12}$$

$$\frac{R}{R_T} = \frac{2}{3}$$

As shown in Fig. 2.7 the maximum error ϵ occurs not at mid-scale but at a setting which is two-thirds of the way away from the lower terminal.

It is advantageous, therefore, from the accuracy standpoint, to increase the resistance of the load resistor to a very large value. However, other considerations limit the maximum which might be used in practice. These include stability of resistance value with time, noise in the resistor, and loading effects caused by the instrumentation used to sense e_o.

While in Fig. 2.3 one variable (e_x) appears as a voltage and the other as a shaft rotation, frequently both variables appear as shaft rotations. In this case two potentiometers are cascaded to perform the multiplication, as illustrated in Fig. 2.8. A constant voltage E is supplied to one
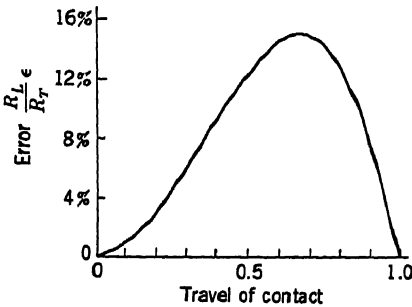
Fig. 2.7
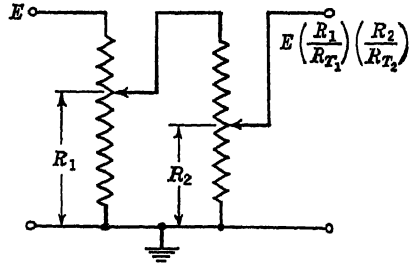
Fig. 2.8

end of the first potentiometer. The shaft rotation representing the first variable sets off a proportionate resistance R_1 on the first potentiometer which has a total resistance R_{T_1}. The shaft rotation representing the second variable sets off a correspondingly proportionate resistance R_2 on the second potentiometer, of total resistance R_{T_2}. The voltage at the brush of the first potentiometer is (neglecting the loading effect of the second potentiometer on the first) $E(R_1/R_{T_1})$, while the voltage at the brush of the second potentiometer (again neglecting loading effects) is $E(R_1/R_{T_1})(R_2/R_{T_2})$. The product $R_1 R_2$ is thus obtained.

The same rules regarding loading effects which were discussed in connection with Fig. 2.4 apply in Fig. 2.8. The second potentiometer should have a large resistance compared with the first potentiometer, while the loading device fed by the second brush should have a large resistance as compared with the second potentiometer. In cascaded potentiometers, therefore, the successive resistances used tend to grow very rapidly in magnitude in order to keep errors down. This is disadvantageous from the point of view of succeeding instrumentation and of noise.[3]

2.3. Minimization of Potentiometer Loading Errors. The best way to eliminate potentiometer loading errors is to set the potentiometer so as

to provide the correct voltage ratio, with the load resistor already connected to its tap. This involves disconnecting the potentiometer input from the circuit and applying a fixed voltage E. The potentiometer, with the load in place, is then adjusted until the voltage at the moving tap, as measured with a precision voltmeter, bears the specified relationship to E. This method cannot be employed when it is necessary to vary the potentiometer setting in the course of solving a problem.
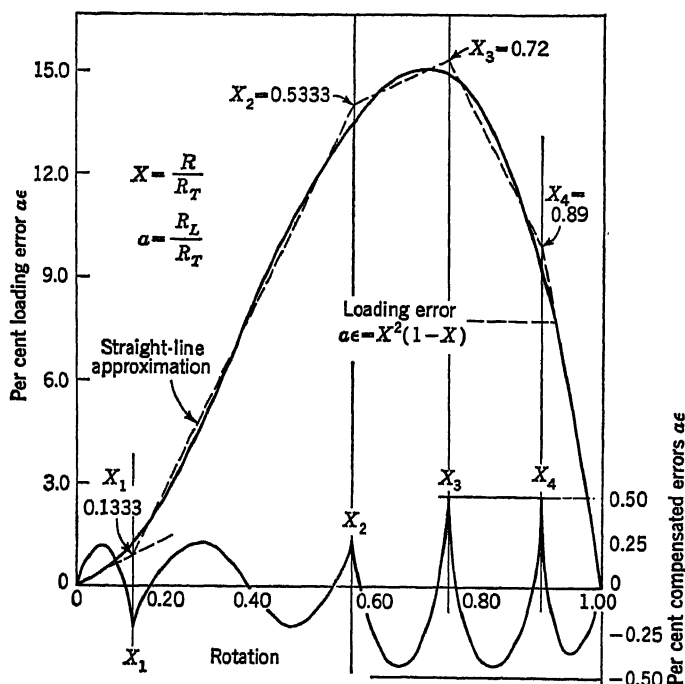
Fig. 2.9. [*J. Gilbert, Use Taps to Compensate Pot Loading Errors, Control Eng., 3:78–82 (1956).*]

A straightforward method of minimizing potentiometer loading errors is to increase the load resistance R_L until the voltage error falls within the prescribed tolerance. Should such an approach be impractical, modified potentiometric multipliers can be employed. One method for attaining this objective involves the inclusion of taps, spaced at intervals along the potentiometer resistance element.[4] Graphical techniques have been developed to optimize the placement of taps and resistors to secure a maximum reduction in the loading error. A plot of the error function is shown in Fig. 2.9. To determine the required number of taps, straight-line segments are drawn through the loading-error curve such that the maximum difference between each straight line and the curve falls within the specified tolerance. The number of straight-line segments required

to approximate the curve and still stay within the desired tolerance determines the number of taps. These taps are located at points corresponding to the intersections of the straight-line segments. In Fig. 2.9, the error curve has been approximated by five line segments, so that four taps are required to reduce the error $(R_L/R_T)\epsilon$, after compensation, to 0.5 per cent. The values of the shunting resistors are then calculated from the approximate relationship[5]

$$\frac{R_i}{a} = \frac{X_j - X_i}{a(S - S_{ji})} \tag{2.13}$$

where X_j, X_i = adjacent tap locations

S = maximum positive slope of any straight-line segment drawn through loading error curve ϵ

S_{ji} = slope of straight-line segment between adjacent taps X_j and X_i

R_i = resistance of shunting resistor across taps X_j and X_i

$a = R_L/R_T$

The general multitap design is illustrated for a four-tap potentiometer in Fig. 2.10. Note that the total number of paralleling resistors is always equal to the number of taps, since no resistor is connected across the two terminals for which the straight-line approximation has a maximum positive slope. A summary of the final design parameters for one-, two-, four-, and five-tap potentiometers is presented in Table 2.1.

Another approach to the elimination of loading effects, particularly where it is necessary to cascade a number of potentiometers, is to make use of constant-resistance attenuating networks.[6] In a typical cell of such a network, the output voltage is a fraction of the input voltage, but

Fig. 2.10. [J. Gilbert, *Use Taps to Compensate Pot Loading Errors*, Control Eng., 3:78–82 (1956).]

the resistance offered by the circuit to both voltages is identical with proper design. One of the simplest of such circuits is the so-called T type of network; a typical cell of this network is illustrated in Fig. 2.11. The input voltage e_i is impressed across the input resistance R, while the output voltage e_o is taken off an equal output resistance, also R. The connecting T-type network, consisting of the resistances R_1, R_2, and R_3, is so designed that each resistance R, when looking toward the other resistance R, sees a resistance always equal to R. This can be shown by

TABLE 2.1. DESIGN PARAMETERS FOR MULTITAP POTENTIOMETERS[*]

	Tap location	Shunt resistor values, $a = R_L/R_T$		Maximum error, $a\epsilon_m$
One tap	$X_1 = 0.74$	$a > 10$ $R_1 = 0.311a$		1.9%
Two taps	$X_1 = 0.20$ $X_2 = 0.80$	$a = 20$ $R_1 = 0.66a$ $R_2 = 0.66a$		0.5%
Four taps	. $X_1 = 0.1333$ $X_2 = 0.5333$ $X_3 = 0.720$ $X_4 = 0.890$	$a = 100$ $R_1 = 0.647a$ $R_2 = 0.831a$ $R_3 = 0.261a$ $R_4 = 0.097a$	$a = 20$ $R_1 = 0.653a$ $R_2 = 0.795a$ $R_3 = 0.261a$ $R_4 = 0.096a$	0.25–0.50%
Five taps	$X_1 = 0.125$ $X_2 = 0.540$ $X_3 = 0.690$ $X_4 = 0.810$ $X_5 = 0.916$	$a = 100$ $R_1 = 0.603a$ $R_2 = 0.707a$ $R_3 = 0.244a$ $R_4 = 0.131a$ $R_5 = 0.072a$		0.25%

[*] J. Gilbert, Use Taps to Compensate Pot Loading Errors, *Control Eng.*, **3**:78–82 (August, 1956).

writing the equations for the effective resistances across the input terminals and across the output terminals. Thus, across the former
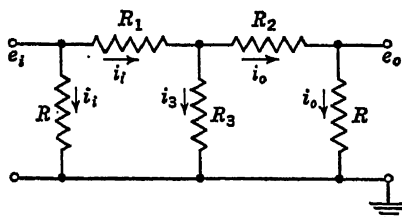
Fig. 2.11

$$R = R_1 + \frac{R_3(R_2 + R)}{R_2 + R_3 + R} \quad (2.14)$$

and across the latter

$$R = R_2 + \frac{R_3(R_1 + R)}{R_1 + R_3 + R} \quad (2.15)$$

The desired voltage ratio (which is also the current ratio through the terminal resistances) is

$$k = \frac{e_i}{e_o} = \frac{i_i}{i_o} \quad (2.16)$$

The current ratio can be obtained in terms of the resistances by referring to Fig. 2.11. At the central junction,

$$i_i = i_o + i_3 \quad (2.17)$$

Since i_o and i_3 are caused by the same voltage drop, they are in inverse

ratio to the resistances through which they flow. Thus

$$\frac{i_3}{i_o} = \frac{R_2 + R}{R_3} \tag{2.18}$$

whence
$$k = \frac{i_i}{i_o} = 1 + \frac{R_2 + R}{R_3} = \frac{R_2 + R_3 + R}{R_3} \tag{2.19}$$

From Eqs. (2.14), (2.15), and (2.19), the values of R_1, R_2, and R_3 can be determined for a given k and a given R. Obviously, $R_1 = R_2$. Then

$$R_1 = R_2 = \frac{k-1}{k+1} R = mR \tag{2.20}$$

$$R_3 = \frac{2k}{k^2 - 1} R = nR \tag{2.21}$$

The resistances R_1, R_2, and R_3 must, therefore, have nonlinear windings if their shaft rotations proportional to $1/k$ are to produce a voltage e_o also proportional to $1/k$. The nature of the windings is shown in Table 2.2, where the values of m and n are shown tabulated for various values of $1/k$.

TABLE 2.2. VALUES OF m AND n IN EQS. (2.20) AND (2.21) FOR VARIOUS ATTENUATIONS*

$1/k$	1	$\frac{1}{2}$	$\frac{1}{3}$	$\frac{1}{4}$	$\frac{1}{5}$	$\frac{1}{6}$	$\frac{1}{7}$	$\frac{1}{8}$	$\frac{1}{9}$	$\frac{1}{10}$	$\frac{1}{100}$
m	0	$\frac{1}{3}$	$\frac{1}{2}$	$\frac{3}{5}$	$\frac{2}{3}$	$\frac{5}{7}$	$\frac{3}{4}$	$\frac{7}{9}$	$\frac{4}{5}$	$\frac{9}{11}$	$\frac{99}{101}$
n	∞	$\frac{4}{3}$	$\frac{3}{4}$	$\frac{8}{15}$	$\frac{5}{12}$	$\frac{12}{35}$	$\frac{7}{24}$	$\frac{16}{63}$	$\frac{9}{40}$	$\frac{20}{99}$	$200/9{,}999$

* P. K. McElroy, Designing Resistive Attenuating Networks, *Proc. IRE*, **23**:213–233 (1935).

The shafts of R_1, R_2, and R_3 must be coupled in such a manner that, for increasing attenuation, R_1 and R_2 increase in resistance while R_3 decreases
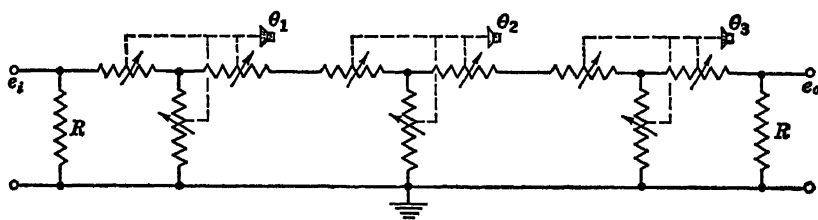
Fig. 2.12

in resistance, according to Table 2.2. The complete circuit for multiplying three variables represented by shaft rotations θ_1, θ_2, θ_3 is shown in Fig. 2.12. For this circuit

$$e_o = C\theta_1\theta_2\theta_3 \tag{2.22}$$

where C is a scale factor.

A modification of the T type of attenuator, which requires only two ganged variable resistors per section, is the bridged-T attenuator.[6] A typical section of this attenuator is shown in Fig. 2.13. For an attenuation by an amount k (that is, $e_o = e_i/k$), R_1 and R_2 are related to R by the expressions
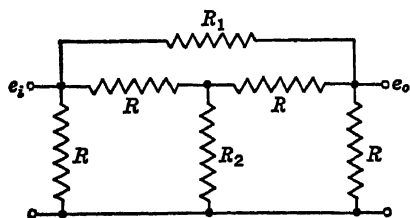
Fig. 2.13

$$R_1 = (k - 1)R = pR \quad (2.23)$$

$$R_2 = \frac{1}{k - 1} R = qR \quad (2.24)$$

Corresponding values of $1/k$, p, and q are shown in Table 2.3 for the bridged-T attenuator.

TABLE 2.3. VALUES OF p AND q IN EQS. (2.23) AND (2.24) FOR
VARIOUS ATTENUATIONS*

$1/k$	1	$\frac{1}{2}$	$\frac{1}{3}$	$\frac{1}{4}$	$\frac{1}{5}$	$\frac{1}{6}$	$\frac{1}{7}$	$\frac{1}{8}$	$\frac{1}{9}$	$\frac{1}{10}$	$\frac{1}{100}$
p	0	1	2	3	4	5	6	7	8	9	99
q	∞	1	$\frac{1}{2}$	$\frac{1}{3}$	$\frac{1}{4}$	$\frac{1}{5}$	$\frac{1}{6}$	$\frac{1}{7}$	$\frac{1}{8}$	$\frac{1}{9}$	$\frac{1}{99}$

* P. K. McElroy, Designing Resistive Attenuating Networks, *Proc. IRE*, **23**:213–233 (1935).

The resistances R_1 and R_2 must be ganged so that they change in opposite directions as the common shaft rotates in accordance with changes in the variable. A circuit producing an output voltage proportional to the product of three shaft rotations is shown in Fig. 2.14.
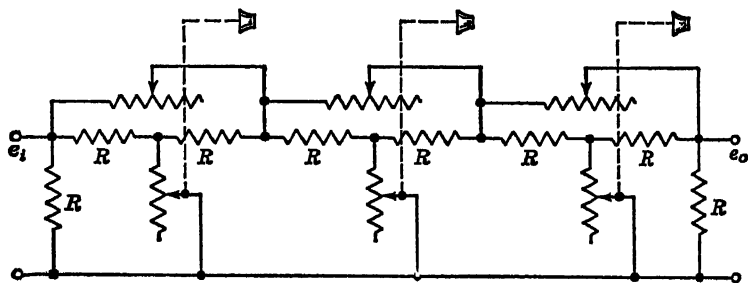
Fig. 2.14

2.4. Multiplication Using Alternating Current. The potentiometric multipliers described above can be used either with direct current or with alternating current.

If alternating current is used, multiplication of variables represented by shaft rotations can also be accomplished with autotransformers.[7]

Such a transformer consists of a single layer of wire wound on a toroidal iron core. A brush rides on the exposed parts of the winding, as in a standard potentiometer. By exciting a portion of the winding with a source of a-c voltage (e_i), the core becomes magnetized, and a voltage is developed across the entire winding. This voltage is equal to the exciting voltage times the ratio between total turns and input turns. The voltage varies linearly with brush position. Schematically, the arrangement is as shown in Fig. 2.15. Within the capacity of the unit, the voltage at a brush position is not affected by the attached load. Hence, autotransformers can be cascaded for multiplication without using amplifiers or other devices to prevent loading effects.
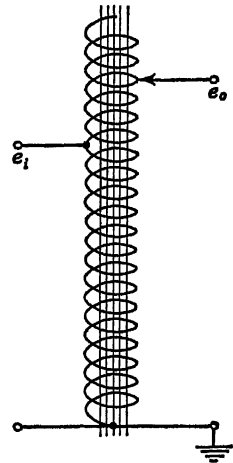
2.5. Addition and Subtraction. Variables appearing as voltages or currents can be summed in simple circuits. Figure 2.16 shows three such circuits. In (a) batteries E_1 and E_2 are shunted by center-tapped potentiometers. The voltages e_1 and e_2, representing the variables to be added, are set to their proper values by mechanical rotation of

Fig. 2.15

the potentiometer shafts. The variables are thus actually shaft rotations, the potentiometers serving to convert these rotations into equivalent voltages. The center tap in each case permits setting e_1 and e_2 either plus or minus, depending on which side of the tap the potentiometer brush is set. Assuming that no appreciable current flows to ground

(a)   (b)   (c)
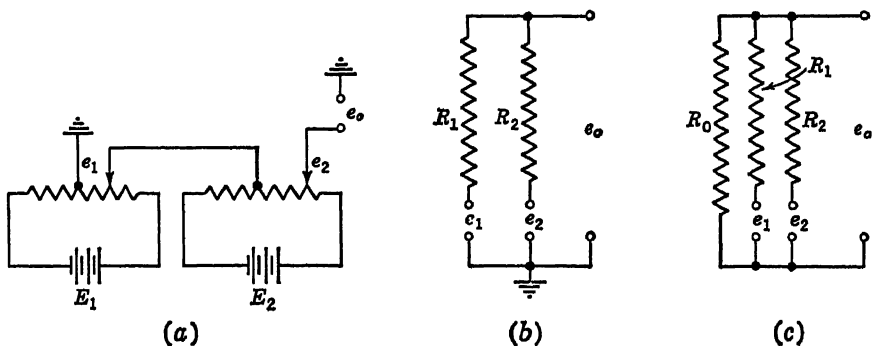
Fig. 2.16

through e_o, the voltages e_1 and e_2 are directly proportional to the geometrical settings of the potentiometer brushes. The output voltage is the algebraic sum of e_1 and e_2.

Instead of batteries to provide direct current, a-c sources of identical

phase can be used to furnish a-c voltages. The voltages on either side of a center tap are in phase opposition, so that plus and minus a-c voltages are obtained as in the case of the d-c circuit. Although resistive potentiometers constitute the most accurate and convenient means for setting e_1 and e_2, any other type of impedance can be used, except that the phase angles must be kept identical to ensure proper addition of the voltages.

A common method for adding voltages is illustrated in Fig. 2.16b. The voltage sources e_1 and e_2 are connected in series with resistors R_1 and R_2. The other ends of the resistors are tied to a common terminal. If the voltage sources have constant internal resistances regardless of voltage variation, the internal resistances may be lumped in R_1 and R_2. In many cases, however, e_1 and e_2 may be values picked off potentiometers by brushes. The internal resistances of such sources vary between wide limits as the brush moves from one end to the other of the potentiometer. In such cases the maximum value of the internal resistance should be low in relation to the external resistance in order that each branch present a constant resistance regardless of variations in its voltage source.

Assuming again that there is no current drain through e_o to ground, the current sum at the node for R_1 and R_2 (e_1 and e_2 having negligible internal resistances or else constant resistances included in R_1 and R_2) is

$$\frac{e_1 - e_o}{R_1} + \frac{e_2 - e_o}{R_2} = 0 \qquad (2.25)$$

whence

$$e_o = \frac{R_2}{R_1 + R_2} e_1 + \frac{R_1}{R_1 + R_2} e_2 \qquad (2.26)$$

The summation thus includes coefficients on e_1 and e_2, which can be adjusted by assigning appropriate values to R_1 and R_2. The variation of both numerator and denominator with variations in R_1 and R_2 somewhat complicates the process of setting coefficients.

If $R_1 = R_2 = R$, the usual case, then

$$e_o = \tfrac{1}{2}(e_1 + e_2) \qquad (2.27)$$

In general, for the addition of n voltages, n parallel resistances are required. The expression for the sum is

$$e_o = \frac{\displaystyle\sum_{k=1}^{n} \frac{e_k}{R_k}}{\displaystyle\sum_{k=1}^{n} \frac{1}{R_k}} \qquad (2.28)$$

If the resistances are identical, then

$$e_o = \frac{1}{n}(e_1 + e_2 + \cdots + e_n) \qquad (2.29)$$

Equation (2.29) clearly shows that e_o is the arithmetical mean of all the voltages, the n identical resistances serving as an averaging circuit.

Other impedance elements can be used in the case of a-c voltages, but phase equality must be maintained for accurate summation.

A variation[8] of the adding network is shown in Fig. 2.16c. This variation consists simply of the insertion of another resistance from the node to ground. The output voltage in this case is

$$e_o = \frac{\dfrac{1}{R_1} e_1 + \dfrac{1}{R_2} e_2}{\dfrac{1}{R_0} + \dfrac{1}{R_1} + \dfrac{1}{R_2}} \tag{2.30}$$

For n voltages to be added, making use of all equal resistances,

$$e_o = \frac{1}{n+1} (e_1 + e_2 + \cdots + e_n) \tag{2.31}$$

If n voltages are to be added in one circuit, m voltages to be added in another circuit, and the two resulting sums are to be added, unless means are provided for equalizing the scale factors resulting from the separate summations, the scale factor on the final result would be indeterminate. Thus, if e_{o1} and e_{o2} result from the summations

$$e_{o1} = \frac{1}{n} (e_1 + e_2 + \cdots + e_n) \quad e_{o2} = \frac{1}{m} (e_1' + e_2' + \cdots + e_m') \tag{2.32}$$

then

$$e_o = \frac{e_{o1} + e_{o2}}{2} = \frac{1}{2n} (e_1 + e_2 + \cdots + e_n)$$
$$+ \frac{1}{2m} (e_1' + e_2' + e_3' + \cdots + e_m') \tag{2.33}$$

Equalization of scale factors can be accomplished by inserting $n - m$ shunt resistors of the type R_0 in Fig. 2.16c into the adding network for e_{o2} (on the assumption that $n > m$). This results in a further loss of scale factor on the part of e_{o2}, a loss which may be excessive if n is much greater than m.

Such loss in scale factor can be avoided, and at the same time constant multipliers conveniently introduced, through the use of a d-c operational amplifier, discussed in Sec. 2.11.

2.6. Transformers as Adders. When alternating current is used in a computing circuit, transformers may be used for addition. For precision, such transformers must have negligible core loss, negligible exciting current (i.e., extremely high core permeability), and negligible leakage inductance[9] (i.e., the coils are so closely coupled that all the flux of each

coil links with the other coil). Actual transformers deviate from the ideal, although modern core materials and special design[10,11] point to a practicable ratio of magnetizing to leakage inductance in excess of 100,000. The shortcomings of real transformers may also be corrected by providing compensating circuits. For example, in the Mallock simultaneous-equation solver,[12] a separate compensating transformer is used to supply nearly all the magnetizing flux to the computer transformer.

Assuming that ideal transformers are available, the adding circuit making use of them is shown in Fig. 2.17a. With e_1 and e_2 the voltages

(a)

(b)   (c)
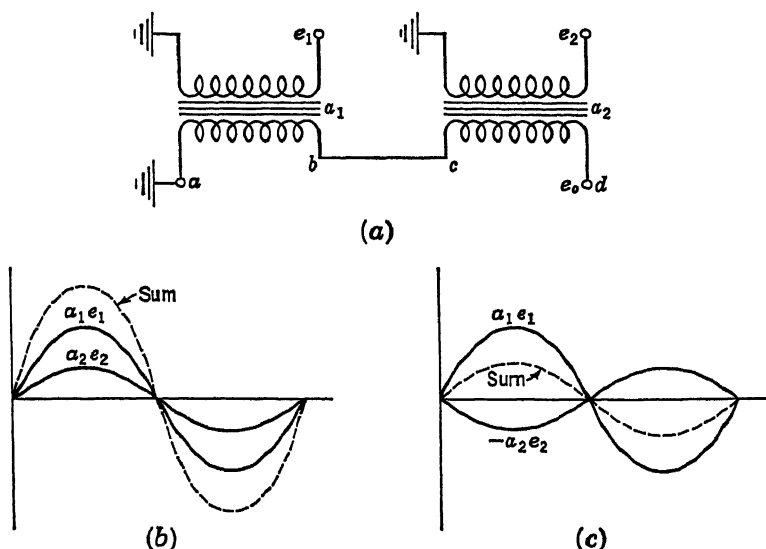
Fig. 2.17

applied to the primary windings, the secondaries act as sources of voltage which can be connected in series to provide the sum $a_1e_1 + a_2e_2$, where a_1 and a_2 are the turns ratios of secondary to primary. In alternating current plus and minus voltages are recognized by a 180° difference in phase between the two alternating voltages being compared. Thus, in Fig. 2.17a, if e_1 and e_2 are of the same phase (same algebraic sign), the output voltage e_o will also be of the same phase and equal in absolute value to the sum of the absolute values of the two inputs multiplied by their appropriate turns ratios. If e_2, however, is provided 180° out of phase with respect to e_1, the output voltage will be in phase with the larger of a_1e_1 or a_2e_2 and will have an absolute value which is the difference of their absolute values. This merely indicates that the output of the adding unit of Fig. 2.17a is always the *algebraic* sum of the two inputs. The corresponding in-phase and out-of-phase wave forms and their sums for one cycle of alternation are shown in (b) and (c), respectively.

The algebraic difference of a_1e_1 and a_2e_2 can be effected simply by connecting b to d instead of to c and taking the output from terminal c.

2.7. Integration. In electric analog computers, the integration (and differentiation) of a variable is performed directly with respect to time. It is shown in Chap. 4 that integration with respect to some variable in the machine other than time can be accomplished by making use of time integrations.

Fundamentally, integration is a process of accumulation. Any device capable of receiving and storing physical quantities and indicating the quantity stored can be used as an integrator. One example of such a device is the disk-and-wheel integrator described in Chap. 5, where the

(a)   *(b)*   *(c)*
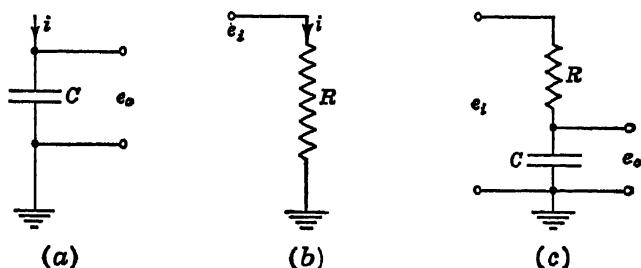
Fig. 2.18

rotations of a wheel are accumulated and represented by the displacement of a nut on a lead screw or by a number in a counter. Revolution counters themselves are integrating devices. Flowmeters, anemometers, watthour meters, etc., are often based on integration.

In electrical circuit theory an ideal capacitance will store electric charge and indicate the quantity stored by the voltage existing across its plates. While the output of a capacitor integrator is a voltage, the input is the charging current which determines the rate at which electric charge enters the storage unit. Thus, for a pure capacitance (Fig. 2.18a) with zero initial voltage

$$e_o = \frac{1}{C} \int_0^t i \, dt \qquad (2.34)$$

For computers in which variables may appear as currents and voltages, a capacitor alone is sufficient for the integration process in accordance with Eq. (2.34). In most computers the variables are voltages, so that the input current must be made proportional to the voltage to be integrated. A direct proportionality between current and voltage drop exists in an ideal resistance (Fig. 2.18b). Hence, by using the series circuit shown in Fig. 2.18c, a charging current *approximately* proportional to e_i will flow into C, provided that e_o is kept small enough to avoid affecting i beyond the allowable degree of approximation. This immediately raises

the problem of the time constant of the circuit. If the time during which integration is occurring is sufficiently great, the capacitor voltage will build up to a point at which the current flow will be seriously reduced, thereby introducing a considerable error into the proportionality relation between e_i and i.

The analysis of this problem is conveniently carried out on the basis of a step input voltage. Thus, in Fig. 2.18c, a voltage e_i is suddenly impressed on the circuit at the time $t = 0$ and remains for an indefinite period. The integration of a constant voltage results in an output voltage increasing uniformly with time. If i were strictly proportional to e_i, then Eq. (2.34) for this case would appear as

$$e_o = \frac{1}{RC} \int_0^t e_i \, dt = e_i \frac{t}{RC} \tag{2.35}$$

For $e_o = 0$ at $t = 0$ the product RC determines the rate at which the voltage e_o builds up with time and hence is called the "time constant" for the circuit. A large time constant means that it takes a long time (relatively) for e_o to build up in value. When $RC = 1$, the integrator is operating on a unit time base, so that $e_o = \int_0^t e_i \, dt$. The actual relationship between e_i and i is given by

$$i = \frac{e_i - e_o}{R} \tag{2.36}$$

whence

$$e_o = \frac{1}{RC} \int_0^t (e_i - e_o) \, dt \qquad \text{or} \qquad \frac{de_o}{e_i - e_o} = \frac{1}{RC} dt \tag{2.37}$$

from which

$$e_o = e_i(1 - \epsilon^{-(t/RC)}) \tag{2.38}$$

The curves for e_o given by Eqs. (2.35) and (2.38) are shown in Fig. 2.19 for comparison. For t approaching infinity, the exponential term
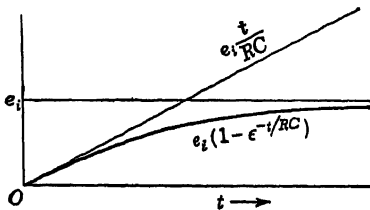
Fig. 2.19

approaches zero. Hence, e_o approaches e_i asymptotically. The discrepancy between the desired linear build-up curve for e_o and the actual exponential build-up, as a ratio δ to the desired build-up, is

$$\delta = 1 - \frac{RC}{t} (1 - \epsilon^{-(t/RC)}) \tag{2.39}$$

For a given tolerable error δ, and for a given integration time t, the circuit time constant RC may be determined from Eq. (2.39).

If a sinusoidal voltage $e_i \sin \omega t$ is applied as an input, a true integral

output would be

$$e_o = -\frac{e_i}{RC\omega}\cos\omega t \qquad (2.40)$$

which lags e_i by exactly 90°.

The actual output of the integrator can be determined by solving the differential equation for the circuit. Thus the charge q in the circuit at any instant of time is governed by the equation

$$R\dot{q} + \frac{1}{C}q = e_i\sin\omega t \qquad (2.41)$$

The steady-state solution is

$$q = \frac{-Ce_i}{[1 + (RC\omega)^2]^{\frac{1}{2}}}\cos(\omega t + \phi) \qquad \tan\phi = \frac{1}{RC\omega} \qquad (2.42)$$

The voltage across the capacitor is q/C, or

$$e_o = -\frac{e_i}{\sqrt{1 + (RC\omega)^2}}\cos(\omega t + \phi) \qquad (2.43)$$

Equations (2.40) and (2.43) agree closely for very large values of $RC\omega$, for then $\tan\phi$ approaches zero, which means that ϕ approaches zero, and the term $(RC\omega)^2$ is large compared with unity.

Thus, for the same degree of accuracy in the integral, signals having different frequencies require different time constants RC. For a signal composed of a superposition of harmonic components of different frequencies, the time constant must be chosen so as to give the required accuracy in the lowest frequency component.[13] All the other components then contribute terms of higher precision to the integral. The time duration of the integrating process, which is important in determining the error in the step-function integral, does not affect the steady-state sinusoidal process directly. The integration can be carried on for an indefinite period of time, accuracy being dependent only on the criterion that $RC\omega$ be large. The time factor enters, of course, in the frequency ω.

A commercially manufactured and widely used integrating device which has also been used in the solution of mathematical problems[14,15] is the watthour meter. As used in measuring electrical consumption, the rotation of the watthour disk is coupled to a mechanical indicating counter exerting very little resistance to rotation. In a mathematical machine, the integrator must be able to drive other units which may offer a very considerable resistance to displacement. As in the case of the mechanical integrators described in Chap. 5, torque amplifiers are necessary when watthour meters are the integrating elements of a computer.[16]

In such a torque amplifier, a motor of sufficient power to drive all the attached computing elements follows the motion of the watthour meter disk without exerting appreciable drag on the disk. In the continuous integraph[14] mercury drop contacts between platinum-tipped terminals on the rotating meter disk and nickel-plated strips on a servo-operated follower disk provide the torque-free electrical connection necessary to operate a relay servo. For his all-electric integrator, Varney[16] mounted a three-legged electromagnet on the motor-driven follower-disk, with a coil of wire wound on each leg, the central leg being excited from a 60-cycle source. The coils on the two outer legs, wound in opposite directions, were connected in series, with their free ends connected to a high-gain power amplifier. The watthour-meter disk, mounted on a separate but collinear shaft, carried a small piece of iron at its periphery in close proximity to the electromagnet. Any tendency of the meter disk to carry the iron out of register with the electromagnet developed a signal in the outer coils of the magnet which was amplified and was used to drive a two-phase induction motor in the correct direction to maintain the two disks in register.

2.8. Differentiation. As indicated in the opening sentence of Sec. 2.7, differentiation in electrical computers is performed directly with respect to time. Differentiation is a rate-of-change process, so that any device which will indicate a rate of change of some quantity is a differentiator.

The rate of build-up of voltage in a capacitor is proportional to the current flow into it. Hence, a capacitor may be used as a differentiating device, as well as an integrating device, if the appropriate measurements are taken. For a capacitor, the derivative form of the voltage-current relation is

$$i = C \frac{de_o}{dt} \tag{2.44}$$

Thus, by measuring the current i, the time derivation of e_o is obtained. For the reason mentioned in Sec. 2.7, it is desirable to convert i into a voltage. This is done in the usual manner, by passing i through an ideal resistor across which the voltage drop is measured. The differentiating circuit is, therefore, as shown in Fig. 2.20a. The voltage drop across the capacitor is $e_i - e_o$. It is changing at a rate proportional to the current flow $i = e_o/R$. Thus, for this case Eq. (2.44) becomes

$$\frac{e_o}{R} = C \frac{d}{dt}(e_i - e_o) \tag{2.45}$$

If the voltage across the capacitor is changing at a uniform rate, a constant current flows through R and the voltage drop e_o does not vary with time. Hence, for this case $de_o/dt = 0$ and $e_o = RC\, de_i/dt$. If deriva-

tives of higher order than the first are present in e_i, which would be the usual situation, then e_o will also change with time and its value will not give the true derivative of e_i.

The study of the accuracy of the differentiation process is based in the following discussion on both a step change in the derivatives (*i.e.*, an input voltage suddenly starting to increase at a uniform rate, say K) and a sinusoidal variation in the derivative (which also means a sinusoidal variation in the input voltage).

Consider, first, the sudden uniform rate of increase K of e_i. If the differentiator accurately reproduces the derivative, e_o will suddenly

(a)   (b)
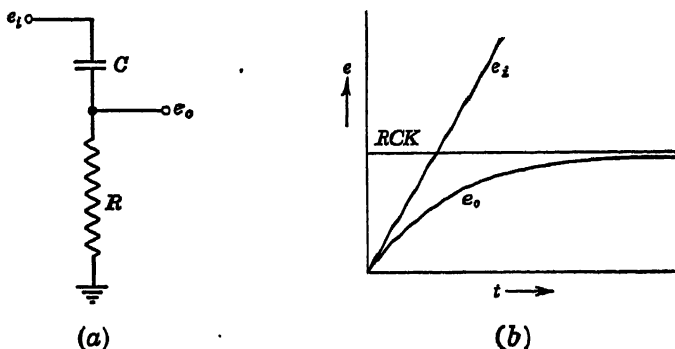
Fig. 2.20

rise stepwise to a value RCK and remain at that value as long as e_i kept increasing at the rate K. This step derivative is shown in Fig. 2.20b. This means that a constant current CK will be developed immediately in the resistor R. Obviously, such a current cannot be produced instantaneously, since, at the initial instant there is a zero drop in potential across R and some time must elapse before e_i builds up to a sufficient value to produce the required current. Meanwhile, the charge on the capacitor is also building up, thereby reducing the rapidity with which e_o approaches its required value. The actual rate of build-up of e_o is also shown in Fig. 2.20b. It approaches the value RCK asymptotically with time. Equation (2.45) for this case is

$$e_o = RCK - RC \frac{de_o}{dt} \tag{2.46}$$

Its solution is

$$e_o = RCK(1 - \epsilon^{-(t/RC)}) \tag{2.47}$$

As in the study of the integration process, RC is the time constant which determines the rate at which e_o approaches its correct value RCK. The discrepancy at any instant of time between RCK and e_o, as a ratio to

RCK, is

$$\delta = \epsilon^{-(t/RC)} \tag{2.48}$$

Equation (2.48) shows that for best results (least error) the differentiation time should be long and the time constant of the circuit short, in contrast to the conclusions arrived at for the integration process, where the reverse is true.

Considering, now, the case of sinusoidal input, the true derivative of $e_i \sin \omega t$ is given by

$$\frac{e_o}{RC} = \omega e_i \cos \omega t \tag{2.49}$$

The actual output of the differentiator is found from the steady-state solution of Eq. (2.45),

$$\frac{de_o}{dt} + \frac{1}{RC} e_o = e_i \omega \cos \omega t \tag{2.50}$$

The solution of this equation, obtained by usual methods, is

$$e_o = e_i \frac{RC\omega}{\sqrt{1 + (RC\omega)^2}} \cos (\omega t - \phi) \tag{2.51}$$

$$\tan \phi = RC\omega \tag{2.52}$$

For very small values of $RC\omega$, the phase angle ϕ between the true derivative represented by Eq. (2.49) and the indicated derivative represented by Eq. (2.51) is also very small, and the circuit produces a voltage which is closely proportional to the true derivative. The extent of the deviation can be measured by the size of the phase angle ϕ.

The requirement that $RC\omega$ should be small in the differentiating circuit also leads to very small output voltages e_o. The smaller the output, on this basis, the more accurately is this output proportional to the derivative of the input. This is consistent with Eq. (2.45). If e_o is maintained very small for a given rate of change of e_i, it is clear that e_o cannot change as rapidly as it might if it were allowed to take on larger values. Ideally, e_o should be kept close to zero. This, in turn, requires the use of a computing amplifier to amplify e_o to a usable and measurable value.

It is well to mention at this time that differentiation is a "peaking" process; i.e., it serves to accentuate irregularities in a function being differentiated. Such irregularities usually result from "noise" developed internally (e.g., backlash in gears, poor electrical contacts, etc.) or picked up externally (e.g., stray fields) and tend to be of relatively high frequency (changing rapidly). Since the output of a differentiation process is directly proportional to frequency, the noise output is likely to be all

out of proportion to the desired signal output and may completely mask the desired signal.

Integration, on the other hand, is a smoothing process which tends to iron out irregularities caused by high-frequency noise. Consequently, if a choice is to be made between using differentiation or integration in a given process, the latter method should certainly be adopted.

ACTIVE (ELECTRONIC) COMPUTING ELEMENTS

2.9. Simple Electronic Circuits. It is apparent from the above discussion that virtually all passive electrical computing elements suffer from loading errors. In general these devices operate correctly only if the input impedance of the circuitry at the output of the computing element is very high. Since vacuum-tube amplifiers have input impedances often in excess of several megohms, it is natural that they should find application in electric-analog-computing operations. The use of vacuum tubes makes it necessary to equip the computer with high-voltage and filament power supplies and to replace the vacuum tubes periodically. The use of such devices, therefore, inevitably increases the first cost and the operating expense of the computer. In general, this expense is well justified by the increase in accuracy and precision attainable with active computing elements. For most general-purpose analog-computing operations, the d-c operational amplifier discussed in detail in Sec. 2.10 is used almost exclusively. It is possible, however, to attain satisfactory results in varied special-purpose applications by employing relatively simply vacuum-tube circuits.[17]

Addition and subtraction can be carried out either by employing a multiple-input vacuum tube or by employing a separate vacuum tube for each input. Figure 2.21a illustrates a simple double-input vacuum-tube circuit suitable for subtraction. In this case the output voltage e_o is equal to $A(e_1 - e_2)$, where A is the gain of the amplifier. Figure 2.21b illustrates a double-input adding circuit in which case the output is proportional to the sum of e_1 and e_2. Parallel-plate adding circuits have the advantage of high input impedance and virtually no coupling between inputs. A typical circuit is shown in Fig. 2.22a. Here the output voltage is proportional to $e_1 + e_2 + e_k + \cdots + e_n$ and appears across the load resistor R_L. Figure 2.22b shows a parallel adding circuit employing a common cathode resistor and having a relatively low output impedance. A differential amplifier circuit for subtraction is shown in Fig. 2.23. Here the output voltage, proportional to the difference $(e_1 - e_2)$, appears between the plates of the two triodes.

To reduce the error that is characteristic of the simple RC integrators discussed in Sec. 2.7, the circuit shown in Fig. 2.24 is sometimes employed.

(a) (b)

Fig. 2.21

(a) (b)
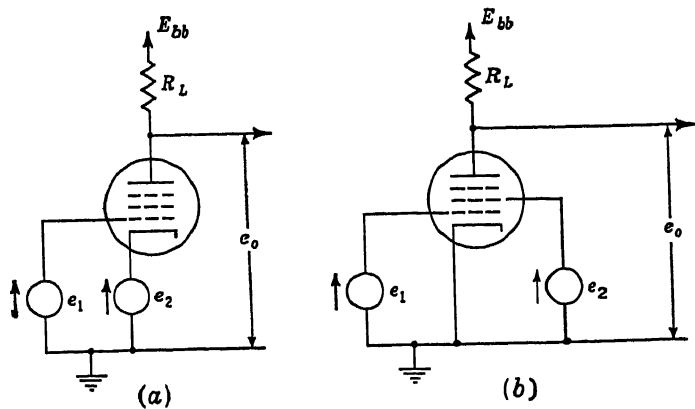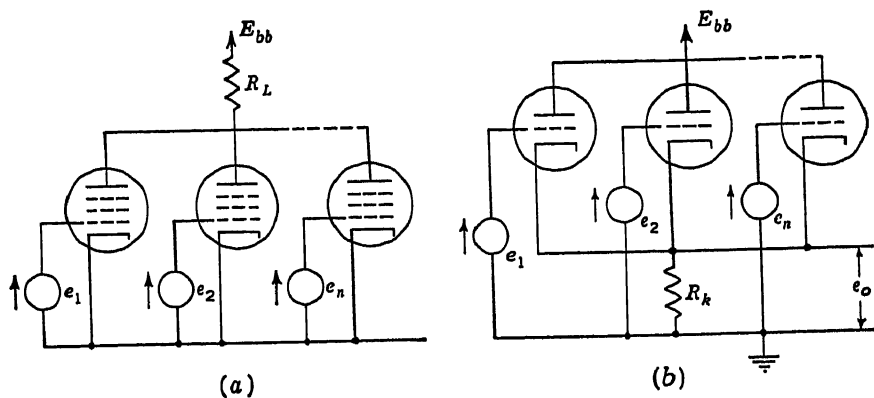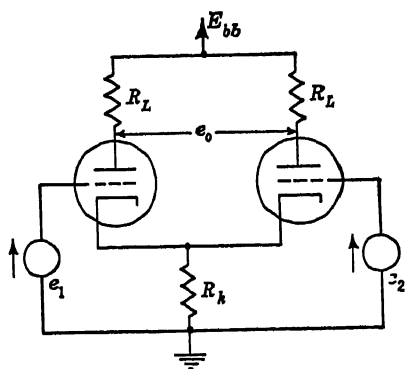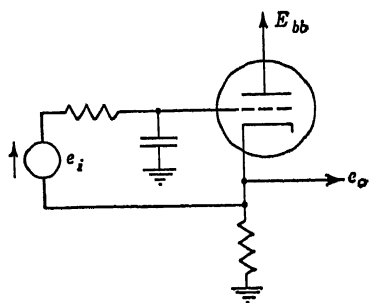
Fig. 2.22

Fig. 2.23

Fig. 2.24

This circuit is known as a "bootstrap" circuit and requires that neither terminal of the input generator be connected to ground. The feedback action of the circuit makes the input current effectively independent of the voltage across the integrating capacitor.

The shortcomings of the simple differentiator of Fig. 2.20 are also alleviated by means of a cathode follower,[18] which serves as a constant-current device and prevents interaction between the capacitor and the resistor of the differentiating circuit. In the cathode-follower circuit shown in Fig. 2.25, the voltage e_k follows the input voltage e_i. The gain through the follower is somewhat less than unity, being given by

$$A = \frac{g_m R}{1 + g_m R} \qquad (2.53)$$

Fig. 2.25

where g_m is the transconductance of the tube.

For circuits employing tubes with high transconductance, A is very close to unity. Whence, the approximation $e_k \approx e_i$ is justified.

The use of a cathode follower in differentiating and integrating circuits and for other computing operations has been described by Philbrick.[19] The differentiating circuit is shown in Fig. 2.26. Since $e_k = e_i$, as e_i varies, the current i through the capacitor C will be precisely proportional to de_i/dt. Exactly the same current flows through R, so that the voltage drop across R is proportional to i and thus to de_i/dt.

Other forms of this circuit have been developed in an effort to obtain an output voltage of the same order of magnitude as the input voltage in a sine-wave differentiator. One such circuit[20] suitable for operation from 100 to 20,000 cps with inputs up to 1 volt is shown in Fig. 2.27a. Typical operating curves for $e_i = 0.2$ volt
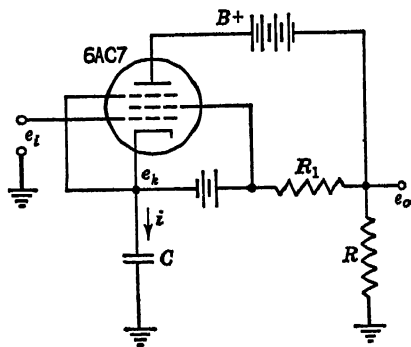
Fig. 2.26. [G. A. Philbrick, *Designing Industrial Controllers by Analog*, *Electronics*, 21(6):108–111 (1948).]

rms, $C = 400$ $\mu\mu$f, and various values of R are shown in (b). The error resulting from the voltage drop across R is compensated in the circuit shown in Fig. 2.28a. An adjustable resistor R_4 feeds back a voltage equal to that across R, but of opposite phase. Typical operating curves for this differentiator are shown in (b) for an input of 0.06 volt rms, $R = 25,000$ ohms, $C = 400$ $\mu\mu$f with varying values of R_4. Ideal differentiation occurs
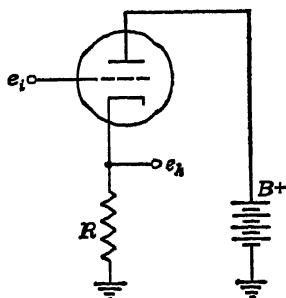
in this case for $R_4 = 6{,}500$.   For values of R above 6,500, undercompensation occurs, while for those below 6,500, overcompensation takes place.   If R or C were changed, the amount of feedback through R_4 would also be changed in order to compensate properly for the voltage drop across R.

All the above circuits suffer from a number of serious shortcomings. The accuracy of the computing operation is generally severely limited by nonlinearities in the tube characteristics.   In multiple-tube circuits,
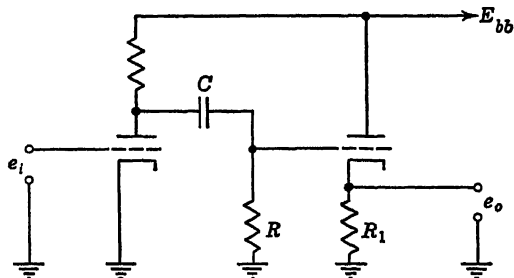
(a)
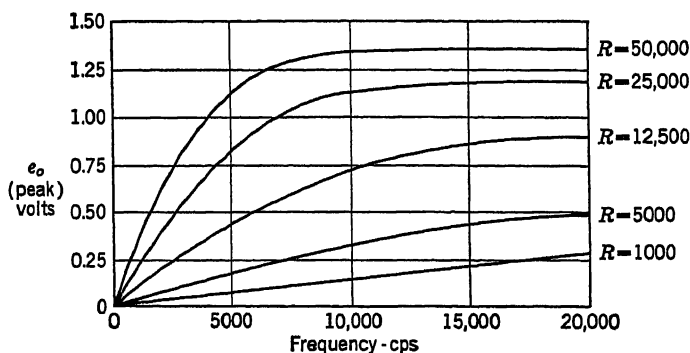
(b)

Fig. 2.27. [A. H. Schmitt and W. E. Tolles, *Electronic Differentiation, Rev. Sci. Instr.*, 13:115–118 (1942).]

the tubes taking part in the computing operation must be carefully matched.   In most of the circuits, the polarity of the output voltage is limited to positive voltages.   For these reasons, d-c operational-amplifier techniques, which make the accuracy of the computing operations essentially independent of the vacuum-tube characteristics and variations in these characteristics, are preferred whenever it is desirable to limit errors to less than 5 per cent.

2.10. The D-C Operational Amplifier.   For most accurate computation work, d-c electrical voltages are employed as the problem variables. In order to permit the performance of the desired mathematical operations

with sufficient accuracy and precision, the electronic amplifiers used in the computing process must have the following properties:

1. High gain (in excess of 10,000; sometimes over 100,000,000)
2. Linearity over a wide region of operation; generally from -100 to $+100$ volts at the output
3. Flat frequency response from direct-current to several hundred cycles per second (sometimes up to several kilocycles)
4. Zero output voltage for zero input voltage
5. Very high input impedance
6. Reversal in polarity between the input and output of the amplifier
7. Very low noise level within the amplifier

The severity of the above requirements, particularly regarding linearity and frequency response, delayed the realization of practical general-

(a)

(b)
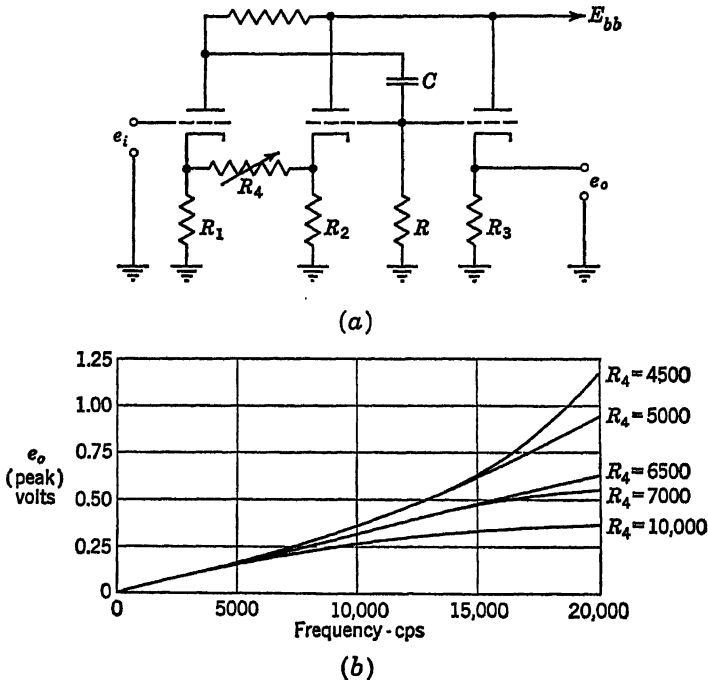
Fig. 2.28. [A. H. Schmitt and W. E. Tolles, *Electronic Differentiation, Rev. Sci. Instr.*, 13:115–118 (1942).]

purpose electronic analog computers until after World War II. Ragazzini[21] presented the first complete description of a satisfactory operational amplifier in 1947. Since then, a large number of modifications of his circuits have been introduced. The basic circuit elements comprising such an operational amplifier are shown in Fig. 2.29a. Note that the coupling between the amplifier stages is entirely by means of resistors.

The use of coupling capacitors would cause the gain of the amplifier to fall off at the low-frequency end when the reactances of the capacitors approach infinity. In the more usual amplifier circuits, the coupling capacitor acts to isolate the grid of an amplifier tube from the positive d-c potential at the plate of the preceding stage. To maintain the amplifier grids at the required slightly negative potentials without the aid of coupling capacitors, it is necessary to include a negative power supply $(B-)$ as well as the customary positive supply $(B+)$. The variable cathode resistor R_K in the first stage is adjusted prior to computation in order to make the output voltage e_o equal to zero when no signal is applied at the input terminal. Since an odd number of amplification
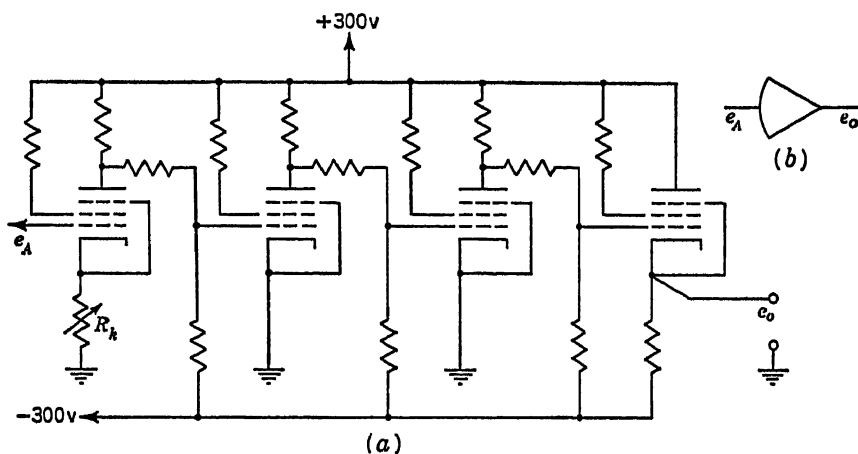
Fig. 2.29

stages are employed, the voltage e_o at the output terminal with respect to ground is $-A$ times the voltage e_A at the grid of the first stage, where A is a very large number. The symbol shown in Fig. 2.29b is employed to represent a high-gain operational amplifier. Since all voltages are measured with respect to ground, the ground bus is generally omitted from the circuit diagram.

The main source of error attending the use of d-c operational amplifiers is their tendency to "drift." Prior to use as a computing element, the amplifier is carefully "zeroed" by connecting the input terminal to ground and by adjusting the variable resistor R_K to give a zero output voltage. If the setting of this resistor is left unchanged and the input voltage maintained at zero, the output voltage will be found to deviate or drift gradually away from zero. The causes for this phenomenon include variations in the power supplies and filament voltages, as well as transient variations in the properties of the tubes and other circuit elements.

Much effort has gone into the design of operational amplifiers with a minimum of drift errors. The most successful and widely used devices of this type employ so-called chopper stabilization.[22,23] This method is based on the recognition that an a-c amplifier is not subject to drift in the same manner as a d-c amplifier. A separate a-c amplifier is provided. The voltage appearing at the input of the operational amplifier is transformed into an alternating signal by means of a vibrator driven by the a-c line voltage and is applied to this a-c amplifier. The output of the a-c amplifier is therefore a signal whose amplitude is proportional to the summing-point voltage e_A. This output is rectified and filtered to transform it back into a d-c voltage. This voltage is then applied as a correcting signal to the d-c amplifier chain. The frequency response of the chopper amplifier is such that it reacts to the slow drift-voltage variations but not to the variations of the computing signal voltage. A
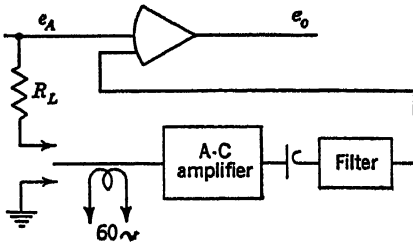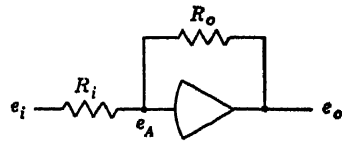
Fig. 2.30   Fig. 2.31

block diagram of such a system is shown in Fig. 2.30. The resistor R_L isolates the stabilizing circuits from the computing circuits to prevent any interference with the computing operation.

Another source of error in electronic operations is the grid current drawn by the input stage of the operational amplifier. This can be minimized by the use of special types of vacuum tubes. In order to avoid instability and oscillations at the high-frequency end of the amplifier characteristics, a number of small capacitors are usually added to the basic circuit. These cause the amplifier gain to fall off as the frequency is increased in such a manner that stability is assured.

2.11. Electronic Sign Change and Addition. When the d-c operational amplifier, described in the preceding section, is applied to the performance of linear mathematical operations, external elements are connected to the amplifier as shown in Fig. 2.31. The resistors R_i and R_o are termed the input and the feedback resistors, respectively. The operation of this circuit depends upon the fact that the amplifier terminal voltage e_A is maintained essentially at ground potential for all practical purposes. This follows from the fact that the forward gain $-A$ of the amplifier is very large. The voltage e_A is related to the output voltage

through the equation

$$e_A = -\frac{e_o}{A} \tag{2.54}$$

A reasonable maximum value for e_o is 50 to 100 volts. The gain A is easily of the order of 10,000, and frequently, it may be as high as 100,000,000. Taking the lower figure (and bearing in mind that e_o is negative when e_A is positive), the largest value e_A might have is $100/10,000 = 0.01$ volt.

Since the terminal e_A is the grid of a vacuum tube, there is no current drain into the amplifier. Instead, all the current flowing through R_i also flows through R_o. The relationship established between e_i and e_o (considering $e_A = 0$) is therefore

$$\frac{e_i}{R_i} = -\frac{e_o}{R_o} \quad \text{or} \quad e_o = -\frac{R_o}{R_i} e_i \tag{2.55}$$

The amplifier thus serves as a means for scale changing (that is, stepping e_i up or down in accordance with the ratio R_o/R_i) as well as for inverting (changing sign). If $R_o = R_i$, only a change in sign of the voltage results.

In a more general sense, the input and feedback elements need not be pure resistances but may be any reasonable complex impedances Z_i and Z_o. In the latter case, assuming $A \gg 1$,

$$e(s)_o = -\frac{Z_o}{Z_i} e(s)_i \tag{2.56}$$

Depending on the nature of Z_o and Z_i, a large variety of relations ("transfer functions") can be established between e_o and e_i. Such relations are considered in Sec. 2.13.

The high-gain negative-feedback d-c amplifier can be used in the "star-mixing" network of Fig. 2.16c for addition by inserting the amplifier into the circuit, so that the resistance R_o is the feedback element. The circuit for adding two voltages e_1 and e_2 is shown in Fig. 2.32a. Bearing in mind that e_A is substantially at ground potential, e_o is given by

$$e_o = -\left(\frac{R_o}{R_1} e_1 + \frac{R_o}{R_2} e_2\right) \tag{2.57}$$

The ratios R_0/R_1 and R_0/R_2 can be employed to adjust scale factors, to represent the coefficients of e_1 and e_2, or both. Any number of inputs can be used in the circuit typified in Fig. 2.32a. For n inputs, the output voltage is

$$e_o = -\left(\frac{R_0}{R_1} e_1 + \frac{R_0}{R_2} e_2 + \cdots + \frac{R_0}{R_n} e_n\right) \tag{2.58}$$

The only restriction is that e_o does not exceed the amplifier range.

The amplifier may also feed any number of loads, provided the resultant impedance to ground is not less than the design value of the load impedance Z_l for the amplifier range. Referring to Fig. 2.32b and making use of the more general impedance concept Z, the above restric-
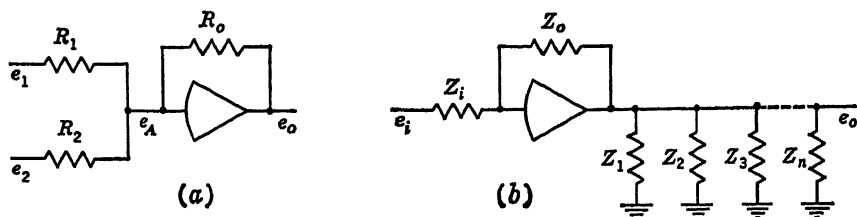
Fig. 2.32

tion is expressed by the equation

$$\frac{1}{Z_o} + \frac{1}{Z_1} + \frac{1}{Z_2} + \cdots + \frac{1}{Z_n} \gtreqless \frac{1}{Z_l} \qquad (2.59)$$

Note that Z_o is part of the load on the amplifier, since one end of Z_o is substantially at ground potential.

2.12. Electronic Integration and Differentiation. In order to apply d-c operational amplifiers to the mathematical operation of integration, the circuit shown in Fig. 2.33 is employed. The current through the input resistor R is given by

$$i = \frac{e_i - e_A}{R} \qquad (2.60)$$
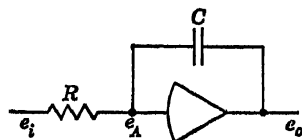
Fig. 2.33

Since the amplifier draws negligible grid current, this current i is also the charging current for the capacitor C. The voltage across C at any instant of time is

$$e_A - e_o = (1 + A)e_A \qquad (2.61)$$

where $-A$ is the gain of the amplifier. Since A is a very large number (10^4 to 10^8), unity can be neglected by comparison, so that the voltage across the capacitor can be written as Ae_A or $-e_o$. Hence, for zero initial conditions,

$$Ae_A = -e_o = \frac{1}{C} \int_0^t i \, dt$$

$$= \frac{1}{RC} \int_0^t (e_i - e_A) \, dt$$

$$= \frac{1}{RC} \int_0^t \left(e_i + \frac{e_o}{A} \right) dt \qquad (2.62)$$

In differential equation form,

$$-\frac{de_o}{Ae_i + e_o} = \frac{1}{RCA} dt \tag{2.63}$$

the solution of which for a step input e_i is

$$e_o = -Ae_i[1 - \epsilon^{-(t/RCA)}] \tag{2.64}$$

for $e_o = 0$ at $t = 0$, remembering that e_o is negative when e_i is positive. The exponential term may be expanded in terms of a power series in t and only the first two terms of the series used for small values of t/RCA:

$$\epsilon^{-(t/RCA)} \cong 1 - \frac{t}{RCA} + \cdots \tag{2.65}$$

whence Eq. (2.64) becomes

$$e_o \cong -e_i \frac{t}{RC} \tag{2.66}$$

This is the same as Eq. (2.35) so that, for small t/RCA, the integration is performed with precision. Thus, when a negative-feedback amplifier of large gain A is used, the time constant of the integrating unit is effectively increased by the factor A, since the capacitor has an effective capacitance of AC, and the output is similarly increased. Hence, for the same degree of accuracy in the final result, the amplifier may integrate a step input for a period A times as long as the simpler network of Fig. 2.20a. Or, for the same integration time, the error in the result is reduced to about $1/A$ times its magnitude for the simpler network.

On the basis that the effective capacitance of the feedback capacitor is A times as great as its actual capacitance, the steady-state output of this integrator to a sinusoidal input voltage $e_i \sin \omega t$ is

$$e_o = \frac{Ae_i}{\sqrt{1 + (RCA\omega)^2}} \cos(\omega t + \phi) \qquad \tan \phi = \frac{1}{\omega RCA} \tag{2.67}$$

Referring back to Eq. (2.62), it is evident that for a large amplification factor A, the ratio e_o/A will be small in comparison with e_i, so that Eq. (2.62) might just as well be rewritten as follows:

$$e_o = -\frac{1}{RC} \int_0^t e_i \, dt \tag{2.68}$$

When expressed in this fashion, the significance of the amplifier in magnifying the time constant and improving the accuracy of the circuit is not so readily evident.

Several inputs to a single integrating amplifier can be summed and integrated in one operation. Thus, in Fig. 2.34, three input voltages are

to be added in different proportions and the integral of the sum obtained. The output voltage is

$$e_o = -\frac{1}{C} \int_0^t \left(\frac{e_1}{R_1} + \frac{e_2}{R_2} + \frac{e_3}{R_3} \right) dt - K \qquad (2.69)$$

where K is an initial condition, and represents the voltage to which capacitor C is charged at time $t = 0$.

The accuracy of the differentiation operation is likewise improved through the use of operational amplifiers. For the circuit of Fig. 2.35,
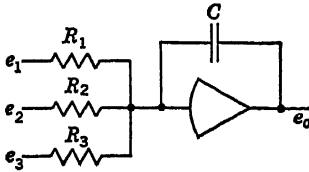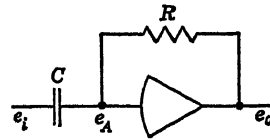
Fig. 2.34   Fig. 2.35

the capacitor charging current is

$$i = C \frac{d}{dt} (e_i - e_A) = \frac{e_A - e_o}{R} \qquad (2.70)$$

Since $e_o = -Ae_A$, and since A is very large compared with unity, Eq. (2.70) can be written as

$$C \frac{d}{dt} \left(e_i - \frac{e_o}{A} \right) = -\frac{e_o}{R} \qquad (2.71)$$

A comparison of Eq. (2.71) with Eq. (2.45) shows that the error caused by the rate of change of e_o has been reduced by a factor of A. Thus, for the same magnitude of error as in the simple RC circuit, the output of the amplifier circuit can be made A times as great.

2.13. Complex Transfer Functions. The feedback and input elements of computing circuits utilizing operational amplifiers need not necessarily be limited to single resistors or capacitors. In general, both the input and feedback impedances may be four-terminal networks as shown in Fig. 2.36a. In accordance with Eq. (2.56) the output voltage is related to the input voltage by the factor $-Z_o/Z_i$. Since the amplifier draws no current, the output current i_1 of Z_i and the input current i_2 of Z_o are identical. Furthermore, since the voltage e_A is always very small (effectively at ground potential), the output terminals of Z_i and the input terminals of Z_o can be considered as being short-circuited. In the general case, therefore, these impedances refer to the short-circuit transfer impedances given by

$$Z_i = \frac{e_i}{i_{sc}} \qquad Z_o = \frac{e_o}{i_{sc}} \qquad (2.72)$$

where all quantities are expressed as functions of s and where

$$|i_{sc}| = |i_1| = |i_2|$$

as illustrated in Fig. 2.36b.

The complex transfer impedances obtainable with RC input and feedback networks are best expressed in terms of the Laplace-transform operator s. It may help readers unfamiliar with Laplace-transform techniques to recognize that for quiescent initial conditions the operator s signifies the operation d/dt, and $1/s$ signifies the operation $\int_0^t dt$. As an example of the derivation of such transfer functions, consider the circuit
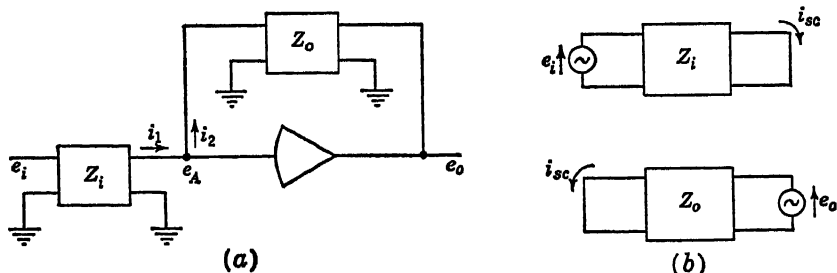
Fig. 2.36
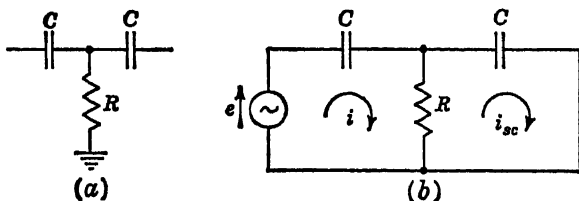
Fig. 2.37

of Fig. 2.37a. The problem is to find the current between the right-hand terminal and ground when a voltage source is applied to the left-hand terminal, as shown in Fig. 2.37b. The loop equations for the two loops of the latter figure are

(a)
$$e = i\left(\frac{1}{C}\int_0^t dt + R\right) - i_{sc}R$$

$$e(s) = i(s)\left(\frac{1}{sC} + R\right) - i(s)_{sc}R$$

(b)
$$0 = -iR + i_{sc}\left(\frac{1}{C}\int_0^t dt + R\right)$$

$$0 = -i(s)R + i(s)_{sc}\left(\frac{1}{sC} + R\right)$$

(2.73)

Solving Eqs. (2.73a and b) simultaneously for the short-circuit transfer

impedance

$$Z = \frac{e(s)}{i(s)_{so}} = \frac{(1/sC + R)^2}{R} - R$$

$$= \frac{1}{sC}\frac{1 + 2sCR}{sCR} \qquad (2.74)$$

The transfer impedances of 40 useful networks are tabulated in Table A1.1.

These networks may be used as input or feedback elements, as desired. For example, the circuit of Fig. 2.38 has an over-all voltage transfer ratio of

$$\frac{e(s)_o}{e(s)_1} = -\frac{Z_o(s)}{Z_1(s)}$$

$$= -\frac{1}{sC}\frac{(1 + 2sCR)/sCR}{R_1/(1 + R_1C_1s)}$$

$$= -\frac{R_1}{sC}\frac{(1 + 2sCR)(1 + R_1C_1s)}{sCR} \qquad (2.75)$$

Occasionally, networks which permit feedback to occur along several separate paths are useful. For the circuit of Fig. 2.39a, a simple node analysis leads to the relationship between the input and output voltages:

Fig. 2.38

$$\frac{e_o}{e_i} = -\frac{R_2R_4}{R_2R_3 + R_1(R_2 + R_3 + R_4)} \qquad (2.76)$$
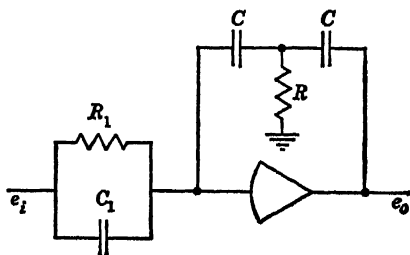
Replacing R_4 by a capacitance C_2 results in schematic (b). The voltage relations for (b) are

$$C_2\left(R_2 + R_3 + \frac{R_2R_3}{R_1}\right)\frac{de_o}{dt} + e_o = -\frac{R_2}{R_1}e_i \qquad (2.77)$$

Transforming gives

$$\frac{e(s)_o}{e(s)_i} = -\frac{R_2}{R_1}\frac{1}{1 + (R_2 + R_3 + R_2R_3/R_1)C_2s} \qquad (2.78)$$

If the node between R_1 and R_3 is grounded through a capacitor C_1 [schematic (c)], the differential equation of the circuit and the transform relation between the output and input voltages are

$$R_2C_2R_3C_1\frac{d^2e_o}{dt^2} + C_2\left(\frac{R_2R_3}{R_1} + R_2 + R_3\right)\frac{de_o}{dt} + e_o = -\frac{R_2}{R_1}e_i \qquad (2.79)$$

and $$\frac{e(s)_o}{e(s)_i} = -\frac{R_2}{R_1}\frac{1}{1 + (R_2 + R_3 + R_2R_3/R_1)C_2s + R_2C_2R_3C_1s^2} \qquad (2.80)$$

where s^2 indicates the operation d^2/dt^2.

When use is made of capacitors in both feedback loops in schematic (b), schematic (d) results. Its equations are

$$R_1 C_2 R_3 C_3 \frac{d^2 e_o}{dt^2} + (R_1 C_2 + R_3 C_2 + R_1 C_3) \frac{de_o}{dt} = -e_i \qquad (2.81)$$

and

$$\frac{e(s)_o}{e(s)_i} = - \frac{1}{(R_1 C_2 + R_3 C_2 + R_1 C_3 + R_1 C_2 R_3 C_3 s)s} \qquad (2.82)$$

In schematic (e) a capacitor C_1 is used to replace the resistor R_3 used in (a). The equations for this case are

$$R_4 C_1 R_1 \frac{R_2 + R_4}{R_2 R_4} \frac{de_o}{dt} + R_1 \frac{R_2 + R_1}{R_1 R_2} e_o = -R_4 C_1 \frac{de_i}{dt} \qquad (2.83)$$

and $$\frac{e(s)_o}{e(s)_i} = - \frac{R_4 C_1 s}{R_4 C_1 R_1[(R_2 + R_4)/R_2 R_4]s + R_1[(R_2 + R_1)/R_1 R_2]} \qquad (2.84)$$

A tabulation of the transfer functions of a wide variety of circuits of this type is provided in Table A1.2.
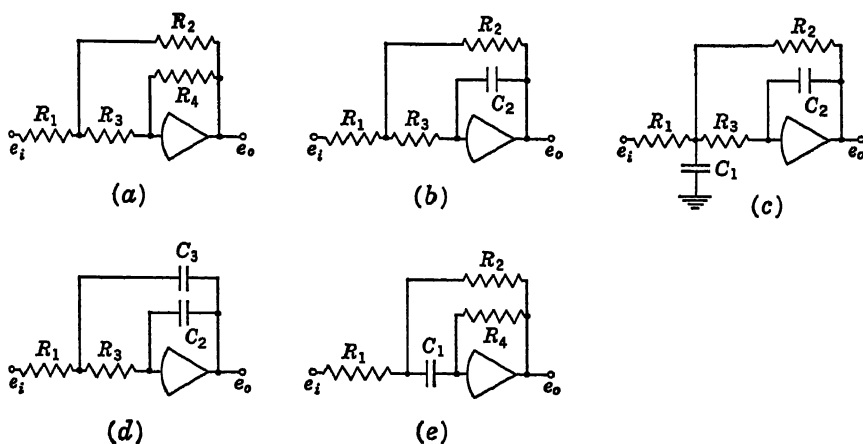
Fig. 2.39

2.14. Errors in Electronic Operations. Errors in the performance of the operations of addition and integration by use of operational amplifiers may result from imperfect operation of the input and feedback elements as well as from shortcomings in the operational amplifiers. In general, sufficiently high-quality resistors are available so that errors from this source are negligible. Capacitors, however, invariably have a small amount of leakage conductance. For analysis purposes, this leakage conductance may be regarded as represented by a large resistor R_C in parallel with each capacitor. As a result, the transfer function of the

simple integrator shown in Fig. 2.40 is actually

$$\frac{e(s)_o}{e(s)_i} = -\frac{R_C}{R}\frac{1}{1 + R_C Cs}$$

$$= -\frac{1}{RCs + R/R_C} \tag{2.85}$$

whereas the desired transfer function is

$$\frac{e(s)_o}{e(s)_i} = -\frac{1}{RCs} \tag{2.86}$$

The presence of R_C, the leakage resistor, therefore introduces an error, which grows as the integration proceeds. For accurate computation it is imperative to employ high-quality capacitors with a minimum of leakage conductance.

More serious errors in computing operations result from shortcomings in the operational amplifiers. Here, most errors are attributable to insufficient input impedance, excessive output impedance, and phase shifts in the amplifier stages. Discussions
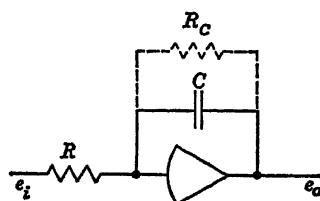
Fig. 2.40

of the effect of these sources of error, particularly upon the operations of addition and integration, have been presented by MacNee,[24] Korn,[25] and Wass.[26]

To estimate the effect of drift and grid current, it is useful to refer all drift phenomena arising in the operational amplifier to the grid of the first amplifier stage. The entire drift effect can then be represented by a single voltage source e_D of such a magnitude that it has the same
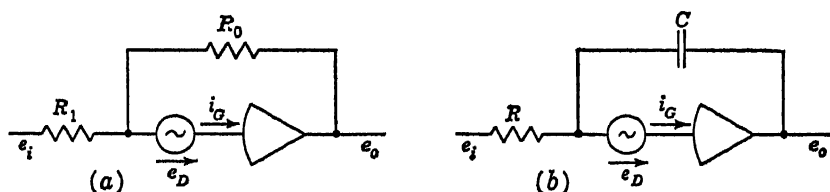
Fig. 2.41

effect as all sources of drift within the amplifier combined. In a similar manner, a current i_G can be visualized as representing the grid current drawn by the amplifier stage, as well as the current flowing through any stray shunt impedance from the input terminals to ground. Figures 2.41a and b illustrate a sign changer and an integrator modified in this manner. A simple node analysis of these circuits reveals that the output

voltage of the sign changer is given by

$$e_o = -\frac{R_0}{R_1} e_i + R_0 i_G + \frac{R_1 + R_0}{R_1} e_D \qquad (2.87)$$

where R_1 and R_0 are the input and feedback resistors, respectively, while that of the integrator becomes

$$e(s)_o = -\frac{e(s)i}{RCs} + \frac{i(s)G}{Cs} - \left(1 + \frac{1}{RCs}\right) e(s)_D \qquad (2.88)$$

In both of these equations, the first term on the right-hand side represents the desired output, while the following two terms represent errors due to grid current and drift, respectively.
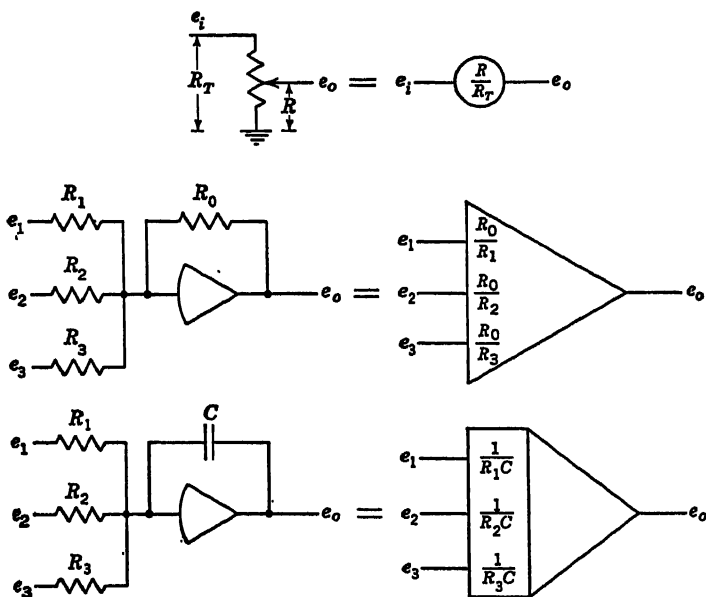
Fig. 2.42

Ideally, operational amplifiers should introduce zero attentuation and phase shift at all frequencies. Because of the presence of stray capacity within the d-c amplifier, such a situation is not physically realizable. For an imperfect sign changer

$$\frac{e(s)_o}{e(s)_i} = -\frac{1}{1 + Ts} \qquad (2.89)$$

where T is determined by the stray capacitance.

In the case of the integrator, the ideal response to a sinusoidal excitation

of frequency ω can be found from Eq. (2.86) by letting s become $j\omega$,

$$e_o = -\frac{e_1}{j\omega RC} \tag{2.90}$$

For ω equal to zero, Eq. (2.90) indicates an infinite voltage gain for the circuit. The best that can be achieved with physically realizable amplifiers is a large but finite gain. Integrators therefore inevitably introduce an error at the low-frequency end. The effect of errors in adders and integrators upon the solution of differential equations is considered in Chap. 6.

2.15. Alternative Notation. In order to conserve space and permit the drawing of more readable circuit diagrams, particularly of intricate systems, the schematic notation for simple adders, integrators, and potentiometers is frequently abbreviated as shown in Fig. 2.42.

REFERENCES

1. Duncan, D. C.: "Characteristics of Precision Servo Computer Potentiometers," paper presented at AIEE Conference on Feedback Control Systems, Atlantic City, N.J., December, 1951.
2. Williams, R. W.: Potentiometers for Computing Circuits, *Electronic Eng.*, **20**:358–360 (1958).
3. Shannon, W.: Electronic Computers, *Electronics*, **19**(8):110–113 (1946).
4. Gilbert, J.: Use Taps to Compensate Pot Loading Errors, *Control Eng.*, **3**:78–82 (August, 1956).
5. Gilbert, J.: Here's a Short Cut in Compensating Pot Loading Errors, *Control Eng.*, **2**:36–39 (February, 1955).
6. McElroy, P. K.: Designing Resistive Attenuating Networks, *Proc. IRE*, **23**:213–233 (1935).
7. Karplus, E.: Design of Variac Transformers, *Elec. Eng.*, **63**:508–513 (1944).
8. Mynall, D. J.: Electrical Analogue Computing, Part I, *Electronic Eng.*, **19**:178–180 (1947).
9. Crowhurst, N. H.: Leakage Inductance, *Electronic Eng.*, **21**:129–134 (1949).
10. MacNeal, R. H.: The Solution of Elastic Plate Problems by Electrical Analogies, *J. Appl. Mechanics*, **18**:59–67 (1951).
11. Weiss, G., and N. I. Linder: Where You Should Use Series or Parallel Summation, *Control Eng.*, **3**:77–83 (June, 1956).
12. Mallock, R. R. M.: An Electrical Calculating Machine, *Proc. Roy. Soc. (London)*, (A)**140**:457–483 (1933).
13. Jeffries, R. J.: Time-constant Selection in the Application of *RC* Differentiating and Integrating Circuits, *Instruments*, **22**:1106 (1949).
14. Bush, V., F. D. Gage, and H. R. Stewart: A Continuous Integraph, *J. Franklin Inst.*, **230**:63–84 (1927).
15. Bush, V., and H. L. Hazen: Integraph Solution of Differential Equations, *J. Franklin Inst.*, **204**:575–615 (1927).
16. Varney, R. N.: An Electric Integrator for Solving Differential Equations, *Rev. Sci. Instr.*, **13**:10–16 (1942).

17. Chance, B., et al. (eds.): "Waveforms," pp. 640–666, McGraw-Hill Book Company, Inc., New York, 1949.
18. Valley, G. E., Jr., and H. Wallman (eds.): "Vacuum Tube Amplifiers," p. 107, McGraw-Hill Book Company, Inc., New York, 1948.
19. G. A. Philbrick, Designing Industrial Controllers by Analog, *Electronics*, **21**(6): 108–111 (1948).
20. Schmitt, O. H., and W. E. Tolles: Electronic Differentiation, *Rev. Sci. Instr.*, **13**:115–118 (1942).
21. Ragazzini, J. R., R. H. Randall, and F. A. Russell: Analysis of Problems in Dynamics by Electronic Circuits, *Proc. IRE*, **35**:444–452 (1947).
22. Goldberg, E. A.: Stabilization of Wide-band Direct Current Amplifiers for Zero and Gain, *RCA Rev.*, **11**:296–300 (1950).
23. Williams, A. J., Jr., W. G. Amey, and W. McAdam: Wide-band D-C Amplifier Stabilized for Gain and for Zero, *Trans. AIEE*, **68**:811–815 (1949).
24. MacNee, A. B.: Some Limitations on the Accuracy of Electronic Differential Analyzers, *Proc. IRE*, **40**:303–308 (1952).
25. Korn, G. A., and T. M. Korn: "Electronic Analog Computers," 2d ed., McGraw-Hill Book Company, Inc., New York, 1956.
26. Wass, C. A. A.: "Introduction to Electronic Analogue Computers," McGraw-Hill Book Company, Inc., New York, 1955.

3

ELECTRICAL MULTIPLIERS AND DIVIDERS

3.1. General Remarks.   The basic operations of addition, subtraction, and constant multiplication are sufficient for the solution of linear algebraic and differential equations with constant coefficients. Frequently, however, it is necessary in the treatment of engineering problems to multiply two quantities, both of which vary with time. Since the basic potentiometric multipliers described in Sec. 2.2 require the manual setting of the sliding arm of the potentiometer, this method can be used to multiply only a variable voltage by a constant. The multiplication of two variables requires additional equipment and techniques.

Although well over 25 different analog-multiplication methods have been proposed and tried out in the past years, only a small number of these have achieved any considerable importance in general-purpose analog computation. The oldest of these involves primarily the mechanization of the manual potentiometer multiplier, so that the position of the sliding arm is automatically made proportional to the magnitude of one of the variables to be multiplied. A second approach to multiplication involves the application of nonlinear electronic elements to approximate parabolic and logarithmic transfer functions. The desired multiplication can be carried out by suitably interconnecting several such function generators. The third major category of multipliers, the time-division or electronic multipliers, performs the computing operation by integrating a wave train of pulses whose amplitudes and widths are made proportional, respectively, to the two variables. These three methods of multiplication are considered in detail in this chapter. A brief survey of a number of other lesser used techniques is included. Finally, the extension of these methods to the problem of dividing one dependent variable by another dependent variable is considered.

3.2. Servo Multipliers.   Automatic potentiometric multipliers constitute one of the oldest and most widely used methods of electrical function multiplication. A combination of the following instruments is employed: an operational amplifier, a servo amplifier, a two-phase induction motor,

and several multiturn potentiometers, all the shafts of which are ganged
and coupled to the rotor shaft of the motor.   Figure 3.1 is a schematic
diagram of such a multiplier.   The dotted line indicates mechanical but
not electrical connection.   One of the variables to be multiplied, e_1, is
applied to one input terminal of an electronic adder, while the voltage
appearing at point B in the diagram is applied to another input terminal
of the same operational circuit.   Point B is at the moving arm of a multi-
turn potentiometer I, one end of which is grounded while the other end is
connected to a fixed d-c voltage source E, the polarity of which is opposite
to that of e_1.   The voltage appearing at B is therefore equal to XE, where
X is the position of the potentiometer arm, as a fraction of full scale.

The signal appearing at the output of the operational amplifier at
point A is therefore equal to $(-e_1 - XE)$.   The servo amplifier effectively
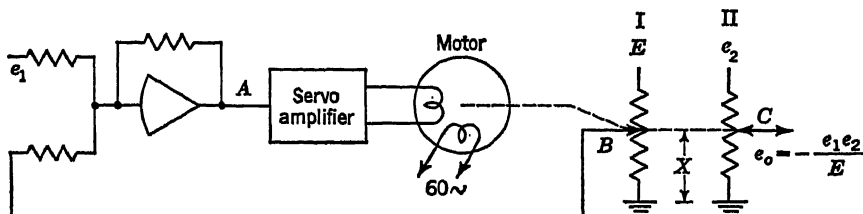
Fig. 3.1

transforms the d-c potential at point A into a 60-cps signal, the magnitude
of which is proportional to the voltage at A; the phase of the signal is
determined by the polarity of the voltage at A.   This a-c signal is applied
to one winding of the motor, while a fixed a-c reference signal is applied
to the other winding.   The motor characteristics are such that rotation
takes place as long as both windings are excited.   The direction of
rotation is determined by the phase relationship of the voltages in the
two windings.   As a result of the mechanical coupling of the motor
shaft and the potentiometer arm, the rotation of the motor effects an
alteration in the potential at point B and, consequently, in the voltage
at A.   The motor finally comes to rest when the potential at point A is
equal to zero, that is, when the voltage at point B is equal to $-e_1$, or
$XE = -e_1$.   The angular positions X of both ganged potentiometers as
a fraction of full scale are then equal to $|e_1/E|$.   If a variable voltage
e_2 is applied to potentiometer II in Fig. 3.1, the potential appearing
at its moving arm is equal to e_1e_2/E and the desired multiplication is
accomplished.

The circuit described above is useful only for multiplying voltages
having a specified polarity.   For the circuit shown in Fig. 3.1, e_1 must
have a polarity opposite that of E, and the output e_o necessarily has the
same polarity as e_2.   To permit multiplication in four quadrants (*i.e.*,

either variable may be of either sign, and the resulting product will be of the correct sign) a modification of the basic circuit is required.

Figure 3.2 shows a four-quadrant servo multiplier. For convenience, the operational amplifier, the servo amplifier, and the motor have been represented by a single block, labeled servo. The lower terminal of potentiometer I, rather than being grounded, is connected to a d-c voltage source $-E$. In a similar manner, a sign changer applies a voltage proportional to $-e_2$ to the lower terminal of potentiometer II. The mid-point of both potentiometers is, therefore, always at zero potential. To reduce the noise level and for slightly increased accuracy, the mid-points of both potentiometers may be connected to ground through
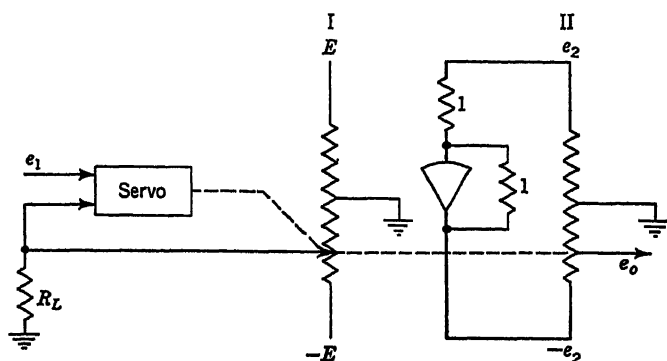
Fig. 3.2

center taps without affecting the operation of the circuit. The resistor R_L is included to compensate potentiometer loading errors. The magnitude of this resistor should be equal to the input impedance of the device connected to the moving arm of potentiometer II. The load on potentiometer I will then introduce a position error in the setting of both potentiometers which will compensate exactly the voltage error in potentiometer II, so that the output voltage is unaffected by loading. If desired, a number of additional potentiometers can be ganged mechanically to potentiometers I and II. In this manner, e_1 can be multiplied separately by several variable electrical voltages, e_2, e_3, e_4, etc.

If the gain of the servo amplifier is sufficiently large, the accuracy of servo multiplication is limited only by the resolution and nonlinearity of the potentiometers, provided that the voltage variation of e_1 is sufficiently slow. Since the servomotor necessarily has some inertia, there is a limit to the rapidity with which the follow-up potentiometer I can follow voltage variations. In multiplying two voltages, it is good practice to apply the slower changing one of the two to the servo amplifier (e_1). To suppress undesirable oscillations and hunting, tachometer

feedback is sometimes included in the multiplier circuit. The tachometer is coupled mechanically to the motor shaft. Its output, which is proportional to the motor velocity, is applied to the input of the operational amplifier. The effect is to damp out any sudden changes in the system and to increase stability.

If both variables to be multiplied are represented by shaft rotations, the multiplier circuit shown in Fig. 3.3a can be employed. The two variables are the shaft rotations of the variable resistors x and y located in diagonally opposite sides of the bridge. The side adjacent to both x

(a)   (b)
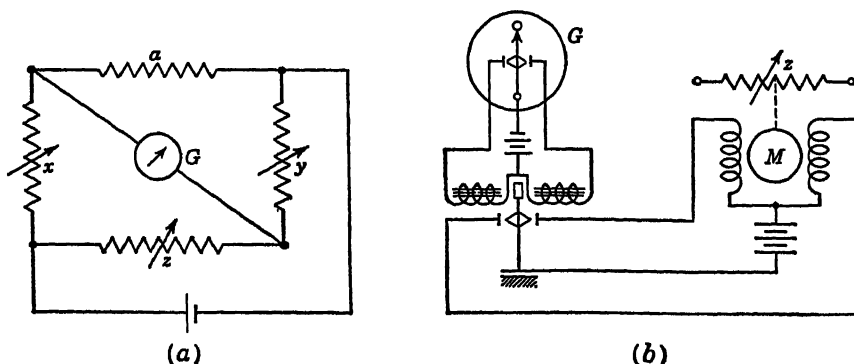
Fig. 3.3

and y has a fixed resistance a. The fourth side is used to balance the bridge, the rotation of this z shaft representing the desired product. Thus, the equation of operation of the unit is

$$z = \frac{1}{a} xy \qquad (3.1)$$

The rotations x and y can be produced manually, and the bridge correspondingly balanced by manual operation. If the rotations x and y are produced automatically, it is desirable to maintain the bridge in balance also by automatic means. A relay servo provides perhaps the simplest of such schemes. Automatic balancing with a relay servo is illustrated schematically in Fig. 3.3b. Any unbalance in the bridge circuit causes the galvanometer pointer to close the circuit through one relay. Current then flows through one of the two field windings of the servomotor coupled to the z resistor shaft and rotates this shaft in the direction to reduce the unbalance. Because of the gap between contactors, inertia in the circuit, and various time delays, unstable operating conditions may arise, causing excessive hunting in the balancing operation or actually increasing the unbalance instead of decreasing it. For the usual slow-speed operation of such relay servos, these difficulties do not arise. The

conditions of stable and unstable operation are discussed in a number of papers.[2-4]

3.3. Quarter-square Multipliers. The principle of operation of another important class of electrical multipliers is based upon the following equation:

$$xy = \tfrac{1}{4}[(x + y)^2 - (x - y)^2] \tag{3.2}$$

Provided the squares of the sum and the difference of the two variables can be generated, the product can be obtained by the simple combination of two such squaring circuits and three adding circuits as shown in Fig. 3.4. A number of devices are available for the squaring operation.
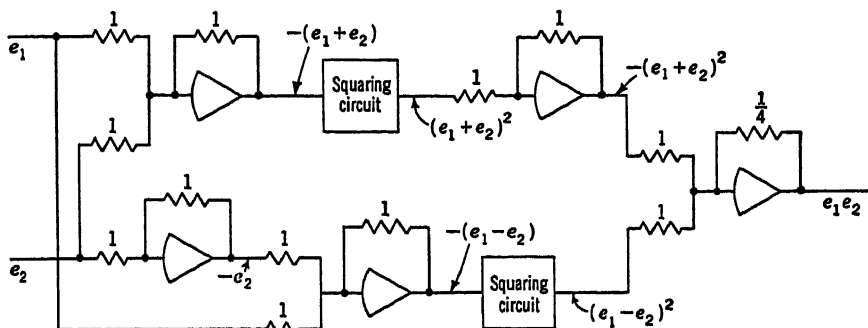
Fig. 3.4

The most important of these involve the use of vacuum-tube or semiconductor diodes.[5,6]

An arrangement of diodes, bias supplies, and series conductances necessary to produce an output current approximately proportional to the square of the input voltage is shown in Fig. 3.5a. The nonlinear-current-vs.-voltage curve is shown in Fig. 3.5b.

Six conductances are shown in parallel. Five of these are in series with diodes, which are biased by batteries E_1 through E_5, of progressively increasing emf. Thus, for low values of e (below E_1), current flows only through G_0, to the amount $G_0 e$. The current-voltage relationship is a linear one, so that the first segment of the "parabola" is a straight line of constant slope G_0. The desired function, $i = ke^2$, may be satisfied by a segmented curve of straight lines only at a limited number of points, e.g., at the junctions of the segments. Thus, to satisfy the parabola at $e = E_1$, G_0 must be so chosen that

$$i = G_0 E_1 = k E_1^2 \quad \text{or} \quad G_0 = k E_1 \tag{3.3}$$

During the next interval, when both G_0 and G_1 are conducting, the

current-voltage curve assumes a steeper slope.   When $e = E_2$,

$$i = G_0E_2 + G_1(E_2 - E_1) = kE_2{}^2 \qquad (3.4)$$

from which corresponding values of G_1 and E_2 can be determined.
   When $e = E_3$,

$$i = G_0E_3 + G_1(E_3 - E_1) + G_2(E_3 - E_2) = kE_3{}^2 \qquad (3.5)$$

from which corresponding values of G_2 and E_3 can be determined.   Thus,
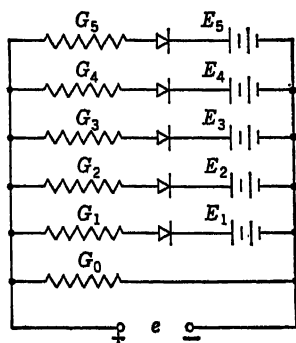
(a)
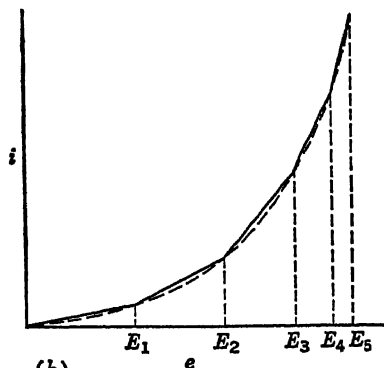
(b)
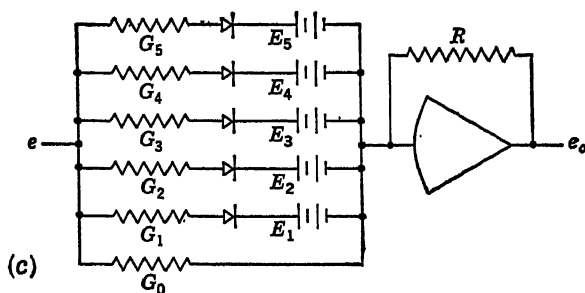
(c)

Fig. 3.5

in successive steps, all the conductances and biasing voltages can be
evaluated to provide a current proportional to the square of the impressed
voltage.

   To convert from current to voltage, the total current i must be passed
through a resistance whose magnitude is small enough so that Eqs. (3.3)
to (3.5) are not appreciably affected by its presence.

   The coupling between the bank of conductances and diodes producing
the current i and the resistance converting this current to a voltage drop
may be substantially eliminated by using a high-gain negative-feedback
amplifier, as shown in Fig. 3.5c.   The need for making the latter resist–

ance very low is thereby obviated, and a convenient value for R can be used.

To satisfy the parabola at $e = E_1$, E_2, E_3, etc., the conductances G_0, G_1, G_2, etc., are still chosen in accordance with Eqs. (3.3) to (3.5). The current i in each case must pass through R to e_0. Thus, when $e = E_1$,

$$i = kE_1{}^2 = -\frac{e_o}{R} \quad \text{or} \quad e_o = -kRE_1{}^2 \qquad (3.6)$$

When $e = E_2$,

$$i = kE_2{}^2 = -\frac{e_o}{R} \quad \text{or} \quad e_o = -kRE_2{}^2 \qquad (3.7)$$

Similar relations hold at E_3, E_4, E_5, etc., so that the parabolic relation between input and output voltage is satisfied at the chosen points.

Fig. 3.6

A square-law curve may be approximated to within ± 2 per cent with 3 line sections, to within ± 1 per cent with 5 line sections, and to within less than 0.4 per cent with 15 segments.

The circuit of Fig. 3.5c accepts only positive input voltages. To permit four-quadrant multiplication it is necessary to modify this circuit to accept negative inputs as well. This is accomplished by employing two sets of diodes and bias supplies as shown in Fig. 3.6. Fisher[7] has described detailed analytical techniques for optimizing the approximation of nonlinear functions by straight-line segments. If the length and slope of each segment are carefully selected, the truncation error can be kept to a minimum. It is also possible to improve the operation of diode circuits by superimposing a small a-c voltage upon the desired signal.

This has the effect of rounding off the corners at the intersection of adjacent line segments, thereby obviating the effect of the sharp changes in slope of the e_o/e_i curve.

Another useful method of generating the square of a voltage (and of generating, as well, many other arbitrary functions of a voltage) is the "photoformer."[8] The operating method of the photoformer is illustrated in Fig. 3.7. The function to be generated is represented by the edge of a mask on the face of a cathode-ray tube. In this case the mask is
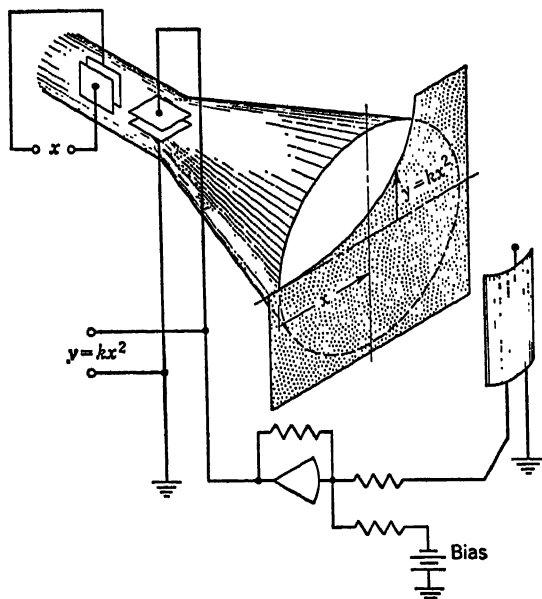
Fig. 3.7

parabolic, to that the vertical distance to a point on its edge is proportional to the square of the horizontal distance to the point in question. The fluorescent spot on the screen is displaced horizontally in proportion to the x voltage. By means of a phototube and a bias supply, the y voltage is made to vary in such a fashion as to keep the spot riding on the edge of the mask, with half the dot hidden behind the mask. Any variation in light intensity caused by the spot tending to leave the edge of the mask either up or down is passed on to the d-c amplifier as a variation in input voltage, which in turn causes a change in the vertical deflecting voltage to maintain the spot on the edge of the screen.

Cathode-ray tubes specially designed for producing any desired single-valued transfer characteristics (such as the parabolic characteristic mentioned above) have been developed.[9] Called "monoformers," these tubes are 8 in. long, $1\frac{3}{4}$ in. in diameter, employing standard cathode-ray-

tube bases. The target is an aluminum disk 1 in. in diameter. The function to be reproduced is printed on the disk with a coating of carbon ink. The operation of the tube depends on the fact that aluminum and carbon have different secondary-emission ratios. An electrode is provided to collect the secondary electrons emitted from the target plate as a result of impingement by the electron stream. If the beam, in sweeping across the target, tends to ride too far into the uncoated area or into the coated area, it causes a variation in secondary electron emission. The corresponding variation in target current produces a variation in voltage drop across a load, this voltage drop being fed back through a network (either an amplifier or simply a resistor) to the vertical deflecting plates of the tube. The result is to keep the electron beam directed against the boundary between the coated and uncoated areas of the target.
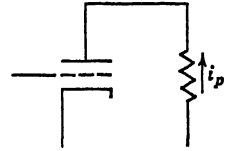
Fig. 3.8

The accuracy of the unit is considered to be 1 per cent. Without amplification in the feedback loop, a response time of 400 microseconds (μsec) to a step input is developed. With sufficient amplification in the feedback loop, this response time may be reduced to 1 μsec.

The transfer characteristic between grid voltage and plate current in a vacuum tube provides a somewhat approximate method of obtaining the square of a voltage. The instantaneous plate current of a triode with negative grid voltage, constant amplification factor, and resistive load on the plate (Fig. 3.8) may be expressed as a power series in terms of the grid exciting voltage e:

Fig. 3.9

$$i_p = a_1e + a_2e^2 + a_3e^3 + \cdots \quad (3.8)$$

For certain tubes[10] the plate-current-vs.-grid-voltage characteristic is approximately parabolic in form over a limited range of grid-voltage values. For such tubes, the voltage across the output resistance will be proportional to the square of the grid voltage.
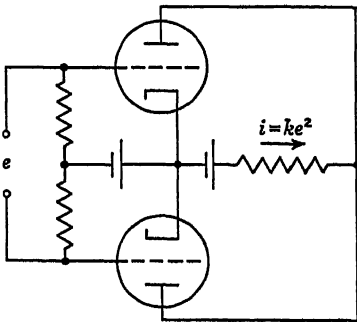
A more precise parabolic transfer characteristic can be obtained by using two triodes in a balanced circuit designed to cancel odd-power terms in the series expansion.[11] This type of circuit is shown in Fig. 3.9. The current through the load resistance and the voltage drop across the load resistance are proportional to the square of the input voltage e.

Circuits have been developed in which the logarithmic relation between a low-level applied voltage and the resistance of a rectifier (such as a selenium-cell rectifier) is used to generate an output voltage proportional

to the square of an input voltage. For low voltages it has been found[12] that

$$R = K\epsilon^{-qe} \tag{3.9}$$

where R is the rectifier resistance, e the applied voltage, and K and q constants of the rectifier. Referring to Fig. 3.10, in which R_1 is small compared with R, the current i is given by

$$i = \frac{e}{R} = \frac{e}{K}\,\epsilon^{qe} = \frac{e}{K}\,(1 + qe + \cdots) \tag{3.10}$$

where the exponential is expressed in series form, neglecting quadratic and higher-order terms on the assumption of small voltages. Hence

$$i \cong \frac{1}{K}\,(e + qe^2) \tag{3.11}$$

This is the circuit suggested by Draper.[12] The voltage drop across the pure resistance R_1 is

$$R_1 i = \frac{R_1 e}{K} + \frac{R_1 q}{K}\,e^2 \tag{3.12}$$

By subtracting from this voltage drop the linear term $R_1 e/K$, a voltage proportional to e^2 results. The subtracting is done by shunting the
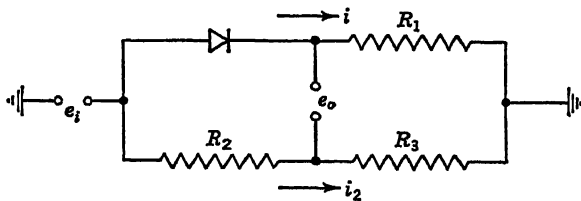
Fig. 3.10

input e with a series pair of resistors, R_2 and R_3, and adjusting the magnitudes of R_2 and R_3 so that the voltage drop across R_3 equals $R_1 e/K$. The necessary values of R_2 and R_3 are obtained from the equations

$$i_2 = \frac{e}{R_2 + R_3} \qquad i_2 R_3 = \frac{R_1 e}{K} \tag{3.13}$$

whence

$$R_3 = \frac{R_1 R_2}{K - R_1} \tag{3.14}$$

The output voltage e_o is then given by

$$e_o = \frac{R_1 q}{K}\,e^2 \tag{3.15}$$

provided that the output circuit does not load the squaring circuit.

A square-law relation can also be generated by means of a galvanometer whose mirror reflects a rectangular spot of light into a triangular opening.[13] The voltage to be squared is applied to the galvanometer, resulting in a proportional deflection of the beam of light. The amount of light passing through the triangular opening and impinging on a photocell is proportional to the square of the beam deflection. Hence, the output of the cell is proportional to the square of the voltage input to the galvanometer.

3.4. Logarithmic Multipliers. Another approach to the multiplication of two variables is based upon the following identity:

$$xy = \text{antilog} (\log x + \log y) \tag{3.16}$$

Both of the two variables to be multiplied must first be transformed into logarithmic form by suitable function-generating equipment. These
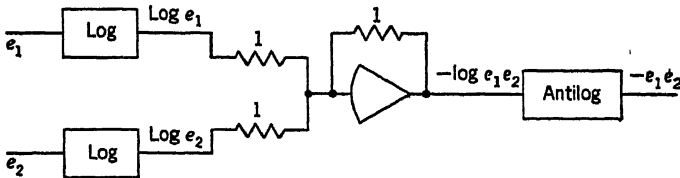
Fig. 3.11

voltages are then added to obtain log xy, and the resulting quantity must be passed through another function generator to obtain the antilog as shown in Fig. 3.11. Three separate function generators are therefore required for this operation. In general, this method is advantageous only in problems in which it is necessary to perform a large number of multiplications and such operations as raising variables to powers and extracting roots of variables. It then becomes feasible to operate entirely in a logarithmic domain. On the other hand, the otherwise simple operations of addition and subtraction become rather cumbersome under these conditions.

A logarithmic function between input and output voltage may be generated by means of conductances and biased diodes, as shown in Fig. 3.12a. The function to be represented is shown in (b). It is

$$e_o = k \log e \tag{3.17}$$

and is to be satisfied at $e = E_1, E_2, E_3$, etc. Since the curve does not pass through the origin, but has unit offset when $e_o = 0$, the first conductance G_0 and the bias E_1 serve to establish the starting point E_1 for the logarithmic function. The values of e between 0 and E_1, therefore, have no significance in so far as Eq. (3.17) is concerned.

The minimum value of E_1 is determined by the line drawn through the

origin and tangent to the logarithmic curve. The slope of this line is $(k \log E_1)/E_1$. The slope of the curve is

$$\frac{d}{de}\,(k \log e) = \frac{k}{2.303e} \tag{3.18}$$

Thus, at $e = E_1$,

$$\frac{k \log E_1}{E_1} = \frac{k}{2.303E_1} \quad \text{or} \quad E_1 = 2.718 \tag{3.19}$$

Between $e = E_1$ and $e = E_2$, the first diode conducts, so that both G_0 and G_1 carry current. G_1 must be chosen so Eq. (3.17) is satisfied
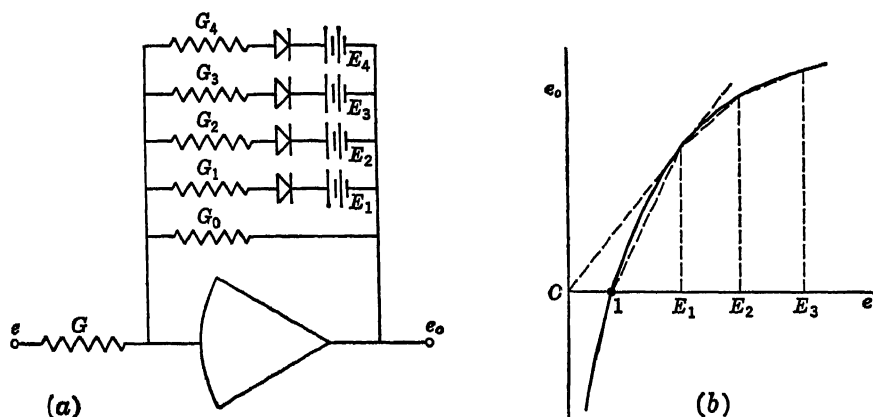
Fig. 3.12

when $e = E_2$. The current through G must equal the sum of the currents through G_1 and G_0. Thus

$$E_2G = -e_oG_0 - (e_o - E_1)G_1 \tag{3.20}$$

or

$$e_o = -\frac{E_2G - E_1G_1}{G_0 + G_1} \tag{3.21}$$

Since for this instant $e_o = -k \log E_2$,

$$G_1 = \frac{E_2G - G_0k \log E_2}{k \log E_2 + E_1} \tag{3.22}$$

Proceeding in a similar manner, the value of G_2, corresponding to the bias E_3, the value of G_3, corresponding to the bias E_4, etc., can be found.

Variable-mu tubes (such as the 6SK7) produce a plate current proportional to the logarithm[14,15] of the grid input voltage within a limited range of the input voltages. It was found[15] by operating a 6SK7 in an inverted circuit, *i.e.*, with the input voltage applied to the plate and cur-

rent withdrawn at the grid, that the output current is proportional to the antilogarithm of the voltage input to the plate.

3.5. Time-division Multipliers. Another method of function multiplication makes use of a train of rectangular pulses as shown in Fig. 3.13. The repetition rate of the pulses is fairly high, approximately 10,000 cps. The height of each pulse is made proportional to one of the variables, while the width of each pulse is a function of the other variable. The average height of the series of pulses is then proportional to the product of the two variables and can be found by integrating the pulse train electronically. To permit multiplication for positive as well as negative values of e_2, the pulse periods T_1 and T_2 are adjusted so that

$$e_2 = k\frac{T_1 - T_2}{T_1 + T_2} \qquad (3.23)$$

where k is a constant, or

$$\frac{T_1}{T_2} = \frac{k + e_2}{k - e_2} \qquad (3.24)$$
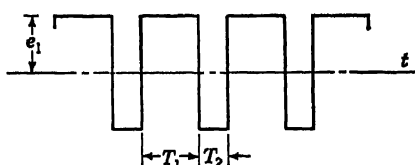
Fig. 3.13

For e_2 positive, T_1 is larger than T_2, while T_2 is larger than T_1 if e_2 becomes negative. Sophisticated models of such time-division multipliers employ two electronic switches, a bistable multivibrator (flip-flop), as well as electronic integrators and adders. Designs such as those by Morrill[16] are finding increasing application in general-purpose computers.

Another multiplier based on this principle is due to Walters.[17] A self-gated Miller integrator circuit[18] is used for time modulation, i.e., for controlling the width of the rectangular pulse. This is accomplished by integrating a step voltage change until the resulting integral equals e_2, at which instant the pulse is cut off by a voltage matching circuit. The pulses are repeated at the frequency of the trigger circuit (e.g., 1,000 cps) and are averaged in an RC smoothing network. The multiplier operates only for positive e_1 and e_2 and is inaccurate when the product is near zero. Both effects can be counteracted by shifting the level of the input by some constant amount. If, for example, a positive voltage e_3 is added to e_1 and e_2, then

$$(e_1 + e_3)(e_2 + e_3) = e_1e_2 + e_1e_3 + e_2e_3 + e_3{}^2 \qquad (3.25)$$

The last three terms are then subtracted, and the product e_1e_2 results. If e_3 is large enough, the resulting inputs will always be positive, well away from zero, and within the range of the multiplier.

A multiplier making use of combined frequency and amplitude modulation has been developed at MIT.[19] The dynamic range in output product is 2,500:1, and the operating frequency ranges from 0 to 10 kc.

While early models of the time-division multiplier suffered from drift problems and other inaccuracies introduced by the relatively complex electronic circuitry, later improvements have made these units the most accurate of all available function multipliers. Accuracies of the order of 0.02 per cent of full scale can be obtained by employing chopper-stabilized amplifiers, high pulse-repetition rates, and carefully stabilized electronic switches. The time-division multiplier therefore combines the high accuracy of the servo multipliers with the rapid frequency response of the biased diode devices.

3.6. Miscellaneous Multipliers. Many other types of electrical function multipliers have been suggested and designed. Most of them
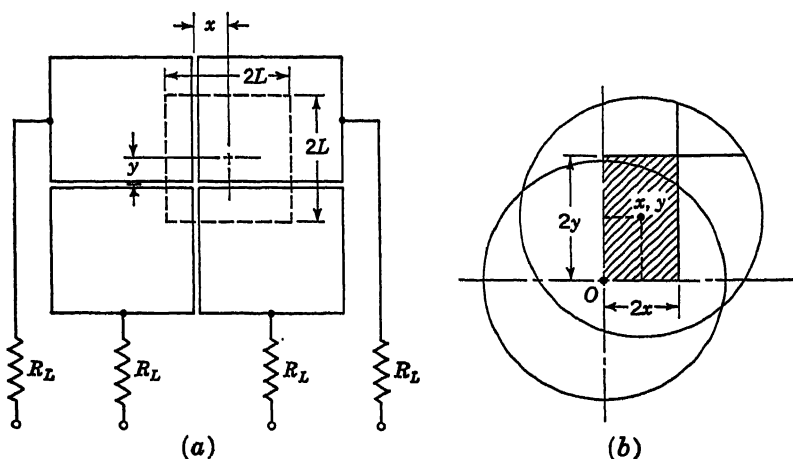
Fig. 3.14

have found application in special-purpose analog computers. Some of the more prominent of these are considered in this section.

An interesting type of multiplier[20] is based on the theory of probability. The probability of the simultaneous occurrence of two independent events having probabilities of occurrence x and y, respectively, is the product xy. Thus, if two pulse generators produce constant-amplitude pulses of time durations proportional to x and y, respectively, and if the pulse frequencies are irrationally related, the fraction of time in which both pulses coincide is proportional to xy. The pulses are added in a mixing circuit and impressed on the grid of a tube which conducts only when the two pulses coincide. The time during which the tube conducts is therefore proportional to the desired product.

Another multiplier[21] makes use of a square beam of electrons, which is deflected horizontally by an x input voltage and vertically by the y input voltage (Fig. 3.14a). The deflection causes the beam to fall eccen-

trically on four square collector plates, the current from each plate passing through a load resistor R_L. If the beam current density at impingement is constant over the area $2L \times 2L$, the current through each load resistor is proportional to the area of impingement on the corresponding collector plate, which in turn, is a function of both the x and the y voltages. These areas are

$$
\begin{aligned}
(L - x)(L + y) &= L^2 + (y - x)L - xy \\
(L - y)(L - x) &= L^2 - (y + x)L + xy \\
(L + x)(L + y) &= L^2 + (x + y)L + xy \\
(L + x)(L - y) &= L^2 - (y - x)L - xy
\end{aligned}
\tag{3.26}
$$

If the sum of the first and fourth equations is subtracted from the sum of the second and third, the net current is found to be, for unit current density at the collector plates,

$$
i = 4xy \tag{3.27}
$$

i.e., proportional to the product of the voltages x and y. Practical difficulties of attaining a strictly uniform current density, linear deflection characteristics, and secondary electron emission may lead to serious inaccuracies.

A similar multiplier making use of a circular beam of electrons was developed by Angelo.[22] Referring to Fig. 3.14*b*, it is clear that by the same connections as those made for the square beam, the currents contained in the clear areas of the deflected beam cancel each other, the resultant current being collected from the crosshatched rectangular area $2x$ by $2y$. The current is again given by $4xy$ on the basis of unit density at the collector plates.

The crossed-fields multiplier[23] is based on the principle that the force exerted on an electron in a magnetic field is given by

$$
\mathbf{F} = e(\mathbf{v} \times \mathbf{B}) \tag{3.28}
$$

where e is the electron charge, $\mathbf{v}$ the electron velocity component in the vertical direction, and $\mathbf{B}$ an axial magnetic field intensity. The multiplier (Fig. 3.15) is a cathode-ray tube with the addition of a magnetic coil around the horizontal deflection plates to produce the axial magnetic field intensity $\mathbf{B}$ between the plates. A current i, proportional to one of the variable voltages, produces the magnetic field. The velocity $\mathbf{v}$ is proportional to the other variable voltage, which is impressed on the vertical deflection plates. The force given by Eq. (3.28) is in the x direction and may be balanced by a voltage applied to the x deflection plates so that the x deflection of the beam is zero. A photocell corrects the spot position to maintain it on the vertical line at $x = 0$ by feeding an error signal back through an amplifier to the x deflection plates. Thus,

the voltage on these deflection plates is at all times proportional to the product of the two voltages representing the input variables.

The strain-gauge multiplier[24] was developed at MIT to meet the requirements of 0.1 per cent accuracy and an effective time constant of about 1 msec. In principle, a strain-gauge multiplier can be arranged as shown in Fig. 3.16. An a-c voltage of constant frequency, representing

$i = kx$

Kxy

Fig. 3.15

Magnet

$e_0 = kxy$ y

x
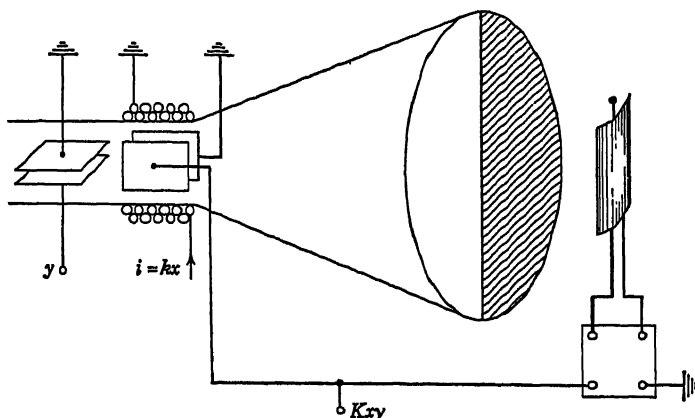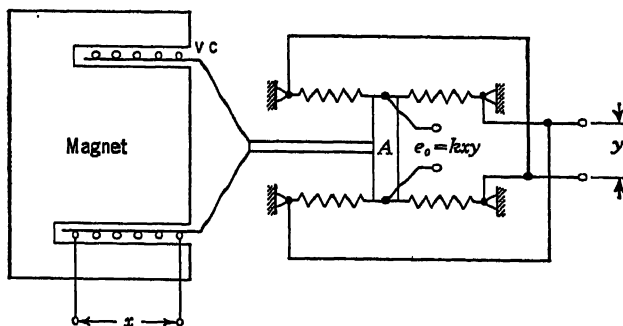
Fig. 3.16

the variable x, is impressed on the voice coil of a loudspeaker unit. The amplitude of the resulting deflection of the voice coil and attached arma-ture A is proportional to x, thereby producing in the strain gauges strains that are also proportional to x. The a-c voltage representing the variable y is impressed across the strain-gauge bridge, so that the bridge output is proportional to both the strain and the bridge exciting voltage; *i.e.,*

$$e_o = kxy \qquad (3.29)$$

By making all four gauges active (*i.e.*, subject to strain), the bridge out-

put is double that of an arrangement in which only two gauges in the bridge are active.

3.7. Servo Dividers. The division of two variable voltages is generally a more difficult task than the multiplication operation. In dividing two quantities, it is clear that if the divisor approaches zero, the quotient approaches infinity. Since the voltage output of any electrical device is limited, it is possible to perform division only if the quotient does not exceed a certain specified value; it is impossible if the divisor approaches or crosses zero. At best, therefore, division is restricted to two quadrants. In the application of servo devices[1] to this problem, two distinct approaches can be employed.

The circuit of Fig. 3.1 can readily be modified to facilitate the division operation. It is only necessary to employ a fixed voltage at the input of the servo amplifier and to apply one of the variables at one terminal

Fig. 3.17

of the follow-up potentiometer. A circuit of this type is shown in Fig. 3.17. The output of this circuit is then given by

$$e_o = \frac{E e_2}{e_1} \tag{3.30}$$

where E is a fixed voltage. In practice, this circuit is subject to erratic behavior. Any change in the variable e_1 effects a change in the feedback loop gain, resulting in instability and loss of accuracy. Occasionally, automatic-gain control circuits are included in the servo amplifier to minimize this difficulty. The variable e_1 is then applied to the automatic-gain control circuit, which in turn maintains the loop gain at a fairly constant value.

A method termed *implicit* division is based upon the instrumentation of an equation of the type

$$e_2 + k e_1 e_o = 0 \tag{3.31}$$

In this equation, the desired solution as specified by Eq. (3.30) is implied. One manner of instrumenting this equation is shown in Fig. 3.18. In this circuit, the angular position X of potentiometer II is given by

$$X = \frac{e_1}{E} \tag{3.32}$$

The voltage at the moving arm of this potentiometer is applied to the input of summing amplifier 1. The dividend e_2, as well as a feedback voltage from amplifier 2, is also applied to this summing amplifier. The
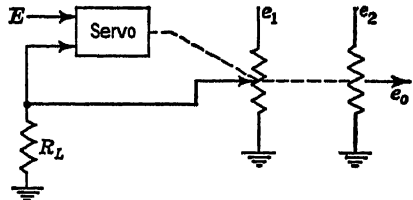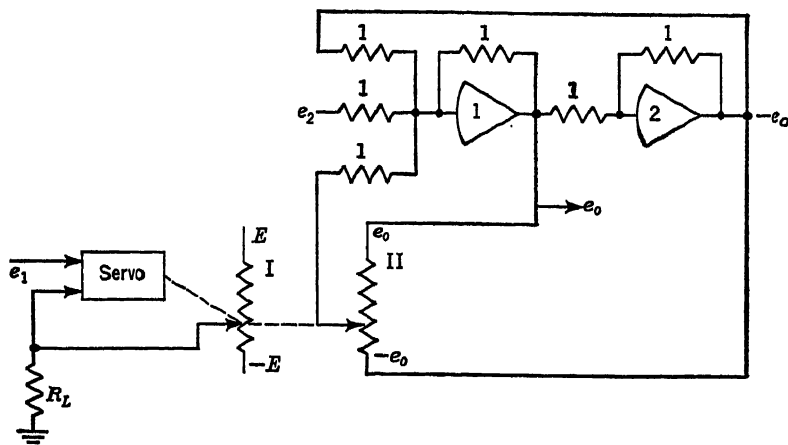
Fig. 3.18

output voltage of this amplifier is passed through the sign changer, amplifier 2, and is applied to one terminal of potentiometer II. The output voltage e_o of amplifier 1 is therefore given by

$$e_o = -(-e_o + e_2 + Xe_o) \tag{3.33}$$

or

$$e_o = e_o - e_2 - \frac{e_1 e_o}{E} \tag{3.34}$$

which can be rearranged as

$$e_o = -\frac{E e_2}{e_1} \tag{3.35}$$

so that the desired division has been accomplished.

Another implicit division circuit, which requires only one operational amplifier, is shown in Fig. 3.19. Here no feedback impedance is used in
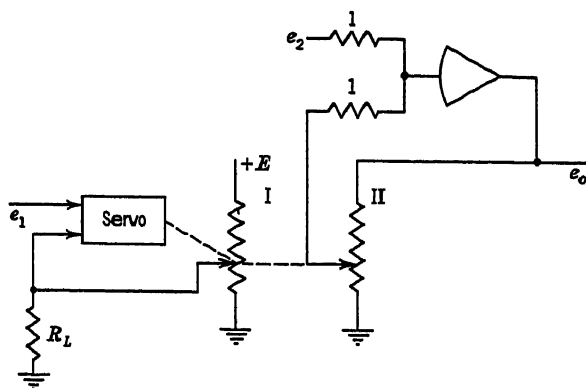
Fig. 3.19

conjunction with the operational amplifier, so that the voltage at the output of this amplifier is given by

$$e_o = -A(e_2 + Xe_o) \tag{3.36}$$

where X is the angular position of potentiometer II and the amplifier gain A is a very large number. Since the output voltage e_o is limited to 100 volts by available power supplies, this expression can be rearranged as

$$e_2 + Xe_o = -\frac{e_o}{A} \approx 0 \tag{3.37}$$

or since $X = e_1/E$

$$e_o = -\frac{Ee_2}{e_1} \tag{3.38}$$

In effect, the high-gain amplifier acts to make the sum of the voltages applied to its input equal to zero, so that the desired division is again accomplished.

3.8. Miscellaneous Dividers. The implicit method of division illustrated in Fig. 3.19 can be generalized to accommodate any multiplier
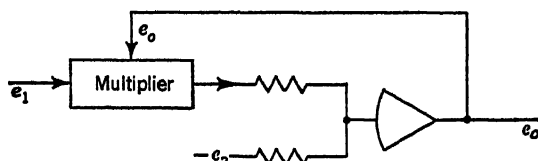
Fig. 3.20

described in the preceding sections. Such a general circuit is shown in Fig. 3.20. For improved frequency response, an electronic multiplier can be used in place of the servo multiplier. In that event, a small stabilizing capacitor, approximately 0.01 μf, should be tied across the high-gain amplifier to attenuate any high-frequency components which may lead to instability.

One of the simplest of the dividing circuits is the Wheatstone bridge. Referring to Fig. 3.3, if z is introduced as the dividend and x as the divisor, the output y is given by

$$y = a\frac{z}{x} \tag{3.39}$$

Another simple dividing circuit is shown in Fig. 3.21. The dividend appears as a voltage e_i, while the divisor enters as a shaft rotation of the variable resistor R_1. The output voltage e_o is given by

$$e_o = \frac{e_i R_2}{R_1 + R_2} \tag{3.40}$$

Potentiometric division can be accomplished by multiplication of the reciprocal of the divisor into the dividend. A potentiometer can be so wound[21] that its shaft rotates in proportion to the value of the divisor, the output voltage of the potentiometer being proportional to the reciprocal of the shaft rotation.

Figure 3.22 shows a developed strip of potentiometer card of variable width w. Assuming a closely spaced winding of fine uniform wire dis-
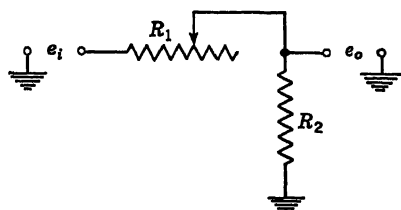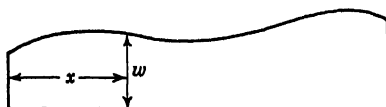
Fig. 3.21   Fig. 3.22

tributed along the card, at any position x from the reference end, the change in resistance of the winding due to one turn of wire is

$$R = 2w\rho \tag{3.41}$$

where ρ is the resistance per unit length of the wire.

The output voltage of the potentiometer at this point is

$$e_o = \frac{R}{R_T} E \tag{3.42}$$

where R_T is the total potentiometer resistance, E the voltage applied across it, and R the winding resistance at the brush position. It is desired to make e_o a particular function of the potentiometer-brush position x.

The rate of change of output voltage with potentiometer setting is obtained by differentiating Eq. (3.42). Thus

$$\frac{de}{dx} = \frac{d}{dx}[f(x)] = \frac{E}{R_T}\frac{dR}{dx} \tag{3.43}$$

Since in the usual wire-wound potentiometer the change occurs in small, but finite steps as the brush traverses the windings, Eq. (3.43) can be expressed in terms of the change in resistance of a single winding occupying the space Δx on the card. Thus

$$\frac{\Delta e}{\Delta x} \approx \frac{d}{dx}[f(x)] \approx \frac{E}{R_T}\Delta R \tag{3.44}$$

In Eq. (3.44) the ΔR must be understood to mean the change in resistance per Δx change in position of the brush (a one-winding change in length

of the wire). Thus, substituting Eq. (3.41) into Eq. (3.44), the card width becomes

$$w \approx \frac{R_T}{2E\rho} \frac{d}{dx} [f(x)] \tag{3.45}$$

The width of the card is thus seen to be proportional to the derivative of the function which it is desired to mechanize.

In order to generate the reciprocal,

$$f(x) = \frac{1}{x} \tag{3.46}$$

$$\frac{d}{dx} [f(x)] = -\frac{1}{x^2} \tag{3.47}$$

The width of the card must be proportional, then, to the square of the reciprocal of the potentiometer-shaft displacement. The negative
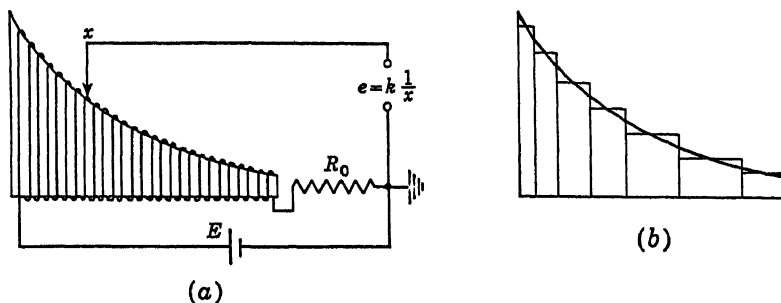
Fig. 3.23

sign in Eq. (3.47) means that the voltage source across the potentiometer terminals must be reversed in polarity. Obviously, x can go neither to zero nor to infinity. The potentiometer must mechanize a given finite range of x. The potentiometer resistance from the higher limiting value of $x(= x_0)$ to $x = \infty$ may be represented by a fixed resistor of magnitude

$$R_0 = k \frac{1}{x_0} \tag{3.48}$$

where k is the net scale factor for the potentiometer. The potentiometric reciprocal generator is, then, as shown in Fig. 3.23a. In this connection it should be mentioned that difficulty may be experienced in winding cards which change in width too rapidly. The turns of wire tend to slip down the card slope. In such cases, the smoothly varying card width may be approximated by a stepped card as shown in (b).

The logarithmic method of multiplication described in Sec. 3.4 is readily adapted to division by subtracting the logarithms of the two variables instead of adding them.

3.9. Summary. In the selection of a device to multiply two variable electrical quantities, the following characteristics are of greatest interest:

1. The static error, that is, the error introduced into the solution when both of the variables are changing slowly or are constant with respect to time.

2. The dynamic error, that is, the error introduced because of relatively rapid variations in one or both of the variables being multiplied.

3. The number of quadrants which can be handled, that is, whether either or both of the variables are permitted to have positive as well as negative polarities.

4. The complexity of equipment and the amount of adjustment and calibration which must precede the operation.

Of the major types of multipliers described above, the time-division multiplier is capable of the highest static and dynamic accuracy. With sufficient care, static errors can be kept below 0.02 per cent of full scale, and with the use of rapid pulse rates, frequencies well in excess of 100 cps can be handled without additional errors. Multiplication in all four quadrants is readily achieved. Until very recently, time-division multipliers suffered from serious zero-point instability or drift problems. These have now been largely overcome, so that this type of multiplier appears to offer the most promise for general-purpose high-quality analog computations.

The servo multiplier also is capable of very high static accuracies, limited only by the characteristics of the potentiometers being used. The frequency response of these devices, however, is usually limited to approximately 10 cps by the inertia of the servomotor and the frictional drag introduced by the mechanical couplings and in the ganged potentiometers, although recently developed 400-cps servos are accurate up to 30 cps. Four-quadrant multiplication is achieved by applying positive as well as negative voltage supplies to the follow-up potentiometer and by employing additional sign changers.

The static accuracy of the biased-diode quarter-square multipliers is limited by the number of straight-line segments employed to approximate the parabolic curve. On the other hand, the frequency response of these devices excels that of any of the other multipliers discussed in this chapter. These units are attractive because they lend themselves to the generation of many other nonlinear functions as described in the following chapter. In the case of photoformers, the persistence of the screen as well as the amplifier responses may set an upper limit on the speed with which the curve can be scanned.

REFERENCES

1. Frost, S.: Compact Analog Computer, *Electronics*, **21**(7):116–120 (1948).
2. Weiss, H. K.: Analysis of Relay Servomechanisms, *J. Aeronaut. Sci.*, **13**:364–376 (1946).
3. Kochenburger, R. J.: A Frequency Response Method for Analyzing and Synthesizing Contactor Servomechanisms, *Trans. AIEE*, **69**:270–284 (1950).
4. Rogers, T. A., and W. C. Hurty: Relay Servomechanisms, *Trans. ASME*, **72**:1163–1172 (1950).
5. Whitehead, D. L.: Analog Computer—New Techniques, New Components, *Westinghouse Engr.*, **10**:235–239 (1950).
6. Chance, B., F. C. Williams, C. Yang, J. Busser, and J. Higgins: A Quarter-square Multiplier Using a Segmented Parabolic Characteristic, *Rev. Sci. Instr.*, **22**:683–688 (1951).
7. Fisher, M. O.: Optimum Design of Quarter-squares Multipliers with Segmented Characteristics, *J. Sci. Instr.*, **34**:312–316 (1951).
8. British Thomson-Houston Co., Ltd., and D. J. Myna: Computing-apparatus, British Patent, Group XIX, Specification 607, 397, No. 3285, Feb. 1, 1946.
9. Munster, A. C.: The Monoformer, *Radio Electronic Eng.*, **44**(10):8A–9A (1950).
10. Chance, B., F. C. Williams, V. Hughes, D. Sayre, and E. F. MacNichol: "Waveforms," McGraw-Hill Book Company Inc., New York, 1949.
11. Michels, W. C.: A Double Tube Vacuum Tube Voltmeter, *Rev. Sci. Instr.*, **9**:10–12 (1938).
12. Draper, J. H. P.: A Square-law Circuit, *J. Sci. Instr.*, **24**:257–258 (1947).
13. Germans, F. H.: Automatic Computation of the Standard Deviation, *Nature*, **163**:25 (1949).
14. Muller, R. H., and G. F. Kinney: A Photoelectric Colorimeter with Logarithmic Response, *J. Opt. Soc. Am.*, **25**:342–346 (1950).
15. Snowden, F. C., and H. T. Page: An Electronic Circuit Which Extracts Antilogarithms Directly, *Rev. Sci. Instr.*, **21**:179–181 (1950).
16. Morrill, C. O., and R. V. Baum: A Stabilized Time-division Multiplier, *Electronics*, **25**(12):139–141 (1952).
17. Walters, L. G.: "A Study of the Series-motor Relay Servomechanism," Ph.D. Thesis, University of California, Los Angeles, 1951.
18. Briggs, B. H.: The Miller Integrator, *Electronic Eng.*, **20**:243–247, 279–284, 325–330 (1948).
19. Price, R.: An FM-AM Multiplier of High Accuracy and Wide Range, *Mass. Inst. Technol., Research Lab. Electronics, Tech. Rept.* 213, Oct. 4, 1951.
20. Hardy, A. C., and E. C. Dench: An Electronic Method for Solving Simultaneous Equations, *J. Opt. Soc. Am.*, **38**:308–312 (1948).
21. Somerville, A.: A Beam-type Tube That Multiplies, *Proc. Natl. Electronics Conf.*, **6**:145–154 (1950).
22. Angelo, E. J., Jr.: "An Electron-beam Tube for Analogue Multiplication," Sc.D. Thesis, Department of Electrical Engineering, Massachusetts Institute of Technology, 1952.
23. MacNee, A. B.: An Electronic Differential Analyzer, *Proc. IRE*, **37**:1315–1324 (1949).
24. Hall, A. C.: A Generalized Analogue Computer for Flight Simulation, *Trans. AIEE*, **69**:308–320 (1950).
25. Rippere, R. O.: An Electrical Computer for Flight Training, *Bell Labs. Record*, **25**:78–81 (1947).

4

ELECTRICAL FUNCTION GENERATORS

4.1. General Remarks. For a wide variety of analog computations, it is necessary to provide operational units which will furnish or generate special electrical functions. Such function generators are classified as generators of *functions of dependent variables* if the output voltage bears some specified relationship to the input voltage and generators of *functions of the independent variables* if the output voltage is some special function of time. Dependent variable-function generators are important particularly in the analysis of nonlinear systems. In general, such nonlinearities arise because the magnitudes of the system parameters or characteristics are governed by the system variables. For example, in a heat-transfer system, the thermal conductivity of a metal conductor may be a function of the temperature of that conductor. Time-function generators are needed most often to simulate special types of excitation or driving functions. A number of the devices described in Chaps. 2 and 3 can be used directly to generate such time functions.

In this chapter, more elaborate devices for generating nonlinear functions are considered. For the most part these devices employ as basic building blocks the operational adding and integrating circuits described in Chap. 2, as well as the biased-diode and servo devices described in Chap. 3. Excellent summaries of the application of electronic analog computers to function generation have been prepared by Bekey.[1,2] Much of the material in this chapter is based upon his excellent work.

FUNCTIONS OF DEPENDENT VARIABLES

4.2. Discontinuous Functions. In many cases, particularly in the study of dynamics and control systems, it is necessary to employ computing units in which the output vs. input voltage curve has sharp breaks or discontinuities. Biased-diode devices are by far the most widely used generators of such functions. Occasionally relays and servomechanisms also find application. The utilization of diode circuits is considered first.

One of the most important of the discontinuity devices is the *limiter*. Such a unit has a linear transfer characteristic over a specified range e_1 to e_2. If the input voltage e_i exceeds e_2 in the positive direction or e_1 in the negative direction, the slope of the e_o/e_i curve undergoes an abrupt change. The yield point of a material, magnetic saturation, airplane control surface position, etc., introduce such limiting values. The circuit shown in Fig. 4.1a can be employed to generate the transfer function of Fig. 4.1b. When $e_1 < e_i < e_2$, neither diode V_1 nor diode V_2 conducts. The output voltage is then a linear function of the input voltage and has a slope determined by the gain of the two sign changers. If e_i is more
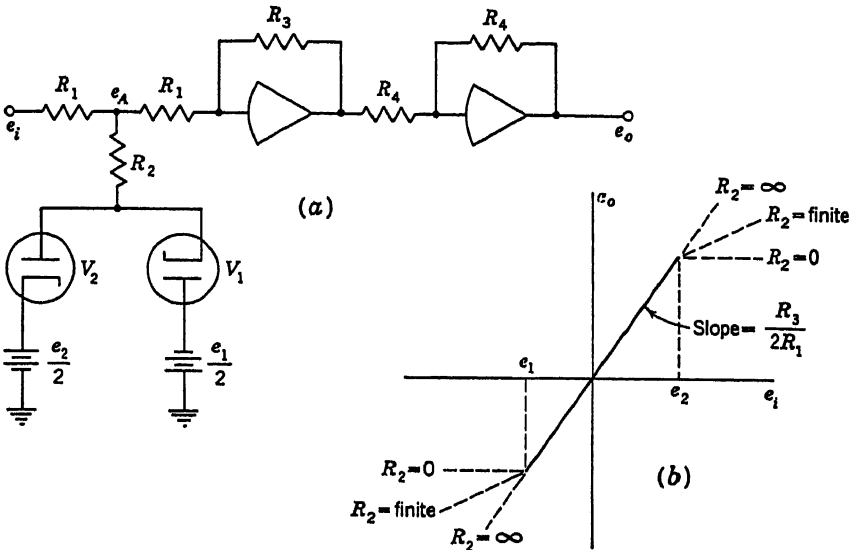
Fig. 4.1

negative than e_1, diode V_1 becomes conductive and a portion of the input current is bypassed through R_2 and V_1. The slope of the e_o/e_i curve is thereby reduced. If R_2 is zero, the voltage e_A cannot rise above $e_i/2$. Similarly, if e_i becomes more positive than e_2, diode V_2 conducts, again resulting in a discontinuity of the curve.

An alternative method of simulating limiter action is to employ the circuit of Fig. 4.2a to obtain the transfer function shown in Fig. 4.2b. Here diode V_2 is cut off until the output voltage e_o exceeds e_2. At that point, resistor R_3 is effectively placed in parallel with R_2 so that the voltage gain of the entire circuit is reduced and the slope of the transfer-function curve is abruptly changed. A similar effect occurs when e_o becomes more negative than e_1. Then R_2 is placed in parallel with R_4,

thereby limiting the output. If R_3 and R_4 are omitted from the circuit, the output voltage is prevented from exceeding e_2 and e_1.

Dead zones are simulated with the circuit shown in Fig. 4.3a. When $e_1 < e_i < e_2$, neither diode V_1 nor diode V_2 conducts and the transfer characteristic has a slope $R_4/(R_i + R_3)$. When e_i becomes more negative than e_1, V_1 conducts and R_2 is effectively placed in parallel with R_i, thereby increasing the effective gain of the network. The slope of the e_o/e_i

(a)

(b)
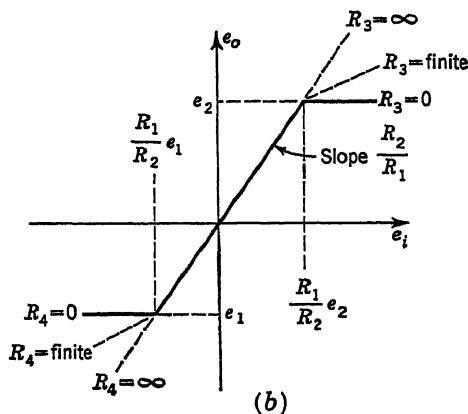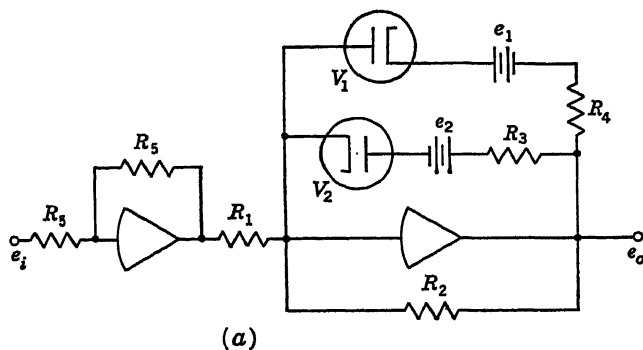
Fig. 4.2

curve is thereby made more positive. A similar effect takes place when e_i becomes more positive than e_2, placing R_1 in parallel with R_i. In Fig. 4.3b, the angles α_1 and α_2 are determined by the magnitudes of R_1 and R_2. The locations of the break points are determined by the magnitudes of the bias voltages e_1 and e_2.

The *comparator* circuit for simulating Coulomb friction is shown in Fig. 4.4a. As a result of the high gain of the operational amplifier, if e_i assumes even a very small positive value, the output voltage e_o immediately jumps to a negative value such that diode V_2 is rendered conductive

and the output is clamped at a fixed voltage by the biased source e_2. Similarly if e_i becomes slightly negative, e_o becomes very positive and the output is maintained at a positive value determined by e_1, as shown in Fig. 4.4b.
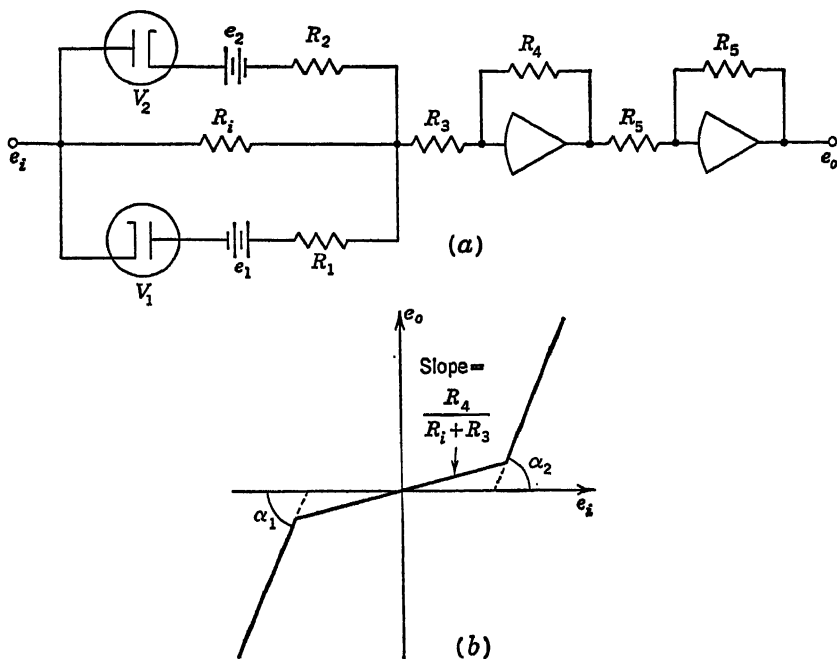
Fig. 4.3
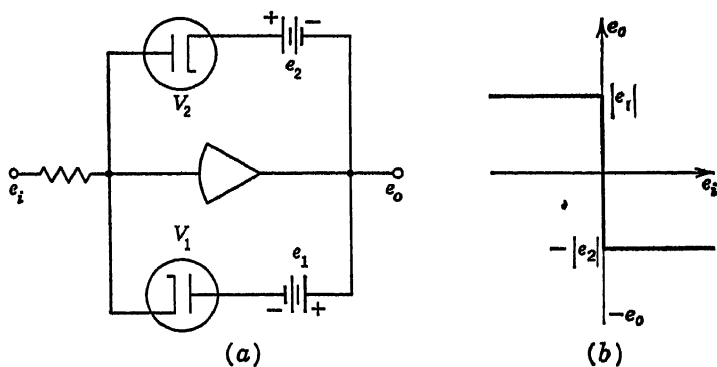
Fig. 4.4

Absolute values can be obtained with the circuit shown in Fig. 4.5a. If e_i is negative, V_1 conducts, but not V_2. The slope of the output curve is therefore determined by R_2/R_1. If e_i is positive, V_2 conducts while V_1 is cut off. The output is then proportional to R_4/R_3. If all the resistors

are equal in magnitude, $e_o = |e_i|$. The input-output relation is shown in Fig. 4.5b.

Another special unit which deserves mention is the *backlash* simulator. This circuit is useful in the study of mechanical systems, in which gears are not tightly coupled, and in the study of electromagnetic systems

(a)   (b)

Fig. 4.5

(a)
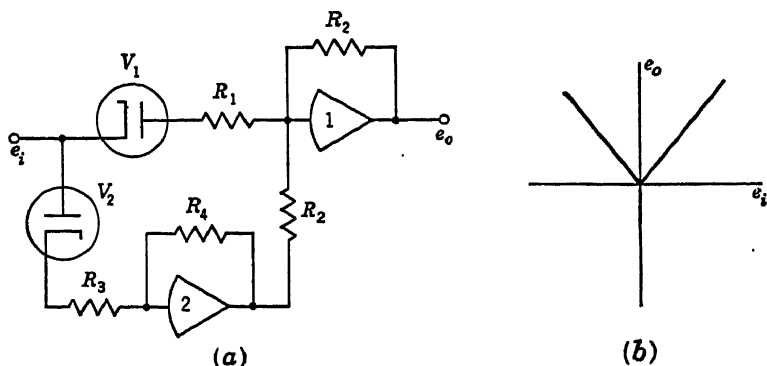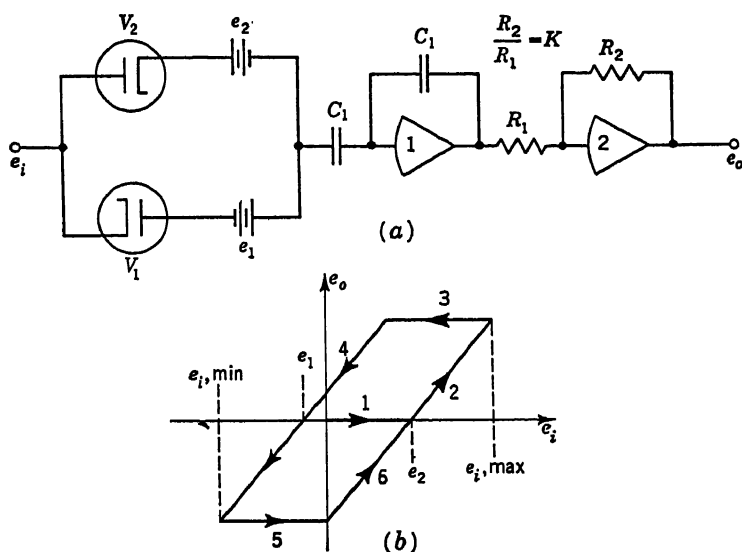
Fig. 4.6

having hysteresis. The circuit shown in Fig. 4.6a can be employed to generate the transfer function shown in Fig. 4.6b. If the two capacitors are discharged at time $t = 0$, the output voltage e_o will remain zero while e_i becomes positive until e_i exceeds e_2 in magnitude. Amplifier 1 then acts as a simple sign changer until e_i reaches its maximum positive magnitude. When e_i begins to decrease (step 3), both diodes are biased

beyond cutoff and both capacitors retain their voltage ($e_{i,max} - e_2$), since they have no discharge paths. This condition is maintained until e_i drops below the voltage on the capacitors. Then V_1 conducts, giving a linear transfer function until e_i reaches a minimum negative value (step 4). A summary of the relationship between e_o, e_i, and e_c (the voltage of C_1) as e_i goes through a complete cycle is given in Table 4.1.

TABLE 4.1. OPERATION OF BACKLASH SIMULATOR[1]

e_i	e_c	e_o
1. $0 \leq e_i \leq e_2$	0	0
2. $e_2 < e_i < e_{i,max}$	$(e_i - e_2)$	$K(e_i - e_2)$
3. $(e_1 + e_{i,max} - e_2) < e_i < e_{i,max}$	$e_{i,max} - e_2$	$K(e_{i,max} - e_2)$
4. $e_{i,min} < e_i < [e_1 + (e_{i,max} - e_2)]$	$e_i - e_1$	$K(e_i - e_1)$
5. $e_{i,min} < e_i < [e_2 + (e_{i,min} - e_1)]$	$e_{i,min} - e_1$	$K(e_{i,min} - e_1)$
6. $e_2 + (e_{i,min} - e_1) \leq e_i \leq e_2$	$e_i - e_2$	$K(e_i - e_2)$

A major source of error in the application of diodes to the generation of discontinuous function lies in the fact that the forward resistance of a diode is not zero and the backward resistance is not infinite. For this reason, relays are occasionally used in function-generating circuits. The response time of a relay is limited by mechanical as well as electrical
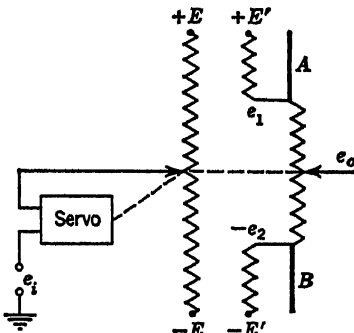
Fig. 4.7
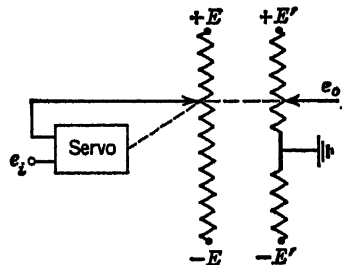
Fig. 4.8

considerations, so that such elements cannot be used where a high-frequency response is required. Occasionally relays have a tendency to vibrate, or "chatter," thereby introducing error signals. Comparator circuits of the type shown in Fig. 4.4a are frequently used in conjunction with relays to provide a more positive and rapid response.

Discontinuity functions can also be obtained with servo-driven potentiometric function generators. To obtain simple limiter action, for example, the servo-driven potentiometer is arranged as shown in Fig. 4.7. After traversing the appropriate range of resistance on the

output potentiometer, the brush is made to ride on solid conductors A and B, which are connected to voltage sources corresponding to the limiting values e_1 and e_2, respectively. Dead-zone responses can be generated with a servo-driven potentiometer by placing the solid conductors A and B at the center of the potentiometer, as shown in Fig. 4.8. Backlash functions are generated by actually providing the required amount of backlash B between the brush and the shaft, and by driving it as shown in Fig. 4.9a. While the motor is moving the brush upward, the contact is pressed against the upper face of the brush carrier P. Upon reversal of the direction of motion, the shaft F traverses the distance $2B$ before
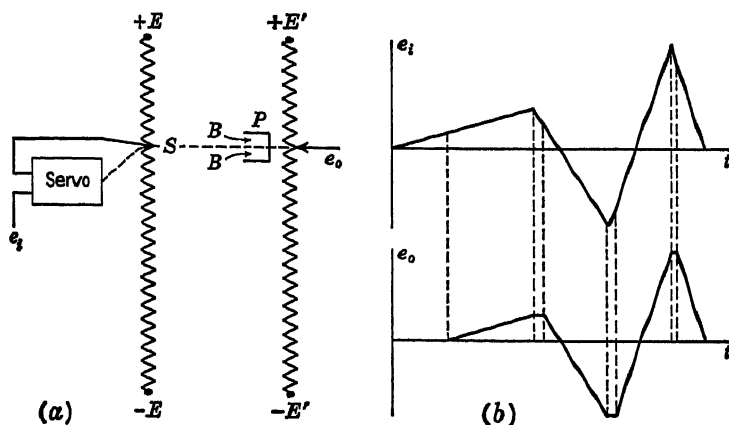
Fig. 4.9

contacting the lower surface of the brush carrier and driving the brush downward. Servo-driven function generators are capable of great accuracy but are limited in frequency response by the inertia of the servomotor and of the other moving mechanical parts.

4.3. Power and Roots. In the solution of engineering problems, it frequently becomes desirable to raise variable voltages to powers such that $e_o = e_i{}^n$, where n may be larger or smaller than unity. The application of Maclaurin and Taylor series expansions permits the expression of numerous transcendental functions in terms of power series. For rapidly converging series, only the first few terms need be included. Table 4.2 lists a number of useful series expansions.

The biased diode and photoformer methods for obtaining parabolic transfer functions can be applied directly to the generation of cubes, fourth powers, square roots, etc. The implicit function techniques, discussed in connection with servo dividers in Sec. 3.7, are particularly useful for this purpose.

For example, in order to extract square roots and cube roots, the desired

TABLE 4.2

$f(x)$	Series expansion	Range of x for which series is convergent
e^{e^x}	$1 + \dfrac{x}{1!} + \dfrac{x^2}{2!} + \dfrac{x^3}{3!} + \cdots$	$-\infty < x < +\infty$
e^{-x}	$1 - \dfrac{x}{1!} + \dfrac{x^2}{2!} - \dfrac{x^3}{3!} + \dfrac{x^4}{4!} - \cdots$	$-\infty < x < +\infty$
$\log_e x$	$(x-1) - \dfrac{(x-1)^2}{2} - \dfrac{(x-1)^3}{3} - \cdots$	$2 < x < +\infty$
$\cos x$	$1 - \dfrac{x^2}{2!} + \dfrac{x^4}{4!} - \dfrac{x^6}{6!} + \cdots$	$-\infty < x < +\infty$
$\sin x$	$x - \dfrac{x^3}{3!} + \dfrac{x^5}{5!} - \dfrac{x^7}{7!} + \cdots$	$-\infty < x < +\infty$
$\tan x$	$x + \dfrac{x^3}{3} + \dfrac{2x^5}{15} + \dfrac{17x^7}{315} + \cdots$	$-\dfrac{\pi}{2} < x < +\dfrac{\pi}{2}$
$\sin^{-1} x$	$x + \dfrac{x^3}{6} + \dfrac{3x^5}{40} + \dfrac{5x^7}{112} + \cdots$	$-1 \leq x \leq +1$
$\tan^{-1} x$	$x - \dfrac{x^3}{3} + \dfrac{x^5}{5} - \dfrac{x^7}{7} + \cdots$	$-1 \leq x \leq +1$
$\cosh x$	$1 + \dfrac{x^2}{2!} + \dfrac{x^4}{4!} + \dfrac{x^6}{6!} + \cdots$	$-\infty < x < +\infty$
$\sinh x$	$x + \dfrac{x^3}{3!} + \dfrac{x^5}{5!} + \dfrac{x^7}{7!} + \cdots$	$-\infty < x < +\infty$
$\sinh^{-1} x$	$x - \dfrac{x^3}{6} + \dfrac{3x^5}{40} - \dfrac{5x^7}{112} - \cdots$	$-1 < x < +1$

functions are

$$e_o = e_i^{\frac{1}{2}} \tag{4.1}$$
$$e_o = e_i^{\frac{1}{3}} \tag{4.1a}$$

The corresponding implicit equations are

$$e_o{}^2 - e_i = 0 \tag{4.2}$$
$$e_o{}^3 - e_i = 0 \tag{4.2a}$$

The circuits for realizing these functions are modifications of the general division circuit of Fig. 3.20 and are shown in Fig. 4.10a and b. Figure 4.10c shows in more detail such an implicit square-root circuit, using a servo divider. One of the important applications of this circuit is the calculation of the length L of vectors given the x, y, and z components according to

$$L = \sqrt{x^2 + y^2 + z^2} \tag{4.3}$$

Expressing the components as e_1, e_2, and e_3, respectively, the desired

implicit relationship is

$$e_o{}^2 - e_1{}^2 - e_2{}^2 - e_3{}^2 = 0 \qquad (4.4)$$

A circuit suitable for this computation is shown in Fig. 4.11. When using this method, it is first necessary to generate the squares of the three components.
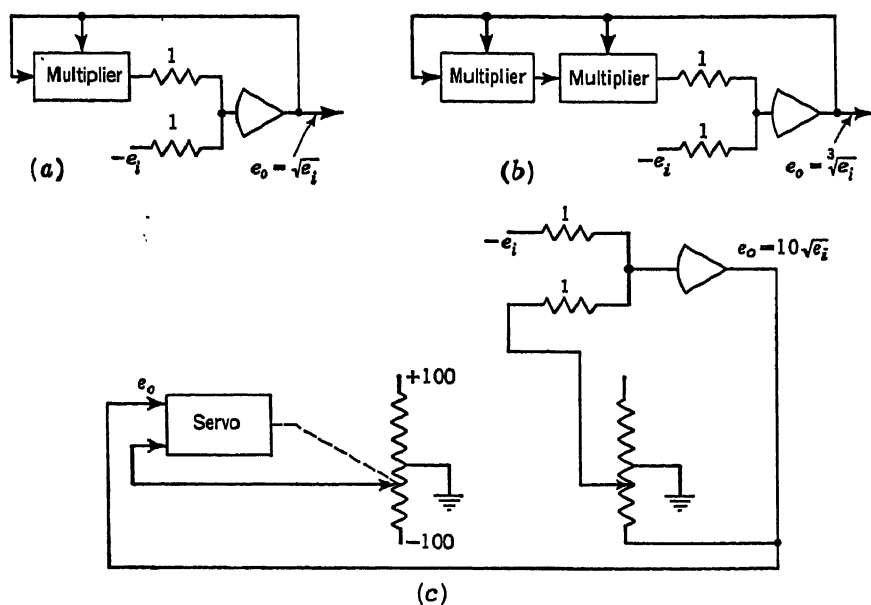
Fig. 4.10
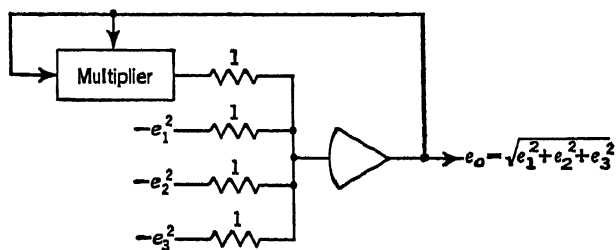
Fig. 4.11

Figure 4.12 shows a standard servo-multiplier circuit for the simultaneous generation of squares, cubes, and higher powers of e_i. Over nine potentiometers can be ganged for this purpose.

Richmond[3] presents a useful technique for the generation of fractional powers, using servo multipliers with accessible center-taps. Consider

the circuit shown in Fig. 4.13 whose output voltage is given by

$$e_o = e_2 - \frac{e_1 e_2}{100} \qquad \text{for } e_1 \geq 0 \tag{4.5}$$

Such a circuit can be applied to obtain fractional powers of a dependent variable by performing continued multiplications of the desired root $e_1^{1/n}$ by itself until one obtains the form $e_1^{(n-1)/n}$. All the terms obtained are then summed in such a manner that all intermediate or undesired exponential terms are eliminated. For example, e_1^{3} and e_1^{4} are generated
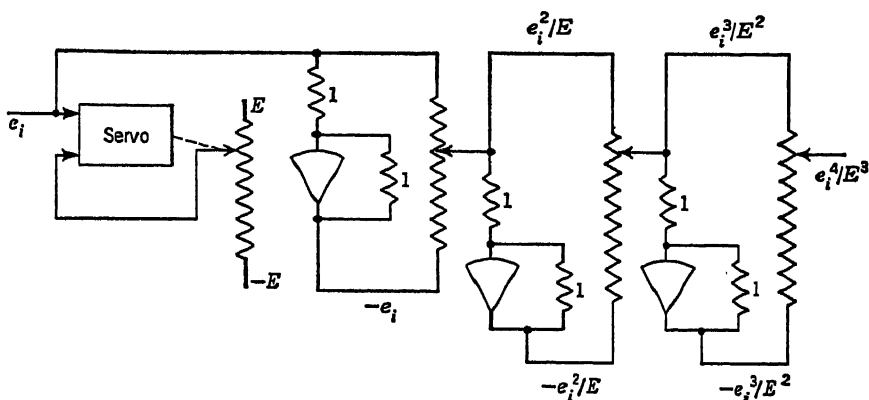
Fig. 4.12
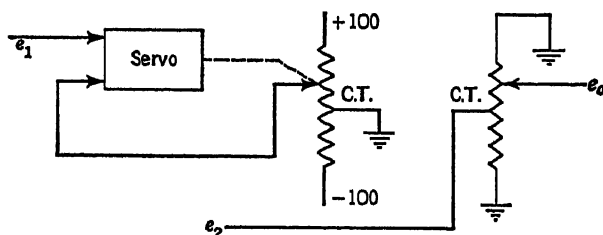
Fig. 4.13

by the circuit of Fig. 4.14. Higher-order numerators and denominators require additional ganged potentiometers.

4.4. Trigonometric Functions—Passive Generators. The generation of voltages proportional to the sine and cosine of a variable appearing as a mechanical rotation is accomplished with potentiometers and resolvers. If the width of a potentiometer card is made proportional to the cosine of the angle of rotation from a given reference position, as shown developed in a plane in Fig. 4.15, the voltage output at the potentiometer brush is equal to the sine of the angle of rotation. When the ends of the card are brought around into contact, a cylinder is formed with two

lobes. The high points are grounded, while the low points are subjected to a positive and a negative voltage of equal absolute magnitudes. Thus, continuous rotation of the potentiometer shaft is possible, and the brush produces voltages proportional to the sine of any angle, including multiple angles.[4]   If the reference point for angle measurement
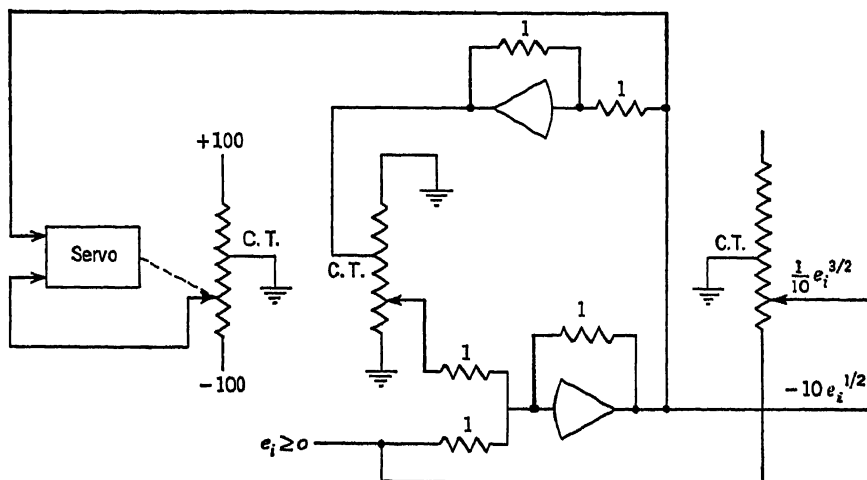
Fig. 4.14
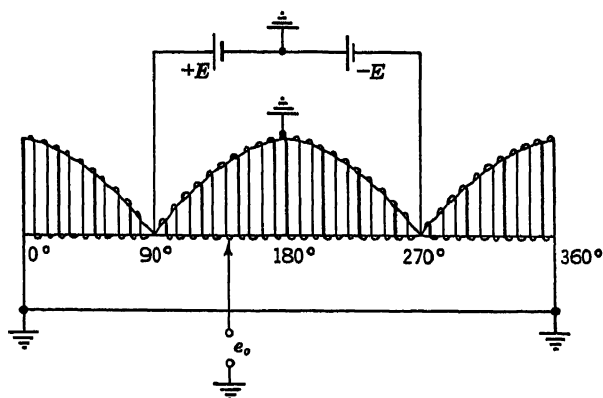
Fig. 4.15

is shifted by 90°, the same potentiometer produces the cosine of the angle. Both sine and cosine are available if two brushes spaced 90° apart are used. The shafts driving the two brushes must be electrically isolated, although acting mechanically as a single unit.

A simple potentiometric sine-cosine generator[4] can be built up from a flat rectangular card, around which a single continuous layer of resistance wire is wound. The wound card is shown in Fig. 4.16. When

voltages of opposite polarities are impressed at the two ends of the wires, a constant potential gradient is made to exist along the card in the direction perpendicular to the turns of the wire. The voltage gradient along the wire should be of negligible magnitude. If the wire is grounded at the center of the card and a brush is caused to move in a circular path about this point, the voltage at the brush is a sinusoidal function of the angle of rotation. Another contact situated at 90° from the first produces the cosine. Brushes situated at diametrically opposite positions produce voltages of opposite signs. Loading problems arise, as with other potentiometric devices, so that only high-resistance loads should be connected to the brushes, or isolating amplifiers should be used between the brushes and the load.

A simple potentiometric circuit which provides a voltage closely approximating the tangent function has been described by Hofstadter.[5] The circuit in Fig. 4.17a shows a circular potentiometer. The angular rotation of the potentiometer tap from the mid-position setting is the angle the tangent of which is desired. The output voltage of this device is given by
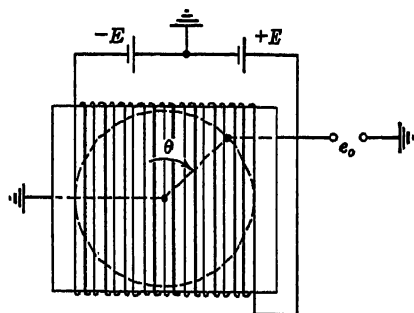
Fig. 4.16

$$e_o = K \frac{\phi}{1 - \phi^2 \gamma} \approx K \tan \phi \tag{4.6}$$

where

$$K = \frac{E}{(R_0/R_1 + R_2/R_1 + 2)\phi_0} \tag{4.7}$$

and

$$\gamma = \frac{1}{(R_2/R_0 + 2R_1/R_0 + 1)\phi_0^2} \tag{4.8}$$

The function $\phi/(1 - \gamma\phi^2)$ represents $\tan \phi$ to a close approximation over limited ranges of ϕ. The fractional error in this value, as compared with $\tan \phi$, is given by

$$\delta = 1 - \frac{\phi}{(1 - \gamma\phi^2)\tan \phi} \tag{4.9}$$

The error depends on ϕ and on the value of γ. In turn, γ depends on the values chosen for the resistances and for the maximum rotational half angle of the potentiometer. Error curves with γ as a parameter are plotted in Fig. 4.17b for a wide range of ϕ. A γ of 0.36 yields a tangent value, correct within 1 per cent over a range of ϕ, from zero to approximately 60. If the allowable error is permitted to go to 3.7 per cent, the circuit produces the tangent within this limit from zero to approximately 80.
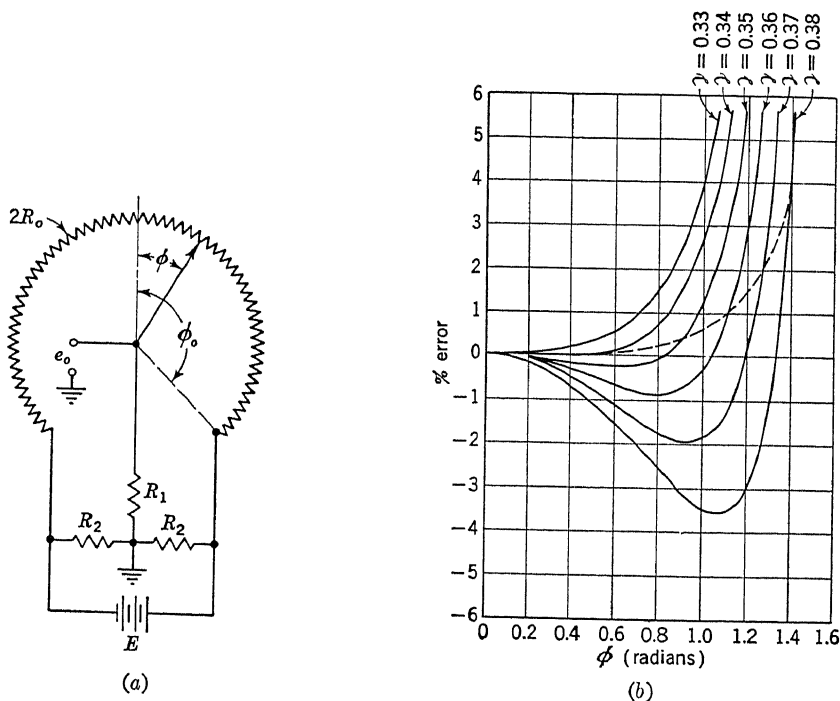
Fig. 4.17. [R. Hofstadter, *A Simple Potentiometer Circuit for Production of the Tangent Function, Rev. Sci. Instr.*, 17:298–300 (1948).]
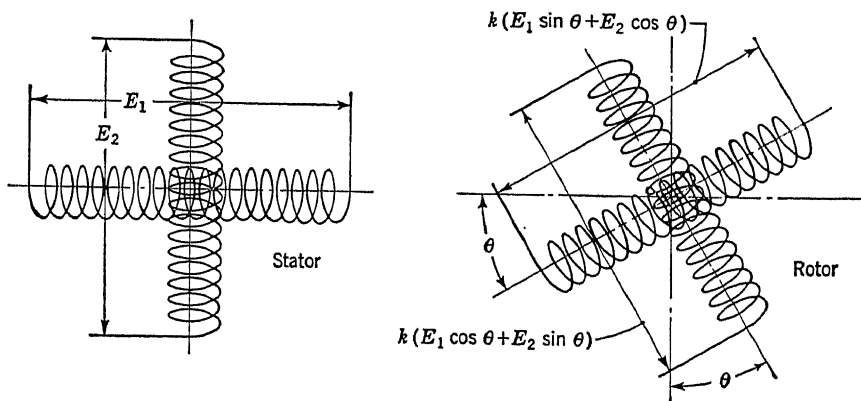
Fig. 4.18

In a-c computing circuits, electromagnetic resolvers[6] are commonly used for the generation of sines and cosines. A typical electromagnetic resolver consists of a rotor and stator, each wound with two separate coils situated precisely at right angles to each other, as shown in Fig. 4.18. Alternating-current voltages E_1 and E_2, applied at the terminals of the

two coils of the stator, cause voltages e_1 and e_2 to appear at the terminals of the rotor coils. When the rotor is situated at an angle θ with respect to the stator, these output voltages are

$$e_1 = k(E_1 \cos \theta + E_2 \sin \theta) \qquad (4.10)$$
$$e_2 = k(E_1 \sin \theta + E_2 \cos \theta) \qquad (4.11)$$

If E_2 is made zero (*i.e.*, the corresponding winding is shorted), the rotor outputs become

$$e_1 = E_1 \cos \theta$$
$$e_2 = E_1 \sin \theta \qquad (4.12)$$

The secant, cosecant, tangent, and cotangent can be obtained from the outputs e_1 and e_2 by taking reciprocals and by dividing one voltage by the other.
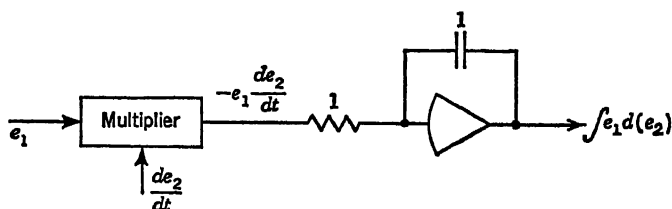
Fig. 4.19

4.5. Trigonometric Functions—Active Generators. Trigonometric functions of dependent variables can be generated by means of standard multipliers, integrators, and sign changers and by using a generalized integration technique. In order to perform an integration with respect to a dependent variable, the following identity is employed:

$$\int y \, dx \equiv \int y \left(\frac{dx}{dt}\right) dt \qquad (4.13)$$

The time derivative of one of the dependent variables is obtained, and this quantity is multiplied by the other variable. The product is then integrated with respect to time, as shown in Fig. 4.19.

The sine and cosine functions are obtained by solving the equation

$$\frac{d^2y}{dx^2} + y = 0 \qquad (4.14)$$

The solution of differential equations of this type involves the use of feedback loops, a subject discussed in considerable detail in Chap. 6. The circuit for solving Eq. (4.14) requires two multipliers, two integrators, and a sign changer as shown in Fig. 4.20. Howe[7] has suggested modifications in this circuit to minimize errors due to phase shifts in the amplifiers and multipliers.
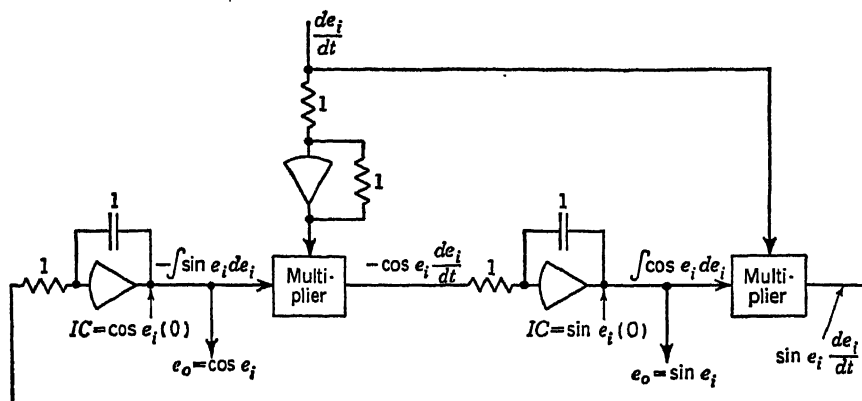
Fig. 4.20
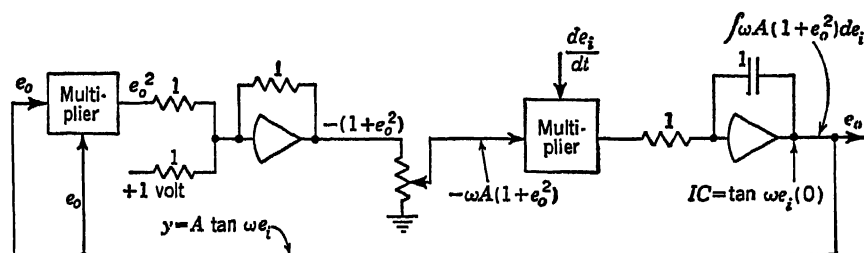
Fig. 4.21
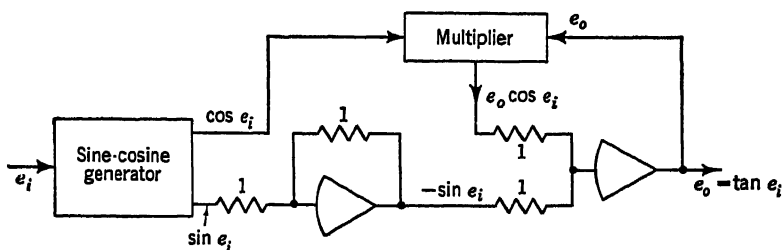
Fig. 4.22

A voltage proportional to the tangent of a dependent variable is obtained by solving the equation

$$\frac{dy}{dx} = \omega A(1 + y^2) \tag{4.15}$$

and by recognizing that

$$\tan x = \int (1 + \tan^2 x)\, dx + \text{const} \tag{4.16}$$

The circuit for solving this equation is shown in Fig. 4.21. Another circuit for generating a tangent is shown in Fig. 4.22. Here, the desired

function is generated by solving the implicit equation

$$z \cos x - \sin x = 0 \qquad (4.17)$$

so that
$$z = \frac{\sin x}{\cos x} = \tan x \qquad (4.18)$$

The circuit of Fig. 4.20 can be employed to generate the necessary sine and cosine functions.

Implicit function techniques can be employed to generate inverse trigonometric functions. For example, the circuit shown in Fig. 4.23 solves the implicit relationship

$$\sin z - x = 0 , \qquad (4.19)$$

so that $z = \sin^{-1} x \qquad (4.20)$

Fig. 4.23

Inverse cosines and tangents can be obtained in a similar manner.
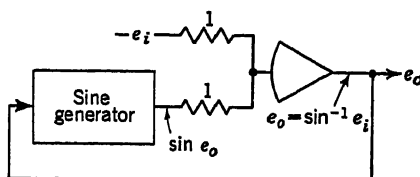
4.6. Exponential, Logarithmic, and Error Functions. The generation of functions in which the dependent variable appears as an exponent can also be achieved by using the generalized integration technique. To obtain the function

$$y = A\epsilon^{-kx} \qquad (4.21)$$

the differential equation

$$\frac{dx}{dy} = -kx \qquad (4.22)$$

is solved by closed-loop methods. The appropriate circuit is shown in Fig. 4.24. In this circuit the constant A is introduced into the solution
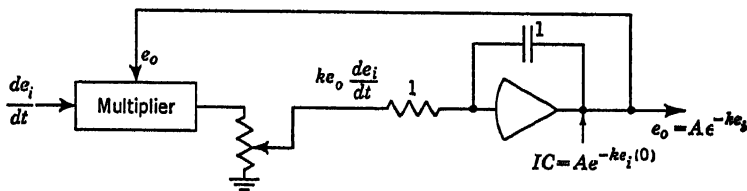
Fig. 4.24

as an initial condition on the integrator. That is, the feedback capacitor is charged to a voltage of A volts at time $t = 0$.

To obtain the function

$$y = \log_\epsilon x \qquad (4.23)$$

the differential equation

$$\frac{dx}{dy} = \frac{A}{x} \qquad (4.24)$$

is solved, say, by means of the circuit shown in Fig. 4.25. In this case, a divider is required. The feedback capacitor is given an initial charge proportional to the product of A and the logarithm of e_i at $t = 0$.
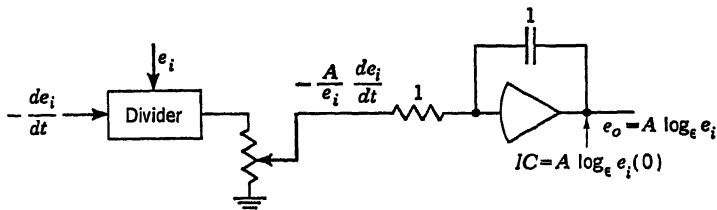
Fig. 4.25

Another important analytical function, which can be generated by electric analog techniques, is the error function defined by

$$\operatorname{erf} x = \frac{2}{\sqrt{\pi}} \int_0^x \epsilon^{-\alpha t^2} \, dt \tag{4.25}$$

This function is generated by solving the equation

$$\frac{dy}{dt} = -2\alpha t y \tag{4.26}$$

where $y = \epsilon^{-\alpha t^2}$. The circuit for the solution of this equation is shown in Fig. 4.26.
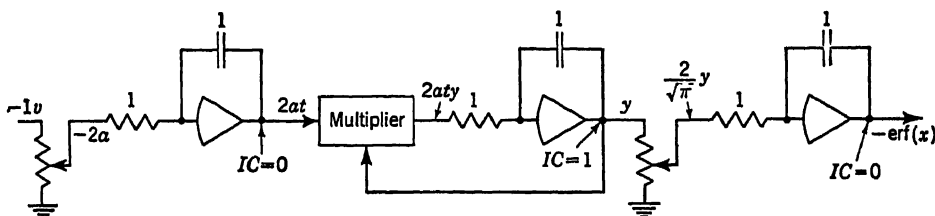
Fig. 4.26

4.7. Arbitrary Functions. The simplest types of function generators are the potentiometric generators. If the independent variable appears in a computer as a shaft rotation, the shaft can be arranged to drive a function potentiometer, which will yield the desired function as a voltage.

The taper- or step-wound potentiometers are often used for the generation of the square and reciprocal functions. By appropriate taper or sequence of steps various other arbitrary functions of shaft roation can be developed. By combining the coarse settings of a multitapped potentiometer with the fine setting of a wire-wound rheostat, high precision can be attained in function generation. One such potentiometer[8] designed for use in radar range determination developed the exponential function to 1 part in 4,000.

The change in voltage distribution produced in a linear potentiometer by tapping off current has been discussed in Sec. 2.2 in connection with "loading" effect.   With a sufficient number of taps provided on a linear potentiometer, the degree of loading at each tap can be adjusted to give the required arbitrary function.[9]   This form of arbitrary function generator may be represented as shown in Fig. 4.27a.   The actual construction can take a variety of forms.   In Fig. 4.27a a plus and minus voltage source is shunted by a low-resistance voltage divider.   A second potentiometer, preferably of much higher resistance, is connected to the first at a number of positions which may be adjustable on either one or both potentiometers.   A brush on the second potentiometer picks off the

(a)

(b)
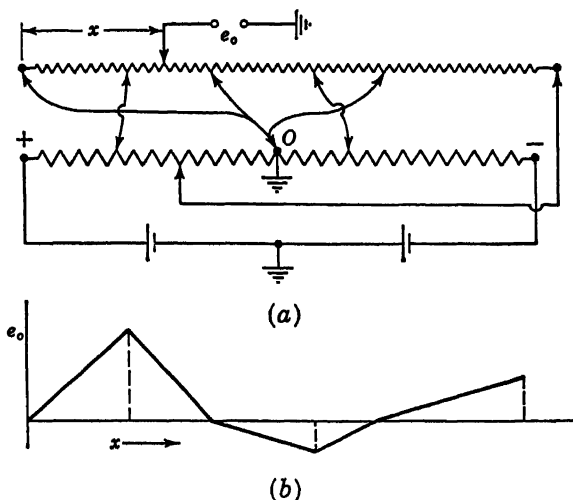
Fig. 4.27

voltage existing at any position x.   It is assumed in this case that the pickoff does not load the second potentiometer.   With the connections as shown, e_o as a function of x is shown in Fig. 4.27b.   The variation in voltage between taps is substantially linear.

Instead of using a tapped linear potentiometer, an untapped linear potentiometer can be used with a pickoff whose position on the potentiometer is the desired function of potentiometer rotation.[10]   This method is illustrated in Fig. 4.28.   A curve C is laid out on an electrically nonconducting surface, so that horizontal distances from reference (indicated by the vertical line through O) represent the desired function of the independent variable.   The independent variable is represented by the vertical distance along the sheet.   If the curve C is formed from a copper wire glued to the sheet, the voltage in the wire will be that in the potentiometer at the point of contact with the wire.   Thus, as the sheet is moved

relative to the potentiometer in proportion to the value of the variable, the point of contact on the potentiometer will be displaced in proportion to the value of the function being generated. The corresponding voltage can be picked off the wire.

In one apparatus, the wire representing the desired function is mounted on a nonconducting cylinder, which rotates against a linear potentiometer. In another, a peep sight is lined up on a plotted curve by means of a hand crank. The hand crank shifts the potentiometer brush, making it unnecessary to cement a wire along the plotted curve. A serious disadvantage of the hand-crank method is the fact that it requires the
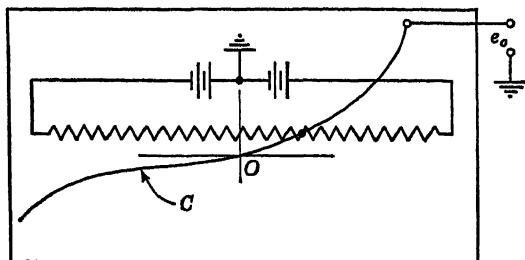
Fig. 4.28

constant attention of an operator. Another disadvantage is the human error involved in tracking the curve.

If the input variable is a voltage instead of a shaft rotation, the use of potentiometers for arbitrary function generation requires servos to convert the input voltage into mechanical displacement of a potentiometer brush or into rotation of function cylinder. Such conversion has been described in connection with servo multipliers and servo dividers.

Biased diodes provide a high-speed and exceptionally flexible method for developing arbitrary functions. It has already been shown how biased-diode circuits can be arranged to give any desired variation in slope from point to point along a curve.

The photoformer has been described earlier and is a means for rapidly introducing arbitrary functions into a computer. In general, the photoformer can be used to represent any single-valued function as long as the hills and valleys of the mask are sufficiently larger in both dimensions than the spot of light that traces them. In some cases multiple-valued functions can be used, the spot selecting the appropriate value in accordance with its previous history.[11]

4.8. Functions of Two Variables. Frequently, it is desired to generate functions which are themselves functions of two or more dependent variables. Occasionally, it is possible to express this functional relationship analytically and to employ combinations of multipliers and other forms of function generators. Sometimes, however, the functional

relationship is available only in graphical form. Examples of the latter condition are the familiar vacuum-tube characteristic curves. The plate current of a triode depends upon both the plate voltage and the grid voltage, and this relationship is generally represented as a family of empiric curves. A number of methods for treating problems of this type have been suggested. These are summarized in considerable detail by Stanley.[12]

Special devices which have been developed for this purpose include three-dimensional cams, the height of the cams being proportional to
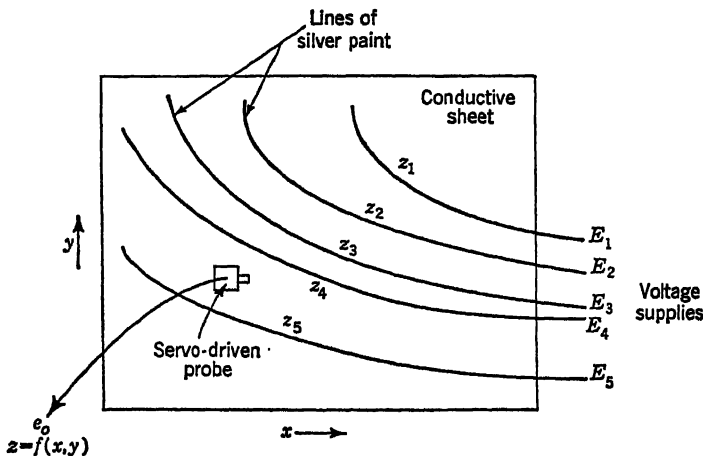
Fig. 4.29

the desired output voltage. The cam is moved by a servo system in the x and y directions corresponding to the two variables, and a cam follower is used to move the tap of a potentiometer, thereby generating the desired voltage. Semiconducting sheets, such as the Teledeltos resistance paper described in Chap. 11, can be applied as shown in Fig. 4.29. A family of curves corresponding to $z = f(x,y)$ is drawn on this paper with conductive ink such as silver paint. A separate electrical potential is applied to each one of these curves. The conductive sheet then acts as an interpolator between these curves. A probe arm is moved over the conductive sheet by means of servos which regulate the x and the y position of the probe.

Servo or biased-diode function generators can be employed as shown in Fig. 4.30. A number of function generators are employed to generate output voltages proportional to $f(x,y_1)$, $f(x,y_2)$, etc. These outputs are fed to the fixed taps of a servo-driven potentiometer. The position of the moving arm of this potentiometer is determined by the variable y.

Elliott[13] employs a graphical technique for matching families of curves
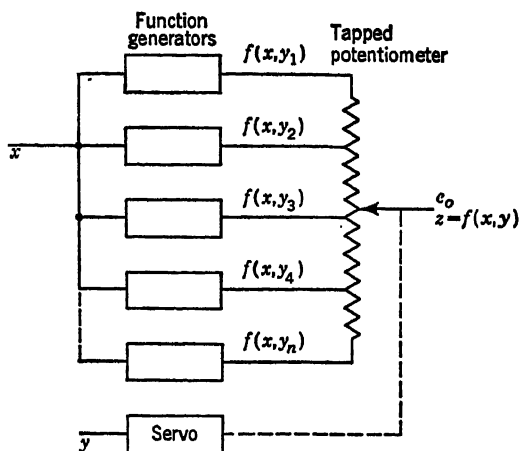
Fig. 4.30
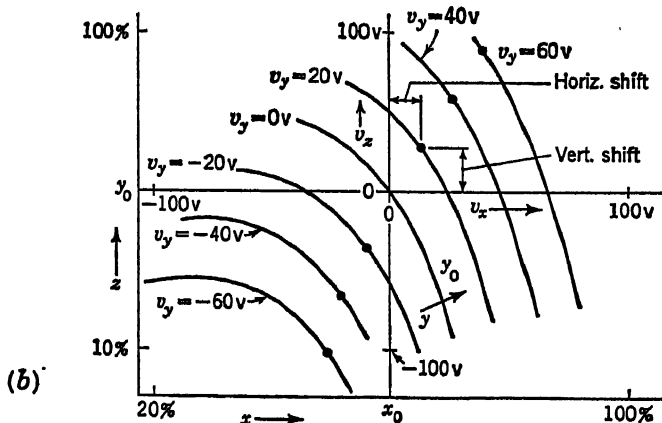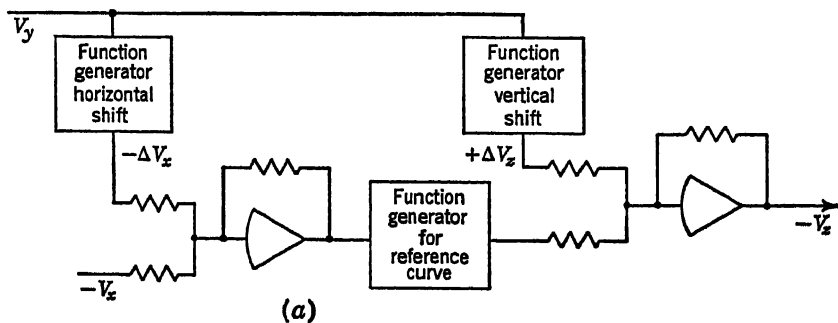
Fig. 4.31. [D. A. Elliott, *Representation of Nonlinear Function of Two Input Variables on Analog Equipment*, *Trans. ASME*, 79:489–495 (1957).]

having reasonably regular characteristics. His method involves the use of a diode function generator to match accurately one of the curves of the family. By means of the addition of suitable voltages to the input and output of this function generator, the basic curve can be translated in the horizontal or vertical directions, as shown in Fig. 4.31. Combined horizontal and vertical translations are achieved by adding voltages to the input as well as the output of the function generator. More sophisticated versions of this technique make it possible to rotate as well as to translate the basic reference curve in order to permit the approximation of a wider variety of families of curves.

FUNCTIONS OF TIME

4.9. Exponential and Logarithmic Functions. Most analytic functions of time are generated by solving differential equations, the solutions of which constitute the desired function. The characteristic equation is constructed by successively differentiating the function, and the highest order derivative is expressed in terms of lower-order derivatives and functions of time. A closed-loop electronic-analog-computer circuit is then constructed to generate the desired function by successive integrations.

To obtain the simple ramp function

$$e_o = kt \tag{4.27}$$

The equation

$$\frac{de_o}{dt} = k \tag{4.28}$$

is instrumented as shown in Fig. 4.32. If the switch is closed at time $t = 0$, the output voltage increases linearly with the time until the output voltage limit of the amplifier is reached. If the feedback capacitor is initially discharged, the ramp function starts from the origin. An initial voltage on the capacitor displaces this straight line in the vertical direction.
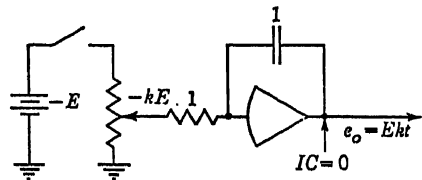
Fig. 4.32

Higher powers of time are generated by applying the output of the circuit of Fig. 4.32 to one or more integrators, as shown in Fig. 4.33. In this circuit all feedback capacitors are discharged at time $t = 0$. The generation of fractional or other nonintegral powers of time can be accomplished by means of the circuit in Fig. 4.34. The desired function

$$e_o = k(t + a)^n \tag{4.29}$$

is differentiated

$$\frac{de_o}{dt} = nk(t + a)^{n-1} \tag{4.30}$$

Substituting Eq. (4.29) into Eq. (4.30) yields

$$\frac{de_o}{dt} = \frac{ne_o}{t + a} \tag{4.31}$$

Equation (4.31) is instrumented as shown in Fig. 4.34 by means of a closed loop, including a divider. Since the first derivative in Eq. (4.31)
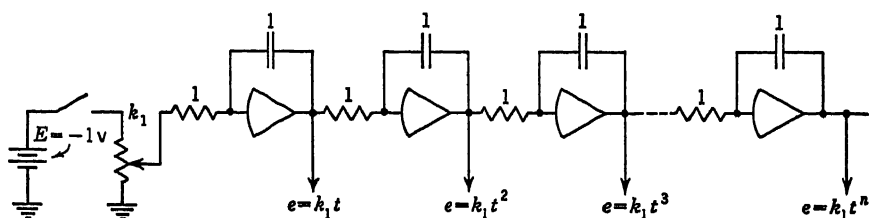
Fig. 4.33
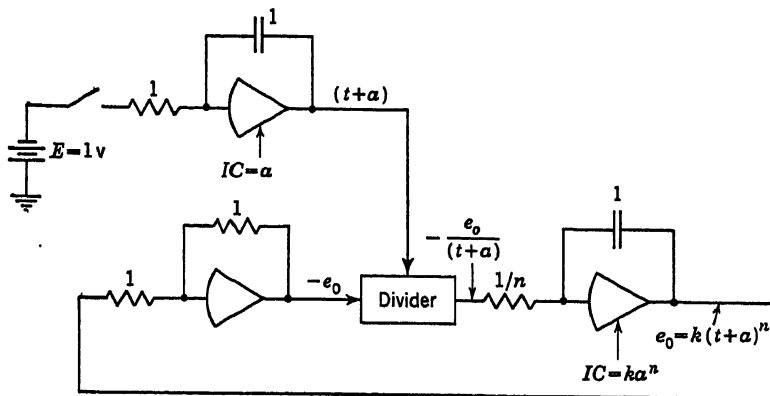
Fig. 4.34

varies inversely as t, it is infinite for $t = 0$ and $a = 0$. In view of the limited voltage outputs available from operational amplifiers, the function generation can only be commenced a short time a after $t = 0$. If n is negative rather than positive, the sign changer in front of the divider is omitted from the circuit.

The expression

$$e_o = A\epsilon^{-kt} \tag{4.32}$$

is generated by solving the differential equation obtained by differentiating Eq. (4.32)

$$\frac{de_o}{dt} = -kA\epsilon^{-kt} \tag{4.33}$$

and by applying an initial condition $e_o = A$ at time $t = 0$, as shown in Fig. 4.35. If the constant k is positive rather than negative, a sign changer is introduced into the feed-back loop.

In order to generate the function

$$e_o = Am^{-kt} \qquad (4.34)$$

where m is an arbitrary constant, the derivative relationship

$$\frac{d(m^x)}{dx} = m^x(\log_e m) \qquad (4.35)$$

is employed. Differentiating Eq. (4.34) yields

Fig. 4.35

$$\frac{de_o}{dt} = -Ak(\log_e m)m^{-kt}$$

$$= -k(\log_e m)e_o \qquad (4.36)$$

Equation (4.36) can be solved by means of the circuit of Fig. 4.35 by making the potentiometer setting equal to $k \log_e m$.
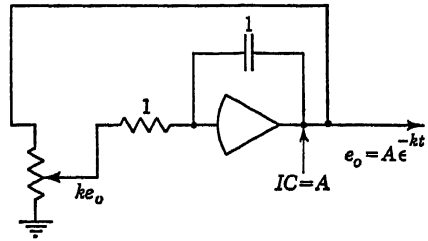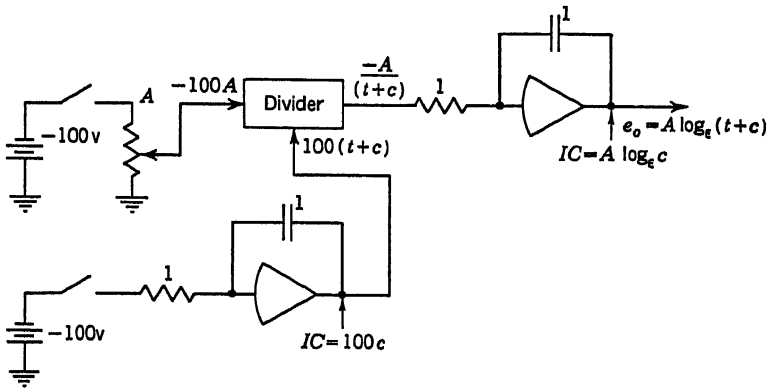
Fig. 4.36

The function

$$e_o = A \log_e (t + c) \qquad (4.37)$$

is instrumented by solving the equation

$$\frac{de_o}{dt} = \frac{A}{t + c} \qquad (4.38)$$

by means of the division circuit shown in Fig. 4.36. As c approaches zero, the output required of the divider approaches infinity for small t.

To generate the logarithm to some arbitrary base m, the relationship

$$\frac{d(\log_e t)}{dt} = \frac{1}{t + c} (\log_e m) \tag{4.39}$$

is employed. The potentiometer in Fig. 4.36 is then given a setting proportional to $A \log_m \epsilon$.

4.10. Periodic Functions. Periodic functions of time are frequently used in analog work as the driving or exciting functions of dynamic systems. The most widely used of these are the trigonometric functions
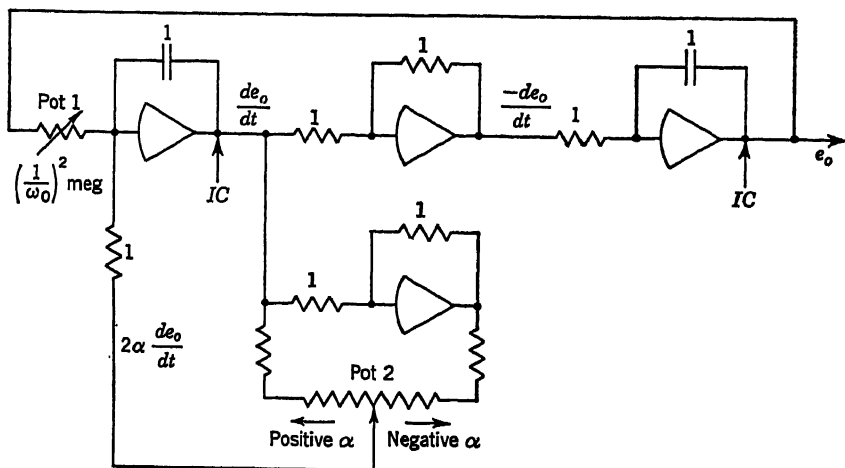
Fig. 4.37

$\sin \omega t$ and $\cos \omega t$. These are generated by solving the equation

$$\frac{d^2 e_o}{dt^2} + 2\alpha \frac{de_o}{dt} + \omega_0^2 e_o = 0 \tag{4.40}$$

where α is the damping constant and ω_0 is the undamped or natural frequency. The solution of Eq. (4.40) is

$$e_o = \epsilon^{-\alpha t} \sin \omega_d t \tag{4.41}$$

where ω_d is the damped frequency, defined by $\omega_d = \sqrt{\omega_0^2 - \alpha^2}$. The four-amplifier closed-loop circuit of Fig. 4.37 is particularly useful for generating this function. Potentiometer 1 is used to adjust the natural frequency, while the setting of potentiometer 2 determines the magnitude and sign of the damping constant. The initial conditions on the two integrators determine the initial amplitude and slope of the output voltage and therefore can be used to adjust the phase of the periodic function. In this way, either a sine or a cosine function can be obtained.

To generate square waves and triangular waves, the circuit of Fig. 4.38

can be used.[1] This circuit includes an integrator, an adder, and a comparator circuit of the type described in Sec. 4.2. At some time $t = 0$, the normally closed switch is opened. Any transient noise appearing at point A immediately sets the comparator circuit in action, and the output voltage e_o becomes either E_1 or E_2. Assume, for the moment, that the output voltage has become positive (E_2). The integrator immediately begins to integrate this constant voltage, so that a negative ramp voltage appears at point B. The adder tends to make the voltage at A equal to
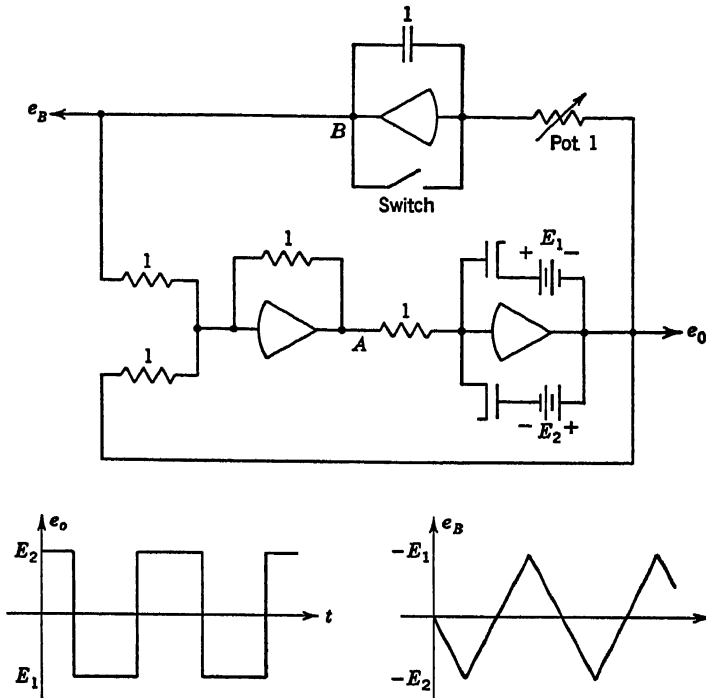
Fig. 4.38

$-(e_o + e_B)$. As long as e_B is smaller than e_o, the voltage at point A remains negative and the output voltage remains positive. After a sufficient time has elapsed, the negative output of the integrator becomes slightly larger than E_2. At that instant, the voltage at point A becomes slightly positive and the comparator circuit flips over, so that the output voltage becomes negative (E_1). The integrator then proceeds to integrate this voltage, eventually generating a positive ramp. This process is repeated periodically and automatically, causing a square wave A to be generated at the output terminal and a triangular wave to be generated at point B. The repetition rate of these waves can be adjusted by means of potentiometer. The waves can be made asymmetric with respect to

the time axis by making E_1 different from E_2. A saw-tooth wave can be obtained from the above circuit by applying the voltage at point B to the absolute-value circuit shown in Fig. 4.5a.

4.11. Time Delays. Occasionally in analyzing engineering systems, it becomes necessary to simulate time delays. For example, in studying transmission processes through hydraulic or pneumatic lines or in studying the motion of radioactive particles in nuclear reactors it is necessary to produce an output voltage which is identical with an input voltage but displaced in time by a specified amount.

A direct and accurate method for generating such time delays is to employ magnetic tape recorders in which the space between the recording and the reading heads is adjustable. By suitably controlling the relative location of the two heads and the speed of the tape, a wide range of time delays can be simulated.

Approximate methods which do not require special auxiliary equipment are based upon the Laplace-transform relationship

$$Lf(t - \tau) = F(s)\epsilon^{-s\tau} \qquad (4.42)$$

To generate a time delay, it is therefore necessary to approximate the function $\epsilon^{-s\tau}$. The Taylor series expansion of this function is

$$\epsilon^{-s\tau} = 1 - \tau s + \frac{(\tau s)^2}{2!} - \frac{(\tau s)^3}{3!} + \frac{(\tau s)^4}{4!} \cdots \qquad (4.43)$$

The generation of the terms of this series would require successive differentiations with attendant noise problems. The rate of convergence of Eq. (4.43) is furthermore relatively slow, particularly for large values of τ or high frequencies.

A more practical approach to the generation of the time-delay function is to employ the so-called Padé approximation as described by Teasdale[14] and Morrill.[15] In this method, the exponential is approximated as the ratio of two polynomials in s, according to

$$\epsilon^{-s\tau} = \frac{P_n(s)}{Q_m(s)} \qquad (4.44)$$

where the subscripts m and n refer to the highest power of s in the numerator and denominator, respectively. For $n = m = 2$

$$\epsilon^{-s\tau} \cong \frac{a_0 + a_1 s + a_2 s^2}{b_0 + b_1 s + b_2 s^2} \qquad (4.45)$$

The coefficients are then selected so as to make the series expansion equation (4.44) approximate the Taylor series expansion equation (4.43). The higher the powers of the numerator and denominator, the more terms of the series can be matched and the smaller the error in the time-

delay function. For the case of Eq. (4.45), $a_0 = b_0 = 1$, $b_1 = -a_1 = \frac{1}{2}$, and $a_2 = b_2 = \frac{1}{12}$. Either the required transfer function can be realized by means of two integrators and two adders, or the complex transfer-function networks described in Sec. 2.13 can be employed. In the latter case, only two operational amplifiers are necessary.

Higher-order Padé approximations provide improved accuracy and frequency response. A circuit for generating time delays of 0.2 to over 30 sec is shown in Fig. 4.39. The circuit generates the function

$$\frac{e_o}{e_1} = \frac{1{,}680 + 840s\tau + 180s^2\tau^2 + 20s^3\tau^3 + s^4\tau^4}{1{,}680 - 840s\tau + 180s^2\tau^2 - 20s^3\tau^3 + s^4\tau^4} \approx \epsilon^{-s\tau} \quad (4.46)$$

The time delay τ in seconds is determined by the magnitudes of the input resistors to the four integrators. Such a circuit works well only in a
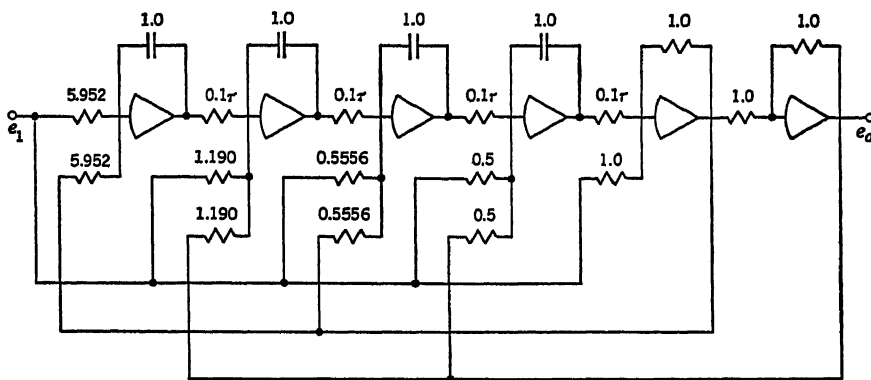
Fig. 4.39

limited frequency range (direct-current to approximately 50 cps). Instability results if the variation of the input signal e_1 is too rapid. It is therefore not feasible to apply a step function to this circuit. In case e_1 is not equal to zero at the commencement of the computer run, it is necessary to apply appropriate initial conditions to the integrators.

The time-delay devices described thus far are limited to applications in which the delay time τ remains constant throughout the computer run. More elaborate equipment is necessary if τ is a function of time or of voltage. Kozak[16] describes an analog memory based on the capacitor-storage method, which can be employed for this purpose. A string of capacitors are charged to discrete voltage levels, and these voltages are read off at some time interval later. The capacitors are mounted radially on a rotating disk, and commutators, mounted along the periphery of the disk, contact recording and reading heads; the position of these heads is controlled by a servo unit. The delay time is then a function of the angular velocity of the disk and the angular displacement of the heads.

4.12. Random Noise Generators.   To analyze the behavior of non-linear dynamic systems in the presence of noise, it is necessary to employ special electronic units for which the magnitude of the output voltage is a random function of time.   The construction and application of such random noise generators are described in some detail by Low.[17]   As primary sources of noise, most analog-computer units utilize either radioactive samples in combination with Geiger-Müller tubes or gas-discharge tubes.

The block diagram of a radioactive-type generator is shown in Fig. 4.40. Gamma and beta radiations are emitted by the radioactive sample and pass through the Geiger-Müller tube.   These particles effect a discharge
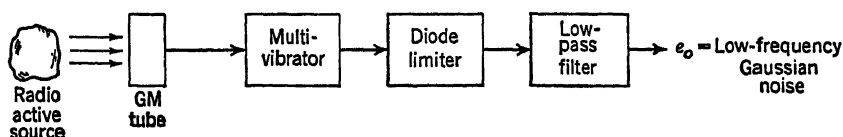
Fig. 4.40

in the Geiger-Müller tube, thereby triggering a voltage pulse at the tube output.   It can be shown that the pulse sequence is random in nature and characterized by a Poisson probability distribution.   The voltage pulse output of the Geiger-Müller tube is employed to trigger a bistable multivibrator circuit.   The output of this multivibrator provides equal positive and negative voltage signals.   This signal is then passed through a low-pass filter, the output of which has an amplitude probability density distribution which is approximately gaussian.   The power spectral density of the output is essentially uniform, from zero frequency to several hundred cycles per second.

Noise is generated in a thyratron-type gas tube by fluctuations in the density of the layer of positive ions around the cathode.   The noise is characterized by a normal-probability density distribution, with resonance peaks due to the natural oscillation frequencies of the ions.   Frequency-shifting techniques are employed to extend the probability distribution into the low-frequency range.   The noise spectrum of commercial thyratrons extends from 30 cps to approximately 3 kc.   If so-called sampling or demodulation techniques are employed, output spectra which are exceedingly uniform from zero to 50 cps can be obtained.

REFERENCES

1. Bekey, G. A.: "Preparing Problems for Solution on an Analog Computer," Beckman Instruments, Inc., Berkeley Division, Richmond, Calif., January, 1957.
2. Bekey, G. A.: "Generation of Analytic Functions on the Analog Computer," Beckman Instruments, Inc., Berkeley Division, Richmond, Calif., January, 1958.

3. Richmond, W. F.: "REAC Techniques," Project Cyclone Symposium I, Reeves Instrument Corp., New York, March, 1951.
4. Greenwood, I. A., Jr., J. V. Holdam Jr., and D. MacRae, Jr.: "Electronic Instruments," McGraw-Hill Book Company, Inc., New York, 1948.
5. Hofstadter, R.: A Simple Potentiometer Circuit for Production of the Tangent Function, *Rev. Sci. Instr.*, **17**:298–300 (1948).
6. "Arma Electrical Resolvers," Bulletin of the Arma Corporation, Brooklyn.
7. Howe, R. M., and E. G. Gilbert: Trigonometric Resolution in Analog Computers by Means of Multipliers, *IRE Trans. on Electronic Computers*, **6**:86–92 (1957).
8. Hibbard L. U., and J. H. Piddington: A Precision Exponential Potentiometer, *J. Sci. Instr.*, **24**:92–94 (1947).
9. Korn, G. A.: Design and Construction of Universal Function-generating Potentiometers, *Rev. Sci. Instr.*, **21**:77–81 (1950).
10. Reeves Catalog on Electronic Analog Computer and Associated Equipment, RICO-2, Reeves Instrument Corp., New York.
11. Schultz, H. W., J. F. Calvert, and E. L. Buell: The Photoformer in Anacom Calculations, *Proc. Natl. Electronics Conf.*, **5**:40–47 (1949).
12. Stanley, P. E.: "The Generation of Functions for Analog Computing," AIEE Conference Paper 57–661, June, 1957.
13. Elliott, D. A.: Representation of Nonlinear Function of Two Input Variables on Analog Equipment, *Trans. ASME*, **79**:489–495 (1957).
14. Teasdale, R. D.: Time Domain Approximation by Use of Padé Approximants, *IRE Convention Record*, pt. V, pp. 89–94, 1953.
15. Morrill, C. D.: A Sub-audio Time Delay Circuit, *IRE Trans. on Electronic Computers*, **3**:45–49 (1954).
16. Kozak, W. S.: "An Analogue Memory," paper presented at Western Electronic Show and Convention, Los Angeles, 1958.
17. Low, H.: Noise and Statistical Techniques, chap. 26 in "Handbook of Automation, Computation and Control," vol. 2, John Wiley & Sons, Inc., New York, 1959.

5

MECHANICAL COMPUTING ELEMENTS

The indirect computing elements described in the preceding three chapters generate the desired mathematical functions as electrical voltages. In this chapter, computing elements are considered in which the dependent variable is represented by translational or rotational mechanical displacements. Such units are fashioned from shafts, gears, disks, etc. They have the advantages over electrical elements of ruggedness, simplicity, and dependability. They have, however, the disadvantages of greater weight and bulk, lack of flexibility, and difficulty in assembly. These disadvantages outweigh the advantages to such an extent that mechanical computing elements are very rarely used in general-purpose analog computations. There are, however, many special-purpose applications, particularly where reliability and the ability to operate under unfavorable environmental conditions are paramount, in which mechanical elements continue to play an important part.

5.1. Mechanical Addition and Subtraction. The variables to be added and their sum usually appear as translations of specified points in a mechanical adder, as angular displacements of its links, or as turns of its shafts. Two common forms of adders are the differential and the tape devices. Variations of the differential adder are shown in Fig. 5.1. Two forms of linkage differential appear in (*a*) and (*b*). An adder comprising a pair of sliding racks in contact with a common pinion appears in (*c*). The zero positions in each case are shown by dotted lines; the displaced positions by full lines. Two forms of gear differential are shown, the bevel gear (*d*) and the spur gear (*e*).

The tape adder is illustrated in Fig. 5.2. It consists of a series of movable and fixed pulleys with a continuous inextensible chain, wire, or tape threaded through them. Assuming the tape to be kept taut at all times, any vertical displacements of the movable pulleys result in a double displacement of the free end of the tape.

For adding n variables, $n\text{-}1$ differentials of Fig. 5.1 would be cascaded

$$z \approx \frac{x+y}{2}$$

(a)

$$z \approx x+y$$

(b)

$$z = \frac{x+y}{2}$$

(c)

$$z = \frac{x+y}{2}$$

(d)

$$z = \frac{x+y}{2}$$

(e)
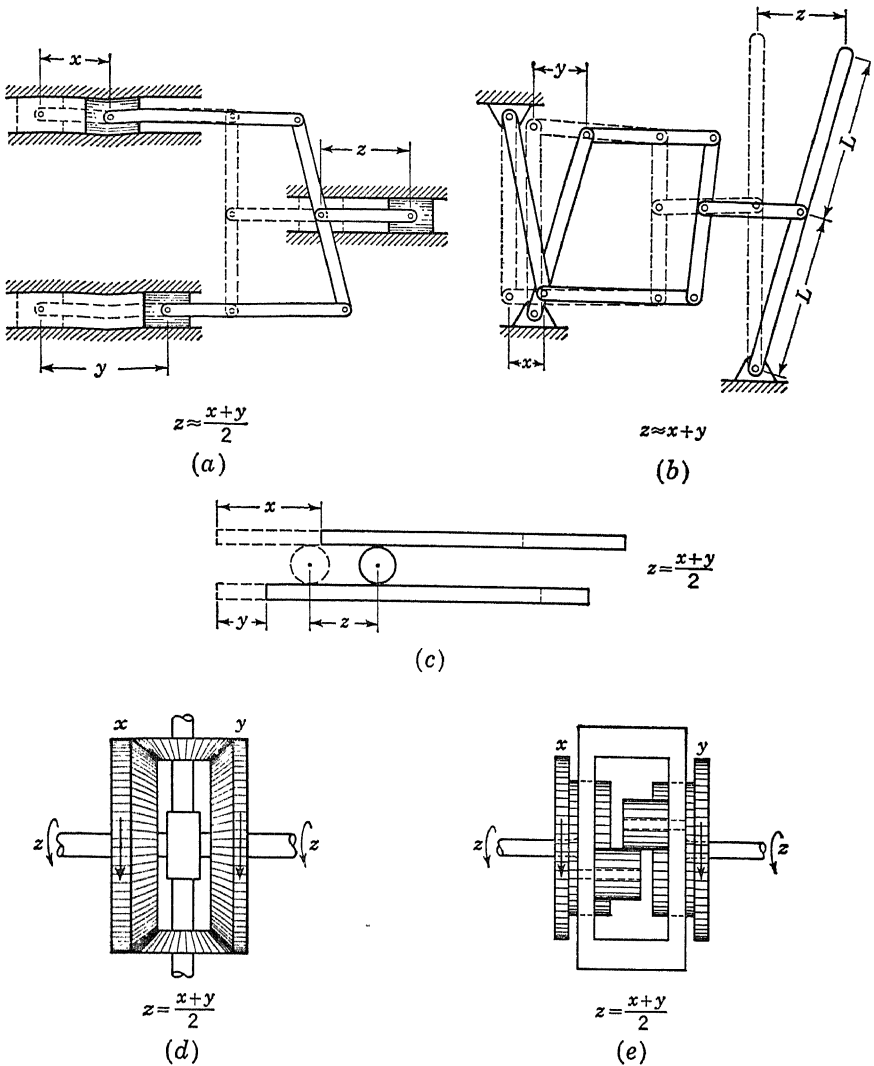
Fig. 5.1

or the tape of Fig. 5.2 would be threaded through n movable and n fixed pulleys.

Subtraction is accomplished simply by reversing the direction of the input having the negative sign.

5.2. Scale Factors. It should be noted that in most cases the direct sum $x + y$ is not obtained but that a scale factor is involved. Thus, adders (a), (c), (d), and (e) have output scale factors of $\frac{1}{2}$, while adder

(*b*) has an output scale factor of unity due to doubling the length of the output link. The adder of Fig. 5.2 has an output scale factor of 2.

In the illustrations all adder inputs were considered to come into the adders with unity scale factors. This is not likely to be the case in most computer applications, where the outputs of other computing elements are used as inputs to adders. In fact, a usual arrangement of computer elements involves the cascading of adders; *i.e.*, the output of an adder is used as the input to another adder. Thus, an adder output at a scale factor of $\frac{1}{2}$ enters directly as an input to another adder. If the other input to the second adder is also at a scale factor of $\frac{1}{2}$, then the second output has a scale factor of $\frac{1}{4}$. If the other input had a scale factor different from $\frac{1}{2}$, then the scale factor of the output would be variable and unknown. This is clear from the following relations
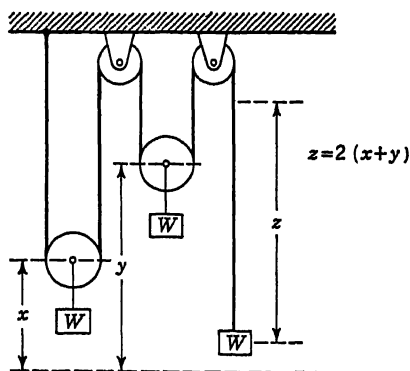
$z = 2(x+y)$

Fig. 5.2

involving two input scale factors S_1 and S_2 and an output scale factor S_3. Thus

$$\tfrac{1}{2}S_1 x + \tfrac{1}{2}S_2 y = S_3(x + y) \tag{5.1}$$

or

$$S_3 = \frac{S_1 x + S_2 y}{2(x + y)} \tag{5.2}$$

Only when $S_1 = S_2$ is it possible to specify S_3 independently of the actual values of x and y. This demonstrates an important rule: namely, both inputs to an adder must have the same scale factor.

5.3. Accuracy. In mechanical computing elements the mechanization of a mathematical relation is subject to the following sources of inaccuracy:

1. Kinematical errors—a result of the inherent approximations of the mechanization. Errors due to this source can be altered only by changes in the geometry of the mechanism. Sometimes such errors are called "theoretical" errors.

2. Fabrication errors—a result of the need for manufacturing tolerances and for clearances to permit proper operation of parts.

3. Slip errors—present to some degree where friction drives are involved, as in integrating units or in belt-connected units.

Referring to the linkage adders of Fig. 5.1, it is clear that the variables x and y cause the links to tilt and so to vary the geometry of the kinematical chain. The resultant effect is that the addition function is not mechanized exactly, and the amount of error introduced increases with

the extent of the tilt. The amount of allowable movement of, say, the y slider relative to the x slider in (a) is determined from the theoretical standpoint by the amount of error which can be tolerated in the output z. Figure 5.3 shows the amount of error ϵ occurring in z as a result of a tilt angle β.

$$\epsilon = L(1 - \cos \beta) \qquad (5.3)$$

The magnitude of β depends on L, a, and γ. In turn, γ depends on the difference of the variables $y - x$. These relations are

$$\sin \beta = \frac{a}{L} (1 - \cos \gamma) \qquad (5.4)$$

$$\sin \gamma = \frac{y - x}{2a} \qquad (5.5)$$

Assuming a required range for the difference $y - x$ (or $x - y$), the angle γ may be reduced by making a as large as may be allowed. This, in turn, reduces the angle β, which may be reduced again by making L large. This is evident from the following

(a)

(b)

Fig. 5.3

approximate analysis. For small angles, letting R be the maximum value of $y - x$,

$$\sin \gamma \approx \gamma \approx \frac{R}{2a} \qquad (5.6)$$

$$\cos \gamma = \sqrt{1 - \sin^2 \gamma} \approx \sqrt{1 - \frac{R^2}{4a^2}} \approx 1 - \frac{R^2}{8a^2} \qquad (5.7)$$

$$\sin \beta \approx \frac{a}{L} \left(1 - 1 + \frac{R^2}{8a^2} \right) = \frac{R^2}{8aL} \qquad (5.8)$$

$$\cos \beta = \sqrt{1 - \sin^2 \beta} \approx \sqrt{1 - \frac{R^4}{64a^2L^2}} \approx 1 - \frac{R^4}{128a^2L^2} \qquad (5.9)$$

$$\epsilon \approx L \left(1 - 1 + \frac{R^4}{128a^2L^2} \right) = \frac{R^4}{128a^2L} \qquad (5.10)$$

By slotting the ends of the connecting link AA (Fig. 5.3b), β may be kept at zero and this source of error avoided.

Fabrication tolerances are costly to control to very close limits. Hence, it is not economical to build a computer of greater precision than that actually required in the problem solution. However, in a complex computer consisting of many elements, each element should have greater precision than the over-all requirement in order to counteract possible accumulation of errors.
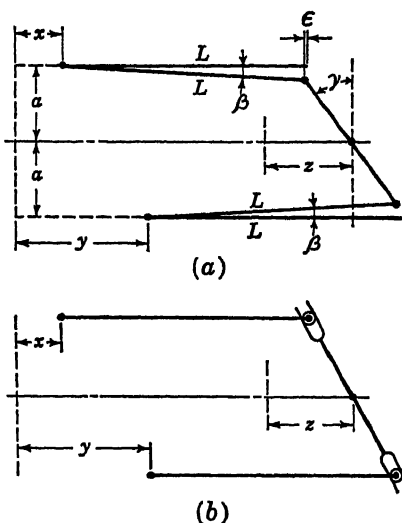
The adders shown in Fig. 5.1c, d, and e and Fig. 5.2 have no kinematical error. Fabrication errors are present, but for the fully rotational systems (d) and (e) their effects may be made arbitrarily small by setting sufficiently large scale factors. Precision is at a premium when an important result in a problem is a small difference of two large numbers.

5.4. Choice of a Mechanical Adder. In deciding on the type of adder to use in a computer, cost, precision, compactnesss, and ranges of variables are important considerations. With linear displacement devices and linkage elements, the amount of movement possible is limited by the allowable space in the computer. A further limitation may be imposed in the case of the linkage elements by the growth of inaccuracy as relative displacements distort the geometry of the mechanism.

However, simplicity, economy, ruggedness, and ability to transmit substantial forces make the linkage computers highly desirable for special purposes.

In computing devices where relatively unlimited displacement and high precision are necessary, the gear differentials provide the best solution to the problem.

5.5. Mechanical Integration. Integration makes possible the mechanical solution of differential equations and the generation of many mathematical functions. It is one of the most important operations in the computing machine field and is a difficult one to perform accurately.

Fig. 5.4

Figure 5.4 shows schematically a disk-and-wheel integrator. The turns of the disk (frequently called "turntable") represent the differential variable x to a suitable scale factor. The distance of the wheel centerplane from the axis of the turntable represents the integrand y, again to some suitable scale factor. These are the two inputs to the integrator.

The turns of the integrating wheel represent the value z of the integral to a scale factor predetermined by the two input scale factors and the actual structural details of the unit. This is the output of the integrator.

A rotation of the disk through an infinitesimal fraction of a turn dx causes the wheel to turn through a correspondingly small part of a turn dz. For a wheel of radius a,

$$dz = \frac{1}{a} y \, dx \tag{5.11}$$

During a finite time interval, the x turntable will turn through a finite number of revolutions, and the distance y will vary, ranging through
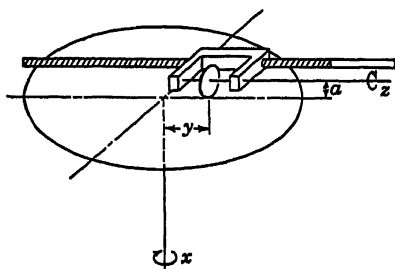
positive (on one side of center) and negative (on the other side of center) values as called for by the problem. The total number of turns registered by the integrating wheel will then be

$$z = \frac{1}{a} \int_{x_0}^{x} y \, dx \qquad (5.12)$$

where x_0 is the initial value of x.

Adequate operation of the integrator requires that the wheel should roll without excessive slip in its plane, that it should slide laterally across the turntable with a minimum of friction, and that its position y should be determinate to the required degree of precision. These conditions are contradictory in some respects, and hence a compromise must be reached.

To locate the plane of the wheel accurately, the rim of the wheel should be as sharp as practicable. This has been accomplished on some differential analyzers by crowning the rim with a radius of 0.002 in.,[1] $\frac{1}{32}$ in.,[2] or by using a 60° rim with its sharp edge ground to a 0.002-in. width.[3] To minimize both wear and resistance to axial displacement of the wheel, hardened steel is used for the wheel rim and either polished hardened steel or polished plate glass for the turntable. The result is a friction drive of very low torque-transmission characteristics, barely sufficient to accelerate and decelerate the integrating wheel. In the MIT differential analyzer,[3] a torque of about 0.07 oz-in. was available at the wheel. Clearly, it would be impossible to drive the other elements of the computing machine without the help of torque amplifiers. Thus, despite the fact that the disk-and-wheel integrator may date back to 1814[4] and that its application to the solution of differential equations was proposed by Thomson[5,6] in two papers in 1876, a successful computer of this type was not built until the development of torque amplifiers[1] in the middle 1920s. These and other forms of torque-amplifying systems are discussed in Sec. 5.29.

The torque amplifier is a one-way device. It enables the integrating wheel to drive a system of shafts and gears absorbing considerable power, with negligible torque reaction on the wheel. The wheel cannot drive the turntable ("inverse integration") except where special provision is made for it (as in the new MIT differential analyzer[3]). The special problem associated with inverse integration is the fact that the wheel and turntable must have the same surface speeds at their point of contact, but the relative rotational speeds of the two may vary arbitrarily from a positive maximum through zero to a negative maximum. The usual servo couples shafts having equal rotational speeds.

However, the equivalent of inverse integration may be obtained with a standard integrator by means of the regenerative connections described

in Sec. 5.21 (see discussion by D. Lebell on page 1370 of Ref. 14).   The inverse of the integration process, by definition, mechanizes Eq. (5.11) in the form $dx = dz/y$ (letting $a = 1$).   This relationship is obtained from Fig. 5.23 if the symbols x and z are interchanged, y taken negative, and unit offset applied to the integrand, as described by Eq. (5.52).

5.6. The Ball-Disk Integrator.   The disadvantage entailed in sliding an integrating wheel axially impressed Maxwell, who saw Sang's planimeter[7] at an exhibition in 1851.   To obtain pure rolling in all directions, Maxwell developed and described an arrangement making use of two equal spheres.[8]   Professor James Thomson, seeking a simpler mechanism than Maxwell's for integrations concerned with wind motions, developed
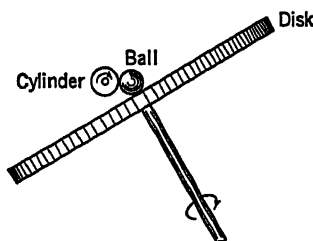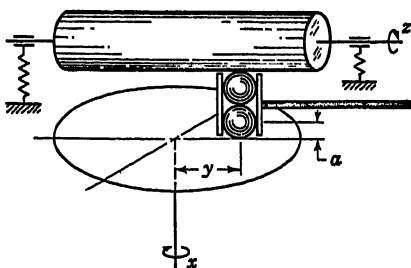
Fig. 5.5   Fig. 5.6

a tilted-disk and rolling-ball integrator,[9] where a loose ball is held by gravity between a disk or cone and a cylinder to which it transmits the rotation of the disk or cone (Fig. 5.5).   The ball is able to roll along the cylinder so that different circumferential elements of the disk (or cone), moving at different surface speeds, become coupled to the cylinder. Professor Thomson suggested that the ball could be positioned by a cage or by a stop if the assembly were tilted sufficiently in a direction allowing the ball to roll downhill parallel to the axis of the cylinder.

A practical arrangement of the ball-disk integrator is shown schematically in Fig. 5.6.   Two hardened steel balls couple the turntable to the output shaft.   A carriage around the balls holds them in vertical alignment and serves to position them along the disk diameter.   Since sliding is replaced by rolling, considerable pressure may be applied to the balls without developing undue resistance to radial movement along the turntable.   Such pressure increases the torque-transmitting capacity of the integrator, thereby enabling drives in many instances without the use of torque amplifiers.   The cylinder may be mounted in ball bearings in a pivoted yoke which is spring loaded to apply the required pressure. Two balls must be used in order that rolling occur on both the cylinder and the turntable during radial movement of the ball carriage.

The design criteria for such an integrator are substantially those for

ball-bearing design with respect to surface finish, hardness, load, and friction. Accurate alignment of the balls and lapped surfaces or roller guides[10] in the ball cage are necessary to minimize lateral thrust and friction in it. Ball size does not affect the integrator output turns. The position of the point of contact between ball and disk is not determined with as great precision as that for the sharp-edged wheel and disk. However, the ruggedness of the ball-disk unit makes its use ideal for instruments and control systems for which extreme precision is not required.

5.7. Integrator Scale Factors. In the integrators described, the turntable input and the integrator output are shaft rotations. The integrand is represented by the position of the wheel (or ball) carriage relative to the center of the turntable. By using a screw to position the wheel, the turns of the screw are related to the wheel position and thus may be used to represent the integrand.

Suppose S_1 to be the scale factor on the turntable variable x, S_2 that on the lead-screw variable y, and S_3 that on the output variable.

If the lead screw has n threads/in., the radial position r of the integrating wheel is given by

$$r = \frac{S_2 y}{n} \tag{5.13}$$

Substituting scale factors into Eq. (5.11),

$$S_3 \, dz = \frac{1}{a} \frac{S_2 y}{n} S_1 \, dx \tag{5.14}$$

Since the actual variables of the problem are x, y, and z, it is desired to mechanize the relation

$$\int dz = \int y \, dx \tag{5.15}$$

A comparison of Eqs. (5.14) and (5.15) shows that when S_1 and S_2 are assigned values, S_3 cannot have an assigned value but is fixed through the relation

$$S_3 = \frac{S_1 S_2}{an} \tag{5.16}$$

It must be borne in mind that the numbers of turns made by each of the three shafts shown in Fig. 5.7 represent the relation (5.14). These are the actual turntable, lead-screw, and wheel shafts. If, for convenience, other shafts connected to these shafts were used to represent x, y, and z, the connections should be 1:1, or else the built-in gear ratio must be taken into account.

For example, suppose in Fig. 5.8 the shaft representing x were connected to the turntable shaft through right-angle gearing having the ratio

$k/1$. The actual turns of the turntable would then be S_1x/k. The relation mechanized would be

$$S_3 \, dz = \frac{1}{a} \frac{S_2 y}{n} \frac{S_1}{k} \, dx \qquad (5.17)$$

from which

$$S_3 = \frac{S_1 S_2}{ank} \qquad (5.18)$$

In one typical integrator, $a = 1$ in., $n = 16$ threads/in., $k = 1$, so that $S_3 = S_1 S_2/16$.

For an integrator lead screw having n threads/in. and a turntable having a usable radius of m in., the number of turns of the lead screw
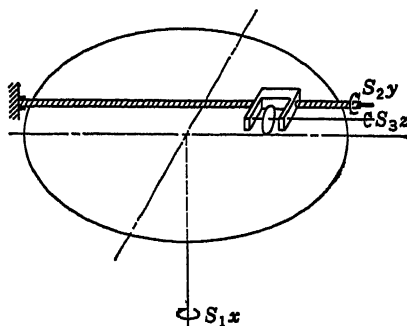
Fig. 5.7
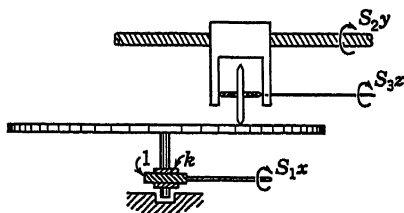
Fig. 5.8

from zero setting to maximum setting is mn. For a lead-screw variable (integrand) whose maximum value is A, the scale factor S_2 is restricted to the range of values

$$S_2 \lesseqgtr \frac{mn}{A} \qquad (5.19)$$

5.8. Multiplication by a Constant. The multiplication of a variable by a constant is accomplished with simple mechanical elements. In linkage computers the mechanical advantage of a lever arm serves to ratio a displacement up or down. Shaft rotations are stepped up or down with simple gear trains.

In a special-purpose machine, the constant multipliers are predetermined and may be built into the machine, rarely, if ever, requiring changing. In machines designed for more general purposes, frequent changes in the constant multiplier may be required. A convenient means for changing the multiplier is then desirable.

For linkage computers, a slide which can be clamped at different positions along a pivoted bar provides the simplest form of adjustment. The similar-triangles multiplier[11,12] shown in Fig. 5.9a may also be readily adjusted. In Fig. 5.9a the constant multiplier C is represented

by the offset of slotted member *de*. The variable x to be multiplied by C is represented by the displacement of a pin j in a fixed slot *mn*. A doubly slotted T bar *acf*, pivoted at b, is connected through pins g and j to these other slots. A is a fixed distance in the mechanism. Figure 5.9*b* shows the two resulting similar triangles. For any position C of the adjustable slide, and for any displacement x of the variable, the position z is determined from the relation

$$\frac{z}{C} = \frac{x}{A} \qquad \text{or} \qquad z = \frac{C}{A} x \qquad (5.20)$$

The number $1/A$ is a scale factor on the product Cx. Actually, multiplying by a constant simply means a scale factor change. Hence, C/A

(*a*)   (*b*)
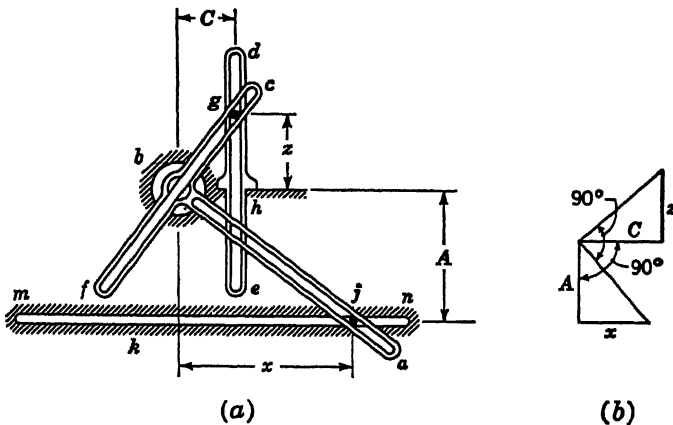
Fig. 5.9

might just as well be considered as the scale factor on x. Thus z and x might be represented by the same displacement, say z in Fig. 5.9*b*, but to different scale factors. Using the new scale factor, the constant multiplier is not needed. However, when two variables, each at a different scale factor, are to be added, the scale factors mut be equalized by means of a constant multiplier. The multiplier C may be positive or negative, depending on which side of pivot b the distance C is laid off.

In shaft computers, the coefficient C may be adjusted conveniently through a gearbox[13] arranged with gearshifts. A decade box is shown schematically in Fig. 5.10*a*. The gears are so arranged that the output shaft turns are a submultiple of input turns. This is done to avoid the high input torques accompanying speed stepups with consequent danger of slip in couplings or clutches and difficult operation. Scale-factor adjustments can usually be made so that no stepups in speed occur.

In Fig. 5.10*a*, the input shaft carries a cone of 8 gears having numbers

of teeth given by $10n$, $9n$, $8n$, . . . , $3n$, where n is some convenient integer. Two shift gears, having $10n$ and $4m$ teeth (m is another convenient integer), operate on a splined countershaft and serve to couple through idlers the input cone to output-cone gears having the teeth $4m$, $6m$, and $12m$. By appropriately shifting the countershaft gears, turns ratios of 0.1, 0.2, 0.3, . . . , 1.0 are obtainable at the output.

The purpose in employing two gear cones and a countershaft is to avoid a ratio greater than 4:1 between any pair of meshing gears. The maximum ratio on the first cone is seen to be $3\frac{1}{3}$, while that on the second cone is 3.
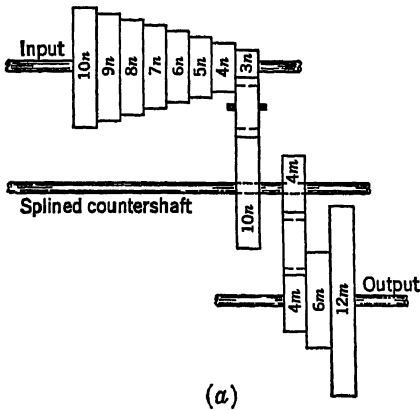
Another possibility is to stop the input cone at $4n$, replace the $4m$ gear on the countershaft with a $9m$ gear, and form the output cone to consist of the four gears $9m$, $12m$, $18m$, and $36m$.

An arrangement permitting a hundred steps from 0.01 to 1.0 is shown schematically in Fig. 5.10b. Two decade boxes of the type in (a) are coupled through a 10:1 reducer gear and a differential. In (b), only the output shafts of the two decades are shown. If p and q are the settings of the two decade boxes, the output of the differential A would be $p + 0.1q$. The inputs of both decades are driven from a common input shaft.

(a)

(b)
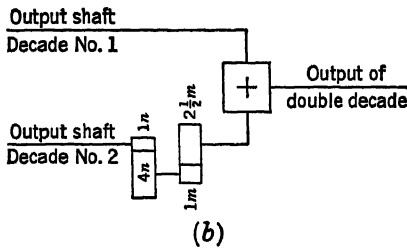
Fig. 5.10

Clearly, three decades and two differentials would yield one thousand steps from 0.0001 to 1.0, etc.

In a multidecade system, any decade not in use (*i.e.*, representing a zero) must be disconnected from the input shaft and locked against turning due to feedback through its differential.

Since an integrator is a variable-speed drive, it might also be used for an adjustable constant multiplier. Such use, in general, would not be warranted where servo-coupled integrators are involved because of their high cost and limited number.

5.9. Mechanical Multiplication of Variables. The ability of a computer to develop the product of two variables opens up to the computer the vast and analytically difficult field of nonlinear differential equation

solving. Various mechanical methods for performing this process are described below.

5.10. The Linkage Multiplier. The similar-triangles constant multiplier of Fig. 5.9 is suitable for the multiplication of variables, as well. The distance C, which was considered adjustable by the operator, may now be under the control of the variable y and represent y. As a result, the output z will be

$$z = \frac{1}{A}xy \qquad (5.21)$$

A variation of this multiplier for use on rotating-shaft computers (*e.g.*, the differential analyzer[14]) is shown in Fig. 5.11. A turntable
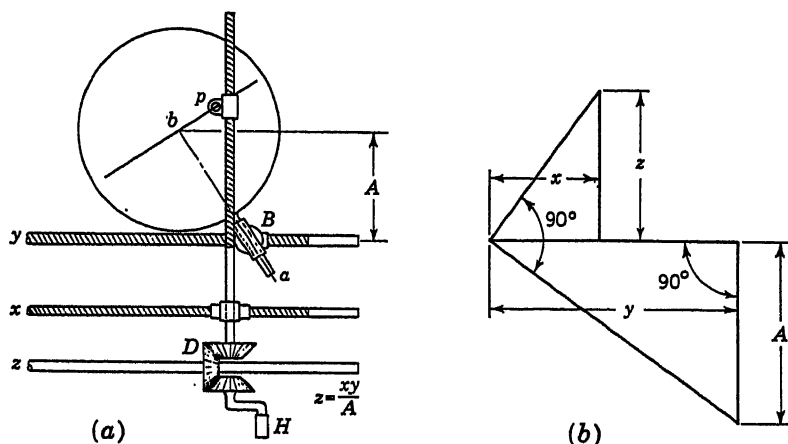
Fig. 5.11

b is inscribed with a diametral line and an arm a is rigidly attached to the turntable, perpendicular to the scribed line. The arm carries a sliding collar to which a nut is attached through a swivel (at B). The nut is moved by rotating the y lead screw. The x lead screw carries a nut to which a collar is rigidly attached at right angles. The z lead-screw shaft is supported in this collar and is thereby carried laterally as the x lead screw rotates. The z lead screw carries a nut with an attached peep sight p. The peep sight is maintained directly over the scribed line at all times, as the x and y screws rotate, by turning the hand crank H. The turns of H, proportional to the product xy, are transmitted to the horizontal z shaft through the right-angle drive D.

The input variables may have either positive or negative values and the product will correspondingly appear as negative or positive, according to the rules of multiplication. Positive or negative values are indicated by the direction of shaft rotation.

A disadvantage of the unit as set up in Fig. 5.11 is that an operator is required to keep the sight trained on the scribed line. However, a photoelectric follower[14] may be used to replace the operator.

5.11. Multiplication by Integration. The product of two variables may be obtained by mechanizing the equation

$$z = xy = \int_{y_0}^{y} x \, dy + \int_{x_0}^{x} y \, dx \tag{5.22}$$

The initial value of the product $x_0 y_0$ is taken into account either as an initial counter setting or as an initial lead-screw setting in the output train of the multiplier.

The mechanization of Eq. (5.22) is shown in Fig. 5.12. Conventional symbols are used to represent the integrators, the adder, and shafting. The shaft representing x is connected to the turntable drive (differential variable) of the left integrator and to the lead-screw drive (integrand) of the right integrator. The output shafts of the integrators (the integrals) are the middle shafts in each case. In order to emphasize the one-way character of the integrators, arrows are shown on the shafts indicating the directions in which the variables are transmitted.
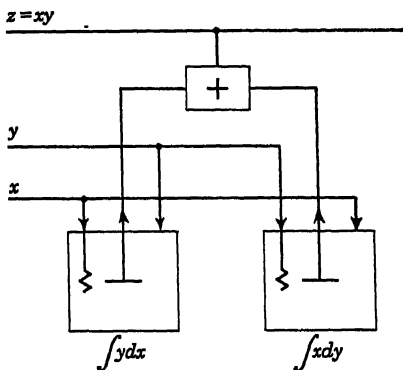
Fig. 5.12

Heavy dots at shaft intersections indicate that the intersecting shafts are connected together. Otherwise, the shafts merely cross without interconnection.

The statement previously made regarding equal scale factors on both inputs to the adder is reiterated here. The outputs from the two integrators will not, in general, have the same scale factor, but before they arrive at the adder inputs, a suitable gear train must be inserted in one or the other of the integrator output shafts to equalize scale factors. In accordance with the criterion adopted in Sec. 5.8, the larger scale factor is reduced to match the smaller one.

To illustrate the application of scale factors to this problem, suppose x and y to have maximum absolute values A and B, respectively. For integrators with lead screws having n threads/in. and allowing a maximum travel of m in. for the integrating wheel along the disk radius, the maximum permissible scale factors S_1 and S_2 for x and y, respectively, at

the lead screws, are [see Eq. (5.19)]

$$S_1 = \frac{mn}{A} \qquad S_2 = \frac{mn}{B} \tag{5.23}$$

The variables x and y are represented in the machine to some other scale factors, say, S_3 and S_4, respectively. Consequently, gear trains having the ratios S_1/S_3 and S_2/S_4 must be inserted in the connections between the x and y shafts and the corresponding integrators, respectively. This is illustrated in Fig. 5.13, in which a gear train is represented
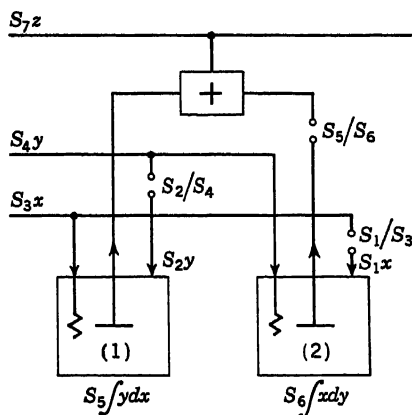
Fig. 5.13

by two open dots with the ratio of output to input turns written between the dots. Since there are no limits on the amount of rotation the turntables can take, no scale factor changes are necessary here.

The output scale factors on integrators 1 and 2 are, respectively [see Eq. (5.16)],

$$S_5 = \frac{S_2 S_3}{an} \qquad S_6 = \frac{S_1 S_4}{an} \tag{5.24}$$

Let us assume that S_6 is larger than S_5. Then S_6 must be reduced to S_5 by means of the gear train S_5/S_6 at the input to the adder. The output of each integrator is shown with its scale factor beneath the schematic representation of the integrator. With the conventional differential gear adder, $S_7 = \frac{1}{2} S_5$.

5.12. Integration of a Product. A slight alteration of the connections of Fig. 5.12 and the elimination of the adder yield a mechanization of the relation

$$x = \int xy \, dx = \int x \, d(\int y \, dx) \tag{5.25}$$

This is shown in Fig. 5.14a. The scale factors may be determined by the procedures described in the previous section.
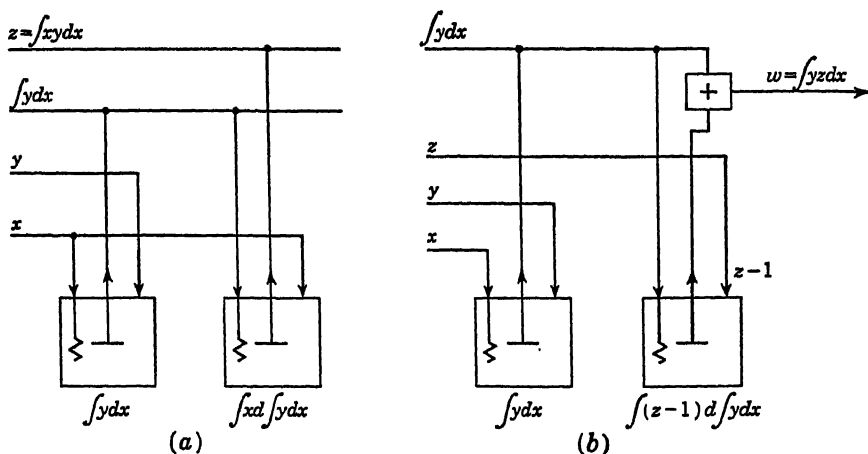
Fig. 5.14

Figure 5.14b shows another modification in which an adder is used and the following relation is mechanized:

$$w = \int yz\, dx \qquad (5.26)$$

5.13. Squaring and the Quarter-squares Multiplier.

A well-known method for obtaining the product of two variables is based on the algebraic relation

$$xy = \tfrac{1}{4}[(x + y)^2 - (x - y)^2] \qquad (5.27)$$
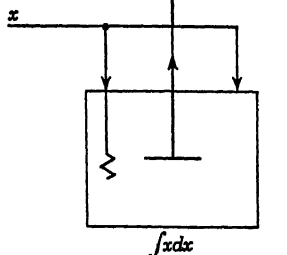
Equation (5.27) points out the fact that three adders are required to obtain the sum and difference of the variables and the difference of the squares. Also a means must be provided for squaring variables.

Since

$$x^2 = \int_0^x 2x\, dx \qquad (5.28)$$

Fig. 5.15

a single integrator suffices for squaring a variable. The connections are shown in Fig. 5.15. The factor 2 in Eq. (5.28) is taken into account in setting scale factors for the various shafts. Consequently, it is not necessary to show a special gear train with a step-up ratio of 2. In actual practice it would be undesirable to include such a stepup in any case.

Because of the connection between the lead screw and turntable of the same integrator, the integrating wheel traces on the turntable a particular

path whose equation in polar coordinates is given by

$$r = k\theta \tag{5.29}$$

where k is a constant determined by the construction of the integrator. This is an Archimedes spiral.

A unit designed solely for squaring a variable might have built into its turntable a special groove, track, or toothed path in order to constrain the integrating wheel to follow this particular path. If the path is laid out as a toothed spiral rack and the integrating wheel is a spur gear in mesh with the rack and guided to remain in mesh with it at all times,
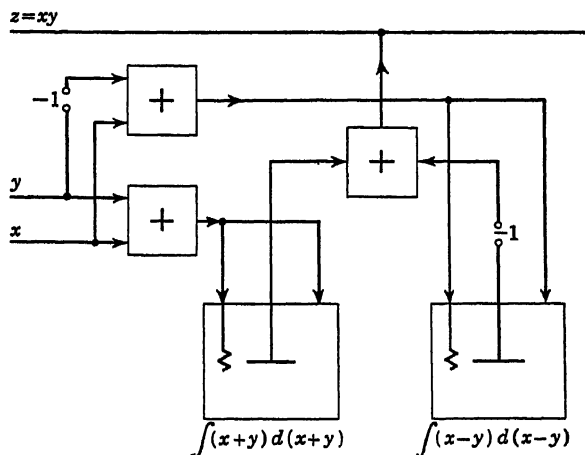
Fig. 5.16

the slippage problem is eliminated and a direct connection to other units can be used.

The mechanization of Eq. (5.27) is shown in Fig. 5.16. Scale factors are not shown but can be determined by the methods described earlier. A gear-cam multiplier based on this principle has been patented.[15]

The all-purpose integrator is capable of squaring negative as well as positive numbers. The gear-cam squaring unit, however, cannot handle directly numbers which change sign, since the spiral gear rack cannot be constructed for both positive and negative values of the variable. This situation is most conveniently handled by adding to $x + y$ and to $x - y$ a number sufficiently large to prevent either from going through zero.[11] If N is that number, the algebraic relation mechanized is

$$(x + y + N)^2 - (x - y + N)^2 = (x + y)^2 - (x - y)^2 + 4Ny$$
$$= 4xy + 4Ny \tag{5.30}$$

To produce the product xy from Eq. (5.30), Fig. 5.16 need be modified

only to the extent of inserting another differential gear to subtract off Ny.

The number N should be made large enough not only to prevent $x + y$ and $x - y$ from going through zero but also to prevent either one from getting close enough to zero to give interference between the wheel and the sharply curved rack.
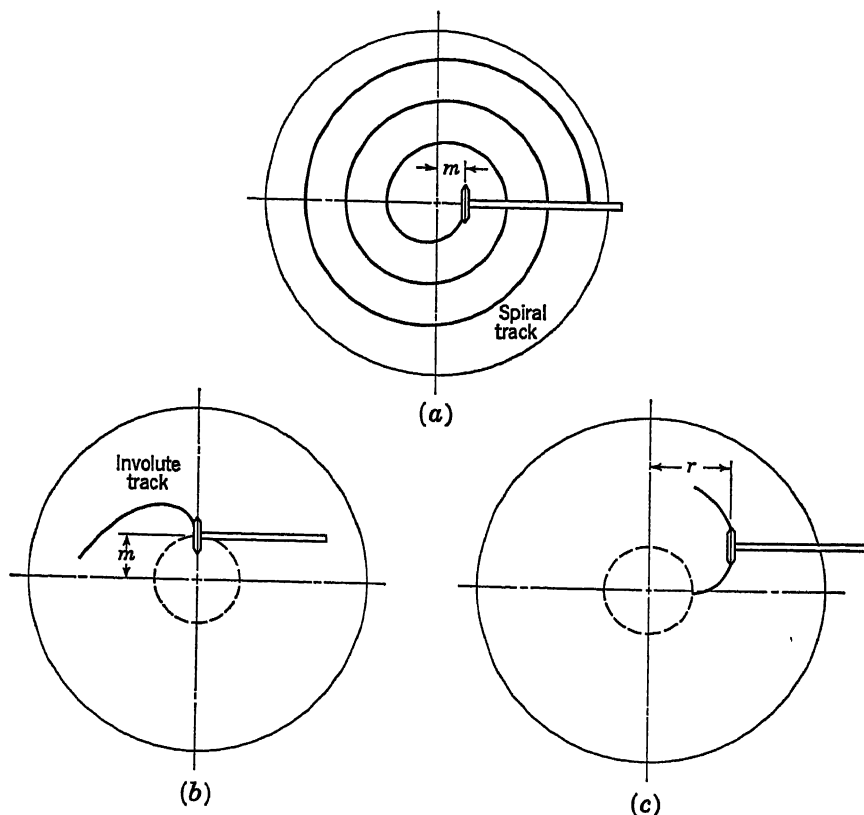
Fig. 5.17

Since the central portion of the gear cam would not be used under these circumstances, the spiral rack would begin at some initial offset m (Fig. 5.17a).

The variable to be squared might still go to (but not through) zero with no interference between wheel and rack if the integrating wheel shaft is offset[11] parallel to itself by a sufficient distance m (Fig. 5.17b). The axis of the wheel does not move radially along the disk, but along a parallel line m in. away. The spiral then becomes an involute curve starting on the periphery of a circle of radius m. The plane of the

integrating wheel always contains the tangent to the involute as the turntable rotates.

The wheel is shown in two positions in Fig. 5.17b and c. Since the involute is a curve developed by a taut string unwinding from the base
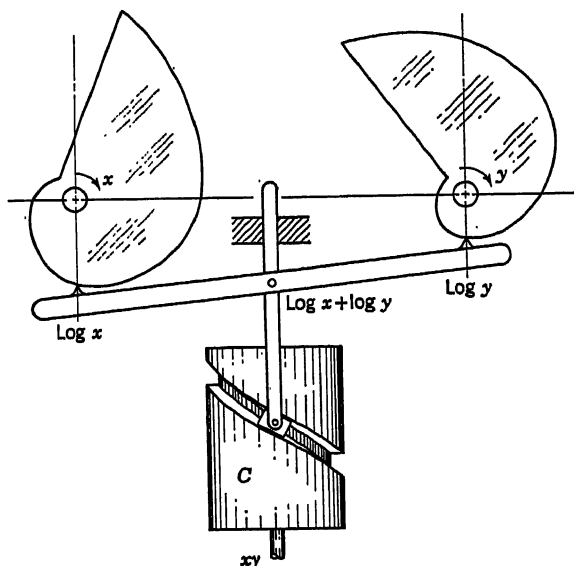
Fig. 5.18

circle, the distance r in (c) is proportional to the angular rotation x, the constant of proportionality being m. The total angular rotation of an integrating wheel of radius a is

$$z = \frac{1}{a} \int_0^x r \, dx = \frac{m}{a} \int_0^x x \, dx = \frac{m}{2a} x^2 \qquad (5.31)$$

The offset m thus enters as part of the scale factor on z.

5.14. Logarithm Generation and Logarithmic Multiplier. The logarithmic multiplier is based on the relation

$$\log xy = \log x + \log y \qquad (5.32)$$

Although logarithms of variables may be generated with integrators, as will be shown later, a more straightforward use of integrators in multiplication has already been described. A computer using Eq. (5.32) for multiplication is likely to be one employing cams for computing elements.

Figure 5.18 shows cams of radii proportional to the logarithms of the angles of rotation. The variables x and y enter as shaft rotations. The logarithms of x and y appear as translations of followers pressing

against the cam surfaces. The logarithms are summed in a linkage differential, whose output link moves in the antilog slot of a cylindrical cam C, thereby producing a rotation of C proportional to the product xy. Variations[12] of this arrangement to suit special purposes are possible.

While the similar-triangles multipliers permit variables to go through zero and have negative values, this is not possible with logarithmic multipliers. To permit the logarithmic multiplication of variables having values ranging through unity and below (including negative values), constants may be added to x and y to bring their minimum values into the desired range of positive values. If m and n are these constants, the cam radii would have lengths proportional to the logarithms of $x + m$ and $x + n$, respectively. The rotation of the cylindrical output cam would then be proportional to

$$(x + m)(y + n) = xy + mx + ny + mn \tag{5.33}$$

The product mn may be automatically subtracted from this result by offsetting the output scale. The x and y variables (which are shaft rotations) are transmitted through gear trains having ratios m and n, respectively, summed in a differential and the sum subtracted from the cylindrical-cam rotation.
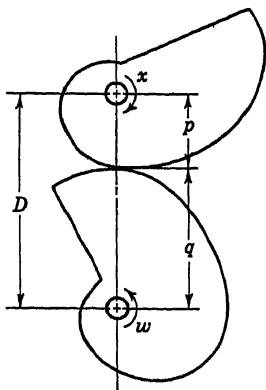
Fig. 5.19

5.15. Logarithm Generation Using Contour Cams. The cam followers in Fig. 5.18 slide on the cams and the action is not reversible. Pairs of contour[16] cams and noncircular gears[17,18] designed to roll on each other without sliding may be designed to generate functions such as the logarithm and may operate in reverse to develop the antilogarithm. A pair of such cams is illustrated in Fig. 5.19.

For two surfaces rotating about fixed centers to roll on each other without sliding, the point of contact of the surfaces must be in line with the centers of rotation and both surfaces must roll on each other through identical distances (*i.e.*, identical velocities both in magnitude and direction exist on both surfaces at the point of contact).

In Fig. 5.19, the instantaneous radii at the point of contact are p and q, the fixed distance between centers being D. If the x cam turns through an elementary angle of dx radians and the w cam through a corresponding angle of dw radians, the point of contact on each cam surface will have moved through the distances $p \, dx$ and $q \, dw$. For a condition of no slip,

$$p \, dx = q \, dw \tag{5.34}$$

Also,
$$p + q = D \tag{5.35}$$

Consequently, the cam profiles must be such that

$$p = \frac{D(dw/dx)}{1 + (dw/dx)} = \frac{D}{1 + (dx/dw)} \tag{5.36}$$

$$q = \frac{D}{1 + (dw/dx)} \tag{5.37}$$

To generate the common log of x,

$$w = \frac{1}{2.303} \ln x \tag{5.38}$$

$$\frac{dw}{dx} = \frac{1}{2.303x} \qquad \frac{dx}{dw} = 2.303x \tag{5.39}$$

$$p = \frac{D}{1 + 2.303x} \qquad q = \frac{2.303xD}{1 + 2.303x} \tag{5.40}$$

Two pairs of cams designed in accordance with Eq. (5.40) can be used to develop log x and log y as shaft rotations. The rotations can be added in a differential gear, and the output of the differential used to drive a third pair of cams of the same sort in reverse to produce the antilogarithm.

Since pure rolling is involved, gear teeth can be cut into the cam faces, the pitch line of the gear teeth being determined by Eqs. (5.40). Much greater torques may be transmitted without danger of slip.

A detailed discussion of cams as computing mechanisms is presented in Sec. 5.30.

5.16. Squaring Mechanisms. Contour cams or noncircular gears may be used to generate the square of a variable. Operated in reverse, the square root is produced. The cam surfaces are determined from the relations

$$w = kx^2 \tag{5.41}$$

$$\frac{dw}{dx} = 2kx \qquad \frac{dx}{dw} = \frac{1}{2kx} \tag{5.42}$$

$$p = \frac{2kxD}{1 + 2kx} \qquad q = \frac{D}{1 + 2kx} \tag{5.43}$$

Contour cams having the shape given by Eq. (5.43) may be used in a quarter-squares multiplier requiring two sets of cams and three adders instead of the three sets of cams and one adder required by the logarithmic multiplier.

A cone and cylinder may be coupled together so that the number of turns of the cylinder is proportional to the square of the number of turns of the cone. Two forms of the cone squaring unit are shown in Fig. 5.20. In (a), an idler is moved axially between the cone and cylinder through a distance proportional to x (that is, proportional to the turns of the cone). If r is the radius of the cone at the point of contact with the idler and

R the radius of the cylinder, a slight rotation dx of the cone produces the rotation

$$dw = \frac{r}{R} \, dx \qquad (5.44)$$

of the cylinder. By means of tracks on the cylinder and cone, or by some other interconnection, the idler position is determined by the relation

$$r = kx \qquad (5.45)$$

Fig. 5.20a

where k is a constant determined by the cone vertex angle and by the amount of advance of the idler per unit of x. Thus

$$dw = \frac{k}{R} x \, dx \qquad w = \frac{k}{2R} x^2 \qquad (5.46)$$
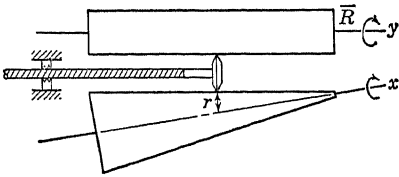
In (b), two flexible wires couple the cone to the cylinder. Grooves cut in the cone and cylinder guide the wires. Two wires are necessary to permit rotation in either direction. While one wire winds up on the drum, the other wire unwinds.
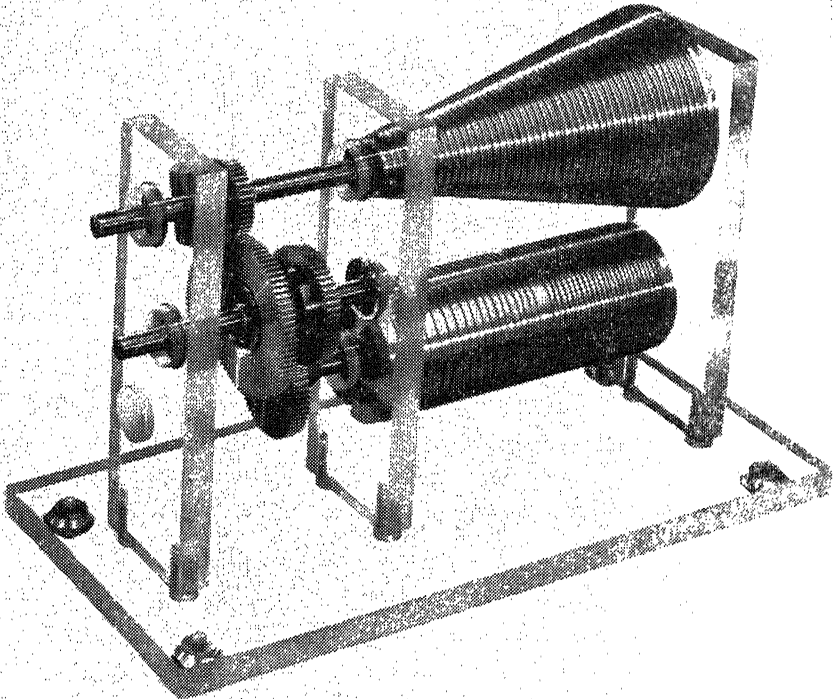
Fig. 5.20b. (Courtesy of Libra scope Inc., Glendale, Calif.)

Neither unit is able to approach zero in r (or x), so that for a variable whose value is likely to approach zero or go negative, a large enough constant should be added to it to keep it within range of the squaring unit. Provision must then be made to subtract the excess value in the square.

The cone squaring units may be operated in reverse and thus produce the square root of a variable.

5.17. Mechanical Division. The process of division is the inverse of that of multiplication. Some of the devices used for multiplication can also be used for division by interchanging the output mechanism with one of the inputs. This may be done, for example, with the similar-triangles multiplier. In the case of the logarithmic multipliers, the only change necessary is to subtract the logarithms of the variables instead of adding them.

An important difference between multiplication and division is the fact that in the former process either or both variables may go to zero without difficulty, whereas in the latter process a divisor approaching zero results in large displacements, undesirably high loads, and the danger of binding.

5.18. Division by Servo-driven Multiplier.[11] In Fig. 5.21 the dividend x enters one side of a mechanical adder. The divisor y enters a
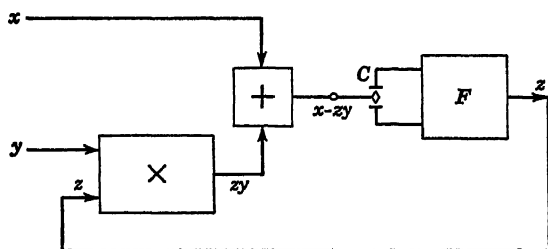
Fig. 5.21

mechanical multiplier where the product zy is developed. zy is subtracted from x in the adder, the difference causing electrical contacts C to close on one side or the other, thereby operating the motor F in one direction or the other in order to keep the adder output at zero. The turning of the motor provides the variable z. The following relation is mechanized thereby:

$$x - zy = 0 \qquad \text{or} \qquad z = \frac{x}{y} \qquad (5.47)$$

5.19. Division by Reciprocal Multiplication. If the divisor can first be converted to its reciprocal form, the methods of multiplication already described may then be used to multiply the reciprocal into the dividend, thereby producing the quotient.

One method of developing the reciprocal is to use a plate cam of appropriate contour. The contour cams or noncircular gears described in Sec. 5.15 cannot be used conveniently because the design criteria in this case call for one radius to be negative when the other is positive.

5.20. Reciprocal and Logarithm Generated by Integration. The reciprocal of a variable can be generated by means of two integrators. In this process, either the logarithm of the variable or the square of the reciprocal is also generated simultaneously. The schematic diagrams are shown in Fig. 5.22a and b.

A general procedure for mechanizing a given function by means of integrators consists in differentiating the given function a sufficient
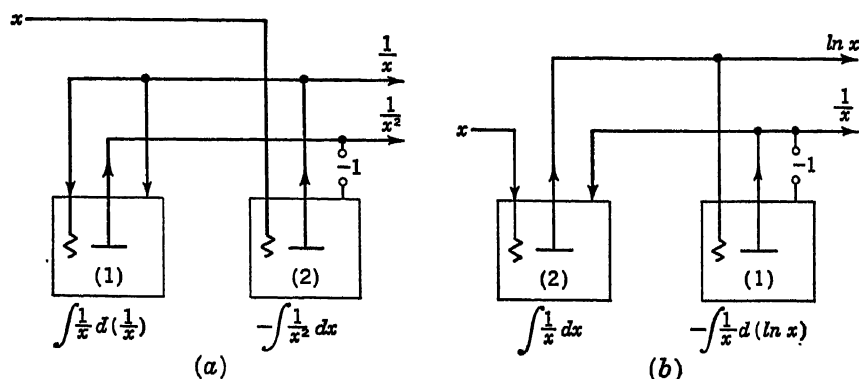
Fig. 5.22

number of times to provide one or more differential relations which might be set up on integrators. This procedure is illustrated here for the reciprocal:

$$d\left(\frac{1}{x}\right) = -\frac{1}{x^2}\,dx = -\frac{1}{x}\frac{dx}{x} = -\frac{1}{x}\,d(\ln x) \qquad (5.48)$$

$$d\left(\frac{1}{x}\right)^2 = \frac{2}{x}\,d\left(\frac{1}{x}\right) \qquad (5.49)$$

Beginning with the known fact that there is a shaft in the machine which represents the variable x, this shaft is to be connected into a system of integrators mechanizing the relations (5.48) and (5.49) to produce $1/x$.

From the first two terms in Eq. (5.48) it seems clear that if $1/x^2$ were available in the machine, an integration would produce $1/x$. Equation (5.49) shows that if $1/x$ were available in the machine an integration would produce $1/x^2$. Actually, the results of each integration may be used simultaneously in the other integration, so that both $1/x$ and $1/x^2$ are simultaneously produced. The schematic diagram for this case is shown in Fig. 5.22a. The factor 2 in Eq. (5.49) is absorbed in the scale factors.

From the first and last terms in Eq. (5.48) it appears that to produce $1/x$ in the machine it must be used as soon as it is produced. In order to make proper use of $1/x$ in the manner indicated, ln x must also be available in the machine. From the third and fourth terms in Eq. (5.48) ln x could be produced if $1/x$ were available. Once again, the results of each integration can be used simultaneously to mechanize the other integration so that $1/x$ and ln x are produced together. The schematic diagram for this case is shown in Fig. 5.22b.

With $1/x$ available, two more integrators can be used to multiply it into y to produce y/x. Such a procedure, requiring four integrators, is not an efficient one unless the reciprocal is required for some other purpose. Division can be accomplished with two integrators, making use of regenerative integrators described in the next section.

5.21. The Regenerative Integrator. A variety of important mathematical processes involving division by one or more variables may be efficiently mechanized by causing the integrator output to contribute to the turntable rotation. The term "regenerative" is applied to such an integrator.[19,20] In Fig. 5.23 the output of the adder

$$z = \int (dx + y\,dz)$$

Fig. 5.23

is both the final result desired and the turntable drive as well. The two variables x and y, between which the integrator is to establish some mathematical relation, are brought into the adder and into the lead screw, respectively. Figure 5.23 mechanizes the differential relation
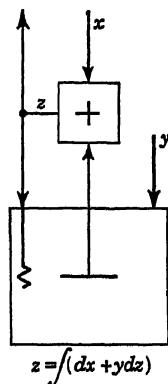
$$dz = dx + y\,dz \qquad dz = \frac{dx}{1-y} \qquad \text{or} \qquad z = \int \frac{dx}{1-y} \quad (5.50)$$

Equation (5.50) points out the danger of unstable operation when y approaches 1. A slight change in x tends to develop an extremely large change in dz and the integrator tends to "run away."

If scale factors S_1, S_2, and S_3 are used for x, y, and z, respectively, the relations between shaft turns become [see Eq. (5.16)]

$$S_3\,dz = S_1\,dx + \frac{S_2 S_3}{an}\,y\,dz$$
$$S_3\,dz = \frac{S_1\,dx}{1 - (S_2 y/an)} \qquad (5.51)$$

Appropriate gear trains must be inserted on one or the other of the adder inputs to make $S_1 = S_2 S_3/(an)$. Equation (5.51) shows that the position of instability of the integrating wheel is $S_2 y = an$ turns of the lead screw.

Looking again at Eq. (5.50), an initial offset of unity in the positive direction on the lead screw will result in

$$dz = dx + (1 + y)\, dz \qquad dz = -\frac{dx}{y} \qquad \text{or} \qquad z = -\int \frac{dx}{y} \quad (5.52)$$

This provides us with the integral of a quotient. The sign may be converted to plus merely by changing the sign of y, so that the lead screw takes the variable $1 - y$ instead of $1 + y$. In either case, the unit offset must be in the positive direction.

Using the scale factors S_1, S_2, and S_3 for x, y, and z, respectively, as before, and S_4 for the scale factor on the unit offset, Eq. (5.52) with scale
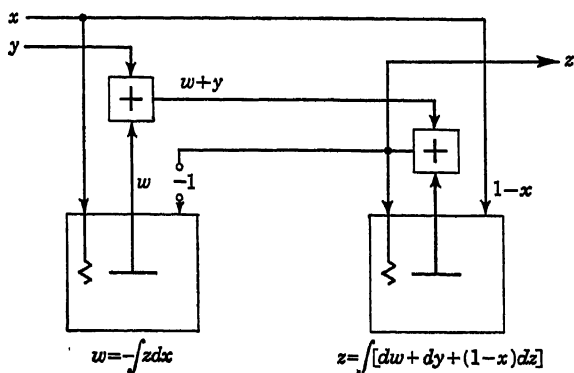
Fig. 5.24

factors included, will become

$$S_3\, dz = S_1\, dx + \frac{S_4 S_3}{an}\, dz + \frac{S_2 S_3}{an}\, y\, dz \qquad (5.53)$$

The condition for cancellation of the terms containing dz as the only variable means that $S_3 = S_4 S_3/an$, or $S_4 = an$. The scale factor S_4 is thus determined by the construction of the integrator and is independent of the scale factor S_2 on y.

To develop a quotient instead of its integral, the circuit of Fig. 5.24 may be used. The relations between the differential inputs and outputs of the integrators are

$$dw = -z\, dx$$
$$dz = dw + dy + (1 - x)\, dz$$

from which

$$dy = z\, dx + x\, dz$$
$$y = xz$$

or

$$z = \frac{y}{x} \qquad (5.54)$$

Other mathematical relations involving division by a variable can be mechanized, using two integrators in a regenerative hookup. Figure 5.25a, b, and c shows the mechanization, respectively, of the processes

$$w = \int \frac{y}{x}\, dz \qquad (5.55)$$

$$w = \frac{1}{x} \int y\, dx \qquad (5.56)$$

$$w = \int \frac{dz}{xy} \qquad (5.57)$$

5.22. Mechanical Differentiation with Respect to Time.

The differentiation of a displacement with respect to time forms the basis of many very common devices, such as speedometers and generators. In such systems the derivatives usually appear as deflections of spring-loaded members. For example, in Fig. 5.26 the viscous drag exerted on the stationary surface A by a concentric surface B through a thin intervening layer of viscous fluid is proportional to the velocity gradient through the layer of fluid, i.e., proportional to the velocity of the moving surface. The drag force is counteracted by forces developed by deflecting springs k. The eddy-current drag on a metal plate spinning between the poles of a magnet is also proportional to velocity. The force reaction on the magnet may be used to indicate the velocity.

The d-c voltage developed in a homopolar generator is proportional to the speed of rotation and its value may be indicated by the deflection of a voltmeter pointer.

$$u = \int y\, dz \qquad w = \int [du + (1-x)\, dw]$$

(a)

$$u = \int (y - w)\, dx \qquad w = \int [du + (1-x)\, dw]$$

(b)

$$u = \int [dz + (1-y)\, du] \qquad w = \int [du + (1-x)\, dw]$$

(c)

Fig. 5.25

One more interesting example of this type of differentiation is typified by the gyroscope (Fig. 5.27). The heavy disk spinning at a high angular velocity Ω about its axis OO has the angular momentum ΩI_o, where I_o
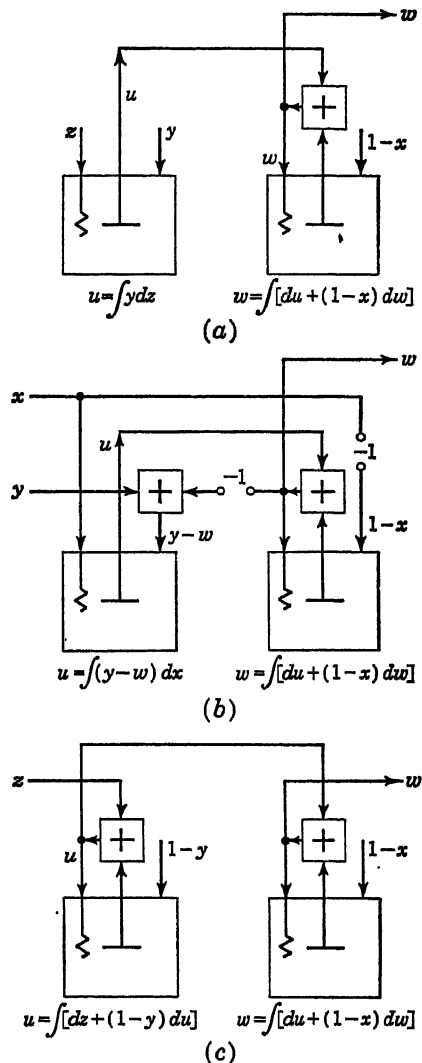
is the polar moment of inertia of the disk. If the variable to be differentiated with respect to time is introduced as a rotation θ about an axis AA perpendicular to the spin axis, then a reacting moment is exerted
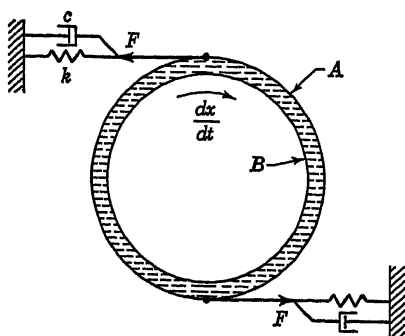
Fig. 5.26
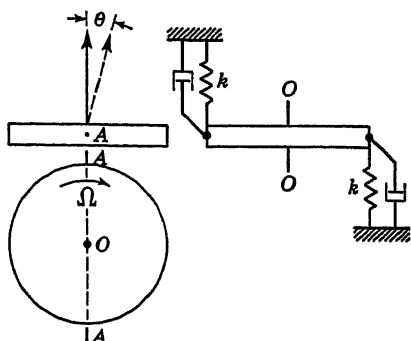
Fig. 5.27

about an axis BB. BB is perpendicular to both OO and AA. This moment is proportional to $d\theta/dt$ and is given by

$$M = \Omega I_o \frac{d\theta}{dt} \tag{5.58}$$

The springs k counteract the moment M, and their deflections are proportional to M.
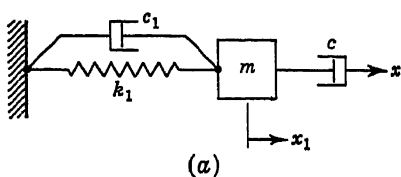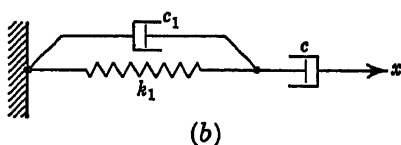
5.23. Response of Mechanical Time Differentiators. The response of mechanical systems, such as those described in Sec. 5.22, to variations in the derivative (*i.e.*, to the presence of higher derivatives) depends on the mass of the response element, on the stiffness of the restraining springs, and on the amount of damping in the system. The equivalent dynamical system for differentiators discussed above is shown in Fig. 5.28a.

(a)

(b)

Fig. 5.28

The velocity across dashpot C is $\dot{x} - \dot{x}_1$, the corresponding force exerted on m being $c(\dot{x} - \dot{x}_1)$. The other forces exerted on m are $-k_1 x_1$ and $-c_1 \dot{x}_1$. Considering m as a free body, the equation of motion for m is

$$m\ddot{x}_1 + c_1\dot{x}_1 - c(\dot{x} - \dot{x}_1) + k_1 x_1 = 0 \tag{5.59}$$

With the system initially at rest, suppose a step change is applied to $\dot{x}$. That is, at $t = 0$, let $x = x_1 = \dot{x}_1 = 0$, and $\dot{x} = K$. Equation (5.59)

becomes

$$m\ddot{x}_1 + (c_1 + c)\dot{x}_1 + k_1 x_1 = cK \tag{5.60}$$

The solution of Eq. (5.60) is[21]

$$x_1 = e^{-\frac{c_1+c}{2m}t}\left(Ae^{\left[\left(\frac{c_1+c}{2m}\right)^2 - \frac{k_1}{m}\right]^{\frac{1}{2}}t} + Be^{-\left[\left(\frac{c_1+c}{2m}\right)^2 - \frac{k_1}{m}\right]^{\frac{1}{2}}t}\right) + \frac{cK}{k_1} \tag{5.61}$$

When $(c_1 + c)/2m$ is less than k_1/m, a decaying transient in x_1 oscillates about the value cK/k_1 at a frequency given by $\left[\frac{k_1}{m} - \left(\frac{c_1+c}{2m}\right)^2\right]^{\frac{1}{2}}$ and with a decay modulus of $2m/(c_1 + c)$. The decay modulus is defined as the time required for the amplitude to decrease by a factor of $1/e$. When $(c_1 + c)/2m$ is greater than k_1/m, oscillation does not take place and x_1 approaches cK/k_1 asymptotically.

If m were so light as to have a negligible effect on response, the term $m\ddot{x}_1$ would be missing from Eq. (5.60). The equivalent system is shown in Fig. 5.28b. The solution for this case is

$$x_1 = \frac{cK}{k_1}\left(1 - e^{-\left(\frac{k_1}{c_1+c}\right)t}\right) \tag{5.62}$$

for $x_1 = 0$ at $t = 0$.

The second term in the parentheses represents the lag in the response of x_1. The lag depends on the ratio $(c_1 + c)/k_1$; the smaller this ratio the more rapid the response.

5.24. Differentiation with Respect to an Arbitrary Variable. The use of time differentiators to produce differentiation with respect to some other variable may be accomplished by dividing dy/dt by dx/dt to produce dy/dx.

The connections for using a mechanical integrator to perform differentiation[22] are shown in Fig. 5.29a. For a slight rotation dx of the turntable the output of the integrating wheel is $z\,dx$. This is subtracted from the slight increment dy, which occurs at the same time, and the difference is used to change the position of the lead screw of the integrator. The lead-screwt urns give the desired output z. The equation mechanized in Fig. 5.29a is

$$dz = dy - z\,dx \qquad z = \frac{dy}{dx} - \frac{dz}{dx} \tag{5.63}$$

In order that z represent dy/dx accurately, the term dz/dx must be kept small. This may be done by using a very large scale factor on the lead-screw input, so that the lead screw makes many turns for slight changes in the adder output. Suppose the scale factors S_1 and S_2 apply, respectively, to x and to z entering the lead screw (Fig. 5.29b). The variable y enters the adder at the same scale factor as does the integrator wheel

output.   For present purposes it may be assumed that the scale factor on the adder output is the same as that on the adder input.   A very large stepup in shaft rotation is provided through a servo-driven unit M, which multiplies the adder output scale factor by a large number N.   The relation mechanized in Fig. 5.29b, including scale factors, is [see Eq. (5.16)]

$$N\left(\frac{S_1 S_2}{an}\,dy - \frac{S_1 S_2}{an}\,z\,dx\right) = S_2\,dz \qquad (5.64)$$

which reduces to

$$z = \frac{dy}{dx} - \frac{an}{S_1 N}\frac{dz}{dx} \qquad (5.65)$$

By making N very large, the error in dy/dx is made correspondingly small.
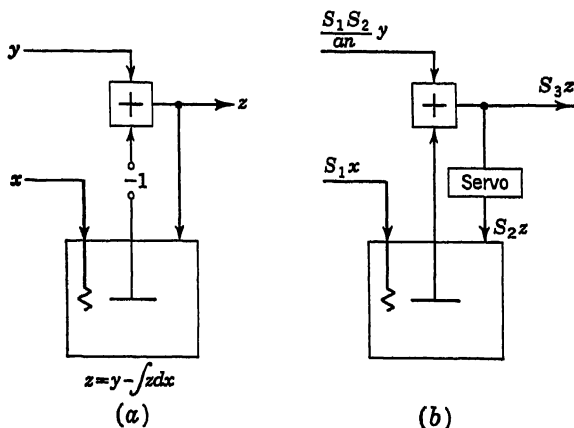
Fig. 5.29

5.25. Differentiation of Plotted Curves.   Data are often obtained in graphical form, from which first and second derivatives are to be obtained. By definition, the derivative at any point on a curve is the slope of the curve at that point.   Some mechanical curve differentiators use this fact directly by positioning a bar by sight to be tangent to the given curve. The bar may have two closely spaced points which can be placed on the curve, giving the slope of the connecting chord as an approximation to the mean slope between the two points.   By means of connecting links a pencil traces the derivative as the pair of points is moved over the given curve.   A differentiator based on this form of construction has been described by Murray.[23]   Another machine[24] based on similar principles makes use of a sharp-edged wheel rolling along the given curve.   The plane of the wheel is kept tangent to the curve, and a pen plots the derivative via a system of links.   A differentiator based on the tangent bar construction, but making use of selsyn transmitters for electrically

coupling the tangent bar to the recording pen, is described by Atkinson and Levens.[25]

Methods requiring the setting of a bar either tangent or orthogonal to a curve are difficult to manipulate and are subject to large human error. A neater method would be one in which an operator need only trace the given curve with a single point, thereby producing through an appropriate mechanism a curve representing the derivative. Such a method is due to Myard[26] and is based on the principle expressed by Eq. (5.63). The movement of a tracing point along the given curve turns both a turntable against which an integrating wheel is pressed and a lead screw on which the integrating wheel is threaded. A pen carried by the integrating wheel then plots the derivative. Assuming a wheel of radius a and an initial offset of the wheel from the disk center of the amount a, for any additional offset z and a differential disk rotation dx, the integrating wheel makes $a^{-1}(z + a)\,dx$ turns. The vertical movement of the tracing point dy and the horizontal movement dx are summed through a differential, the sum rotating the lead screw so as to counteract the displacement z. The relation so enforced is

$$\frac{1}{a}(z + a)\,dx = (dx + dy) \qquad \text{or} \qquad z = a\frac{dy}{dx} \qquad (5.66)$$

5.26. Mechanical Generation of Trigonometric Functions. The generation of trigonometric functions, particularly the sine and cosine, is frequently an important requirement in an analog computer. In mechanical systems the Scotch yoke mechanism illustrated in Fig. 5.30 may be used for sines and cosines. The crank r rotating about a fixed pivot carries a pin which fits snugly into two slotted sliders arranged at right angles to each other. As the crank generates the angle θ, the horizontal slider will have the motion $x = r$

Fig. 5.30

cos θ, the vertical slider the motion $y = r \sin \theta$. Such a unit is often called a "resolver," for it resolves the vector r (represented in direction and magnitude by the crank) into its two rectangular components x and y. There is no theoretical error in this resolver. The fabrication errors can be held to very close limits.
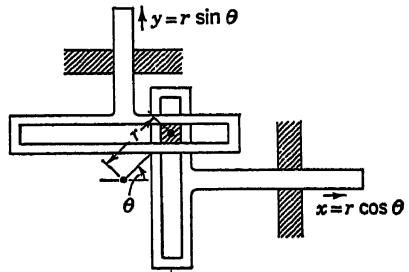
A precision cosine (or sine) generator may be based on the geometrical fact that a point on the circumference of a circle executes simple harmonic motion as the circle rolls internally in another circle of twice the radius. In Fig. 5.31a, the small circle is about to roll clockwise, its center describ-
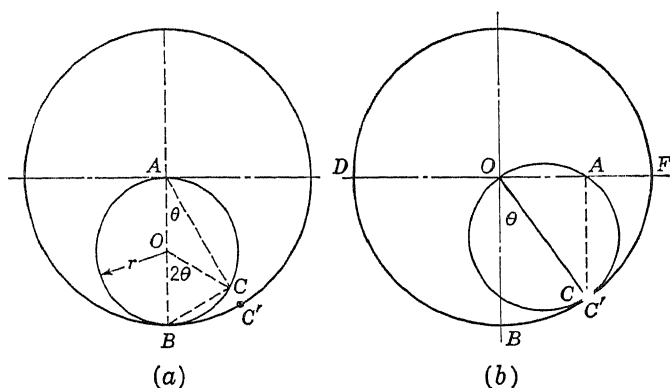
Fig. 5.31
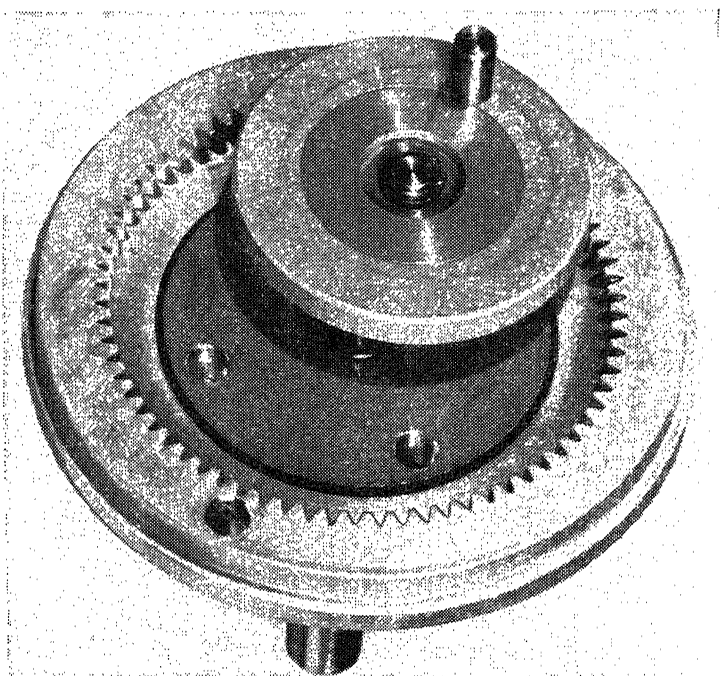
Fig. 5.32. (Courtesy of Librascope Inc., Glendale, Calif.)

ing a circle in the counterclockwise direction. In rolling on the larger circle, a point C on the smaller circle, spaced $2\theta r$ from B, will eventually coincide with a point C' on the larger circle. In the figure, $AC = 2r \cos \theta$ and $CB = 2r \sin \theta$. When C falls on C' [in (b)], the angle $C'OB = \theta$, and the point A on the small circle will have moved a distance OA to the right. It is clear that A remains on the diameter of the large circle at all times since $AC' = 2r \cos \theta$ and $OA = 2r \sin \theta$. Thus, point A moves in

simple harmonic motion across the diameter DF of the large circle.   A mechanism in which toothed surfaces roll on each other to generate the simple harmonic motion is shown in Fig. 5.32.

Approximate mechanization of the sine function may be obtained by means of the slider-crank mechanism or the four-bar linkage of Fig. 5.33 or

(a)

(b)
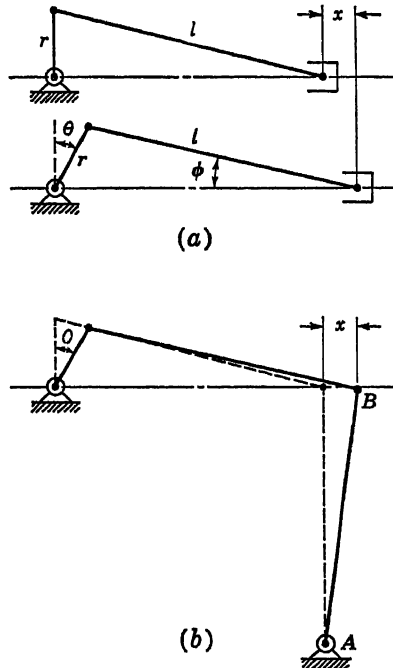
Fig. 5.33

by means of the cam-follower arrangements[27] of Fig. 5.34.   In Fig. 5.33a,

$$x = r \sin \theta + l \cos \phi - \sqrt{l^2 - r^2} \tag{5.67}$$

$$l \sin \phi = r \cos \theta$$

$$\cos \phi = \sqrt{1 - \frac{r^2}{l^2} \cos^2 \theta} \tag{5.68}$$

Hence,

$$x = r \sin \theta + l \left(\sqrt{1 - \frac{r^2}{l^2} \cos^2 \theta} - \sqrt{1 - \frac{r^2}{l^2}} \right) \tag{5.69}$$

The theoretical error [second term in Eq. (5.69)] depends on the crank-to-connecting-rod length ratio r/l.   The smaller this ratio, the smaller will be the theoretical error.   By offsetting the zero position for θ to equalize the maximum errors for the plus and minus values of x, the maximum error may be reduced.

In (b), the movement of the end of the connecting rod is guided by the crank AB. The theoretical error depends on the r/l ratio and also on the length AB. The analysis of this case is left to the reader.

Either disk or cylindrical cams may be profiled to mechanize the sine function exactly. The approximate mechanization shown in Fig. 5.34a makes use of a simple circular disk rotating about an off-center pivot.

(a) (b)
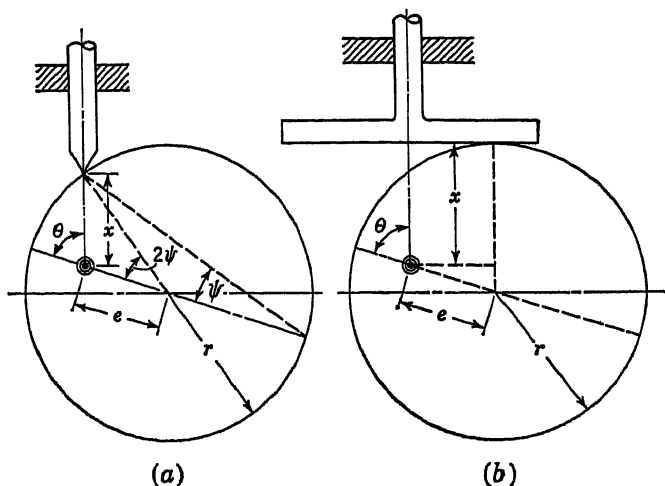
Fig. 5.34

From the geometry of (a), we find

$$x^2 = r^2 + e^2 - 2re \cos 2\psi \tag{5.70}$$

$$\sin 2\psi = \frac{x}{r} \sin \theta$$

$$\cos 2\psi = \sqrt{1 - \frac{x^2}{r^2} \sin^2 \theta} \tag{5.71}$$

from which we obtain the implicit relation for x in terms of θ as

$$x = \sqrt{(r-e)^2 + 2re \left[1 - \sqrt{1 - \frac{x^2}{r^2} \sin^2 \theta}\right]} \tag{5.72}$$

The output desired is not simply x but the variation of x about its mean value. The zero setting for θ must be adjusted, therefore, to equalize the error on either side of the mean value of x for best results.

If, instead of a pointed follower, a flat follower were to be used, as in Fig. 5.34b, the distance of the follower above the pivot would be given by

$$x = r - e \cos \theta \tag{5.73}$$

The mean value of x is r, and the variation about the mean is $e \cos \theta$. Thus the variation represents the sinusoidal function exactly.

The tangent and cotangent can be mechanized[11,27] over a limited range of values by means of the simple linkage shown in Fig. 5.35. The slotted crank A rotates about its pivot to generate θ. The sliding bar has a displacement $x = D \tan \theta$. If ϕ be the variable angle, then $x = D \operatorname{ctn} \phi$.

5.27. Integrators for Generating Circular and Hyperbolic Functions.

The differential relation for $z = \sin x$ is $dz = \cos x \, dx$, and for $w = \cos x$ it is $dw = - \sin x \, dx$. These lead to the integral relation

$$z = \sin x$$
$$= \int (\int - \sin x \, dx) \, dx \quad (5.74)$$

which is mechanized in Fig. 5.36a; $\cos x$, as well as $\sin x$, is developed in this circuit.

To generate $\sin^2 x$, a third integrator may be connected into the circuit in accordance with Fig. 5.15.
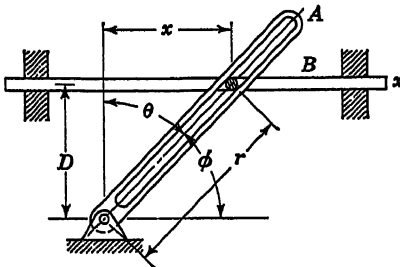
Fig. 5.36
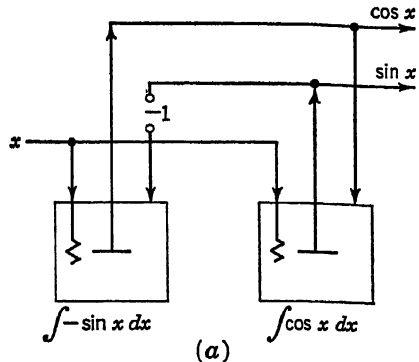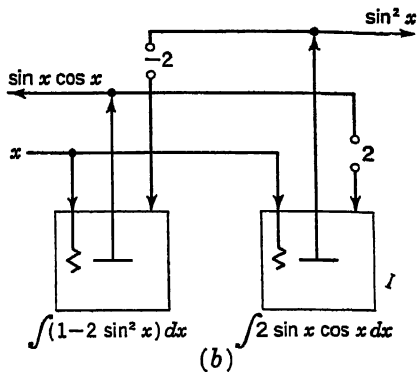
Fig. 5.35

However, by differentiating $\sin^2 x$ a more direct approach to generating the function becomes evident. The relations are

$$d(\sin^2 x) = 2 \sin x \cos x \, dx \qquad d(\sin x \cos x) = (1 - 2 \sin^2 x) \, dx \quad (5.75)$$

The mechanization is shown in Fig. 5.36b.

By dividing the two outputs in Fig. 5.36a, $\tan x$ can be obtained. However, a more efficient mechanization results from an examination of the differential of $\tan x$. Identical relations exist for $\operatorname{ctn} x$, with only a sign change. Thus

$$d(\tan x) = (1 + \tan^2 x) \, dx$$
$$d(\tan^2 x) = 2 \tan x \, d(\tan x) \qquad (5.76)$$

$$d(\operatorname{ctn} x) = -(1 + \operatorname{ctn}^2 x) \, dx$$
$$d(\operatorname{ctn}^2 x) = 2 \operatorname{ctn} x \, d(\operatorname{ctn} x) \qquad (5.77)$$

The connections for Eq. (5.76) are shown in Fig. 5.37. To mechanize

Eq. (5.77) requires merely a reversal of direction of the lead screw in integrator 1.

The differentials of the inverse trigonometric functions given below provide the basis for their mechanization with integrators. For the inverse sine,

$$d(\sin^{-1} x) = (1 - x^2)^{-\frac{1}{2}} dx$$

$$d\left[\frac{d}{dx}(\sin^{-1} x)\right] = x(1 - x^2)^{-1}[(1 - x^2)^{-\frac{1}{2}} dx] \qquad (5.78)$$

$$= x\left[\frac{d}{dx}(\sin^{-1} x)\right]^2 d(\sin^{-1} x)$$

The mechanization of Eq. (5.78) is shown in Fig. 5.38.
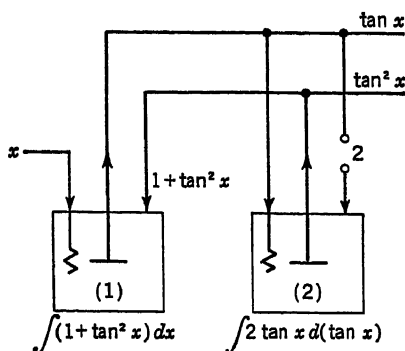
Fig. 5.37

The differential form for the inverse cosine involves merely a change of sign in Eq. (5.78), since

$$d(\cos^{-1} x) = -(1 - x^2)^{-\frac{1}{2}} dx \qquad (5.79)$$

For the inverse tangent,

$$d(\tan^{-1} x) = (1 + x^2)^{-1} dx$$

$$d\left[\frac{d}{dx}(\tan^{-1} x)\right] = -2x(1 + x^2)^{-1}[(1 + x^2)^{-1} dx] \qquad (5.80)$$

$$= -2x\left[\frac{d}{dx}(\tan^{-1} x)\right] d(\tan^{-1} x)$$

The only essential difference between Eqs. (5.78) and (5.80) is the presence of the second power of the derivative in the former in contrast to the first power of the derivative in the latter. Therefore, in mechanizing $\sin^{-1} x$ (or $\cos^{-1} x$) an extra integrator is needed to perform the squaring operation, which is not required when mechanizing $\tan^{-1} x$ (or $\operatorname{ctn}^{-1} x$).

The differential form for the inverse cotangent is

$$d(\text{ctn}^{-1} x) = -(1 + x^2)^{-1} dx \qquad (5.81)$$

involving only a sign change in Eq. (5.80).

The methods for generating hyperbolic functions follow readily from the discussion presented for their counterparts in the circular functions.
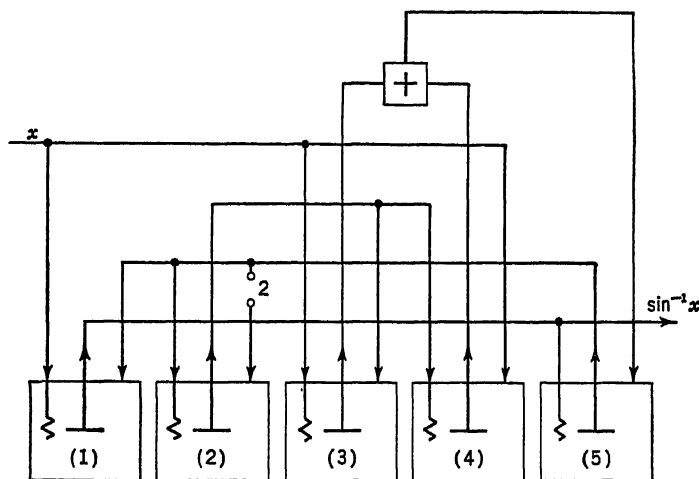
Integrator outputs:

No. 1: $\int \frac{d}{dx}(\sin^{-1} x)\, dx$

No. 4: $\int x\, d\,[\frac{d}{dx}(\sin^{-1} x)]^2$

No. 2: $\int 2\frac{d}{dx}(\sin^{-1} x)\, d\,[\frac{d}{dx}(\sin^{-1} x)]$

No. 5: $\int x\,[\frac{d}{dx}(\sin^{-1} x)]^2\, d(\sin^{-1} x)$

No. 3: $\int [\frac{d}{dx}(\sin^{-1} x)]^2 dx$

Fig. 5.38

Thus, for the hyperbolic sine and cosine,

$$d(\sinh x) = \cosh x\, dx \qquad d(\cosh x) = \sinh x\, dx \qquad (5.82)$$

Figure 5.36a applies to this case, but without the sign reversal indicated in the lead screw of the first integrator.

Differentials for the hyperbolic tangent and cotangent, and for the inverse hyperbolic functions lead to substantially the mechanizations shown in Figs. 5.37 and 5.38.

$$d(\tanh x) = (1 - \tanh^2 x)\, dx \qquad d(\text{ctnh}\, x) = (1 - \text{ctnh}^2 x)\, dx$$
$$d(\sinh^{-1} x) = (1 + x^2)^{-\frac{1}{2}}\, dx \qquad d(\cosh^{-1} x) = (x^2 - 1)^{-\frac{1}{2}}\, dx \quad (5.83)$$
$$d(\tanh^{-1} x) = (1 - x^2)^{-1}\, dx \qquad d(\text{ctnh}^{-1} x) = (1 - x^2)^{-1}\, dx$$

5.28. Miscellaneous and Arbitrary Function Generators. In this section additional mechanical function generators not previously described will be mentioned. The list is by no means complete.

When multiplying a variable x by a very large constant n, a bulky gear train may be necessary. This train can be avoided by using an integrator instead, in the regenerative connection of Fig. 5.39. The output in this case is

$$dz = \left(1 - \frac{1}{n}\right) dz + dx \quad \text{or} \quad dz = n\,dx \quad\quad (5.84)$$

In Sec. 5.20 two integrators are used to generate both the reciprocal and the logarithm (Fig. 5.22b). One regenerative integrator may be used to produce the logarithm without the need for the reciprocal, as shown in

$$z = \int [dx + (1 - \tfrac{1}{n})\,dz]$$

Fig. 5.39

$$z = \int [dx + (1 - x)\,dz]$$
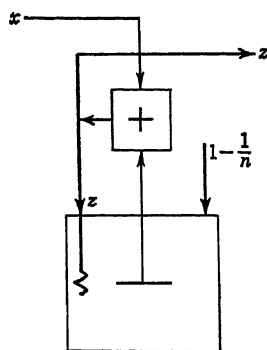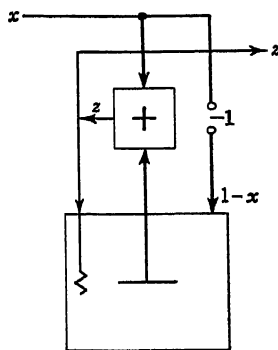
Fig. 5.40

Fig. 5.40. The controlling equation is

$$dz = (1 - x)\,dz + dx$$
$$\text{or} \quad\quad dz = \frac{dx}{x} = d(\ln x) \quad\quad (5.85)$$

A single regenerative integrator can be used to produce the square root (Fig. 5.41). The relation mechanized is $dz = (1 - z)\,dz + dx$, or $z\,dz = dx$. When integrated, this yields

$$\frac{z^2}{2} = x \quad \text{or} \quad z = \sqrt{2x} \quad\quad (5.86)$$

A variable can be raised to any other power by first generating its logarithm (as in Fig. 5.40), and then using an additional integrator to mechanize the relation

$$d(x^n) = nx^{n-1}\,dx = nx^n \frac{dx}{x} = x^n\,d(n \ln x) \quad\quad (5.87)$$

The connections for Eq. (5.87) are shown in Fig. 5.42.

Arbitrary functions can be incorporated in an analog computer by

means of input tables on which such functions are plotted.   Figure 5.43a shows such a table.   The curve $y = f(x)$ is plotted on a sheet of paper which is then fastened to the table.   A pair of lead screws, L_x and L_y, are arranged at right angles to each other. L_x is held to the table in bearings, while L_y is held in a carriage which also serves as a nut on L_x.   Thus, rotation of L_x carries L_y along in the x direction.   Hand crank H moves nut M

$$z = \int [dx + (1-z)dz]$$

Fig. 5.41

$$w = \int [dx + (1-x)d(\ln x)]$$

$$z = n \int x^n d(\ln x)$$

Fig. 5.42

(a) (b)
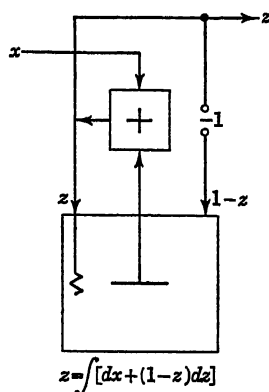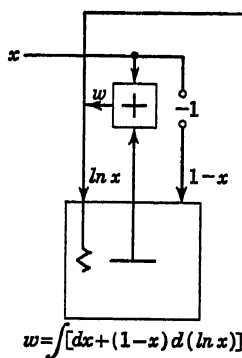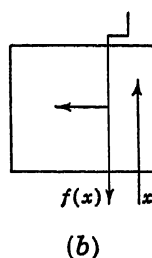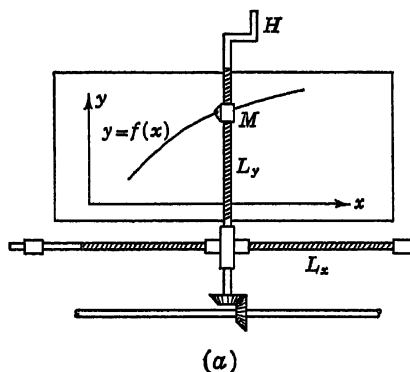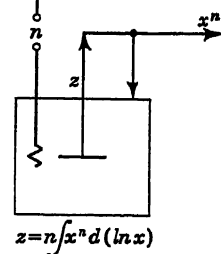
Fig. 5.43

along lead screw L_y and also turns the splined shaft y.   An operator turns H so that a viewer on M is always maintained directly over the curve as the viewer is moved horizontally by L_x.   The turns of H (that is, L_y) are proportional to $f(x)$.   Thus, with the variable x turning L_x, the variable $y[= f(x)]$ will appear as a rotation of the y shaft.

The operator may be replaced by a photoelectric curve follower[14,28] and the stationary table by a rotating drum.[29]

In schematic diagrams for mechanical computers the input table may be represented as shown in Fig. 5.43b.

Since the results of analog computations are usually desired as plotted curves, the input table may also be used as an output table by driving the L_y screw from the y shaft and using a pen in place of the viewer. The output table is symbolized as shown in Fig. 5.44.

Plane cams and three-dimensional cams,[27,30] discussed in Sec. 5.30, are particularly useful function generators for special-purpose computers.

Linkages may be designed to mechanize a wide variety of functions. For a detailed discussion of this very extensive field the reader is referred to Svoboda[31] and to Hrones and Nelson.[32]

A hydraulic method[33] generating fractional powers of a variable is based on the fact that the weight of water displaced by an appropriate
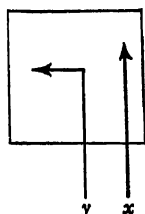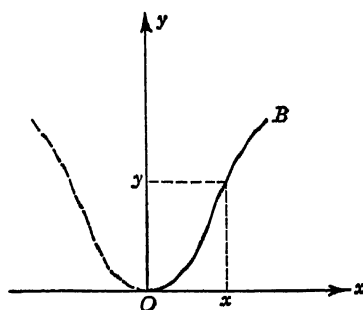
Fig. 5.44   Fig. 5.45

surface of revolution is proportional to a predetermined power of the depth of immersion. If the force W exerted by the displaced water on such a surface of revolution be taken as the independent variable, the resulting depth of immersion y will be the corresponding root of W. Conversely, the force required to produce a given depth of immersion will give the required power of y.

In Fig. 5.45, the curve OB by revolving about Oy generates a surface of revolution. For any submergence y the weight of displaced water is

$$W = w\pi \int_0^y x^2 \, dy = y^n \tag{5.88}$$

where w = weight of water per unit volume

n = required exponent on y

If the generatrix OB is given the form $x = Ay^m$, then

$$A^2 w\pi \int_0^y y^{2m} \, dy = \frac{wA^2\pi y^{2m+1}}{2m + 1} = y^n \tag{5.89}$$

From the last relation in Eq. (5.89), it is clear that

$$\frac{wA^2\pi}{2m + 1} = 1 \qquad 2m + 1 = n \tag{5.90}$$

Therefore the equation for the generatrix OB is

$$x = \left(\frac{n}{w\pi}\, y^{n-1}\right)^{\frac{1}{2}} \tag{5.91}$$

Equation (5.91) specifies the shape of the surface required to extract the nth root of W. It shows that for a square root ($n = 2$) y is proportional to x^2 and the required surface is a paraboloid. For a cube root ($n = 3$) y is proportional to x, so that the required surface is a straight-sided cone.

5.29. Torque Amplifiers. When mechanical computing elements are applied to the solution of differential equations, the integrating wheels
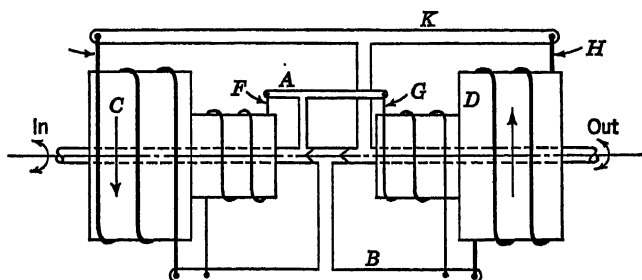
Fig. 5.46

must drive integrator lead screws, turntables, adders, and input and output table lead screws. Relatively large torques are required for this purpose, torques considerably in excess of the frictional torque generated on the sharp-edged wheel by the smooth plate-glass disk. In developing the original MIT differential analyzer it was determined that about a pound-foot of torque would need to be supplied by an integrator output shaft and that only about 0.0001 lb-ft would be available at the wheel. Thus a torque amplification of the order of 10,000 times is required.

Torque amplification of this order of magnitude was obtained with a two-stage capstan-type torque amplifier widely adopted in the various differential analyzers, both large and small, in the 1930s. The principle of such a two-stage amplifier is shown in Fig. 5.46. Two stepped drums, C and D, are driven in opposite directions at constant speed by an electric motor of sufficient capacity to drive the gearing to be coupled to the integrating wheel. The integrating wheel shaft E passes through the hollow core of the left-hand stepped drum. A T bar A fixed to this shaft holds firmly the input ends of two light strings F and G wrapped clockwise and counterclockwise, respectively, about the two small steps on the drums. The other ends (output ends) of the wrapped strings are attached to a freely pivoted T bar B. Heavy cords or metal bands H are wrapped about the larger steps, and the lighter strings are similarly

wrapped about the smaller steps. By means of the T bar B, the outputs of the smaller steps become the inputs to the larger steps. The output ends of the heavy cords on the larger steps are attached to T bar K which is fixed to the output shaft. The whole assembly is put together with slight initial tension in the wraps. When the integrating wheel is at a standstill, equal tensions exist on both sides of T bar A and there is no tendency for T bar K to rotate. Both stepped drums slip at the same rate with respect to their wrappings. If the integrating wheel starts to turn, however, the T bar A would move slightly relative to the drums, tightening one light string and loosening the other. The rate of slippage relative to the tightened string would be reduced, causing the string to rotate with the T bar A. For a given coefficient of friction, the tension in the string builds up exponentially with the angle of wrap. The ratio of tight-side and slack-side tensions of a belt is given by

$$\frac{T_2}{T_1} = e^{f\theta} \tag{5.92}$$

where f is the coefficient of friction and θ the angle of wrap in radians. With a $2\frac{1}{4}$-turn wrap (used in the MIT torque amplifier) and a coefficient of friction of the order of 0.3, T_2/T_1 becomes 110. Thus a multiplication of tension of the order of 100 times occurs through the light string. A further multiplication of 100 times occurs through the heavy cord, thus yielding the over-all amplification of 10,000 required. The reason for doing this in two stages instead of using 5 turns on one drum was to ensure adequate control by minute initial tension and yet provide sufficient power in the output drive with heavy bands.

The constant rotational speed of the stepped drums is greater than the highest speed at which the integrators are to operate, so that all bands are constantly slipping. Clockwise or counterclockwise torques are transmitted to the output shaft by tightening the appropriate bands through the integrating wheel shaft while loosening at the same time the other bands. As the integrating wheel speeds up, it pulls more tension in the driving band, thus increasing the output tension, which speeds up the output shaft to keep up with the wheel.

The polarized-light servomechanism for torque amplification is shown schematically in Fig. 5.47. Integrating wheel A consists of a polarizing disk with a steel rim and steel hub. The direction of polarization is shown by the direction of the crosshatch lines on the wheel. The follow-up system consists of a pair of similar polarizing disks B and C on the motor-driven output shaft D. The two disks are mounted with their planes of polarization at right angles to each other. Two beams of light pass through polarizer A and are polarized in the same direction. One light beam then passes through polarizer B, the other through polarizer C.

The light beams are picked up by separate phototubes which are connected through an amplifier to a split-field series motor. Any difference in light intensity striking the two phototubes will cause the motor to turn in the direction and by the amount necessary to equalize the two incident light intensities. This will occur when the output shaft D is oriented with respect to the wheel A so that the plane of polarization of wheel A bisects the right angle between the two planes of polarization of disks B and C. Any deviation from this position will cause more light to strike one photocell because the plane of polarization of its disk becomes more nearly aligned with that of the wheel, while less light will strike the other photocell because the plane of polarization in its disk comes more
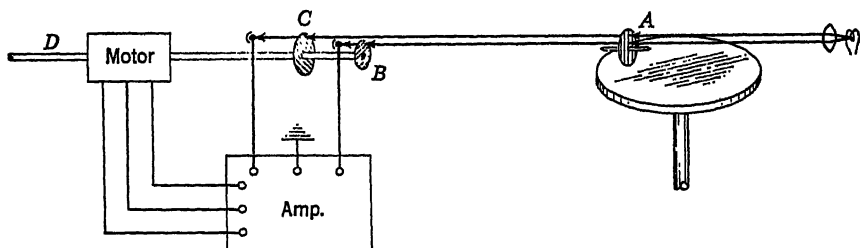
Fig. 5.47

nearly to being at right angles (the extinction position) with that of the wheel. The output shaft D is thus constrained to follow the motions of the integrating wheel, with only two light beams as the coupling medium between them.

A follow-up servomechanism making use of the variation of capacitance due to the rotation of a plate of dielectric material between fixed plates of condensers was developed for the new MIT differential analyzer. The basic unit on both the transmitting shaft (e.g., the integrating wheel shaft) and the receiving shaft (e.g., the integrator output shaft) consists of two capacitance bridges supplied by a 3,000-cps exciting voltage E. The rotation of a dielectric plate common to two capacitors in one bridge produces an output voltage proportional to $E \sin \theta$ with properly shaped capacitor plates and dielectric material. An identical unit in the other bridge with the dielectric plate on the same shaft, but placed at 90° to the first plate, simultaneously has an output proportional to $E \cos \theta$. θ is the angle of rotation of the transmitting shaft. Essentially, the output voltages are transmitted over wires to a receiving shaft whose rotation is to be kept in synchronism with the transmitting shaft by means of an electric motor. The voltages $kE \sin \theta$ and $kE \cos \theta$ serve as the input voltages to the receiving unit capacitance bridges. The connections are such that $kE \sin \theta$ is impressed on the unit generating the cosine component of voltage and $kE \cos \theta$ on the unit generating

the sine component. The bridge output voltages on the receiver end become, therefore,

$$k^2E \sin \theta \cos \phi \quad \text{and} \quad k^2E \cos \theta \sin \phi$$

These are subtracted in a network, so that the output voltage is, finally,

$$\epsilon = k^2E \sin (\theta - \phi) \qquad (5.93)$$

By impressing the voltage ϵ on a servo follower designed to keep ϵ as nearly zero as possible by operating on ϕ through a motor, the angles ϕ and θ are maintained very nearly alike.

Because the information connecting the movements of the input and output shafts is transmitted over wires, any transmitting unit could operate any receiving unit through a switchboard.

5.30. Cams as Computing Mechanisms. The use of cam mechanisms for the generation of special functions has been illustrated in Secs. 5.13 to 5.16. By virtue of their superior accuracy, cam mechanisms are frequently preferred over other types of mechanical computing elements for the generation of arbitrary and nonanalytic functions. The design, construction, and utilization of cams are discussed in considerable detail by Rothbart,[34,35] who also contributed the brief summary below. Fry,[30] Hannura,[36] Lockenvitz,[37] and Davis[38] also have made significant contributions.

When cams are applied to generate arbitrary functions, the cams can be shaped as required by a specific application or an adjustable cam can be used. Adjustable cams are employed either to correct the mechanism action on installation or to correct for changes in parameters with respect to time. Such an adjustable cam may have adjustment screws which are in contact with a thin flexible copper sheet. This sheet is the cam profile which is shaped to suit the application. A follower is, of course, in contact with the cam periphery.

Cams are generally utilized as function generators, *i.e.*, to produce displacements that are definite functions of a number of independent variables. The first step in design is selection of the output scale, the input scale being fixed by the fact that the cam rotates usually less than 360 degrees for full range. Scale choice is an important consideration. From the standpoint of accuracy, it is desirable to have the scale as large as possible, *i.e.*, as few units per inch per revolution as possible. Thus, backlash and dimensional inaccuracy will have a lesser effect.

The second step is to establish the cam size and the sense of the follower movement, *i.e.*, whether to move outward or inward for increasing values. This is chosen so that the steepest portion of the function

curve is at the cam outer radius, permitting smaller cams for the same pressure-angle limit. Generally a maximum pressure angle of 30° is suggested, but angles as high as 45° have been successfully applied.

The basic functional relationship between the variables x and y to be treated by means of the cam mechanism is denoted as

$$y = f(x) \tag{5.94}$$

where x is the input parameter, y is the output parameter, and $f(x)$ is any single-valued continuous function whose derivatives are held within certain limits. The latter restriction on $f(x)$ prevents the cam from becoming too large and impractical.

In Fig. 5.48 are indicated some of the more widely used types of cam mechanisms. The nonpositive-drive types held in contact by springs are not shown. Figure 5.48a shows the general case of two contours in contact, usually with pure rolling action. Figure 5.48b and c shows the input x as a constant-speed rotating cam, with the output y as translating and oscillating followers, respectively. In d a spiral rotating input x with a positive-drive and pin-in-groove output y is shown. Figure 5.48e shows a so-called gear cam, which is similar to the mechanism shown in d except that the output parameter y is a rotating pin-gear meshing with the grooves in the spiral input x. The primary advantage of these two spiral cams is that more than one cam revolution is permitted, thereby providing greater accuracy. Spirals as high as eight revolutions have been employed. Figure 5.48f shows a rotating cylindrical cam input x and a translating output y. Compared with radial cams, cylindrical cams generally have a smaller maximum dimension for a given follower travel. The cylindrical cam shown in Fig. 5.48g differs from all the others in that it is a three-dimensional cam or camoid, the mechanism having two degrees of freedom. The follower is generally a spherical ball in contact with the cam profile. With the camoid, the output parameter y is a function of two parameter inputs x_1 and x_2 according to

$$y = f(x_1, x_2) \tag{5.95}$$

The input x_1 and the output y are translating, while the input parameter x_2 is rotating. In an alternate design, output y may have oscillating action. The three-dimensional cam is used in applications where the relation is so complicated that no analytical solution exists, the function being known only in the form of tabulated data or curves. An example is the computation of various exterior ballistic quantities such as the time of a projectile flight in fire-control work. These three-dimensional cams are generally employed only as a last design possibility because of their
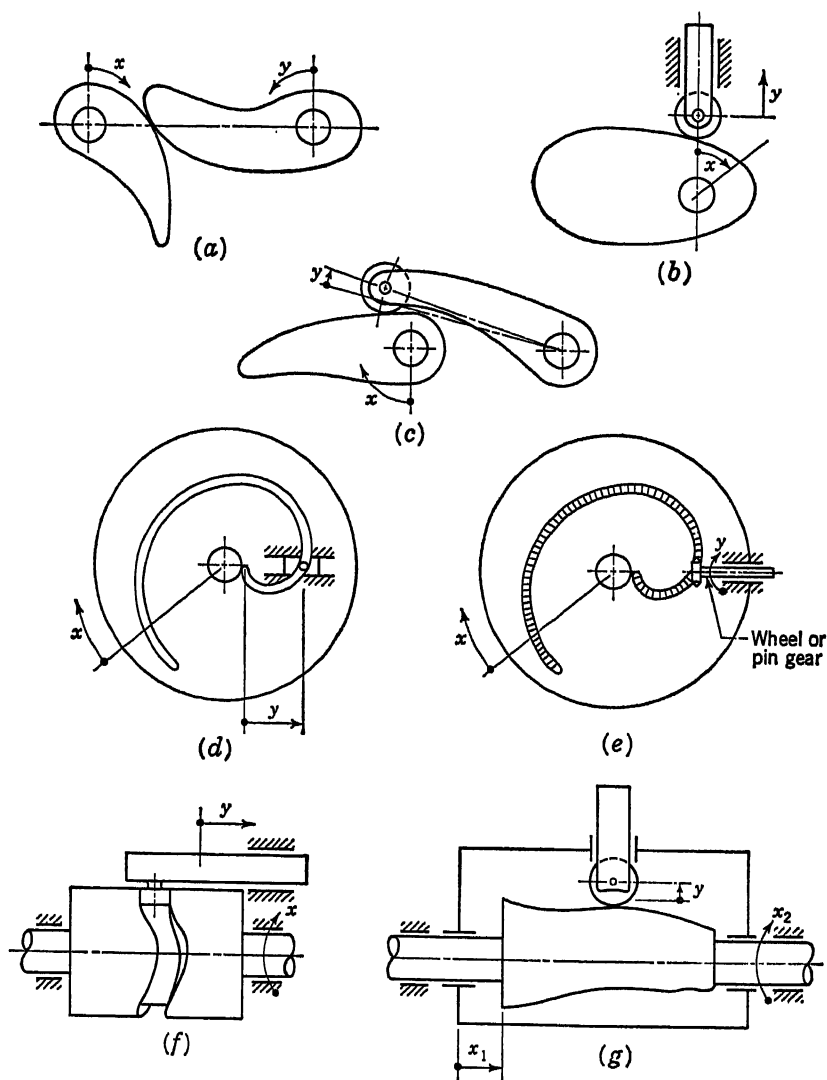
Fig. 5.48

high pressure angle, large size, high friction, and high manufacturing cost. Such cams are often cut on a profiling machine controlled by a master cutter, sometimes requiring 15,000 points with a tolerance of at least ±0.0004 in. After removal from the fixture, the surface is covered with thousands of tiny protuberances between successive cuts. These projections are removed by round files properly selected to conform more or less with the cam surface at the point of filing. Last, the surface is

hand-polished to 20-μin. (root-mean-square) smoothness. Sometimes to simplify fabrication cams have been built up of many thin disks.

Occasionally cams are employed as corrective devices rather than as complete function generators. In such applications they do not perform complete mathematical operations but are used in conjunction with other cams, gears, or linkages. For example, if a linkage alone cannot generate the desired function, a cam may be coupled to the linkage mechanism. High accuracy can be attained in this manner, since the range of cam operation is small compared with the total movement.

REFERENCES

1. Bush, V.: The Differential Analyzer, A New Machine for Solving Differential Equations, *J. Franklin Inst.*, **212**:447–488 (1931).
2. Kuehni, H. P., and H. A. Peterson: A New Differential Analyzer, *Trans. AIEE*, **63**:221–228 (1944). (Discussion, pp. 429–431.)
3. Bush, V., and S. H. Caldwell: A New Type of Differential Analyzer, *J. Franklin Inst.*, **240**:255–326 (1945).
4. Fry, M.: Designing Computing Mechanisms, Part IV, Integration, *Machine Design*, **17**(11):141–145 (1945).
5. Thomson, W.: Mechanical Integration of the Linear Differential Equations of the Second Order with Variable Coefficients, *Proc. Roy. Soc. (London)*, **24**:269–271 (1875–1876).
6. Thomson, W.: Mechanical Integration of the General Linear Differential Equation of Any Order with Variable Coefficients, *Proc. Roy. Soc. (London)*, **24**:271–275 (1875–1876).
7. Sang, J.: Description of a Platometer, An Instrument for Measuring the Areas of Figures Drawn on Paper, *Trans. Roy. Scottish Soc. Arts*, **4**:119–129 (1850–1856).
8. Maxwell, J. C.: Description of a New Form of Platometer, an Instrument for Measuring the Areas of Plane Figures Drawn on Paper, *Trans. Roy. Scottish Soc. Arts*, **4**:420–429 (1850–1856).
9. Thomson, J.: On an Integrating Machine Having a New Kinematic Principle, *Proc. Roy. Soc. (London)*, **24**:262–265 (1875–1876).
10. Ford, Hannibal C.: Mechanical Movement, U.S. Patent 1,317,915, Oct. 7, 1919.
11. Fry, M.: Designing Computing Mechanisms, Part II, Multiplying and Dividing, *Machine Design*, **17**(9):113–120 (1945).
12. Reid, R. R., and D. R. E. Stromback: Mechanical Computing Mechanisms, Part III, *Product Eng.*, **20**(10):126–130 (1949).
13. Grodzinski, P.: Change-gear Box Has Wide Range, *Machine Design*, **24**(5):154 (1952).
14. Cook, A. C., L. K. Krichmayer, and C. N. Weygandt: Special Devices Aid Differential Analyzer Solution of Complex Problems, *Trans. AIEE*, **69**:1365–1370 (1950).
15. Maxson, William L., and Peter J. McLaren: Multiplying Machine, U.S. Patent 2,194,477, Mar. 26, 1940.
16. Yavne, R. O.: High Accuracy Contour Cams, *Prod. Eng.*, **19**(8):134–136 (1948).
17. Temperley, C.: Intermeshing Non-circular Algebraic Gears, *Engineering*, **165**:49–52 (1948).
18. Lockenvitz, A. E., J. B. Oliphant, W. C. Wilde, and J. M. Young: Noncircular Cams and Gears, *Machine Design*, **24**(5):141–145 (1952).

19. Michel, J. G. L.: Extensions in Differential Analyzer Techniques, *J. Sci. Instr.*, **25**:357–361 (1948).
20. Amble, O.: On a Principle of Connexion for Bush Integrators, *J. Sci. Instr.*, **23**:284–287 (1946).
21. Den Hartog, J. P.: "Mechanical Vibrations," 3d ed., p. 63, McGraw-Hill Book Company, Inc., New York, 1947.
22. Fry, M.: Designing Computing Mechanisms, Part V, Differential Equations and Differentiation, *Machine Design*, **17**(12):123–126 (1945).
23. Murray, J. E.: A Differentiating Machine, *Proc. Roy. Soc. Edinburgh*, **25**:277–280 (1903–1905).
24. Elmendorf, A.: Mechanical Differentiation, *J. Franklin Inst.*, **185**:119–130 (1918).
25. Atkinson, C. P., and A. S. Levens: A New Differentiating Machine, *Mathematical Tables and Other Aids to Computation*, **5**:99–102 (1951).
26. Myard, F. E.: Nouvelles solutions de calcul grapho-méchanique. Dérivographes et planimétres, *Génie civil*, **104**:103–106 (1934).
27. Reid, R. R., and D. R. E. Stromback: Mechanical Computing Mechanisms, Part II, *Prod. Eng.*, **20**(9):119–123 (1949).
28. Blackett, P. M. S., and F. C. Williams: An Automatic Curve Follower for Use with the Differential Analyzer, *Proc. Cambridge Phil. Soc.*, **35**:494–505 (1939).
29. Sauer, R., and H. Posch: Integriermaschine fur gewohnliche Differential-gleichungen, *Z. Ver. deut. Ing.*, **87**:221–224 (1943).
30. Fry, M.: Designing Computing Mechanisms, Part III, Cam Mechanisms, *Machine Design*, **17**(10):123–128 (1945).
31. Svoboda, A.: "Computing Mechanisms and Linkages," MIT Radiation Laboratory Series, vol. 27, McGraw-Hill Book Company, Inc., New York, 1948.
32. Hrones, J. A., and G. L. Nelson, "Analysis of the Four Bar Linkage: Its Application to the Synthesis of Mechanisms," John Wiley & Sons, Inc., New York, 1951.
33. Emch, A.: Two Hydraulic Methods to Extract the nth Root of Any Number, *Am. Math. Monthly*, **8**:10–12 (1901).
34. Rothbart, H.: "Cams—Design, Dynamics and Accuracy," John Wiley & Sons, Inc., New York, 1956.
35. Rothbart, H.: Cam Mechanisms for Measurement, Control and Computing, to be published in *Control Eng*.
36. Hannula, F. W.: Designing Noncircular Surfaces, *Machine Design*, **23**:111 (July, 1951).
37. Lockenvitz, E., J. B. Oliphant, W. C. Wilde, and J. M. Young: Geared to Compute, *Automation*, **2**:37 (August, 1955).
38 Davis, S.: Rotating Components for Automatic Control, *Prod. Eng.*, **24**:129 (November, 1953).

Part Two

INDIRECT COMPUTERS

6

DIFFERENTIAL ANALYZERS

6.1. General Remarks. In the preceding four chapters applications of electrical and mechanical analog devices to perform a wide variety of mathematical operations have been considered. Occasionally, these units are in themselves sufficient to perform the entire computational task required of them and therefore constitute special-purpose computers. More frequently, however, it is necessary to interconnect such units in order to permit the solution of algebraic and differential equations or to simulate complex physical systems. In this chapter, the application of these elements to the solution of ordinary differential equations is considered. Analog computers designed for the solution of such equations are known as "differential analyzers," a name coined by W. V. Lyon (see Bush[1]). These machines usually present the results of the solving process as graphs of the desired functions plotted against one or more other variables. Digital computers, of course, provide numerical answers to these problems. The solution of simultaneous and nonlinear algebraic equations and the solution of partial differential equations are considered in subsequent chapters.

A considerable body of mathematical theory applied to ordinary and partial differential equations[2,3] has been developed through the years. While procedures have been standardized for the solution of certain linear differential equations with constant coefficients, modern developments in engineering and the sciences inexorably lead to nonlinear equations[4,5] and to variable coefficients. Formal methods exist only for the solution of a limited number of nonlinear differential equations. In most cases, it is necessary to obtain particular solutions by numerical methods or analog devices. As a result, there has occurred an intense activity in the development of high-speed digital computers and of analog computers for obtaining families of particular solutions of such equations without unreasonable expenditures of time. Such computers are useful, not only for nonlinear equations for which mathematical solutions cannot be found, but also for complex systems of linear equations

the solutions of which, though possible, would be extremely laborious by conventional methods.

Throughout this chapter the application of the so-called "long-time" electronic analog computer is stressed. The solution of simple ordinary differential equations is first demonstrated. Next, the problem of selecting suitable scale factors for the dependent and independent variables of the computer is discussed. The solution of more complex linear and nonlinear differential equations is then considered. The chapter closes with a survey of various other types of differential analyzers.

6.2. Historical Background of Differential Analyzers. The possibility of obtaining machine solutions of ordinary differential equations by successive mechanical integrations was first suggested by W. Thomson[6,7] (Lord Kelvin) in 1876, immediately after the development of a mechanical integrating unit by his brother. No successful machine using this method appears to have been constructed until a group of men at the Massachusetts Institute of Technology, without the knowledge of Thomson's original suggestion, proceeded to develop and construct a series of such machines. The first embryonic computer, employing shaft-rotation principles with torque amplifiers, was the continuous integraph[8] in operation at MIT in 1925. A more flexible and larger machine was constructed and put into operation in 1930.[1] This machine had six mechanical integrating units.

With the MIT differential analyzer pioneering the way, other general-purpose indirect computers began to make their appearance. Mechanical differential analyzers were constructed at the University of Pennsylvania,[9] the University of Manchester in England,[10–12] in Oslo,[13] in Leningrad, and elsewhere. In the early 1940s, the General Electric Company developed and built a new 14-integrator mechanical differential analyzer[14] using beams of polarized light[15] to couple the integrating wheel to the output drive system. Another unit of the same type was installed at the University of California at Los Angeles.[16] The most elaborate mechanical differential analyzer of all was put in operation at MIT in 1942.[17] At that time, mechanical differential analyzers had probably reached the peak of their popularity. With the development of more and more accurate and dependable electronic differential analyzers, the bulky and cumbersome mechanical installations gradually began to give way. By 1958, most of the remaining mechanical units had been dismantled or relegated to classroom demonstration work.

Few fields of analog-computer development have enjoyed such widespread activity as that of the electronic analog computer in the years following World War II. The major reasons for this spurt are the abun-

dance of commercially available electronic components, the ease with which they can be assembled into computing units, and the relative low cost of such units. Additional factors include the rapidity with which a problem can be programmed into such a computer, the speed with which solutions are completed, and the convenience with which parameters can be changed.

C. A. Lovell and G. A. Philbrick[18] are generally credited with the first use of high-gain d-c amplifiers to perform simple mathematical operations. Ragazzini's[19] classic paper in 1947 comprises the first description of a complete general-purpose electronic differential analyzer. The development of this equipment was stimulated by military requirements and contracts during World War II. Since that time, numerous companies, in particular Reeves Instrument Corporation (REAC), Beckman Instruments (EASE), Goodyear (GEDA), Electronic Associates (PACE), and Philbrick (GAP/R), have developed and marketed large-scale and sophisticated general-purpose differential analyzers.

In 1950, a new type of computer employing the general principles of differential analyzers, but using digital techniques to perform the required calculations, was introduced. The earliest model developed by Northrup Aircraft was the MADDIDA (magnetic drum differential digital analyzer). Bendix Aviation Corporation and Litton Industries subsequently marketed commercial digital differential analyzers.

6.3. Problem Preparation. The differential analyzer solves ordinary differential equations. It does not derive them. Thus, somewhere along the line, an analysis has been made of a given situation, an ordinary differential equation has been developed, and appropriate initial or boundary conditions have been specified for the problem. Data are available in tabular or graphical form, representing whatever experimentally determined relationships exist between the parameters which enter into the differential equations. The task remains, then, of obtaining one or more solutions to the differential equations (or equation) subject to the specified conditions. In its most general form an ordinary differential equation is written as

$$f\left(\frac{d^n y}{dx^n}, \frac{d^{n-1} y}{dx^{n-1}}, \cdots, \frac{dy}{dx}, y, x\right) = 0 \tag{6.1}$$

The function is arbitrary; the variables and the derivatives may appear in any fashion—as powers, roots, or cross products or in logarithms, exponentials, trigonometric forms, etc. It is desired to find corresponding values of x and y which satisfy Eq. (6.1). The solution can be obtained, in principle, in either one of two ways:

1. By successive integrations, starting with the highest derivative. The process is indicated by the following series of equations:

$$\frac{d^{n-1}y}{dx^{n-1}} = \int \frac{d^n y}{dx^n} \, dx$$

$$\frac{d^{n-2}y}{dx^{n-2}} = \int \frac{d^{n-1}y}{dx^{n-1}} \, dx \qquad (6.2)$$

$$\cdot \, \cdot \, \cdot \, \cdot \, \cdot \, \cdot \, \cdot \, \cdot \, \cdot \, \cdot$$

$$y = \int \frac{dy}{dx} \, dx$$

2. By successive differentiations starting with the dependent variable. The process is indicated by the following series of equations:

$$\frac{dy}{dx} = \frac{d}{dx} y$$

$$\frac{d^2 y}{dx^2} = \frac{d}{dx} \frac{dy}{dx} \qquad (6.3)$$

$$\cdot \, \cdot \, \cdot \, \cdot \, \cdot \, \cdot \, \cdot \, \cdot \, \cdot$$

$$\frac{d^n y}{dx^n} = \frac{d}{dx} \frac{d^{n-1}y}{dx^{n-1}}$$

In method 1 the highest derivative of Eq. (6.1) is isolated on the left side of the equations such that

$$\frac{d^n y}{dx^n} = f_1 \left(\frac{d^{n-1}y}{dx^{n-1}}, \frac{d^{n-2}y}{dx^{n-2}}, \; \cdot \, \cdot \, \cdot \, , \frac{dy}{dx}, y, x \right) \qquad (6.4)$$

Most of the ordinary differential equations occurring in applied mathematics are of the form permitting this to be done. The highest derivative is thus expressed in terms of the lower derivative and the variables themselves. The right-hand side of Eq. (6.4) can therefore be substituted as the integrand in the first of Eq. (6.2). Since all the variables in this integrand have known initial values, an integrator can be assigned to perform the integration called for by the first of Eq. (6.2). The initial condition on this integrator—the voltage to which the feedback capacitor is charged time $t = 0$ in the case of the electronic analog (or the lead-screw setting of a mechanical integrator)—is adjusted to a value as called for by the right-hand side of Eq. (6.1). As time progresses, the various derivatives and other variables and parameters of the problem correspondingly change their magnitudes in conformance with Eq. (6.1). By summing at the input of the first integrator all the voltage variables which represent the right-hand side of Eq. (6.4), the output of that integrator is made at all times proportional to the $(n - 1)$st derivative. Since the

integrand is also a function of the $(n-1)$st derivative, the output of this integrator must be fed back to its own input to introduce this function.

So far, only the first integrator has materialized, and the suggestion has been made that other voltage variables contributing to the input of this integrator are present in the computer. The various derivatives, of course, must be provided by additional integrators which step down the order of the derivative in successive steps. The biggest hurdle is overcome when the first integrator is properly equipped. After that, the output of this integrator is made the input of a second integrator, the output of which in turn is $(n-2)$nd derivative, in accordance with the second of Eq. (6.2). The initial condition on this second integrator is the initial value of the $(n-1)$st derivative. The output of the second is connected to the output of the first integrator, the input resistor being adjusted so that the function of the $(n-2)$nd derivative called for in Eq. (6.4) is supplied. The output of the second integrator is also connected to a third integrator's input to provide the $(n-3)$d derivative, etc. Each integrator thus feeds into the input of the first integrator to produce the function called for by Eq. (6.4). Each integrator also constitutes the input of the next integrator. Thus, at the nth integrator, the function y finally appears. This output is transmitted to the first integrator as well as to an output device and to any other point in the computer where the value y is required. It may also be desirable to record outputs in addition to or instead of the y output. Any variable voltage in the computer can, of course, be connected to an oscillograph or servo-driven recorder, and the values of the variable it represents so registered.

In electronic analog computers, time is necessarily the independent variable. All derivatives must therefore be with respect to time. This limitation does not exist in mechanical and digital differential analyzers.

In method 2, the procedure calls for isolating the dependent variable on the left-hand side of the equation and putting all the functions of the derivatives and independent variables on the right:

$$y = f_2\left(\frac{d^n y}{dx^n}, \frac{d^{n-1}y}{dx^{n-1}}, \cdots, \frac{dy}{dx}, x\right) \qquad (6.5)$$

Successive differentiations of x are required to mechanize Eq. (6.5), whereas successive integrations of $d^n y/dx^n$ were called for in instrumenting Eq. (6.4). Ultimately, the entire computer system will consist of interconnected differentiators instead of integrators to satisfy the original differential equation.

There are two major reasons why the method of integration (method 1) is universally accepted in differential analyzers: One reason is that the

process of differentiation is difficult to instrument with sufficient precision. The other is that any irregularities (noise) in operation or in input data usually manifest themselves as relatively small changes in absolute value but large changes in slope. A derivative of a slightly irregular curve may have very wide fluctuations indeed. This tends to instability in a differentiating unit, particularly where the differentiators are cascaded to produce higher-order derivatives. Just the reverse process occurs
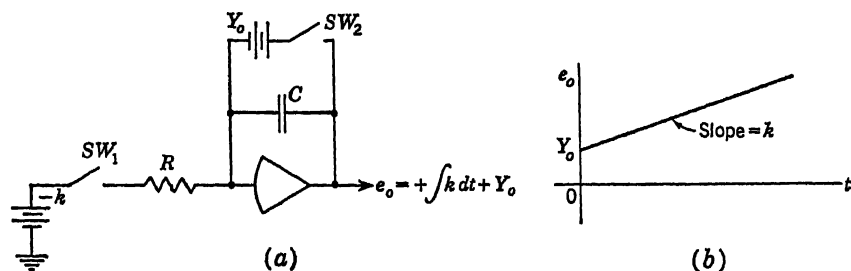
Fig. 6.1

when integrating. Small irregularities in a given curve affect the area under the curve to a very minor degree. The integrator itself thus serves as a smoothing device. This leads to stable operation and accurate results even with cascaded integrators.

6.4. Ordinary Linear Differential Equations. An understanding of differential-analyzer operation is perhaps best obtained by setting up the schematic diagrams for a series of progressively more complex illustrative problems. Consider first the equation

$$\frac{dy}{dt} - k = 0 \tag{6.6}$$

where $y = Y_0$ at $t = 0$. In accordance with the discussion in the previous section, this equation is rearranged as

$$y = \int_0^t k \, dt + Y_0 \tag{6.7}$$

The circuit of Fig. 6-1a is employed to solve this equation. Two switches, one normally open, the other normally closed, possibly both activated by the same relay coil, are employed to apply the initial condition and driving function. At time $t = 0$, the normally open switch SW_1 is closed, applying a fixed d-c voltage proportional to $-k$ to the input of the integrator. At the same instant, the normally closed switch SW_2, through which the capacitor C has been charged to a voltage proportional to Y_0, is opened. The transient voltage at the output of the integrator is then proportional to the desired solution, as shown in Fig.

6.1b. The input resistor R and the feedback capacitor C are selected in such a manner that the product RC is equal to unity. Convenient values for these two circuit elements are 1 megohm and 1 μ respectively. *In applying operational amplifiers, it is always necessary to take into account the sign change inherent in such a circuit.* Thus the input is made proportional to $-k$ rather than $+k$.

Consider now the equation

$$\frac{dy}{dt} + ay - k = 0 \tag{6.8}$$

where $y = Y_0$ at $t = 0$. This expression is rearranged as

$$y = \int_0^t (-ay + k)\, dt + Y_0 \tag{6.9}$$

In this case, the integrator is required to have two inputs, one proportional to $(+ay)$ and the other proportional to $-k$. Since the output of the
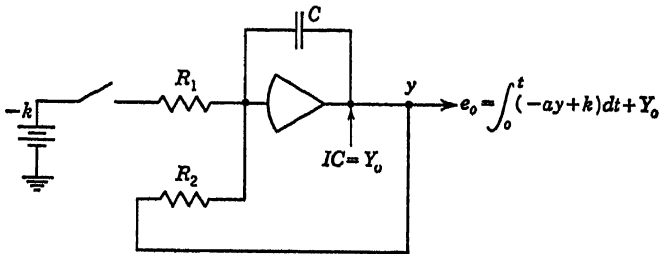
Fig. 6.2

integrator is proportional to y, a simple feedback loop, as shown in Fig. 6.2, can be formed. The values of the resistor R_1 and the capacitor C are again made equal to 1 megohm and 1 μf, respectively. The value of the resistor R_2 is made proportional to $1/a$ megohms. In Fig. 6.2, the initial condition Y_0 is indicated in the more conventional manner. The arrow labeled $IC = Y_0$ has the same significance as the combination of the battery Y_0 and switch SW_2 in Fig. 6.1a.

Consider now the second-order homogeneous equation

$$a\frac{d^2y}{dt^2} + b\frac{dy}{dt} + cy = 0 \tag{6.10}$$

where $y = Y_0$, $dy/dt = \dot{Y}_0$ at $t = 0$. This equation may represent the oscillation of a mass a supported by a spring of spring constant c and damped by a dashpot b, or it may represent the electrical current transient in a series circuit, consisting of an inductor of magnitude a, a capacitor of magnitude $1/c$, and a resistor of magnitude b. The equation is

rearranged as

$$\frac{d^2y}{dt^2} = -\frac{b}{a}\frac{dy}{dt} - \frac{c}{a}y \qquad (6.11)$$

or

$$\frac{dy}{dt} = \int_0^t \left(-\frac{b}{a}\frac{dy}{dt} - \frac{c}{a}y \right) dt + \mathring{Y}_0 \qquad (6.12)$$

where

$$y = \int_0^t \frac{dy}{dt}\, dt + Y_0 \qquad (6.13)$$

The solution of Eq. (6.12) requires two integrations as well as one sign-changing operation. According to Eq. (6.12), dy/dt is formed by integrating the sum of two terms. In order to obtain a voltage proportional to $+dy/dt$ at the output of amplifier 1 in Fig. 6.3 (taking into account the sign change inherent in the integration operation), it is necessary to
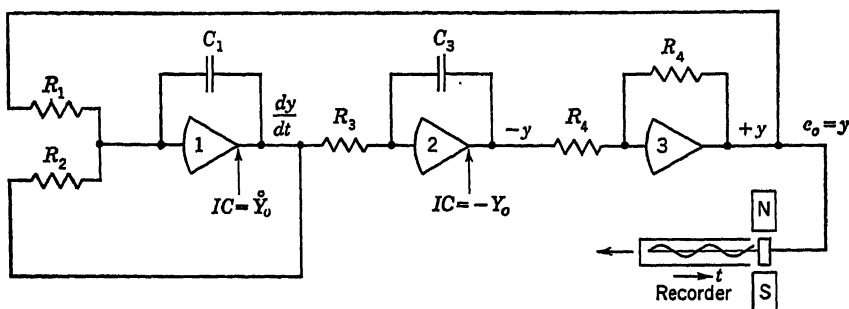
Fig. 6.3

apply to the input terminals voltages proportional to $+y$ and $+dy/dt$, respectively. Resistors R_1 and R_2 are then adjusted to take into account the parameters of the equation. If C_1 is 1 μf, R_1 and R_2 are made equal to a/c and a/b megohms, respectively. The input voltage dy/dt is obtained by feeding back the output of amplifier 1 to its own input resistor R_2; the other input $+y$ is obtained by integrating the output of amplifier 1 to obtain a voltage proportional to $-y$. The product R_3C_3 is made equal to unity. The output of integrator 2 is applied to a sign changer to obtain a voltage proportional to $+y$, and this voltage is then fed back to the input of amplifier 1. Initial conditions proportional to $-y$ and dy/dt at time $t = 0$ are applied to integrators 1 and 2 as specified. The transient voltage at the output of amplifier 3 is proportional at every instant of time to the variable y of the original system and can be recorded by means of a strip-chart recorder or some other output device. If desired, the transient voltage at the output of amplifier 1 can also be recorded.

If the right-hand side of Eq. (6.10) is not equal to zero but is either a constant or a function of time, the circuit of Fig. 6.3 is readily modified,

as shown in Fig. 6.4, by including a third input resistor in the circuit of amplifier 1. The excitation—either a constant d-c voltage or a transient voltage as specified—is then applied to amplifier 1 through this resistor R_1. In Fig. 6.4 the positions of the second integrator and of the sign changer have been interchanged. The operation of this circuit will be similar to that of Fig. 6.3, provided $R_4 = R_5$ and $R_6C_2 = 1$.

The rate at which integration occurs in the computing circuit (Fig. 6.3), in comparison with the rate at which it occurs in the actual problem represented by Eq. (6.10), depends on the value of the fundamental time constant of the computer: $T = R_3C_3 = C_1R_1(a/c)$. If $T = 1$, as has been assumed in the discussion so far, a unit time base results and a
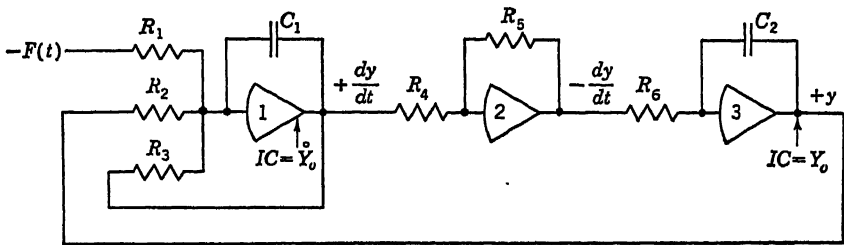
Fig. 6.4

1:1 correspondence of time scale exists between Eq. (6.10) and the computer. If $T = n$, a number either larger or smaller than unity, events in the computer will require intervals of time which are n times as great as the durations of corresponding events in Eq. (6.10). In general, it is necessary to select an appropriate time scale factor n to obtain optimum operation of the computer. A scale factor must also be established for the output voltages of the various computing units in order that the voltages and currents do not exceed the ratings of the amplifiers and are of convenient magnitudes. The problem of scale factoring is examined in some detail in the next two sections.

6.5. Time Scale Factors. Operation on the basis of a unit time scale (*i.e.*, in real time) has certain advantages as well as disadvantages. With a 1:1 correspondence between the rate at which an event occurs in the analog computer and the rate at which the same event occurs in the physical system whose equation is under study, certain of the elements of the physical system can be incorporated into the analog. For example, all the external response characteristics of a flying airplane can be represented on a unit time base electronic analog computer. An actual automatic pilot which is proposed for the given airplane can be incorporated in the system, mounted on a servo-driven table operated by signals received from the computing elements. The movements of the table affect the automatic pilot, which, in turn, sends signals back to the

computing elements just as it would to the control elements of the actual airplane. The computing elements thus *simulate* the airplane, and as far as the automatic pilot is concerned, it appears to be flying the physical airplane whose equation of motion is that represented by the computing unit. Computers applied in this manner are often called "simulators."[20] All the actual characteristics of the automatic pilot, regardless of their complexity, are thus incorporated into the simulated airplane. The interactions between the control unit (automatic pilot) and the simulator are observed. This leads to the proper design of a control unit for air-draft of specified characteristics without entailing the danger and expense of actual flying an untried combination of control unit and airplane. Simulation has been used in countless applications involving controls of various types. Typical of these are an aircraft-engine cooling control study,[21] and a pneumatic process controller.[22]

A disadvantage of operating in real time becomes evident when the solution time for a given equation is long. Amplifier drift and capacitor leakage may then introduce noticeable errors. In addition, the time required for a solution may be undesirably long or even impractical. A limitation also occurs when the real solution time is of extremely short duration (*e.g.*, the travel of a rifle bullet through a gun barrel). In the one case it would be desirable to speed up the solution time by some convenient factor so that families of solutions can be obtained in a reasonably short interval of time. In the other case it would be desir-able to stretch the solution time to a point where the servos, computing amplifiers, and recording instrumentation could follow the solution accu-rately and produce readable results. Obviously, actual control elements could then not be incorporated, so that the entire system must be repre-sented by computing elements.

When it is unnecessary or undesirable to operate on a unit time base, the choice of a computing period will depend at least in part on the nature of the recording and indicating equipment used. Where direct-inking recording equipment is used, the time base must be chosen to meet the frequency-response characteristics of such recording units. In addition, phase shifts in the operational amplifiers and inertia in servo multi-pliers limit the maximum permissible frequencies. Where servo multi-pliers or servo-driven output equipment is employed, the maximum problem frequencies which can be handled rarely exceed 5 cps. Galva-nometer-type oscillographs sometimes have linear frequency-response characteristics to frequencies in excess of 200 cps. Phase-shift errors in commercial electronic equipment begin to appear at frequencies of about 100 cps.

The time-scale-factor problem generally involves two separate phases: First, the problem to be solved must be examined and analyzed to esti-

mate as closely as possible the highest frequencies of interest. If it appears undesirable to operate in real time, it is then necessary either to modify, by effecting suitable changes in variable, the differential equations to be instrumented on the computer, or to effect the time scale change directly by suitably modifying the time constants of all the integrators included in the computer system.

The estimation of the maximum frequencies present in the system under analysis is frequently a difficult matter. If the system behavior is governed by second-order differential equations, however, the following concepts can be used to advantage. The equation

$$a \frac{d^2y}{dt^2} + cy = k \tag{6.14}$$

has a particular solution of the form

$$y = A \sin \omega_n t \tag{6.15}$$

where the natural frequency ω_n is

$$\omega_n = \sqrt{\frac{c}{a}} \qquad \text{rad/sec}$$

If there is damping in the system, a first derivative of y with respect to t will be present, and the equation becomes

$$a \frac{d^2y}{dt^2} + b \frac{dy}{dt} + cy = k \tag{6.16}$$

with a particular solution of the form

$$y = A \epsilon^{-\alpha t} \sin \omega_d t \tag{6.17}$$

The frequency ω_d is then less than the natural frequency and is given by

$$\omega_d = (\omega_n{}^2 - \alpha^2)^{\frac{1}{2}}$$

where

$$\omega_n{}^2 = \frac{c}{a} \qquad \alpha = \frac{b}{2a}$$

Frequently dynamic equations are written directly in the form

$$\frac{d^2y}{dt^2} + 2\zeta\omega_n \frac{dy}{dt} + \omega_n{}^2 y = k \tag{6.18}$$

where ζ is the damping ratio.

Having approximated the frequencies existing in the problem, it remains to effect a suitable time scale factor change. A straightforward technique is to replace the problem time variable t by a new computer time variable τ such that

$$\tau = nt \tag{6.19}$$

Terms involving derivatives with respect to τ then become

$$\frac{dy}{dt} = n\frac{dy}{d\tau}, \qquad \frac{d^2y}{dt^2} = n^2\frac{d^2y}{d\tau^2}, \qquad \cdots \tag{6.20}$$

Effecting such a transformation on Eq. (6.18) yields

$$n^2\frac{d^2y}{d\tau^2} + 2\zeta\omega_n n\frac{dy}{d\tau} + \omega_n^2 y = k \tag{6.21}$$

The natural frequency of Eq. (6.21) is $1/n$ of the natural frequency of Eq. (6.18). To slow the solution rate of a problem, the scale factor n is made larger than unity. If n is smaller than unity, the magnitude of the system frequency in the computer is increased. It is important, of course, to take due account of this time scale factor change in interpreting the results furnished by the computer. The time axis of the computer output curve must be revised by the factor n to permit interpretation of the results in terms of the problem time t.

Example: A machine weighing 80 lb and supported on four vertical springs has an unbalanced rotating element which results in a disturbing force of 80 lb at a repetition rate of 3,000 rpm. The stiffness coefficient of each spring is 1,000 lb/in., and the damping factor is $\zeta = C/C_c = 0.20$, where C is the damping coefficient and C_c is the critical damping coefficient, $C_c = 2m\omega_n$. The vibrating-mass–spring-dashpot system is governed by the equation

$$m\frac{dy^2}{dt^2} + c\frac{dy}{dt} + ky = F\sin\omega t \tag{6.22}$$

where m = mass of vibrating member, lb-sec²/ft
ω = angular velocity, rad/sec, corresponding to the impressed frequency
F = amplitude of the driving force, in lb
m = vibrating mass, lb-sec²/ft
k = stiffness, lb/ft, of spring equivalent to the four springs acting in parallel
y = vertical displacement from position at rest, ft
In the present case

$$k = 1,000 \times 4 \times 12 = 48,000 \text{ lb/ft}$$
$$m = \frac{80}{32.2} = 2.48 \text{ lb-sec}^2/\text{ft}$$
$$\omega = \frac{2\pi \times 3,000}{60} = 314 \text{ rad/sec} \tag{6.23}$$
$$\omega_n = \sqrt{\frac{k}{m}} = \sqrt{\frac{48,000}{2.48}} = 139 \text{ rad/sec} = 22 \text{ cps}$$
$$C = 2m\omega_n\zeta = 2 \times 2.48 \times 139 \times 0.2 = 138 \text{ lb-sec/ft}$$

Inserting these numerical values in Eq. (6.22) gives

$$2.48\frac{dy^2}{dt^2} + 138\frac{dy}{dt} + 48,000y = 80\sin 314t$$

or

$$\frac{d^2y}{dt^2} + 56\frac{dy}{dt} + 19,300y = 32.3\sin 314t \tag{6.24}$$

If Eq. (6.24) were mechanized without a change in time scale, the output equipment would be unable to record the values of ω and ω_n. The problem must be slowed down so that the highest value of ω falls within the recording range, say, $\omega \lesssim 5$ rad/sec. Decreasing the problem frequencies by a factor of 100 will yield $\omega = 3.14$ rad/sec and $\omega_n = 1.39$ rad/sec. The transformation

$$\tau = 100t \tag{6.25}$$

is therefore appropriate. Making this substitution in Eq. (6.24) gives

$$10^4 \frac{d^2y}{d\tau^2} + 5,600 \frac{dy}{d\tau} + 19,300y = 32.3 \sin 3.14\tau$$

or $\quad \dfrac{d^2y}{d\tau^2} + 0.56 \dfrac{dy}{d\tau} + 1.93y = 32.3 \times 10^{-4} \sin 3.14\tau \tag{6.26}$

The mechanization of Eq. (6.26) yields the circuit shown in Fig. 6.4. The magnitudes of the resistors and capacitors in the circuit are evaluated by identifying the coefficient $1/RC$ of each integrator with the corresponding coefficient in the equation. Thus

$$\frac{1}{R_3C_1} = 0.56 \qquad \frac{1}{R_2C_1} = 1.93 \qquad \frac{1}{R_6C_2} = 1 \tag{6.27}$$

for $C_1 = C_2 = 1$ μf, $R_1 = R_2 = R_4 = R_5 = R_6 = 1$ megohm, $R_2 = 0.52$ megohm, and $R_3 = 1.78$ megohms.

An alternate approach to time scale factoring follows from the recognition that, in the case of linear differential equations, the only elements in the computer which are affected by time scale changes are the input resistors of integrators. A time scale change effects a proportional change in the RC product of each integrator unit but leaves all sign changers and adders unchanged. Rather than vary the magnitudes of integrator input resistors to effect time scale changes, it is convenient to connect a separate potentiometer from each integrator input to ground and to connect the moving tap of this potentiometer to fixed integrator input resistors 1 megohm in magnitude, say. Moving the potentiometer tap from full scale toward ground then has the same effect as increasing the magnitude of the integrator input resistor from 1 megohm to infinity. A change in time scale is effected simply by changing the settings of the input potentiometers at each integrator. This method has the further advantage that the necessity for large input resistors is avoided. It is generally inadvisable to employ computer resistors in excess of 10 megohms, since resistances of these magnitudes may be comparable to leakage resistance through wire insulation, leakage resistances across plug-in boards, etc.

A circuit for the solution of Eq. (6.26) using time scale potentiometers is shown in Fig. 6.5a. The alternative method of notation, described in Sec. 2.15, is particularly suitable for this method of problem setup. A circuit diagram for the same problem, using this notation, is shown in Fig. 6.5b. Note that a 10:1 voltage stepup is used in amplifier 3, since

$1/R_2C_1$ in Eq. (6.27) is greater than unity. To reduce further the speed of the solution by a factor of 2, the setting of each potentiometer is reduced by 50 per cent as shown in Fig. 6.5c.
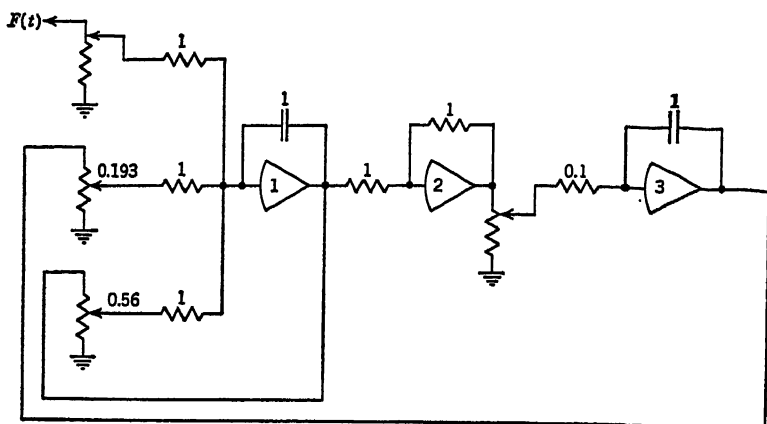
(a)
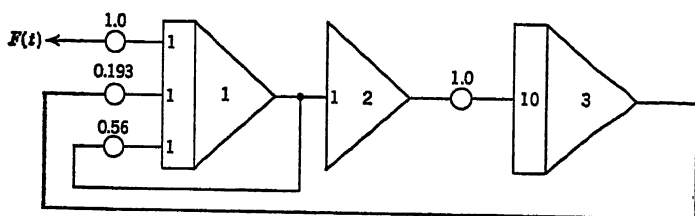
(b)
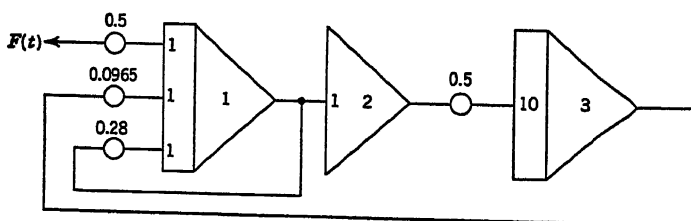
(c)

Fig. 6.5

6.6. Amplitude Scale Factors. In indirect analog computers, the dependent computer variable (*e.g.*, voltage) at the output of each computer unit corresponds to some physical quantity (*e.g.*, displacement, velocity, acceleration, etc.) in the original system under study. In order that the computer results have practical significance, it is necessary to assign amplitude scale factors relating the magnitude of the transient voltage at each point in the computer to the magnitude of the corresponding

problem variable. The selection of amplitude scale factors is governed by two constraints:

1. The output voltage of each operational amplifier is limited by the capabilities of its d-c power supply. In most computers, linear operation is feasible only in the range of −100 to +100 volts. No computer variable must therefore exceed these values at any time during the solution.

2. The accuracy of the computing operation is governed to some extent by the signal-to-noise ratio in the computer. Inevitably, noisy relay contacts, noisy potentiometers, vacuum-tube fluctuations, stray power-line pickup, etc., result in an over-all noise level. For accurate computations, the useful signals should be as large as possible relative to the noise amplitude. In most problems, the dependent variables pass through zero at some time in the computation. Clearly, there is nothing one can do to optimize the signal-to-noise ratio at that point. On the other hand, it is logical to make the maximum amplitudes as large as possible without overloading the amplifiers.

An optimum selection of amplitude scale factors implies a knowledge of the maximum excursion of all the dependent variables of the problem. In general, however, it is the determination of the excursion of the variables which constitutes the solution being sought. It is therefore necessary to make judicious guesses when first programming the computer. Such guesses can be based upon a physical insight into the system under study, a general knowledge of the mathematical characteristics of the governing equations, or a trial-and-error procedure. In the last case, the problem is instrumented on the basis of a first guess and the excursions of the computer variables are noted. If these voltages do not fall in a suitable range, the problem is rescaled and the computer circuit changed accordingly. To assist in the recognition of incorrectly chosen scale factors, a visual indication of amplifier overloading is provided with most general-purpose analog computers. Most commonly, this is accomplished with the aid of neon glow lamps which start to conduct at d-c voltages of the order of 90 volts. A glow lamp is connected between each amplifier output and ground. When an amplifier output reaches or exceeds the breakdown voltage of the lamps, a reddish light is emitted, thereby warning of the overload condition.

Consider the case of the sample problem discussed in the preceding section. According to Eq. (6.26), the driving function is

$$F(t) = 32.3 \times 10^{-4} \sin 3.14t \text{ lb}$$

If a 1:1 relationship between the problem variables and the computer variables were selected, that is, if 1 volt were made proportional to a force of 1 lb, a displacement of 1 ft, and a velocity of 1 ft/sec, it would

be necessary to drive the whole system with a voltage source having a maximum amplitude of 32.3 × 10⁻⁴ volt. Clearly, such a small driving voltage would result in a very unfavorable signal-to-noise ratio and a highly inefficient utilization of the −100- to +100-volt range of the amplifiers. Accordingly, another change in variable such that

$$y = 10^{-4}X \qquad (6.28)$$

is indicated. Equation (6.26) then becomes

$$10^{-4}\frac{d^2X}{d\tau^2} + 0.56 \times 10^{-4}\frac{dX}{d\tau} + 1.93 \times 10^{-4}X = 32.3 \times 10^{-4}\sin 3.14\tau$$

$$\frac{d^2X}{d\tau^2} + 0.56\frac{dX}{d\tau} + 1.93X = 32.3\sin 3.14\tau \qquad (6.29)$$

Now a sinusoidal input voltage having an amplitude of 32.3 volts is specified.

In general, amplitude scale factors can take one of two forms: Either one unit of the problem variable is made to correspond to a specified number of volts, or 100 volts is made to correspond to a specified magnitude of the problem variable. Both methods will yield satisfactory results if applied with logic and care. By either approach, the problem of amplitude scale factoring is not one which lends itself to "cookbook" procedures, and there is no substitute for a careful thinking through and understanding of each step in this scaling operation.

Consider the nonhomogeneous second-order equation

$$m\frac{d^2x}{dt^2} + c\frac{dx}{dt} + kx = F \qquad (6.30)$$

where
$$m = 4 \text{ lb-sec}^2/\text{in.}$$
$$k = 576 \text{ lb/in.}$$
$$c = 9.6 \text{ lb-sec/in.}$$

with initial conditions

$$x = 0 \quad \frac{dx}{dt} = 0 \quad F = 0 \qquad \text{for } t < 0$$

$$x = 0 \quad \frac{dx}{dt} = 0 \quad F = 1{,}000 \text{ lb} \quad \text{for } t = 0$$

$$F = 1{,}000 \text{ lb} \quad \text{for } t > 0$$

The ranges of the variables are approximately $0 < x < 3.5$ in., $-21 < dx/dt < 21$ in./sec, $-250 < d^2x/dt^2 < 250$ in./sec². Rearranging Eq. (6.30),

$$\frac{d^2x}{dt^2} = \frac{F}{m} - \frac{c}{m}\frac{dx}{dt} - \frac{k}{m}x \qquad (6.31)$$

where $F/m = 250$ in./sec^2
$c/m = 2.4$ sec^{-1}
$k/m = 144$ sec^{-2}

The time interval over which the solution is desired is 0.25 sec. Amplifier outputs are to be limited to 100 volts. In numerical form Eq. (6.31) is

$$\frac{dx^2}{dt^2} = 250 - 2.4\frac{dx}{dt} - 144x$$
$$\frac{dx}{dt} = \int_0^t \left(250 - 2.4\frac{dx}{dt} - 144x\right) dt + \dot{x}(0) \tag{6.32}$$

Figure 6.4 is a schematic diagram for the solution of this problem too, provided the function $F(t)$ is made a step input at time $t = 0$. The scale factor on dx/dt may be as high as $S_1 = 100/21$ volts/(in./sec). Let $S_1 = 4.5$, so that the voltage at the output of the first integrator becomes $+4.5\ dx/dt$. The scale factor on x may be as high as $S_2 = 100/3.5$ volts/in. Let $S_2 = 25$, yielding, for the output voltage of amplifier 3, $+25x$. All three quantities at the input of amplifier 1 must have the same scale factor to be added properly. The input and output voltages of this amplifier are related as follows:

$$e_1 = -\int_0^t \left(-\frac{e_o}{R_1C_1} + \frac{e_1}{R_3C_1} + \frac{e_3}{R_2C_1}\right) dt + e_1(0) \tag{6.33}$$

where e_1 and e_3 are the output voltages of amplifiers 1 and 3, respectively, and c_o is the voltage simulating $F(t)$. Comparing with Eqs. (6.32), the following equalities between the actual system and the computer are established (letting $c_o = 250S_3$ and assuming $S_3 = 0.1$ for convenience):

$$250S_3\frac{S_1}{S_3} = \frac{c_o}{R_1C_1}$$
$$2.4S_1\frac{dx}{dt} = \frac{e_1}{R_3C_1} \tag{6.34}$$
$$144S_2x\frac{S_1}{S_2} = \frac{e_3}{R_2C_1}$$

where
$$c_o = 250S_3$$
$$e_1 = S_1\frac{dx}{dt}$$
$$e_3 = S_2x$$

In Eq. (6.34) multiplying factors S_1/S_3 and S_1/S_2 have been employed to give all terms at the input of amplifier 1 the same scale factor. The magnitudes of the input resistors and the feedback capacitors can be found from the equations

$$\frac{S_1}{S_3} = \frac{1}{R_1C_1} \qquad 2.4 = \frac{1}{R_3C_1} \qquad 144\frac{S_1}{S_2} = \frac{1}{R_2C_1} \tag{6.35}$$

so that

$$R_1 C_1 = \frac{0.1}{4.5} = 0.0222$$

$$R_3 C_1 = \frac{1}{2.4} = 0.417 \tag{6.36}$$

$$R_2 C_1 = \frac{25}{144 \times 4.5} = 0.0386$$

If $C_1 = 1\ \mu\text{f}$, then $R_1 = 0.0222$ megohm, $R_3 = 0.417$ megohm, and $R_2 = 38.6K$ ohms.

If amplifier 2 acts as a sign changer, $R_4 = R_5 = 1$ megohm. The output voltage of amplifier 3 is then given by

$$e_3 = -\int_0^t \frac{e_2}{R_6 C_2}\, dt + Y_0$$

$$e_3 = \int_0^t \frac{e_1}{R_6 C_2}\, dt + Y_0 \tag{6.37}$$

where e_2 is the output voltage of amplifier 2. In the actual system, the corresponding relationship is

$$x = \int_0^t \frac{dx}{dt}\, dt + x(0) \tag{6.38}$$

Comparing Eqs. (6.37) and (6.38), the following relations are seen to hold:

$$S_2 x = e_3 \qquad \left(S_1 \frac{dx}{dt}\right)\frac{S_2}{S_1} = \frac{e_1}{R_6 C_2} \tag{6.39}$$

Since $e_1 = +S_1(dx/dt)$, $R_6 C_2 = S_1/S_2 = 0.18$; for $C_2 = 1\ \mu\text{f}$, $R_6 = 0.180$ megohm.

A different technique for the scaling of more complex and nonlinear problems is considered in Sec. 6.9.

6.7. Simultaneous Differential Equations. The dynamic behavior of systems with more than one degree of freedom is characterized by two or more differential equations. These ordinary differential equations must be solved simultaneously. For example, in the analysis of a coupled dynamical system with two degrees of freedom, a set of equations of the following type may arise:

$$\frac{d^2 y_1}{dt^2} + a_1 \frac{dy_1}{dt} + b_1 y_1 = c_1 \frac{d^2 y_2}{dt^2}$$

$$\frac{d^2 y_2}{dt^2} + a_2 \frac{dy_2}{dt} + b_2 y_2 = c_2 \frac{d^2 y_1}{dt^2} \tag{6.40}$$

where, at $t = 0$,

$$y_1 = Y_1 \qquad \frac{dy_1}{dt} = \dot{Y}_1 \qquad y_2 = Y_2 \qquad \frac{dy_2}{dt} = \dot{Y}_2 \tag{6.41}$$

Following the usual procedure of solution, these equations are rearranged as

$$\frac{d^2y_1}{dt^2} = -a_1 \frac{dy_1}{dt} - b_1 y_1 + c_1 \frac{d^2y_2}{dt^2} \tag{6.42}$$

$$\frac{d^2y_2}{dt^2} = -a_2 \frac{dy_2}{dt} - b_2 y_2 + c_2 \frac{d^2y_1}{dt^2} \tag{6.43}$$

$$\frac{dy_1}{dt} = \int_0^t \frac{d^2y_1}{dt^2}\, dt + \dot{Y}_1 \qquad y_1 = \int_0^t \frac{dy_1}{dt}\, dt + Y_1 \tag{6.44}$$

$$\frac{dy_2}{dt} = \int_0^t \frac{d^2y_2}{dt^2}\, dt + \dot{Y}_2 \qquad y_2 = \int_0^t \frac{dy_2}{dt}\, dt + Y_2 \tag{6.45}$$

The mechanization of these relations is shown in Fig. 6.6. Summing amplifiers 4 and 8 satisfy Eqs. (6.42) and (6.43). Integrators 1 and 2
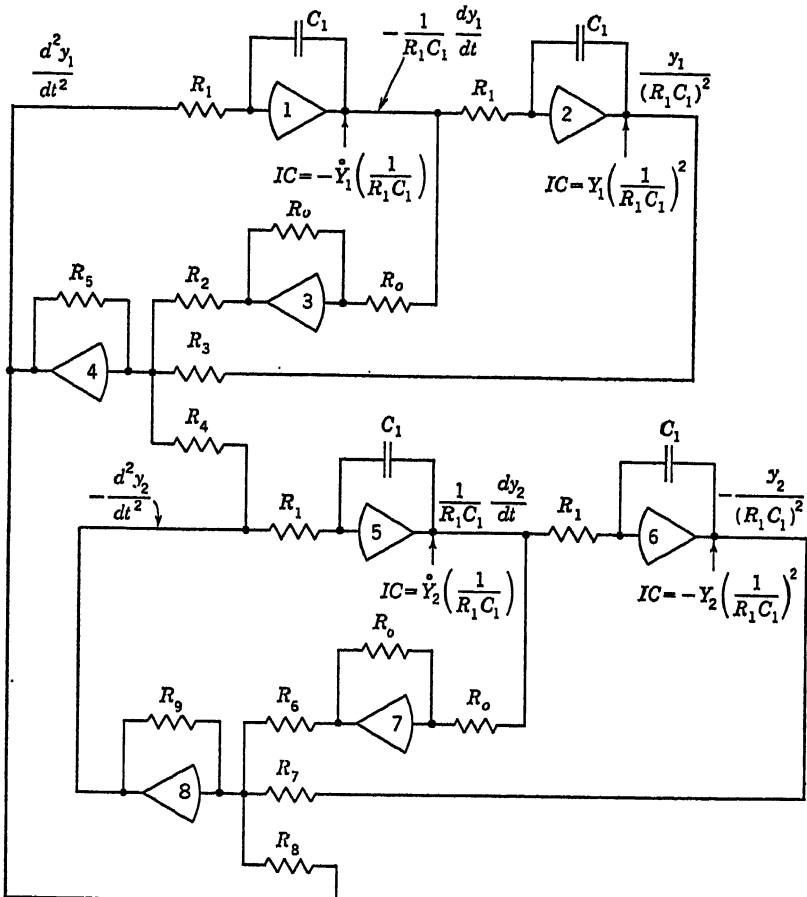
Fig. 6.6

satisfy Eq. (6.44), while integrators 5 and 6 satisfy Eq. (6.45). Amplifiers 3 and 7 serve merely as sign changers with $R_1C_1 = 1$ and a 1:1 time scale. The input and feedback resistors of the circuit are chosen so that $R_5/R_2 = a_1$, $R_5/R_3 = b_1$, $R_5/R_4 = c_1$, $R_9/R_6 = a_2$, $R_9/R_7 = b_2$, and $R_9/R_8 = c_2$. Actually, amplifiers 4 and 8 need not be used because the required summations can be performed simultaneously with the integrations in amplifiers 1 and 5. The two processes are separated in this example to focus attention on the time constant R_1C_1. Notice that this network consists actually of two separate closed loops, satisfying separately each of the two simultaneous equations. These two loops are interconnected through resistors R_4 and R_8 as specified by the equation.

If some time base other than unity is desired in the computer circuit of Fig. 6.6, R_1C_1 would be assigned a value different from unity. Suppose, for example, that the computer is to operate in time τ, where τ and t are related by the equation

$$\tau = nt \tag{6.46}$$

Thus, for $n < 1$, the computer operates in speeded-up time, and for $n > 1$, it operates in slowed-down time. Substitution of Eq. (6.46) into Eqs. (6.40) and (6.41) yields

$$n^2 \frac{d^2y_1}{d\tau^2} + a_1 n \frac{dy_1}{d\tau} + b_1 y_1 = c_1 n^2 \frac{d^2y_2}{d\tau^2}$$
$$n^2 \frac{d^2y_2}{d\tau^2} + a_1 n \frac{dy_2}{d\tau} + b_2 y_2 = c_2 n^2 \frac{d^2y_1}{d\tau^2} \tag{6.47}$$

Equations (6.42) to (6.45) then become

$$\frac{d^2y_1}{d\tau^2} = -\frac{a_1}{n}\frac{dy_1}{d\tau} - \frac{b_1}{n^2}y_1 + c_1 \frac{d^2y_2}{d\tau^2}$$
$$\frac{d^2y_2}{d\tau^2} = -\frac{a_2}{n}\frac{dy_2}{d\tau} - \frac{b_2}{n^2}y_2 + c_2 \frac{d^2y_1}{d\tau^2}$$
$$\frac{dy_1}{d\tau} = \int_0^t \frac{d^2y_1}{d\tau^2} d\tau + \dot{Y}_1 \qquad y_1 = \int_0^t \frac{dy_1}{d\tau} d\tau + Y_1 \tag{6.48}$$
$$\frac{dy_2}{d\tau} = \int_0^t \frac{d^2y_2}{d\tau^2} d\tau + \dot{Y}_2 \qquad y_2 = \int_0^t \frac{dy_2}{d\tau} d\tau + Y_2$$

The mechanization of these relations follows the same pattern as for Eqs. (6.42) to (6.45). It should be noted that $(1/n) dy_1/d\tau$ and $(1/n) dy_2/d\tau$ must be generated by integrators 1 and 5, and $(1/n^2)y_2$ and $(1/n^2)y_1$ must be produced by integrators 2 and 6. This is accomplished by making $R_1C_1 = n$.

6.8. Feedback-system Equations. Electronic analog computers are particularly suited to the simulation and study of closed-loop control systems. Such systems are generally composed of a number of units

which may include electronic amplifiers, electric motors, pneumatic elements, etc. The behavior within the system of each one of these units is compactly expressed in terms of transfer functions relating the output variable of each unit to its input variable. Such a transfer function is ordinarily expressed as a quotient of two polynomials in s, the Laplace-transform parameter. Two approaches can be employed to treat systems of this type: The entire system behavior can be expressed by a series of simultaneous differential equations, and these equations can be solved by the methods indicated in the preceding section. A more economical approach is to utilize the complex transfer-function elements described in Sec. 2.13. The behavior of each complete unit within the automatic control system is then simulated by a single amplifier with complex resistance-capacitance networks as the input and feedback impedances.
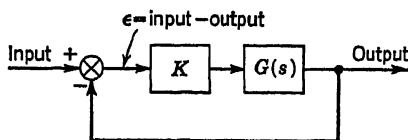
Fig. 6.7

Consider, for example, the automatic control system shown in Fig. 6.7. In this figure, the block labeled $G(s)$ is specified to have a transfer function

$$G(s) = \frac{s+1}{s(2s+1)[(s/20)+1]} \tag{6.49}$$

which can be written as

$$G(s) = \frac{s+1}{2s+1} \frac{1}{s[(s/20)+1]} \tag{6.50}$$

where $(s+1)/(2s+1)$ represents a lag-lead term and $1/s[(s/20)+1]$ represents a motor term. Both of these terms may be considered as unalterable. In this case, the only alterable variable is the amplification K of the amplifier.

Since the transfer function $G(s)$ is fixed, it may be desirable to rearrange the factors in Eq. (6.50) to allow more convenient representation by the transfer functions listed in Appendix 1. If the input and feedback impedances Z_1 and Z_f are made,

$$\begin{aligned} Z_1 &= 2s+1 \\ Z_f &= \frac{s+1}{s[(s/20)+1]} \end{aligned} \tag{6.51}$$

The voltage transfer ratio of the circuit is given by

$$\frac{e(s)_o}{e(s)_1} = -\frac{s+1}{s(2s+1)[(s/20)+1]} = -G(s) \tag{6.52}$$

The negative sign introduced by the operational amplifier can be eliminated, if necessary, by employing an additional amplifier as a sign changer.

A number of the circuits listed in Appendix 1 are suitable for the synthesis of the required transfer functions. Two of these are shown in Fig. 6.8b and c. For the circuit of Fig. 6.8b, the transfer function is

$$Z_1 = 2R_1 \left(\frac{R_1 C_1 s}{2} + 1 \right) \tag{6.53}$$

if R_1 is made 0.5 megohm, and if C_1 is made 8 μf, the transfer impedance specified by Eqs. (6.51) is realized.

(a)

(b)

(c)
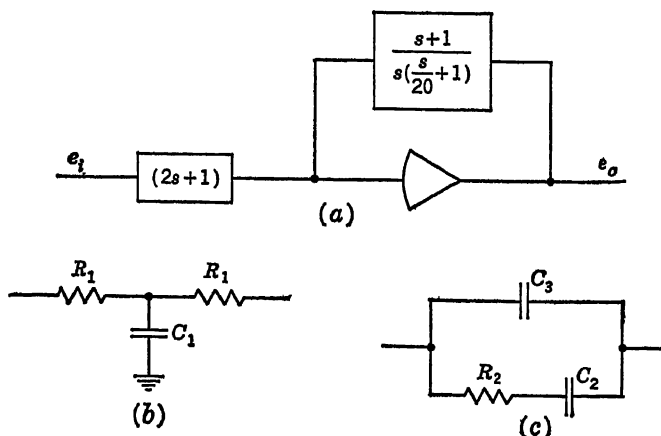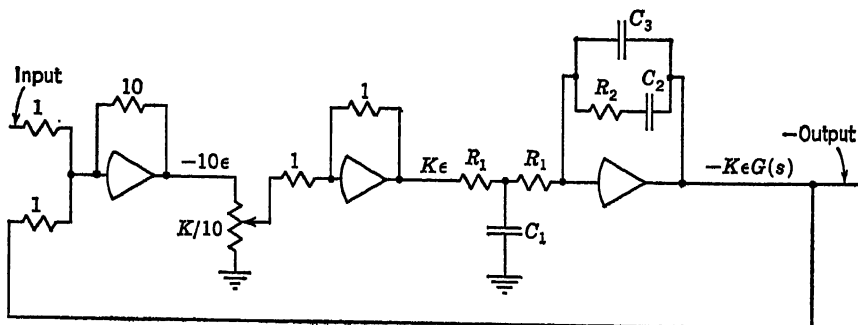
Fig. 6.8

Fig. 6.9

Z_f can be synthesized by means of the circuit shown in Fig. 6.8c, the transfer function of which is given by

$$Z_f = \frac{1}{s(C_2 + C_3)} \frac{1 + R_2 C_2 s}{1 + R_2 C_2 C_3 s / C_2 + C_3} \tag{6.54}$$

To conform to Eqs. (6.51), R_1 should be made 1.025 megohms while C_2 and C_3 are made 0.95 and 0.05 μf, respectively. To obtain more convenient element values, i.e., a smaller C_1 and a larger C_3, identical

constant multipliers can be applied to the expressions of both impedances in Eqs. (6.51). This constant multiplier will cancel out in Eq. (6.52). Or the entire transfer function specified in Eq. (6.49) can be multiplied by a constant and this constant taken into account elsewhere in the analog system.

The final circuit for the system of Fig. 6.7 is shown in Fig. 6.9. It is, of course, not necessary to represent the entire transfer function of each unit by a single amplifier. Each factor in the transfer function can be represented by a separate computer unit.

6.9. Equations with Nonlinear and Time-varying Coefficients. Non-linear differential equations arise most frequently in physical problems,
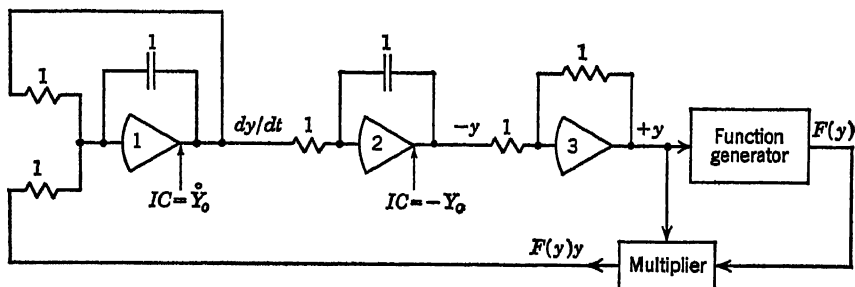
Fig. 6.10

because the system parameters are a function of one or more of the dependent variables. For example, the spring constant of a spring in a dynamic system may depend upon the elongation of the spring, or the thermal conductivity of a heat conductor may be governed by the temperature. Problems of this type can be solved readily on electronic analog computers by augmenting the simple closed-loop circuits, already described, with function generators and multipliers. Units of this type are discussed in considerable detail in Chaps. 3 and 4. Consider, for example, the second-order nonlinear differential equation

$$\frac{d^2y}{dt^2} + \frac{dy}{dt} + F(y)y = 0 \qquad (6.55)$$

where $\qquad y = Y_0 \qquad$ and $\qquad \dfrac{dy}{dt} = \dot{Y}_0 \qquad$ at $t = 0$

The term $F(y)$ may be an analytic function such as y^2, cos y, or log y; it may be a discontinuity function, being constant over certain ranges of y and assuming different values outside these ranges; or it may be a function which is furnished in graphical form. In the design of the analog computer circuit to solve this equation, the choice of the type of function generators to be utilized is governed to a large extent by the nature of $F(y)$. The circuit shown in Fig. 6.10 demonstrates the general

approach to problems of this type. Note the use of the function generator and multiplier to generate the product $F(y)$ to be applied at the input of integrator 1. In all other respects, this circuit is similar to that of Fig. 6.3 for the solution of the linear second-order differential equation. Nonlinear coefficients of the first derivative term or higher derivative terms can be handled in a similar manner.

Occasionally, the parameters of a physical system under study are functions of time or other independent variables. It then becomes necessary to generate a voltage proportional to time and to apply this
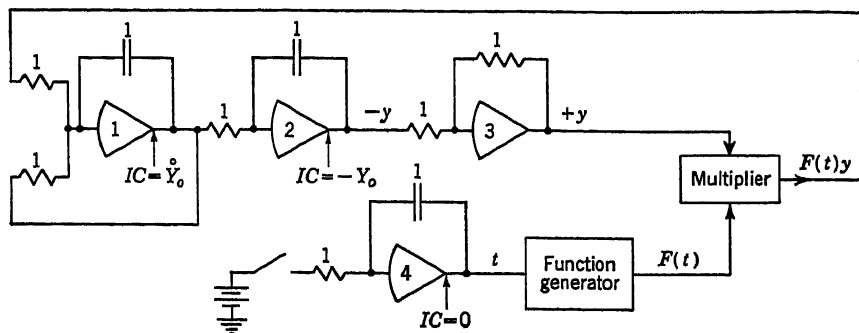
Fig. 6.11

voltage to a suitable function generator. The output of the function generator is then multiplied by the appropriate dependent variable as specified by the problem, and the product is introduced into the feedback loop. A linear function of time, serving as the input to the function generator, is best obtained by integrating a step function, generated by applying a constant d-c voltage source to the input of an integrator at time $t = 0$. Consider the equation

$$\frac{d^2y}{dt^2} + \frac{dy}{dt} + F(t)y = 0 \tag{6.56}$$

where at $t = 0$, $y = Y_0$ and $dy/dt = \dot{Y}$. The computer circuit for the solution of this equation is shown in Fig. 6.11. Integrator 4 serves to generate the linear time function.

Example: To illustrate in detail the problems involved in scaling nonlinear equation and equations with time-varying coefficients, consider the following problem contributed by Bekey.[23] The transient current is to be determined in an electrical circuit consisting of a resistor, an inductor, and a capacitor in series with a sinusoidal voltage source, as shown in Fig. 6.12a. The magnitude of the resistor as a function of time is shown graphically in Fig. 6.12b; the capacitor has a magnitude which is a function of the current i, as shown in Fig. 6.12c. The inductor L has a constant magnitude of 1.2 henrys, while the voltage source has an amplitude of 30 volts and a frequency of 60 cps. i and di/dt are equal to zero at time $t = 0$. It is estimated that

the absolute value of the current never exceeds 25 ma. The Kirchhoff-law equation governing this current is

$$E(t) = L\frac{di}{dt} + R(t)i + \frac{1}{C(i)} \int_0^t i\, dt \tag{6.57}$$

The first step in programming this equation is to select a suitable time scale. The frequency of the applied voltage, 60 cps, is too fast for servo-driven recorders and servo
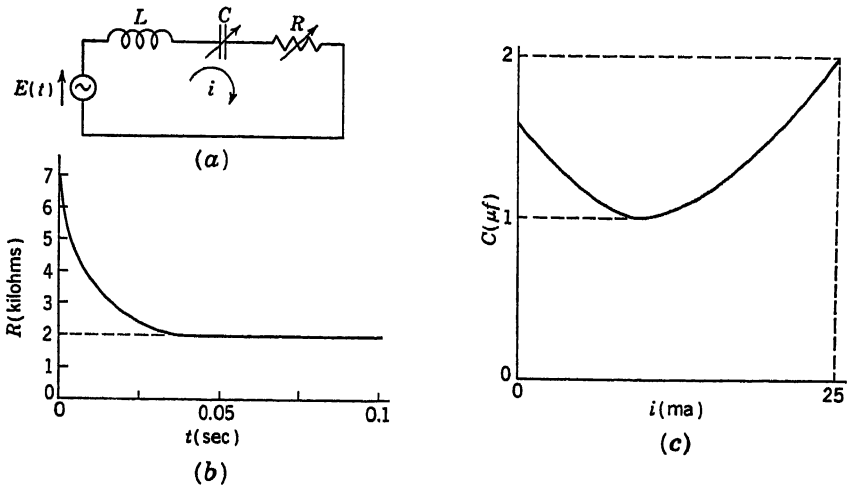
Fig. 6.12

multipliers. If it is desired to view the transient current over several cycles, a solution time of 10 to 20 sec/cycle is probably satisfactory. This suggests using

$$\tau = 10^3 t$$

or

$$t = \frac{\tau}{10^3} \tag{6.58}$$

Effecting this change of variable in Eq. (6.57) and inserting the specified numerical values yield

$$30 \sin\left(\frac{2\pi \times 60}{10^3} \tau\right) = 1.2 \times 10^3 \frac{di}{d\tau} + R\left(\frac{\tau}{10^3}\right) i + \frac{10^{-3}}{C(i)} \int_0^t i\, d\tau \tag{6.59}$$

Rearranging this equation in the customary manner, to solve for the highest-order derivative, and simplifying yields

$$\frac{di}{d\tau} = 0.025 \sin 0.377\tau - \frac{R(\tau/10^3)i}{1.2 \times 10^3} - \frac{1}{1.2 \times 10^6 C(i)} \int_0^t i\, d\tau \tag{6.60}$$

A preliminary block diagram for the solution of this equation is shown in Fig. 6.13. The nonlinear capacitance and time-varying resistance are to be introduced by means of function generators and multipliers. For the generation of the sinusoidal driving function, the circuit illustrated in Fig. 4.37 can be employed.

The next step in the solution of this problem is the selection of suitable amplitude scale factors. This necessitates an estimation of the maximum values attained by all variable quantities of the problem. These can be obtained from specified data and
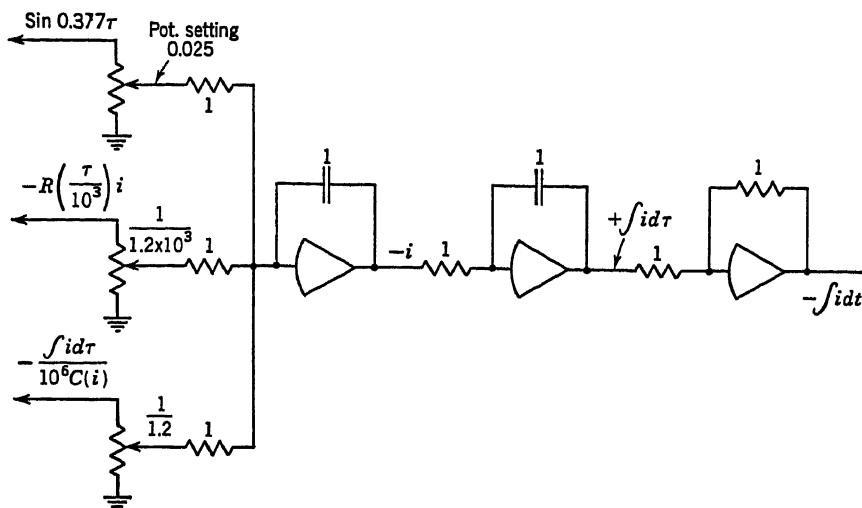
Fig. 6.13

the graphs of Fig. 6.12. An estimate of the maximum value of the quantity $\int_0^t i\,d\tau$ is obtained by assuming that the full applied voltage exists across the capacitor. Since

$$E(t)_{max} = 30 = \frac{1}{C}\int_0^t i\,dt = \frac{1}{10^3 C}\int_0^t i\,d\tau \tag{6.61}$$

and since the capacitor attains the maximum value of 2 μf,

$$\left(\int_0^t i\,d\tau\right)_{max} = 10^3 E(t)_{max} C_{max} = 10^3 \times 30 \times 2 \times 10^{-6} = 0.060 \tag{6.62}$$

Recognizing that the maximum permissible voltage excursions at the output of each amplifier are ± 100 volts, scale factors in volts per unit of variable can now be selected. Table 6.1 represents a summary of the variable quantities of the problem, their estimated maximum values, and the maximum permissible scale factors which can be used.

<div align="center">TABLE 6.1</div>

Quantity	Estimated maximum value	Maximum permissible scale factor, volts/unit
i	25×10^3	4×10^3
R	7×10^3	10^{-2}
C	2×10^{-6}	50×10^6
$\int_0^t i\,d\tau$	0.060	10^3
Ri	175	0.5
$\dfrac{\int_0^t i\,d\tau}{10^6 CL}$	0.050	20×10^2

On the basis of these scale factors, the circuit diagram can now be completed as shown in Fig. 6.14. In this diagram, the significances of the voltage appearing at various points in the circuit, in terms of the problem variables, are indicated directly. The scale factors of coefficients are indicated in parentheses above the potentiometers.
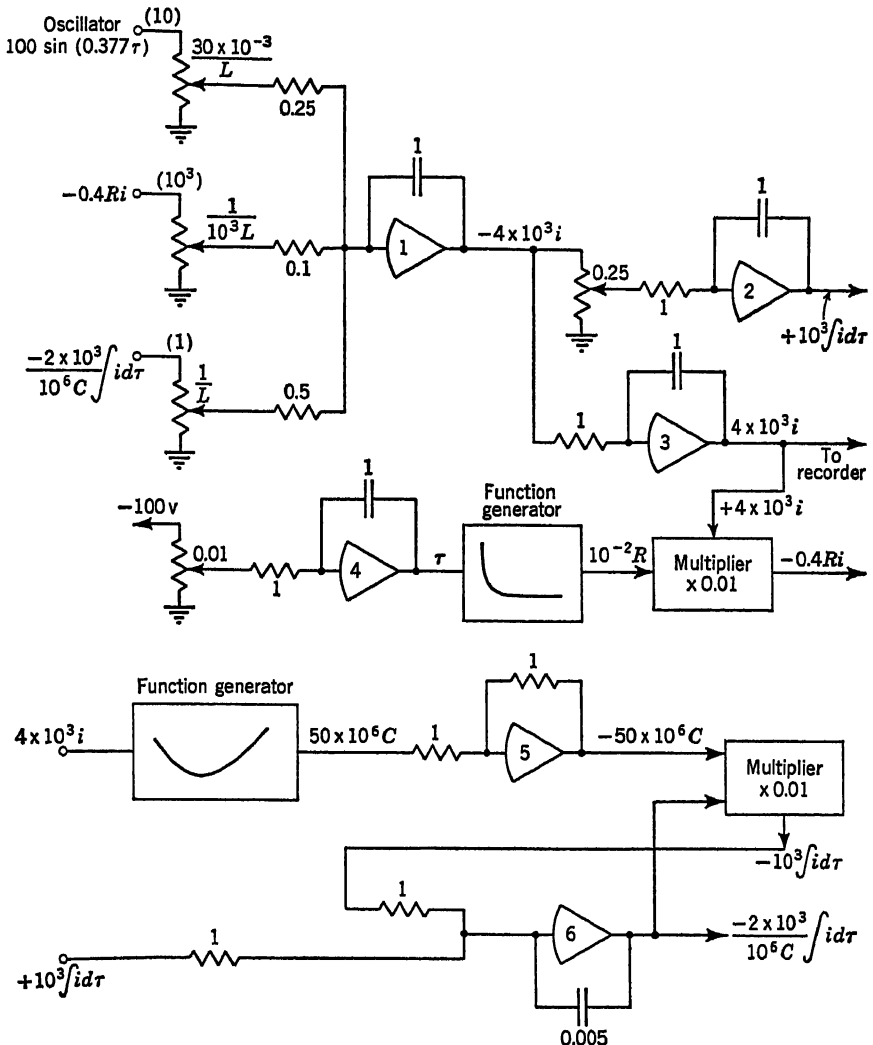
Fig. 6.14

This approach to scale factoring, differing to some extent from that presented in Sec. 6.6, generally results in a clearer and simpler representation of complex problems. In effect, the numerical scale factors are carried along with the variables, rather than assigning new symbols S_1, S_2, etc., to them. In this schematic, it should be noted that amplifiers 3 and 5 can generally be omitted, since most function generators are

capable of generating positive or negative functions directly as required. The solution of this problem as obtained from an actual oscillograph-record chart is shown in Fig. 6.15.

6.10. Two-point Boundary Conditions. Differential analyzers are particularly suited to the solution of a class of differential equations known as "initial-value problems." In such problems, the magnitudes of the dependent variable and its derivatives are all specified for an initial time: $t = 0$. The specified initial conditions are translated directly, in programming the computer, into initial charges on the capacitors of all integrators. Occasionally, in engineering work, there arise problems governed by differential equations for which the dependent variable is specified for two values of the independent variable. For example, the current in an electrical circuit may be specified for two different values of time. If conditions at both ends of an interval of integration are specified, in general not enough is known about the starting condition, so that the correct final conditions will result upon integration. This means that trial solutions must be made for a number of assumed starting conditions; the correct starting condition must be determined by interpolation to satisfy also the required final conditions. In the case of a simple second-order equation such as Eq. (6.11), whose analog-computer solution is illustrated in Fig. 6.3, this means varying in an iterative manner the initial condition applied to one of the integrators. For example, if the variable y is specified to be $y = Y_0$ at time $t = 0$ and $y = Y_{30}$ at $t = 30$ sec, the initial condition on amplifier 2 in Fig. 6.3 is made proportional to $-Y_0$. The initial condition on amplifier 1 is varied, and successive plots of y as a function of t are made. The initial condition $\dot{Y}_0$ is readjusted until the value of y, indicated on the recorder 30 sec after the commencement of the run, corresponds to the specified final condition Y_{30}.

Greenspan[24] has presented a method for transforming a two-point boundary-value problem into two initial-value problems, each of which can be solved separately on the electronic analog computer. The results obtained by these separate solutions are then combined to yield the complete solution of the boundary-value problem. Suppose one has the

Fig. 6.15

equation

$$\frac{d^2y}{dt^2} + P\frac{dy}{dt} + Qy = R \tag{6.63}$$

where

$$\begin{array}{lll} y = c_1 & \text{at } t = a \\ y = c_2 & \text{at } t = b & b > a \end{array}$$

and where P, Q, and R may be functions of time, and a solution of y as a function of time is desired. A subsidiary equation in $u = u(t)$ is formed such that

$$\frac{d^2u}{dt^2} + P\frac{du}{dt} + Qu = R \tag{6.64}$$

where

$$u = d_1 \quad \text{and} \quad \frac{du}{dt} = d_2 \quad \text{at } t = a$$

d_1 and d_2 are arbitrary constants. A second equation in $v = v(t)$ is next constructed, such that

$$\frac{d^2v}{dt^2} + P\frac{dv}{dt} + Qv = R \tag{6.65}$$

where

$$v = e_1 \quad \text{and} \quad \frac{dv}{dt} = e_2 \quad \text{at } t = a$$

Here e_1 and e_2 are again arbitrary constants, which must be different from d_1 and d_2. The functions $u(t)$ and $v(t)$ are readily obtained by means of the analog computer. It can be demonstrated that the required solution $y(t)$ can be formed by combining these two preliminary solutions according to the equation

$$y(t) = \frac{c_1v(b) - c_2e_1}{d_1v(b) - e_1u(b)} u(t) + \frac{c_2d_1 - c_1u(b)}{d_1v(b) - e_1u(b)} v(t) \tag{6.66}$$

where $u(b)$ and $v(b)$ are the values of u and v at time $t = b$ as obtained from the computer runs.

Consider, for example, the simple equation

$$\frac{d^2y}{dt^2} + y = 0$$

where

$$\begin{array}{lll} y = 1 & \text{at } t = 0 \\ y = 2 & \text{at } t = 1 \end{array} \tag{6.67}$$

The subsidiary equations become

$$\frac{d^2u}{dt^2} + u = 0$$

$$u = 1 \qquad \frac{du}{dt} = 0 \qquad \text{at } t = 0 \tag{6.68}$$

$$\frac{d^2v}{dt^2} + v = 0$$

$$v = 0 \qquad \frac{dv}{dt} = 1 \qquad \text{at } t = 0 \tag{6.68a}$$

The initial conditions on u, du/dt, v, and dv/dt were selected arbitrarily and for convenience. These equations are then solved separately on the computer, and the values of u and v at time $t = 1$ are noted. In the present simple example, it is evident that the solution of Eq. (6.68) is $u = \cos t$ and the solution of Eq. (6.68a) is $v = \sin t$. Therefore $u(b) = \cos 1$ and $v(b) = \sin 1$. In terms of the above development, the pertinent constants are

$$\begin{array}{ll} c_1 = 1 & e_1 = 0 \\ c_2 = 2 & e_2 = 1 \\ d_1 = 1 & u(b) = \cos 1 \\ d_2 = 0 & v(b) = \sin 1 \end{array} \tag{6.69}$$

In accordance with Eq. (6.66), the solution of the problem becomes

$$y(t) = u(t) + \frac{2 - \cos 1}{\sin 1} v(t) \tag{6.70}$$

or $\qquad y(t) = u(t) + 1.73v(t)$

The required addition of the two time functions $u(t)$ and $1.73v(t)$ can be performed graphically or with the aid of additional computing equipment.

6.11. Statistical Inputs. Many engineering systems are subject to excitations whose time function can be expressed only in statistical terms. Whenever noise is present in a system, the analysis and design of such systems involve the treatment of inputs which are combinations of predictable and random functions of time. Common sources of noise include thermal noise in vacuum tubes, contact noise in electrical potentiometers and other components, random mechanical vibrations in gear systems, static from atmospheric disturbances, etc. The electronic analog computer has been of great utility in analyzing both linear and nonlinear physical systems subjected to noise.

In the case of nonlinear systems, it is usually necessary to employ electrical noise generators having specified spectral characteristics. Such devices are discussed in Sec. 4.12. Either these units can be employed to generate complete plots of the dependent variables of interest as a

function of time, or by means of repeated runs, the values of the dependent variables at specific instants of time can be obtained. In the latter case, conventional statistical techniques are employed to interpret the ensemble of these solutions.

In the case of linear systems with constant or time-varying parameters, a special method due to Bennett,[25] termed the *adjoint* technique, can be used to advantage. Any linear system can be characterized by a weighting function $h(t_2,t_1)$, which is defined as the system output measured at time t_2, resulting from an excitation in the form of a unit impulse applied at the input terminals of the system at time t_1, where $t_2 > t_1$. Since the superposition principle applies to linear systems, the response to arbitrary inputs can then be expressed in terms of the weighting function.

If the input to the linear system is a function of time $e_1(t)$, the output $e_o(t)$ at a specific instant of time t_2 can be expressed by

$$e_o(t_2) = \int_{-\infty}^{t} e_1(t)h(t_1,t_2)\, dt_1 \qquad (6.71)$$

In the particular case in which the input is white noise of spectral density N, the mean square ensemble output at time t_2 is given by

$$\overline{e_o{}^2(t_2)} = \frac{N}{2} \int_{-\infty}^{t} h^2(t_2,t_1)\, dt \qquad (6.72)$$

The symbol on the left-hand side of Eq. (6.72) signifies the average of the square of the outputs e_o of a large number of identical systems, each subjected to noise having similar statistical characteristics, all measured at time t_2.

The analog computer is employed to determine the appropriate weighting function, which is generally very difficult to determine by analytical methods. To solve Eqs. (6.71) and (6.72) directly would require the introduction of unit impulses at time t_1 into the simulated system. Since t_1 is the variable of integration in these equations, it would be necessary to take a large number of computer runs for various values of t_1. Lanning[26] has demonstrated that, by using a new variable defined as

$$\tau = t_2 - t_1 \qquad (6.73)$$

and by replacing the system under study by a closely related system called the *adjoint*, the desired weighting function can be computed directly. To construct the adjoint system on the analog computer, the original system is first set up in the conventional manner using whatever units such as adders, multipliers, integrators, etc., may be required. The direction of flow through each of these units is then reversed to construct the adjoint system. For example, an adder having three inputs e_1, e_2, and e_3 and whose outputs constitute the input voltages

e_4 and e_5 for two other computer units is replaced by an adder which has two inputs e_4 and e_5 and whose output is applied to three different computer units. The adjoint system has the property that its response to an impulse excitation applied at a given time t_2 is the desired weighting function as defined above. The use of the variable τ instead of t obviates the necessity of having time run backward in the adjoint system.

(a)

(b)
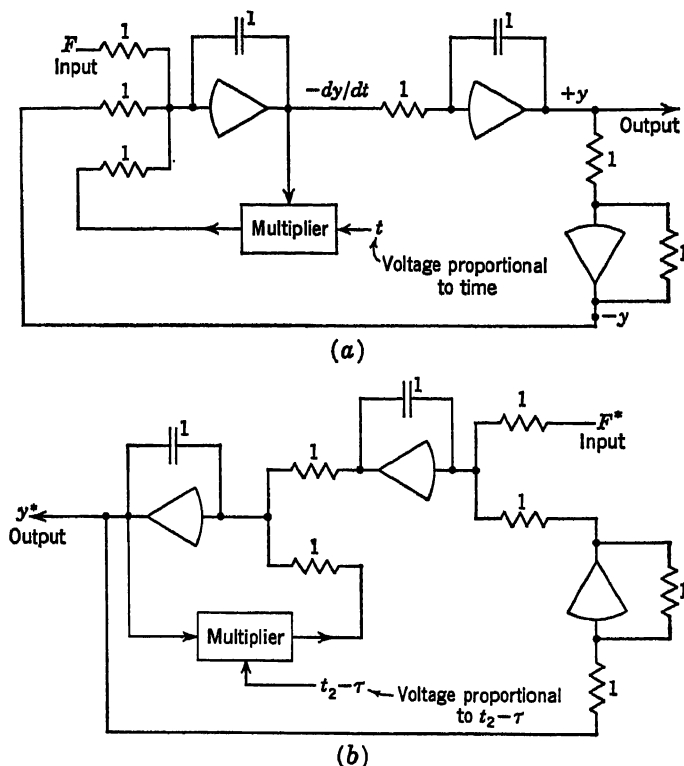
Fig. 6.16

As an example of the application of this technique, consider the treatment of the following second-order differential equation, suggested by Low.[27]

$$\frac{d^2y}{dt^2} + t\frac{dy}{dt} + y = F \qquad (6.74)$$

This system can be simulated in the conventional manner as shown in Fig. 6.16a. In order to obtain the weighting function, as described above, it would be necessary to apply a large number of unit impulses spread over the time domain prior to time t_2 and to measure the output voltage at time t_2 in each case. This would involve a large number of computer

runs. The adjoint system for this problem is obtained by interchanging the inputs and outputs of each of the computing units and by replacing the time variable t by $t_2 - \tau$. The computer diagram for the adjoint system is shown in Fig. 6.16b. The weighting function in this system can be generated by applying a unit impulse at time $\tau = 0$ and by recording the output transient y^*. If the input F^* for this system is white noise of spectral density N, Eq. (6.72) specifies the relationship between the mean square ensemble output of the original system and the weighting function of the adjoint system, as obtained from the computer.

6.12. Errors in Electronic Differential Analyzers. Errors arise in the application of electronic differential analyzers for a wide variety of reasons. Foremost among these are:

1. Gross malfunctioning of the computer, such as failure of relay contacts to close, short circuits in connecting cables, failure of plug-in connectors to make contact, etc.

2. Limitations in the performance of the computer components, such as the band-width characteristics of amplifiers, amplifier drift, non-infinite amplifier input impedance, leakage resistance in the capacitors, and variations in the component magnitudes.

3. Major human errors, such as incorrect instrumentation of the specified differential equations, incorrect scale factoring, etc.

A great deal of analytical work has been devoted to estimating and evaluating errors in the solution of linear and nonlinear differential equations with constant coefficients as a result of operational amplifier limitations. The work of Miller[28] and of Marsocci[29] deserves particular mention. The latter, in generalizing Macnee's[30] classic treatment, demonstrates that the effect of nonideal computer components causes the computers to solve characteristic equations of a higher order than the original characteristic equation whose solution is desired. The error in the solution manifests itself as a displacement in the roots of the original characteristic equation as well as the introduction of some additional roots. The effect of this rearrangement of roots (in the Laplace-transform domain) upon the graphical solutions furnished by the analog computer is discussed in considerable detail. Dow[31] shows that when a given linear differential equation is instrumented on an imperfect computer, the equation actually solved by the machine can be expressed approximately as an equation of the same degree as the given equation with coefficients which are functions of the coefficients of the given equation and the computer imperfections, including particularly leakage resistances and capacitances.

A number of checking procedures have been developed to evaluate experimentally and to minimize errors due to major and minor shortcomings. A number of computer installations have available special

problems boards which, when connected to the computer, put into action all or most of the computer amplifiers and other components to assist in the location of any equipment malfunction. McCoy[32] describes a static and dynamic voltage checking procedure with the aid of which the correctness of setups and proper functioning of components at various levels of input can be analyzed experimentally.

Meissinger[33] describes a substitution method for the verification of analog-computer solutions. The solutions obtained on the analog computer are substituted back in the original differential equation. Errors due to whatever source result in inequalities or remainders in the resulting equation. Iterative and variational procedures can be employed to reduce this remainder and thereby improve the solution accuracy.

6.13. Organization of General-purpose Electronic Computers. Electronic analog computers were first developed for military applications during World War II. Subsequently, numerous manufacturers entered into competition to provide progressively larger, more accurate, and more flexible general-purpose computers. General-purpose electronic differential analyzers are now available in installations ranging from a modest 10 operational amplifiers to well over 500 operational amplifiers. The accuracies of these computers range from 2 per cent of full scale for relatively low-cost devices to better than 0.01 per cent for the most elegant models. Very early in the development of analog computers, it became apparent that there exist two distinct philosophies or approaches to the application of these devices. In one class of computers, the time necessary to obtain a solution varies from approximately 10 sec to several minutes. The initial conditions and driving functions are applied at an instant of time corresponding to $t = 0$, and continuous graphical outputs are obtained from various points in the computer system. This type of computer is termed a "long-time" or "one-shot" computer. The other class of differential analyzers operates on a greatly speeded-up time scale, and solutions of problems are obtained in several milliseconds. The entire problem run is repeated automatically several times a second, and the result of the computation is displayed on a cathode-ray oscilloscope. While both approaches have had their enthusiastic adherents, the long-time computer has assumed a preponderant position by a wide margin, both in terms of number of companies engaged in its production as well as in number of computers actually in use. The salient features of one-shot computers, discussed in considerable detail by Korn,[34] are summarized in this section. Repetitive computers are considered briefly in Sec. 6.14.

Almost all commercial "long-time" installations are designed around a centrally located patch bay located in a control console. Wires leading to the inputs and outputs of all computer units and components are

brought out to an array of several hundred or even thousands of patch tips. Removable problem boards, made of an insulating material, are machined to fit precisely over these plug tips in such a manner that a clearly identified hole in the problem board lies directly over each patch tip. The bulk of the programming and connecting of the computer can then be accomplished by means of patch cords interconnecting the various holes in the problem board. In that manner, the computer installation is not "tied up" by a single problem. Usually a considerable number of problem boards are available with each computer. Problems can be programmed on these boards, which can be stored for subsequent experimental work while the computer is being employed to solve an entirely different problem. A considerable effort has been expended in optimizing the design of problem boards to facilitate their use. Even so, the programming of reasonably complex problems results in a veritable maze of plug-in wires, a factor which not infrequently leads to errors in programming and makes problem checking very difficult. To alleviate this situation, some manufacturers have introduced color-coded plug-in connectors and multicolored problem boards.

In addition to the patch bay, the control console generally includes the principal operating relays for resetting initial conditions and commencing computer runs, the scale factor potentiometers, and the amplifier overload indicators. The rest of the components are mounted in standard racks in such a manner that the computer facility can readily be expanded by purchasing and installing additional racks of equipment. Precision resistors and capacitors are used throughout, and in the more refined high-accuracy installations all resistors and capacitors actually taking part in the computing operation are kept in a temperature-controlled oven to minimize drift errors. The d-c operational amplifiers are almost universally of the chopper-stabilized type. An overload indicator is supplied with each amplifier. This device is generally a neon bulb connected from each amplifier output to ground. If the amplifier is overloaded in either the positive or negative direction, this bulb glows to warn the operator. Occasionally buzzers or bells have been used for the same purpose. All computers have variable d-c power supplies for the application of initial conditions to the integrators and for the generation of excitations. The output devices are generally mounted separately and may include direct-writing oscillographs for relatively high-speed recording, servo-driven recorders, and digital vacuum-tube voltmeters.

In addition, most analog facilities possess several multipliers. Recently, the trend has been in the direction of time-division or electronic multiplication, although servo multipliers and biased-diode multipliers are also in wide use. The latter two units are useful also for the generation of analytic and arbitrary nonlinear functions. Other equipment

which is frequently supplied at the option of the user includes resolvers for the generation of trigonometric functions, polarized relays for simulating various discontinuity functions, gaussian noise generators, and time-delay units for simulating transport lags.

An important feature of all installations is the relay control system. The primary function of this system is to permit the connection of d-c power supplies to the outputs of all integrators for the setting of specified initial conditions. At the commencement of the computer run, at $t = 0$, all these relays open simultaneously, and at the same time other relays connect the specified driving functions into the circuit. To repeat the computer run, the relay control switch is moved from the "compute" to the "reset" position, and the identical initial conditions are again applied. Frequently a relay control unit includes a "hold" setting. In this position, all integrator capacitors are disconnected from the input resistors, so that they tend to maintain whatever charge they possess at the instant the control switch is turned to the "hold" position. The voltages at various points in the circuit can then be examined at leisure, and changes in scale factors can be effected in the middle of a run.

Advanced models of electronic analog computers include automatic devices for eliminating potentiometer loading errors. A special power supply and voltmeter are employed to indicate the ratio of the output to the input voltage of the potentiometer while in the loaded condition. Recently, several manufacturers have introduced automatic punch-tape or punch-card programmers to set all potentiometers automatically to predetermined values. Automatic programmers are particularly useful where a large number of essentially similar and complex problems are to be analyzed.

6.14. Repetitive Computers. As indicated above, "repetitive" or "short-time" electronic analog computers were first conceived and developed about the same time as the "one-shot" electronic differential analyzers. In the United States, repetitive computers are marketed by only one major company, the G. A. Philbrick Researches Inc., which has participated in the application of this technique to a wide variety of engineering problems.[18] A successful short-time electronic analog facility has also been constructed at MIT.[35,36]

In a repetitive computer, the problem is solved over and over again, many times a second (for example, 60 times per second). To make such a computer useful for the solution of physical problems, the following conditions must be met:

1. The time constants of all integrators must be small enough so that a sufficient portion of the dynamic process under investigation has elapsed before the end of the cycle.

2. The specified initial conditions and the driving functions of the problem must be reintroduced at the beginning of each cycle.

3. The output device for recording the voltage transient must have a sufficiently high frequency response to accommodate the very rapid fluctuations in voltage.

The first requirement is met by suitable scale factoring. At the same time the RC product of all integrators is made much smaller than in the case of long-time computers. The feedback capacitors and input resistors of each integrator, in commercial models of repetitive computers, are made equal to 0.0004 μf and 0.1 megohm in magnitude, respectively. This compares with 1 μf and 1 megohm as typical magnitudes for the integrator elements of long-time computers.

To return all integrators to their initial conditions at the beginning of each cycle, it is necessary to discharge each feedback capacitor at the end of each cycle and to recharge it to its initial voltage. Special electronic circuits are supplied for this purpose, and a portion of the cycle is devoted to the establishment of the correct initial conditions. In general, only step-function driving voltages, applied at the beginning of each computing cycle, are employed.

Since the entire solution of the differential equation under study is generated in 4 msec, the output device for displaying the transient of interest must have an extremely high frequency response. No available graphic recording instruments are suitable for this purpose. The cathode-ray oscilloscope appears to be the only practical display device. If the horizontal sweep of the oscilloscope is synchronized with the repetitive computing cycle, and if the vertical input of the oscilloscope is connected to suitable points in the computer system, a stable pattern is observed on the face of the oscilloscope. This pattern then corresponds to a plot of the dependent variable vs. time and can be analyzed visually or photographed if a permanent record is desired. The accuracy of cathode-ray oscilloscopes is limited particularly by the width of the beam and distortions near the edges of the tube face. In general, accuracies of the order of 5 per cent are all that can be expected with such units, although considerably higher accuracies can be obtained by using special time and calibration marking pips. The relatively low accuracy of the output device limits the accuracy of the over-all computing procedure. Repetitive computers are therefore relatively low-accuracy devices. Since the sacrifice of high accuracy permits the use of relatively less expensive resistors, capacitors, and other components, repetitive computers as a whole also represent a less expensive method of computation.

The use of cathode-ray oscilloscopes and repetitive excitations has an important advantage for many applications. Since each individual solu-

tion takes only a fraction of a second and is displayed immediately on the cathode-ray oscilloscope, the effect upon the solution of varying any of the problem parameters by readjusting scale-factor potentiometers results in an immediate change in the oscilloscope pattern. This quality of repetitive computers facilitates their use in problems where the system behavior must be "optimized" through the selection of suitable parameters. This type of computer is therefore particularly useful for problems involving the design of dynamic systems. In the case of long-time electronic differential analyzers, it is necessary to make a new computer run, lasting perhaps 30 sec, after each change in the system parameters.

Until very recently, the Philbrick computer was organized in a manner radically different from the organization of other differential analyzers. Rather than utilizing a centrally located patch bay, the Philbrick featured a modular design. The computing system consisted of a large number of boxes, each a self-contained, complete computing unit. Integrating units, adding units, differentiating units, dead-zone units, function multiplication units, and squaring units represent only a few of the many different components available. To instrument a specific differential equation, these units were interconnected by means of patch cords. A separate power supply and modified square-wave generator was employed to supply initial conditions and driving functions and to initiate the oscilloscope sweep. This approach had the advantage that operators relatively unfamiliar with the detailed operation of an electronic computer could readily instrument complex equations merely by interconnecting the individual units. As engineers became more and more familiar with electronic analog techniques, this feature became less important, and the trend, even in the case of repetitive computers, appears to be toward the more compact and flexible patch-bay-type installation.

6.15. Mechanical Differential Analyzers. As indicated in Sec. 6.2, the first general-purpose machines for solving differential equations were of the mechanical type. Such computers employ the mechanical computing units described in Chap. 5, and the dependent variables of the problem are all represented by shaft rotations rather than by electrical voltages, as in the case of electronic differential analyzers. In most respects, the programming of equations on the mechanical differential analyzer is similar to the procedure employed on the electronic analog computer. The equation is first rearranged to express the highest derivatives in terms of the lower derivatives. Integrators and adders are then connected in closed loops to generate solutions of this equation. The principal conceptual difference between mechanical and electronic differential analyzers is that while the latter must necessarily employ

time as the dependent variable (since capacitors integrate current only with respect to time), no such restriction exists in the case of mechanical differential analyzers.

Integration with respect to dependent variables facilitates the operation of function multiplication. Using the equation

$$xy = \int x \, dy + \int y \, dx \tag{6.75}$$

the variables x and y can be multiplied by using only two integrators and an adder. An additional convenience in mechanical differential analyzers is that the solution can be stopped at any time and rescaled if necessary. Time can also be run backward simply by reversing the direction of the rotation of the main driving shaft.

To illustrate the application of the mechanical differential analyzer consider the following series of progressively more complex problems: One of the simplest problems (for which, of course, a differential analyzer would not be used) is that of finding the area under a curve. Referring to Fig. 6.17, a curve $y = f(x)$ is shown plotted on a sheet of paper fastened on an input table I. The curve starts at some value x_1 of the independent variable and ends at some other value x_2. The curve

$$z = \int_{x_1}^{x_2} y \, dx \tag{6.76}$$

is to be plotted on the output table O over the range x_1 to x_2. The differential equation corresponding to Eq. (6.76) is

$$\frac{dz}{dx} = y \tag{6.77}$$

where y is given as a plotted function of x. Equation (6.77) is thus solved by the process indicated in Eq. (6.76). The variable y displaces the integrating wheel when the hand crank on the input table is turned to keep a peephole on the given curve while the x lead screw shifts the peephole horizontally via the independent variable motor drive. The motor also turns the integrator disk D. The integrating wheel W operates through a torque-amplifying coupling C to drive the vertical lead screw on the output table O. A nut on this lead screw carries a pen P which traces the curve $z = f(x)$, as a nut on the horizontal lead screw traverses the x range. The schematic diagram for the apparatus pictured in Fig. 6.17 is shown in Fig. 6.18.

Consider, now, a simple linear second-order differential equation of the form

$$M \frac{d^2y}{dx^2} + b \frac{dy}{dx} + ky = 0 \tag{6.78}$$

Fig. 6.17

M, b, and k are known constants.   Initial values of y and dy/dx are given. The solving process is as follows:

Fig. 6.18

$$\frac{d^2y}{dx^2} = -\left(\frac{b}{M}\frac{dy}{dx} + \frac{k}{M}y\right) \quad (6.79)$$

$$\frac{dy}{dx} = \int_0^x \frac{d^2y}{dx^2}\,dx + y(0) \quad (6.80)$$

$$y = \int_0^x \frac{dy}{dx}\,dx + \dot{y}(0) \quad (6.81)$$

Two integrations are involved and hence two integrators are required. Equation (6.79) indicates that two variables are to be summed, so that an adder is also required.   No arbitrary functions of x or y, or of the derivatives, are involved, so that no input tables are needed.   As outputs, it may be desired to have y and/or one or both derivatives.   These output values may be plotted against x, against y, or against either of the two derivatives.   To make the problem definite, suppose y and dy/dx are required as functions of x, and also suppose dy/dx is required as a function of y and as a function of d^2y/dx^2.   The schematic diagram will then be as shown in Fig. 6.19.   All the variable shafts are shown as horizontal lines. The integrators are all grouped below; the function tables above.   Adders

and gear trains interconnecting the various shafts are shown at one end. Connections from the various horizontal shafts are carried over to the integrators and output tables by cross shafts.

An equation worthy of a differential-analyzer solution is attained if, in Eq. (6.78), M is a function of x, b a function of dy/dx, and k a function of y. The equation is thus nonlinear (owing to the dependence of b and k upon dy/dx and y, respectively) and has a variable coefficient (M). In
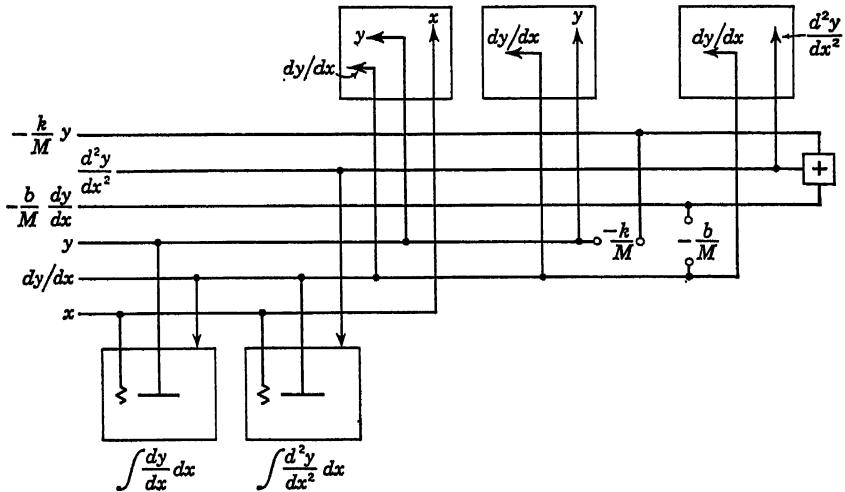
Fig. 6.19

addition, a forcing function $f(x)$ may be present on the right-hand side. With these modifications, the equation becomes

$$f_1(x)\frac{d^2y}{dx^2} + f_2\left(\frac{dy}{dx}\right)\frac{dy}{dx} + f_3(y)y = f(x) \qquad (6.82)$$

The solution procedure is

$$\frac{d^2y}{dx^2} = \frac{1}{f_1(x)}\left\{f(x) - \left[f_2\left(\frac{dy}{dx}\right)\right]\frac{dy}{dx} - [f_3(y)]y\right\} \qquad (6.83)$$

$$\frac{dy}{dx} = \int_0^x \frac{d^2y}{dx^2}\,dx + \dot{y}(0) \qquad (6.84)$$

$$y = \int_0^x \frac{dy}{dx}\,dx + y(0) \qquad (6.85)$$

The various functions in Eq. (6.83) may be experimentally determined and are, therefore, available only as curves rather than as mathematical expressions. Consequently, an input table must be provided for each

function (four input tables). There are two products of variables and
one division. Thus, four integrators are required to produce the two
products, two integrators to perform the division and first integration,
and one more integrator for the second integration, a total of seven inte-
grators, although the equation is only a second-order equation and should
be capable of solution with only two integrators. It could, of course, be
accomplished with two integrators and three multiplying units. How-
ever, these operations can be carried out more conveniently and more
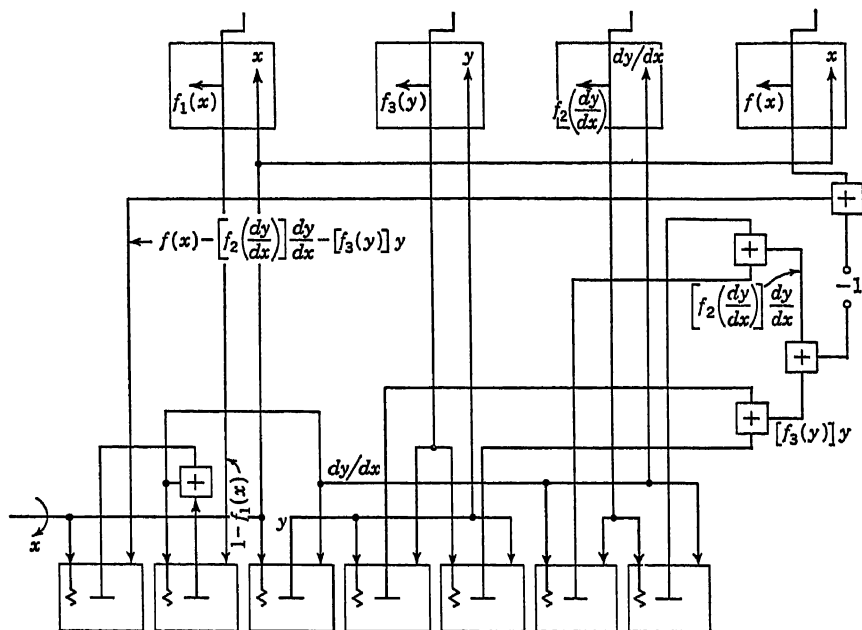
Fig. 6.20

accurately by using integrators. Moreover, if manually operated multi-
pliers and input tables are used, seven operators would be required for
these units alone. At least three operators could be dispensed with by
self-generation of the products.

The schematic diagram for Eq. (6.82) is shown in Fig. 6.20. The out-
put tables are not shown.

Frequently, $f(x)$ is a trigonometric function of x (for example, a sine
or a cosine). In that case the corresponding input table may be elim-
inated and two more integrators used to generate the trigonometric
function (see Chap. 5).

Simultaneous differential equations are mechanized in as straight-
forward a manner as are the individual equations. To illustrate the pro-

cedure, consider the pair of simultaneous equations

$$\frac{d^2y}{dx^2} + a\left(\frac{dy}{dx}\right)^{\frac{1}{2}} + zyx = x^4 + 2$$

$$\frac{d^3z}{dx^3} + \frac{dz}{dx}\frac{dy}{dx} + b(y - z) = \ln x$$

(6.86)

Each equation is solved for the highest derivative:

$$\frac{d^2y}{dx^2} = (x^4 + 2) - a\left(\frac{dy}{dx}\right)^{\frac{1}{2}} - zyx$$

$$\frac{d^3z}{dx^3} = \ln x - \frac{dz}{dx}\frac{dy}{dx} + b(z - y)$$

(6.87)

The methods of generating square roots, powers, and logarithms with integrators have been described in Chap. 5. These methods are now employed to set up the functions in Eqs. (6.87). The schematic diagram is shown in Fig. 6.21.

Although the above methods in general provide the most useful approach to the differential analyzer solution of an ordinary differential equation, it may not be always possible to isolate the highest derivative. A solution by integration may still be performed. As an extreme example, consider the hypothetical equation

$$\frac{d^2y}{dx^2} + \left(\frac{dy}{dx}\right)^{d^2y/dx^2} + \sin\frac{d^2y}{dx^2} = 0$$

(6.88)

It is clear that the highest derivative cannot be isolated. It is possible to set up a machine solution by using two input tables. On one table a family of curves representing values of the second term would be plotted against dy/dx with values of the exponent as parameter. As d^2y/dx^2 is developed in the machine, and as dy/dx drives the horizontal lead screw of this table, an operator would maintain the traveling peephole on the vertical lead screw at those positions in the family of curves corresponding to the value of the d^2y/dx^2 parameter read from a counter on the d^2y/dx^2 shaft. The other table would have plotted on it a curve of the sine term versus d^2y/dx^2. An operator would maintain the peep sight of the vertical lead screw on this curve as the horizontal lead screw is driven by the variable d^2y/dx^2. The inputs from the two tables are added, sign reversed, and then fed to an integrator lead screw. The output of this integrator will then be dy/dx, which may be integrated once more to yield y. The schematic diagram for this problem is shown in Fig. 6.22.

The two input tables may be eliminated by using integrators to generate the functions. Two integrators would be used to generate the sine.
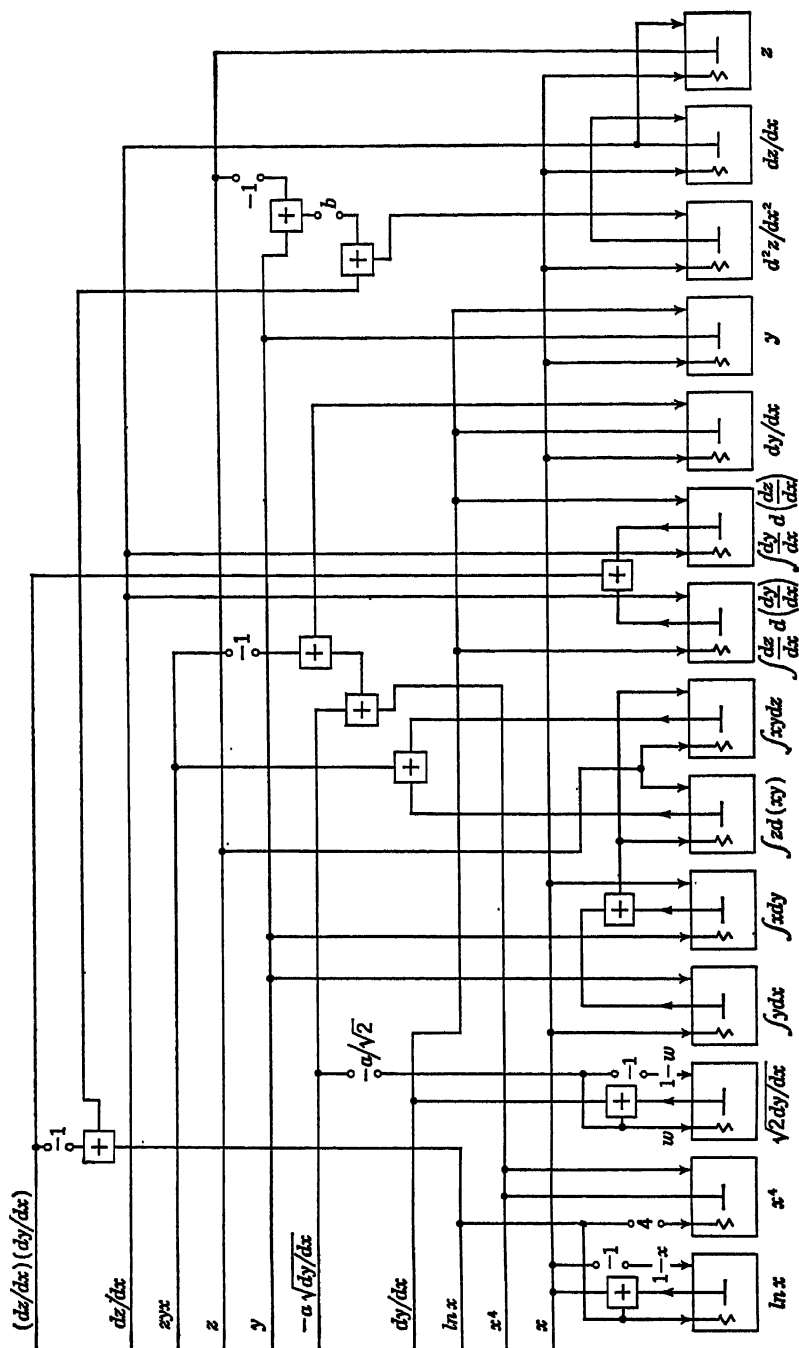
Fig. 6.21

One integrator would be used to generate the logarithm of dy/dx, two to get the product of d^2y/dx^2 into the logarithm of dy/dx, and one more to get the antilogarithm of the product, as described in Chap. 5. The schematic diagram for Eq. (6.88) is shown in Fig. 6.23. The output tables are not shown in Figs. 6.22 and 6.23.

6.16. Digital Differential Analyzers. A recent entry into the general-purpose differential analyzer fields is the result of the combinations of some of the circuit techniques used in digital computers and some of the logical techniques used in analog computations. On the basis of the classification of automatic computers presented in Chap. 1, the digital
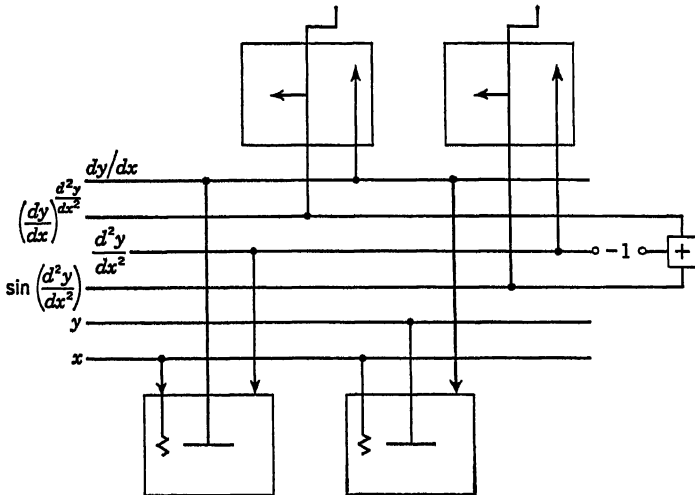
Fig. 6.22

differential analyzer is a digital computer. Everywhere within the machine, the data are carried in discrete or numerical form. On the other hand, the organization of the machine and the philosophy of its utilization are closely akin to that of the electronic and mechanical differential analyzers.

The heart of the digital differential analyzer and indeed of all digital computers is a memory. In commercially available digital differential analyzers, this memory unit is a metal disk termed the magnetic drum. This drum is made to rotate past an array of magnetic recording and reading heads. The recording head serves to place the segment along the periphery of the drum, which is directly adjacent to the head, into one of two stable magnetic states. The reading head senses the magnetic condition of that segment of the magnetic drum which is directly adjacent to it. The periphery of the drum may be viewed as being divided into a large number of adjacent segments, each having a special significance in

terms of the computing operation. The entire drum is rotated contin-
uously and rapidly so that each segment passes the recording and reading
heads many times a second. Numerical data (in binary form) as well
as computing instructions are introduced into the computer by mag-
netizing or demagnetizing appropriate segments along the drum. The
actual programming is done by an operator using keys located on the
front of the computer. The digital information contained along each sec-
tion of the drum can be displayed by means of a cathode-ray oscilloscope.
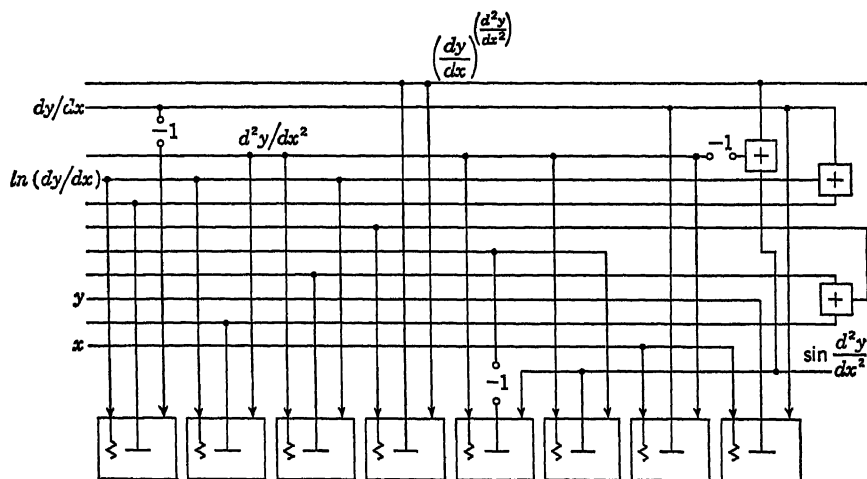
Fig. 6.23

The operation of integration is performed in essence by approximating
the integral

$$z = \int_0^y y\, dx + z(0) \qquad (6.89)$$

by summing a series of finite increments of x and y, according to the
equation

$$z_n = \sum_{i=0}^n y_i\, \Delta x_i \qquad (6.90)$$

Provided that the increments Δx are sufficiently small, Eq. (6.90)
represents a close approximation to the integration process. An even
closer approximation can be obtained by employing such techniques as
trapezoidal integration, as described by Palevsky.[37]

To instrument Eq. (6.90), the periphery of the magnetic drum is
divided into a number of adjacent sections, each containing a number
(for example, 20) of segments. These sections are regarded as inte-
grators; digital differential analyzers having as many as 60 such inte-

grators are available commercially. Each integrator unit in a digital differential analyzer accepts Δx and Δy as inputs and makes available the quantity Δz as an output. The integrator is given the specified initial value of y, and this value is continually modified as the computation proceeds by adding or subtracting discrete Δys. A schematic diagram of an integrating unit is shown in Fig. 6.24.
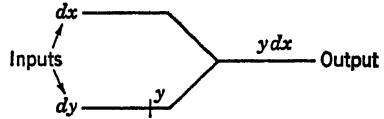
Fig. 6.24

To solve complete equations, the integrators of the digital differential analyzer are "interconnected" by suitable programming instructions in very much the same manner as the integrators of other differential analyzers. Figure 6.25 illustrates the solution of the equation

$$\frac{d^2y}{dt^2} + a\frac{dy}{dt} + by = 0 \qquad (6.91)$$

Note that separate integrators (integrators 2 and 4) are required to perform the multiplications by the coefficients a and b. On the other hand, each integrator can be programmed to furnish either a positive or
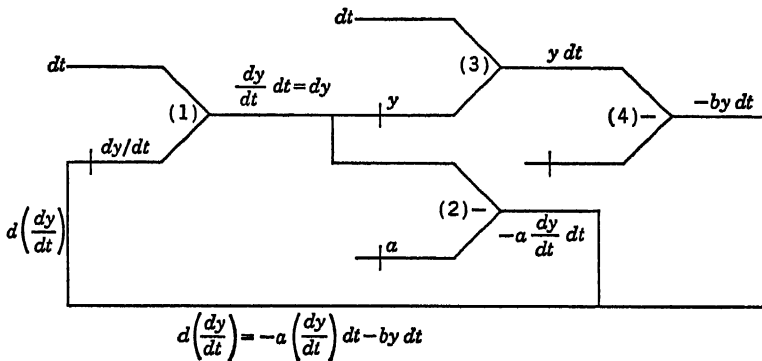
Fig. 6.25

a negative output, so that no sign changers are required. The solution of Eq. (6.91) requires three operational amplifiers on an electronic analog computer, while four integrators are required to solve the same equation on a digital differential analyzer. Note also that the independent variable of the problem need not necessarily be time, so that the integration with respect to a dependent variable is possible with a digital differential analyzer. The solutions of problems are displayed by means of specially designed curve plotters.

With a digital differential analyzer, it is generally possible to sacrifice speed in obtaining the solution to a given problem in order to increase

the accuracy of the solution. Thus, where a solution obtained in, for example, 2 min may have an accuracy of 1 per cent, a 20-min solution time will furnish solutions of the same problem with an accuracy of 0.1 per cent. In general, solution times using the digital differential analyzer are considerably longer than those of long-time electronic analog computers. Great advances have been made in developing digital differential analyzers having very compact designs. For example, a digital differential analyzer manufactured by Litton Industries, having 20 integrators, weighs only 79 lb and occupies only slightly more than 2 cu ft.

Digital differential analyzers have been employed to solve a wide variety of linear and nonlinear differential equations. Forbes[38] describes the application of this computer to such advanced problems as conformal mapping, the solution of partial differential equations, vector transformation and vector algebra, and the generation of a great variety of analytic and discontinuity functions.

Thus far, only serial digital differential analyzers of the type described above have appeared on the market. In these, each segment on the magnetic drum passes by a reading and recording head once during each revolution of the drum (typical drum speed: 60 rev/sec). All computing operations must therefore be performed sequentially as each integrator is processed in turn. This feature reduces the flexibility as well as the rapidity in solving differential equations. For this reason a considerable effort is being expended in devising digital differential analyzers in which all operations are performed simultaneously as in electronic analog computers. Such parallel digital differential analyzers, employing electric delay line memories, promise to effect an important improvement in the applicability and utility of digital differential analyzers.

REFERENCES

1. Bush, V.: The Differential Analyzer, A New Machine for Solving Differential Equations, *J. Franklin Inst.*, **212**:447–488 (1931).
2. Ince, E. L.: "Ordinary Differential Equations," 4th rev. ed., Dover Publications, New York, 1944.
3. Bateman, H.: "Partial Differential Equations of Mathematical Physics," Dover Publications, New York, 1944.
4. Minorsky, N.: "Introduction to Nonlinear Mechanics," Edwards Bros., Inc., Ann Arbor, Mich., 1947.
5. Ku, Y. H.: "Analysis and Control of Nonlinear Systems," The Ronald Press Company, New York, 1958.
6. Thomson, W.: Mechanical Integration of the Linear Differential Equations of the Second Order with Variable Coefficients, *Proc. Roy. Soc. (London)*, **24**:269–271 (1875–1876).
7. Thomson, W.: Mechanical Integration of the General Linear Differential Equa-

tion of Any Order with Variable Coefficient, *Proc. Roy. Soc. (London)*, **24**:271–275 (1875–1876).

8. Bush, V., F. D. Gage, and R. H. Stewart, A Continuous Integraph, *J. Franklin Inst.*, **203**:63–84 (1927).

9. Travis, I.: Differential Analyzer Eliminates Brain Fag, *Machine Design*, **7**(7):15–18 (1935).

10. The Differential Analyzer, *Engineer*, **160**:56–58, 82–84 (1935).

11. Hartree, D. R.: The Mechanical Integration of Differential Equations, *Math. Gaz.*, **22**:342–364 (1938).

12. Hartree, D. R., and A. K. Nuttall: The Differential Analyzer and Its Applications in Electrical Engineering, *JIEE (London)*, **83**:263–647 (1938).

13. Meyer zur Capellen, W.: "Mathematische Instrumente," p. 225, Akademie-Verlag G.m.b.H., Berlin, 1944 (Edwards Bros., Inc., Ann Arbor, Mich., 1947).

14. Kuehni, H. P., and H. A. Peterson: A New Differential Analyzer, *Trans. AIEE*, **63**:221–228 (1924).

15. Berry, T. M.: Polarized-light Servo System, *Trans. AIEE*, **63**:195–197 (1944).

16. "The Differential Analyzer of the University of California," brochure, Department of Engineering, University of California, Los Angeles, 1947.

17. Bush, V., and S. H. Caldwell, A New Type of Differential Analyzer, *J. Franklin Inst.*, **240**:255–326 (1945).

18. Paynter, H. M.: "A Palimpsest on the Electronic Analog Art," G. A. Philbrick Researches Inc., Boston, 1955.

19. Ragazzini, J. R., R. H. Randall, and F. A. Russell: Analysis of Problems in Dynamics by Electronic Circuits, *Proc. IRE*, **35**:444–452 (1947).

20. Hall, A. C.: A Generalized Analogue Computer for Flight Simulation, *Trans. AIEE*, **69**:308–320 (1950).

21. Polisar, G. L.: Analysis of Nonlinear Systems of Autoregulation by the Method of Combination of the Investigated Objects with the Electrointegrator, *Izvest. Akad. Nauk SSSR, Otdel. Tekh. Nauk*, no. 3, p. 384, March, 1949.

22. Eckman, D. P., and W. H. Wannamaker: Electrical Analogy Method for Fundamental Investigation in Automatic Control, *Trans. ASME*, **67**:81–86 (1945).

23. Bekey, G. A.: "Preparing Problems for Solution on an Analog Computer," Beckman Instruments Inc., Berkeley Division, Richmond, Calif., 1957.

24. Greenspan, D., B. Ulrich, and S. Matsuno: On an Analog Simulation of Two-point Boundary Value Problems, *Rev. Sci. Instr.*, **28**:1040–1042 (1957).

25. Bennett, R. R.: Analog Computing Applied to Noise Studies, *Proc. IRE*, **41**:1509–1513 (1953).

26. Lanning, J. H., Jr., and R. H. Battin: "Random Processes in Automatic Control," McGraw-Hill Book Company, Inc., New York, 1956.

27. Low, H.: Use of Noise and Statistical Techniques in Analog Computations, chap. 26 in "Handbook of Automation, Computation and Control," vol. 2, John Wiley & Sons, Inc., New York, 1959.

28. Miller, K. S., and F. J. Murray: The Mathematical Basis for Error Analysis of Differential Analyzers, *J. Math. and Phys.*, **32**:136–144 (1953).

29. Marsocci, V. A.: An Error Analysis of Electronic Analog Computers, *IRE Trans. on Electronic Computers*, **5**:207–212 (1956).

30. Macnee, A. B.: Some Limitations on the Accuracy of Electronic Differential Analyzers, *Proc. IRE*, **40**:303–308 (1952).

31. Dow, P. C., Jr.: An Analysis of Certain Errors in Electronic Differential Analyzers, *IRE Trans. on Electronic Computers*, **6**:255–260 (1957); **7**:17–22 (1958).

32. McCoy, R. D., and B. D. Loveman: "Problem Check for Analog Computers," Reeves Instrument Corp., New York, 1955.

33. Meissinger, H. F.: "Substitution Methods for the Verification of Analog Solutions," paper presented at National Simulation Conference, Dallas, Tex., January, 1956.
34. Korn, G. A., and T. M. Korn: "Electronic Analog Computers," 2d ed., McGraw-Hill Book Company, Inc., New York, 1956.
35. Macnee, A. B.: An Electronic Differential Analyzer, *Proc. IRE*, **37**:1315–1324 (1949).
36. Allen, W. R.: Dynamic System Studies, Part VI, *WADC Tech. Rept.*, **54**:250 (1956).
37. Palevsky, M.: The Design of the Bendix Digital Differential Analyzer, *Proc. IRE*, **41**:1352–1356 (1953).
38. Forbes, G. F.: "Digital Differential Analyzers," published by George F. Forbes, Pacoima, Calif., 1957.

7

MACHINES FOR SIMULTANEOUS LINEAR ALGEBRAIC EQUATIONS

A large range of problems in science and engineering[1] can be conveniently set up in terms of sets of simultaneous linear algebraic equations. Such problems occur, for example, in statistics, quantum mechanics, chemistry, spectrographic analysis, stress analysis, vibration, impact, indeterminate structures, etc. While numerical methods for solving such systems of equations are straightforward, the procedures are often laborious because of the large numbers of equations that would be involved in a comprehensive analysis of a real problem, particularly if the effects of varying a number of different parameters are to be investigated. Machines for solving sets of linear algebraic equations need perform simply the elementary arithmetical operations of multiplying variables by constants and summing the resultant products. The sum may be indicated on an instrument or may be used in a servomechanism or feedback circuit to drive the machine to equilibrium. The constant multipliers and summing devices described in Chaps. 2 and 5 may now be combined to form complete mathematical machines of this important type. Various mechanical, electromechanical, and electrical (including electronic) machines for manual and for automatic solution of such equations are described in this chapter. Since digital computers are ideally suited for solving simultaneous linear algebraic equations, the importance of these analog methods has gradually been diminished in recent years.

7.1. The Gauss-Seidel ("Classical Iterative") Numerical Method. Of the various numerical methods for solving systems of simultaneous linear algebraic equations, the classical iterative method[2] appears most adapted to many forms of manual and automatic machine computation. The method will be described in connection with the following set of equations:

$$a_{11}x_1 + a_{12}x_2 + \cdots + a_{1n}x_n = a_{10}$$
$$a_{21}x_1 + a_{22}x_2 + \cdots + a_{2n}x_n = a_{20}$$
$$\cdots \cdots \cdots \cdots \cdots \cdots \cdots \cdots \cdots \cdots \cdots \cdots \qquad (7.1)$$
$$a_{n1}x_1 + a_{n2}x_2 + \cdots + a_{nn}x_n = a_{n0}$$

The given set of equations must be arranged so that the principal diagonal does not contain any zero coefficients. This is essential, since in the Gauss-Seidel method each equation is solved in order for the unknown appearing along the principal diagonal in the above array. Moreover, to improve the rapidity of convergence,[3] the coefficients along the diagonal should be large and those off the diagonal (particularly the postdiagonal coefficients) should be small.

In the numerical solving procedure, the unknowns $x_2 - x_n$ in the first of Eqs. (7.1) are assigned values and x_1 is calculated to satisfy this equation. All these values except x_2 are carried down into the second equation, which is then solved for the x_2 required to satisfy it. All the values for the unknowns in the second equation, except x_3, are carried down into the third equation, which is then solved for the x_3 required to satisfy it. This procedure is repeated from equation to equation, with all values of x except x_n carried down from the $(n-1)$st equation to the nth, which is then solved for x_n. This completes one cycle of iteration and results, of course, in actually satisfying only the last equation. The second cycle is started by substituting all the values of x, except x_1, from the nth equation back into the first equation and once again solving this equation for x_1. The second cycle is then carried on to completion in a manner identical with that for the first cycle. With each cycle, the unknowns approach their true values more closely. As many iterations are performed as are necessary to attain the desired degree of accuracy in the final answers. While procedures are available for accelerating[2] the numerical process, the simple iterative procedure fits very nicely into some of the manual and automatic techniques of machine computation.

7.2. Analog Methods of Solution. The machine solution with analogs is usually approached from one of the two following points of view.[4]

1. The unknowns are adjusted by successive manual or continuous automatic operation until the sum on the left-hand side of each equation becomes equal to the related constant term.

2. The constant term in each equation is adjusted to its required value, causing thereby the unknowns to attain the values satisfying Eqs. (7.1).

Some machines are reversible, so that either method of solution is possible. Others operate in one direction only, usually in accordance with first method.

7.3. Mechanical Shaft-type Simultaneous-equation Solvers. These mechanical simultaneous-equation solvers have appeared in numerous

and rather ingenious forms.[5]   A straightforward computer consisting of gears, shafts, and adding differentials is shown schematically in Fig. 7.1 for a system of four simultaneous equations.   The unknowns appear as rotations of the shafts $x_1 - x_4$.   Hand cranks on these shafts drive them the required number of turns.   Counters on the x shafts show the number of turns made by each shaft and thus provide the answers.   An inspection of the schematic diagram shows that the summations through
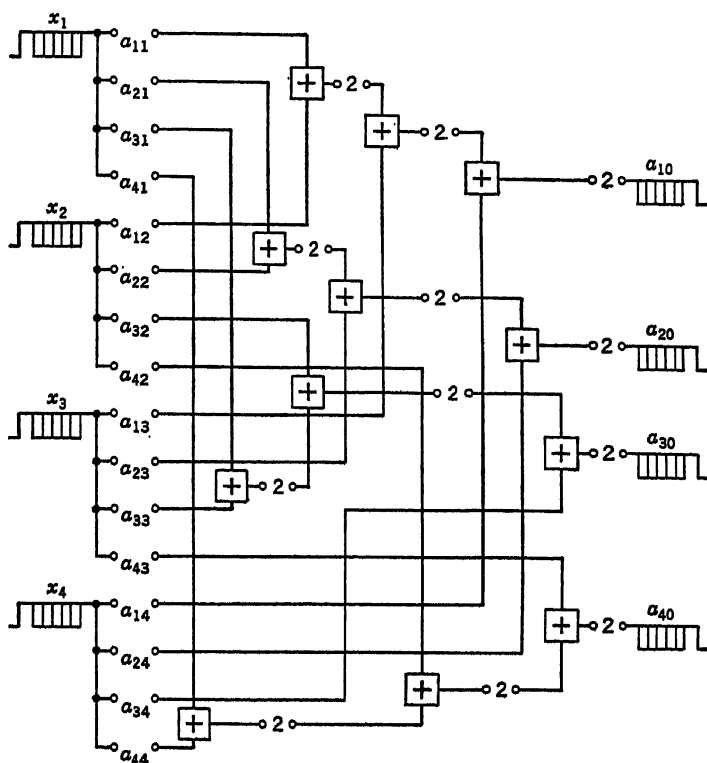
Fig. 7.1

each horizontal string of adders take place in accordance with each of Eqs. (7.1), respectively.   The loss of scale factor through each adding differential is made up immediately by inserting a 2:1 gear stepup after each adder.   This has been done only to emphasize the fact that this loss does occur.   In an actual machine, the step-up gears would not be inserted as shown; instead, gear ratios of $8a_{11}$, $8a_{21}$, $8a_{31}$, $8a_{41}$, $8a_{12}$, $8a_{22}$, $4a_{32}$, $4a_{42}$, $4a_{13}$, $4a_{23}$, $8a_{33}$, $2a_{43}$, $2a_{14}$, $2a_{24}$, $2a_{34}$, $8a_{44}$ would be used on the unknown shafts in place of those indicated in Fig. 7.1.   The loss of scale factor is thus compensated for in advance, so that the true sums of terms show up in the a_{10}, a_{20}, a_{30}, and a_{40} counters.

In preparing a set of equations to be solved on the machine, each equation may be divided by the largest coefficient occurring in that equation so that all coefficients become unity or less. Thus, no gear ratio greater than unity need be provided, and the cranks are not loaded by stepups in the system. Actually, the 8, 4, and 2 factors in the previous paragraph should be incorporated in the coefficients before this reduction is made. It should be borne in mind that the arrangement shown in Fig. 7.1 is only one of several possible arrangements of the summations. The factors on the coefficients shown are applicable only to this particular arrangement. If another arrangement were used, the distribution of factors would be changed, although there would still be eight factors of magnitude 8, four of magnitude 4, and four of magnitude 2. It can be shown that with n simultaneous equations in n unknowns with n^2 coefficients, there will be $2n$ factors of magnitude $2^{(n-1)}$, and n each of the factors $2^{(n-2)}$, $2^{(n-3)}$, $2^{(n-4)}$, . . . , 2.

Once the equations have been reduced to give unity as the largest coefficient (including its scale-compensating factor), the required gear ratios may be set into the machine. This may be done by selecting gears from a stock on hand and manually making up the appropriate gear trains. Or decade gearboxes, such as those described in Chap. 5, might be provided.

The machine is now set for operation. The unknown counters and the constant-term counters are set to zero. One of the x cranks (the one that turns most easily, perhaps) is now turned in either the plus or the minus direction until the counter a_{10} reads its correct value. During this process all cranks must be free to rotate. The constant-term shafts, other than a_{10}, may be free or they may be locked against rotation. It may be preferable to keep them locked. Turning one of the x cranks will also turn all the others because of the shaft interconnections. This must be so since at all times Eqs. (7.1) must be satisfied while the "constant" terms are changing. Having brought the a_{10} counter to its required value (positive or negative), the a_{10} shaft must now be locked to prevent further rotation, and the a_{20} shaft unlocked. Again, any one of the x cranks may be turned until the a_{20} counter attains the specified value, whereupon the a_{20} shaft is locked and the a_{30} shaft unlocked. The same procedure is carried out, then, for the a_{30} counter and the a_{40} counter. Upon completion of the last step, the readings of the x counters give directly the values of the unknowns.

This method is capable of extremely high accuracy since a large number of turns of each x counter may be used to represent one unit of the corresponding x (large scale factor) where necessary. For example, if x_1 is found to be a relatively small number and thus not represented directly in the x_1 counter with sufficient accuracy, the coefficients of x_1 might be

reduced by some suitable factor, such as 10 or 100 in Eqs. (7.1). Upon solving the modified set of equations, the number appearing in the x_1 counter is actually the desired x_1 times the factor by which the coefficients were reduced. Any of the other unknowns could be treated in a similar fashion as necessary.

The procedure described above for causing the values of the constant terms to appear in their counters may be made more direct by operating the machine from the opposite end. By placing the cranks on the constant-term shafts, each of these shafts may be turned directly to produce the required figure in its counter. As before, all the x shafts must be free, while all but one of the constant-term shafts may be locked. The free crank may then be turned to bring its counter to the correct reading. It is then locked to prevent further rotation, while another such shaft is unlocked, rotated to its correct reading, and then locked again. The process is continued until all the constant-term counters read correctly. The x counters then provide the values of the unknowns. The shaft interconnections, of course, remain as in Fig. 7.1. High ratio gear stepups may be encountered in operating the machine in reverse, resulting in high torques and difficult operation. Scale factors may be chosen to avoid stepups in this type of operation.

Since gear ratios capable of wide variation are necessary to generate the products of the coefficients by the unknowns in Eqs. (7.1), integrators may be used for this purpose. Referring to Fig. 5.4, which shows the essential elements of a Kelvin disk-and-wheel integrator, the wheel output turns at constant setting r of the lead screw for x turns of the turntable are

$$w = \frac{r}{a} x \qquad (7.2)$$

The lead-screw setting r is capable of a wide variation in setting, from 0 to plus or minus the maximum travel along the turntable radius. Scale factors appropriate to the particular integrators involved must necessarily be included in determining the actual range of coefficient value.

One integrating unit provides one coefficient. Thus, for a system of n equations with all different coefficients, n^2 integrators must be provided. The system of four equations under consideration in this section requires 16 integrators. It is clear that the use of expensive integrators for setting coefficients is very wasteful.

In general, integrators cannot be operated in reverse, so that it would not be possible to make the constant-term shafts the independent drives or to allow one unknown shaft to drive the other unknowns, as was done in the hand-cranked machine described just previously. The Gauss-Seidel procedure would then be used, in which each unknown is brought to its equilibrium value with all other unknowns fixed at their estimated

or approximated values and by means of successive iterations the values improved to the desired accuracy.

7.4. Tilting-plate Equation Solver. A rather different type of mechanical equation-solving machine, which is based on the simulation of the equations by the geometrical properties of a set of tilted plates, was first proposed by Thomson[6] in 1878. He suggested that a useful machine for 8 or 10 or more equations would not be difficult or overelaborate and that the exceeding ease of application of the machine promised well for its real usefulness. Two machines[7] based on a practical improvement of this principle were constructed at the Massachusetts Institute of Technology in the period 1934 to 1936. The first was a 2-equation machine built as a pilot model, the second a 9-equation machine.

The principle of the Thomson machine is most easily visualized by examining the simple set of two simultaneous linear equations. The conclusions drawn from this analysis are readily applied to any greater sets of equations.
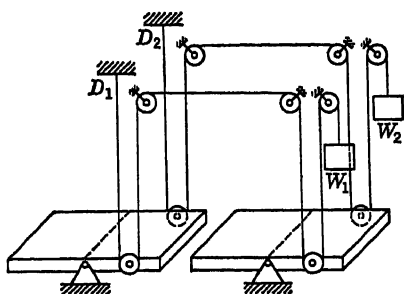
$$a_{11}x_1 + a_{12}x_2 = a_{10} \atop a_{21}x_1 + a_{22}x_2 = a_{20} \quad (7.3)$$

Fig. 7.2

Referring to Fig. 7.2, two plates are shown pivoted along their transverse center lines. Two pulleys in each plate are positioned in slots in the plates so that their distances from the plate pivots are proportional to the coefficients in Eqs. (7.3). Two inextensible cords are fixed to points D_1 and D_2 at one end, pass around the plate pulleys and other fixed guide pulleys, and end at balancing weights W_1 and W_2. The fixed points D and the guide pulleys should be capable of adjustment so that the cords leading to and from the coefficient pulleys would always be perpendicular to the plates for any coefficient settings, either plus or minus. Positive coefficients may be set as shown in Fig. 7.2. Negative coefficients would be set on the other side of the pivot. Springs and additional weights may be required on the plates so that after all coefficients are set and the plates leveled, the entire system is in balance. The weight W_1 is then pulled down a distance proportional to a_{10} and W_2, a distance proportional to a_{20}. If consistent constants of proportionality (*i.e.*, scale factors) have been used in each equation, the angle of tilt of each plate would be proportional to the unknown it represents.

Thus, suppose that the counterclockwise angles of tilt are θ_1 and θ_2. The two pulleys on plate 1 then move vertically through the distances $a_{11}\theta_1$ and $a_{21}\theta_1$, assuming small deflections so that $\sin \theta_1 = \theta_1$. The pairs

of parallel cord lengths on each plate pulley are correspondingly shortened by these amounts. The slack so generated is taken up by lowering the weights W_1 and W_2 by the amounts $2a_{11}\theta_1$ and $2a_{21}\theta_1$. A similar situation holds at plate 2, except that the pairs of parallel cord lengths on each plate pulley are shortened by $a_{12}\theta_2$ and $a_{22}\theta_2$. The additional slack generated by the tilt θ_2 is taken up by a further lowering of W_1 and W_2 by the amounts $2a_{12}\theta_2$ and $2a_{22}\theta_2$. Thus, if m_1 and m_2 are the distances W_1 and W_2 are moved by tilting the plates, the relations between plate tilt and the other geometrical values in the system are

$$
\begin{aligned}
2a_{11}\theta_1 + 2a_{12}\theta_2 &= m_1 \\
2a_{21}\theta_1 + 2a_{22}\theta_2 &= m_2
\end{aligned}
\tag{7.4}
$$

It is clear that to solve Eqs. (7.3), m_1 and m_2 should be $2a_{10}$ and $2a_{20}$, respectively. The plates would be tilted in practice by pulling (or pushing) on the weights W_1 and W_2.

To use this method for n equations with n unknowns, there must be n plates (one for each unknown), n pulleys on each plate (one for each coefficient), and n cords to tilt the plates. Means must be provided for measuring the angle of tilt of each plate.

Thomson also suggested at this point that the unknowns found by a first application of the machine may be substituted back into the original equations, the residual errors calculated by numerical means (he proposed Crelle's multiplication tables), and the machine used a second time, without resetting any of the coefficient pulleys, to calculate corrections on the unknowns. By successive applications of the machine, any desired degree of precision may be obtained in the final answers, the limit being set by the accuracy with which residual errors are calculated.

The corrective procedure occurs as follows. Suppose that x_1' and x_2' are the values of x_1 and x_2 determined upon a first application of the machine. The residual errors in the left-hand sides of Eqs. (7.3) are, then,

$$
\begin{aligned}
r_1' &= a_{10} - (a_{11}x_1' + a_{12}x_2') \\
r_2' &= a_{20} - (a_{21}x_1' + a_{22}x_2')
\end{aligned}
\tag{7.5}
$$

Because the equations are linear, the residual errors are related to the corrections on the unknowns by the same equations as are the constant terms and the unknowns themselves. Thus, if the corrections are $\Delta x_1'$ and $\Delta x_2'$,

$$
\begin{aligned}
a_{11}\,\Delta x_1' + a_{12}\,\Delta x_2' &= r_1' \\
a_{21}\,\Delta x_1' + a_{22}\,\Delta x_2' &= r_2'
\end{aligned}
\tag{7.6}
$$

In general, r_1' and r_2' would be small numbers, so that for an accurate determination of the corrections, the residuals should be increased by

some factor, such as 100. Equations (7.6) then become

$$a_{11}(100 \, \Delta x_1') + a_{12}(100 \, \Delta x_2') = 100r_1'$$
$$a_{21}(100 \, \Delta x_1') + a_{22}(100 \, \Delta x_2') = 100r_2' \qquad (7.7)$$

Thus, by realigning the plates and then pulling the cords through the distances $200r_1'$ and $200r_2'$, the angles of tilt of the plates would represent $100x_1'$ and $100x_2'$. The final answers would then become

$$x_1 = x_1' + \Delta x_1' \qquad x_2 = x_2' + \Delta x_2' \qquad (7.8)$$

It seems hardly likely that more than one corrective application, if any, would be required in practical problems. However, the procedure may
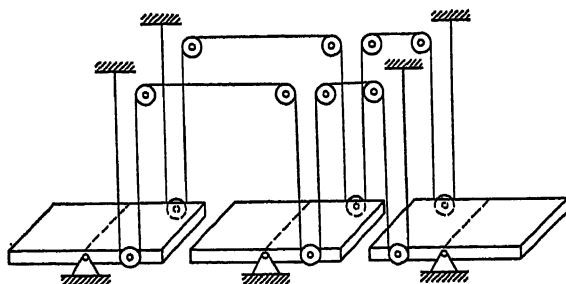
Fig. 7.3

be continued with corrections superimposed on corrections as far as need be.

Wilbur's[7] improvement of this machine consists in introducing one more tilting plate holding a set of pulleys representing the constant terms. Thus, no loose cord ends are present to be pulled or pushed. Both ends of the cord are now fixed (Fig. 7.3).

As before, the cords entering and leaving each coefficient pulley should be vertical. The same is true for the cords on the constant-term pulleys. With all plates horizontal and the pulleys set to their appropriate distances from the pivots, both ends of the cords are clamped. One of the plates is then tilted manually. Which one makes little difference. In practice the one easiest to move would be tilted.

Suppose, for example, that plate 3 (the constant-term plate) were tilted in a counterclockwise direction. Plates 1 and 2 would correspondingly tilt in a counterclockwise direction (as set up in Fig. 7.3). Small slopes need not be specified now. However, as the plates tilt, the tape supports should be able to shift enough to maintain the tapes in a vertical position. The elongation of the tapes at the constant-term pulleys must be exactly equal to the total shortening occurring at the coefficient pulleys,

since the total lengths of the tapes are invariable. Thus, the relations satisfied by the pulley positions are

$$2a_{11} \sin \theta_1 + 2a_{12} \sin \theta_2 = 2a_{10} \sin \theta$$
$$2a_{21} \sin \theta_1 + 2a_{22} \sin \theta_2 = 2a_{20} \sin \theta$$

(7.9)

or

$$a_{11} \left(\frac{\sin \theta_1}{\sin \theta} \right) + a_{12} \left(\frac{\sin \theta_2}{\sin \theta} \right) = a_{10}$$
$$a_{21} \left(\frac{\sin \theta_1}{\sin \theta} \right) + a_{22} \left(\frac{\sin \theta_2}{\sin \theta} \right) = a_{20}$$

(7.10)

The unknowns x_1 and x_2 are given, therefore, by the ratios of the slopes of the unknown plates to the slope of the constant-term plate.

The nine-equation machine built at MIT consisted of a heavy steel frame containing 10 rotatable slotted steel plates. Each plate had 10
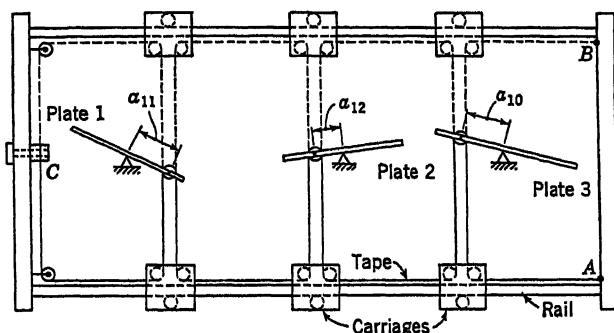
Fig. 7.4

longitudinal parallel slots. Slides were provided in 9 slots in order to set the constants of the equations. The tenth slot was used for reading the sine of the plate angle. Nine steel tapes, each about 60 ft long, were passed around the plate pulleys and were supported between the clamped ends on freely sliding carriages carried on rails in the steel frame. The carriages thus ensured that the tapes to and from the plate pulleys remained vertical during operation of the machine. The system of tapes and pulleys was repeated above and below the tilting plates in order to maintain tension during machine movement. The arrangement[7] used is shown schematically in Fig. 7.4.

The slides in the plates could be set by micrometer screws to 0.002 in., corresponding to four significant figures in the constants. In operation the plate turning through the greatest angle was rotated to about 40° one way and then to the same value the other way. The sums of the sine readings in the two positions for the unknown plates divided by the corresponding sum for the constant-term plate provided the values of the unknowns. The total time to solve nine equations for nine unknowns

to three significant figures was estimated to be from 1 to 3 hr on this machine, as compared with possibly 8 hr on a desk calculator. A major portion of time on this and on other simultaneous-equation machines is consumed in setting coefficients. Once these have been set, the solution occurs rapidly. Successive solutions are also rapidly obtained if some coefficients are given successive values, while in the main most of the coefficients remain fixed.

7.5. The Mallock Transformer-type Machine. The use of transformers for multiplication of voltages by constants and for the addition of voltages has been described in the previous chapter. Thus transformers provide the essential elements for the electrical solution of simultaneous algebraic equations. Such a machine was developed by Mallock.[8] The
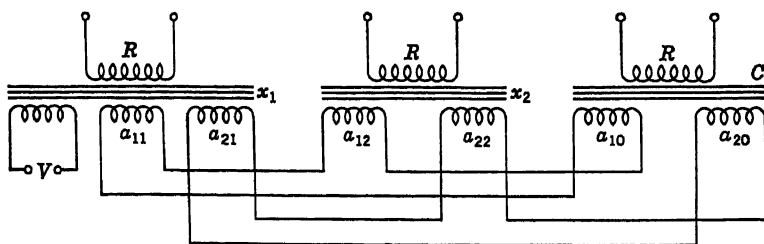
Fig. 7.5

operation of the machine may be described in principle by referring to Eqs. (7.3) and to Fig. 7.5.

Suppose three transformers are wound as shown in Fig. 7.5. The first transformer, which is labeled x_1, has two coils having the numbers of turns proportional to the x_1 coefficients of Eqs. (7.3), namely, a_{11} and a_{21}. The x_2 transformer, similarly, is wound with two coils whose turns are proportional to a_{12} and a_{22}. The third transformer is wound with two coils whose turns are proportional to the constant terms a_{10} and a_{20}. All three transformers are provided with identical reference coils R, which are used for determining the relative magnetic flux densities in the three transformer cores. An additional coil V is provided to one of the transformers (the x_1 transformer, for example) in order to excite the whole system.

Thus, if an alternating voltage were applied across the exciting coil V, magnetic flux would be developed in the core of the x_1 transformer. This in turn would generate alternating voltages in the coils a_{11}, a_{21}, and R. Assuming that ideal transformers are used, the voltages generated in the three coils would be proportional to the numbers of turns in the coils.

. Because of the interconnections between the three transformers, currents will flow through all the coefficient and constant-term coils, thus generating alternating magnetic fields in the other two cores. In these

other transformers the voltages generated in the coils are also proportional to the numbers of turns and the flux densities in the cores.

Thus, suppose that when the steady state is reached the flux density in the first core is X_1, that in the second core is X_2, and that in the third core is C. Then the voltages across the terminals of the coils would be as shown below (where m is the constant of proportionality):

Coil	Voltage at terminals
a_{11}	$ma_{11}X_1$
a_{21}	$ma_{21}X_1$
R (on x_1)	mRX_1
a_{12}	$ma_{12}X_2$
a_{22}	$ma_{22}X_2$
R (on x_2)	mRX_2
a_{10}	$ma_{10}C$
a_{20}	$ma_{20}C$
R (on C)	mRC

The sum of the voltage drops across each closed loop of Fig. 7.5 must be zero. The sums for the two loops shown are

$$ma_{11}X_1 + ma_{12}X_2 - ma_{10}C = 0$$
$$ma_{21}X_1 + ma_{22}X_2 - ma_{20}C = 0 \tag{7.11}$$

or, dividing through by mC,

$$a_{11}\frac{X_1}{C} + a_{12}\frac{X_2}{C} - a_{10} = 0$$
$$a_{21}\frac{X_1}{C} + a_{22}\frac{X_2}{C} - a_{20} = 0 \tag{7.12}$$

Equations (7.12) correspond exactly to Eqs. (7.3). Thus

$$x_1 = \frac{X_1}{C} \qquad x_2 = \frac{X_2}{C} \tag{7.13}$$

Measurements of the voltages in the identical R coils on each transformer permit the evaluation of the ratios in Eqs. (7.13). The voltage across R on x_1 divided by the voltage across R on C is x_1, and that across R on x_2 divided by that across R on C is x_2.

The exciting coil V could be placed on any one of the three transformers. In the Mallock machine for 10 simultaneous equations there are 11 main transformers with an exciting coil on each. In operation, the core having the greatest flux density (largest root) is excited. This is determined after an initial trial.

Each coefficient winding on each transformer is variable between 1

and 1,000 turns, requiring 16 separate coils to provide this range. Coefficients can thus be set to three significant figures.

The transformers themselves are made of continuous figure-eight Mu-metal stampings 0.008 in. thick. The coils are wound on the central limb. An elaborate arrangement of compensating coils, transformers, and amplifiers permits the magnetization of the cores by the auxiliary coils without requiring any appreciable magnetizing current to flow in the coefficient coils, thus yielding a corresponding increase in accuracy of the machine.

7.6. The Potentiometric Simultaneous-equation Solver. Because of its simplicity and economy, the potentiometric method of multiplication by a constant and addition has been widely used in simultaneous-equation solving machines. Equations (7.3) will again be used to demonstrate the principles of these computers. The extension to greater sets of equations will be obvious.

Figure 7.6 shows the two complete circuits for solving the two simultaneous equations. The first circuit imposes on its voltages the relations existing in the first of Eqs. (7.3). The second circuit does the same thing with respect to the second of Eqs. (7.3). In each circuit a potentiometer is required to represent each coefficient, each unknown, and the constant term. The coefficient and constant-term potentiometers are all subjected to a constant voltage $\pm E$ (depending on the algebraic signs of the terms in the equations). For this purpose two identical batteries may be connected in series and the common terminal grounded. A switch at the input end of each coefficient and constant-term potentiometer permits reversal of sign at will.

Assuming that the constants in Eqs. (7.3) have been normalized (*i.e.*, each equation divided through by the largest constant occurring in the equation), the constants a_{11}, a_{12}, a_{10}, a_{21}, a_{22}, a_{20} then have values which do not exceed unity. They may be set on the coefficient potentiometers as fractions of the total travel of the potentiometer brushes and the voltages at the brushes will be the same fractions of the input voltage E, provided that the loading effects described in the previous chapter are avoided. The voltages $a_{11}E$, $a_{21}E$ are the input voltages to the two x_1 potentiometers, and the voltages $a_{12}E$ and $a_{22}E$ the inputs to the two x_2 potentiometers. At this point we do not know what x_1 and x_2 are. However, for any settings of the x_1 and x_2 potentiometers as fractions x_1 and x_2 of the total travel, the brush voltages will be $a_{11}x_1E$, $a_{12}x_2E$, $a_{21}x_1E$, and $a_{22}x_2E$, again provided loading effects are avoided. By means of adding resistors R_0, the output voltages of the pairs of x potentiometers may be added to the corresponding output voltages of the constant-term potentiometers. It should be noted at this point that the sign of the constant-term coefficient should be reversed so that upon addition the constant

term is actually subtracted from the sum of the other two terms. This reversal of sign is accomplished, of course, by the plus-or-minus switch at the potentiometer input terminal. Each circuit then provides a resultant output voltage V given by

$$\frac{E}{3} (a_{11}x_1 + a_{12}x_2 - a_{10}) = V_1$$

$$\frac{E}{3} (a_{21}x_1 + a_{22}x_2 - a_{20}) = V_2$$

(7.14)

If x_1 and x_2 are exactly the roots of the normalized Eqs. (7.3), then V_1 and V_2 become zero. The solving procedure, therefore, would be to manipulate the x_1 and x_2 potentiometer settings until the readings of the two voltmeters (or galvanometers) V_1 and V_2 become zero. If the x_1 or x_2 potentiometers, or both, go off scale, the values of x_1 and/or x_2 are greater than unity and scale factors must be applied to reduce them to magnitudes which will appear on the potentiometers.

To illustrate in a simple way the method of setting up a problem, suppose Eqs. (7.15) are to be solved on the simultaneous-equation machine of Fig. 7.6.

$$4x_1 + 5x_2 = 20$$
$$3x_1 + 9x_2 = 4.5$$

(7.15)

In normalized form these equations are

$$0.2x_1 + 0.25x_2 = 1.0$$
$$0.33x_1 + 1.0x_2 = 0.5$$

(7.16)

The coefficient potentiometers would then be set at the values $a_{11} = 0.2$, $a_{12} = 0.25$, $a_{21} = 0.33$, $a_{22} = 1.0$, and the constant-term potentiometers at the values $a_{10} = 1.0$, $a_{20} = 0.5$. If x_1 and x_2 are now manipulated in an attempt to bring voltmeters V_1 and V_2 to zero, it would be found that these potentiometers go off scale. A numerical solution of Eqs. (7.16), which would not be available in an actual situation, shows that $x_1 = 7.45$ and $x_2 = 2.51$, an obvious reason for the unknown potentiometers being pushed up to their stops.

With this advance knowledge and a determination to make the equation solver work, Eqs. (7.16) may be rewritten in the form

$$0.2 \left(\frac{x_1}{10}\right) 10 + 0.25 \left(\frac{x_2}{3}\right) 3 = 1$$

$$0.33 \left(\frac{x_1}{10}\right) 10 + 1.0 \left(\frac{x_2}{3}\right) 3 = 0.5$$

(7.17)
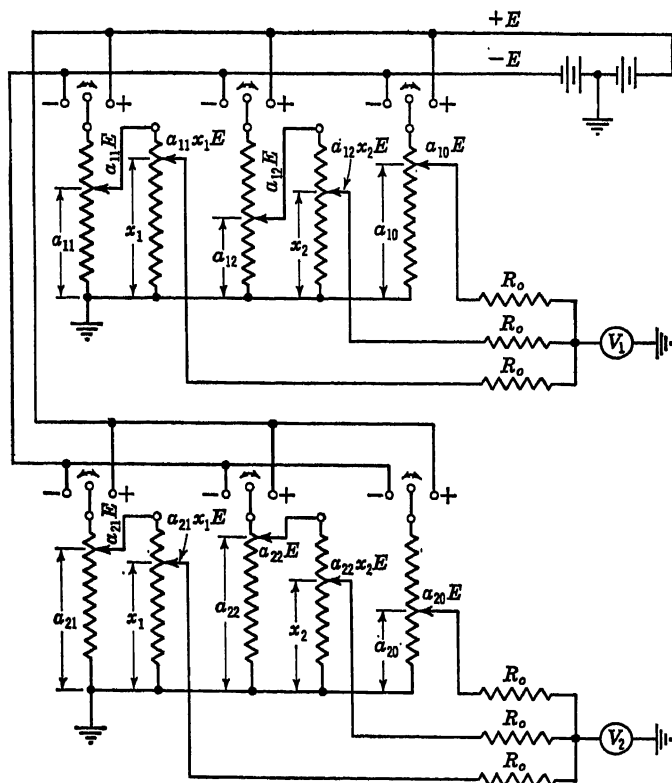
Fig. 7.6

or, with $X_1 = x_1/10$ and $X_2 = x_2/3$,

$$2.0X_1 + 0.75X_2 = 1.0$$
$$3.3X_1 + 3.0X_2 = 0.5 \qquad (7.18)$$

These equations must be normalized again to give

$$X_1 + 0.375X_2 = 0.5$$
$$X_1 + 0.9X_2 = 0.15 \qquad (7.19)$$

Now resetting the coefficient and constant-term potentiometers to the values 1, 0.375, 1, 0.9, 0.5, and 0.15, the X_1 and X_2 potentiometers will balance out at the settings 0.754 and 0.84.

An alternative procedure would be to use Eqs. (7.16) as they stand on the left-hand side but to reduce the constant terms by some factor such as 10 (*i.e.*, set the constant-term potentiometers at 0.1 and 0.05).

This is equivalent to rewriting Eqs. (7.16) in the form

$$0.2\left(\frac{x_1}{10}\right) + 0.25\left(\frac{x_2}{10}\right) = \frac{1.0}{10}$$
$$0.33\left(\frac{x_1}{10}\right) + 1.0\left(\frac{x_2}{10}\right) = \frac{0.5}{10} \tag{7.20}$$

or

$$0.2Y_1 + 0.25Y_2 = 0.1$$
$$0.33Y_1 + 1.0Y_2 = 0.05 \tag{7.21}$$

for which the Y_1 and Y_2 potentiometers will balance at the settings 0.745 and 0.251.

Since the first of Eqs. (7.20) has all coefficients less than unity, it may be multiplied through by a factor as large as 4. This would change the coefficient and constant-term potentiometer settings for this particular equation to 0.8, 1.0, and 0.4, respectively, without affecting the Y_1 and Y_2 readings.

Another alternative would be to divide the coefficients in Eqs. (7.15) by 10, to give values which could be set on the potentiometers, yielding the equations

$$0.4Z_1 + 0.5Z_2 = 20$$
$$0.3Z_1 + 0.9Z_2 = 4.5 \tag{7.22}$$

The network will now be used to sum *only the left sides* of Eqs. (7.22), the voltmeters being used to show when the sums are equal to the constant term. The exciting voltage E must be adjusted to the correct value so that settings of the Z_1 and Z_2 potentiometers which give readings of 20 and 4.5 volts for V_1 and V_2, respectively, may be properly interpreted in terms of x_1 and x_2. To get Z_1 and Z_2 into the desired range of potentiometer settings, suppose we put $Z_1 = x_1/10$ and $Z_2 = x_2/10$. The exciting voltage E must then be adjusted to the value satisfying all the relations of the type

$$a_{11}x_1 = \frac{a_{11}}{10}\frac{x_1}{10}E\frac{1}{2} \tag{7.23}$$

or $E = 200$ volts. Now, the Z potentiometer readings will be found to be 0.745 and 0.251 when V_1 reads 20 volts and V_2 reads 4.5 volts. Whereupon, $x_1 = 7.45$ and $x_2 = 2.51$. Equation (7.23) is based on the fact that an increase in E will make up for decreases in the coefficients and in unknowns (a factor of 100 here) when the actual sums on the left-hand sides are to be produced. An additional factor of 2 is involved, because, in the method of summation adopted, the result is an *average* rather than a true sum. Consequently, if n terms were involved, instead of only 2, the last fraction in Eq. (7.23) would be $1/n$ instead of $\frac{1}{2}$.

Both x_1 potentiometers must, obviously, have identical settings. So

must the two x_2 potentiometers. This is most easily accomplished if the two x_1 potentiometers are ganged together on the same shaft and thus are constrained to move together. The x_2 potentiometers would be similarly arranged.

The duplication of x potentiometers in machines for large numbers of simultaneous equations may be a serious matter in regard to both expense and bulk.

On this basis, a machine designed for n equations with n unknowns will require n^2 coefficient potentiometers, n constant-term potentiometers, and n sets of unknown potentiometers with n identical potentiometers ganged together in each set, or a total of $n(2n + 1)$ potentiometers. For a 20-equation machine, for example, the total number of potentiometers required would be $20(41) = 820$ potentiometers. Also, $n(n + 1)$ adding resistors are required (420 for the 20-equation machine).

By means of an appropriate multiple-pole switching arrangement[9] a single potentiometer to represent each unknown suffices, thereby decreasing the total number of potentiometers required by the amount $n(n - 1)$, or, in the case of the 20-equation machine, by 380 potentiometers. With this arrangement the number of adding resistors is also reduced by the same amount. The switching arrangement for positive and negative values of $a_{ij}x_j$ remains unchanged.

The number of coefficient potentiometers can also be drastically reduced by providing a single potentiometer with n independently adjustable taps for each column in the matrix of coefficients of Eqs. (7.1) and for the column of constant terms. A single coefficient potentiometer would thus be matched with its corresponding unknown potentiometer. Switching from equation to equation would be merely a matter of switching from tap to tap on each of $(n + 1)$ potentiometers, instead of switching from potentiometer to potentiometer in a system of $n(n + 1)$ potentiometers. This more compact arrangement is shown in Fig. 7.7 for a system of four simultaneous equations. Note that only nine potentiometers, that is, $2n + 1$, and five adding resistors, that is, $n + 1$, are required. Multiple taps and multiple switches eliminate the need for additional units. Plus and minus coefficients are obtained from a single coefficient potentiometer by preset switches P and an equation selector switch S at each of the multitapped potentiometers. Plus and minus values of x are provided by the double-pole double-throw switches D.

With n unknown potentiometers to be manipulated, a random series of manipulations to bring all equations into balance would be impractical. A practical procedure is the mechanical equivalent of the Gauss-Seidel numerical process. After all coefficient potentiometers have been set, the x potentiometers are set to arbitrary values (estimated as closely as possible, if a basis for judgment exists). With the first set of coefficients

connected into the system, the x_1 potentiometer is adjusted to bring about a balance. If necessary, the sign switch may be flipped over to reverse the sign of x_1. Then, the second set of coefficients is connected into the system and the x_2 potentiometer adjusted to a balance. The procedure is repeated with the third set of coefficients and x_3, etc., until in the end the nth set of coefficients will have been introduced into the system and balance attained with x_n. This completes one iteration. At
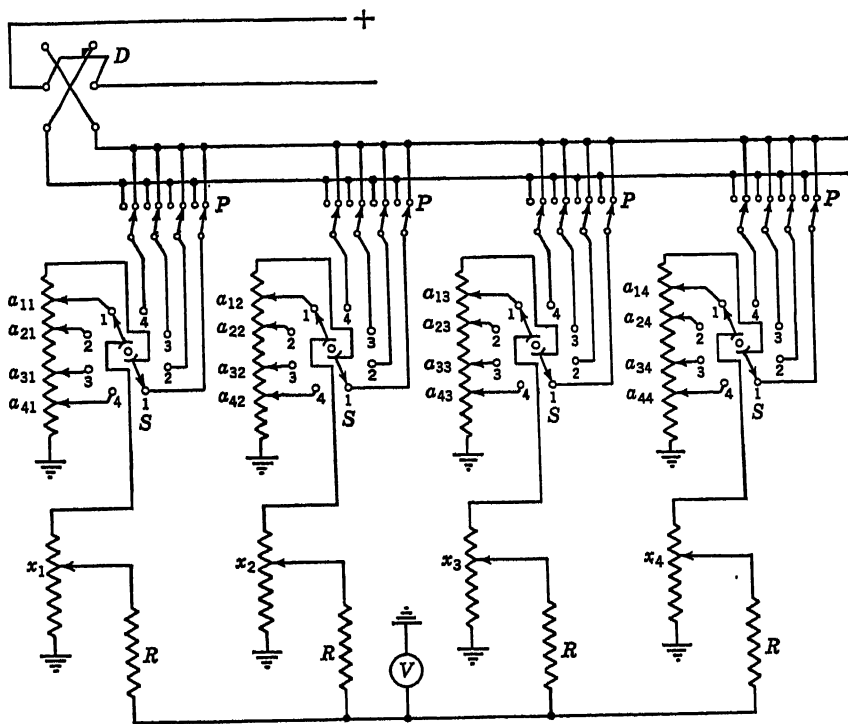
Fig. 7.7

this point only the nth equation is now in balance, since the successive readjustments have thrown previous equations out of balance again. Therefore, starting once again with the first set of coefficients connected into the system, x_1 is readjusted to a balance. Then, with the second set of coefficients inserted, x_2 is readjusted, etc., through the nth equation. This completes the second iteration. As many iterations are performed as are necessary to bring about a balance in all equations, so that as each set of coefficients is inserted into the system in turn, no further adjustment in the x potentiometers is required. The readings of the x potentiometers, when corrected in accordance with scale factors introduced in the solving process, give the required roots of the set of equations.

While Fig. 7.6 shows a d-c supply consisting of two identical batteries with the common terminal grounded, an alternative procedure for a plus-minus supply with respect to ground may be that illustrated in Fig. 7.8a. A single battery is shunted by means of a linear resistance. Since the voltage drop across the resistance is linear, the central point of the resistance may be grounded, thus providing equal and opposite voltages at its two ends with respect to ground. An identical arrangement is possible for an alternating voltage supply, where the a-c source would replace the battery in Fig. 7.8a. With an a-c source each terminal voltage will alternate between plus and minus values; however, the two ends will always assume values of opposite sign with respect to ground, so that if one side is labeled plus, the other will be minus. With either the d-c or a-c source, problems of overloading one side or the other of the resistance might arise. In that case the geometrical center of the resistance and its electrical center (equal potential drops on the two sides) will not coincide. Such a loading effect can be compensated by using a potentiometer in place of the fixed resistance. The brush of the potentiometer would then be the grounded tap and, for any unbalanced loading conditions, it would be shifted up or down to equalize the voltages on either side.
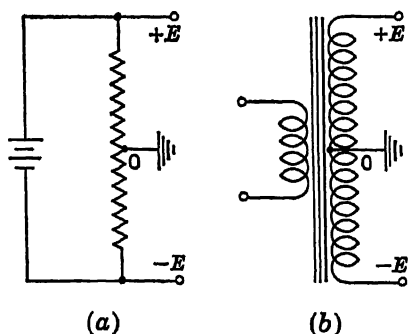
(a)   (b)

Fig. 7.8

Instead of a resistance, a center-tapped transformer can be used to supply plus-minus a-c voltages, as shown in Fig. 7.8b. The a-c voltage drop across the secondary coil is divided into two equal parts of opposite sign with respect to ground by grounding the central tap of this transformer.

In evaluating the accuracy and rate of convergence of such an instrument, the inherent nature of the set of equations must be considered. Such sets of equations may be "well-conditioned" or "ill-conditioned." In the numerical solution of such equations it is often necessary to carry a large number of digits during calculation in order to obtain relatively few significant digits in the answer.[10,11] Some unknowns in the set may be very sensitive to small variations in values of the coefficients. Thus, if coefficients are accurate to four figures, the roots may be accurate to only two or three figures even when many more digits are carried in the calculating procedure. If, upon substituting the roots back into the equations, the discrepancies between the sums on the left sides and the constant terms are of the same order as the

uncertainties in the constant terms, the roots are then as accurate as the known data.

Let us consider the determinant of the coefficients of n simultaneous equations. If the elements in two rows or two columns are identical or proportional, these equations or variables are not independent and a unique solution for the n unknowns cannot be obtained. The system of equations has a zero determinant and is singular (indeterminate). If a determinant is small (almost singular, *i.e.*, ill-conditioned), some of the unknowns will be sensitive to slight changes in the constants of the equation and the rate of convergence to a solution is likely to be slow. The conditions for convergence discussed in Sec. 7.1 for the numerical process also apply to this mechanical process. The equations should be arranged, before starting the solution, to make the elements on the principal diagonal large and those off the diagonal small.

In bringing each equation to a balance by adjusting one of its unknowns, some advantage might well accrue if an indication were provided of the effect of this adjustment on the error present in all the equations. The successive adjustments of the unknowns may then be carried out with the objective of reducing the *over-all* error of the system of equations, rather than reducing the error in only one equation at a time. Since errors may be plus or minus, a direct summation of errors would not provide the necessary criterion. Instead, the error in each equation may be squared and the sum of the squares taken. Each unknown is then adjusted in the direction to reduce continuously this sum of the squares of errors.[12,13] Either all equations must be simultaneously represented in order that their errors be available simultaneously or else rapid switching from equation to equation must be used in order to sample the errors in turn and display their cumulative squared effect on galvanometer or voltmeter.

7.7. Electronic Simultaneous-equation Solver. Automatic balancing of potentiometric simultaneous-equation solvers may be accomplished by feedback across high-gain computing amplifiers.[14] The application of negative-feedback amplifiers to summation and multiplication by constants has been described previously in Chap. 2. The interconnections necessary to solve Eqs. (7.3) will be discussed below. The extension to more than two equations will be obvious, as in the previous cases.

Referring to Fig. 7.9, suppose $-e_1$ and $-e_2$ to be the output voltages, respectively, of two high-gain negative-feedback amplifiers. These output voltages will be negative with respect to the inputs and will be A times as large, where A is the absolute gain through each amplifier. Of these output voltages, portions are fed back to the inputs of both amplifiers. Thus, the fraction a_{11} of the output of amplifier 1 and the fraction a_{12} of the output of amplifier 2 are both fed back through identical

resistors R to the input of amplifier 1. (Large enough values must be assigned to R to avoid loading effects.) Similarly, the fraction a_{21} of the output of amplifier 1 and the fraction a_{22} of the output of amplifier 2 are both fed back through another pair of resistors identical with the first pair to the input of amplifier 2. External voltages v_1 and v_2 excite the amplifiers through input resistors also of magnitude R. With the amplifier input terminal substantially at ground potential, the sum of the currents flowing through the three resistances R is given by
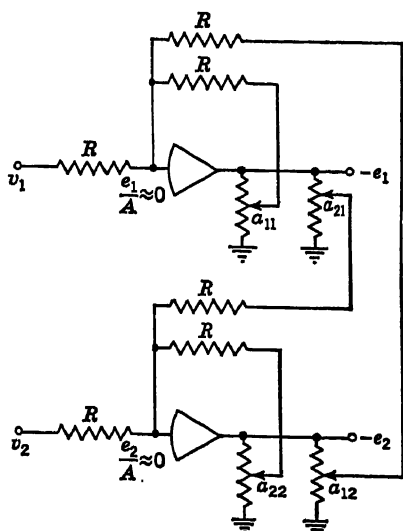
Fig. 7.9

$$\frac{v_1}{R} - \frac{e_1 a_{11}}{R} - \frac{e_2 a_{12}}{R} = 0$$
$$\frac{v_1}{R} - \frac{e_1 a_{21}}{R} - \frac{e_2 a_{22}}{R} = 0$$

(7.24)

or

$$a_{11}e_1 + a_{12}e_2 = v_1$$
$$a_{21}e_1 + a_{22}e_2 = v_2$$

(7.25)

Comparing Eqs. (7.25) with Eqs. (7.3), it will be clear that the input voltages v_1 and v_2 should be the constant-term values a_{10} and a_{20}. Then e_1 and e_2 will be the values of x_1 and x_2. The voltages v_1 and v_2 representing the constant terms may be obtained from input potentiometers supplied with a constant voltage $\pm E$.

Since the potentiometers serve as voltage dividers, permitting settings from 0 to 100 per cent of the input voltage, the usual equation reduction procedures must be adopted, as in the case of the nonelectronic potentiometric equation solvers. Whatever actual value of voltage is found convenient for E may be taken as the unit of voltage for the equation solver and the output voltages e_1 and e_2 expressed in terms of this unit.

7.8. Stability of Electronic Equation Solvers. The lack of perfection in amplifiers limiting the accuracy obtainable in operations such as adding and integrating has been mentioned in Chap. 2. With feedback, amplifiers may also become unstable. The gain through an amplifier not only varies in magnitude with frequency but is accompanied by a phase shift which also varies with frequency. Such a phase shift can lead to a condition of self-oscillation (instability) in the amplifier output.

While Eqs. (7.24) express the relations between input and output voltages on the basis of a stable system, these relations may be written more accurately in terms of the actual gain characteristic $A(s)$ of the amplifier,[14] where $A(s)$ relates both the amplification and the phase to

the frequency ω. In general, $s (= \sigma + j\omega)$ is a complex number, whose real part σ determines the rate of growth or decay of a transient oscillation, and whose imaginary part ω is the natural frequency of the oscillation. Usually s is called the "complex frequency" and may be represented by the positions of points in the complex frequency plane. Values of σ are represented along the axis of reals and values of ω along the axis of imaginaries. Thus, amplifier behavior, including its stability characteristics, may be depicted in the complex frequency plane.[15] A positive real part in s denotes oscillation increasing with time and hence instability of the amplifier.

With $e_1/A(s)$ and $e_2/A(s)$ as the voltages at the input terminals of the two amplifiers in Fig. 7.9, the current sums at these terminals considered as nodes are

$$\frac{1}{R}\left[\left(v_1 - \frac{e_1}{A(s)}\right) - \left(\frac{e_1}{A(s)} + a_{11}e_1\right) - \left(\frac{e_1}{A(s)} + a_{12}e_2\right)\right] = 0$$
$$\frac{1}{R}\left[\left(v_2 - \frac{e_2}{A(s)}\right) - \left(\frac{e_2}{A(s)} + a_{21}e_1\right) - \left(\frac{e_2}{A(s)} + a_{22}e_2\right)\right] = 0 \tag{7.26}$$

where e_1 and e_2 are functions of s; or

$$v_1 = \left(a_{11} + \frac{3}{A(s)}\right)e_1 + a_{12}e_2$$
$$v_2 = a_{21}e_1 + \left(a_{22} + \frac{3}{A(s)}\right)e_2 \tag{7.27}$$

If v_1 and v_2 are set equal to zero, the resulting homogeneous set of equations will describe the transient response characteristics of the amplifier system. They have a solution only if the determinant of the coefficients of e_1 and e_2 is zero. Thus the characteristic equation is

$$\left(\frac{3}{A(s)}\right)^2 + (a_{11} + a_{22})\left(\frac{3}{A(s)}\right) + a_{11}a_{22} - a_{12}a_{21} = 0 \tag{7.28}$$

and the two characteristic roots are

$$\frac{3}{A(s)} = -\frac{1}{2}(a_{11} + a_{22}) \pm \frac{1}{2}\sqrt{(a_{11} + a_{22})^2 - 4(a_{11}a_{22} - a_{12}a_{21})} \tag{7.29}$$

Values of s can be calculated from Eq. (7.29). If a positive real part occurs in any one of the values of s, the system of amplifiers will be unstable.

While only two equations have been considered above, the analysis may be extended to any number of equations. However, a stability analysis for a large system on this basis would be very laborious. Goldberg and Brown[14] make use of a stabilizing technique which always works,

namely, to write the system of simultaneous equations in matrix form and develop a new set of equations by multiplying both sides of the matrix equation by the transpose of the matrix of coefficients. Let the given set of equations be written

$$\mathbf{Ax} = \mathbf{a} \qquad (7.30)$$

where $\mathbf{A}$ is the square matrix of coefficients, $\mathbf{x}$ the column matrix of unknowns, and $\mathbf{a}$ the column matrix of constant terms. Then the new stable set of equations may be written

$$\mathbf{A'Ax} = \mathbf{A'x} \qquad (7.31)$$

where $\mathbf{A'}$ is the transpose of $\mathbf{A}$ (that is, $\mathbf{A'}$ is obtained by interchanging the rows and columns of $\mathbf{A}$).

The transformation from Eq. (7.30) to Eq. (7.31) may be done on a desk calculator and the Eq. (7.31) solved in the analog computer, or both the transformation and solution may be accomplished simultaneously in the computer if the computer capacity is double that required for the original set of equations.

Korn[16] has developed a simple condition of stability applicable to a system of equations whose matrix of coefficients is positive definite, a situation which commonly occurs in physical systems. Under this condition, if a single amplifier with simple feedback can be shown either analytically or experimentally to be stable, then a computer employing n such amplifiers for the given set of equations will also be stable.

A unique approach to the stability problem has been developed at the Naval Research Laboratory.[17] It is based essentially on the common practice of introducing appropriate amounts of damping into dynamical systems which tend to become self-excited (unstable). The system of computing amplifiers with its multitude of feedback paths is such a dynamical system. The damping effect is introduced by inserting into the given system of equations where necessary first derivative terms of the proper magnitude and sign. These cause the transient effects (which are responsible for instability) to die out rapidly, leaving finally only the steady-state condition which is the solution of the given set of algebraic equations. This device positively ensures stability in electronic linear-simultaneous-equation solvers.

7.9. Simultaneous Equations with Complex Coefficients and Roots. Equations frequently encountered in practice have complex coefficients and, of course, complex roots. A set of linear simultaneous algebraic equations of this sort may be converted to a set of equations of twice the order, but with real coefficients and real roots, by separating the real and imaginary parts of the original set of equations. Thus suppose that in Eqs. (7.3) the constants are complex (that is, $a = b + ic$, where

$i = \sqrt{-1}$). The roots will also be complex (that is, $x = y + iz$). The equations may then be written as follows:

$$\begin{aligned}(b_{11} + ic_{11})(y_1 + iz_1) + (b_{12} + ic_{12})(y_2 + iz_2) &= b_{10} + ic_{10} \\ (b_{21} + ic_{21})(y_1 + iz_1) + (b_{22} + ic_{22})(y_2 + iz_2) &= b_{20} + ic_{20}\end{aligned} \quad (7.32)$$

Upon multiplying out and separating real and imaginary parts, Eqs. (7.32) become

$$\begin{aligned}b_{11}y_1 + b_{12}y_2 - c_{11}z_1 - c_{12}z_2 &= b_{10} \\ b_{21}y_1 + b_{22}y_2 - c_{21}z_1 - c_{22}z_2 &= b_{20} \\ c_{11}y_1 + c_{12}y_2 + b_{11}z_1 + b_{12}z_2 &= c_{10} \\ c_{21}y_1 + c_{22}y_2 + b_{21}z_1 + b_{22}z_2 &= c_{20}\end{aligned} \quad (7.33)$$

The original set of two equations with two complex unknowns has now become a set of four equations with four real unknowns and may be solved by any of the procedures described so far. Once y_1, y_2, z_1, and z_2 have been determined from Eqs. (7.33), the absolute magnitudes of x_1 and x_2 will be

$$x_1 = \sqrt{y_1{}^2 + z_1{}^2} \qquad x_2 = \sqrt{y_2{}^2 + z_2{}^2} \qquad (7.34)$$

The components y_1 and z_1 form the two sides of a right triangle, of which x_1 is the hypotenuse. A similar situation prevails for x_2 in connection with y_2 and z_2 and for the coefficients. It is thus possible to study geometrically not only the magnitudes of the roots and coefficients but also their phase angles.

Some equations with complex coefficients and complex roots may be solved directly[18] on an a-c network calculator. The equations must have symmetrical determinants (that is, $a_{ij} = a_{ji}$) and the real parts of the coefficients must be positive. The latter condition prevails because resistance is used to represent the real part of the coefficient, inductive reactance the positive imaginary part, and capacitive reactance the negative imaginary part. Negative resistances are not, in general, convenient to represent in the circuit.

7.10. Secular-equation Computers. Vibrations of mechanical, electrical, and molecular systems, problems in quantum mechanics, in statistics, and in other fields frequently involve indeterminate sets of linear algebraic equations of the form:

$$\begin{aligned}(a_{11} - \lambda^2)x_1 + a_{12}x_2 + \cdots + a_{1n}x_n &= 0 \\ a_{21}x_1 + (a_{22} - \lambda^2)x_2 + \cdots + a_{2n}x_n &= 0 \\ a_{n1}x_1 + \cdots + a_{n,n-1}x_{n-1} + (a_{nn} - \lambda^2)x_n &= 0\end{aligned} \quad (7.35)$$

To simplify the discussion of the problem without restricting its generality, a system of two equations of the above type will be considered

below, namely,

$$(a_{11} - \lambda^2)x_1 + a_{12}x_2 = 0$$
$$a_{21}x_1 + (a_{22} - \lambda^2)x_2 = 0 \tag{7.36}$$

In these equations λ is a characteristic value ("eigenvalue") of the particular system for which the equations are written. Thus, in a mechanical or electrical oscillatory system, λ would be a natural frequency of the system. The values of x_1 and x_2 satisfying the above equations are the characteristic functions ("eigenfunctions") of the given system. In the mechanical or electrical system mentioned they would be the relative amplitudes of free vibration of the elements of the system [two elements in Eqs. (7.36)] at a natural frequency λ; that is, they represent the "mode shape" at this frequency. In such oscillatory systems $a_{12} = a_{21}$.

The values of λ and the relative values of the xs are to be determined from Eqs. (7.36). For x_1 and x_2 to have values other than zero, the determinant of the coefficients of x_1 and x_2 must be zero. The values of λ are, therefore, determined from the equation

$$\begin{vmatrix} a_{11} - \lambda^2 & a_{12} \\ a_{21} & a_{22} - \lambda^2 \end{vmatrix} = 0 \tag{7.37}$$

Equation (7.37) is called the "secular" equation, or, in vibration-engineering terminology, the "frequency" equation. The determinant may be expanded to yield the frequency equation in the form:

$$\lambda^4 - (a_{11} + a_{12})\lambda^2 + (a_{11}a_{22} - a_{12}{}^2) = 0 \tag{7.38}$$

remembering that for linear oscillatory systems $a_{12} = a_{21}$.

Equation (7.38) is a second-degree equation in λ^2. Two values of λ^2 are thus available, providing the two natural frequencies (positive values of λ, only) of the system represented by the two Eqs. (7.36). For the system of Eqs. (7.35), the secular determinant would be of the nth order, and the expanded equation would be of nth degree in λ^2, providing for this system n different natural frequencies.

For each natural frequency, a characteristic function (or mode shape) exists. These may be calculated by substituting into Eqs. (7.36) in turn the values of λ^2 determined from the frequency equation. It should be noted that any characteristic value substituted into Eqs. (7.36) will make both equations identical, so that absolute values of x_1 and x_2 cannot be determined from these equations alone, but only the ratios of the xs may be determined for each characteristic value of λ. Consequently, the characteristic functions are frequently "normalized" by assuming one of the xs, say x_1, to be unity and then determining all the other xs as ratios with respect to unity. Such a procedure defines a set of normal modes having unit amplitudes at the same fixed location in the system. The actual

amplitude of each normal mode at this location would then be determined from initial conditions.

The expansion of an nth-order determinant of the form given in Eq. (7.37), followed by a solution of an nth-degree algebraic equation in λ^2, and then by the solution of $n - 1$ linear simultaneous algebraic equations to obtain the characteristic functions, is a very laborious task indeed if n is of the order of 8 or more. A solution of the original set of indeterminate equations [Eqs. (7.35)] by direct application of a simultaneous-equation-solving machine would offer decided advantages. The literature shows considerable activity has already been directed toward this end, and a number of different machines have been developed to meet this problem.

Frost and Tamres[19] have approached the problem by separation of terms involving λ^2. This method applied to Eqs. (7.36) converts the equations to the form:

$$a_{11}x_1 + a_{12}x_2 = \lambda^2 x_1$$
$$a_{21}x_1 + a_{22}x_2 = \lambda^2 x_2 \tag{7.39}$$

Since λ^2 has values between 0 and infinity, the range for λ^2 is covered in two steps, from 0 to 1 and from 1 to infinity. Following the method of Frost and Tamres, this may be done by introducing multipliers A and B into Eqs. (7.39) and dropping the λ^2, as follows:

$$A(a_{11}x_1 + a_{12}x_2) = Bx_1$$
$$A(a_{21}x_1 + a_{22}x_2) = Bx_2 \tag{7.40}$$

In these equations the ratio B/A is λ^2. Thus, if A is unity and B is varied from 0 to 1, all values of λ^2 from 0 to 1 would be covered. Now, if B is unity and A is varied from 1 to 0, all values of λ^2 from 1 to infinity would be covered.

The circuit for solving Eqs. (7.40) is shown in Fig. 7.10. In this case the exciting voltage is applied directly to the x potentiometers, instead of the coefficient potentiometers. The outputs of the x potentiometers are then fed to the input ends of the paralleled associated coefficient potentiometers. A three-gang double-pole switch serves to select one or the other of Eqs. (7.40) for consideration. The terms in the parenthesis on the left side of the equation selected are then summed through the resistors R. The voltage representing this sum is the input to the A potentiometer, where it is multiplied by the factor A. The corresponding x voltage for the selected equation is similarly fed through an identical R resistor to the B potentiometer, where it is multiplied by the factor B. A galvanometer or null detector G connecting the brushes of the A and B potentiometers indicates when balance is reached between the two sides of the equation under investigation. Each time

such balance is attained in both equations for the same settings of the x_1, x_2, and A or B potentiometers, these settings provide both a characteristic value and the associated characteristic function for Eqs. (7.39). Both A and B potentiometers are not varied simultaneously. When one is being varied, the other is maintained at unit position (brush at top of potentiometer). Since the xs are determined only as ratios with respect to one of the xs, one of the x potentiometers may be set at any arbitrary
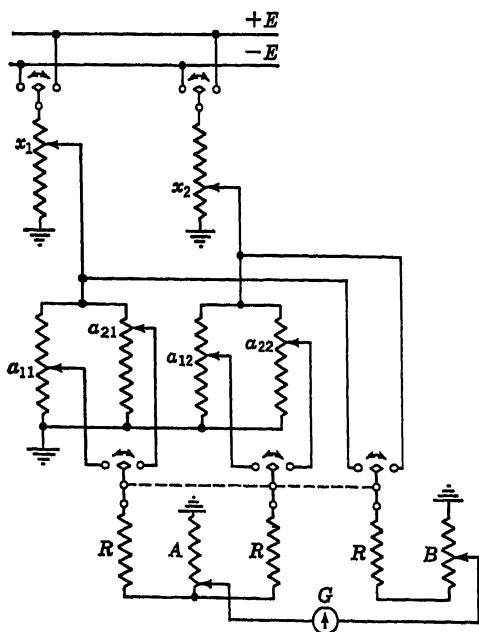
Fig. 7.10

position (*e.g.*, unity, if convenient) and the others (in an n-equation system) then used to balance out the electrical system in conjunction with the A and B potentiometers. In general, however, it would not be possible to set an arbitrary x potentiometer to unity because the required settings on some of the others may then be in excess of unity. Under those circumstances, the arbitrary setting must be reduced until all potentiometers will balance on scale. Ideally, if one could by inspection determine which x would be a maximum, the corresponding potentiometer could then be set to unity.

Machines requiring successive manual operations on the variable potentiometers to bring about balance result in a considerable expenditure of time in performing these operations. Automatic operation is, of course, a desirable improvement if the increased initial costs of such machines could be justified on the basis of time saved. An automatic

motor-driven secular-equation solver for four linear equations is described by Adcock.[20]   The principle of the method will be described in a simplified form in connection with Eqs. (7.36); the extension to more than two equations is straightforward.   Referring to Fig. 7.11, voltages labeled x_1 and x_2 (and their negative values) are shown applied to the ends of potentiometers representing the coefficients and frequencies in Eqs. (7.36).   It is not clear yet how x_1 and x_2 have been obtained, but that will become evident after the rest of the circuit has been described.   The summations indicated by the left sides of Eqs. (7.36) are performed through identical adding resistors R.   These sums will differ from zero until x_1,
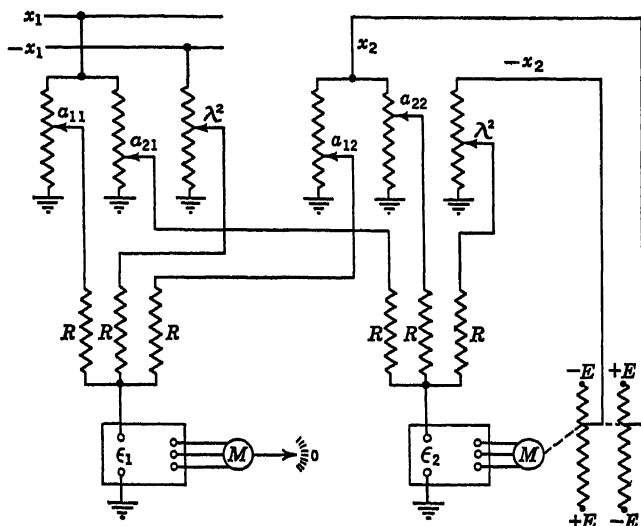
Fig. 7.11

x_2, and λ^2 have attained their correct values.   Consequently, error voltages ϵ_1 and ϵ_2 will be present at the summing ends.   These errors are amplified and drive motors M which attempt to provide from potentiometers connected to them the necessary voltages to reduce the errors to zero.   Since the secular equations involve only ratios of the xs, either x_1 or x_2 can be chosen arbitrarily.   Thus, suppose x_1 to be arbitrarily set to some convenient value, and a guess made as to a value of λ^2.   Because of the errors present in the system the motors M will turn in an effort to readjust the input voltages to values satisfying the circuit.   The input voltage x_2 will change, but x_1 will not, since it is disconnected from the motor-driven potentiometers.   Now by varying λ^2, the motor detecting errors in the first equation sum may be returned to zero position, thus indicating that the chosen x and the λ^2 found in this manner satisfy the first of Eqs. (7.36).   Meanwhile, the second motor will readjust itself

so that the output from its potentiometers will be x_2. Each value of λ^2 may be found in succession in this manner. For systems of more than two equations, the basic circuits are repeated as many times as are necessary to provide for all the equations. The manner of operating will be identical with that for the two-equation system. The λ^2 potentiometers would be ganged to a common shaft in order that they might be turned simultaneously.
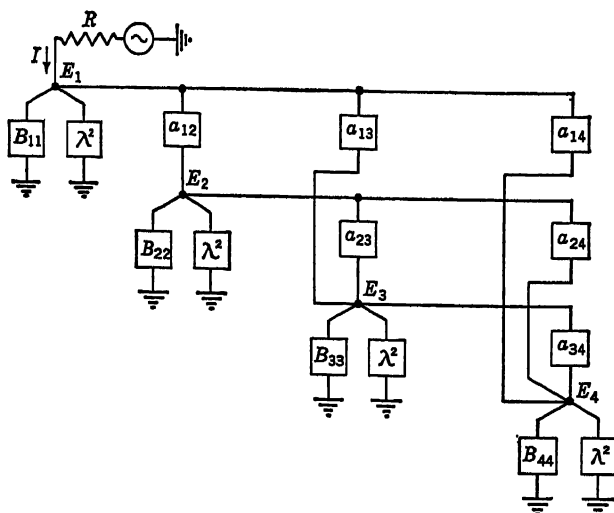
Fig. 7.12

The secular equation may also be mechanized by means of a network of inductances and capacitances.[21] The method will be described for the fourth-order secular equation shown below.

$$
\begin{vmatrix}
a_{11} - \lambda^2 & a_{12} & a_{13} & a_{14} \\
a_{21} & a_{22} - \lambda^2 & a_{23} & a_{24} \\
a_{31} & a_{32} & a_{33} - \lambda^2 & a_{34} \\
a_{41} & a_{42} & a_{43} & a_{44} - \lambda^2
\end{vmatrix} = 0 \qquad (7.41)
$$

The network for solving Eq. (7.41) is shown in Fig. 7.12, in which four nodes are connected to each other and to ground through admittances represented by blocks. The voltages at the four nodes are $E_1 - E_4$. The system is excited by an alternating current I supplied to one of the four nodes (node 1 in the figure).

Applying Kirchhoff's first law to each node, the current sum entering a typical node, say node 3, is (remembering that $a_{ij} = a_{ji}$)

$$
a_{31}(E_1 - E_3) + a_{32}(E_2 - E_3) + B_{33}(0 - E_3) + \lambda^2(0 - E_3)
$$
$$
+ a_{34}(E_4 - E_3) = 0 \qquad (7.42)
$$

Rearranging terms,

$$a_{31}E_1 + a_{32}E_2 + (-B_{33} - a_{31} - a_{32} - a_{34} - \lambda^2)E_3 + a_{34}E_4 = 0 \quad (7.43)$$

Let
$$B_{33} = -(a_{31} + a_{32} + a_{33} + a_{34}) \quad (7.44)$$

Then Eq. (7.43) becomes

$$a_{31}E_1 + a_{32}E_2 + (a_{33} - \lambda^2)E_3 + a_{34}E_4 = 0 \quad (7.45)$$

Similar equations may be written for all the other junctions. The equation for the first junction will contain one additional term, namely, the current I being supplied by the current generator. This current, however, will be small compared with the other currents flowing at the junction when the circuit is operated at resonance, and thus may be neglected. The result is a set of four homogeneous algebraic equations of the form of Eq. (7.45). In order that such a set have solutions for the Es other than zero, the determinant of the coefficients of the Es must be zero. Consequently, Eq. (7.41) results.

Based on the analysis leading to Eq. (7.44), the remaining B admittances are found to be

$$B_{11} = -(a_{11} + a_{12} + a_{13} + a_{14})$$
$$B_{22} = -(a_{21} + a_{22} + a_{23} + a_{24}) \quad (7.46)$$
$$B_{44} = -(a_{41} + a_{42} + a_{43} + a_{44})$$

The various admittances in the network are set, therefore, in accordance with the coefficients of Eq. (7.41) and in accordance with Eqs. (7.46). Positive values of a and B are conveniently represented by capacitance and negative values by inductance. The values of λ^2 are positive, and hence are set by capacitors. The four λ^2 capacitors are set identically, and thus should be ganged on a common shaft. The circuit is excited with a constant-frequency input through a large resistor R to ensure constancy in the input current as the set of ganged capacitors is adjusted through the four resonant states of the network. At each resonant point the admittance of one of the capacitors gives the characteristic value λ^2. The corresponding characteristic function is given by the voltage distribution from node to node. Theoretically, at resonance these voltages should go to infinity, since the theoretical system for which Eq. (7.41) are written is lossless. However, losses do occur in the actual system, so that finite values of voltage are established at the junction points in the steady state. In this representation of the secular equation, a dynamical analogy is actually set up for the physical system yielding Eq. (7.41).

REFERENCES

1. Dennis, P. A., and D. G. Dill: Application of Simultaneous Equation Machines to Aircraft Structure and Flutter Problems, *J. Aeronaut. Sci.*, **17**:107–113, 127 (1950).
2. Hotelling, H.: Some New Methods in Matrix Calculation, *Ann. Math. Stat.*, **14**:1–34 (1943).
3. Berry, C. E.: A Criterion of Convergence for Classical Iterative Method of Solving Linear Simultaneous Equations, *Ann. Math. Stat.*, **16**:398–400 (1945).
4. Murray, F. J.: Linear Equation Solvers, *Quart. Appl. Math.*, **7**:263–274 (1948).
5. Fairthorne, R. A.: Mechanical Instruments for Solving Simultaneous Equations, Aeronautic Research Council (England), *R. and M.* 2144, August, 1944.
6. Thomson, W.: On a Machine for the Solution of Simultaneous Linear Equations, *Proc. Roy. Soc. (London)*, **28**:111–113 (1878–1879).
7. Wilbur, J. B.: The Mechanical Solution of Simultaneous Equations, *J. Franklin Inst.*, **222**:715–724 (1936).
8. Mallock, R. R. M.: An Electrical Calculating Machine, *Proc. Roy. Soc. (London)*, (A)**140**:457–483 (1933).
9. Berry, C. E., D. E. Wilcox, S. M. Rock, and H. W. Washburn: A Computer for Solving Linear Simultaneous Equations, *J. Appl. Phys.*, **17**:262–272 (1946).
10. Tuckerman, L. A.: On Mathematically Significant Figures in the Solution of Simultaneous Linear Equations, *Ann. Math. Stat.*, **12**:307–316 (1941).
11. Satterthwaite, F. E.: Error Control in Matrix Calculations, *Ann. Math. Stat.*, **15**:373–387 (1944).
12. Walker, R. M.: An Analogue Computer for the Solution of Linear Simultaneous Equations, *Proc. IRE*, **37**:1467–1473 (1949).
13. Ackerman, S.: Precise Solutions of Linear Simultaneous Equations Using a Low Cost Analog, *Rev. Sci. Instr.*, **22**:746–748 (1951).
14. Goldberg, E. A., and G. W. Brown: An Electronic Simultaneous Equation Solver, *J. Appl. Phys.*, **19**:339–345 (1948).
15. Lynch, W. A.: The Stability Problem in Feedback Amplifiers, *Proc. IRE*, **39**:1000–1008 (1951).
16. Korn, G. A.: Stabilization of Simultaneous Equation Solvers, *Proc. IRE*, **37**:1000–1002 (1949).
17. McCool, W. A.: D-c Analog Solution of Simultaneous Linear Algebraic Equations: Circuit Stability Considerations, *NRL Rept.* 3533, Sept. 9, 1949.
18. Haupt, L. M.: Solution of Simultaneous Equations through Use of the A.C. Network Calculator, *Rev. Sci. Instr.*, **21**:683–686 (1950).
19. Frost, A. A., and M. Tamres: A Potentiometric Secular Equation Computer, *J. Chem. Phys.*, **15**:383–390 (1947).
20. Adock, W. A.: An Automatic Simultaneous Equation Computer and Its Use in Solving Secular Equations, *Rev. Sci. Instr.*, **19**:181–187 (1948).
21. Hughes, R. H., and E. B. Wilson, Jr.: An Electrical Network for the Solution of Secular Equations, *Rev. Sci. Instr.*, **18**:103–108 (1947).

8

ANALOG SOLUTION OF NONLINEAR ALGEBRAIC EQUATIONS

Polynomial equations often occur in physical and mathematical situations and require a solution. While general methods of solution for equations as high as the fourth degree are available in handbooks, Abel[1] showed many decades ago that general solutions for algebraic equations of degree higher than the fourth cannot be obtained. For these equations of higher degree numerical procedures are well developed,[2] but each equation must be treated as an individual case and its own particular solution obtained. For high-degree equations, e.g., an eighth degree or higher, the labor of numerical solution becomes great indeed, particularly if complex roots are involved. Machines for the solution of such equations have attracted the attention of mathematicians and scientists since the latter part of the eighteenth century.[3]

A typical polynomial of high degree is the following:

$$a_n z^n + a_{n-1} z^{n-1} + \cdots + a_2 z^2 + a_1 z + a_0 = 0 \qquad (8.1)$$

Its solution by machine methods involves the generation of powers of z, their multiplication by coefficients, and the summation of resulting terms to equal the negative of a_0.

Schemes for performing the basic operations mechanically and electrically have been described in Chaps. 2 to 5. It remains to assemble these mechanisms into a compatible unit satisfying Eq. (8.1).

In Eq. (8.1) the coefficients may be real or complex. Even if the coefficients are real, the roots may still be complex. This places rather stringent requirements on the machine, which must be capable of finding both the real and imaginary parts of each root.

8.1. Potentiometric Machines. If the coefficients and roots of Eq. (8.1) are real, the simple potentiometric procedures of multiplication and

summation used in Chap. 7 may be used. The circuit is shown in Fig. 8.1 for the fourth-degree equation:

$$a_4 z^4 + a_3 z^3 + a_2 z^2 + a_1 z + a_0 = 0 \qquad (8.2)$$

Since potentiometers are to be used, it will be assumed that the coefficients in Eq. (8.2) have been derived from the coefficients of an earlier equation by dividing by the largest coefficient. Hence, in Eq. (8.2) no coefficient is larger than unity. Four ganged and cascaded potentiometers identically set by a single knob provide the four powers of z present in Eq. (8.2). Four independent potentiometers set to the coefficients
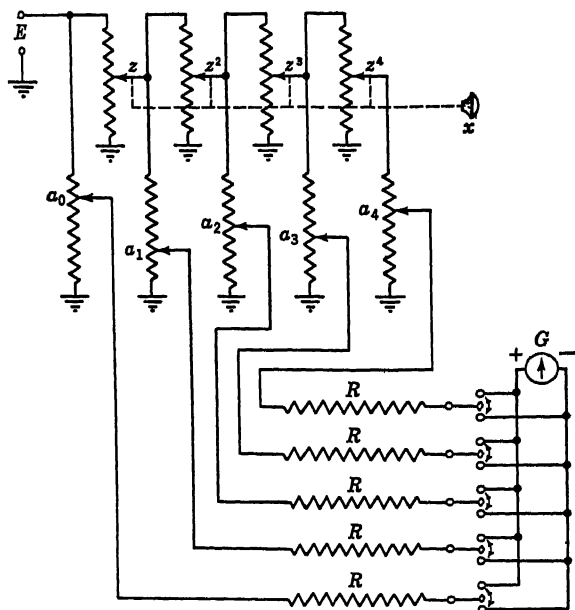
Fig. 8.1

of Eq. (8.2) are tapped off the brushes of the z potentiometers. A fifth independent potentiometer is supplied directly from the battery, and its brush is set to supply the constant term a_0. The outputs of the five independent potentiometers are connected to the input ends of identical adding resistors R. Plus-minus switches are provided at the output ends for balancing the sum of the plus terms in Eq. (8.2) against the sum of the minus terms with the aid of a galvanometer or null detector G. Such a procedure makes unnecessary a source of plus and minus voltage. If a positive value is presumed for z, then those terms with negative coefficients are switched into the negative side of the galvanometer, the others into the positive side. If balance cannot be attained with positive z, then z is presumed to be negative and the switches on

all the odd-powered terms would be reversed in polarity.   Even-powered terms are, of course, unaffected by a change in the sign of z.   Loading effects may become critical because of the large number of cascaded and paralleled potentiometers.   Appropriate means to avoid them should be taken.

In balancing plus and minus sums against each other in the adding circuit of Fig. 8.1, it should be noted that scale factors depending on the number of terms in each sum are involved.   For a null on the galvanometer to indicate the correct solution to Eq. (8.2), the scale factor for the positive sum should be the same as that for the negative sum, or, alternatively, differences in scale factor should be compensated for by altering the settings on the coefficient potentiometers.   The scale factors may be equalized by doubling the number of adding resistors and using double-pole double-throw switches, as shown in Fig. 8.2.   The grounded resistors add nothing to the actual sums, but provide for equal numbers of adding resistors on both sides of the galvanometer.   Switching a voltage from plus to minus automatically switches a grounded resistor from minus to plus.   Actually, one could do with fewer grounded resistors, using only enough to make up for the difference between the numbers of plus and of minus terms.
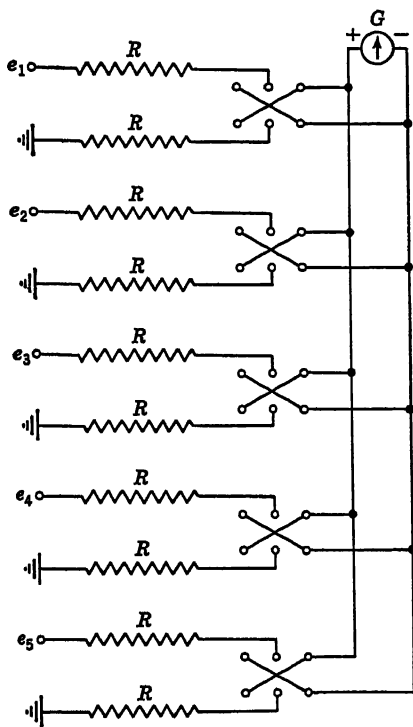
Fig. 8.2

Alternatively, if m voltages are to be added on the plus side and n on the minus side, scale-factor differences may be compensated by multiplying the coefficients of the plus terms by m/n and correspondingly changing the potentiometer settings, or by multiplying the coefficients of the minus terms by n/m and correspondingly changing these potentiometer settings.

Since potentiometers are used for the zs, the maximum value of z obtainable in terms of the potentiometer maximum displacement is unity. Consequently, scale factors may be introduced somewhat as in the potentiometric computers of Chap. 7 whenever z tends to go beyond unity.

Another method for readily taking into account values of z exceeding unity is to transform Eq. (8.1) so that the reciprocal of z appears in the transformed equation.   By making the substitution $z = 1/Z$ and multi-
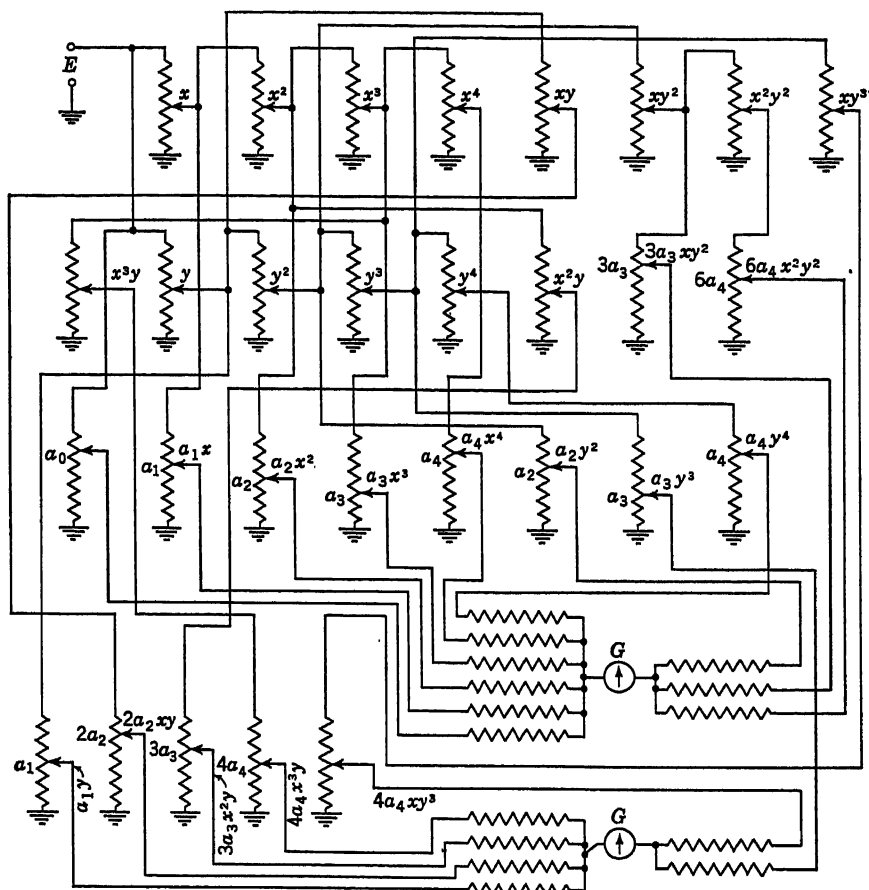
Fig. 8.3

plying the equation through by Z^n, the following equation results instead of Eq. (8.1):

$$a_0 Z^n + a_1 Z^{n-1} + a_2 Z^{n-2} + \cdots + a_{n-1} Z + a_n = 0 \quad (8.1a)$$

The roots of Eq. (8.1a) between 0 and 1 are the reciprocals of the roots of Eq. (8.1) between 1 and ∞.

If complex roots are present in Eq. (8.2), the equation may be converted into a pair of simultaneous equations by substituting in place of z the relation

$$z = x + iy \qquad (8.3)$$

Thus

$$a_4(x + iy)^4 + a_3(x + iy)^3 + a_2(x + iy)^2 + a_1(x + iy) + a_0 = 0 \quad (8.4)$$

Upon expanding the binomials, collecting terms, and separating real and imaginary parts, the resulting equations are

$$a_4x^4 + a_3x^3 + a_2x^2 + a_1x - 3a_3xy^2 - 6a_4x^2y^2 - a_2y^2 - a_4y^4 + a_0 = 0 \quad (8.5)$$

$$4a_4x^3y + 3a_3x^2y + 2a_2xy - 4a_4xy^3 - a_3y^3 + a_1y = 0$$

A potentiometric computer to solve this set of equations is shown schematically in Fig. 8.3. The relations shown in Eqs. (8.5) are represented by connecting the various potentiometers in accordance with
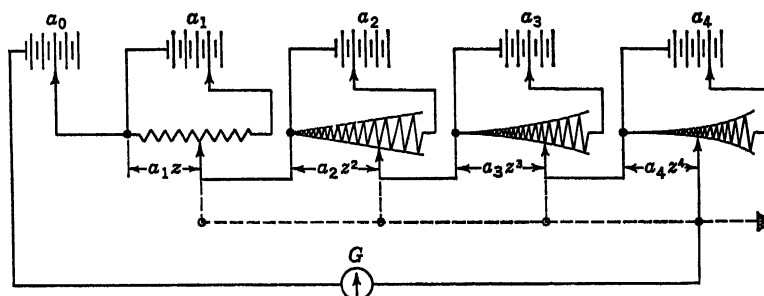
Fig. 8.4

the methods already discussed. The mechanization of both equations is shown. Again it should be emphasized that in dispensing with a negative voltage source, provision must be made for scale-factor differences in the positive and negative sums being balanced.

In the operation of this computer, for each value of x the range of y would be searched for a balance. Values of x may be either negative or positive. There will always be both a positive and a negative value of y because complex roots occur in conjugate pairs. Hence, only the positive range of y need be investigated, whereas both positive and negative values of x must be searched.

The various powers of z may be developed by means of tapered resistance potentiometers instead of cascaded potentiometers. Such a circuit using independent batteries instead of potentiometers to produce voltages proportional to the coefficients is described by Schooley.[4] A circuit diagram is shown in Fig. 8.4 for Eq. (8.2) in which both coefficients and roots are real. Instead of tapering the resistances and ganging all brushes on one shaft, all linear resistances can be used, with brushes geared up to give the shaft rotations z, z^2, z^3, etc.
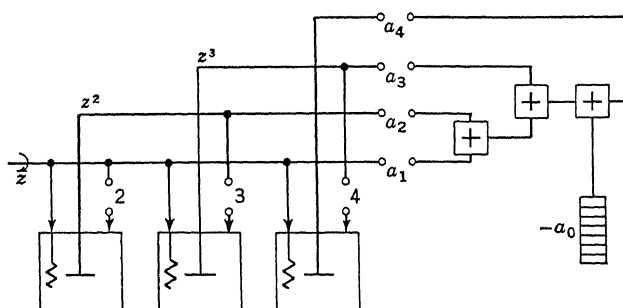
Fig. 8.5
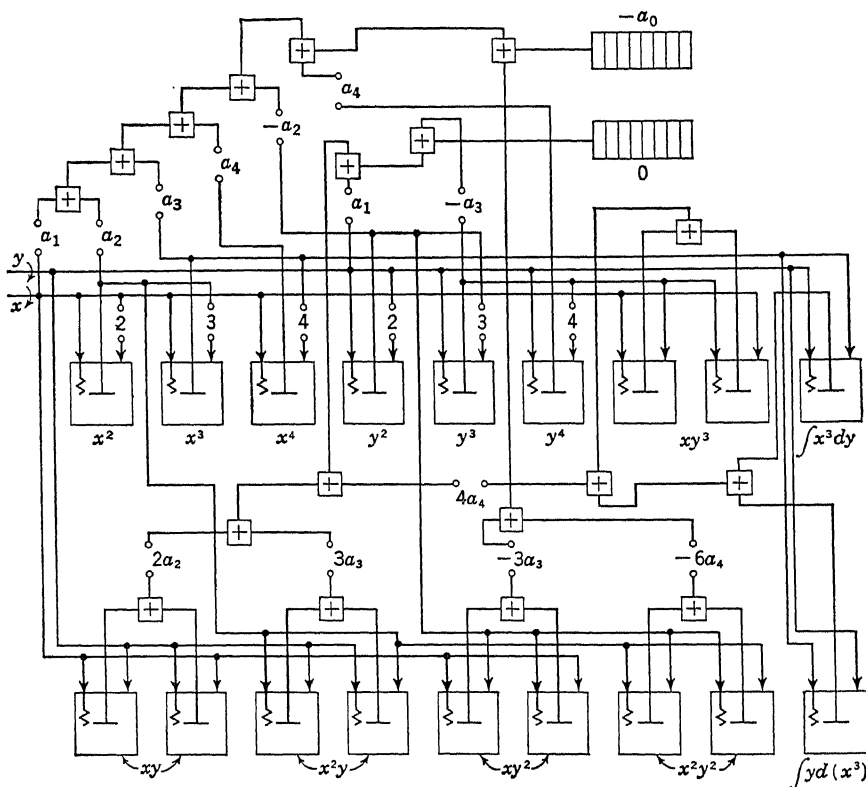
Fig. 8.6

8.2. Integrator Solution of Algebraic Polynomials. Since the solution of algebraic polynomials is based on the generation of the various powers of the variable, multiplication by constants, and subsequent addition, mechanical integrators, gears, and differentials may be used for this purpose. If coefficients and roots are real, the schematic diagram for connecting the units is as shown in Fig. 8.5. If complex coefficients

and roots are involved, the equation must be transformed to a pair of simultaneous equations with real roots and real coefficients. The integrator and gear connections would then be as shown in Fig. 8.6. The constant term a_0 is initially set into a counter with sign reversed. Each value of z at which a zero appears in the counter of Fig. 8.5 is a real root of Eq. (8.2). Each pair of values of x and y at which zeros appear simultaneously in both counters of Fig. 8.6 is a complex root of Eq. (8.2).

In a method suggested by Prof. C. P. Atkinson an nth-degree polynomial is converted into an nth-order ordinary differential equation and

$$\int \frac{d^4w}{dz^4}\,dz \qquad \int \frac{d^3w}{dz^3}\,dz \qquad \int \frac{d^2w}{dz^2}\,dz \qquad \int \frac{dw}{dz}\,dz = w$$

$$IC = 24a_4 \qquad IC = 6a_3 \qquad IC = 2a_2 \qquad IC = a_1$$
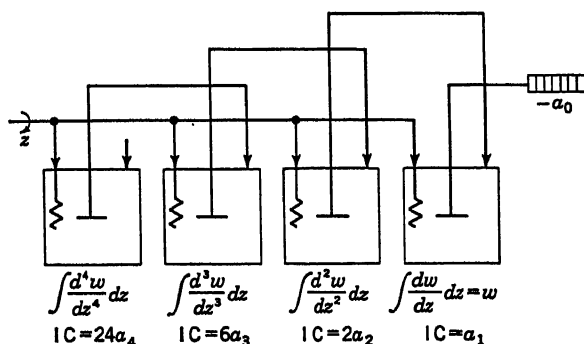
Fig. 8.7

then integrated to arrive at the various roots involved. Thus, suppose Eq. (8.2) to be written in the form

$$w = a_4 z^4 + a_3 z^3 + a_2 z^2 + a_1 z + a_0 \qquad (8.6)$$

Values of z for which $w = 0$ are the roots which are wanted. Differentiating Eq. (8.6) four times, the following equations result:

$$\frac{dw}{dz} = 4a_4 z^3 + 3a_3 z^2 + 2a_2 z + a_1$$

$$\frac{d^2w}{dz^2} = 12a_4 z^2 + 6a_3 z + 2a_2$$

$$\frac{d^3w}{dz^3} = 24a_4 z + 6a_3 \qquad\qquad (8.7)$$

$$\frac{d^4w}{dz^4} = 24a_4$$

These equations may now be solved for w by successive integrations as z is varied through the necessary range of values. Each value of z which makes w zero in this process is a root of the equation. The schematic diagram for interconnecting integrators to perform this operation is shown in Fig. 8.7. Initial positions of the integrator lead screws are shown on each integrator. In operation, the z shaft would be turned

as required through plus and minus values while a counter on the w shaft is observed, or the w versus z curve is plotted. Zeros in the counter, or crossings of the z axis by the curve, indicate the roots of Eq. (8.2). Complex roots can be handled in a similar manner via Eqs. (8.5) by considering one variable, say y, to be constant during each run of the machine. Thus, for different settings of y, a series of pairs of curves will be drawn (one curve for each equation). Those values of x and y at which *both* curves in a pair cross the axis *simultaneously* are the roots of the equation.

8.3. Solution by Harmonic Synthesis. Numerous machines have been constructed for solving high-degree algebraic equations by the process of harmonic synthesis. This approach has been particularly effective for determining complex roots. The possibility of using precise mechanical means for this purpose was suggested by Kempner.[5]
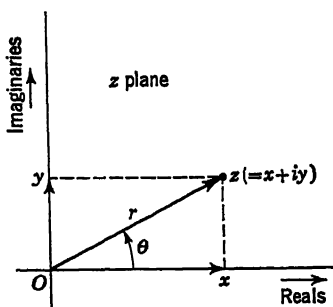
If complex roots are to be expected, we may write $z = x + iy$, as has already been mentioned. Each value of z then represents a point in the z plane (Fig. 8.8) having the coordinates x (along the real axis) and y (along the imaginary axis). The same point can be located by the end of a vector of length r and angular anticlockwise displacement θ from the axis of reals. This location in terms of r and θ is given by

$$z = x + iy = re^{i\theta} = r(\cos \theta + i \sin \theta) \qquad (8.8)$$

where $r = (x^2 + y^2)^{\frac{1}{2}}$ and $\theta = \tan^{-1}(y/x)$

Equation (8.8) is the transformation equation by which a high-degree algebraic equation may be converted to a trigonometric form permitting the application of harmonic synthesis methods for its solution. Upon substituting Eq. (8.8) into (8.1), terms of the following form will result:

$$z^n = a_n r^n (\cos \theta + i \sin \theta)^n = a_n r^n e^{in\theta} \qquad (8.9)$$
$$\text{or} \qquad z^n = a_n r^n (\cos n\theta + i \sin n\theta) \qquad (8.10)$$

and the equation becomes

$$\{a_n r^n \cos n\theta + a_{n-1} r^{n-1} \cos [(n-1)\theta] + \cdots + a_2 r^2 \cos 2\theta + a_1 r \cos \theta\}$$
$$+ i\{a_n r^n \sin n\theta + a_{n-1} r^{n-1} \sin [(n-1)\theta] + \cdots$$
$$+ a_2 r^2 \sin 2\theta + a_1 r \sin \theta\} = -a_0 \qquad (8.11)$$

or, in simpler notation,

$$u + iv = -a_0 \qquad (8.12)$$

Fig. 8.8

where u represents the sum of all the terms in the first set of braces and v the sum in the second set of braces. The variables u and v are the coordinates of a point in a plane we can call the w plane, by analogy with x and y as coordinates in the z plane. In the z plane, the locus of points having a constant value of r, but θ varying from 0 to 360°, will be a circle. In the w plane, n harmonics of θ will be present, as well as r raised to all powers through the nth. Thus the corresponding locus of points for constant r with θ sweeping through 360° will be a complicated curve, in general, in the w plane (Fig. 8.9).

The advantage of using the w plane in solving for the roots of Eq. (8.1) resides in the fact that an inspection of the complicated curves drawn
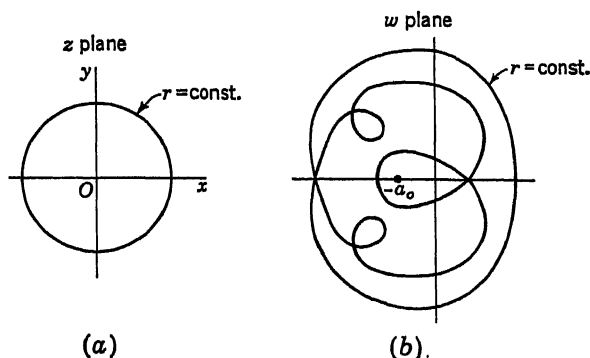
Fig. 8.9

for various constant values of r serves to bracket the roots,[6] which may then be evaluated by successively closing down the brackets. It is clear from Eq. (8.11) that each pair of values for r and θ which makes $u + iv = w = -a_0$ provides a root of Eq. (8.1). Thus, if in Fig. 8.9b the value $-a_0$ is spotted on the real axis, the value of r for which the curve passes through $-a_0$ and the value of θ at which this occurs provide both the modulus and the angle of a root. The real and imaginary parts of the root can then be found from the relations defining Eq. (8.8). If a trial value of r results in a curve in the w plane, which does not enclose $-a_0$, then there are no roots having as small a modulus as the trial value. A larger value of r should then be tried. Upon plotting the $r =$ const locus in this case, suppose the curve in Fig. 8.9b to be obtained. It is found that this curve makes three complete closed loops around $-a_0$. This signifies that three roots exist, whose moduli are less than the second trial value. Furthermore, the intersection of two of the loops with each other on the real axis indicates that a pair of complex conjugate roots may be expected. The third root is, of course, real. All three roots may be tracked down by successively changing r until curves are obtained which pass through $-a_0$.

If additional roots are present in the equation, then larger values of r must be taken. Successive increases in r might be arranged to isolate each real root or each pair of complex conjugate roots in turn.

The mechanization of this process merely requires the generation of sines and cosines of θ and its multiples, the production of r and its powers, the multiplication of these factors, and the summation of the products.

8.4. The Linkage Machine of Kempe. When only real roots are to be found in Eq. (8.1), a special case of harmonic synthesis is involved. The application of a linkage computer to this form of equation appears to have been first suggested by Kempe.[7] For purposes of illustration, the fourth-degree Eq. (8.2) will be considered. Kempe proposed that in such an equation z be replaced by

$$z = c \cos \theta \qquad (8.13)$$

yielding

$$a_4 c^4 \cos^4 \theta + a_3 c^3 \cos^3 \theta + a_2 c^2 \cos^2 \theta + a_1 c \cos \theta + a_0 = 0 \quad (8.14)$$

The powers of $\cos \theta$ are related to cosines of multiples of θ as follows:[8]

$$\cos^4 \theta = \tfrac{1}{8} \cos 4\theta + \tfrac{1}{2} \cos 2\theta + \tfrac{3}{8}$$
$$\cos^3 \theta = \tfrac{1}{4} \cos 3\theta + \tfrac{3}{4} \cos \theta \qquad (8.15)$$
$$\cos^2 \theta = \tfrac{1}{2} \cos 2\theta + \tfrac{1}{2}$$

Thus, Eq. (8.14) may be written finally as

$$c_4 \cos 4\theta + c_3 \cos 3\theta + c_2 \cos 2\theta + c_1 \cos \theta + c_0 = 0 \qquad (8.16)$$

where
$$c_4 = \frac{a_4 c^4}{8}$$
$$c_3 = \frac{a_3 c^3}{4}$$
$$c_2 = \tfrac{1}{2}(a_4 c^4 + a_2 c^2) \qquad (8.17)$$
$$c_1 = \tfrac{3}{4} a_3 c^3 + a_1 c$$
$$c_0 = \frac{3}{8} a_4 c^4 + \frac{a_2 c^2}{2} + a_0$$

A value for c in Eq. (8.13) must be assumed in order to evaluate the constant c_0 to c_4. Since $\cos \theta$ cannot exceed unity in value, in order to get the largest root z, c must be assigned a value greater than this largest value of z. However, if only some of the smaller roots are required, c need be chosen only large enough to produce the largest of these roots. In fact, a different c may be chosen for evaluating each root if it turns out to be convenient to do so.

Equation (8.16) may be mechanized by means of series of links of different lengths forming an incomplete equiangular polygon. The

principal features of this linkage are shown in Fig. 8.10. The linkage consists of five links OA, AB, BC, CD, DE of lengths c_0, c_1, c_2, c_3, c_4, respectively. Link OA is always constrained to be horizontal. Link AB may be tilted clockwise to assume any angle θ between 0 and π. Link BC is geared to link AC in such a fashion that the angle formed by BC with the horizontal is always 2θ, measured anticlockwise. Similarly, CD is geared to BC in such fashion that the angle formed by CD with the horizontal is always 3θ, measured anticlockwise. The angle between DE and the horizontal is likewise maintained at 4θ.

It is clear from Fig. 8.10 that the algebraic sum of the horizontal projections of the five links is represented by the horizontal distance W from the end E of the last link to the vertical axis OY. As θ is varied from 0 to π, the end E will describe a path which will intersect, eventually, the axis OY. The value of θ at which this occurs satisfies Eq. (8.16). The point E will intersect the OY axis as many times as there are real roots in Eq. (8.16) during the rotation of AB through 180°, provided that c has been chosen large enough.

Negative as well as positive constants in Eq. (8.16) may be represented in these links. Thus, if c_0 is negative, OA would be taken to the left from O, instead of to the right. If c_1 were negative, then AB would be taken downward to the left instead of upward to the right.

Fig. 8.10

That is, since OA, AB, BC, CD, and DE are all positive vectors as shown in Fig. 8.10, any such vector that becomes negative would be drawn in the opposite direction along the same line of action.

A linkage construction designed to maintain such equiangularity between links as the link AB is rotated is described by Blakesley.[9] It consists of a series of similar four-sided kite-shaped figures with each length OA, AB, BC, etc., as the length of a diagonal in the corresponding kite. Each kite is built on the extensions to the sides of the adjacent kite to give a "lazy-tongs" type of structure capable of being pulled around in an arc, as in Fig. 8.10. For this linkage to work properly, the kites must be geometrically similar. While the diagonals OA, AB, BC, etc., remain in proper ratio as the kites are rotated, their lengths necessarily change, tending to become zero as the angle θ approaches zero and tending to infinity as θ approaches 90°. The construction has, therefore, obvious limitations. These limitations may be removed, if desired, by means of geared systems for maintaining equal angles between adjacent
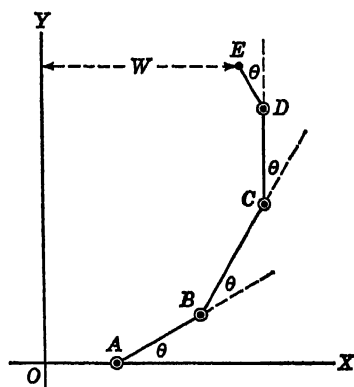
sides, or by means of the tape-and-wheel constructions used in drafting machines.

8.5. Mechanical Harmonic Synthesizers. In these machines the u and v summations indicated by Eq. (8.12) are accomplished mechanically, and the resultant w is found by plotting u along one axis and v along an orthogonal axis. The sine and cosine components are almost invariably generated by Scotch yoke mechanisms (Fig. 8.11), while the summation is accomplished in such cases by a continuous tape, cord, or chain, much as in Thomson's simultaneous-equation-solving machine and his tide-predicting machine.[10] The connections for a fourth-degree equation are shown in Fig. 8.12. Cranks 1, 2, 3, and 4 are set, respectively, to values

Fig. 8.11

Fig. 8.12

a_1r, a_2r^2, a_3r^3, a_4r^4, where r is an assumed value for crank-length setting to start the solving process. A continuous tape threads through all the cosine term pulleys. It is fixed at one end and attached to a drawing
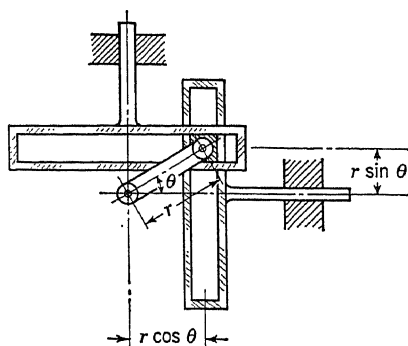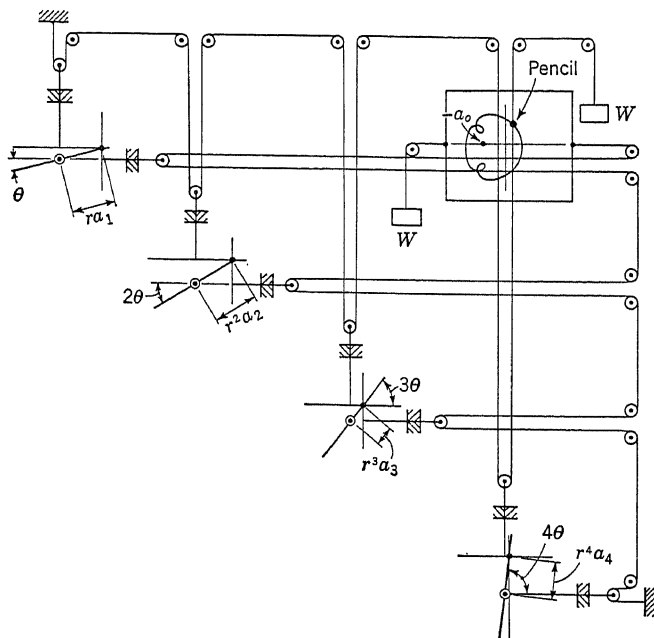
board at the other.   A weight W maintains the tape taut at all times. The cosine summation causes the board to move back and forth horizontally in appropriate guides.   A similar tape threads through all the sine-term pulleys and causes a pencil to move up and down vertically in appropriate guides.   The position of the pencil point on the board with respect to a set of coordinate axes drawn on the board is at all times determined by the vector sum of the sine and the cosine terms.   Thus, as both the board and pencil point move in their respective orthogonal directions, curves such as those in Fig. 8.9b are plotted.   The curve shown on the board in Fig. 8.12 indicates that there is one root (real) whose modulus is less than the value of r used in setting the cranks.   The procedures for finding this root, as well as the other three roots of this equation, have been described in Sec. 8.3.

One of the first precise mechanical machines built to solve these equations by harmonic synthesis is the Bell Telephone Laboratories Isograph, containing 10 sine-cosine units[11,12] and thus capable of solving a tenth-degree algebraic polynomial.   Equations up to this order of complexity were occurring in the calculation of resonant frequencies of electrical circuits.   The time for the determination of the eight complex roots of an eighth-degree equation was reduced from four days by previous methods, to one day by means of the Isograph.   Emphasis is to be placed on the fact, also, that special skills are not required for the operation of the machine; no mental fatigue is involved, and costly errors are thereby avoided.

Although this is one of the early machines built specifically for the solution of algebraic equations, the 32-element synthesizer of Miller[13] and the 40-harmonic synthesizer of Krantz[14] were forerunners of precision harmonic synthesizers.   The latter machines were used in the studies of sound.

In the Isograph, gears were fitted to the bearings with an accuracy of one ten-thousandth of an inch for play and concentricity.   Slide bars were lapped and fitted individually to their bronze guides to minimize friction and play.   Ball bearings were used in all the pulleys.

In the Isograph, as in many of the computing machines described so far, the labor of calculating the coefficients to be set on the machine, and then setting them, may be a large portion of the total time required to obtain a solution.   In the solving process described in this section, this requires the calculation of powers of r through the nth (10th in the case of the Isograph) and then multiplications by the corresponding coefficients.   A unique device is incorporated in the Isograph to reduce this time to a minimum.   It consists of a set of 10 cylindrical slide rules having 10-in. scales, located close to the cranks whose settings must be in accordance with the products $a_k r^k$.   The slide rules are geared to

each other in the same ratios as are the cranks. Thus, assuming all slide rules have been "zeroed" on unity at the start (friction clutches in the slide-rule drive system permit these adjustments to be made), turning the first slide rule to a chosen value for r causes all the other slide rules to indicate their appropriate values of the powers of r. If, instead of being set to unity, the initial settings of the slide rules are the coefficients of the terms, then the initial setting actually corresponds to the coefficient multiplied into powers of $r = 1$. Thereupon, any resetting of the first slide rule in the interconnected auxiliary computer to allow for a different choice of r will yield new settings on all the other slide rules in accordance with $a_k r^k$. These readings may then be used to set the crank lengths manually. The scale by which the latter settings are made can be read to 0.001-in. with a vernier and with skill can be set even more closely.

A machine of the same general type, but of considerably greater capacity, was constructed at the University of Texas.[15] It consists of 15 sine and 15 cosine units, so that polynomials up to the fifteenth degree could be solved. The application to the solution of polynomials is described by Brown and Wheeler.[16]

Complex coefficients in Eq. (8.8) may be handled by setting not only an initial radius $a_k r^k$ on each crank but also an initial angular displacement θ_k given by

$$\tan \theta_k = \frac{c_k}{b_k} \qquad (8.18)$$

where the corresponding complex coefficient is

$$a_k = b_k + i c_k \qquad (8.19)$$

Since the constant term a_0 may also be complex, the reference point through which the final curves must pass will not be located on the real axis under these circumstances but will have the position $-b_0 - i c_0$ in the plane (b_0 to the left of the origin and c_0 down from the real axis). The solving procedure then occurs as before, except that θ is measured from the initially displaced position of the first crank instead of from the axis of reals.

To obtain only the *real* roots of a polynomial, the procedure of Kempe may be applied to the Scotch yoke type of machine. This is the "real root method" of Brown and Wheeler. The substitutions denoted by Eqs. (8.13) and (8.15) are made to arrive at Eq. (8.16). The summation of the cosine terms of Eq. (8.16) is represented by a vertical movement of the recording pencil, while the angle θ is represented by a horizontal movement of the drawing board. By scribing a horizontal line on the board at a distance c_0 below the origin of coordinates, the intersections

of the curve representing the sums of the cosines with this horizontal line at $-c_0$ will give all the real roots of the equation, provided that c was chosen large enough in Eq. (8.13) to encompass all these roots.   A typical solution curve of this sort is shown in Fig. 8.13.   It is clear that all real roots could be obtained with only one run of the machine.

8.6. Electromechanical Harmonic Synthesizers. A potentiometric equation solver has been described in Sec. 8.1 for obtaining real roots of a high-degree equation. Such a device is adaptable to the determination of complex roots if alternating voltages of adjustable phase are provided to excite the

Fig. 8.13

system.   This is the system developed by Hart and Travis[17] and similarly described by Schooley.[4]   The basic feature of this system that is different from the other electrical system described is the incorporation of $n + 1$ identical a-c generators, of which n are provided with rotatable stators.   The generators alone are shown in Fig. 8.14, since the connections to the other components of the system are as in the cases previously studied.   The n rotatable stators are connected to a common
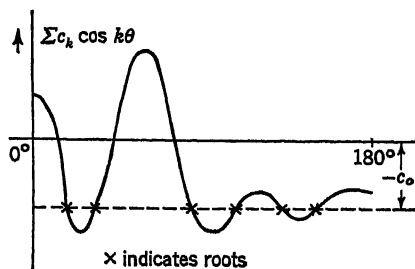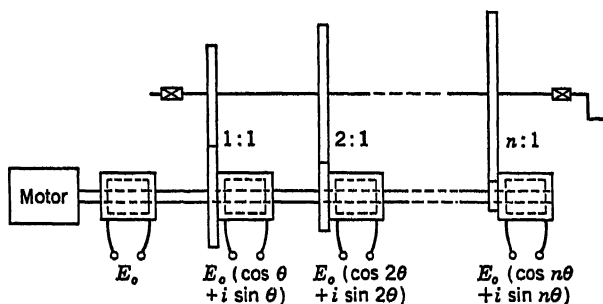
Fig. 8.14

shaft through gear ratios of $1:1$, $2:1$, . . . , $n:1$, so that as the hand crank is slowly turned, the first stator would turn through the angle θ, the second through 2θ, etc., down the line to the nth stator, which would turn through $n\theta$.   The a-c voltage outputs of the various generators would have the phase relations indicated in Fig. 8.14.   These may now be impressed across coefficient potentiometers set to the fractional values $a_1, a_2, \ldots, a_n$.   The outputs of these coefficient potentiometers would then be impressed across corresponding modulus potentiometers as in Fig. 8.4, using either ganged potentiometers with tapered windings to

produce the various powers of the modulus or geared potentiometers with uniform windings on which the brushes are geared up to move through distances proportional to the powers of the modulus.

In the operation of such a machine for solving an equation with *real* coefficients, all generators are aligned so that their outputs are identical and in phase. The coefficients are set on the coefficient potentiometers. An estimated value of the modulus and its powers are set on the modulus potentiometers. The outputs of the modulus and constant-term potentiometers are connected in series through a galvanometer used to indicate a null, as in Fig. 8.4. Then, the crank on the stators (θ) is slowly turned

$E_o \cos 0°$ $E_o \cos 90°$ $E_o \cos 180°$
or $E_o \sin 90°$ or $E_o \cos 270°$ or $E_o \sin 270°$
                or $E_o \sin 0°$
                or $E_o \sin 180°$
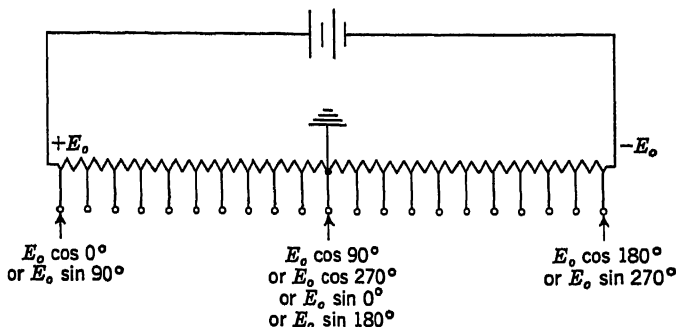
Fig. 8.15

through 180° while observing the galvanometer for a null. The first setting of the modulus is not likely to produce a null; consequently, the modulus is changed and the procedure repeated until a null is attained. The setting of the modulus potentiometers and the position of the stator crank determine both the modulus and phase of the root. This procedure would be repeated until all the roots have been found. The Hart and Travis machine was designed to solve an eighth-degree equation, determining all the roots of such an equation in about $\frac{1}{2}$ hr with a stated accuracy within 2 per cent in modulus and 1 per cent in angle.

If complex coefficients are involved, these may be set by making a separate phase setting on each generator after the initial alignment and before turning the hand crank.

Another form of circuit[18] which might be used for harmonic synthesis involves the generation of sine and cosine terms with resistive voltage dividers. Referring to Fig. 8.15, a center-tapped resistance is shunted across a battery. Taps are taken at points for which voltages correspond to the sines and cosines of uniformly spaced values of angle. Thus, for any setting θ, voltages are available to represent $\cos \theta$, $\cos 2\theta$, . . . , $\cos n\theta$. These may be connected into coefficient and summing networks by standard procedures to complete the solving network.

Other possibilities include the use of rectangular resistance cards or resolvers (Sec. 4.4), for generating the harmonic values of voltage necessary in these equation solvers.

A unique approach to the problem of developing multiples of a base frequency for use in a polynomial-equation solver makes use of square-wave generators of the rotating-commutator type.[19] Cascaded ganged potentiometers supplied from a d-c source develop the various powers of r involved in Eq. (8.11). In the given reference, 10 such potentiometers are cascaded, with unit-gain isolating amplifiers between potentiometers to avoid loading effects; 10 commutators having, respectively, from 1 to 10 segments are driven at 3,600 rpm, yielding output square-wave frequencies in multiples of 60 cps up to 600 cps, and are supplied from the ganged potentiometers. Filtering circuits shape the waves into sinusoidal form, and potentiometers serve to bring in the coefficients a_k of the equation. The outputs, $a_k r^k e^{ik\omega t}$, are split electrically into sine and cosine components, summed separately, and displayed on the vertical and horizontal axes of an oscilloscope, much as the mechanical isograph does it on a drawing board.

Since the use of potentiometers for developing r^k limits r to a maximum value of unity, the range of r from 1 to ∞ may be obtained by the same type of transformation as that used in arriving at Eq. (8.1a).

8.7. Other Harmonic Synthesizers. A resistive d-c voltage divider for generating sines and cosines is described in Sec. 8.6. A similar voltage divider employing alternating current makes use of tapped auto-transformers.[20] If taps are taken on the transformer windings at equal intervals (Fig. 8.16a), the voltage amplitudes at these taps have the spatial distribution shown in (b), a cosine curve. At each tap the voltage varies sinusoidally with time through the amplitude shown in (b). The more windings are tapped, the more accurately the spatial cosine curve which is reproduced.

In another synthesizer[21] a rotating disk of photographic film has concentric rings, each ring having a varying light and dark area corresponding to a sine or cosine wave. The two innermost rings represent the sine and cosine of the fundamental, with each succeeding pair going out along the radius representing the sine and cosine of the next integral multiple of the fundamental. A narrow slit of light impinges along a radius of the disk, with filters provided for reducing light intensity through each ring in proportion to the corresponding Fourier coefficient. The light passing through each ring is focused on a photoelectric cell, whose output is then the sum of the Fourier series. In application to a polynomial solver, the sines and cosines would be summed in separate photoelectric cells and displayed on the horizontal and vertical axes of an oscilloscope or plotted against each other in a recorder.

In another form of the photoelectric harmonic synthesizer[22] rotating disks were placed between photoelectric cells and constant light sources, the edges of the disks having sinusoidal variations corresponding to the fundamental and its harmonics.   Phase angle relative to the fundamental was varied by shifting each light source and photoelectric cell along the edge of its respective disk.   The output of each cell was passed through a potentiometer to permit setting the appropriate Fourier coefficients.

A summing device for Fourier series, based on the multiple reflection of a beam of light from a series of tilted mirrors, is due to Robertson.[23] A set of miniature stepped-cone pulleys rotated small drums through

(a)   (b)
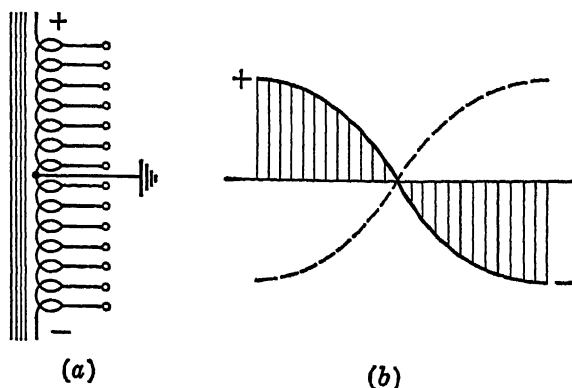
Fig. 8.16

connecting threads at speeds which were integral multiples of the slowest speed.   Each drum had a peg whose radial distance was adjustable in accordance with the Fourier coefficient corresponding to it.   A thread from each peg to a pivoted mirror served as a connecting rod to tilt the mirror harmonically as the peg rotated.   By placing successive mirrors alternately in two rows facing each other, a beam of light started at one end of the mirror system was reflected successively from mirror to mirror, finally impinging on a measuring screen.   The displacement of the light beam on the screen gave at any instant the sum of the Fourier series.

8.8. Solution of Trigonometric and Transcendental Equations by Harmonic Synthesis.   A procedure that is often useful in solving trigonometric and transcendental equations consists in expanding the given functions in a power series in which terms of sufficiently higher power may be neglected.   The resulting polynomial may then be solved by the methods discussed.   Another possibility is that of transforming a given trigonometric equation by means of suitable identities directly into an equation involving only sines and cosines of multiple angles.   Equations involving logarithms, exponentials, and hyperbolic functions may often be transformed to a suitable form for solution by harmonic synthesis.

Brown and Wheeler[24] discuss a variety of trigonometric and transcendental equations.

8.9. Force-Balance Methods of Solution. Emch[25] and Meslin[26] developed independently a hydrostatic balance method of solving a high-degree algebraic equation with real roots and real coefficients. The method consists in distributing solids of revolution of appropriately varying cross section on levers jutting out from a pivot. By immersing the ends of the solids in water, buoyant forces are exerted on the lever arms, which result in moments about the pivot. For each depth of immersion which produces a state of balance in the total system of moments, a solution to the equation is obtained.

If this method were to be applied to Eq. (8.2), four solids of revolution would be necessary. The first would be a cylinder (volume varying linearly with z), the second a paraboloid (volume varying as the square of z), the third a cone (volume varying as the cube of z), the fourth a cusplike solid whose generatrix is given by the equation $r = az^{\frac{3}{2}}$ (volume varying as the fourth power of z). The solids are mounted on lever arms of lengths a_1, a_2, a_3, and a_4, respectively, from a common fulcrum. The weights of these solids times their respective distances from the pivot exert a moment which may be balanced by another weight placed at the appropriate distance on the other side of the pivot. The solids in such an arrangement may, therefore, be considered as weightless from now on.

The system is now unbalanced by placing a weight on the negative side of the fulcrum of such magnitude and at such a distance that its moment about the pivot is a_0. With the lever arms horizontal and all weight tips at the same level in a tank, water is brought up in the tank until the tips become immersed. A force proportional to the amount of displaced water will act on each solid. If the solids are designed so that this force is equal to z, z^2, z^3, z^4 for each solid, respectively (other scale factors are, of course, just as good), the total moment M exerted by the system of buoyant forces on the lever will be

$$M = a_1z + a_2z^2 + a_3z^3 + a_4z^4$$

To this must be added the moment a_0 exerted by the added weight. When the depth of water has reached the point where the system is in balance within itself, that depth satisfies Eq. (8.2) and hence is a root of that equation. If the depth is increased still further, the system will be thrown out of balance again, but at a greater depth will again attain a balance, thus giving the next root to the system of equations. This procedure may be continued until all the real positive roots have been found.

It should be remarked that the solids will be distributed on the positive

and negative sides of the fulcrum in accordance with the signs of the coefficients. Only positive values of z are obtained this way, since negative depths of immersion are not practical. To get negative roots, $-z$ would be substituted in Eq. (8.2) in place of $+z$ and the solids redistributed (*i.e.*, solids representing odd-powered terms would be transferred to the opposite side of the pivot). The depths of immersion at balance now represent the negative roots of Eq. (8.2).

The balancing of an interconnected system of levers by means of dead weights and a varying moment arm[27] may be made to satisfy Eq. (8.2) in a somewhat similar manner as in the hydraulic system, although the appearance of this mechanism is quite different. Referring to Fig. 8.17, two sets of lever arms are shown. The spacing between the two sets of pivots is $z + 1$, where z is the variable in Eq. (8.2). As z is varied, the lever system will attain a balance within itself for particular settings of z. These are the roots of Eq. (8.2). At all other values of z the system will be out of balance. As in the case of the hydraulic model, this mechanical linkage model serves to locate all the positive real roots of an algebraic equation. Negative real roots are obtained as in the hydraulic model by substituting $-z$ into Eq. (8.2) and solving the resulting equation for z.
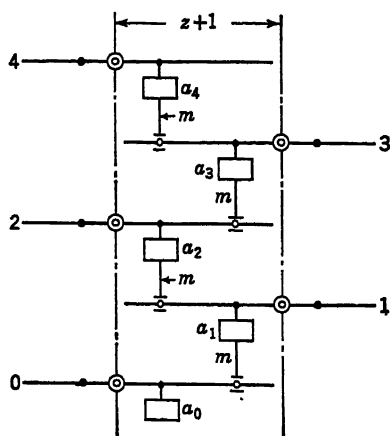
Fig. 8.17

In Fig. 8.17, a weight a_4 placed on a pan 4 unit to the right of pivot 4 will exert the moment a_4 about that pivot. Since the pivot is assumed frictionless and the arm is initially in balance, the arm will tend to tilt clockwise, thereby bearing down on arm 3 through a connecting link m at a distance z from its pivot. Thus, it causes a moment about pivot 3 of magnitude a_4z. Arm 3 tends to tilt and exerts through another connecting link m a moment $(a_4z)z = a_4z^2$ about the pivot on arm 2. The moment is thus cascaded from arm to arm. When it reaches the arm 0, the total clockwise moment exerted by the weight a_4 about the pivot 0 is a_4z^4. Similarly, a weight a_3 placed on arm 3 at unit distance from pivot 3 cascades through the system of levers to cause a clockwise moment of a_3z^3 about the pivot 0. A weight a_2 placed on arm 2 at unit distance from pivot 2 produces a clockwise moment a_2z^2 about pivot 0. The weight a_1 produces a moment a_1z, and finally the weight a_0 produces the moment a_0. These are all additive, so that the total clockwise

moment M about pivot 0 is

$$M = a_4z^4 + a_3z^3 + a_2z^2 + a_1z + a_0$$

By shifting the two sets of pivots relative to each other (*i.e.*, changing z) until the sum of the moments given in the above expression is zero, a real positive root of Eq. (8.2) is obtained. This balance will be attained as many times (each at a different value of z) as there are real positive roots in the given equation. As before, to obtain real negative roots, $-z$ is substituted into the equation in place of $+z$, and the resulting expression solved for its positive roots, which will be the desired negative roots.

8.10. Electric Field Representation of Analytic Functions Applied to Solution of Algebraic Equations. Maxwell[28] showed that functions of the complex variable may be represented by the potential distribution due to current flow in a conducting sheet of uniform thickness. Lucas, in a series of six papers,[29] described the development of a method for applying these relations of function theory to the experimental solution of algebraic polynomials. The method remained relatively dormant until a rebirth of this approach occurred in connection with studies of the steady-state and transient response of electrical networks and amplifiers.[30,31]

The following development shows how the method might be applied. Consider the polynomial

$$f(z) = a_nz^n + a_{n-1}z^{n-1} + \cdots + a_1z + a_0 = 0 \qquad (8.20)$$

If it were possible to factor this polynomial conveniently, it could be written in the equivalent factored form:

$$f(z) = (z - z_1)(z - z_2)(z - z_3) \cdots (z - z_n) = 0 \qquad (8.21)$$

where $z_1, z_2, \ldots, z_n$ may be complex quantities. If z is made equal to z_1, or $z_2, \ldots$, or z_n, one of the factors in Eq. (8.21) will become zero, which makes the whole product zero. Thus, Eq. (8.20) is satisfied by these values of z, and $z_1, z_2, \ldots, z_n$ are the roots of the equation. It is our intention to evaluate these roots.

In the conducting-sheet approach to the problem it is necessary to set up an auxiliary function $F(z)$, which is at least one degree higher than Eq. (8.20). $F(z)$ should have real roots which are known. The need for this auxiliary function will become clear during the succeeding development.

The easiest way to set up $F(z)$ is to assign arbitrarily convenient numbers to $Z_1, Z_2, \ldots, Z_{n+1}$, in the factored form of $F(z)$:

$$F(z) = (z - Z_1)(z - Z_2) \cdots (z - Z_{n+1}) \qquad (8.22)$$

Since $Z_1, Z_2, \ldots, Z_{n+1}$ are assigned real numbers, the expansion of the

product in Eq. (8.22) will give the polynomial whose roots are real and known.

A new function may now be formed by dividing the original function $f(z)$ by the auxiliary function $F(z)$. Thus

$$G(z) = \frac{f(z)}{F(z)} = \frac{(z - z_1)(z - z_2) \cdots (z - z_n)}{(z - Z_1)(z - Z_2) \cdots (z - Z_{n+1})} \qquad (8.23)$$

The function $G(z)$ goes to zero when $z = z_1, z_2, \ldots,$ or z_n. These values are called the "zeros" of $G(z)$. They are, of course, the roots to be found in Eq. (8.20). Because the denominator is one degree higher than the numerator, a value of $z = \infty$ will also make $G(z) = 0$, so that a zero is also located at infinity. The function $G(z)$ goes to infinity when $z = Z_1, Z_2, \ldots, Z_{n+1}$. These values of z are called the "poles" of $G(z)$. Since the latter values were arbitrarily chosen to begin with, the locations of the poles of $G(z)$ are known. The locations of the zeros of Eq. (8.23) are related to the known locations of the poles. The relationship is found from the following considerations.

Since $G(z)$ is a proper fraction (denominator of higher degree than the numerator) and also since the numbers $Z_1, Z_2, \ldots, Z_{n+1}$ are all different, $G(z)$ can be expressed as a sum of partial fractions in the following manner:[32]

$$G(z) = \frac{f(z)}{F(z)} = \frac{A_1}{z - Z_1} + \frac{A_2}{z - Z_2} + \cdots + \frac{A_{n+1}}{z - Z_{n+1}} \qquad (8.24)$$

The numerators $A_1, A_2, \ldots, A_{n+1}$ may be determined by clearing fractions in Eq. (8.24), expanding the resulting products, and equating coefficients of like powers of z. This results in $n + 1$ linear simultaneous equations from which $A_1, A_2, \ldots, A_{n+1}$ may be evaluated.

A more direct method of evaluating the numerators was used by Lucas.[33] It consists in dividing the value of the original function at a pole location by the value of the *derivative* of the auxiliary function at the same pole. If this is done for each pole location, all the values $A_1, A_2, \ldots, A_{n+1}$ will be obtained. Thus, for the kth pole

$$A_k = \frac{f(Z_k)}{F'(Z_k)} \qquad (8.25)$$

Consider, now, an infinite conducting sheet in which a set of reference axes is drawn. Suppose that point electrodes are placed at the predetermined pole locations along the x axis (axis of reals). If a current $2\pi A_k$ is supplied through the electrode at the kth pole in Fig. 8.18, it will flow radially from this pole (Z_k) toward infinity. The rate of current flow

through a point z on the circumference of a circle of radius $|z - Z_k|$ is

$$I_{sk} = \frac{A_k}{|z - Z_k|} \qquad (8.26)$$

Equation (8.26) is seen to correspond to the kth term of Eq. (8.24). The total rate of current flow through the point z due to all poles will be, therefore,

$$I_z = \frac{A_1}{z - Z_1} + \frac{A_2}{z - Z_2} + \cdots + \frac{A_{n+1}}{Z - z_{n+1}} \qquad (8.27)$$

Some values of A will be negative and others positive. Thus, at some points in the z plane the vector sum represented in Eq. (8.27) reduces to
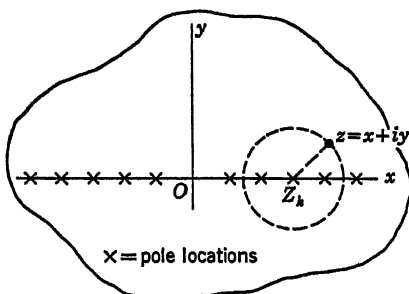
Fig. 8.18
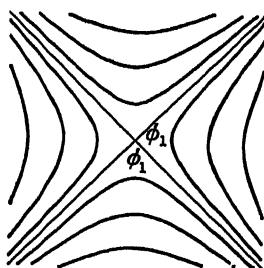
Fig. 8.19

zero. The values of z at these points are the zeros of $G(z)$ and hence the roots of Eq. (8.20).

Since the zero points are points through which there is no current, they are also points of zero voltage gradient. If equipotential lines are plotted on this sheet, the zeros would be indicated by intersections of a given equipotential with itself. The other equipotentials skirt by the point. A typical isotropic point of this sort is shown in Fig. 8.19. The locations of the zeros may be determined, therefore, either by locating points of zero voltage gradient with a pair of closely spaced probes or by locating isotropic points by plotting equipotentials.

The theory requires a conducting sheet of infinite extent, for only then will the flow lines from each pole be strictly radial. Hence, a finite size of tank will introduce some error. By using only a small central area of a large conducting sheet such errors may be reduced to tolerable magnitudes. Hansen and Lundstrom[30] used a 16-in.-diameter circular tank containing a $\frac{3}{8}$-in. depth of dilute copper sulfate solution. The rim of the tank was a conductor. Boothroyd, Cherry, and Makar[31] simulated an infinite conducting sheet by using an 18-in.-inside-diameter insulated tank in which the electrolyte was divided into two 18-in. layers

by a $\frac{1}{8}$-in.-thick circular plate glass disk of $17\frac{1}{2}$-in. diameter.   The center of the bottom layer then simulates the required infinite boundary.

8.11. Electromagnetic Field Solution of Algebraic Equations. Following his development of the conducting-sheet method for obtaining the roots of polynomial equations, Lucas[33] also described the use of an electromagnetic field for the same purpose. A detailed description of apparatus making use of the earth's magnetic field in this connection is given by Russell and Alty.[34] In the latter paper the authors adopted a somewhat different method for resolving Eq. (8.20) into partial fractions. The auxiliary function chosen is of the same degree as the given polynomial. The known real roots, while still chosen for convenience, are not entirely arbitrary, but must satisfy the relation

$$Z_1 + Z_2 + \cdots + Z_n = \frac{-a_{n-1}}{a_n} \qquad (8.28)$$

The reduction into partial fractions then takes the following form:

$$G(z) = \frac{f(z)}{F(z)} = a_n + \frac{A_1}{z - Z_1} + \frac{A_2}{z - Z_2} + \cdots + \frac{A_n}{z - Z_n} \qquad (8.29)$$

where $$A_1 = \frac{f(Z_1)}{(Z_1 - Z_2)(Z_1 - Z_3) \cdots (Z_1 - Z_n)}$$

$$A_2 = \frac{f(Z_2)}{(Z_2 - Z_1)(Z_2 - Z_3) \cdots (Z_2 - Z_n)}$$

$$\cdots \cdots \cdots \cdots \cdots \cdots \cdots \cdots \cdots \cdots \cdots$$

$$A_n = \frac{f(Z_n)}{(Z_n - Z_1)(Z_n - Z_2) \cdots (Z_n - Z_{n-1})}$$

It will be found that $A_1 + A_2 + \cdots + A_n = 0$.

Suppose now that a sheet of paper be placed parallel to the earth's magnetic field. A pair of coordinate axes are drawn on the sheet so that the positive Y axis is in the direction of the field (Fig. 8.20). Long vertical wires perpendicular to the paper sheet penetrate through the sheet and extend above and below it at positions on the x axis given by $Z_1, Z_2, \ldots, Z_n$. Let the current through the wire at position Z_k be porportional to A_k. Thus

$$I_k = CA_k \qquad (8.30)$$

where C is the constant of proportionality. The magnetic field developed around the long wire as a result of current flow is cylindrical, with an intensity varying inversely with distance from the wire. Thus, at a point z in the plane of the paper there is a magnetic field intensity of

$$H_{zk} = \frac{2I_k}{|z - Z_k|} \qquad (8.31.)$$

The magnetic field intensity is defined as the force exerted on a hypothetical unit pole placed at the point in question. It is the magnetic potential gradient and is expressed in the cgs absolute unit system as oersteds, or gilberts per centimeter. Thus, in Eq. (8.31) I_k is in abamperes (1 abampere = 10 amperes), $|z - Z_k|$ is in centimeters, and H_{zk} is in oersteds. If the current through the wire is to be expressed in the mks unit amperes, then a factor of 10 must be introduced into the denominator of Eq. (8.31), resulting in the expression

$$H_{zk} = \frac{I_k}{5|z - Z_k|} \qquad (I_k \text{ in amperes}) \qquad (8.32)$$

While Eq. (8.32) shows the denominator as an absolute value, it will be remembered that the magnetic force H_{zk} is directed perpendicularly to the radius vector $z - Z_k$, as shown in Fig. 8.20.

The earth's magnetic field intensity is expressed by the symbol H_e and is considered to be uniform over the region of the paper sheet.

The resultant intensity of the magnetic field at z as a result of the current I_k and the earth's magnetic field H_e will be the vector

$$iH_e + i\,\frac{I_k}{5|z - Z_k|} \qquad (8.33)$$
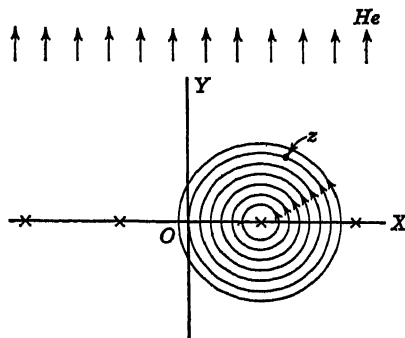
Fig. 8.20

The imaginary i has been inserted in expression (8.33) to indicate that the earth's magnetic field vector is directed in this problem along the y axis (imaginary axis) and to indicate that the magnetic force vector at z due to I_k is rotated 90° clockwise with respect to the radius vector $z - Z_k$.

The total magnetic field intensity at z due to all the wires will be

$$H_z = iH_e + i\left[\frac{I_1}{5(z - Z_1)} + \frac{I_2}{5(z - Z_2)} + \cdots + \frac{I_n}{5(z - Z_n)}\right] \qquad (8.34)$$

The i in Eq. (8.34) may be transferred to the left side of the equation, so that the right side of Eq. (8.34) will be of identical form with the right side of Eq. (8.29). Since the earth's magnetic field is not subject to adjustment, Eq. (8.29) should be multiplied by the factor H_e/a_n to make the constant terms of both equations agree. The result is

$$\frac{H_e}{a_n}G(z) = H_e + \frac{A_1 H_e}{a_n(z - Z_1)} + \frac{A_2 H_e}{a_n(z - Z_2)} + \cdots + \frac{A_n H_e}{a_n(z - Z_n)} \qquad (8.35)$$

Equations (8.34) and (8.35) will agree on their right-hand sides if the currents through the wires are chosen as follows:

$$I_1 = \frac{5A_1H_e}{a_n} \qquad I_2 = \frac{5A_2H_e}{a_n} \qquad \cdots \qquad I_n = \frac{5A_nH_e}{a_n} \qquad (8.36)$$

The locations of the zeros of Eq. (8.29), and hence of Eq. (8.35), are the roots of Eq. (8.20). The points of zero magnetic field intensity defined by Eq. (8.34) are the same zeros if the currents are in accordance with Eq. (8.36). Thus, the roots of Eq. (8.20) may be found experimentally by searching for points of zero magnetic force in Fig. 8.20. A small compass (as suggested by Russell and Alty) or a small search coil[35] might be used for this purpose.

8.12. Impedance Network Representation of Partial Fractions. Each term in Eq. (8.27) can be considered as a current flowing through an impedance represented by the value of the denominator under the influence of a voltage represented by the numerator.[36] A typical form of the network representing the kth term of Eq. (8.24) is shown in Fig. 8.21. A constant-frequency source of alternating voltage is shunted by a low-resistance potentiometer with center-tap grounded. The brush on the potentiometer may thus be set to give positive or negative values of A_k. The voltage A_k is fed to one end of a variable resistor labeled $r \pm R_k$. The variable resistor has a large resistance compared with the voltage-dividing potentiometer to keep loading effects down. In series with the variable resistor is an inductor L and a variable capacitor C. The circuit to ground is completed through an ammeter reading the current I_k.

The impedance through the resistor-capacitor series circuit is

$$(r - R_k) + i\left(\omega L - \frac{1}{\omega C}\right) \qquad (8.37)$$

If r is adjusted to equal the real part of z, $\omega L - 1/\omega C$ adjusted to the imaginary part of z, and R_k to the assigned real root Z_k, then the current to ground would be

$$I = \frac{A_k}{z - Z_k} \qquad (8.38)$$

Positive and negative values of the imaginary part of z are obtained, respectively, by adjusting $1/\omega C$ to values smaller and larger than L. Positive values of $r - R_k$ are obtained, as shown in Fig. 8.21. Negative values of $r - R_k$ may be simulated by reversing the sign of the input voltage. This, of course, also reverses the sign of the imaginary part of z as set in Fig. 8.21. To represent Eq. (8.27), $n + 1$ circuits of the form shown in Fig. 8.21 must be set up. Although each circuit would have a

different value for R_k, all circuits would have the same values of r and of C, so that these elements could be ganged on common shafts. The lower ends of all branches would meet in a common node which is grounded through an ammeter. By adjusting r and C until no current flows from

the node to ground, a zero of Eq. (8.23) is obtained. These values of r and C then give the real and imaginary parts of a root of Eq. (8.20). The procedure is repeated, changing signs as necessary, until all the roots are obtained.

Since the Z_ks are arbitrarily chosen real roots of the auxiliary function, they might all be chosen negative and large enough so that $r + R_k$ remains positive even when r assumes its largest possible negative value.
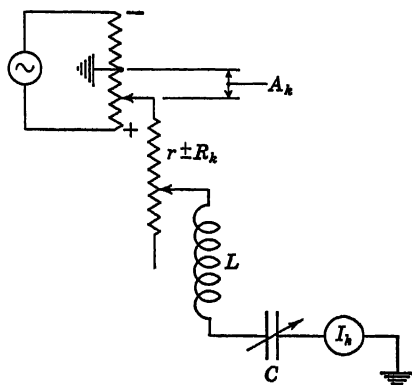
Fig. 8.21

8.13. Miscellaneous Algebraic-equation Solvers. The Wheatstone bridge (Fig. 8.22a) when in balance establishes the algebraic relation

$$\frac{x_1}{x_2} = \frac{x_3}{x_4} \qquad \text{or} \qquad x_1 x_4 = x_2 x_3 \qquad (8.39)$$

between the resistances of its four arms. By inserting into the arms

(a)   (b)
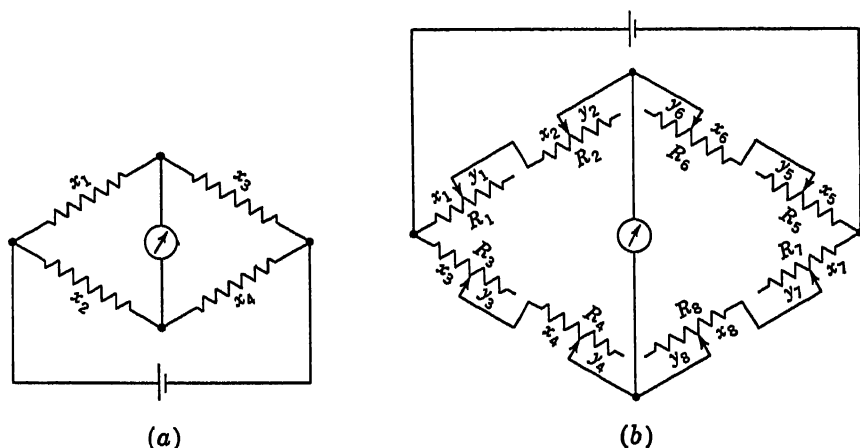
Fig. 8.22

of the bridge resistances which depend on linear combinations of variables, more general types of equations can be satisfied.[37] As an example, refer to the bridge in (b). Depending on whether the resistance being

inserted or removed from the circuit is measured from the right or left end of each variable resistor, quadratic equations of the following form are satisfied when the bridge is in balance:

$$(x_1 + x_2)(x_7 + x_8) = (x_3 + x_4)(x_5 + x_6) \qquad (8.40)$$

or

$$(x_1 + R_2 - y_2)(x_7 + R_8 - y_8) = (x_3 + R_4 - y_4)(x_5 + R_6 - y_6) \quad (8.41)$$

Other combinations of x, y, and R may be written by inspection. Obviously more elaborate combinations of resistances may be used. With alternating current, complex impedances provide further latitude in developing algebraic relations amongst the variables involved.

An interesting application of electrodynamometers for developing the squares and square roots of algebraic terms occuring in strain-gauge work appears in a principal strain computer.[38]   In investigating general strain distributions on the surface of a body by means of rectangular rosettes, the principal strains e_p and e_q are related to the strains e_1, e_2, e_3, indicated by the three gauges of the rosette, as follows:

$$\begin{aligned}
e_p &= \frac{1-t}{2}(e_1 + e_3) + \frac{1-t}{\sqrt{2}}[(e_1 - e_2)^2 + (e_2 - e_3)^2]^{\frac{1}{2}} \\
e_q &= \frac{1-t}{2}(e_1 + e_3) - \frac{1-t}{\sqrt{2}}[(e_1 - e_2)^2 + (e_2 - e_3)^2]^{\frac{1}{2}}
\end{aligned} \qquad (8.42)$$

where t is a factor representing the sensitivity of a gauge to transverse strain.

The strains e_1, e_2, e_3 are indicated by voltage outputs of the order of a few millivolts.   These may be fed through amplifiers into a computer mechanizing the right sides of Eqs. (8.42), providing as outputs the voltages e_p and e_q proportional to the principal strains.

In the computer referenced, the amplified voltages at 400 cps are fed into transformers, and the sums and differences called for in Eqs. (8.42) obtained by in-phase or out-of-phase series connections of signals attenuated in accordance with the coefficients.

The squares of the difference terms are generated by an electrodynamometer, both coils of which are connected in series.   The torque developed in the dynamometer shaft is thus proportional to the square of the current, and the current is proportional to a voltage difference. By placing two (or more) such dynamometers on a common shaft, the torques developed in each are summed in the shaft, producing thereby the sums of the squares appearing under the radical in each of Eqs. (8.42). An additional dynamometer on the same shaft is used in a servo loop to counterbalance the sum of the torques produced by the other dynamometers.   The balancing current is supplied by a high-gain amplifier oper-

ated through a phototube illuminated by light reflected from a mirror on the shaft. This current is thus proportional to the square-root term in Eqs. (8.42). The current is converted into a voltage by passing it through a resistance.

Equations for vapor-liquid equilibrium in multicomponent mixtures at a given temperature and pressure are of the form:

$$\sum_1^n x_m = \sum_1^n \frac{z_m}{1 + (K_m - 1)v} = 1$$

$$\sum_1^n y_m = \sum_1^n \frac{K_m z_m}{1 + (K_m - 1)v} = 1$$

(8.43)

where x_m, y_m are mole fractions of the mth component in the liquid and vapor phases, respectively, z_m the mode fraction of this component in the
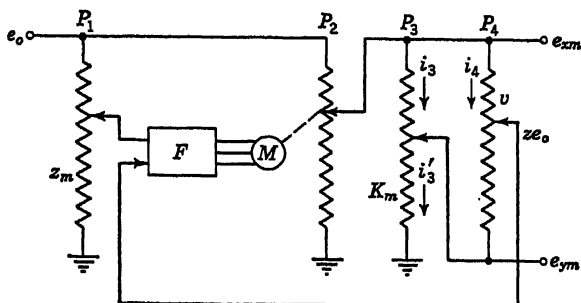
Fig. 8.23

mixture, K_m its equilibrium constant, and v the mole fraction of vapor in the mixture. The unknowns in Eqs. (8.43) are x_m, y_m, and v.

In an analog computer designed to solve these equations,[39] the magnitudes z_m, v, and K_m are set on potentiometers and a voltage-matching servo is used to drive the electrical system to the proper equilibrium state. The principle of the computer is illustrated in Fig. 8.23. The fraction z_m is set on a potentiometer P_1 provided with a d-c voltage e_0. The voltage from P_1 is compared with the voltage from P_4 in a servo amplifier, any differences between them causing the servomotor M to move the contact on P_2 to wipe out this difference. The resistance R of P_4 is large compared to the resistance r of P_3. Applying Kirchhoff's laws to the network consisting of P_3 and P_4, and observing that no current is drawn at e_{zm} and e_{ym}, or at v,

$$e_{zm} - e_{ym} = (1 - K_m)ri_3 = Ri_4$$
$$e_{ym} = K_m i_3' r$$
$$i_3 + i_4 = i_3'$$
$$z_m e_0 = e_{ym} + (e_{zm} - e_{ym})(1 - v)$$

(8.44)

Solving for e_{xm}/e_o and e_{ym}/e_o and remembering that $r/R \approx 0$, we find

$$\frac{e_{xm}}{e_o} = \frac{z_m e_o}{1 + (K_m - 1)v}$$
$$\frac{e_{ym}}{e_o} = \frac{z_m e_o K}{1 + (K_m - 1)v} \qquad (8.45)$$

Equations (8.45) are identical with the components of Eqs. (8.43). Thus, n cells of the type in Fig. 8.23 are connected to adding resistors and the two sums so obtained constrained to satisfy Eqs. (8.43). For different settings of v, the concentrations in the liquid and gas phases for each component may be determined from the voltage readings e_{xm} and e_{ym}.

Simultaneous algebraic equations occurring in automatic color correction of color printing involve products of three independent variables. In a computer[40] designed to solve these equations the triple product was obtained by a method based on the theory of probability. The probability of the simultaneous occurrence of three independent events whose probabilities of occurrence are x, y, and z, respectively, is the product xyz. Thus, if three pulse generators produce constant amplitude pulses of time duration proportional to x, y, and z, respectively, and if the pulse frequencies are irrationally related, the fraction of time in which all three pulses coincide is proportional to xyz. The pulses are adding in a mixing circuit and impressed on the grid of a tube which conducts only when the three pulses coincide. The time during which the tube conducts is thus proportional to the product xyz.

REFERENCES

1. Abel, N. H.: "Oeuvres completes," Christiania (Oslo), vol. 1, p. 28, 1881.
2. Scarborough, J. B.: "Numerical Mathematical Analysis," 2d ed., p. 185, Johns Hopkins Press, Baltimore, 1950.
3. Frame, J. S.: Machines for Solving Algebraic Equations, *Mathematical Tables and Other Aids to Computation*, 1(9):337–353 (January, 1945).
4. Schooley, A. H.: An Electro-mechanical Method for Solving Equations, *RCA Rev.*, 3:86–96 (1938).
5. Kempner, A. J.: On the Separation and Computation of Complex Roots of Algebraic Equations, *Univ. Colo. Studies*, 16:75–87 (1927–1929).
6. Kempner, A. J.: On the Complex Roots of Algebraic Equations, *Bull. Am. Math. Soc.*, 41:809–843 (1935).
7. Kempe, A. B.: On the Solution of Equations by Mechanical Means, *Messenger Math.*, 2(2):51–52 (1873).
8. Pierce, B. O.: "A Short Table of Integrals," 3d rev. ed., p. 75, Ginn & Company, Boston, 1929.
9. Blakesley, T. H.: A Kinematic Method of Finding the Roots Which Are Less than Unity of a Rational Integral Equation of Any Degree: Followed by a More General Method of Finding the Roots of Any Value, *Phil. Mag.*, 23(6):892–900 (1912).

10. Thomson, W., and P. G. Tait: "Treatise on Natural Philosophy," new ed., vol. 1, part 1, pp. 379, 482, The University Press, Cambridge, England, 1879.

11. Dietzold, R. L.: The Isograph—A Mechanical Root-finder, *Bell Labs. Record*, 16:130–134 (1937–1938).

12. Merener, R. O.: The Mechanism of the Isograph, *Bell Labs. Record*, 16:135–140 (1937–1938).

13. Miller, D. C.: A 32-element Harmonic Synthesizer, *J. Franklin Inst.*, 181:51–81 (1916).

14. Krantz, F. W.: A Mechanical Synthesizer and Analyzer, *J. Franklin Inst.*, 204: 245–262 (1927).

15. Brown, S. L.: A Mechanical Harmonic Synthesizer-Analyzer, *J. Franklin Inst.*, 228:675–694 (1939).

16. Brown, S. L., and L. L. Wheeler: A Mechanical Method for Graphical Solution of Polynomials, *J. Franklin Inst.*, 231:223–243 (1941).

17. Hart, H. C., and I. Travis: Mechanical Solution of Algebraic Equations, *J. Franklin Inst.*, 225:63–72 (1938).

18. Rymer, T. B., and C. C. Butler: An Electrical Circuit for Harmonic Analysis and Other Calculations, *Phil. Mag.*, 35(7):606–616 (1944).

19. Marshall, B. O., Jr.: The Electronic Isograph for Roots of Polynomials, *J. Appl. Phys.*, 21:307–312 (1950).

20. Hagg, G., and T. Laurent: A Machine for the Summation of Fourier Series, *J. Sci. Instr.*, 23:155–158 (1946).

21. Furth, R., and R. W. Pringle: A New Photo-electric Method for Fourier Synthesis and Analysis, *Phil. Mag.*, 35(7):643–656 (1944).

22. Ferrara, G., and R. L. Nadeau: A Complex Wave Synthesizer, *Elec. Eng.*, 70:585 (1951).

23. Robertson, J. H.: A Simple Machine Capable of Fourier Synthesis Calculation, *J. Sci. Instr.*, 27:276–278 (1950).

24. Brown, S. L., and L. L. Wheeler: The Use of a Mechanical Synthesizer to Solve Trigonometric and Certain Types of Transcendental Equations, and for the Double Summations Involved in Patterson Contours, *J. Appl. Phys.*, 14:30–36 (1943).

25. Emch, A.: Hydraulic Solution of an Algebraic Equation of the *n*th Degree, *Am. Math. Monthly*, 8:58–59 (1901).

26. Meslin, G.: Sur une machine a résoudre les équations, *J. phys. radium*, 9:(3):339–343 (1900).

27. Boys, C. V.: On a Machine for Solving Equations, *Phil. Mag.*, 21(5):241–245 (1886).

28. Maxwell, J. C.: "A Treatise on Electricity and Magnetism," 3d ed., vol. II, p. 286, Oxford University Press, New York, 1892.

29. Lucas, F.: Généralization du théorème de Rolle, *Compt. rend.*, 106:121–122; Détermination électrique des racines réeles et imaginaires de la derivée d'un polynôme quelconque, 106:195–197; Résolution électrique des équations algébriques, 106:268–270; Détermination électrique des lignes isodynamiques d'un polynôme quelconque, 106:587–589; Résolution immédiate des équations au moyen de l'électricite, 106:645–648; Résolution des équations par l'électricité, 106:1072–1074 (1888).

30. Hansen, W. W., and O. C. Lundstrom: Experimental Determination of Impedance Functions by the Use of an Electrolytic Tank, *Proc. IRE*, 33: 528–534 (1945).

31. Boothroyd, A. R., E. C. Cherry, and R. Makar: An Electrolytic Tank for the Measurement of Steady-state Response, Transient Response, and Allied Properties of Networks, *Proc. IEE (London)*, part I, 96:163–177 (1949).

32. Keller, M. W.: "College Algebra," p. 399, The Riverside Press, Cambridge, Mass., 1946.
33. Lucas, F.: Résolution électromagnétique des équations, *Compt. rend.*, **111**:965–967 (1890).
34. Russell, A., and J. N. Alty: An Electromagnetic Method of Studying the Theory of and Solving Algebraical Equations of Any Degree, *Phil. Mag.*, **18**(6):802–811 (1909).
35. Taylor, P. L.: Electronic Fluxmeter, *Wireless World*, **57**:161–162 (1951).
36. Borsellino, A.: Un metodo electtrico per la determinazione approsimata delle radici reali o complesse di una equazione algebrica, *Nuovo cimento*, **5**:23–28 (1948).
37. Ergen, W. K.: Bridge Type Electrical Computers, *Rev. Sci. Instr.*, **18**:564–567 (1947).
38. Hathaway, C. M., and R. C. Eddy: Rosette Principal Strain Computer, *Proc. Natl. Electronics Conf.*, **6**:295–307 (1950).
39. Bubb, F. W., R. G. Nisle, and P. G. Carpenter: An Electronic Analog Computer for Solving the Flash Vaporization Equilibrium Equation, *Trans. AIMME* (Petroleum Division), **189**:143–148 (1950).
40. Hardy, A. C., and E. C. Dench: An Electronic Method for Solving Simultaneous Equations, *J. Opt. Soc. Am.*, **38**:308–312 (1948).

Part Three

DIRECT COMPUTERS (SIMULATORS)

9

DYNAMICAL ANALOGIES

Dynamical analogy refers to the well-established correspondence among the equations of motion of dynamical (mechanical) systems, electrical circuits, and acoustical systems. The theory of the dynamic behavior of mechanical systems was well developed by the time electrical circuits came under consideration. The early concept that electrical phenomena were fundamentally dynamic[1] in character led to the study of electrical circuit by means of these equations. The presence of electromagnetic energy in association with moving charges and of electrostatic energy in association with static charges naturally led to the association of electromagnetic energy with the kinetic energy of a mechanical system and of electrostatic energy with the potential energy of the mechanical system. Later it was shown[2] that the analogy may be likewise drawn between electrostatic energy and kinetic energy and between electromagnetic energy and potential energy.

The fact that the behavior of mechanical systems may be visually observed and easily comprehended proved highly useful in visualizing the behavior of analogous electrical systems. As a result there has been considerable development of mechanical models for demonstrating to students electrical principles which would be difficult to grasp by mathematical reasoning alone. An extensive review of the older models was published in 1926.[3] More recent additions include a mechanical model of a vacuum-tube oscillator[4] and one[5] representing the "new" analogy developed by Firestone.

It is but a short step from the use of mechanical models for illustrating electrical principles to the use of electrical circuits for modeling complex mechanical and electromechanical systems. Starting with Nickle's fundamental paper[6] on the application of electrical circuits to the solution of problems in dynamics, this field of experimental analysis was rapidly developed.

This chapter is concerned with the derivation of the analogous relations between electrical and mechanical systems and with the application

of such electrical circuits to the solution of mechanical, electromechanical, and acoustical systems.

9.1. Analogy between Electrical and Mechanical Elements. New-ton's laws of motion provide the basis for the analysis of dynamical systems; Kirchhoff's laws give the basis for the analysis of electrical net-works. Both sets of laws are versions of the more general concepts of equilibrium and continuity.
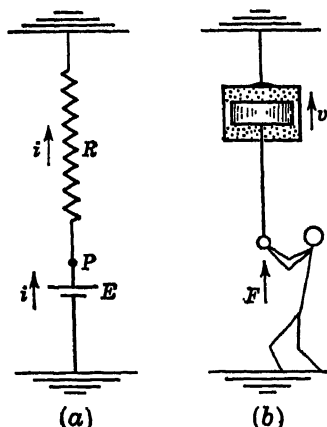
Considering, first, electrical-circuit ele-ments, suppose a voltage E to be suddenly applied across a resistance R (Fig. 9.1a). Immediately a current i will flow. Because of this current flow a back emf Ri is gen-erated in the resistor and is of such magni-tude that it balances the impressed voltage E. Thus a condition of equilibrium is established, which is given by the relation

$$E - Ri = 0 \qquad (9.1)$$

The rate at which work is being done by E in forcing i through R is

$$P = Ei \qquad (9.2)$$

(a)   (b)

Fig. 9.1

With E in volts and i in amperes, P is given in watts.

Equation (9.1) may be rewritten in the form

$$i - \frac{1}{R} E = 0 \qquad (9.3)$$

This is an equation of continuity in that it states that the current i entering node P from source E equals the current E/R leaving node P.

The resistance is an energy-dissipating element. Consequently, its mechanical counterpart must similarly be an energy-dissipating element. Such is the dashpot, which forces a damping fluid, e.g., oil, through a restricted opening and dissipates energy through viscous friction and turbulence in the oil. While the dashpot (shock absorber) is intentionally designed as an energy dissipator, mechanical equipment has many other sources of energy dissipation which are inherent in the design of the equipment and which designers seek to reduce to a minimum. Such sources, for example, include the areas of contact of sliding and rotating surfaces. Although proper lubrication minimizes these losses, they are nevertheless present and might well exercise a real influence on the dynamic behavior of the systems. Other sources, which may or may not be desirable according to the purpose of the machine, include the internal dissipation (hysteresis) of the material from which the equipment

is constructed. Rubber compounds, for example, have notable internal energy-loss rates. Cast iron also has a high internal damping and is frequently used in those applications where energy dissipation is desirable. Other materials, such as high-strength alloy steels, have very low energy-dissipation rates. Riveted and welded joints, although seemingly rigid, also contribute to damping because of slippage or relative movement of the jointed parts. Much of the damping in aircraft structures is due to this source. In electromechanical systems, eddy currents are often major sources of energy dissipation.

In taking damping into account in mechanical systems it is frequently convenient to consider the losses as concentrated in an equivalent viscous dashpot in which the damping force is proportional to velocity. This is the type of dashpot shown in Fig. 9.1b. A solid piston is shown fitted with a predetermined amount of clearance in a cylinder filled with oil. Motion of the piston results in transfer of oil from one side to the other through the small clearance annulus, and consequently in a pressure drop which depends on the rapidity with which the transfer is made.

Consider, now, a force F to be suddenly applied to the piston rod in (b). Assuming the weight of the moving parts to be negligible, the piston will immediately acquire a velocity v such that the viscous friction of the displaced fluid will exactly balance the impressed force F. The resulting equilibrium is expressed by the equation

$$F - cv = 0 \tag{9.4}$$

where c is the damping coefficient of the dashpot. The rate at which the force F is doing work is

$$P = Fv \tag{9.5}$$

A comparison of the equilibrium relations given by Eqs. (9.1) and (9.4) and of the power relations given by Eqs. (9.2) and (9.5) shows that the two systems of Fig. 9.1 are completely analogous. The analogy is even indicated by the similarity in appearance of parts (a) and (b) of the figure. It is clear that a force cannot be exerted without a "ground" to take up the reaction.

The equations show that voltage is analogous to force, current to velocity, and resistance to dashpot coefficient.

If, however, Eq. (9.3) is included in the comparison instead of Eq. (9.1), it is clear that the two systems are still completely analogous, but that the analogy now exists in a different form. In this case current is analogous to force, voltage to velocity, and conductance to dashpot coefficient.

Although in so far as the dashpot alone is concerned either analogy is equally valid, and that convenience and available equipment are the

only criteria for the choice of one analogy in preference to the other, such analogies are useful as experimental or computing devices only when systems become too complex to be handled readily by conventional numerical methods. With such complex systems it is sometimes found that one analogy can be realized in a physical electrical circuit, whereas the other cannot be realized. This point is covered in more detail later in this chapter.

Consider, now, another electrical circuit element—the inductance coil. It has been experimentally established that whenever a magnetic field
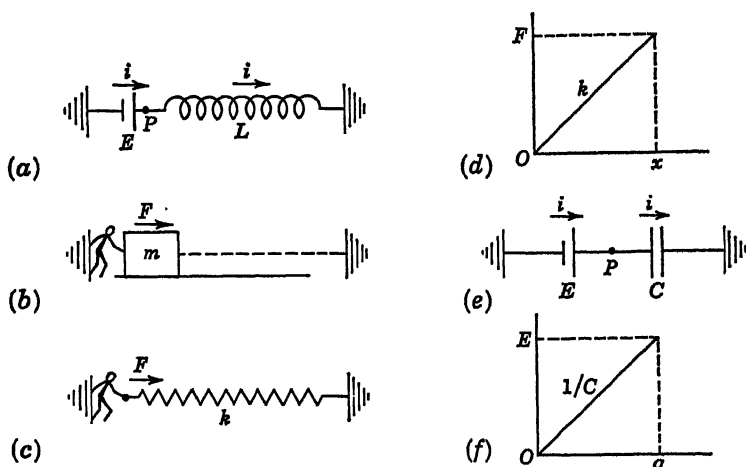
Fig. 9.2

linking an electrical circuit changes for any reason, an electromotive force is induced in that circuit. If the changing magnetic field is due to changing current flow in the coil itself, then the emf is "self-induced." This induced, or "back," emf acts in such a direction as to oppose the phenomenon causing the change in current. The magnitude of the back emf is proportional to the rate of change of the current and the constant of proportionality is called the self-inductance (or, simply, "inductance") L of the coil. The magnitude of L depends on the extent of the flux linking and on the flux density per ampere-turn, and thus on the form of the winding and on the core material. The design of coils is discussed at length by Grover.[7]

Suppose a voltage E to be suddenly impressed across a coil of inductance L (Fig. 9.2a). The equation of equilibrium requires that the impressed voltage must be equaled by the back emf at every instant of time. The equation is

$$E - L\frac{di}{dt} = 0 \tag{9.6}$$

An equivalent form of Eq. (9.6) is obtained by integration and by assuming zero energy stored in the inductor at $t = 0$.

$$i - \frac{1}{L} \int_0^t E\, dt = 0 \tag{9.7}$$

Again, this is the equation of continuity, stating that the flow of current into node P is equal to the flow out of node P.

These equations strictly apply only to an ideal inductor (no resistance, and no capacitance between coils). With a constant voltage E applied to the coil, the current increases indefinitely at a constant rate E/L. With E in volts and L in henrys, this rate is in amperes per second. Actually, however, resistance is invariably present in the wire of the coil. Hence, after the initial rate of increase given by E/L, the rate of increase begins to drop off and either reaches zero (constant current equal to E/R) or else the current becomes heavy enough to burn out the coil before attaining its steady-state value.

If, at any instant of time, the voltage is suddenly reduced to zero without disrupting the circuit (*i.e.*, by shorting across E), the current present at that instant in the purely inductive circuit would persist indefinitely at full value. Actually, of course, it would be dissipated in heat because of the resistance inherently present in the circuit.

The energy stored in the electromagnetic field of the coil is given by the work done by E in establishing the current i. Thus

$$W = \int_0^t Ei\, dt = \int_0^i Li\, di = \tfrac{1}{2}Li^2 \tag{9.8}$$

With L in henrys and i in amperes, W is given in wattseconds. Note that P [Eq. (9.2)] is a *rate* expressed in watts, while W is an *energy* expressed in wattseconds.

In a mechanical system consisting only of a mass on a frictionless plane, subjected to a suddenly applied force F (Fig. 9.2b), the equation of motion is

$$F = m \frac{dv}{dt} \tag{9.9}$$

In accordance with D'Alembert's principle, Eq. (9.9) can be rewritten as an equation of force equilibrium in statics. The mass times acceleration term is to be considered as an "inertia force" which opposes the force producing the acceleration. The equation of equilibrium on this basis may, therefore, be written as follows:

$$F - m \frac{dv}{dt} = 0 \tag{9.10}$$

In view of the simplicity of the problem now under study, the approach to Eq. (9.10) seems somewhat artificial at first glance, since one could go directly from Eq. (9.9) to Eq. (9.10) merely by transposing the right side of Eq. (9.9) to the left. The concept of an inertia force, however, has practical value in permitting unrestricted application of the methods of statics to the analysis of complex problems in dynamics. Also, by considering Eq. (9.10) as an equation of equilibrium, the analogy with Eq. (9.6) representing the equilibrium of voltages is more clearly understood physically.

If a constant force F is suddenly applied to the mass m, in the absence of friction the velocity of the mass will increase at a constant rate given by F/m. If at any instant of time F is suddenly reduced to zero, m will continue to move indefinitely at a constant speed. However, friction is invariably present and the mass is eventually brought to a standstill.

The kinetic energy of the mass at any instant of time is given by

$$W = \tfrac{1}{2}mv^2 \qquad (9.11)$$

A comparison of Eqs. (9.6) and (9.8) with Eqs. (9.10) and (9.11) points out strikingly the dynamical analogy which exists between a pure inductance and a pure mass.

Voltage and force, current and velocity, inductance and mass, electromagnetic energy and kinetic energy are seen to be analogous quantities. These are consistent with the analogy shown to exist between Eqs. (9.1) and (9.2) and Eqs. (9.4) and (9.5).

The analogy appears more realistic in Fig. 9.2 by associating with the applied force F a ground terminal which must absorb the reaction and also by associating with the mass m a ground terminal (shown dotted) to indicate that the concept of mass is based on gravitational attraction.

In a mechanical system consisting only of a spring with one end attached to ground and a force F applied to the other (Fig. 9.2c), the equation of equilibrium is

$$F - kx = 0 \qquad (9.12)$$

where k is the spring stiffness (i.e., the force required to produce unit deflection, usually expressed in pounds per inch) and x the amount of deflection of the spring as a result of the action of F.

In the study of idealized mechanical systems, springs are often considered as being weightless, or else the weight of the spring, if significant, is lumped with other attached masses and the spring then considered as weightless. The spring of Fig. 9.2c is to be considered as having elasticity only, but no mass. Thus, a force F, no matter how rapidly applied, must build up linearly from 0 to its value F while the spring deflects from 0

to the value x. The load-deflection diagram is, therefore, the straight line shown in Fig. 9.2d, having the slope $F/x = k$. If the load F is suddenly applied, then the deflection x is just as suddenly attained, with no overshoot and no lag, since there is no mass or friction associated with the idealized spring. The suddenly applied force builds up even in zero time only along the deflection curve in Fig. 9.2d.

The elastic energy stored in the spring is equal to the work done by F in deflecting the spring. This is equal to the average force times the distance through which the force is moved and is independent of how rapidly the force is applied. Since the force-distance relation is linear (Fig. 9.2d), the average force is $F/2$. The work done is

$$W = \tfrac{1}{2}Fx \tag{9.13}$$

This is, of course, the area under the load-deflection curve of Fig. 9.2d. Since $F = kx$, Eq. (9.13) may be written as

$$W = \frac{1}{2}\frac{1}{k}F^2 \tag{9.14}$$

Since during the build-up of F the end of the spring must move through a distance x, a velocity must be associated with this end of the spring in order to cover the distance x in the same interval of time that the applied force attains its value F. Consequently, x may be written as an integral of the velocity over this time interval. The relation is

$$x = \int_0^t v \, dt \tag{9.15}$$

Substituting into Eq. (9.12), we obtain

$$F - k \int_0^t v \, dt = 0 \tag{9.16}$$

We may now compare Eqs. (9.7) and (9.8) with Eqs. (9.16) and (9.14). The analogy, again, is very striking and complete. Current and force, voltage and velocity, inductance and compliance (the reciprocal of stiffness), and electromagnetic energy and potential (elastic) energy are seen to be analogous quantities. These are consistent with the analogy shown to exist between Eqs. (9.3) and (9.2) and Eqs. (9.4) and (9.5).

Thus a self-inductance may be used to represent either a mass or a compliance in a mechanical system, depending on the approach which one wishes to adopt and on other factors which remain yet to be considered.

The capacitor is another basic element in electric circuits. It stores electric charges just as a tank stores water. If a voltage E is impressed across a capacitor (Fig. 9.2e), a current i will transport a charge q into

the capacitor, creating a back emf in the capacitor dielectric of magnitude q/C volts, where q is the charge in coulombs and C is the capacitance in farads. When dealing with an ideal capacitance (perfect dielectric, zero inductance and zero resistance in leads), the back emf is at all instants in equilibrium with the impressed voltage, following all variations in this voltage without lag or defect. The equation of equilibrium is

$$E - \frac{1}{C} q = 0 \qquad (9.17)$$

The charge q is transported by a flow of current and is equal to the time integral of the current flow into the capacitor. Thus

$$q = \int_0^t i \, dt \qquad (9.18)$$

and Eq. (9.17) may be rewritten as

$$E - \frac{1}{C} \int_0^t i \, dt = 0 \qquad (9.19)$$

Equation (9.19) may be presented in differential, instead of integral, form. Differentiating the equation and rearranging yields

$$i - C \frac{dE}{dt} = 0 \qquad (9.20)$$

This is, again, the equation of continuity stating that the current i entering node P equals the current $C(dE/dt)$ leaving node P.

The electrostatic energy stored in the capacitor dielectric is given by the work done by E in forcing charge into the capacitor. It is equal to the average voltage across the capacitor times the amount of charge and is independent of how rapidly the voltage is applied. Since the voltage-charge relation is linear (Fig. 9.2f), the average voltage is $E/2$. The work done is

$$W = \tfrac{1}{2}Eq \qquad (9.21)$$

Since $E = q/C$, Eq. (9.21) may be written as

$$W = \tfrac{1}{2}CE^2 \qquad (9.22)$$

A comparison of Eqs. (9.17) to (9.19), (9.21), and (9.22) with Eqs. (9.12) to (9.16) strikingly reveals the complete analogy which exists between the mechanical compliance and the electrical capacitance. This is the force-voltage (or mass-inductance) analogy, in accordance with common terminology. The electrostatic energy of the capacitor is analogous to the potential energy of the spring. Also, it is apparent that the quantity of electric charge q is analogous to the displacement x.

If Eqs. (9.20) and (9.22) are compared with Eqs. (9.10) and (9.11) the other analogy clearly holds. Known as the force-current (or mass-capacitance) analogy, the capacitance is shown to be analogous to mass and electrostatic energy to kinetic energy.

An approach to perfection in capacitors is much more easily realizable physically than it is in inductors. A detailed discussion of capacitor construction and characteristics is given by Brotherton.[8]

9.2. Relations for Simple Vibrating Systems. Single-degree-of-freedom damped mechanical systems are shown in Fig. 9.3a and b. In (a) the system is rectilinear. A mass m (lb-sec^2/in.) is attached to one end of a spring of stiffness k (lb/in.). The other end of the spring is fixed to a ceiling. A dashpot having the damping coefficient c (lb-sec/in.) is similarly attached between the mass and the ceiling. A time-varying force $F(t)$ acts on m, resulting in a displacement x which is taken to be positive in the downward direction. In (b) a torsional system is shown. A disk having the mass moment of inertia I (lb-sec^2-in.) is attached to a shaft of torsional stiffness k (in.-lb/rad). The other end of the shaft is fixed

(a)   (b)

(c)   (d)

Fig. 9.3

to the ceiling. A dashpot having the damping coefficient c (in.-lb-sec/rad) acts on the disk. A time-varying torque $T(t)$ (in.-lb) acts in the plane of the disk, producing an angular displacement θ, positive as shown.
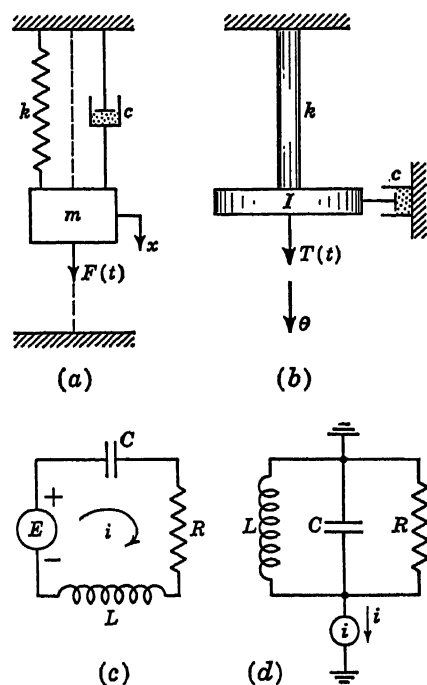
Making use of D'Alembert's principle, the equations of equilibrium may be set up for the mass of the rectilinear system and the inertia of the torsional system. These equations are

$$\Sigma F - m\ddot{x} = 0 \tag{9.23}$$

$$\Sigma T - I\ddot{\theta} = 0 \tag{9.24}$$

The indicated summations must include all forces acting on each inertia considered as a free body. For positive displacements and positive velocities, negative forces are exerted by the springs and dashpots. The externally applied forces are independent of the motion and are assigned

a positive sign.   Equations (9.23) and (9.24) become, therefore,

$$F(t) - kx - c\dot{x} - m\ddot{x} = 0 \qquad (9.25)$$
$$T(t) - k\theta - c\dot{\theta} - I\ddot{\theta} = 0 \qquad (9.26)$$

These equations are written in terms of the displacements.   They may also be written in terms of velocities:

$$F(t) - k \int_0^t v \, dt - cv - m \frac{dv}{dt} = 0 \qquad (9.27)$$

$$T(t) - k \int_0^t \Omega \, dt - c\Omega - I \frac{d\Omega}{dt} = 0 \qquad (9.28)$$

where Ω is the instantaneous angular velocity of I.

It should be pointed out that Eq. (9.25) is based on displacements with respect to the static equilibrium position of mass m hanging on spring k. The weight of m is exactly balanced by tension in the spring in this position so that it need not appear in the equations of motion.   If x_0 is the deflection of the spring as a result of hanging the weight mg upon it, the total deflection of the spring as a result of the weight mg and the action of the force $F(t)$ is $x_0 + x$.   The equation of equilibrium corresponding to Eq. (9.25) then becomes

$$F(t) + mg - k(x_0 + x) - c(\dot{x}_0 + \dot{x}) - m(\ddot{x}_0 + \ddot{x}) = 0 \quad (9.28a)$$

Since x_0 is a constant quantity, equal to mg/k, its derivatives are zero. Moreover, since $mg = kx_0$, these terms cancel each other in Eq. (9.28a). As a result Eq. (9.28a) becomes Eq. (9.25).

The electrical elements discussed in Sec. 9.1 may be combined either in series or in parallel.   The first arrangement is shown in (c), the second in (d), in Fig. 9.3.   A voltage source is used in (c) and a current source in (d).   In (c) it is desired to sum voltage drops around the closed loop.   In (d) it is desired to sum the currents entering and leaving a node.   According to Kirchhoff's first law the sum of the currents entering and leaving a node must equal zero (the equation of continuity).   According to Kirchhoff's second law the sum of the voltage drops (a voltage rise is a negative drop) around a closed loop must be zero.   Thus, applying Kirchhoff's second law to (c) and his first law to (d) the following equations result:

$$E - \frac{1}{C} \int_0^t i \, dt - Ri - L \frac{di}{dt} = 0 \qquad (9.29)$$

$$i - \frac{1}{L} \int_0^t E \, dt - \frac{1}{R} E - C \frac{dE}{dt} = 0 \qquad (9.30)$$

where E is the voltage at the lower node.

Comparing Eqs. (9.29) and (9.30) with Eqs. (9.27) and (9.28) shows that either circuit (c) or (d) may be used to represent the rectilinear mechanical system or the torsional system. Which to use in this case is entirely a matter of convenience. In general, simpler instrumentation is involved in supplying and measuring voltages, so that circuit (c), representing the mass-inductance analogy, is often preferred. On the other hand, the resemblance in the physical arrangement of the elements in (a) and (d) has led to a vigorous advocacy[2] of the mass-capacitance analogy represented in (d) because of the much lesser likelihood of errors in setting up the equivalent circuits of complex mechanical systems. If the mass and the force are both referred to ground, as indicated by the dotted lines in (a), the mass-capacitance circuit (d) may be drawn directly by sight.

The natural frequencies of the mechanical systems (a) and (b) are

$$\omega_m = \left[\frac{k}{m} - \left(\frac{c}{2m}\right)^2\right]^{\frac{1}{2}} \tag{9.31}$$

$$\omega_m = \left[\frac{k}{I} - \left(\frac{c}{2I}\right)^2\right]^{\frac{1}{2}} \tag{9.32}$$

Substituting into these equations the analogous electrical quantities, the corresponding frequencies of the analogous electrical circuits are

$$\omega_e = \left[\frac{1}{LC} - \left(\frac{R}{2L}\right)^2\right]^{\frac{1}{2}} \tag{9.33}$$

$$\omega_e = \left[\frac{1}{LC} - \left(\frac{1}{2RC}\right)^2\right]^{\frac{1}{2}} \tag{9.34}$$

for the mass-inductance and mass-capacitance analogies, respectively. If L is in henrys, C in farads, and R in ohms, the frequencies are in radians per second.
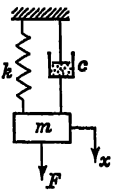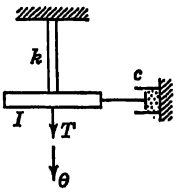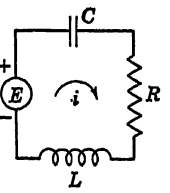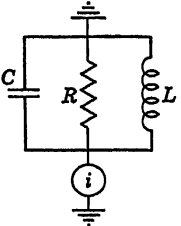
The formal similarity between Eqs. (9.29) and (9.30) suggests that the circuits of Fig. 9.3c and d may be considered to be analogs of each other. The analogy between systems belonging to the same physical area carries a special name: *duality*. Duality is recognized by writing the loop equations for one circuit and the node equations for the second circuit. If for every term in one set of equations there exists a corresponding term (same order of differentiation) in the other set, the two circuits are duals.

In summary, the analogous quantities developed so far are presented in Table 9.1.

In general, in a dynamical system the variables of interest are the displacements of the masses and the stresses in the connecting springs. These are related, since the stress in a spring such as that in Fig. 9.3a is proportional to the relative displacement of the two ends. The load

(force) in this spring may be obtained by measuring the voltage drop across capacitor C. The displacement of mass m is then obtained by dividing this force by the spring stiffness k. Another, and more complicated, way of measuring in the electrical circuit a value which gives the mechanical displacement is to measure the total quantity of charge which has passed through inductance L (and hence through all the other elements of this series circuit). This may be done with a current-integrating meter. The force in the spring may also be obtained by

TABLE 9.1. SUMMARY OF ANALOGOUS ELECTRICAL AND MECHANICAL QUANTITIES

Rectilinear mechanical system		Torsional mechanical system		Mass-inductance analogy		Mass-capacitance analogy
Force F	$\doteqdot$	Torque T	$\doteqdot$	Voltage E	$\doteqdot$	Current i
Mass m	$\doteqdot$	Inertia I	$\doteqdot$	Inductance L	$\doteqdot$	Capacitance C
Damping c	$\doteqdot$	Damping c	$\doteqdot$	Resistance R	$\doteqdot$	Conductance $\frac{1}{R}$
Velocity v	$\doteqdot$	Velocity Ω	$\doteqdot$	Current i	$\doteqdot$	Voltage E
Compliance $\frac{1}{k}$	$\doteqdot$	Compliance $\frac{1}{k}$	$\doteqdot$	Capacitance C	$\doteqdot$	Inductance L
Displacement x	$\doteqdot$	Displacement θ	$\doteqdot$	Charge q	$\doteqdot$	$\int_{o}^{t} E\,dt$

measuring the current flowing through inductance L in Fig. 9.3d, where the force-current analogy is in use. This would be used to obtain the displacement of m. However, one could also obtain the displacement of m by integrating the voltage across C in (d). This, however, requires more complicated instrumentation. If the velocity of the mass is desired for any reason, it may be obtained by measuring either the current through L in (c) or the voltage across C in (d).

The manner of exciting the electrical system must naturally correspond with the type of excitation expected in the mechanical system. For example, suppose that the mechanical system in (a) is initially at rest and then a constant force F is suddenly applied to mass m. The mass will execute a damped sinusoidal oscillation, finally coming to rest at a displacement $x = F/k$. In the electrical system (c) this process would be simulated as shown in Fig. 9.4. With the capacitor C in the uncharged state, at time $t = 0$ the switch S is suddenly closed. The charge q would oscillate through the circuit and finally reach a constant value given by

EC. At this instant all current will have ceased to flow (system at rest). The voltage drop across the capacitor will be a constant value *E*, corresponding to the constant force *F* in the mechanical spring. The source *E* must, of course, have sufficient capacity so that its voltage would not be affected by current drain. At the same time its internal resistance either should be negligible or else should be considered as part of the required resistance *R*. Similarly, resistance in *L* should be included in calculating *R*. To excite the analog in Fig. 9.3*d* in a similar manner requires a constant current generator *i* whose output will not be affected by the voltage surges occurring through the system during the decaying transient phase of the motion. When the steady state is finally reached, there will be zero voltage drop through the circuit (corresponding to a stationary system) and a constant current *i* will be flowing through *L*, corresponding to the constant force existing finally in spring *k*. Since coil *L* has zero resistance, theoretically all the current in the system will pass through *L* in the steady state without any voltage drop, and none will flow through *C* or *R*. During the transient motion, however, the self-inductance of *L* offers impedance to current flow, so that current will also flow through *R* and *C*. Actually, *L* will have some resistance, so that a slight voltage drop will exist across the passive elements. This would correspond in the mechanical system to a slight constant velocity of *m*.
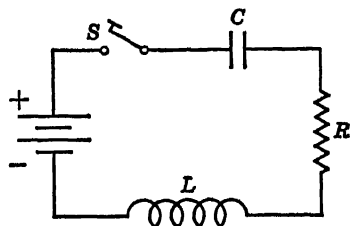
Fig. 9.4

Other forms of excitation of mass *m* may be easily reproduced electrically.[9] The forms include a rectangular pulse, square wave, sawtooth wave, sinusoidal pulse, decaying sine wave, etc. Sinusoidal forces of variable frequency are useful in studying resonance phenomena and frequency-response characteristics of mechanical systems. Such forces are easily simulated by the outputs of electronic oscillators.

In many problems the point of support of the spring (*e.g.*, the ceiling) is excited by a time-varying displacement. Such excitation, for example, is that experienced by buildings during an earthquake. Associated with this is a time-varying velocity of the support point. Referring to Fig. 9.5*a*, the ceiling is subjected to a displacement x_1. As a result, mass *m* will acquire a displacement x and velocity $\dot{x}$. All of these vary with time. The equation of equilibrium for *m* is written

$$m\ddot{x} + c(\dot{x} - \dot{x}_1) + k(x - x_1) = 0 \qquad (9.35)$$

Since x and x_1 represent charge and $\dot{x}$ and $\dot{x}_1$ current in a mass-inductance analog circuit, Eq. (9.35) indicates that the electrical elements represent-

ing c and k must be in a branch common to two loops.   In one loop the current $\dot{x}$ and charge x are circulating; in the other loop the current $\dot{x}_1$ and charge x_1 are circulating.   The inductance representing m is in the loop in which the charge x circulates.   The corresponding electrical circuit is shown in Fig. 9.5b.   If a voltage E is used to excite the circuit, its time-varying value must be so adjusted that it represents the combined time-varying reaction of spring k and dashpot c on the ceiling.   To meet any arbitrary variation of x_1 by this means would require a series of trial variations in E until one is obtained in which the charge q_1 (or
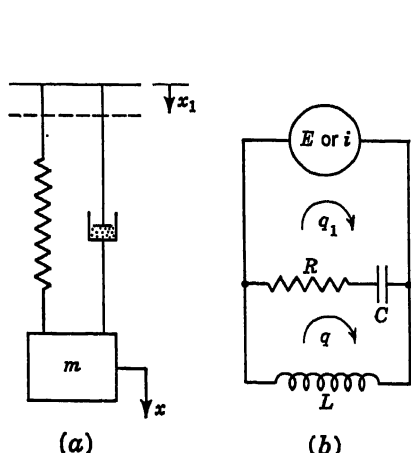
Fig. 9.5
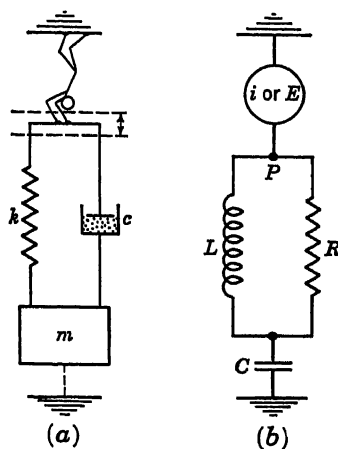
Fig. 9.6

current $\dot{q}_1$) will agree with the ceiling displacement x_1 (or velocity $\dot{x}_1$). A more direct method would be to use a current source in place of the voltage source and to vary the output of this current source in accordance with the variation assigned to $\dot{x}_1$.

The mass-capacitance analogy may be drawn directly by inspection if Fig. 9.5a is altered somewhat to show the mass m with a terminal to ground and to indicate a source of excitation at the top ends of the spring and dashpot.   The altered form of Fig. 9.5a is shown in Fig. 9.6a.   The corresponding analog circuit is shown in Fig. 9.6b.   If a current source is used, it would have to be adjusted by trial until the voltage at the junction P followed the required velocity variation imposed on the support point of the mechanical system.   A voltage source may be used, instead, and output varied directly in accordance with the prescribed variation in $\dot{x}$.

Another possible form of excitation of a flexible mechanical system is that caused by the sudden arrest of the system at the end of a free fall.   The problem of packaging radio tubes to withstand drops during shipment has been studied by this means.[10]   Figure 9.7a illustrates a

drop involving "perfect" rebound, and Fig. 9.7b shows a drop without rebound. In the latter case an auxiliary mass M, whose weight exceeds the maximum upward force to be expected in the spring-dashpot combination, serves to clamp the end of the falling system to the ground at the instant of contact, thereby preventing rebound. By specifying plastic impact between M and the ground, there will be no rebound of mass M.

In both cases, just before contact with the ground the systems will be traveling with an initial velocity of $\sqrt{2gh}$. At the instant of contact,
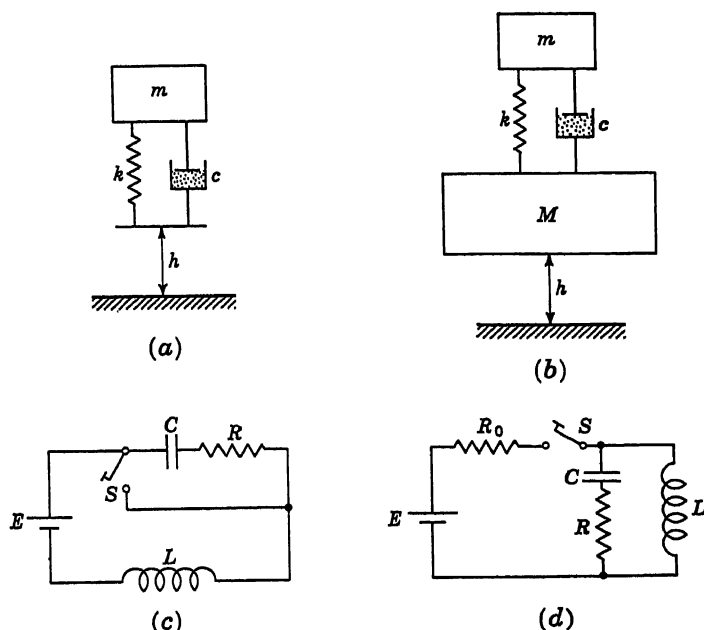
Fig. 9.7

the lower ends of the springs and dashpots will be suddenly stopped. These initial conditions must be reproduced in the analogies. It should be remembered that in the electrical analogies only the *relative* motions of the two ends of a spring or of a dashpot are manifested. Thus, if the mass-inductance analogy is to be used in Fig. 9.7, the velocity just *before* contact would be represented by a current through the coils representing masses m and M, but *no current* through the capacitor and resistors representing k and c. At the instant of contact, the relative velocities of the two ends of each spring and dashpot become at once equal to the velocity of m, and thus the same current must flow through all these elements. The required currents may be produced in either one of two ways. In one method, illustrated in Fig. 9.7c, a voltage E, proportional

to the weight (gravitational force) of m, is applied to the circuit with the switch S closed for the length of time representing the drop period of the system. During this period a uniformly increasing current flows through L, corresponding to the uniformly increasing velocity of m. There is, properly, no voltage across C and R. When the current reaches the prescribed value, the switch is instantly opened. The full current in L is then diverted into R and C, and the voltage variation across C will be a measure of the combined dynamic and static load in the spring, and hence also a measure of the displacement of m relative to the unloaded position of the free end of the spring. During the initial surge, the voltage across the capacitor will increase to a maximum and then decrease. The instant this voltage becomes zero, the "bouncing" phase sets in. This means that the switch must be instantly closed again, since the spring and dashpot are ineffective when not in contact with the ground. During this phase, the current will drop linearly to zero in the direction opposing the battery output and then pick up linearly in the direction of the battery output. When this current reaches the same value it had at the time the switch was closed, the condition of contact with the ground is once again reestablished and the switch must be opened again. Another way of looking at the bounce phase is to time the interval during which the current drops to zero (top of the bounce) and at an equal interval later (back to earth again) open the switch. The switching arrangement is rather complicated to reproduce the bouncing condition faithfully. The steps must be repeated as many times as there are bounces in the system.

If the switch is opened on first contact with the ground and is left there throughout the period of current flow, the condition of no bounce, illustrated by Fig. 9.7b, will be reproduced. The presence of M is only incidental to the problem, in that it acts as a clamping device on the system, just like the open switch in the electrical system. Thus, in so far as the electrical system is concerned, M need not be simulated by a large inductance.

When either system finally comes to rest, the spring k will have a load in it equal to the weight of m. Correspondingly, the capacitor C will have a constant voltage across it equal to E.

The other method of exciting this system is illustrated in Fig. 9.7d. With switch S closed, the current in the circuit is allowed to reach a steady value given by E/R_0. This corresponds to the velocity of m at the instant of impact. Since a steady current is flowing, there is no voltage drop across the branch containing C and R (assuming that the resistance of the inductance coil is negligible). The switch S is then opened suddenly, and the current is diverted through R and C. This condition corresponds to the case of no rebound and provides only the

dynamic loads (*i.e.*, when the system finally comes to rest there will be no voltage across the condenser corresponding to the dead weight of m).

9.3. Scale Factors. Whenever a mechanical system is to be represented by an electrical model, a decision must be made regarding the magnitudes of the electrical elements to be used. Economy and practicability are important factors.

In view of the fact that the dimensions of all the quantities involved in the dynamics of mechanical systems may be expressed in terms of three fundamental units, *e.g.*, mass, length, and time, the selection of analogous electrical elements is really concerned with modeling these fundamental units. Once the mass, length, and time ratios have been established, all the other quantities involved are automatically determined.

Consider, first, the mass-inductance analogy. The scale factors relating inductance, charge, and electrical time to mass, displacement, and mechanical time are S_1, S_2, and S_3 in the following set of equations:

$$L = S_1 m \qquad q = S_2 l \qquad t_e = S_3 t_m \qquad (9.36)$$

The scale factors for all other quantities may now be determined in terms of S_1, S_2, and S_3. To do this, first express the dimensions of each new quantity in terms of the dimensions of the fundamental quantities and scale factors adopted in Eq. (9.36). The combination of the fundamental scale factors occurring in each such expression is the true scale factor for that quantity. Thus

Current $= i$ amp $= S_4 \times v$ in./sec $\approx (S_2 l S_3^{-1} t^{-1})$

$$\text{or} \qquad S_4 = \frac{S_2}{S_3} \qquad (9.37)$$

Voltage $= E$ volts $= S_5 \times F$ lb $\approx (S_1 m S_2 l S_3^{-2} t^{-2})$

$$\text{or} \qquad S_5 = \frac{S_1 S_2}{S_3^2} \qquad (9.38)$$

Resistance $= R$ ohms $= S_6 \times c$ lb-sec/in. $\approx (S_1 m S_3^{-1} t^{-1})$

$$\text{or} \qquad S_6 = \frac{S_1}{S_3} \qquad (9.39)$$

Capacitance $= C$ farads $= S_7 \times \frac{1}{k}$ in./lb $\approx (S_3^2 t^2 S_1^{-1} m^{-1})$

$$\text{or} \qquad S_7 = \frac{S_3^2}{S_1} \qquad (9.40)$$

Frequency $= \omega_e$ rad/sec $= S_8 \omega_m$ rad/sec $\approx (S_3^{-1} t^{-1})$

$$\text{or} \qquad S_8 = \frac{1}{S_3} \qquad (9.41)$$

The times t_e and t_m are the instants at which corresponding events occur in the two systems and are expressed for convenience in seconds.

It is by no means necessary, or even desirable, to make $t_e = t_m$. In general, mechanical systems tend to be massive and slow moving. To reproduce such a time constant in an electrical circuit would require impractical values for the circuit components. Usually, therefore, it will be found that S_3 is much less than unity, and the electrical system operates at many times the frequency of the mechanical system.

As an example of the application of scale factors, consider the simple mechanical oscillatory system shown in Fig. 9.8. The 4-ft rigid bar OA pivoted at O has a spring, dashpot, weight, and externally applied force spaced, respectively, at 1-ft intervals. The system is to execute small

$W=$10 lb $c=$1 lb sec/in.
$F_0 =$1 lb $\omega=$62.8 rad/sec
$k=$40 lb/in.
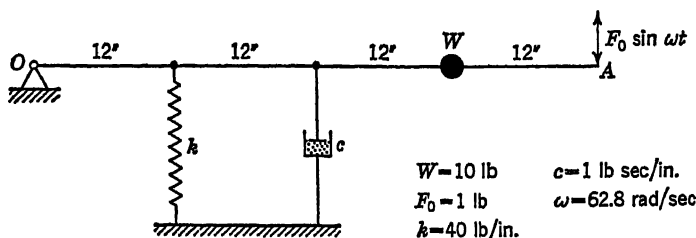
Fig. 9.8

oscillations about O. Considered as a rotational system, the weight W executes torsional oscillations about O under the influence of torques provided by the other units. Thus

$$I = \frac{W}{g}(36)^2 = \frac{10}{386} \times 1{,}296 \text{ lb-in.-sec}^2$$
$$k_t = k(12)^2 = 40 \times 144 \text{ in.-lb/rad} \qquad (9.42)$$
$$c_t = c(24)^2 = 1 \times 576 \text{ in.-lb-sec/rad}$$
$$T_0 = F_0(48) = 1 \times 48 \text{ in.-lb}$$

The equivalent torsional system may be represented, therefore, as shown in Fig. 9.3b, with subscripts t applied to k_t and c_t to distinguish them from the linear values. It should be noticed that the system of Fig. 9.3a is, similarly, the equivalent of Fig. 9.8. Equations (9.42) imply that if the weight W is moved down to a point 1 in. from O, it must be increased by a factor of $(36)^2$ to 1^2 to be equally effective. The same ratio applied to the effectiveness of the mass. This is one aspect of the term "effective mass" frequently found in connection with mechanical vibration problems.

Similarly, from Eqs. (9.42) it may be concluded that the "effective stiffness" of the system at the 1-in. location is k times the ratio $(12)^2:1^2$, the "effective damping coefficient" at the same location is c times the ratio $(24)^2:1^2$, and the "effective force" is F times the ratio $48:1$.

While the effective values at the 1-in. location were obtained directly

from the simple mathematics of Eqs. (9.42) there is a basic physical reason why they are obtained in terms of such ratios. To be equally effective in any position, each element of the system at any chosen point must do exactly the same amount of work for a given change in position of the bar OA as it would do in its original position with the same change in position of the bar. With this fundamental principle in mind, it is clear that the effective values of the various elements may be obtained at any position along the bar, and not solely at the 1-in. or 1-ft positions. To show that this approach does produce the equivalent values indicated in Eqs. (9.42), suppose the bar to move through a small angle $\Delta\theta$, with an average velocity $\dot\theta$ and an average acceleration $\ddot\theta$. The work done by F_0 is $F_0 \times 48\Delta\theta$, that by the spring is $\frac{1}{2}k(12\Delta\theta)^2$, that by the dashpot $c(24\dot\theta)(24\Delta\theta)$, that by the inertia force $m(36\ddot\theta)(36\Delta\theta)$. If an equivalent mass, dashpot, spring, and applied force were all concentrated at the 1-in. position and the bar executed the same motion as above in order to do the same amount of work, the values of the elements located at this point are found from

$$F_e \times 1 \times \Delta\theta = F_0 \times 48\Delta\theta$$
$$\tfrac{1}{2}k_e(1 \times \Delta\theta)^2 = \tfrac{1}{2}k(12\Delta\theta)^2$$
$$c_e(1 \times \dot\theta)(1 \times \Delta\theta) = c(24\dot\theta)(24 \times \Delta\theta) \qquad (9.43)$$
$$m_e(1 \times \ddot\theta)(1 \times \Delta\theta) = m(36\ddot\theta)(36 \times \Delta\theta)$$

or

$$F_e = \frac{48}{1}F_0 \qquad k_e = \frac{12^2}{1}k \qquad c_e = \frac{24^2}{1}c \qquad m_e = \frac{36^2}{1}m \qquad (9.44)$$

In Eqs. (9.43), instead of using the 1-in. location for concentrating all the elements, any other location could be used, the only criterion being that the values of the elements be scaled up by the ratios of the old locations to the new locations (measured from the pivot), either to the first power for applied forces or squared for elements which generate forces proportional to the movement of the bar. For example, the effective values of all elements at the original mass location (36 in. from pivot) would be

$$F_e = \tfrac{48}{36}F_0 \qquad k_e = (\tfrac{12}{36})^2k \qquad c_e = (\tfrac{24}{36})^2c \qquad m_e = (\tfrac{36}{36})^2m = m \qquad (9.45)$$

The principles involved in setting up equivalent simplified mechanical systems before proceeding with an analogy are important in analyzing complex geared systems. Hence, a rather detailed discussion of the basic problem has been given above.

Returning, now, to the development of the dynamical analogy, any one of the equation sets, Eqs. (9.42), (9.44), or (9.45), may be used to evaluate scale factors and values of elements in the equivalent electrical

circuit. Using, say, Eqs. (9.44), suppose the effective mass m_e to be represented by a 1-henry inductance. From Eq. (9.46) we find

$$1 = S_1 \frac{36^2}{1} \times \frac{10}{386} \quad \text{or} \quad S_1 = 0.0298 \tag{9.46}$$

Suppose the effective spring stiffness k_e to be represented by a 1-μf capacitance. Then, from Eq. (9.40), we find

$$10^{-6} = S_7 \times (\tfrac{1}{12})^2 \times \tfrac{1}{40} \quad S_7 = 0.00576 \tag{9.47}$$

Also, $\qquad\qquad\qquad S_8 = (S_1 S_7)^{\frac{1}{2}} = 0.0131 \tag{9.48}$

Equation (9.41) points out that the frequency ratio between the electrical and mechanical systems is

$$\frac{\omega_e}{\omega_m} = S_8 = \frac{1}{S_3} = \frac{1}{0.0131} = 76.3 \tag{9.49}$$

Thus, the electrical system will operate at frequencies which are 76.3 times as high as those of the mechanical system. Once the inductance and capacitance have been chosen, the time scale of the dynamical analogy becomes fixed. By reducing either the inductance or the capacitance by a factor of 4, the operating frequency of the analog would be doubled. In general, the operator has considerable latitude in the choice of time scales and other scale factors. In the present case, with $\omega_m = 62.8$ rad/sec, or $f_m = 10$ cps, the exciting frequency of the electrical circuit would be $f_e = 763$ cps.

Fixing the inductance and capacitance also fixes the scale factor on the damping coefficient. From Eq. (9.39), we find

$$S_6 = \frac{0.0298}{0.0131} = 2.27 \quad \text{or} \quad R = 2.27 \times \frac{24^2}{1} = 1{,}310 \text{ ohms} \tag{9.50}$$

One more arbitrary choice of scale factor is left. Either S_4 or S_5 may be chosen to suit one's convenience. Suppose a 12-volt (peak value) source is chosen to represent F_e. Then, from Eq. (9.38),

$$12 = S_5 \times \tfrac{48}{1} \times 1 \quad S_5 = \tfrac{12}{48} = 0.25 \tag{9.51}$$

from which

$$S_2 = \frac{S_3^2 S_5}{S_1} = S_5 S_7 = 0.00144 \tag{9.52}$$

From Eq. (9.37), we have

$$S_4 = \frac{S_2}{S_3} = \frac{0.00144}{0.0131} = 0.11 \tag{9.53}$$

so that a velocity v_e of 1 in./sec is represented by a current of 0.11 amp. A displacement x_e of 0.01 in. produces a force of

$$0.01 \times 144 \times 40 = 57.6 \text{ lb}$$

in the spring k_e. Consequently, the voltage appearing across C, which would be a measure of the displacement, would be $57.6 \times S_b = 14.4$ volts.

9.4. Multi-degree-of-freedom Lumped Systems.

A lumped system consists of concentrated masses connected by weightless springs and dashpots. There is a separate equation of equilibrium for each junction (node) of such a system, and consequently its dynamical analogy will
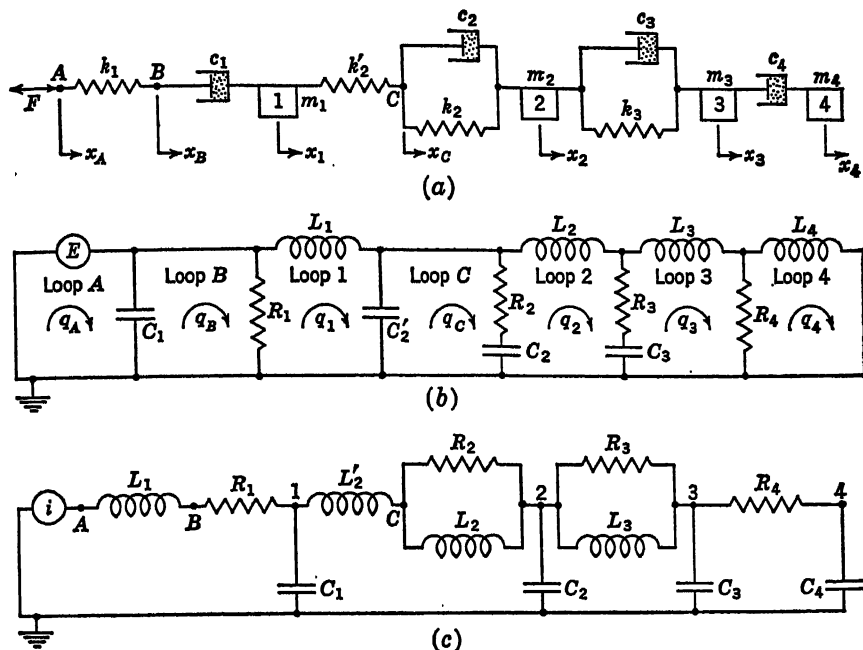
Fig. 9.9

have as many loops (mass-inductance analogy) or nodes (mass-capacitance analogy) as there are junctions. For example, consider the lumped system of Fig. 9.9. A force F excites the system through a spring k_1 and a dashpot c_1. The masses m_1 through m_4 are interconnected through an array of weightless springs and dashpots. Each mass is a junction (or node) in the mechanical circuit. In addition, points A, B, and C are also points for which equations of equilibrium must be written and consequently are nodes of the system. Thus, seven equations are involved. The mass-inductance analogy will contain seven loops, the mass-capacitance analogy seven nodes.

The equations of equilibrium for Fig. 9.9a are

Node A $F - k_1(x_A - x_B) = 0$ (9.54)

Node B $k_1(x_A - x_B) - c_1(\dot{x}_B - \dot{x}_1) = 0$ (9.55)

Node 1 $c_1(\dot{x}_B - \dot{x}_1) - m_1\ddot{x}_1 - k_2'(x_1 - x_C) = 0$ (9.56)

Node C $k_2'(x_1 - x_C) - k_2(x_C - x_2) - c_2(\dot{x}_C - \dot{x}_2) = 0$ (9.57)

Node 2 $k_2(x_C - x_2) + c_2(\dot{x}_C - \dot{x}_2) - m_2\ddot{x}_2 - k_3(x_2 - x_3)$
$$- c_3(\dot{x}_2 - \dot{x}_3) = 0 \quad (9.58)$$

Node 3 $k_3(x_2 - x_3) + c_3(\dot{x}_2 - \dot{x}_3) - m_3\ddot{x}_3 - c_4(\dot{x}_3 - \dot{x}_4) = 0$ (9.59)

Node 4 $c_4(\dot{x}_3 - \dot{x}_4) - m_4\ddot{x}_4 = 0$ (9.60)

The corresponding loops of the mass-inductance analogy for Eqs. (9.54) to (9.60) are shown in Fig. 9.9b.

The common branch of each pair of adjacent loops always contains the electrical counterparts of the mechanical elements which connect corresponding pairs of nodes. This is clearly seen on the basis of force considerations. The force F acts through spring k_1 and is consequently represented by a voltage E across capacitance C_1. The force in k_1 acts through the dashpot c_1. Hence, the voltage existing across C_1 must be impressed across R_1. The force in c_1 acts on m_1 and k_2'. Therefore, the voltage across R_1 must be impressed across inductance L_1 and capacitance C_2' in series. The force in k_2' acts through k_2 and c_2, whence the voltage across C_2' must be impressed across C_2 and R_2 in series. The sum of the forces in k_2 and c_2 acts on m_2, spring k_3, and dashpot c_3. Hence, the voltage across the C_2R_2 branch must be impressed across L_2, C_3, and R_3 in series. The sum of the forces in k_3 and c_3 acts on m_3 and c_4. The voltage across C_3 and R_3 must be impressed, therefore, across L_3 and R_4 in series. Finally, the force in dashpot c_4 acts on m_4, and in the electrical circuit the voltage across R_4 must be impressed across L_4. This completes the electrical analogy as shown in Fig. 9.9b.

The mass-capacitance analogy for the same mechanical system is shown in Fig. 9.9c. The nodes in (c) are labeled to correspond with the nodes in (a). The current-equilibrium relations at each node of (c) are identical with the force-equilibrium equations at each node in (a). The similarity in appearance of circuits (a) and (c) is very striking.

Branched mechanical systems are common in engineering practice. A branched system is shown in Fig. 9.10a. Its mass-inductance and mass-capacitance analogies are easily obtained by the methods already outlined, and are shown in (b) and (c) of Fig. 9.10. The automobile torque converter is an example of a branched system for which practical equivalent circuits have been developed.[11]

Geared torsional systems in which shaft speeds are geared up or down in going from one end of the system to the other are usually first reduced to an equivalent single speed system, and then the latter system is studied either analytically or by analogies. A geared and branched system is shown schematically in Fig. 9.11a. Prime movers, having moments of inertia I_1 and I_2, drive pinions of inertia I_p through connecting shafts of stiffnesses k_1 and k_2. The pinions mesh with larger gears of inertia

I_3 and I_4. The rotational speed of I_3 is $1/n_1$ that of its pinion, and the rotational speed of I_4 is $1/n_2$ that of its pinion. Shafts of stiffnesses k_3 and k_4 drive gears I_5 and I_6 through which a further reduction in rotational speed occurs to a common gear of inertia I_7. The speed of I_7 is
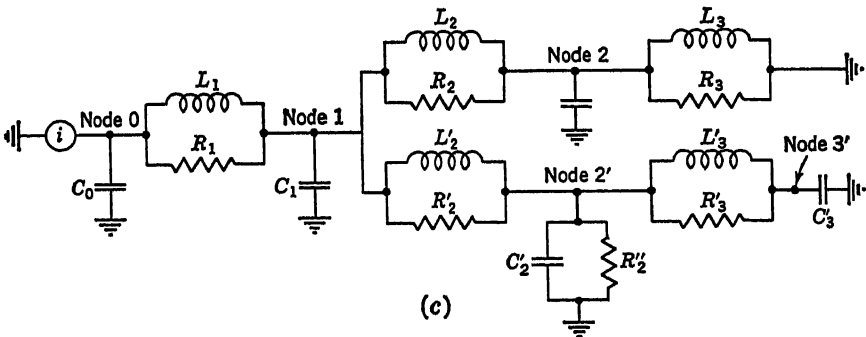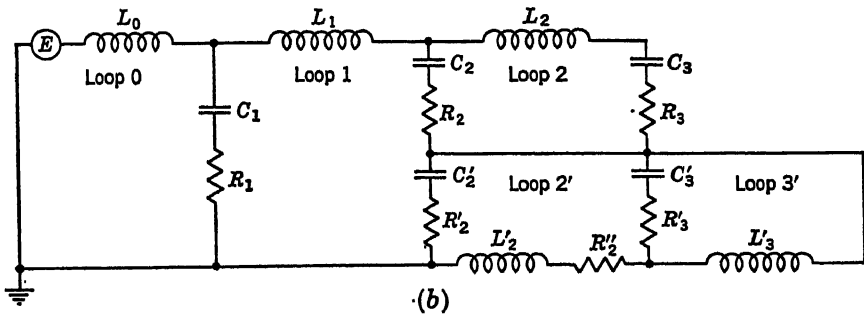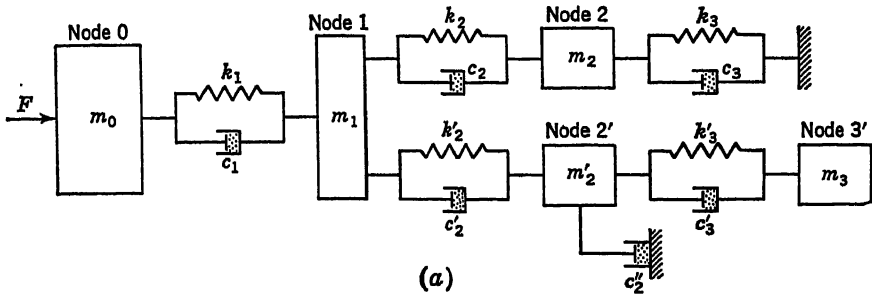
Fig. 9.10

$1/n_5$ that of I_5 and is $1/n_6$ that of I_6. The shaft of stiffness k_5 finally drives a load-absorbing device having the mass moment of inertia I_8.

Bearing in mind the principle set forth in converting Fig. 9.8 to its equivalent shown in Fig. 9.3a, a conversion on the same basis may be made from (a) of Fig. 9.11 to the simpler *constant-speed* system in (b) in which all gears have been eliminated. The system (b) may be designed

to operate at any speed. Usually the reference speed is taken to be that of the prime mover or that of the load-absorbing device. Suppose that in this case the system (b) is to operate at the speed of inertia I_8. Thus, I_8 and k_5 will be the same in both (a) and (b). I_9 is composed of I_7 and the lower speed equivalents of I_5 and I_6. The moment of inertia
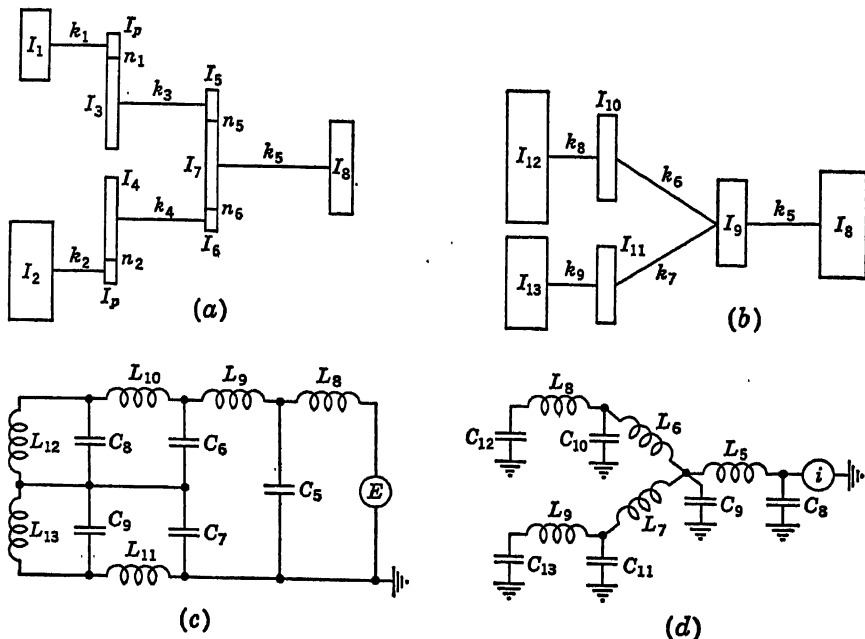
Fig. 9.11

must be increased by the square of the speed ratio. Thus

$$I_9 = I_7 + n_5{}^2I_5 + n_6{}^2I_6 \tag{9.61}$$

Similarly, shaft stiffnesses must be increased by the same factor. Thus

$$k_6 = n_5{}^2k_3 \qquad k_7 = n_6{}^2k_4 \tag{9.62}$$

The remaining equivalents are

$$I_{10} = n_5{}^2I_3 + n_1{}^2n_5{}^2I_p \qquad I_{11} = n_6{}^2I_4 + n_2{}^2n_6{}^2I_p \tag{9.63}$$
$$k_8 = n_1{}^2n_5{}^2k_1 \qquad k_9 = n_2{}^2n_6{}^2k_2 \tag{9.64}$$
$$I_{12} = n_1{}^2n_5{}^2I_1 \qquad I_{13} = n_2{}^2n_6{}^2I_2 \tag{9.65}$$

We have in Fig. 9.11b a branched system similar to that already treated in Fig. 9.10, but without damping. The mass-inductance and mass-capacitance analogies are shown in (c) and (d), respectively, in Fig. 9.11, with excitation being produced at I_8.

Voltage measurements made in tests on the mass-inductance analog

(c) may be interpreted as follows: A reading across capacitor C_8, for example, gives the torque in shaft k_8 of the equivalent system (b). But this is the torque with k_8 operating at the reduced speed. The torque really desired is that in shaft k_1. This is obtained by dividing the torque in k_8 by the over-all speed ratio $n_1 n_5$. That the speed ratio only, and not the square of that ratio, is involved may be seen from the fact that the quantity of work done by a shaft per unit of time depends on the product of torque into speed for that shaft. Thus, if the speed is increased by a factor $n_1 n_5$, then the torque must be reduced by the same factor in order to keep the work unchanged.
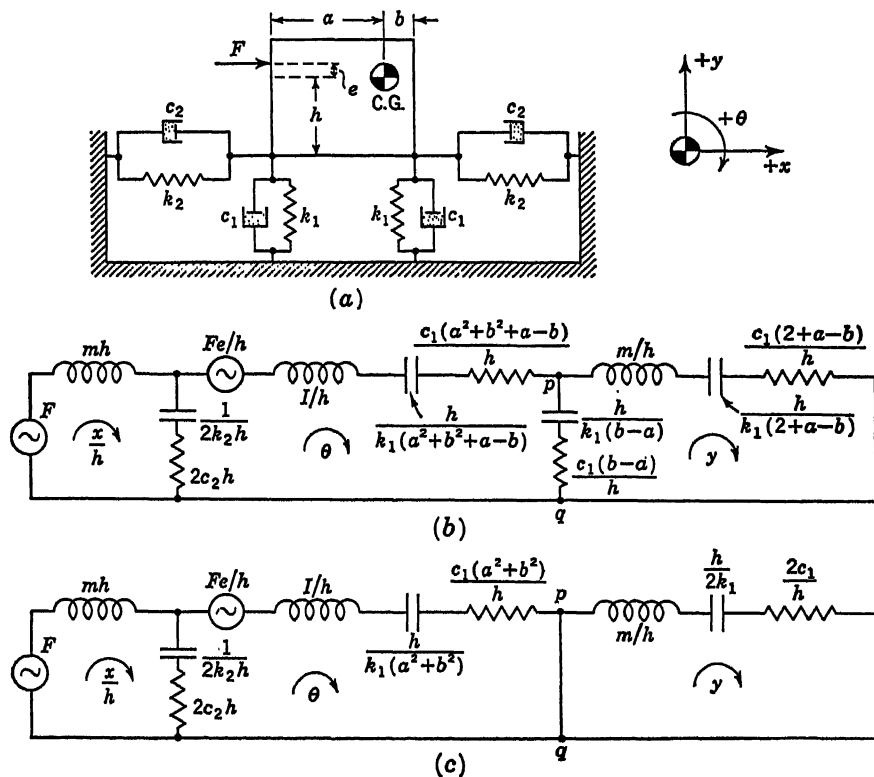
Fig. 9.12

9.5. Coupled Translation and Rotation.

The rigid bodies considered in the mechanical systems to this point were permitted only translational or only rotational motions. In many of the most common mechanical systems rigid bodies are subject to combined translation and rotation. Figure 9.12a illustrates one example of such a coupled system.

It shows a machine flexibly mounted in order to reduce transmission of force F to the supporting structure. The machine is subject to translations in the x and y directions and rocking (rotation) in the xy plane, the three motions being coupled together by the springs and dashpots, so that all exist simultaneously. The system thus has three degrees of freedom.

The coupling effects are easily observed in the equations of dynamic equilibrium for the system. Suppose the center of gravity of the machine to be subjected to a small displacement in each of its degrees of freedom, namely, x to the right, y upward, and θ clockwise. The forces and moments which must act on the center of gravity to maintain this displaced position are equal and opposite to the restoring forces and moments exerted by the springs. If, in addition, the center of gravity is also subjected to the velocities instantaneously given by $\dot{x}$, $\dot{y}$, and $\dot{\theta}$, additional forces and moments would be required to overcome the viscous drag effects of the dashpots paralleling the springs.

The additional forces acting on the spring-mounted machine consist of the force F along the x direction and the associated moment Fe, and the inertia forces of the center of gravity. The equations of equilibrium for this system may therefore be written:

$$-F + m\ddot{x} + 2k_2 x + 2c_2 \dot{x} - 2k_2 h\theta - 2c_2 h\dot{\theta} = 0 \qquad (9.66)$$

$$m\ddot{y} + 2k_1 y + 2c_1 \dot{y} - k_1(b-a)\theta - c_1(b-a)\dot{\theta} = 0 \qquad (9.67)$$

$$-Fe + I\ddot{\theta} - 2k_2 hx - 2c_2 h\dot{x} - k_1(b-a)y - c_1(b-a)\dot{y} + 2k_2 h^2\theta$$
$$+ 2c_2 h^2\dot{\theta} + k_1(a^2 + b^2)\theta + c_1(a^2 + b^2)\dot{\theta} = 0 \quad (9.68)$$

Adding $k_1(b-a)y - k_1(b-a)y + c_1(b-a)\dot{y} - c_1(b-a)\dot{y}$ to Eq. (9.67) and $k_1(b-a)\theta - k_1(b-a)\theta + c_1(b-a)\dot{\theta} - c_1(b-a)\dot{\theta}$ to Eq. (9.68), and rearranging terms in all three equations, the following equivalent forms appear:

$$-F + mh\frac{\ddot{x}}{h} + 2k_2 h\left(\frac{x}{h} - \theta\right) + 2c_2 h\left(\frac{\dot{x}}{h} - \dot{\theta}\right) = 0 \qquad (9.69)$$

$$m\frac{\ddot{y}}{h} + k_1\frac{2+a-b}{h}y + c_1\frac{2+a-b}{h}\dot{y} + k_1\frac{b-a}{h}(y-\theta)$$
$$+ c_1\frac{b-a}{h}(\dot{y}-\theta) = 0 \quad (9.70)$$

$$-\frac{Fe}{h} + \frac{I}{h}\ddot{\theta} + 2k_2 h\left(\theta - \frac{x}{h}\right) + 2c_2 h\left(\theta - \frac{\dot{x}}{h}\right) + k_1\frac{b-a}{h}(\theta - y)$$
$$+ c_1\frac{b-a}{h}(\theta - \dot{y}) + k_1\frac{a^2 + b^2 + a - b}{h}\theta$$
$$+ c_1\frac{a^2 + b^2 + a - b}{h}\dot{\theta} = 0 \quad (9.71)$$

Equations (9.69) and (9.71) show the coupling existing between x and θ through the $(x/h - \theta)$ and $(\dot{x}/h - \dot{\theta})$ terms, which are of identical magnitudes but of opposite signs in the two equations. Similarly, Eqs. (9.70) and (9.71) show the coupling existing between y and θ through the $(y - \theta)$ and $(\dot{y} - \dot{\theta})$ terms, which are also of identical magnitudes but of opposite signs.

The mass-inductance analogy for Eqs. (9.69) to (9.71) is shown in Fig. 9.12b, the coupling elements being condensers (springs) and resistors (dashpots). The charges circulating in the three loops of this network represent x/h, θ, and y, respectively.

If the springs are so mounted that $a = b$, that is, the center of gravity is halfway between the points of attachment of the springs and dashpots at the base, all the $(a - b)$ terms become zero and the y motion becomes uncoupled from the x and θ motions. The capacitance in the branch pq of Fig. 9.12b becomes infinite (a short circuit) and the resistance in that line becomes zero. The dynamical analogy then appears as in Fig. 9.12c. The y loop is shorted across its points of connection to the θ loop and consequently cannot be excited by any currents in the θ loop. A horizontal force F could not excite vertical motion in the mechanical system under such circumstances, even though it does excite rocking motion.

As the distance h becomes smaller (i.e., the center of gravity approaches alignment with the supports), the coupling between the rocking and horizontal motions should diminish, while that between the rocking and vertical motions remains unchanged. That this does happen is clear from Fig. 9.12b, for the impedances in the x/h loop are decreasing toward zero, while those in the θ and y loops are correspondingly increasing toward infinity.

With h equal to zero, the electrical elements in this circuit acquire impractical values. For this special case (represented by Fig. 9.13a), the horizontal motions are completely uncoupled from the vertical motions and need not be considered in dealing with the coupled vertical motion and rotation. This case has been generalized below by making the supporting springs unequal in stiffness. The dashpots also have unequal coefficients.

With y and θ as the vertical and rotational movements of the center of gravity, the equations for Fig. 9.13a are obtained as were those for Fig. 9.12a. Thus

$$-F + m\ddot{y} + (k_1 + k_2)y + (c_1 + c_2)\dot{y} + (k_1a - k_2b)\theta$$
$$+ (c_1a - c_2b)\dot{\theta} = 0 \quad (9.72)$$
$$-Fe + I\ddot{\theta} + (k_1a - k_2b)y + (c_1a - c_2b)\dot{y} + (k_1a^2 + k_2b^2)\theta$$
$$+ (c_1a^2 + c_2b^2)\dot{\theta} = 0 \quad (9.73)$$

The translational and rotational motions of the center of gravity may be
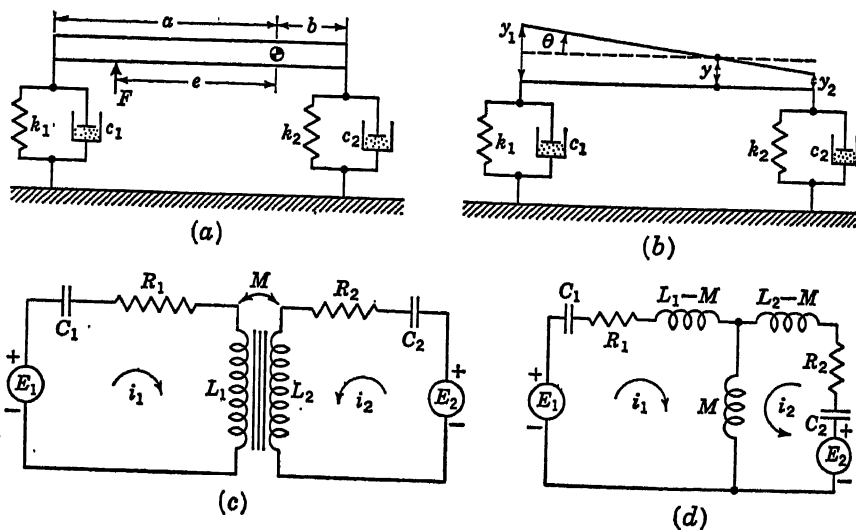
Fig. 9.13

expressed more conveniently in terms of the translational motions of the points of attachment of the supporting springs and dashpots. Thus, referring to Fig. 9.13b,

$$y = y_1 - \frac{a}{a+b}(y_1 - y_2) = \frac{by_1 + ay_2}{a+b} \tag{9.74}$$

$$\dot{y} = \dot{y}_1 - \frac{a}{a+b}(\dot{y}_1 - \dot{y}_2) = \frac{b\dot{y}_1 + a\dot{y}_2}{a+b} \tag{9.75}$$

$$\ddot{y} = \ddot{y}_1 - \frac{a}{a+b}(\ddot{y}_1 - \ddot{y}_2) = \frac{b\ddot{y}_1 + a\ddot{y}_2}{a+b} \tag{9.76}$$

$$\theta = \frac{y_1 - y_2}{a+b} \tag{9.77}$$

$$\dot{\theta} = \frac{\dot{y}_1 - \dot{y}_2}{a+b} \tag{9.78}$$

$$\ddot{\theta} = \frac{\ddot{y}_1 - \ddot{y}_2}{a+b} \tag{9.79}$$

Substituting these relations into Eqs. (9.72) and (9.73), the following results are obtained:

$$-F + \frac{mb}{a+b}\ddot{y}_1 + \frac{ma}{a+b}\ddot{y}_2 + k_1y_1 + k_2y_2 + c_1\dot{y}_1 + c_2\dot{y}_2 = 0 \tag{9.80}$$

$$-Fe + \frac{I}{a+b}(\ddot{y}_1 - \ddot{y}_2) + k_1ay_1 - k_2by_2 + c_1a\dot{y}_1 - c_2b\dot{y}_2 = 0 \tag{9.81}$$

If Eqs. (9.80) and (9.81) are considered as the equations for charge in electrical loops, they show the presence of inductive coupling ($\ddot{y}_1$ and

$\ddot{y}_2$ terms), resistive coupling ($\dot{y}_1$ and $\dot{y}_2$ terms), and capacitive coupling (y_1 and y_2 terms) between the loops. It is possible to eliminate the capacitive-resistive coupling terms, obtaining a pair of equations which are coupled inductively only. Thus, if Eq. (9.80) is multiplied by b and then added to Eq. (7.81), the y_2 and $\dot{y}_2$ terms will not be present in the resulting equation. Similarly, if Eq. (9.80) is multiplied by a and then Eq. (9.81) subtracted from it, the y_1 and $\dot{y}_1$ terms will not be present in the resulting equation. The only terms common to both equations are now the $\ddot{y}_1$ and $\ddot{y}_2$ terms. These equations are

$$-F(b+e) + \frac{mb^2+I}{a+b}\ddot{y}_1 + \frac{mab-I}{a+b}\ddot{y}_2 + k_1(a+b)y_1$$
$$+ c_1(a+b)\dot{y}_1 = 0 \quad (9.82)$$

$$-F(a-e) + \frac{ma^2+I}{a+b}\ddot{y}_2 + \frac{mab-I}{a+b}\ddot{y}_1 + k_2(a+b)y_2$$
$$+ c_2(a+b)\dot{y}_2 = 0 \quad (9.83)$$

The equivalent electrical circuit representing the mass-inductance analogy for this case is shown in Fig. 9.13c. The equations for the voltage drops across each loop are[12]

$$-E_1 + \frac{1}{C_1}\int_0^t i_1\,dt + R_1 i_1 + L_1\frac{di_1}{dt} + M\frac{di_2}{dt} = 0 \quad (9.84)$$

$$-E_2 + \frac{1}{C_2}\int_0^t i_2\,dt + R_2 i_2 + L_2\frac{di_2}{dt} + M\frac{di_1}{dt} = 0 \quad (9.85)$$

Thus if the electrical elements are chosen so that

$$E_1 = F(b+e) \qquad \frac{1}{C_1} = k_1(a+b)$$

$$E_2 = F(a-e) \qquad \frac{1}{C_2} = k_2(a+b)$$

$$L_1 = \frac{mb^2+I}{a+b} \qquad R_1 = c_1(a+b) \qquad (9.86)$$

$$L_2 = \frac{ma^2+I}{a+b} \qquad R_2 = c_2(a+b)$$

$$M = \frac{mab-I}{a+b} \qquad i_1 = \frac{dy_1}{dt}$$

$$i_2 = \frac{dy_2}{dt}$$

Eqs. (9.84) and (9.85) will be identical with Eqs. (9.92) and (9.83). The positive directions of the currents in the loops are shown in Fig. 9.13c. The positive current i_1 flows clockwise, while positive i_2 flows counterclockwise. These directions were chosen in order to make the

back emf generated by the mutual inductance between loops act in the same direction as the back emfs of the other elements.[13]

A transformer having self-inductances and mutual inductances may be replaced by an equivalent T network[14] consisting of three self-inductances of magnitudes $L_1 - M$, $L_2 - M$, and M, respectively, the last one forming the leg of the T. Thus, if the equivalent circuit for the transformer is now used to replace the actual transformer in Fig. 9.13c, the circuit of Fig. 9.13d will result. The effect of mutual inductance on both loops is more easily visualized in this equivalent circuit.
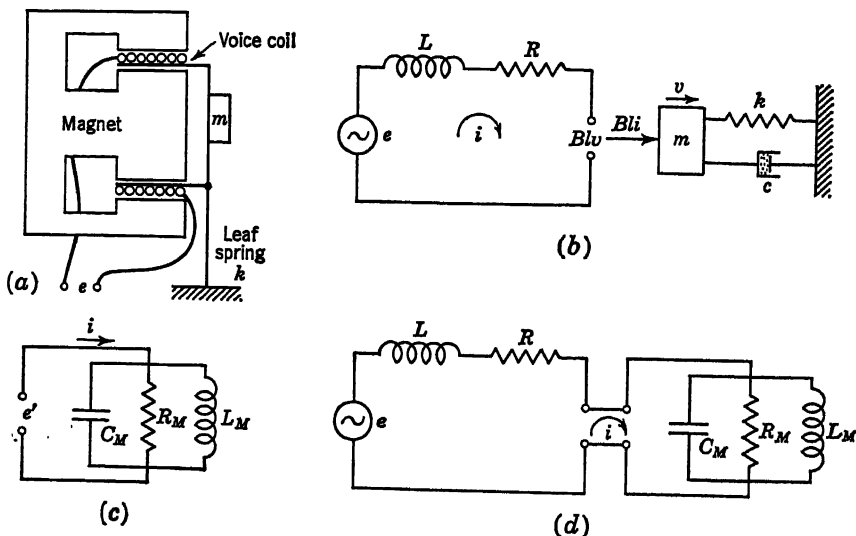
Fig. 9.14

Transformers may be wound on iron cores to predetermined values of L_1, L_2, and M.[15] The coupling factor between coils L_1 and L_2 may be adjusted from nearly zero to nearly 100 per cent. With complete coupling, the mutual inductance will have its maximum value given by $M = (L_1 L_2)^{\frac{1}{2}}$.

9.6. Dynamical Analogies for Electromechanical Systems.

Detailed studies of the dynamical properties of systems consisting of combined electrical and mechanical elements may be made on analogous all-electric systems. Included in such electromechanical systems are electromechanical transducers,[16] positioning servomechanisms,[17,18] voltage regulators,[19] speed regulators,[20] and interconnected synchronous motors and generators.[21,22]

Consider, as a first example, a transducer of the type shown in Fig. 9.14a. If a voltage e is impressed across the voice coil placed in the narrow gap between the magnet pole pieces, a current i will flow through

the coil and a force F will be exerted on it. The force is given by Bli, where B is the strength of the magnetic field and l the total length of wire.[23] The force F serves to accelerate the total mass m of the mechanical system and to counteract the spring force and dissipative forces. On the other hand, if an external force is exerted on m, causing the voice coil to attain a velocity v across the magnetic field, a voltage will be induced within the coil, given by Blv. The system acts as a loudspeaker, or force generator, in the former case, and as a velocity pickup, or electrodynamic microphone, in the latter case. Considered as a force generator (loudspeaker), Fig. 9.14a will be governed by the following set of differential equations:

$$e - L\frac{di}{dt} - Ri - Bl\dot{x} = 0 \tag{9.87}$$

$$-Bli + m\dot{v} + cv + k\int_0^t v\,dt = 0 \tag{9.88}$$

where L is the self-inductance of the voice coil and R its resistance. Figure 9.14b shows the electrical exciting circuit and the excited mechanical system. The fact that the force in the mechanical system is coupled to current in the electrical system and that voltage in the electrical system is coupled to velocity in the mechanical system inexorably leads to the force-current mass-capacitance analogy for this electromechanical system.[24] The equivalent circuit for the mechanical system is thus shown in (c). If the electrical circuit of (b) is to be joined to the analog circuit (c), then the voltages Blv and e' must match. Thus, in Eq. (9.88), v is replaced by e'/Bl, yielding,

$$-Bli + \frac{m}{Bl}\frac{de'}{dt} + \frac{c}{Bl}e' + \frac{k}{Bl}\int_0^t e'\,dt = 0 \tag{9.89}$$

Similarly, the current i in circuit (b) must also be the current i in the parallel network of (c). Thus, Eq. (9.89) will now become

$$-i + \frac{m}{(Bl)^2}\frac{de'}{dt} + \frac{c}{(Bl)^2}e' + \frac{k}{(Bl)^2}\int_0^t e'\,dt = 0 \tag{9.90}$$

Thus if we put

$$C_M = \frac{m}{(Bl)^2} \qquad R_M = \frac{(Bl)^2}{c} \qquad L_M = \frac{(Bl)^2}{k} \tag{9.91}$$

the e' and the i of the network (c), which represents the mechanical system, are equal to the Blv and the i in the electrical part of (b). Consequently, the two may be joined to form the complete analogy shown in (d).

Thus, for electromagnetic coupling between electrical and mechanical systems (illustrated by the speaker of Fig. 9.14a), the "electromagnetic analogy" (force-current, mass-capacitance) must be used.

Additional factors which may be included in the equivalent circuits of Fig. 9.14 are the inertia effects of the air outside the unit and inside the cavity, the elasticity of the air in the cavity, the resistance to airflow through the slot around the voice coil, the radiation of acoustical energy into the surrounding air, other masses, springs, or dissipative elements in the mechanical system, and other auxiliary circuits which may be made a part of the voice-coil electrical circuit. Thus, equivalent circuits of high complexity to account for many electrical, mechanical, and acoustical properties combined in any given real system may be developed and
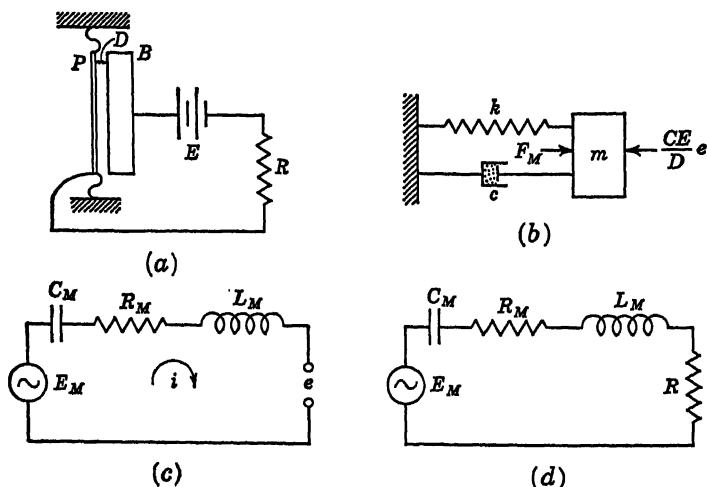
Fig. 9.15

studied in a purely electrical form. Jones[25] describes the development of improved telephone transmitter and receiver units with the aid of equivalent circuits for these units. The analogies provided a means for predicting their response characteristics and for evaluating interactions between elements. It is pointed out, also, that the analogy was useful in tracing causes of variations in transmitter performance observed during manufacture.

Equivalent circuits for acoustical systems are considered in more detail in Sec. 9.7.

Consider, now, the case of electrostatic coupling (Fig. 9.15a), represented by the case of a condenser microphone. If a flexible plate P is spaced a distance D from a charged stationary plate B, the capacitance of the air capacitor so formed is[28]

$$C = \frac{A \epsilon_0}{4\pi D} \tag{9.92}$$

where A is the area of one side of one plate and ϵ_0 is the permittivity of air.

If, as the result of an externally applied mechanical force F acting on P, the plate moves with a velocity v, a current of magnitude

$$i = \frac{CE}{D} v \qquad (9.93)$$

will flow through the capacitor. The voltage across the capacitor will differ from the impressed value by the amount e, where e is related to F through

$$F = \frac{CE}{D} e \qquad (9.94)$$

Equations (9.93) and (9.94) clearly demonstrate the analogy between current and velocity, force and voltage, so that an equivalent circuit which is to represent the mechanical properties of the diaphragm (force, mass, elasticity, and damping) in combination with the electrical properties of the attached circuit must necessarily be based on the mass-inductance ("electrostatic") analogy.[24]

The equation for the diaphragm motion is (see Fig. 9.15b)

$$F_M - \frac{CE}{D} e - k \int_0^t v\, dt - cv - m \frac{dv}{dt} = 0 \qquad (9.95)$$

Replacing v by iD/CE, dividing through by CE/D, and letting $\phi = D/CE$, Eq. (9.95) becomes

$$\phi F_M - e - k\phi^2 \int_0^t i\, dt - c\phi^2 i - m\phi^2 \frac{di}{dt} = 0 \qquad (9.96)$$

The equivalent circuit for the mechanical system is shown in (c), in which

$$E_M = \phi F_M \qquad C_M = \frac{1}{k\phi^2} \qquad R_M = c\phi^2 \qquad L_M = m\phi^2 \qquad (9.97)$$

The voltage e shown as the output voltage of this circuit is the output of the condenser microphone and is impressed on whatever circuit is used with the microphone. If a resistive load alone is used, as in (a), the equivalent circuit of the combined electromechanical system will be that shown in (d). The voltage source E does not appear in the equivalent circuit because it serves merely as the charging device which makes the condenser microphone operate as a source of the voltage e and the current i.

Another important electromechanical system to be considered from the standpoint of a dynamical analogy is the positioning servomechanism. As shown in Fig. 9.16a, a positioning motor M is supposed to follow the movements of a shaft θ_0, so that regardless of how θ_0 may rotate or oscillate, θ_1 will correspondingly rotate or oscillate in an effort to keep the difference $\theta_1 - \theta_0$ as nearly zero as possible. To accomplish this, an error detector ϵ measures the difference in angular position of θ_1 and θ_0 and

converts this difference to a voltage, which is then amplified and impressed on the field winding F of a constant-speed generator. Either one field winding or the other is energized, depending on the sign of $\theta_1 - \theta_0$. A voltage of the proper sign is then generated by G in order to drive motor M in the direction to reduce $\theta_1 - \theta_0$ toward zero. A separately excited d-c field is applied to the motor. Kirchhoff's second law applied to the
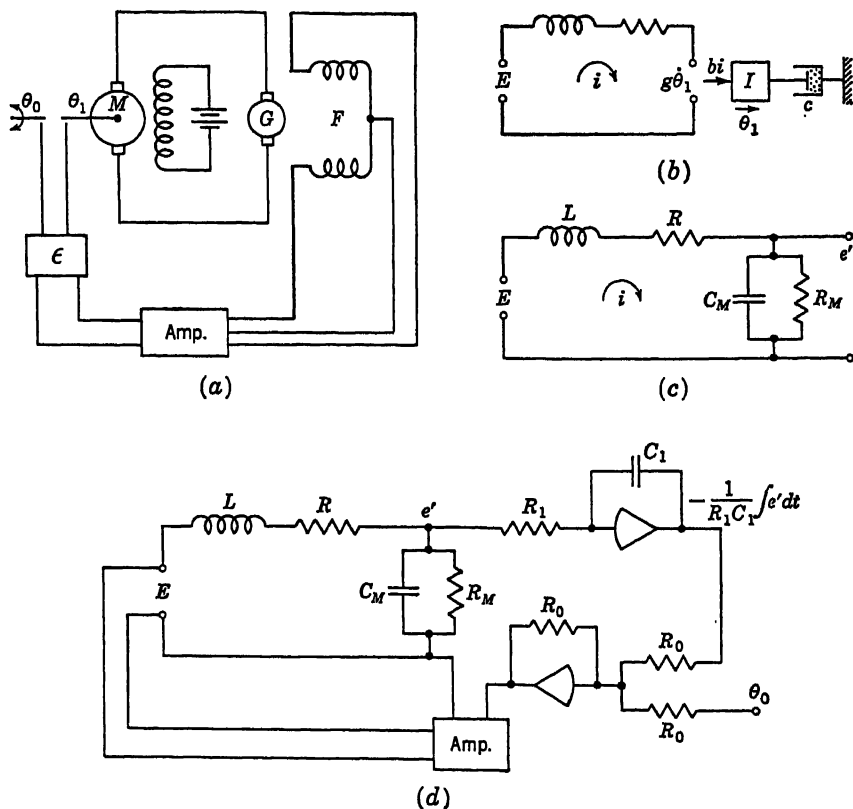
Fig. 9.16

armature circuit of the motor-generator set yields

$$E = L \frac{di}{dt} + Ri + g \frac{d\theta_1}{dt} \tag{9.98}$$

where E = output voltage of generator

    L = armature circuit inductance

    R = armature circuit resistance

    g = back emf developed in motor, volts per rad/sec

    i = armature current

A torque directly proportional to armature current will be developed by the motor. This will be used to overcome armature mechanical inertia and frictional resistance. The torque equation will be, therefore,

$$T = bi = I \frac{d^2\theta_1}{dt^2} + c \frac{d\theta_1}{dt} \tag{9.99}$$

where b = motor constant (torque per unit of armature current)

I = mass moment of inertia of the motor rotor

c = viscous damping coefficient of motor

The generator voltage output is taken proportional to the error $\theta_1 - \theta_0$:

$$E = K(\theta_1 - \theta_0) \tag{9.100}$$

As far as Eqs. (9.98) and (9.99) are concerned, we have almost exactly the same situation as in the case of the loudspeaker given by Eqs. (9.87) and (9.88). The only difference is the absence of an elastic force in the torque equation. The coupling is electromagnetic, and so the mass-capacitance analogy will be used. In Fig. 9.16b the armature circuit and the mechanical circuit represented by Eqs. (9.98) and (9.99) are shown. By setting $e' = g\theta_1$, Eq. (9.99) becomes

$$i = \frac{I}{bg} \frac{de'}{dt} + \frac{c}{bg} e' \tag{9.101}$$

Thus, the combined circuit for Eqs. (9.98) and (9.101) becomes that in (c), with

$$C_M = \frac{I}{bg} \qquad R_M = \frac{bg}{c} \tag{9.102}$$

The input voltage E is developed by an amplifier in proportion to the difference between θ_1 and θ_0. Since in the proposed analogy $\theta = e'/g$, we must have

$$\theta_1 = \frac{1}{g} \int_0^t e' \, dt \tag{9.103}$$

The voltage corresponding to θ_0 enters from an external source which reproduces the variations of θ_0. By applying e' to an integrating amplifier of time constant g, θ_1 will be produced. This may be subtracted from θ_0 in a summing amplifier and the result applied to the servo amplifier, which will then supply the voltage E in Eq. (9.100) to the circuit. The complete circuit is shown in Fig. 9.16d.

9.7. Lumped Acoustical Systems. A typical element of a lumped acoustical system is shown in Fig. 9.17. It is a Helmholtz resonator[26] in which the volume of fluid V (usually air) acts as a spring and the slug of fluid in the neck l acts as an inertia. Dissipation of energy (dashpot loss)

is due to frictional resistance in the neck and at the edges and is also due to the radiation of acoustical energy from the open end of l. Often the neck is packed with porous material to increase frictional damping.

The dimensions of the resonator are small compared with the wavelength of the sound exciting it. The fluid in l is, therefore, considered to act like a rigid piston in a wall represented by the surface of the container V. It can be shown (see p. 193 of Ref. 26) that for a rigid piston of radius a oscillating at low frequency (long wavelength) in a wall of infinite extent, the effect of the fluid on either side of the piston is to increase, effectively, the mass of the piston by the amount $8\rho a^3/3$, where ρ = mass density of the air. This is equivalent to adding to the length l an end correction $\Delta l = 8a/3\pi$, so that the effective length of the oscillating slug of fluid is $l + 2\Delta l$. Since the resonator is often mounted in a surface which is not large enough to behave like an infinite baffle, the actual end correction is likely to be 10 to 15 per cent less than the above value.
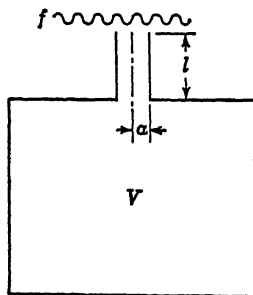
Fig. 9.17

By analogy with the rigid piston, the rate at which acoustic energy is radiated from the open end of l is $\frac{1}{2}\pi\rho a^4\omega^2 v/s$, where s is the velocity of sound in the given fluid and v the instantaneous piston velocity.

If the slug of fluid in l is displaced downward a distance x, V will change by the amount $\pi a^2 x$, and the pressure inside the resonator will increase by the amount $p = K\pi a^2 x/V$, where K is the adiabatic bulk modulus of the fluid (that is, K is the constant of proportionality relating pressure to volume strain). For a fluid, the sound velocity is given by $(K/\rho)^{\frac{1}{2}}$. Hence, for the displacement x, the restoring force acting on the slug of fluid is $p\pi a^2$, or $\rho s^2\pi^2 a^4 x/V$. The effective spring stiffness of the resonator volume (force per unit displacement of the fluid slug) is $\rho s^2\pi^2 a^4/V$.

In the expression for energy radiated, $v = \dot{x}$. Hence the damping coefficient for the resonator is $\frac{1}{2}\pi\rho a^4\omega^2/s$.

Excitation is provided by means of a sound wave impinging on the resonator. For an acoustic pressure $F \sin \omega t$ in the exciting wave, the force on the fluid slug is $\pi a^2 F \sin \omega t$. The equation of motion of the system of Fig. 9.17 is, therefore,

$$\left[\left(l + \frac{16a}{3\pi}\right)\pi a^2\rho\right]\ddot{x} + \left(R_d + \frac{\pi\rho a^4\omega^2}{2s}\right)\dot{x} + \left(\frac{\pi^2\rho a^4 s^2}{V}\right)x$$
$$= \pi a^2 F \sin \omega t \quad (9.104)$$

The damping term in this equation includes both the friction loss (R_d) and the radiation loss.

The equivalent mechanical and electrical circuits for Eq. (9.104) are

those shown in Fig. 9.3. The correspondence between the mechanical and electrical circuits has already been established. The correspondence between the acoustical and electrical circuit is clear if in Fig. 9.3c one sets

$$L = \left(l + \frac{16a}{3\pi}\right)\pi a^2 \rho \qquad R = R_d + \frac{\pi \rho a^4 \omega^2}{2s}$$
$$C = \frac{V}{\pi^2 \rho a^4 s^2} \qquad E = \pi a^2 F \qquad x = q \tag{9.105}$$

The radiation loss from the mouth of the resonator makes R dependent on the frequency of excitation. When the resonator is used as a side branch on a pipe, it does not radiate into an infinite medium, and the radiation loss is substantially zero.

The length l of the neck may be reduced to a small value (*e.g.*, simply the thickness of the container material). In such a case the end corrections constitute the major portion of the oscillating mass.

Instead of particle displacement x in Eq. (9.104), volume displacement $w(= \pi a^2 x)$ is often used as the dependent variable, and the forcing function expressed as a pressure instead of a force. Equation (9.104) then becomes

$$\left[\left(\frac{l}{a} + \frac{16}{3\pi}\right)\frac{\rho}{\pi a}\right]\ddot{w} + \frac{1}{\pi}\left(\frac{R_d}{\pi a^4} + \frac{\rho \omega^2}{2s}\right)\dot{w} + \frac{\rho s^2}{V} w = F \sin \omega t \tag{9.106}$$

The equivalent electrical circuit is then set up on the basis of

$$L = \left(\frac{l}{a} + \frac{16}{3\pi}\right)\frac{\rho}{\pi a} \qquad R = \frac{1}{\pi}\left(\frac{R_d}{\pi a^4} + \frac{\rho \omega^2}{2s}\right)$$
$$C = \frac{V}{\rho s^2} \qquad E = F \qquad q = w \tag{9.107}$$

If the acoustical element consists merely of a short length of tube l in a large baffle (Fig. 9.18), the same equations apply as in the case of the resonator with the exceptions that V goes to infinity (zero spring stiffness) and radiation occurs from both ends of l. If the short tube is used as a side branch on a pipe, radiation of energy will take place from the outside opening only.
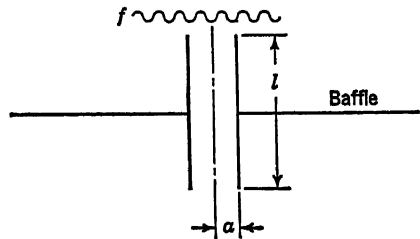
Fig. 9.18

Networks of resonators or orifices form acoustical filters of the low-pass, high-pass, band-pass, or band-elimination types. Typical idealized acoustical networks and corresponding electrical analogies are shown in Fig. 9.19 (damping neglected).

9.8. Continuously Distributed Mass and Elasticity.

Longitudinal or torsional waves in elastic bars, plane waves in organ pipes or hydraulic systems, and transverse waves in wires or strings under tension are phenomena which obey the same form of wave equation. Any differences between the systems are usually those of boundary conditions.
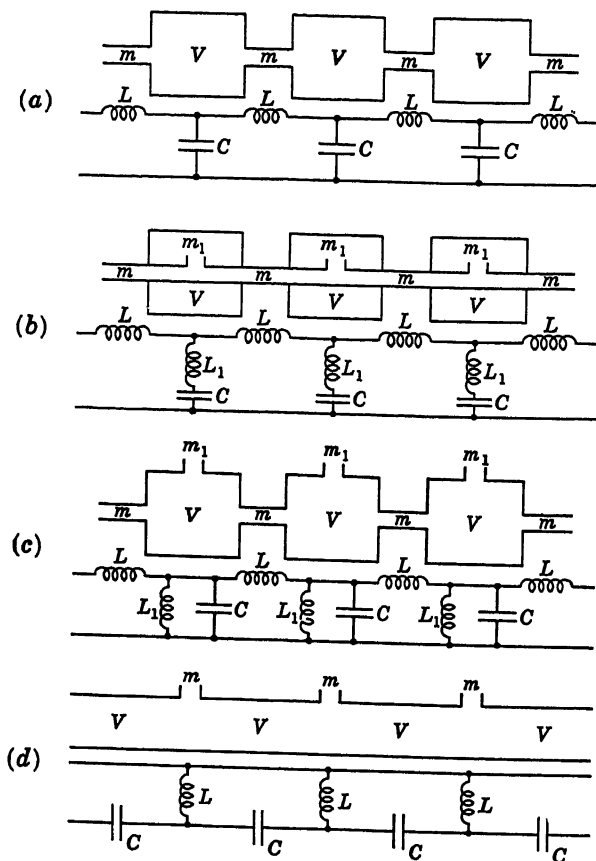
Fig. 9.19

Such continuous systems may be readily transformed to lumped systems of approximately the same dynamical properties, and the lumped systems in turn represented by either one or the other of the two dynamical analogies.

Consider, for example, the case of longitudinal elastic waves in a bar. In Fig. 9.20a an unloaded elementary element dx is shown in an elastic bar. When longitudinal vibrations occur, the edges of the element dx will move back and forth, the displacements being represented by u and $u + (\partial u/\partial x)\, dx$ in (b). At the edge $x + u$ (or simply x, since u is a

minute quantity as compared with x), a gradient $\partial u / \partial x$ exists at any instant of time. This gradient is the *strain* in the material and consequently must be accompanied by a *stress*. If the bar has a cross-sectional area A and a Young's modulus E, the total force S acting on the cross section at x would be

$$S = AE \frac{\partial u}{\partial x} \qquad (9.108)$$

Similarly, at the cross section at $x + dx$, the strain is

$$\frac{\partial u}{\partial x} + \left(\frac{\partial^2 u}{\partial x^2} \right) dx,$$

and the force is

$$S + dS = AE \left(\frac{\partial u}{\partial x} + \frac{\partial^2 u}{\partial x^2} dx \right) \quad (9.109)$$

The only other force acting on the element dx is the inertia force

$$\left(\frac{\partial^2 u}{\partial t^2} \right) dm$$
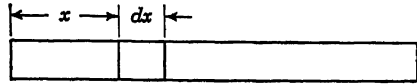
(a)
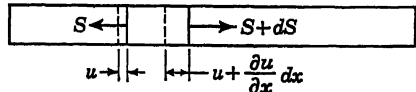
(b)

Fig. 9.20

where dm is the mass of the element dx. The equation of equilibrium for the element dx may be written, therefore, as follows:

$$dS - \frac{\partial^2 u}{\partial t^2} dm = 0 \qquad \text{or} \qquad s^2 \frac{\partial^2 u}{\partial x^2} - \frac{\partial^2 u}{\partial t^2} = 0 \qquad (9.110)$$

where $s = (E/\rho)^{\frac{1}{2}}$ and ρ = mass density of the bar material. The parameter s is seen to be the acoustic velocity in the material. For solids there is also a lateral strain in the bar due to the Poisson-ratio effect. However, for waves which are long compared with the dimensions of the cross section, the lateral strain effects are of minor consequence and may be neglected in the interest of simplicity.

(a)

(b)

Fig. 9.21

If the bar consists of a material like air, whose properties vary markedly with pressure and temperature, the parameter s must be evaluated for the conditions of interest. Suppose the short length of bar L (air) in Fig. 9.21a to be at given conditions p, T of pressure and temperature. The corresponding volume of the bar is V. Suppose the bar to be subjected to a small increment in pressure dp, as in Fig. 9.21b. The length will change by a small amount $-dL$, and the volume by a small amount $-dV$. Since the mass of material present remains unchanged, but the volume has decreased, the density of the material must increase by an amount
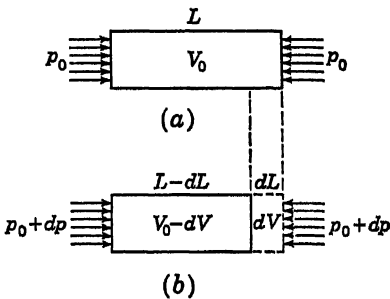
$d\rho$, such that

$$d(V\rho) = 0 \qquad \text{or} \qquad V\, d\rho + \rho\, dV = 0 \tag{9.111}$$

or
$$\frac{d\rho}{\rho} = -\frac{dV}{V} \tag{9.112}$$

By definition, $E = $ stress/strain, and strain $= $ elongation/original length. Thus

$$E = \frac{dp}{-dL/L} = \frac{dp}{-dV/V} = \rho\,\frac{dp}{d\rho} \tag{9.113}$$

Thus, the expression for the acoustic velocity becomes

$$s = \left(\frac{dp}{d\rho}\right)^{\frac{1}{2}} \tag{9.114}$$

The pressure and volume are related by the adiabatic process

$$pv^k = \text{const} = K_1$$

where v is the specific volume. Thus, $v = 1/\rho g$, and we have the equation $p = K_1(\rho g)^k$, from which

$$\frac{dp}{d\rho} = kK_1 g^k \rho^{k-1} \tag{9.115}$$

The adiabatic temperature-volume relation is $Tv^{k-1} = \text{const} = K_2$, or $(g\rho)^{k-1} = T/K_2$. Whence Eq. (9.115) becomes

$$\frac{dp}{d\rho} = kg\,\frac{K_1}{K_2}\,T \tag{9.116}$$

But $K_1 = pv^k$ and $K_2 = Tv^{k-1}$, so that $K_1/K_2 = pv/T = R$, the perfect gas constant. Thus

$$\frac{dp}{d\rho} = kgRT \tag{9.117}$$

and the velocity of sound in a perfect gas is

$$s = (kgRT)^{\frac{1}{2}} \tag{9.118}$$

a function only of absolute temperature for any one gas or gas mixture.

Thus, for gas-containing systems such as ventilating ducts, engine intake and exhaust systems, organ pipes, etc., for which the perfect gas relations apply with sufficient accuracy in dealing with small oscillations, Eq. (9.110) will apply with $s^2 = kgRT$.

For shafts subject to torsional wave propagation, a cross section A (Fig. 9.22a) will have at any given instant an angular displacement θ with respect to its static equilibrium position. An adjacent cross section

B will have an angular displacement differing by the amount $(\partial\theta/\partial x)\,dx$. An angular strain $\partial\theta/\partial x$ exists at A and one differing by the amount $(\partial^2\theta/\partial x^2)\,dx$ at B. These angular strains are related to the torques M acting on the surfaces A and B through the expressions

$$\frac{\partial\theta}{\partial x} = \frac{M}{GI_p} \qquad \frac{\partial\theta}{\partial x} + \frac{\partial^2\theta}{\partial x^2}\,dx = \frac{M + dM}{GI_p} \qquad (9.119)$$

where $I_p = \pi r^4/4$ is the polar moment of inertia of the cross section of the bar (assuming a circular cross section) and G is the shear modulus (or modulus of rigidity). The inertia torque is $-dI\,\partial^2\theta/\partial t^2$. For a cylindrical element about its axis,

$$dI = \frac{r^2\,dm}{2} = \frac{\pi r^4 \rho}{2}\,dx = \rho I_p\,dx \qquad (9.120)$$

(a)

Thus the equation of equilibrium for torsional waves in a shaft is

$$s^2\frac{\partial^2\theta}{\partial x^2} - \frac{\partial^2\theta}{\partial t^2} = 0 \qquad (9.121)$$

(b)
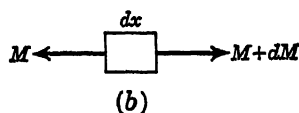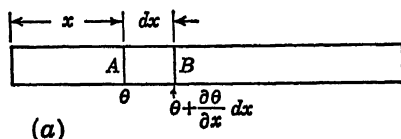
Fig. 9.22

where $s = (G/\rho)^{\frac{1}{2}}$ is the velocity of a shear wave in the material. For steels, G is usually about $0.4E$, so that shear waves travel at a speed roughly 65 per cent of that of the longitudinal (or acoustic) waves.

The equation of equilibrium of a vibrating string is obtained from Fig. 9.23. In (a) a string is shown under tension T. The vibrational displacements z are assumed small so that T remains substantially constant at all times. The element of string dx at location x is shown enlarged in (b). The slope at end A is $\partial z/\partial x$ (a partial derivative is used because z also varies with time) at any instant of time. Thus, for small slopes, the downward pull on the elements dx of string is $T\,\partial z/\partial x$ at A. Similarly, the upward pull at B is $T[\partial z/\partial x + (\partial^2 z/\partial x^2)\,dx]$. The inertia force is $-\mu\,dx\,\partial^2 z/\partial t^2$, where μ is the mass per unit length of string. The equation of equilibrium is, therefore,

(a)

(b)

Fig. 9.23

$$s^2\frac{\partial^2 z}{\partial x^2} - \frac{\partial^2 z}{\partial t^2} = 0 \qquad (9.122)$$
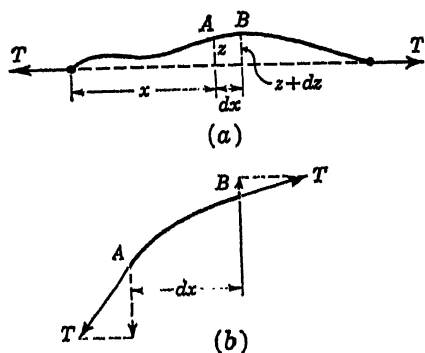
where $s = (T/\mu)^{\frac{1}{2}}$ is the velocity of transverse wave propagation along the string. The dependence of this velocity on the tension in the string and on the weight of the string per unit of length is clearly seen.

Equations (9.110), (9.121), and (9.122) may be represented by the same dynamical analogy. Since lumped electrical elements are used, the continuous mechanical systems must be converted to lumped form, *i.e.*, be replaced by systems consisting of finite numbers of discrete masses connected by massless springs. Consider, for example, the vibrating
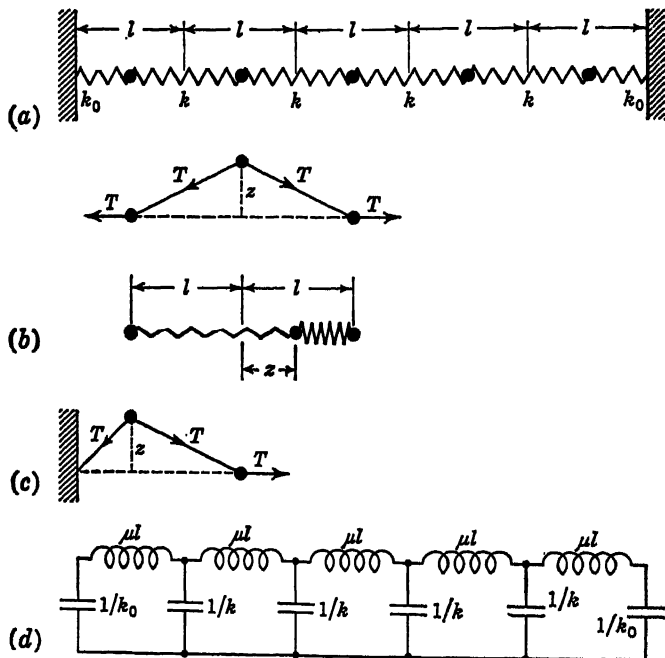
Fig. 9.24

string. In Fig. 9.24a the string is shown separated into five equal segments l, the mass of each segment being considered as concentrated at its center. The elasticity of the string is represented by rectilinear springs interconnecting the masses. Since the elasticity is due to a uniform tension in the string, all springs will have flexibilities proportional to the lengths of the strings between masses. Each mass will be of magnitude μl. The spring stiffnesses are such that the forces acting on any one mass displaced alone are the same as the forces acting at the corresponding point on the string when that point is moved the same distance with the adjacent points held. The comparison is shown in Fig. 9.24b for a mass other than an end mass. The downward force due to each side tension is $(T/l)z$. The force to the left in each spring

is kz, where k is the spring stiffness.   Thus

$$k = \frac{T}{l} \qquad (9.123)$$

The end conditions are illustrated in (c).   The downward force due to the tension in the string to the left is $2(T/l)z$; consequently,

$$k_0 = \frac{2T}{l} \qquad (9.124)$$

The mass-inductance analogy for the five-lump string is shown in (d). The number of lumps to be used depends on the number of modes which one desires to develop and on the accuracy with which the modes are required.   Although a string has an infinite number of transverse modes and natural frequencies, a five-lump representation can provide at the most the first five modes, and these are only rough approximations beyond perhaps the second or third mode.   Thus, for higher modes or greater accuracy, more lumps (finer subdivisions) must be taken in the string.

If a torsional problem is involved, instead of the string, the same general procedures for lumping would be employed.   The end conditions, however, may be different in that either end or both ends of the shaft may be free, whereas for the string under tension both ends are held (zero deflection).   In a torsional system the spring stiffness is found from Eq. (9.119).   Thus, if l is the distance between concentrated inertias and θ the angle of rotation of one inertia relative to an adjacent one, then

$$k = \frac{M}{\theta} = \frac{GI_p}{l} \qquad (9.125)$$

At the ends, the distance to the inertia is $l/2$, so that

$$k_0 = \frac{2GI_p}{l} \qquad (9.126)$$

If either end is free, the corresponding spring k_0 is omitted.   Thus, Fig. 9.25a represents the mass-inductance analogy for an equivalent lumped torsional system with both ends fixed, (b) with one end free, and (c) with both ends free.

Acoustic systems are also lumped in the same fashion, so that exhaust systems, mufflers, etc., may be represented by circuits such as those in Fig. 9.25a for analysis and design purposes.   Typical acoustical networks are shown in Fig. 9.19.
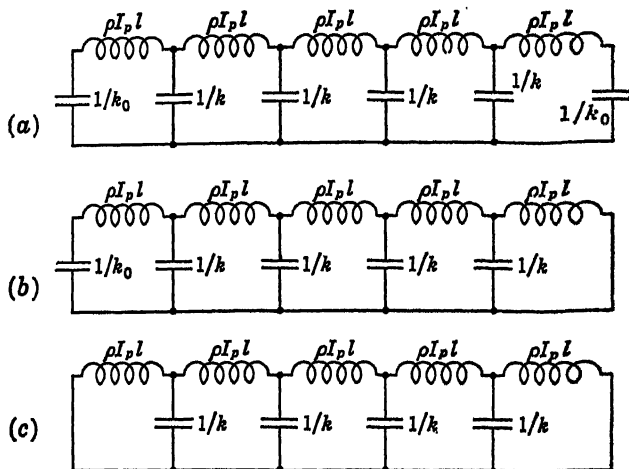
Fig. 9.25

9.9. Lumped Networks for Beams in Bending.

The transverse vibrations of beams either with distributed mass or with several concentrated attached masses present a radically different problem from that of the vibrating string under tension, or that of the torsional system. Figure 9.26a represents a beam vibrating about its static equilibrium position indicated by the dotted line. Any element dx of the beam is in dynamic equilibrium. This element is shown with the forces acting upon it in (b). From common beam theory the bending moment M is related to the deflection y as follows:
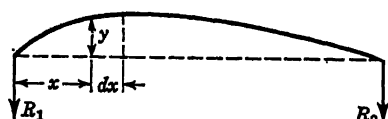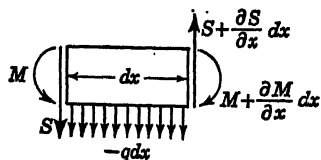
(a)

(b)

Fig. 9.26

$$EI \frac{d^2y}{dx^2} = -M \qquad (9.127)$$

where EI is the flexural rigidity (Young's modulus times the moment of inertia of the cross section about the neutral axis). The positive directions for M and the shear S are shown in (b). The inertia loading per unit of length is $-q$. Equilibrium of the vertical forces yields

$$\frac{\partial S}{\partial x} = -q \qquad (9.128)$$

Equilibrium of moments of the element in (b) yields

$$\frac{\partial M}{\partial x} = S \qquad (9.129)$$

Thus, equilibrium of the vertical forces may be expressed in terms of y as follows:

$$\frac{\partial}{\partial x}\left(-EI\,\frac{\partial^2 y}{\partial x^2}\right) = S \tag{9.130}$$

$$\frac{\partial^2}{\partial x^2}\left(EI\,\frac{\partial^2 y}{\partial x^2}\right) = q \tag{9.131}$$

With $q = -\rho A(\partial^2 y/\partial t^2)$, Eq. (9.131) becomes

$$\frac{\partial^2}{\partial x^2}\left(EI\,\frac{\partial^2 y}{\partial x^2}\right) + \rho A\,\frac{\partial^2 y}{\partial t^2} = 0 \tag{9.132}$$

where ρ is the mass density of beam material and A is the cross-sectional area. Equation (9.132) is quite different from Eqs. (9.110), (9.121), or (9.122) and requires in consequence a different analog circuit.

A convenient approach to an equivalent lumped system may be taken through the influence coefficient concept. As an example, consider the fixed-hinged beam of Fig. 9.27. Suppose for the time being that the mass of the beam is negligible in comparison with three concentrated masses m_1, m_2, m_3 attached to the beam. This is a case, therefore, of *distributed stiffness*, but *lumped masses*. If a unit vertical force be applied in turn to each of the masses, vertical deflections of all three masses would take place in each case. The nine deflections so obtained are the "influence" coefficients, determining the influence of a load at any one location on deflections at various locations. For present purposes, the locations of interest are at the concentrated masses.

In Fig. 9.27a, the subscripts on the influence coefficients are so arranged that the first subscript indicates the point at which the unit load is applied, while the second indicates the point at which the corresponding deflection is being considered. Thus a_{12} represents the deflection at mass 2 due to a unit load applied at mass 1, while a_{21} represents the deflection at mass 1 due to a unit load applied at mass 2. For small deflections (*i.e.*, for linear systems) the Maxwell reciprocity rule[27] states that $a_{12} = a_{21}$. Similarly, $a_{13} = a_{31}$, $a_{23} = a_{32}$, so that actually only six independent influence coefficients are involved in Fig. 9.27a, instead of nine.

Influence coefficients may be determined[28] by the conventional processes of calculation used in static stress analysis. Frequently, the coefficients are obtained by direct measurement in static tests conducted on the given structure or on a model of the structure.

The three masses and six influence coefficients in (a) may be represented by the three masses and six springs of the equivalent lumped system in (b). The spring stiffnesses are so chosen that the influence coefficients in (b) are identical with those in (a). If a unit load is applied to each
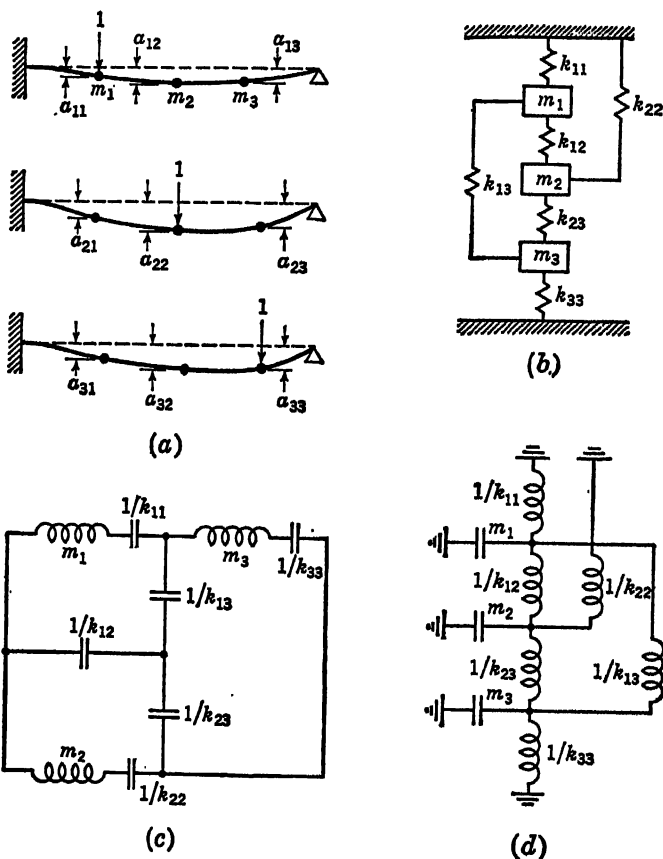
Fig. 9.27

mass in turn in (b) and the equations of static equilibrium written in each case for the entire system and for each mass individually, six equations are obtained, as follows:

$$a_{11}k_{11} + a_{12}k_{22} + a_{13}k_{33} = 1$$
$$a_{21}k_{11} + a_{22}k_{22} + a_{23}k_{33} = 1 \qquad (9.133)$$
$$a_{31}k_{11} + a_{32}k_{22} + a_{33}k_{33} = 1$$

$$a_{11}k_{11} + (a_{11} - a_{12})k_{12} + (a_{11} - a_{13})k_{13} = 1$$
$$(a_{22} - a_{21})k_{21} + a_{22}k_{22} + (a_{22} - a_{23})k_{23} = 1 \qquad (9.134)$$
$$(a_{33} - a_{31})k_{31} + (a_{33} - a_{32})k_{32} + a_{33}k_{33} = 1$$

The first set of equations provides values for k_{11}, k_{22}, and k_{33}. These may be substituted into Eqs. (9.134), which may then be solved for the remaining spring stiffnesses, k_{12}, k_{23}, and k_{13}. The system (a) is thus transformed to the equivalent system (b) and either the mass-

inductance analogy or the mass-capacitance analogy may be used to represent the latter system. The mass-inductance analogy is shown in (c), the mass-capacitance analogy in (d). The linear simultaneous algebraic equation solving machines described in Chap. 7 may be used to solve the two sets of Eqs. (9.133) and (9.134).

It should be mentioned at this time that these equations are likely to yield some negative values of spring stiffness. Although this poses no problem if a linear-algebraic-equation solver is to be used for analysis, it is troublesome if a dynamical analogy is to be set up. For example, the influence coefficients for a cantilever bar (Fig. 9.28a) are

$$a_{11} = \frac{l^3}{3EI} \qquad a_{22} = \frac{8l^3}{3EI} \qquad a_{33} = \frac{9l^3}{EI}$$

$$a_{12} = \frac{5l^3}{6EI} \qquad a_{23} = \frac{14l^3}{3EI} \qquad a_{13} = \frac{4l^3}{3EI} \qquad (9.135)$$

The corresponding spring stiffnesses are

$$k_{11} = \frac{138EI}{13l^3} \qquad k_{22} = -\frac{54EI}{13l^3} \qquad k_{33} = \frac{9EI}{13l^3}$$

$$k_{12} = \frac{138EI}{13l^3} \qquad k_{23} = \frac{48EI}{13l^3} \qquad k_{13} = -\frac{36EI}{13l^3} \qquad (9.136)$$

Thus, of the six springs required, two of them, k_{22} and k_{13}, are negative.

With constant-frequency sinusoidal excitation of a circuit, an inductance will serve as the equivalent of a negative capacitance, and vice versa. If the frequency of excitation is changed, the absolute values of the impedances of a positive inductance and the capacitive equivalent of a negative inductance change in opposite directions. This, of course, must not occur in the desired circuit. Hence, in an experimental setup to be operated in the steady state but at a number of different exciting frequencies, variable units must be used for the elements representing the negative stiffnesses. Then, each time the exciting frequency is changed, the magnitude of the negative unit would also be changed to bring its impedance at that frequency to the appropriate value. As a matter of fact, the entire system may be operated at constant frequency at all times and the effect of operation at
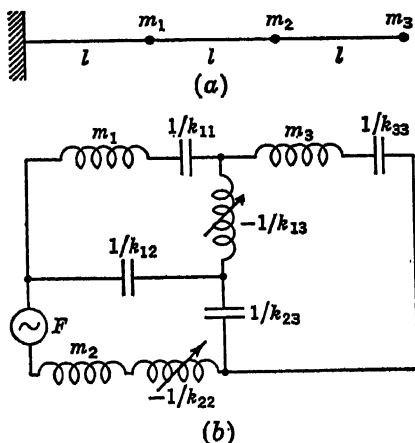
Fig. 9.28

different steady-state frequencies obtained by changing the magnitudes of the Ls and Cs. These changes would produce the same impedances that would exist with constant L and C at the different frequencies. This is the basis for the network-analyzer approach.[29] Such a procedure has certain advantages if the inductance, resistance, or capacitance values in the circuit are frequency-sensitive, or if only a single precise frequency is available. When large numbers of elements are involved, the procedure becomes very cumbersome. The circuit is not suitable for transient or impact simulation because in such problems many different frequencies are present simultaneously and the circuit can be set up to satisfy only one of them.

Negative a-c impedances can be effectively obtained with electronic circuits, thereby circumventing the difficulty mentioned above in using inductance as a substitute for negative capacitance. Referring to Fig. 9.29, the current i through C is given by
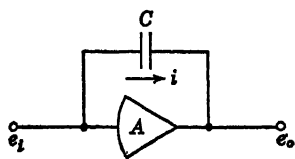
Fig. 9.29

$$i = \frac{e_i - e_o}{-(1/\omega C)} = e_i(1 - A)\omega C \quad (9.137)$$

where i, e_i, and e_o are functions of ω. As far as the input terminal e_i is concerned, it sees an impedance given by

$$Z_i = \frac{e_i}{i} = \frac{1}{(1 - A)\omega C} \quad (9.138)$$

If the amplification A through the amplifier is a real positive number greater than 1, the input impedance of this circuit is a negative capacitive reactance.

Brunetti and Greenough[30] describe a two-stage amplifier circuit for obtaining negative capacitance. By making use of inverse feedback, stable negative impedances (resistance, capacitance, inductance) are obtainable.[31] Such methods are also described in Chap. 10.

For a particular frequency of excitation applied to, say, m_2 of the cantilever beam, the equivalent circuit will be that shown in Fig. 9.28b. The negative springs k_{13} and k_{22} are represented by variable inductors whose values would be reset when the exciting frequency is changed. Or the negative capacitance unit of Fig. 9.29 may be used for these elements.

If more than three concentrated masses are involved in the beam problem, the mass-inductance analogy cannot be used directly because the mechanical circuit now becomes nonplanar, i.e., connections between elements or to ground are found to cross over each other. The mass-capacitance analogy, however, may be used equally well for either planar or nonplanar systems.[32]

To illustrate this point, suppose the beam of Fig. 9.30a to be vibrating under the influence of its own distributed weight and stiffness. The beam will be divided into five parts, each of length l, and the mass of each part will be considered as concentrated at its mid-point. The corresponding lumped system is shown in (b). Five direct influence coefficients (a_{11}, a_{22}, . . . , a_{55}) and twenty cross influence coefficients
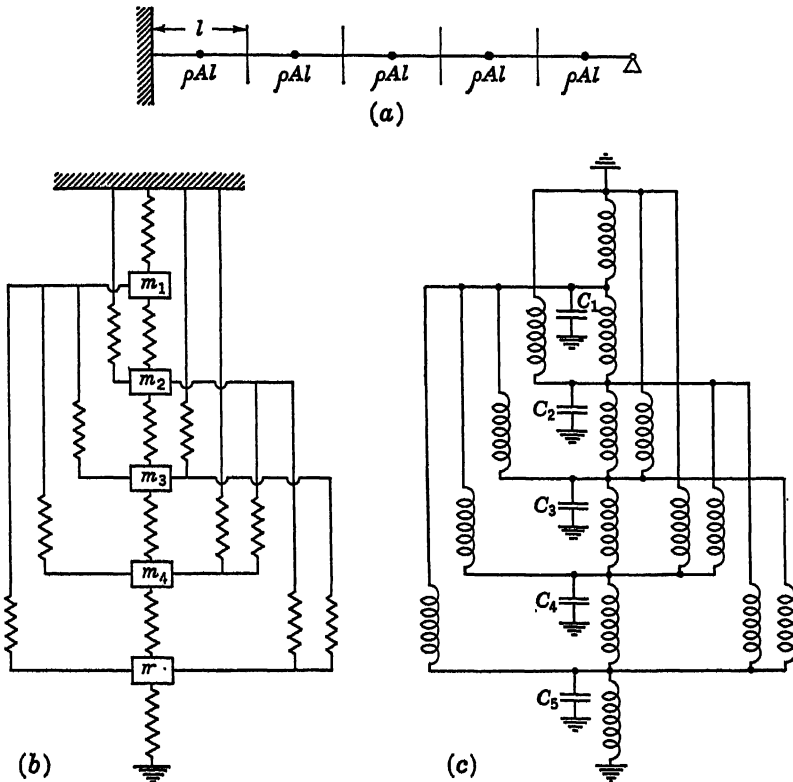
Fig. 9.30

(a_{12}, a_{21}, . . . , a_{13}, a_{31}, . . . , a_{45}, a_{54}) are involved. By Maxwell's reciprocity rule, only 10 of the cross influence coefficients are different, so that a system of only 5 springs to ground and 10 between-masses springs are necessary in (b) to represent the lumped beam in (a).

It is apparent from (b) that a number of crossovers occur. If it is remembered that each mass must be referred to ground (i.e., an imaginary connecting line should be drawn between each mass and the ground), additional crossovers will be evident. Attempts to set up a mass-inductance analogy for such a system are doomed to failure because short circuits will occur. It will be shown in the next chapter how

transformers may be used with this analogy and short circuits thus avoided. The mass-capacitance analogy, however, is applicable directly without the use of transformers, although it also may be used with transformers. This analogy for the system in (b) is shown in (c). Of course, the problem of contending with negative springs still remains. The use of transformers to be indicated in Sec. 10.11 avoids the need for negative springs.

9.10. Plasticity, Creep, and Nonlinearity. When an ideal weightless spring is subjected to a suddenly applied massless force, it stretches immediately to its equilibrium position and stays there. Actual materials, however, do not behave in this ideal manner, even exclusive of their
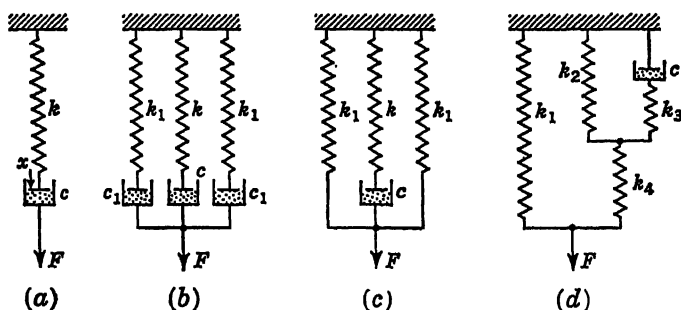
Fig. 9.31

weight effect. They are subject to internal friction, plasticity, and creep.[33] Rubberlike materials are particularly noticeable in their departure from the ideal spring. For metals, the departure is usually not noticeable except for high loadings or high temperatures.

In setting up analogous systems, it is often desirable to model the actual behavior of materials to a reasonable extent. As a result, research workers have developed mechanical models[34] of various degrees of complexity to represent these phenomena. For some materials, a suddenly applied load leads to an equally sudden elastic deflection, followed by a period of creep as the load is maintained. If the creep continues indefinitely, the mechanical model of this material would be as represented in Fig. 9.31a. The sudden application of the load F causes the spring k to deflect immediately to its equilibrium value, $x = F/k$. At the same time a velocity, $v = F/c$, is developed across the dashpot. This velocity persists while F remains applied. Thus the point of application of F continues to move steadily (creep), while the elastic deflection x remains constant. If F is suddenly removed, the spring k will immediately contract to its original position; but the amount of creep remains unchanged, since there are no forces acting to restore the dashpot to its original configuration.

Some creep recovery may be simulated in a model consisting of three spring-dashpot units symmetrically arranged as in Fig. 9.31b. The application of a sudden force F causes initial transient deflections of the springs which tend to be equal at the first instant, but later readjust themselves to conform with dashpot coefficients. Thus in the steady creep condition, the rate of creep is $v = F/(2c_1 + c_2)$ and the loads in the springs are $cF/(2c_1 + c_2)$ in k and c_1F ($2c_1 + c_2$) in k_1. The deflections are thus proportional to dashpot coefficient and inversely proportional to spring stiffness. If, after the steady-state creep has been established, the force F is suddenly removed, the springs will tend to contract. The least extended spring (or springs) will reach its unextended position first, whereupon the other spring (or springs) will continue to contract, thereby causing a viscous force to act through its dashpot in a direction to recover some creep.

In Fig. 9.31c, the dashpots c_1 have been omitted. Under a sudden force F, an initial deflection $F/(2k_1 + k)$ will occur, after which F will continue to creep down until its deflection becomes $F/(2k_1)$. At this point creep stops. Upon removal of the load there is a sudden elastic contraction which puts spring k into compression, followed by a gradual and complete recovery of creep. This model has been used to develop mathematical expressions for the one-dimensional plastic deformation of solid materials.[35]

A model of the type proposed to explain the behavior of rubber isolation mounts is shown in Fig. 9.31d.[36]

There are unlimited combinations of springs and dashpots from which a combination may be developed to meet a specific stress-strain characteristic of a viscoelastic solid. For additional models, see Halsey and Roscoe.[37,38]

Equivalent electrical circuits for the mechanical models are easily set up on the basis of the force-voltage or force-current analogies.

Nonlinear load-deflection characteristics are often purposely incorporated in otherwise linear spring systems by means of elastic stops, clearances, and preloaded springs. Some possible arrangements for linear systems are shown in Fig. 9.32. Torsional systems of this sort are illustrated in Wilson.[39]

In Fig. 9.32a, clearance (or backlash) in the amount of $2a$ is provided between a vibrating mass and linear springs of stiffnesses k_1 and k_2, respectively, against which the mass oscillates. The load-deflection characteristic for this system is described by the equations

$$\begin{aligned}
f &= 0 & &\text{for } -a < x < a \\
f &= k_2(x - a) & &\text{for } x > a \\
f &= k_1(x + a) & &\text{for } x < -a
\end{aligned} \qquad (9.139)$$
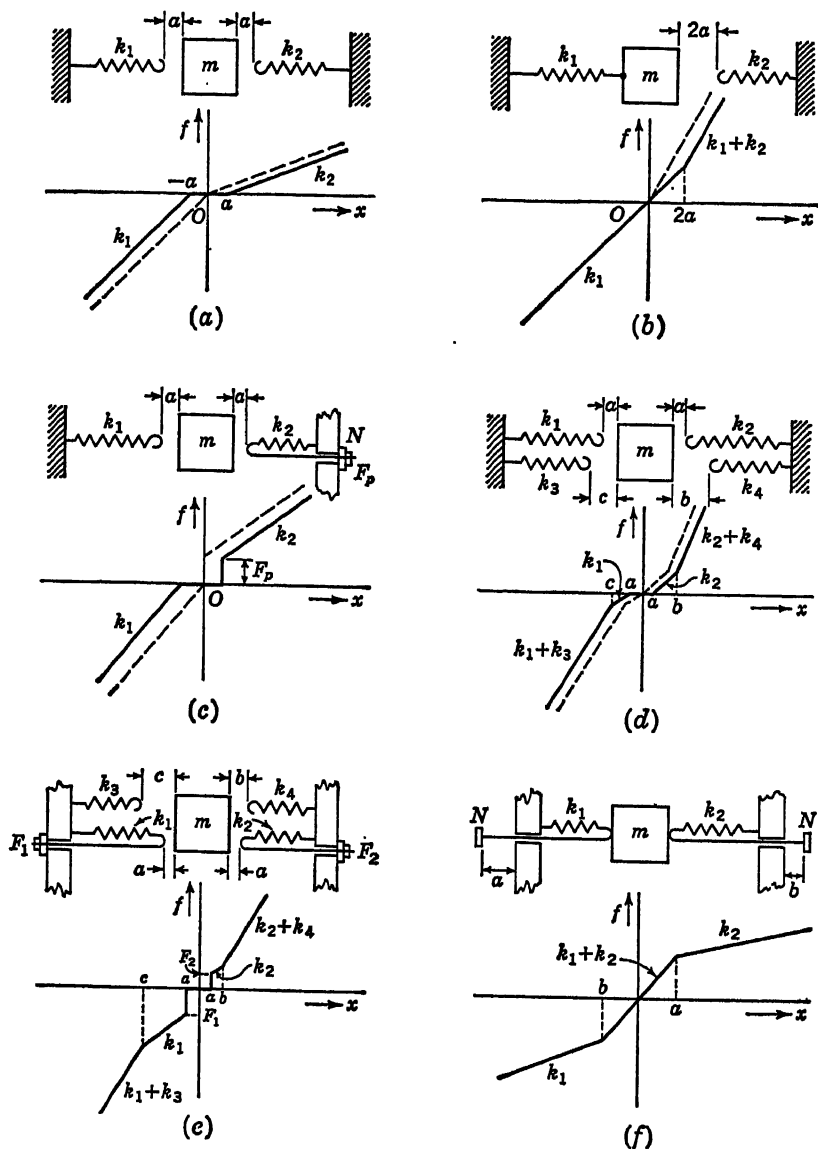
Fig. 9.32

If this backlash is reduced to zero, the dotted characteristic in Fig. 9.32a will be obtained. By fastening one of the springs to m, so that it may be extended as well as compressed (Fig. 9.32b), the load-deflection relations become

$$
\begin{aligned}
f &= 2ak_1 + (k_1 + k_2)(x - 2a) && \text{for } x > 2a \\
f &= k_1 x && \text{for } x < 2a
\end{aligned}
\qquad (9.140)
$$

One (or both) of the springs may be preloaded (preset). In Fig. 9.32c this is done by running the free end of the spring back through the spring holder and pulling it up to any desired degree of preload F_p by means of nut N. The nut is free to move to the right with the spring, but both are stopped by the spring holder on their return. The load-deflection equations for this case are

$$
\begin{array}{lll}
f = 0 & \text{for } -a < x < a \\
f = F_p + k_2(x - a) & \text{for } x > a & (9.141) \\
f = k_1(x + a) & \text{for } x < -a
\end{array}
$$

If the free end of k_1 is fastened to m and all the backlash is assigned to positive x, the load-deflection equations become

$$
\begin{array}{lll}
f = 2ak_1 + F_p + (k_1 + k_2)(x - 2a) & \text{for } x > 2a \\
f = k_1 x & \text{for } x < 2a
\end{array} \quad (9.142)
$$

Figure 9.32d illustrates the case of backlash plus elastic stops, the latter being provided by springs k_3 and k_4. The load-deflection characteristic shown in (d) is given by the equations

$$
\begin{array}{lll}
f = 0 & \text{for } -a < x < a \\
f = k_2(x - a) & \text{for } a < x < b \\
f = k_2(x - a) + k_4(x - b) & \text{for } x > b & (9.143) \\
f = k_1(x + a) & \text{for } -c < x < -a \\
f = k_1(x + a) + k_3(x + c) & \text{for } x < -c
\end{array}
$$

As in the previous cases, the backlash may be reduced to zero, and/or one or both springs k_1, k_2 may be attached to m. The consequent changes in the load-deflection characteristics of the system are easily determined.

In Fig. 9.32c a spring system is shown having backlash, preset springs with preloads F_1 and F_2, and elastic stops. The load-deflection equations are

$$
\begin{array}{lll}
f = 0 & \text{for } -a < x < a \\
f = F_2 + k_2(x - a) & \text{for } a < x < b \\
f = F_2 + k_2(x - a) + k_4(x - b) & \text{for } x > b & (9.144) \\
f = -F_1 + k_1(x + a) & \text{for } -b < x < -a \\
f = -F_1 + k_1(x + a) + k_3(x + c) & \text{for } x < -c
\end{array}
$$

Here again, various modifications in spring arrangement are possible to arrive at variations of the characteristic shown in (e).

One more spring system is illustrated in Fig. 9.32f. The free ends of the springs are brought around through the spring holders and are provided with nuts N. Before the mass m is inserted between the springs, the nuts may be pulled up just enough to rest against the spring

holders without preloading the springs, or they may be pulled up sufficiently to preload one or both springs as desired. In the case illustrated, the former condition is assumed.

The system has been designed so that in order to insert the mass between the springs it is necessary to pry the springs apart, so that the nuts become spaced distances a and b, respectively, from the holders. These distances are predetermined, since we must have $k_1a = k_2b$ for equilibrium. The load-deflection curve for the mass m, shown in (e), is described by the equations

$$
\begin{aligned}
f &= (k_1 + k_2)x && \text{for } -b < x < a \\
f &= k_2x && \text{for } x > a \\
f &= k_1x && \text{for } x < -b
\end{aligned}
\tag{9.145}
$$

The simulation of broken-linear characteristics with biased diodes in electronic-analog-computer circuits is discussed in Chap. 4. Another method which has been used in a dynamical analogy[40] develops the breaks in the simulated spring characteristics by inserting or removing condensers with high-speed relays. Referring to Fig. 9.32b, the dynamical analogy for this system under forced vibration is shown in Fig. 9.33a. Capacitors C_1 and C_2 are both active for the period during which $x < 2a$. When increasing x reaches the value $2a$, the relay R is activated to disconnect C_2 from the circuit, whereupon the steeper load-deflection characteristic takes hold until decreasing x again reaches the value $2a$ and causes relay R to insert C_2 back into the circuit again.
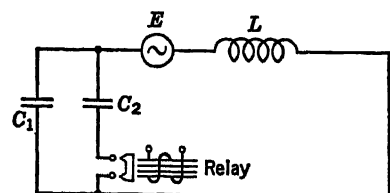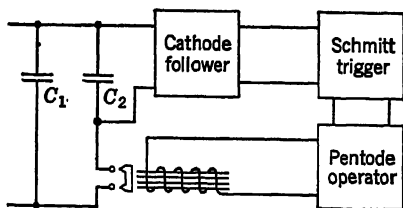
(a)

(b)

Fig. 9.33

High-speed relay action with proper timing was obtained with a relay-operating circuit indicated by the block diagram of Fig. 9.33b. A cathode follower senses the voltage (proportional to x) across capacitor C_1 without loading the circuit. When this voltage reaches a value determined from $x = 2a$, the Schmitt trigger circuit suddenly switches on the pentode circuit which provides rapid relay operation. Capacitor C_2 is thereby removed from the circuit, but retains its charge. The voltage across C_1 continues to rise to a maximum, and then begins to fall. When the decreasing voltage drops to the value corresponding to $x = 2a$, the

Schmitt trigger cuts off the pentode operator and the relay closes to reinsert condenser C'_2.

As many relays and relay-operating circuits (b) are required as there are breaks in the load-deflection curve being simulated.

9.11. Further Applications of Dynamical Analogies. The bands observed in infrared spectra of complex molecules are explained in terms of resonant modes and frequencies of the molecule considered as a dynamical system. For example, a band near 3.5μ in organic compounds is considered due to the vibration of the H atom against the C atom, while one near 28μ due to vibration of one C atom against another C atom.[41] The natural frequencies of a molecule lead to the determination of the force constants of the valence bonds and specific-heat curves.

To study the dynamics of the molecule on a large scale, mechanical models consisting of masses and interconnecting springs have been constructed.[42,43] Such models have also been represented by analogous electrical circuits.[44,45]

Mechanical analogies have been used to represent color vision and to explain color blindness. Resonators are assumed in the retina to account for the sensitivity of the eye to the limited range of wavelengths from about 4×10^{-5} cm to 7.6×10^{-5} cm.[46,47] The early theories of color vision, due to Young, Helmholtz, Maxwell, and others, were designed to show that any color can be built up from three fundamental colors, e.g., red, green, and blue or red, green, and violet. Accordingly, Barton and Browning set up a mechanical analogy for color vision, making use of three pendulums tuned to frequencies proportional to those of red, green, and violet light and properly damped. When subjected to stimulation, the resonators appeared to simulate most of the known fundamentals of color vision.

In an earlier paper[48] Barton and Browning also simulated the characteristics of hearing over the range of an octave by making use of 13 pendulum resonators. A modern theory of the dynamics of the cochlea, accounting for the hydrodynamics of the cochlear ducts and the dynamics of the basilar membrane, has been proposed[49] and an electrical analogy developed[50] to check the theory. The "analog ear" is a transmission line made up of 175 sections, each section consisting of two inductances (to represent the mass of a slice of fluid and that of the duct) and four capacitors (to represent duct stiffness).

An interesting dynamical analog, suggested for possible application in control systems involving a human operator as an element, is that for a muscle.[51] The rate of shortening of a muscle depends on the tension being developed in it, high rates being associated with small tensions and low rates with large tensions. Experiments indicate this relationship to be hyperbolic. The electrical analogy set up by Wilkie for the muscle of

the arm pulling against a constant external force applied to the hand made use of a rectifier for developing the proper voltage-current relation corresponding to the given force-velocity muscle characteristic.

REFERENCES

1. Mason, W. P.: Electrical and Mechanical Analogies, *Bell System Tech. J.*, **20**: 406–414 (1941).
2. Firestone, F. A.: A New Analogy between Mechanical and Electrical Systems, *J. Acoust. Soc. Am.*, **4**:249–267 (1932–1933).
3. Models and Analogies for Demonstrating Electrical Principles, Parts I-XIX, *Engineer*, **142**:167–168, 194–196, 228–229, 242–244, 273–274, 299–301, 339–340, 354–356, 380–382, 408–410, 447–448, 464–466, 503–504, 518–519, 548–549, 574–·576, 602–603, 628–629, 655–657 (1926).
4. Blake, G. G.: A Mechanical Model Analogous to an Oscillatory Electrical Circuit, *Engineer*, **181**:535–536 (1946).
5. Rogers, E. M.: Demonstration Experiments: Mechanical Analogs of Electric Circuits, *Am. J. Phys.*, **14**:318–319 (1946).
6. Nickle, C. A.: Oscillographic Solution of Electromechanical Systems, *Trans. AIEE*, **44**:844–856 (1925).
7. Grover, F. W.: "Inductance Calculations," D. Van Nostrand Company, Inc., Princeton, N.J., 1946.
8. Brotherton, M.: "Capacitors," D. Van Nostrand Company, Inc., Princeton, N.J., 1946.
9. Criner, H. E., G. D. McCann, and C. E. Warren: A New Device for the Solution of Transient-vibration Problems by the Method of Electrical-Mechanical Analogy, *J. Appl. Mechanics*, **12**:135–141 (1945).
10. Mindlin, R. D.: Dynamics of Package Cushioning, *Bell System Tech. J.*, **24**:353–461 (1945).
11. Sandeman, E. K.: Multiple Reactive Gears, *Phil. Mag.*, **5**(7):946–958 (1928).
12. Schelkunoff, S. A.: Methods of Electromagnetic Field Analysis, *Bell System Tech. J.*, **27**:487–509 (1948).
13. Electrical Engineering Staff, MIT, "Principles of Electrical Engineering—Magnetic Circuits and Transformers," John Wiley & Sons, Inc., New York, 1943.
14. Casper, W. L.: Telephone Transformers, *Trans. AIEE*, **43**:443–456 (1924).
15. Barrett, J. O. G.: The Design of Iron-cored Transformers with Specified Self and Mutual Inductances, *Electronic Eng.*, **17**:676–678 (1945).
16. Olson, H. F.: "Elements of Acoustical Engineering," D. Van Nostrand Company, Inc., Princeton, N.J., 1940.
17. Herward, S. W., and G. D. McCann: Dimensionless Analysis of Servomechanisms by Electrical Analogy, *Trans. AIEE*, **65**:636–639 (1946).
18. McCann, G. D., and S. W. Herward: Dimensionless Analysis of Servomechanisms by Electrical Analogy, I, *Trans. AIEE*, **66**:111–118 (1947).
19. Carleton, J. T.: The Transient Behavior of the Two-stage Rototrol Main Exciter Voltage Regulating System as Determined by Electrical Analogy, *Trans. AIEE*, **68**:59–63 (1949).
20. McCann, G. D., W. O. Osbon, and H. S. Kirschbaum: General Analysis of Speed Regulators under Impact Loads, *Trans. AIEE*, **66**:1243–1252 (1947).
21. Concordia, C., S. B. Crary, and G. Kron: The Doubly Fed Machine, *Trans. AIEE*, **61**:286–289 (1942).

22. Kron, G.: Equivalent Circuits for Hunting of Electrical Machinery, *Trans. AIEE*, **61**:290–296 (1942).

23. Electrical Engineering Staff, MIT, "Principles of Electrical Engineering—Electric Circuits," John Wiley & Sons, Inc., New York, 1940.

24. Miles, J.: Applications and Limitations of Mechanical-Electrical Analogies, New and Old, *J. Acoust. Soc. Am.*, **14**:183–192 (1943).

25. Jones, W. C.: Instruments for the New Telephone Sets, *Bell System Tech. J.*, **17**:338–357 (1938).

26. Kinsler, L. E., and A. R. Frey: "Fundamentals of Acoustics," chap. 8, John Wiley & Sons, Inc., New York, 1950.

27. Van Den Broek, J. A.: "Elastic Energy Theory," 2d ed., p. 198, John Wiley & Sons, Inc., New York, 1942.

28. Myklestad, N. O.: A Simple Tabular Method of Calculating Deflections and Influence Coefficients of Beams, *J. Aeronaut. Sci.*, **13**:23–28 (1946).

29. Morgan, W. A., F. S. Rothe, and J. J. Winsness: An Improved A-C Network Analyzer, *Trans. AIEE*, **68**:891–897 (1949).

30. Brunetti, C., and L. Greenough: Negative Capacitance, *Communications (N.Y.)*, **24**(3):28–31 (March, 1944).

31. Ginzton, E. L.: Stabilized Negative Impedances, parts I, II, III, *Electronics*, **18**:141–150 (July), 138–148 (August), 140–144 (September, 1945).

32. Abbott, W. R.: Comment on Engineering Design Analysis, *Mech. Eng.*, **72**:252 (1950).

33. Jeffreys, H.: On Plasticity and Creep in Solids, *Proc. Roy. Soc. (London)*, (A)**138**:283–297 (1932).

34. Leaderman, H.: "Elastic and Creep Properties of Filamentous Materials and Other High Polymers," chap. 2, The Textile Foundation, Washington, D.C., 1943.

35. Thorne, C. J.: On Plastic Flow and Vibrations, *J. Appl. Mechanics*, **17**:84–90 (1950).

36. "Engineering Report on Resilient Mountings for Reciprocating and Rotating Machinery," Illinois Institute of Technology, ONR Contact N7-ONR-32904, June 15, 1948, to June 15, 1949.

37. Halsey, G.: Non-linear Viscous Elasticity and the Eyring Shear Model, *J. Appl. Phys.*, **18**:1072–1097 (1947).

38. Roscoe, R.: Mechanical Models for the Representation of Visco-elastic Properties, *Brit. J. Appl. Phys.*, **1**:171–173 (1950).

39. Wilson, W. K.: "Practical Solution of Torsional Vibration Problems," 2d ed., vol. II, p. 412, John Wiley & Sons, Inc., New York, 1941.

40. Gross, W. A., and W. W. Soroka: Electrical Analogy for Dynamical Systems Containing Broken-linear Unsymmetrical Elasticity, *Proc. 1st Natl. Congr. Appl. Mechanics (U.S.)*, 1952, pp. 133–138.

41. Lewis, A. B.: Coupled Vibrations with Applications to the Specific Heat and Infrared Spectra of Crystals, *Phys. Rev.*, **36**:568–586 (1930).

42. Kettering, C. F., L. W. Shutts, and D. H. Andrews: A Representation of the Dynamic Properties of Molecules by Mechanical Models, *Phys. Rev.*, **36**:531–543 (1930).

43. Yates, R. C.: Study of the Small Vibrations of Six Particles in a System Analogous to the Benzene Ring, *Phys. Rev.*, **36**:563–567 (1930).

44. Kron, G.: Electric Circuit Models for the Vibration Spectrum of Polyatomic Molecules, *J. Chem. Phys.*, **14**:19–31 (1946).

45. Carter, G. K., and G. Kron: Network Analyzer Tests of Equivalent Circuits of Vibrating Polyatomic Molecules, *J. Chem. Phys.*, **14**:32–34 (1946).

46. Houstoun, R. A.: A Theory of Colour Vision, *Phil. Mag.*, **36**(6):402–417 (1918).
47. Barton, E. M., and H. M. Browning: A Syntonic Hypothesis of Colour Vision with Mechanical Illustrations, *Phil. Mag.*, **38**(6):338–348 (1919).
48. Barton, E. M., and H. M. Browning: The Resonance Theory of Audition Subjected to Experiments, *Phil. Mag.*, **38**(6):164–173 (1919).
49. Peterson, L. C., and B. P. Bogert: A Dynamical Theory of the Cochlea, *J. Acoust. Soc. Am.*, **22**:369–381 (1950).
50. Bogert, B. P.: A Network to Represent the Inner Ear, *Bell Labs. Record*, **28**:481–485 (1950).
51. Wilkie, D. R.: The Circuit Analogue of Muscle, *Electronic Eng.*, **22**:435–437 (1950).

10

FINITE-DIFFERENCE NETWORKS

10.1. General Remarks. In Chap. 6 the solution of differential equations by indirect analog techniques is discussed. Computer units, each capable of performing such elementary operations as addition, integration, and multiplication, are interconnected to form a computer system, termed a differential analyzer. Differential analyzers are very useful for the solution of differential equations with only one independent variable (ordinary differential equations), in which the dependent variable and its derivative are specified for an initial value of independent variable (for example, x and dx/dt given for $t = 0$). In this chapter, a basically different approach to the analog treatment of differential equations is considered. This method is based upon a direct analogy between the physical system under study and the analog simulator. The electric analog model consists of an array of passive electric elements, particularly resistors and capacitors. Only rarely are active electronic elements such as operational amplifiers and multipliers required. Direct analogs are capable of furnishing solutions of very high accuracies and precisions and are frequently less expensive to build and to maintain than corresponding differential analyzers. Moreover, the use of direct analogs permits the solution of differential equations having more than one independent variable (partial differential equations), as well as ordinary differential equations for which the dependent variable or its derivatives are specified at two or more points in space.

The mathematical basis for direct network analog simulators lies in the calculus of finite differences. This approach permits the approximation of ordinary and partial differential equations by a set of algebraic equations. Techniques for the numerical solution of such a set of finite-difference equations are well known.[1,2] It has also been demonstrated[3] that the network models used in the direct simulation can be designed directly by analyzing the physical system under study without recourse to mathematics. Both techniques involve the dividing or splitting up of the domain of one or more of the independent variables into a finite number

of elements. A coordinate grid is visualized as being superimposed upon the field under study, so that a straight line becomes a series of adjacent line segments, a two-dimensional field is divided into an array of rectangles, and a three-dimensional field is represented by an array of rectangular solids. If noncartesian coordinate systems are appropriate, the discrete elements of the field will assume other shapes. In solving a problem, attention is limited to the points of intersection of the grid lines, the node points of the grid, and solutions are obtained only for values of the independent variables corresponding to the node points. Solutions for other values of the independent variables can then be obtained by interpolation.

The electrical analog model is constructed by recognizing the formal similarity between the finite-difference equation applying to any node point in the discretized system and Kirchhoff's current-law equation for a node formed by passive electrical elements. Each grid line of the finite-difference grid can then be replaced by one or more electrical elements in such a manner that the current-law equation for each node of the network is similar in form to the finite-difference equation for each corresponding node of the finite-difference grid. Voltage in the electrical network then becomes analogous to the dependent variable of the original system under study.

Network analyzers, though occasionally useful for ordinary differential equations, have found their widest application in the solution of partial differential equations. Equations that have been treated successfully by network models include the important Laplace equation, Poisson's equation, the diffusion equation, the wave equation, and the biharmonic equation characterizing beam problems. Network models can also be employed to treat more complex modified forms of these equations, including equations with first space derivatives and mixed derivatives and equations with nonlinear, space-varying, or time-varying parameters.

The underlying principles of network analyzers are first demonstrated by applying them to simple ordinary differential equations. This is followed by the treatment of progressively more complex partial differential equations by direct analog methods.

10.2. Linear Ordinary Differential Equations. Ordinary differential equations have only one independent variable. The discretization of
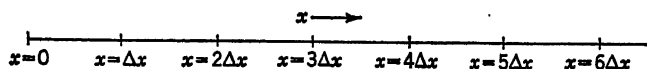
Fig. 10.1

this dependent variable therefore leads to an array of line segments, as shown in Fig. 10.1. Typical nodes in this discretized system can be identified by the subscript 0 and adjacent nodes by the subscripts 1 and 2

as shown in Fig. 10.2. The transient or steady-state values of the dependent variable y at these three adjacent node points are indicated by y_0, y_1, and y_2.

The first derivative or slope of the dependent variable can be approximated by taking the difference between the value of y at two adjacent nodes and dividing by the node spacing. This furnishes an approximation for the first derivative at the points midway between the two nodes, that is, at $+\frac{1}{2}$ and at $-\frac{1}{2}$:

$$\left(\frac{dy}{dx}\right)_{x=+\frac{1}{2}} = \frac{y_1 - y_0}{h} \qquad (10.1)$$

$$\left(\frac{dy}{dx}\right)_{x=-\frac{1}{2}} = \frac{y_0 - y_2}{h} \qquad (10.2)$$
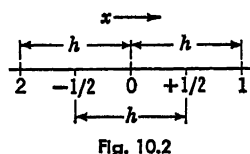
Fig. 10.2

where $\Delta x \equiv h$. The approximation for the first derivative at node 0 is obtained by averaging the first derivatives at locations $+\frac{1}{2}$ and $-\frac{1}{2}$, according to

$$\left(\frac{dy}{dx}\right)_{x=0} = \frac{(dy/dx)_{x=+\frac{1}{2}} + (dy/dx)_{x=-\frac{1}{2}}}{2}$$

$$= \frac{y_1 - y_0}{2h} + \frac{y_0 - y_2}{2h} = \frac{y_1 - y_2}{2h} \qquad (10.3)$$

The second derivative of y with respect to x is defined as the rate of change of the first derivative and can be found by taking the difference between dy/dx at $+\frac{1}{2}$ and at $-\frac{1}{2}$ and by dividing by the grid spacing:

$$\left(\frac{d^2y}{dx^2}\right)_{x=0} = \frac{(dy/dx)_{x=+\frac{1}{2}} - (dy/dx)_{x=-\frac{1}{2}}}{h}$$

$$= \frac{y_1 - y_0}{h^2} + \frac{y_2 - y_0}{h^2} = \frac{y_1 + y_2 - 2y_0}{h^2} \qquad (10.4)$$

Consider now the second-order differential equation:

$$\frac{d^2y}{dx^2} = 0 \qquad y(0) = A \qquad y(X) = B \qquad (10.5)$$

where A is the end condition specified for y at $x = 0$ and B is the value specified for y at $x = X$. In accordance with Eq. (10.4), this equation can be approximated by

$$\frac{y_1 - y_0}{h^2} + \frac{y_2 - y_0}{h^2} = 0 \qquad (10.6)$$

Consider now the node formed in an electrical circuit by the junction of two resistors as shown in Fig. 10.3a. According to Kirchhoff's current

law

$$i_1 + i_2 = 0 \qquad (10.7)$$

or

$$\frac{V_1 - V_0}{R} + \frac{V_2 - V_0}{R} = 0 \qquad (10.8)$$

A comparison of Eqs. (10.6) and (10.8) reveals that the typical node of Fig. 10.3a is analogous to a typical node of the finite-difference grid if R is made proportional to h^2. The voltage V_0 at node 0 is then the proportional to y_0.

To solve Eq. (10.5), a number of typical elements are connected together to form a one-dimensional network analog, as shown in Fig.
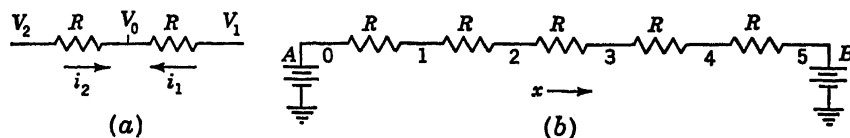
Fig. 10.3

10.3b. End conditions are applied to this circuit in accordance with the boundary conditions specified by Eq. (10.5).

Consider now the nonhomogeneous second-order differential equation

$$\frac{d^2y}{dx^2} = F \qquad (10.9)$$

whose finite-difference approximation in electrical analog terms is

$$\frac{V_1 - V_0}{R} + \frac{V_2 - V_0}{R} = F \qquad (10.10)$$

In accordance with the above development, each term of the left-hand side of the equation represents a current flowing into the typical node 0.
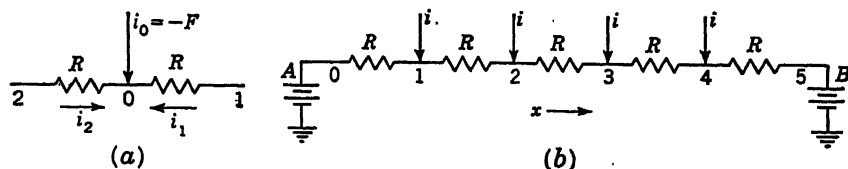
Fig. 10.4

The term F must therefore be represented by a current i flowing out of the node, or a current $-F$ in magnitude can be fed into each node of the network analog. A typical node of the resulting network is shown in Fig. 10.4a, while the complete network is shown in Fig. 10.4b. The value of F in Eq. (10.9) need not be a constant but may be a function of x. In that event, the magnitudes of the currents introduced at each node in

Fig. 10.4*b* are determined by the coordinates of that node. Thus, for example, in solving the equation

$$\frac{d^2y}{dx^2} + ky = 0$$

or

$$\frac{d^2y}{dx^2} = -ky \tag{10.11}$$

The current introduced at node 2 is made twice as large as the current introduced at node 1; the current at node 3 is made three times that of node 1; etc.

The feed-in currents required for the network of Fig. 10.4*b* can each be generated by separate current sources. It is generally more con-
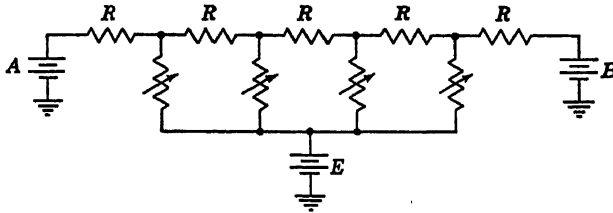
Fig. 10.5

venient, however, to employ a single voltage source and to apply the currents through potentiometers as shown in Fig. 10.5. Each potentiometer must be adjusted until the current through it assumes the specified magnitude. Since the current through each potentiometer affects to some extent the current through every other potentiometer, such an adjustment must proceed iteratively. If, however, the voltage source E is made large in magnitude, and if the potentiometer resistances are large compared with the magnitudes of the network resistors R, little interaction occurs between the potentiometers. If the parameter k in Eq. (10.11) is negative, a current proportional to y must flow *out* of every node. This is accomplished readily by connecting a resistor having a magnitude proportional to $|1/k|$ from each network node to ground.

The presence of a first derivative in the differential equation introduces a peculiar difficulty in the analog simulation procedure. Consider the second-order differential equation

$$\frac{d^2y}{dx^2} + \frac{dy}{dx} = F \tag{10.12}$$

In accordance with Eqs. (10.3) and (10.4),

$$\frac{y_1 - y_0}{h^2} + \frac{y_2 - y_0}{h^2} + \frac{y_1 - y_0}{2h} - \frac{y_2 - y_0}{2h} = F \tag{10.13}$$

Collecting terms involving common differences,

$$\left(\frac{1}{h^2} + \frac{1}{2h}\right)(y_1 - y_0) + \left(\frac{1}{h^2} - \frac{1}{2h}\right)(y_2 - y_0) = F \qquad (10.14)$$

or in terms of analogous voltages for a typical node of the type shown in Fig. 10.4a,

$$\frac{V_1 - V_0}{R_1} + \frac{V_2 - V_0}{R_2} = I_0 \qquad (10.15)$$

Comparing Eqs. (10.15) and (10.14), the magnitudes of the electrical parameters are seen to be

$$\frac{1}{R_1} = \frac{1}{h^2} + \frac{1}{2h} \qquad (10.16)$$

$$\frac{1}{R_2} = \frac{1}{h^2} - \frac{1}{2h} \qquad (10.17)$$

$$I_0 = F \qquad (10.18)$$

The term $1/2h$ in Eqs. (10.16) and (10.17) is due to the presence of the first derivative in Eq. (10.12). The fact that it is added in Eq. (10.16)
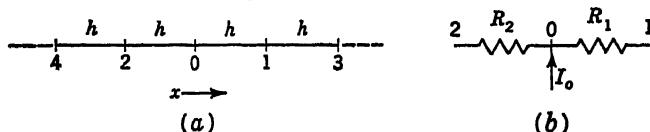
Fig. 10.6

and subtracted from Eq. (10.17) is of considerable significance because this means that the conductances connecting the nodes ("series" conductances) have different values, depending on which ends of the conductances are being considered as the node. Thus, in Fig. 10.6, with the node at the right of R_2, the value of $1/R_2$ is given by Eq. (10.17). When the left end R_2 is considered to be the node, then the value of R_2 is

$$\frac{1}{R_2} = \frac{1}{h^2} + \frac{1}{2h} \qquad (10.19)$$

A conductance which has unequal values depending on whether it is viewed from one end or the other is termed "unilateral." If its value is the same regardless of the end from which it is viewed, it is "bilateral." For numerical methods of analysis, no difficulty is introduced by the presence of unilateral conductances. If, however, it is desired to represent the finite-difference equation in the form of a physical electrical circuit, special consideration must be given to unilateral elements.

The simplest method, presented by Johnson,[4] for obtaining bilateral values in the present case is to introduce multiplying factors into the

equations for each node. Suppose the equation for node 2, Fig. 10.6a, be written out

$$\left(\frac{1}{h^2} + \frac{1}{2h}\right)(y_0 - y_2) + \left(\frac{1}{h^2} - \frac{1}{2h}\right)(y_4 - y_2) = F \qquad (10.20)$$

Equation (10.20) can be multiplied through by a constant K_2 without changing its significance. Similarly, Eq. (10.14) can be multiplied through by a constant K_0. If the constants are so chosen that their ratio is given by

$$\frac{K_2}{K_0} = \frac{(1/h^2) - (1/2h)}{(1/h^2) + (1/2h)} \qquad (10.21)$$

then

$$\frac{1}{R_2} = \left(\frac{1}{h^2} - \frac{1}{2h}\right)K_0 \qquad (10.22)$$

regardless of which end of R_2 is taken as the node. Factors can be chosen in the same manner for all the nodes of the network. Since only the ratios of the factors are involved and not their magnitudes, a convenient choice can be made for the initial node and then the factors for succeeding nodes obtained by ratios of the type given by Eq. (10.21).

A method for obtaining unilateral conductances when necessary (as

Fig. 10.7

with simultaneous differential equations discussed subsequently) consists in introducing isolating cathode-follower stages between nodes as shown in Fig. 10.7a, as suggested by E. L. Cordell. The voltage at node A is closely reproduced at the cathode of tube 1. Similarly, the voltage at node B is reproduced at the cathode of tube 2. When located at node A, an observer views the resistance R_A; when located at node B, he views R_B.

Two-stage, unity-voltage-ratio, isolating power amplifiers can be used in much the same manner as the cathode followers for obtaining unilateral resistances. The circuit is shown in Fig. 10.7b. By appropriate feedback connections, the voltages at A' and B' are maintained equal to those at A and B, respectively. An observer at A then sees the resistance R_A, while one at B sees the resistance R_B.

Positive conductances are represented by simple resistors. Consequently, it is desirable to keep the coefficients in Eq. (10.14) positive if
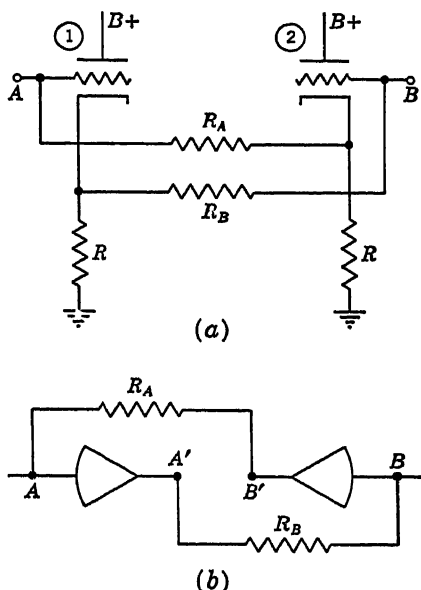
possible. If negative resistors are required, active electronic circuits will be necessary. A method for synthetizing such negative circuit elements using electronic analog-computer units is described in Sec. 10.13. Another means for introducing positive and negative impedances or admittances has been mentioned in the preceding chapter. This involves the use of constant-frequency alternating current and capacitors for positive admittances, inductors for negative admittances, or vice versa.

10.3. Nonlinear Ordinary Differential Equation. If some of the terms of the differential equation under study have coefficients which are themselves functions of the dependent or independent variables of the problem, these terms can also be simulated by introducing currents of suitable magnitudes at each node of the network. If the magnitudes of the currents depend upon the dependent variable, the solution of the equation must be known before the correct current can be determined. One must resort therefore to a series of successive approximations in which the first measurement of the voltage distribution along the network nodes leads to a first adjustment of the current inputs. This, in turn, leads to a new distribution of voltages, which are used for further adjustment of current inputs. The procedure is continued until the current input and the voltage distributions match, in accordance with the specified nonlinear terms.

As an example of a relatively complex ordinary differential equation, consider

$$\frac{d^2y}{dx^2} + f(x)\frac{dy}{dx} - ky + F(x,y) = 0 \tag{10.23}$$

whose finite-difference form is

$$\frac{y_1 - y_0}{h^2} + \frac{y_2 - y_0}{h^2} + \frac{f_0}{2h}(y_1 - y_0) - \frac{f_0}{2h}(y_2 - y_0) - ky_0 + F(x_0,y_0) = 0 \tag{10.24}$$

which can be arranged as

$$\left(\frac{1}{h^2} + \frac{f_0}{2h}\right)(y_1 - y_0) + \left(\frac{1}{h_2} - \frac{f_0}{2h}\right)(y_2 - y_0) - ky_0 + F(x_0,y_0) = 0 \tag{10.25}$$

The term ky_0 is simulated by connecting a resistor $R_0 = 1/k$ from each network node to ground. The feed-in currents at node 0 are made equal to $f(x_0,y_0)$, and the series resistances are given by

$$\frac{1}{R_1} = \frac{1}{h_2} + \frac{f_0}{2h} \tag{10.26}$$

$$\frac{1}{R_2} = \frac{1}{h^2} - \frac{f_0}{2h} \tag{10.27}$$

These are now multiplied by suitable multiplying factors to permit the use of bilateral circuit elements.

If boundary conditions are specified as prescribed voltages at both ends of the interval over which the equation is to be solved, it is only necessary to supply the end nodes of the network with these voltages. As an example, a six-section network for Eq. (10.23) is shown in Fig. 10.8. It consists of five nodes and two terminals. The boundary conditions call
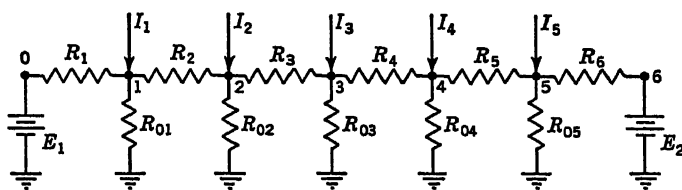
Fig. 10.8

for voltages E_1 at $x = 0$ and E_2 at $x = L$. In this circuit $h = L/6$. Starting with node 1, the appropriate conductances and currents are

$$\frac{1}{R_1} = K_1\left(\frac{1}{h_2} - \frac{f_1}{2h}\right) \qquad \frac{1}{R_2} = K_1\left(\frac{1}{h^2} + \frac{f_1}{2h}\right) \qquad \frac{1}{R_{01}} = K_1 k$$

$$I_1 = K_1 F(x_1, y_1) \qquad \frac{1}{R_3} = K_2\left(\frac{1}{h^2} + \frac{f_2}{2h}\right) \qquad \frac{1}{R_{02}} = K_2 k$$

$$I_2 = K_2 F(x_2, y_2) \qquad \frac{1}{R_4} = K_3\left(\frac{1}{h^2} + \frac{f_3}{2h}\right) \qquad \frac{1}{R_{03}} = K_3 k \qquad (10.28)$$

$$I_3 = K_3 F(x_3, y_3) \qquad \frac{1}{R_5} = K_4\left(\frac{1}{h^2} + \frac{f_4}{2h}\right) \qquad \frac{1}{R_{04}} = K_4 k$$

$$I_4 = K_4 F(x_4, y_4) \qquad \frac{1}{R_6} = K_5\left(\frac{1}{h^2} + \frac{f_5}{2h}\right) \qquad \frac{1}{R_{05}} = K_5 k$$

$$I_5 = K_5 F(x_5, y_5)$$

In these equations K_1 may have any convenient value. Once this has been selected, the remaining Ks have definite values related to it. Thus

$$K_2 = \frac{K_1[(1/h^2) + (f_1/2h)]}{(1/h^2) - (f_2/2h)} \qquad K_3 = \frac{K_2[(1/h^2) + (f_2/2h)]}{(1/h^2) - (f_3/2h)}$$

$$K_4 = \frac{K_3[(1/h^2) + (f_3/2h)]}{(1/h^2) - (f_4/2h)} \qquad K_5 = \frac{K_4[(1/h^2) + (f_4/2h)]}{(1/h^2) - (f_5/2h)} \qquad (10.29)$$

If the boundary conditions specify both the dependent variable and its first derivative at the start of the interval of integration, the settings on the electrical network are not so easily made. The voltage E_2 in this case may be made variable and adjusted until the voltage difference across the first interval h provides the correct first derivative $(V_1 - V_0)/h$. This means that an additional adjustment must be coordinated with the current adjustments I_1 to I_5.

10.4. Simultaneous Ordinary Differential Equations. When dealing with a set of simultaneous ordinary differential equations, a separate network is developed for each dependent variable. The coefficients of the coupling terms in the equations appear in the admittances coupling the networks to each other. This type of an arrangement restricts the form of the coupling between equations to that proportional to the difference of the dependent variables. A set of, say, three simultaneous equations of the following form may be represented:

$$\frac{d^2\phi}{dx^2} + f(x)\frac{d\phi}{dx} - k_1\phi - A_1(\phi - \psi) - A_2(\phi - \eta) + F_1(x,\phi,\psi,\eta) = 0$$

$$\frac{d^2\psi}{dx^2} + f_2(x)\frac{d\psi}{dx} - k_2\psi - A_3(\psi - \phi) - A_4(\psi - \eta) + F_2(x,\phi,\psi,\eta) = 0$$

$$\text{(10.30)}$$

$$\frac{d^2\eta}{dx^2} + f_3(x)\frac{d\eta}{dx} - k_3\eta - A_5(\eta - \phi) - A_6(\eta - \psi) + F_3(x,\phi,\psi,\eta) = 0$$

The finite-difference forms of these equations may be written directly from Eq. (10.25) with the addition of the difference terms and a change in the nonlinear terms to include the other dependent variables. A typical triple node for these equations is shown in Fig. 10.9. With 0 in the ϕ network as node,
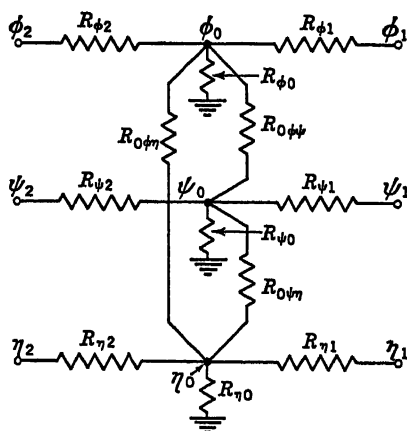
Fig. 10.9

$$\frac{1}{R_{\phi 1}} = \frac{1}{h^2} + \frac{f_{10}}{2h}$$

$$\frac{1}{R_{\phi 2}} = \frac{1}{h^2} - \frac{f_{10}}{2h}$$

$$\frac{1}{R_{\phi 0}} = k_1 \qquad \text{(10.31)}$$

$$I_{\phi 0} = F_1(x_0,\phi_0,\psi_0,\eta_0)$$

Similar relations may be written for 0 in the ψ network and for 0 in the η network. Since the same independent variable applies to all equations, the same interval h must be used in all three networks, and the points 0 must be corresponding nodes in the three networks. The coupling conductances between the networks are the reciprocals of the resistances $R_{0\phi\psi}$ between the ϕ and ψ networks, $R_{0\phi\eta}$ between the ϕ and η networks, and $R_{0\psi\eta}$ between the ψ and η networks. Their values are

$$\frac{1}{R_{0\phi\psi}} = A_1 \text{ or } A_3 \qquad \frac{1}{R_{0\phi\eta}} = A_2 \text{ or } A_5 \qquad \frac{1}{R_{0\psi\eta}} = A_4 \text{ or } A_6 \quad \text{(10.31a)}$$

In linearly coupled systems the coupling coefficients are equal. Namely,

$A_1 = A_3$, $A_2 = A_5$, and $A_4 = A_6$. Under the circumstances it might appear offhand that the coupling conductances would be bilateral. However, it should be remembered that the series conductances in each network are unilateral and that they are made bilateral only by means of a multiplying factor at each node. Because $f_1(x)$, $f_2(x)$, and $f_3(x)$ are different functions, a different multiplying factor would be needed at the same nodal location in the three networks. Thus the coupling conductances would become unilateral after the multiplication, even if they were bilateral before. To solve simultaneous differential equations, therefore, devices like those in Fig. 10.7, at least for the coupling conductances of the network, are required.

The adjustment of the currents corresponding to the nonlinear terms of the equation must follow the same successive approximations procedure described in connection with the single equation, except that any given current now depends on voltage values at three nodes instead of at only one. This, of course, greatly multiplies the problems of adjustment.

10.5. Laplace's and Poisson's Equations in Cartesian Coordinates. Two- and three-dimensional equations of the form

$$\nabla^2 \phi = f \tag{10.32}$$

occur frequently in engineering applications involving field problems of various types, e.g., stress fields, thermal fields, fluid-flow fields, electric fields, etc. The reason for the wide occurrence of Eq. (10.32) is that it expresses the condition of equilibrium, or continuity, in continuous systems in which force, flow rate, or current density can be expressed as the gradient of a potential function. For example, if u and v are flow rates in the x and y directions, respectively, at a point x, y in a given area and we can express them as

$$u = -k \frac{\partial \phi}{\partial x} \qquad v = -k \frac{\partial \phi}{\partial y} \tag{10.33}$$

then, for an element $dx\, dy$ of the area, the flow at x across the edge dy is $-k(\partial\phi/\partial x)\, dy$, that at $x + dy$ across dy is $-k[\partial\phi/\partial x + (\partial^2\phi/\partial x^2)\, dx]\, dy$, and the net quantity stored in $dx\, dy$ due to flow in the x direction is the difference, yielding, $k(\partial^2\phi/\partial x^2)\, dx\, dy$. Similarly, the net quantity stored in $dx\, dy$ due to flow in the y direction is $k(\partial^2\phi/\partial y^2)\, dx\, dy$. If no accumulation is to be permitted in $dx\, dy$, the outflow must equal the inflow, with the result that

$$\frac{\partial^2\phi}{\partial x^2} + \frac{\partial^2\phi}{\partial y^2} = 0 \tag{10.34}$$

If, in addition to flow across the boundaries, there is a sink of strength f per unit of area, the accumulation due to flow across the boundaries is

absorbed in the sink, so that Eq. (10.34) becomes

$$\frac{\partial^2\phi}{\partial x^2} + \frac{\partial^2\phi}{\partial y^2} = f \tag{10.35}$$

Thus Eq. (10.32) for rectangular coordinates in a two-dimensional field is

$$\nabla^2\phi = \frac{\partial^2\phi}{\partial x^2} + \frac{\partial^2\phi}{\partial y^2} = f(x,y) \tag{10.36}$$

For the three-dimensional field, it is

$$\nabla^2\phi = \frac{\partial^2\phi}{\partial x^2} + \frac{\partial^2\phi}{\partial y^2} + \frac{\partial^2\phi}{\partial z^2} = f(x,y,z) \tag{10.37}$$

In either case the function f is known, the boundary distribution of ϕ is known, and the problem is one of evaluating ϕ at all other points within the given region. Equation (10.32) is the Poisson equation. If the function f is everywhere zero, Eq. (10.32) reduces to the Laplace equation:

$$\nabla^2\phi = 0 \tag{10.38}$$

Considering, first, the two-dimensional Laplace equation, the numerical approach to its solution due to Liebmann[5] consists in developing a network of squares over the area in question and then by simple iterative steps satisfying the finite-difference equation at each network junction. Thus, the area in Fig. 10.10a is shown laid out in a network of squares of side h. If any junction (or node) within the boundaries of the area is labeled 0, and the four nearest neighbors 1, 2, 3, 4 as shown in the figure, Eq. (10.38) may be expressed as a linear algebraic relation between the values of ϕ at the five nodes. In accordance with procedures already discussed, we may write the approximations:

$$\left(\frac{\partial^2\phi}{\partial x^2}\right)_0 \approx \frac{\phi_1 + \phi_3 - 2\phi_0}{h^2} \qquad \left(\frac{\partial^2\phi}{\partial y^2}\right)_0 \approx \frac{\phi_2 + \phi_4 - 2\phi_0}{h^2} \tag{10.39}$$

$$\left(\frac{\partial^2\phi}{\partial x^2} + \frac{\partial^2\phi}{\partial y^2}\right)_0 \approx \frac{\phi_1 + \phi_2 + \phi_3 + \phi_4 - 4\phi_0}{h^2} = 0 \tag{10.40}$$

Thus
$$\phi_0 = \frac{\phi_1 + \phi_2 + \phi_3 + \phi_4}{4} \tag{10.41}$$

This simple algebraic expression is to be satisfied at every interior point spaced a distance h from its nearest neighbors. Points near the boundary may have unequal spacing relative to the adjacent points because of curvature of the boundary, choice of the magnitude of h, or for some other reason. These points may be treated in one of two ways when using the square mesh. The simplest way is to fit the curved boundary with a

jagged line which maintains complete squares everywhere. The method is illustrated in Fig. 10.10b. Although this results in a change in the boundary configuration, the error introduced may be no greater than the approximation already involved in the finite-difference procedure. This method of fitting the boundaries has considerable appeal from the numerical manipulation standpoint because it involves no change in the basic equation, Eq. (10.41), even for points adjacent to the "curved" boundary.

(a)   (b)

(c)
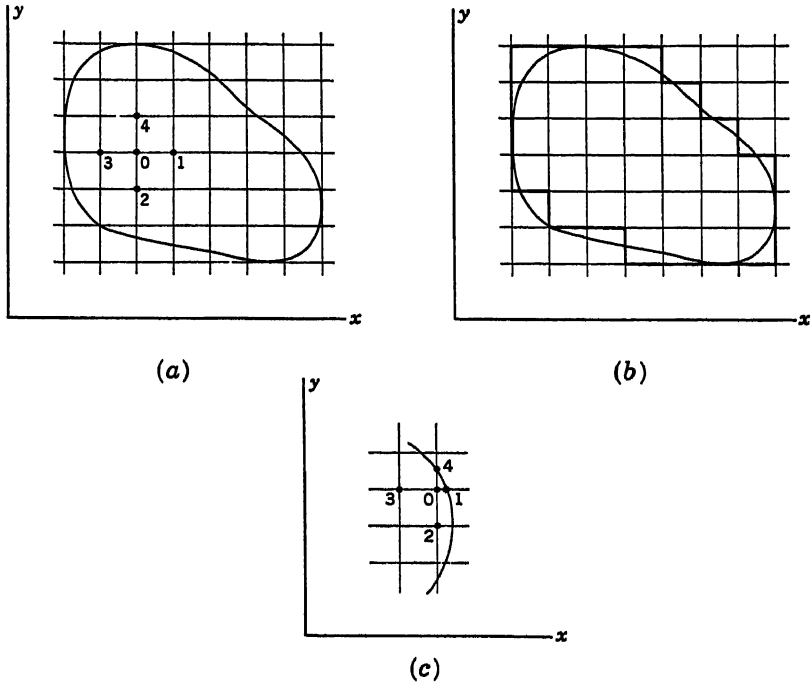
Fig. 10.10

If it appears desirable to maintain the network points on the actual boundary, Eq. (10.41) must be modified to account for decreased spacing. Referring to Fig. 10.10c, a section of a curved boundary is shown. The network point 0 is spaced distances ah and bh from points 1 and 4, respectively, where a and b are less than unity. The first derivatives at the mid-points of 0-2 and 0-3 are the same as before, namely, $(\phi_0 - \phi_2)/h$ and $(\phi_0 - \phi_3)/h$. The first derivatives at the mid-points of 0-1 and 0-4 are, approximately, $(\phi_1 - \phi_0)/ah$ and $(\phi_4 - \phi_0)/bh$. In determining the value of the second derivative at 0, the approximate approach is to assume that the second derivative is constant along x from the mid-point of 0-3 to that of 0-1 and is given by the difference in the first derivatives

at these points divided by the distance between.   Thus

$$\left(\frac{\partial^2 \phi}{\partial x^2}\right)_0 \approx \frac{[(\phi_1 - \phi_0)/ah] - [(\phi_0 - \phi_3)/h]}{(h/2) + (ah/2)} \tag{10.42}$$

Similarly,

$$\left(\frac{\partial^2 \phi}{\partial y^2}\right)_0 \approx \frac{[(\phi_4 - \phi_0)/bh] - [(\phi_0 - \phi_2)/h]}{(h/2) + (bh/2)} \tag{10.43}$$

Since the sum of the second derivatives must be zero to satisfy Laplace's equation, the above gives

$$\frac{\phi_1 - \phi_0}{a(1 + a)} - \frac{\phi_0 - \phi_3}{1 + a} + \frac{\phi_4 - \phi_0}{b(1 + b)} - \frac{\phi_0 - \phi_2}{1 + b} = 0 \tag{10.44}$$

from which[6]

$$\phi_0 = \frac{ab}{a + b}\left[\frac{\phi_1}{a(1 + a)} + \frac{\phi_2}{1 + b} + \frac{\phi_3}{1 + a} + \frac{\phi_4}{b(1 + b)}\right] \tag{10.45}$$

In the numerical application of this method to the solution of Laplace's equation for a specific problem, the true values of ϕ must be known around the boundaries involved and hence may be written down for all the network intersection points on the boundary. To start the iterative process going, values are either estimated or arbitrarily assigned for all interior points. The value at each interior point is then readjusted in accordance with the improvement formula Eq. (10.41) or, where necessary, Eq. (10.45). After the first corrective traverse of all points, the calculated values on the average are nearer the correct values. By repeating the corrective procedure over and over again, the values tend to stationary values which give the approximate solution to the Laplace equation. The error of the solution is proportional to h^2, so that doubling the number of squares into which a given area is divided tends to reduce the error by a factor of 4. With the smaller interval, however, the labor of obtaining a solution goes up by a similar factor. Various schemes have been devised to speed up the rate of convergence of the numerical process. For these the reader is referred to the literature.[1,2,6,7]

An electrical network may be devised which will perform the iterations instantaneously and provide the values of ϕ at the nodes as voltage readings.[8,9] Suppose the network of equal lines in Fig. 10.10b be replaced by a network of equal resistors. With voltages applied to the boundary points, currents will be instantly established and the network points will acquire steady values of voltage. Either direct or alternating current may be used. The relations between the voltages may be determined by summing the currents at a node. If a point 0 and its four nearest neighbors are connected by four resistances R (Fig. 10.11a), the currents

flowing through the resistors, and the sum of the currents at the node 0 are given in terms of the voltages as follows:

$$i_1 - i_2 - i_3 + i_4 = 0$$

or

$$\frac{V_1 - V_0}{R} - \frac{V_0 - V_2}{R} - \frac{V_0 - V_3}{R} + \frac{V_4 - V_0}{R} = 0 \qquad (10.46)$$

From which

$$V_0 = \frac{V_1 + V_2 + V_3 + V_4}{4} \qquad (10.47)$$

The analogy between Eqs. (10.47) and (10.41) is evident. The simple resistance network to solve Laplace's equation must have the same geometrical form as the grid overlay on the given area, for example, as in
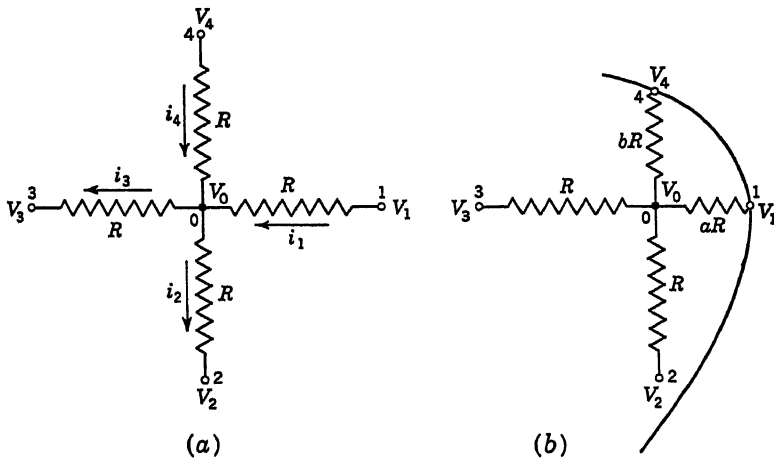
Fig. 10.11

Fig. 10.10b. The voltages applied to the boundary nodes must be proportional to the values of ϕ on the actual boundary. Since the Laplace equation is linear, the interior voltage values will bear the same ratio to the interior values of ϕ as do the boundary voltages to the boundary values of ϕ.

To represent curved boundaries more faithfully in the analog, the resistances corresponding to the shortened lines of the network may be correspondingly reduced in magnitude. Thus the resistors replacing the network lines of Fig. 10.10c are shown in Fig. 10.11b, with aR and bR (a and b both less than unity) being the resistance values from 0 to the boundary points 1 and 4, respectively. The current summation at the node 0 for this particular point is

$$\frac{V_1 - V_0}{aR} - \frac{V_0 - V_2}{R} - \frac{V_0 - V_3}{R} + \frac{V_4 - V_0}{bR} = 0 \qquad (10.48)$$

from which

$$V_0 = \frac{ab}{a + 2ab + b}\left(\frac{V_1}{a} + V_2 + V_3 + \frac{V_4}{b}\right) \tag{10.49}$$

Equation (10.49) differs some from Eq. (10.45) because the resistance network does not conform exactly to the restraints imposed on the system by the numerical procedure used in deriving Eq. (10.45). The resistances meeting at node 0 in Fig. 10.11b form a weighted averaging circuit. If in Eq. (10.45) each of the factors $1 + a$ and $1 + b$ occurring in the denominators be replaced by an average value given by $1 + \frac{1}{2}a + \frac{1}{2}b$, an equation identical with Eq. (10.49) will result.

The difference in values for ϕ_0 obtained from Eqs. (10.45) and (10.49) may be illustrated by substitution of numerical values. If $\phi_1 = \phi_2 = \phi_3 = \phi_4$, both equations give ϕ_0 the same value, as they should, for all values of a and b. If $\phi_1 = 3$, $\phi_2 = 2$, $\phi_3 = 4$, and $\phi_4 = 1$, for $a = \frac{1}{4}$ and $b = \frac{3}{4}$, Eq. (10.45) yields $\phi_0 = 2.76$, while Eq. (10.49) yields $\phi_0 = 2.63$. If $a = \frac{3}{4}$ and $b = \frac{1}{4}$, keeping the same values for $\phi_1 - \phi_4$, Eq. (10.45) yields $\phi_0 = 1.76$, while Eq. (10.49) yields $\phi_0 = 1.91$.

Since the resistance network simulates the actual field problem more closely than does the numerical process near the boundaries, Eq. (10.49) is probably more accurate than (10.45).
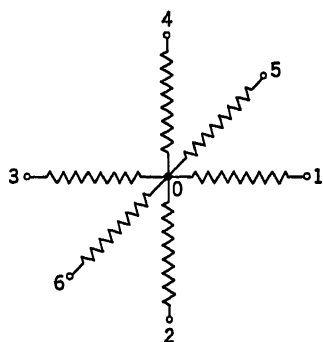
Fig. 10.12

The extension of the two-dimensional network to three dimensions is easily accomplished, the most important factor being the multiplication of the number of resistances required. A typical node for such a network is shown in Fig. 10.12. The numerical procedure yields (for uniform spacing h in the three directions)

$$\left(\frac{\partial^2\phi}{\partial x^2} + \frac{\partial^2\phi}{\partial y^2} + \frac{\partial^2\phi}{\partial z^2}\right)_0 \approx \frac{\phi_1 + \phi_2 + \phi_3 + \phi_4 + \phi_5 + \phi_6 - 6\phi_0}{h^2} = 0 \tag{10.50}$$

or

$$\phi_0 = \frac{1}{6}(\phi_1 + \phi_2 + \phi_3 + \phi_4 + \phi_5 + \phi_6) \tag{10.51}$$

Equation (10.51) is also the relation between the voltages in the resistive network of Fig. 10.12. At irregular boundaries the network resistors may be reduced in value in proportion to the shortening of the corresponding lines of the latticework drawn through the solid, or the same device may be used in the three-dimensional system as is shown in Fig. 10.10b for a two-dimensional system.

In the application of the finite difference approach to Poisson's equa-

tion, the first part of Eq. (10.40) still holds. However, instead of being equal to zero, this expression is equal to $f(x_0,y_0)$. Thus the Poisson equation in finite difference form for Fig. 10.10a is

$$\left(\frac{\partial^2\phi}{\partial x^2} + \frac{\partial^2\phi}{\partial y^2}\right)_0 \approx \frac{\phi_1 + \phi_2 + \phi_3 + \phi_4 - 4\phi_0}{h^2} = f(x_0,y_0) \quad (10.52)$$

from which

$$\phi_0 = \frac{\phi_1 + \phi_2 + \phi_3 + \phi_4 - h^2 f(x_0,y_0)}{4} \quad (10.53)$$

The numerical procedures occur as for the Laplace equation, but taking into account the term $f(x,y)$, which may vary from point to point. Electrically, the term $h^2 f(x_0,y_0)$ may be included in the analog as a feed-in current. The sum of the currents flowing through the equal resistors R of Fig. 10.11a is no longer equal to zero, but to a current I being drained from node 0. Equation (10.46) thus becomes

$$\frac{V_1 + V_2 + V_3 + V_4 - 4V_0}{R} = I \quad (10.54)$$

or

$$V_0 = \frac{V_1 + V_2 + V_3 + V_4 - RI}{4} \quad (10.55)$$

Consequently, for the analogy to hold between the numerical result required in Eq. (10.53) and the electric volt-
age obtained in Eq. (10.55), we see that

$$RI = h^2 f(x_0,y_0) \quad \text{or} \quad I = \frac{h^2}{R} f(x_0,y_0)$$
$$(10.56)$$

A typical node for this circuit is shown in Fig. 10.13.

Fig. 10.13

For nodes near boundaries where the network spacing is incomplete (Fig. 10.10c), the current withdrawn should be less than that given by Eq. (10.56). Since the current must be proportional to the area served by a given node, the current flowing from the node in Fig. 10.11b may be taken as

$$I = \frac{h^2(1 + a)(1 + b)}{4R} f(x_0,y_0) \quad (10.57)$$

When $a = b = 1$, Eq. (10.57) becomes Eq. (10.56).

Usually some scale factor would be involved in setting up the boundary voltages to represent the boundary values of ϕ. The same scale factor would also apply to the current I. The discussion of scale factors given
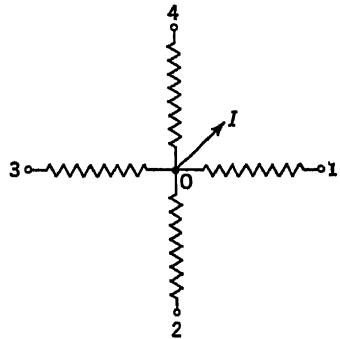
in Sec. 11.6 for the membrane analogy is equally valid for the network analogy.

In a practical application of the network to a solution of Poisson's equation, the adjustment of the currents I to their required values may present a problem unless interactions between the various current
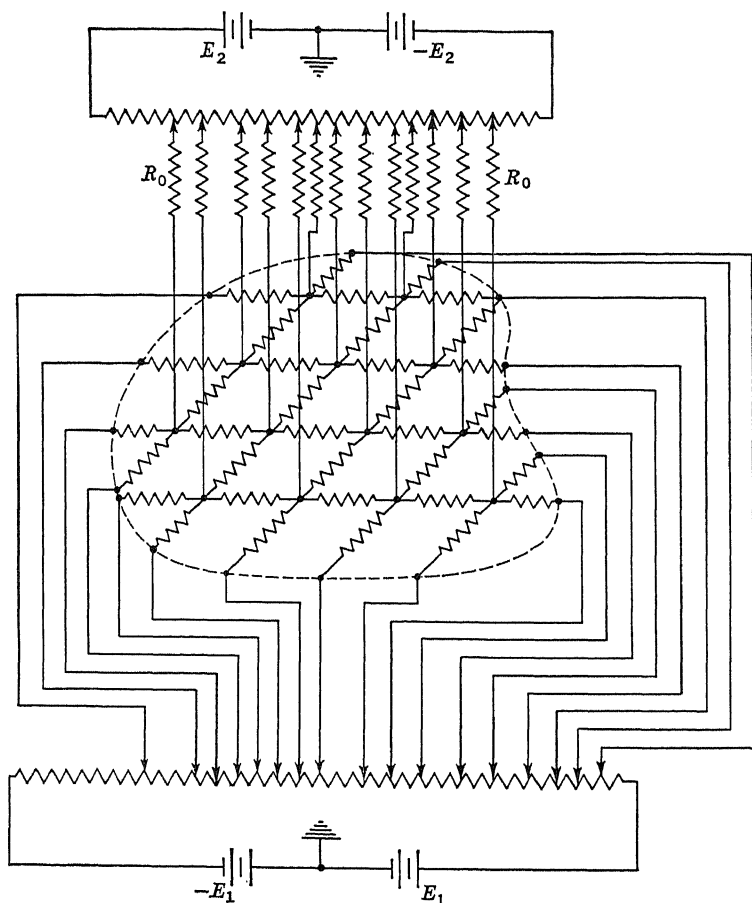
Fig. 10.14

sources (or sinks) are avoided. This may be done if the interconnected resistors R have low values while the currents I are introduced to the nodes through nodal resistors R_0 having values many times R. Then the possible variations in voltage within the network would be small compared to the voltage drops through the nodal resistors, and the currents could be adjusted to the required values from node to node without the necessity of successive readjustments due to interactions. A network illustrating this execution of the analogy is shown in Fig. 10.14. The area

of interest is shown as a dotted line, and the resistance network representing it (a very coarse network is shown for clarity) is contained within the boundaries. A battery E_1, through a low-resistance voltage divider, supplies boundary potentials to the loose ends of the network resistors. Since they may be either plus or minus, the source E_1 is arranged to provide both positive and negative voltages. Another battery E_2, also through a low-resistance voltage divider, supplies current to the nodal resistors R_0. R_0 might be conveniently taken as $100R$ or $1,000R$. The correct amount of current flowing through each R_0 is obtained by connecting R_0 to the appropriate point on the voltage divider. When the various currents are switched on, the voltage readings at the nodes immediately supply the solution to Poisson's equation in two dimensions. The extension to three dimensions is straightforward.

The accuracy of finite-difference solutions of partial differential equations may be improved by taking into account a fourth-order corrective term directly, as proposed by Fox,[10] or by using first a coarse net, then a net with spacing halved, and then extrapolating the results to values they would have if the spacing were halved again. The latter method, due to Richardson,[11] is often more convenient both in numerical applications and in electrical network applications of finite differences. Liebmann[9] discusses the effect of resistor tolerance on errors.

10.6. Laplace's Equation in Curvilinear Coordinates. In this section the discussion will be restricted to cylindrical coordinates and the two special cases of cylindrical coordinates, namely, polar coordinates and axial symmetry. Laplace's equation in cylindrical coordinates is easily derived if one bears in mind the physical significance of the equation. More generally, Laplace's equation in any set of orthogonal curvilinear coordinates[12] is given by

$$\nabla^2 \phi = \frac{1}{h_1 h_2 h_3} \left[\frac{\partial}{\partial q_1} \left(\frac{h_2 h_3}{h_1} \frac{\partial \phi}{\partial q_1} \right) + \frac{\partial}{\partial q_2} \left(\frac{h_3 h_1}{h_2} \frac{\partial \phi}{\partial q_2} \right) + \frac{\partial}{\partial q_3} \left(\frac{h_1 h_2}{h_3} \frac{\partial \phi}{\partial q_3} \right) \right] \quad (10.58)$$

where h_1, h_2, h_3, and q_1, q_2, q_3 are defined through linear distances along each of the coordinate lines. Thus, if ds_1, ds_2, and ds_3 are these distances,

$$ds_1 = h_1 \, dq_1 \qquad ds_2 = h_2 \, dq_2 \qquad ds_3 = h_3 \, dq_3 \qquad (10.59)$$

For cylindrical coordinates r, θ, z, Eqs. (10.59) are $ds_1 = dr$, $ds_2 = r \, d\theta$, $ds_3 = dz$ so that $h_1 = 1$, $h_2 = r$, $h_3 = 1$. A substitution into Eq. (10.58) yields for this case

$$\frac{1}{r} \left[\frac{\partial}{\partial r} \left(r \, \frac{\partial \phi}{\partial r} \right) + \frac{1}{r} \frac{\partial^2 \phi}{\partial \theta^2} + r \frac{\partial^2 \phi}{\partial z_2} \right] = 0 \qquad (10.60)$$

A direct application of the condition of continuity to an elementary volume in cylindrical coordinates might provide a better physical under-

standing of this important form of Laplace's equation. Thus, referring to Fig. 10.15, the flow quantity across the face $r \, d\theta \, dz$ is

$$-k \frac{\partial \phi}{\partial r} r \, d\theta \, dz$$

The flow across the face $(r + dr) \, d\theta \, dz$ is

$$-k \left(\frac{\partial \phi}{\partial r} + \frac{\partial^2 \phi}{\partial r^2} dr \right) (r + dr) \, d\theta \, dz$$

Fig. 10.15

The net quantity remaining in the elementary volume is the difference, given by

$$k \left[r \frac{\partial^2 \phi}{\partial r^2} + \frac{\partial \phi}{\partial r} \right] dr \, d\theta \, dz \quad (10.61)$$

The flow quantities in and out of the elementary volume through the faces $r \, d\theta \, dr$ are

$$-k \frac{\partial \phi}{\partial z} r \, d\theta \, dr \qquad \text{and} \qquad -k \left(\frac{\partial \phi}{\partial z} + \frac{\partial^2 \phi}{\partial z^2} dz \right) r \, d\theta \, dr$$

The net amount remaining is

$$k \frac{\partial^2 \phi}{\partial z^2} r \, dr \, d\theta \, dz \tag{10.62}$$

Similarly, the flow quantities through the faces $dr \, dz$ are

$$-k \frac{\partial \phi}{r \, \partial \theta} dr \, dz \qquad \text{and} \qquad -k \left(\frac{\partial \phi}{r \, \partial \theta} + \frac{\partial^2 \phi}{r^2 \, \partial \theta^2} r \, d\theta \right) dr \, dz$$

The net amount remaining is

$$k \frac{\partial^2 \phi}{r^2 \, \partial \theta^2} r \, dr \, d\theta \, dz \qquad (10.63)$$

Since nothing is to be left behind, the sum of Eqs. (10.61) to (10.63) must equal zero, and Eq. (10.60) is obtained.

For polar coordinates, the function ϕ is independent of z, so that Eq. (10.60) reduces to

$$\frac{1}{r} \frac{\partial}{\partial r} \left(r \frac{\partial \phi}{\partial r} \right) + \frac{\partial^2 \phi}{r^2 \, \partial \theta^2} = 0 \quad (10.64)$$

Fig. 10.16

For axial symmetry, the function ϕ is independent of θ, so that Eq. (10.60) reduces to

$$\frac{1}{r} \frac{\partial}{\partial r} \left(r \frac{\partial \phi}{\partial r} \right) + \frac{\partial^2 \phi}{\partial z^2} = 0 \tag{10.65}$$

To convert Eq. (10.60) into finite-difference form, a grid of uniformly spaced points is chosen along the r, θ, and z axes. Figure 10.16 is an end
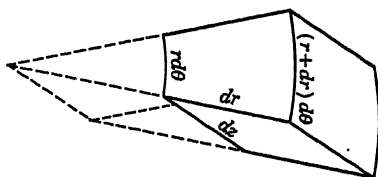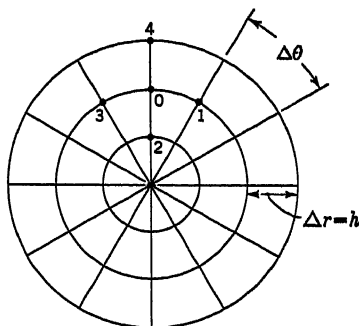
view of the grid, showing the points spaced a distance h apart along r and $r \, \Delta\theta$ apart circumferentially. The points are also spaced a distance h apart in the z direction. For these points, we have the approximate relations

$$\left(r \, \frac{\partial\phi}{\partial r} \right)_{0-4} = \left(r_0 + \frac{h}{2} \right) \frac{\phi_4 - \phi_0}{h} \tag{10.66}$$

$$\left(r \, \frac{\partial\phi}{\partial r} \right)_{2-0} = \left(r_0 - \frac{h}{2} \right) \frac{\phi_0 - \phi_2}{h} \tag{10.67}$$

$$\frac{\partial}{\partial r} \left(r \, \frac{\partial\phi}{\partial r} \right)_0 = \frac{2r_0 + h}{2h^2} (\phi_4 - \phi_0) - \frac{2r_0 - h}{2h^2} (\phi_0 - \phi_2) \tag{10.68}$$

$$\left(\frac{\partial\phi}{r \, \partial\theta} \right)_{0-1} = \frac{\phi_1 - \phi_0}{r_0 \, \Delta\theta} \tag{10.69}$$

$$\left(\frac{\partial\phi}{r \, \partial\theta} \right)_{3-0} = \frac{\phi_0 - \phi_3}{r_0 \, \Delta\theta} \tag{10.70}$$

$$\left(\frac{\partial^2\phi}{r^2 \, \partial\theta^2} \right)_0 = \frac{1}{r^2 \, \Delta\theta^2} (\phi_1 - \phi_0) - \frac{1 \cdot}{r^2 \, \Delta\theta^2} (\phi_0 - \phi_3) \tag{10.71}$$

$$\left(\frac{\partial^2\phi}{\partial z^2} \right)_0 = \frac{1}{h_2} (\phi_5 - \phi_0) - \frac{1}{h^2} (\phi_0 - \phi_6) \tag{10.72}$$

The finite-difference form of Eq. (10.60) is, therefore,

$$\frac{1}{r_0} \left[\frac{2r_0 + h}{2h^2} (\phi_4 - \phi_0) - \frac{2r_0 - h}{2h^2} (\phi_0 - \phi_2) + \frac{\phi_1 - \phi_0}{r_0 \, \Delta\theta^2} \right.$$
$$\left. - \frac{\phi_0 - \phi_3}{r_0 \, \Delta\theta^2} + \frac{r_0(\phi_5 - \phi_0)}{h^2} - \frac{r_0(\phi_0 - \phi_6)}{h^2} \right] = 0 \tag{10.73}$$

If the ϕs of Eq. (10.73) are to be represented by voltages in a resistance network, the coefficients in this equation must be the conductances of the network. A typical node of the network is shown in Fig. 10.17. With current flows as indicated by the arrows, the sum of the currents at the node is

$$\frac{V_4 - V_0}{R_4} - \frac{V_0 - V_2}{R_2} + \frac{V_1 - V_0}{R_1} - \frac{V_0 - V_3}{R_2} + \frac{V_5 - V_0}{R_5}$$
$$- \frac{V_0 - V_6}{R_6} = 0 \tag{10.74}$$

Thus

$$R_4 = \frac{2h^2 r_0}{2r_0 + h}$$

$$R_2 = \frac{2h^2 r_0}{2r_0 - h} \tag{10.75}$$

$$R_1 = R_3 = r_0{}^2 \, \Delta\theta^2$$
$$R_5 = R_6 = h^2$$

If sources or sinks are present in the element of Fig. 10.15, the extension of the network of Fig. 10.17 to include this factor is made as in the case for cartesian coordinates.

For polar coordinates, the distribution of resistances in the z direction is eliminated, the network becoming a two-dimensional network for which the typical node is that in Fig. 10.17 with R_5 and R_6 removed. For axial symmetry, there is no variation in the θ direction. Consequently, a two-dimensional network again results, representing a wedge of included angle $\Delta\theta$, the typical node being that of Fig. 10.17 with resistors R_1 and R_3 removed.
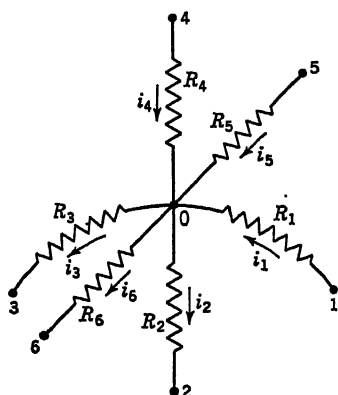
Fig. 10.17

10.7. The Diffusion Equation. One-, two-, and three-dimensional equations of the form

$$\nabla^2\phi = \frac{1}{\alpha}\frac{\partial\phi}{\partial t} \qquad (10.76)$$

where $\nabla^2\phi$ is the Laplacian of the potential function, are of particular importance in the study of heat transfer but occur also in the analysis of the flow of compressible fluids through porous media, the diffusion of particles in air, and numerous other applications. The most widely used network analogs for the solution of the diffusion equation[13-15] employ a dynamic analogy to simulate the time derivative in Eq. (10.76). The left-hand side of the diffusion equation is then represented in finite-difference form, but the right-hand side is retained as a time derivative. The finite-difference equation for node 0 in a typical one-dimensional system is

$$\frac{\phi_1 - \phi_0}{h^2} + \frac{\phi_2 - \phi_0}{h^2} = \frac{1}{\alpha}\frac{d\phi_0}{dt} \qquad (10.77)$$

and for a two-dimensional system

$$\frac{\phi_1 - \phi_0}{h^2} + \frac{\phi_2 - \phi_0}{h^2} + \frac{\phi_3 - \phi_0}{h^2} + \frac{\phi_4 - \phi_0}{h^2} = \frac{1}{\alpha}\frac{d\phi_0}{dt} \qquad (10.78)$$

where the subscripts 1, 2, 3, and 4 represent adjacent nodes in the x and the y directions. Just as in the simulation of Laplace's equation, the terms on the left side of Eqs. (10.77) and (10.78) represent current flow through resistors of magnitude h^2. The term on the right-hand side of these equations must therefore also be represented by a current. This is accomplished by connecting a capacitor of magnitude $1/\alpha$ from each network node to ground. Typical nodes of the network analog circuits

for Eqs. (10.77) and (10.78) are shown in Fig. 10.18a and b. Kirchhoff's current law then specifies for the one-dimensional case that

$$\frac{V_1 - V_0}{R} + \frac{V_2 - V_0}{R} = C\frac{dV_0}{dt} \qquad (10.79)$$

and for the two-dimensional case

$$\frac{V_1 - V_0}{R} + \frac{V_2 - V_0}{R} + \frac{V_3 - V_0}{R} + \frac{V_4 - V_0}{R} = C\frac{dV_0}{dt} \quad (10.80)$$

The formulation of engineering problems governed by the diffusion equation demands the specification of boundary conditions as well as initial conditions. The boundary conditions are, in general, similar to those specified for Laplace's equation and may include equipotential boundaries, streamline boundaries, and boundaries for which the normal
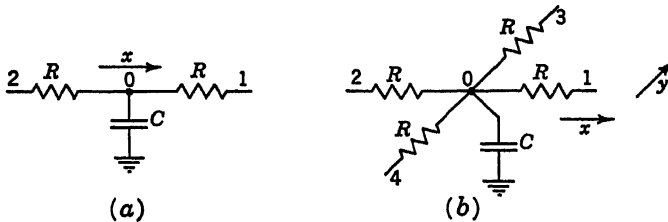
Fig. 10.18

derivative of the potential function is specified. In addition, the magnitude of the potential function at all points within the field must be specified for some instant of time (usually at $t = 0$). In analog terms, this involves the application of specified voltages to all the boundaries of the network and the charging of all capacitors to a specified initial voltage. The transient electrical voltages at each network node are then analogous to the transient potential at the corresponding points in the field being simulated. The time required for a specific diffusion process to go to completion in the electric analog depends on the magnitude of the RC product. In designing an electric analog for this type of problem it is necessary, therefore, to select a scale factor to relate time in the original system and time in the analog.

Just as in the case of the differential analyzers described in Chap. 6, there are two philosophies or approaches to the time scaling problem. Time constants may be selected to be of the order of several seconds or minutes. In that case, suitable switching devices are employed to give all capacitors the correct initial charge at time $t = 0$, and strip-chart or other "one-shot" output devices are employed to record the voltage transient at each node. On the other hand, time constants may be of the order of milliseconds, and initial conditions applied periodically many

times a second.   In that case, the transient voltage at each node can be displayed by means of a cathode-ray oscilloscope.   The latter repetitive network analyzers require special switching circuits to return the charge on each capacitor to its initial condition many times a second.   On the other hand, the small time constants required in repetitive computers permit the use of capacitors which have relatively small magnitudes and which are therefore less expensive and less subject to leakage errors.

In order to scale completely a network analog of a *thermal* system, it is necessary to select scale factors relating voltage and temperature, current and heat flux, electrical charge and thermal energy, electrical resistance and thermal resistance, electrical capacitance and thermal capacitance, and time for analog circuit and time for the thermal system. These scale factors are not independent but are related by three basic equations.   In the case of the electrical circuit, these equations include the following:

(a)
$$i = \frac{v}{R}$$

(b)
$$i = C\,\frac{dv}{dt}$$
(10.81)

(c)
$$i = \frac{dq}{dt}$$

Similar relations exist for the thermal circuits.   It is apparent, therefore, that only three of the six scale factors relating the thermal system to the electrical system can be independent.   It is also apparent that the three independent scale factors cannot be chosen arbitrarily.   For example, basic scale factors relating current, voltage, and resistance in the electrical system to the corresponding variables in the thermal system could not constitute an independent set, because all three of these quantities appear in Eq. (10.81a).   To assure complete independence of basic scale factors, the parameters and variables involved are divided into two groups:

(a)	(b)
Time	Voltage (temperature)
Resistance	Charge (heat energy)
Capacitance	Current (heat flux)

A basic requirement of the scaling process is that two scale factors be selected from group (a) and that only one be selected from group (b). Further limitations on the selection of scale factors are imposed by such practical considerations as the range of available power supplies, the magnitudes of available electrical circuit elements, and the characteristics of available input-output equipment.   Most frequently the scaling operation proceeds as follows:

A scale factor l is first selected to relate the node voltages of the electric circuit to the temperature of the corresponding points of the thermal system. A scale factor m is next chosen to relate the electrical and thermal capacitances. The third independent scale factor n is selected to relate time in the electric analog and the time in the thermal system. The three basic scale factors are defined by

$$v = lT$$
$$C_e = \frac{1}{m} Ct \qquad (10.82)$$
$$t_e = n\tau_t$$

where the subscripts e and t refer to the electrical and thermal systems respectively, v is the voltage, and T the temperature. Relationships

(a)

(b)
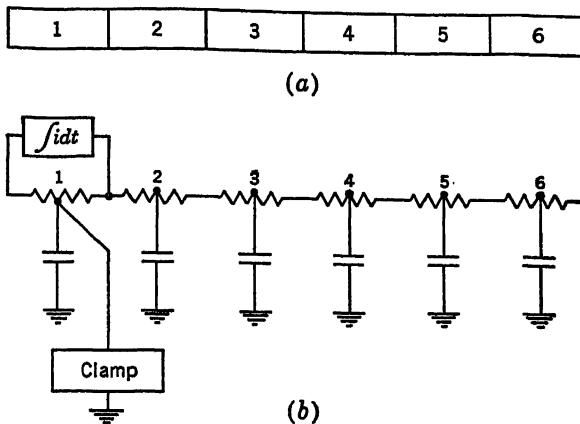
Fig. 10.19

between the other parameters and variables of the two systems in terms of l, n, and m, derived by dimensional analysis, are

$$i = \frac{l}{mn} q_t \qquad q_e = \frac{1}{m} Q_t \qquad R_e = mnR_t \qquad (10.83)$$

where q_t and Q_t represent, respectively, the rate of heat flow and the heat energy in the thermal system, while q_e is the stored charge in the electrical system. R_e and R_t are the electrical and thermal resistances, respectively. The scaling process for other types of field problems governed by the diffusion equation is accomplished in a manner similar to that described above for heat transfer problems.

Transient heat flow problems often involve not only thermal capacity but also heat of fusion. The melting of ice is an example.[16] Considering the case of one-dimensional heat flow again, Fig. 10.19a shows a block of

ice cut full depth from a slab. The left end of the block is subjected to a temperature above 32°F, and the progress of melting of the slab is to be observed.

In the finite-difference representation of the process, the block of ice is divided into a number of lumps, the thermal capacity of each lump being represented by a capacitor and its thermal resistance by an electric resistor, as in Fig. 10.19b. As heat flows into block 1 and raises its temperature to 32°F, block 1 is considered to remain at 32°F until it is entirely melted. The resulting block of water is then allowed to rise in temperature in accordance with its thermal capacity, meanwhile heating block 2 to 32°F. Block 2 remains at 32°F until melted before block 3 starts to melt. The process is repeated from block to block until the block of ice completely melts and the resulting water attains the desired temperature. Only conduction is considered in this analysis. Convection effects in the liquid are neglected.

In the electrical analog, when the voltage at node 1 reaches a value corresponding to 32°F, a clamping circuit keeps the voltage from going any higher. During the clamped period, the current flowing into 1, less that flowing into 2, is integrated. Since electric charge is analogous to quantity of heat, the clamping period lasts until the current integrator indicates the amount of charge corresponding to the heat of fusion of lump 1. At this point the clamping device is switched by a relay to node 2, the integrator discharged, and then switched across node 2 when the clamping device senses 32°F at this point. The process is thus repeated step by step until the last lump of ice is melted.

Liebmann[17,18] describes an interesting method for employing network analogs containing only resistors to simulate fields governed by the diffusion equation. His method is based upon the complete finite-difference expansion of Eq. (10.76). For fields in one space dimension,

$$\frac{\phi_1 - \phi_0}{\Delta x^2} + \frac{\phi_2 - \phi_0}{\Delta x^2} = \frac{1}{\alpha}\frac{\phi_0 - \phi_{t_0 - \Delta t}}{\Delta t} \tag{10.84}$$

Note that the Laplacian as well as the time derivative have been discretized and that the "backward difference" is employed for the time function. The term $\phi_{t_0 - \Delta t}$ refers to the potential existing at node 0, one time increment (Δt) previous to the instant of time for which measurements are being made. The node equation for the analogous resistance network is

$$\frac{V_1 - V_0}{R_x} + \frac{V_2 - V_0}{R_x} = \frac{V_0 - V_{t_0 - \Delta t}}{R_t} \tag{10.85}$$

as illustrated in Fig. 10.20.

This network permits the prediction of the potential at all nodes at a

time $t = t_0 + \Delta t$ if the potentials at time $t = t_0$ are known. To solve a typical problem, the resistors R_t are made to correspond to a convenient $\alpha \Delta t$ and the given initial conditions for time $t = 0$ are applied at their lower terminals. The potentials at time $t_0 + \Delta t$ are then obtained by measuring the voltages at the network nodes. The feed-in voltages E_f to all feed-in resistors R_t are then readjusted to correspond to the network voltages for time $t = t_0 + \Delta t$. The voltages now appearing at the network nodes correspond to the potentials at time $t = t_0 + 2\Delta t$. The
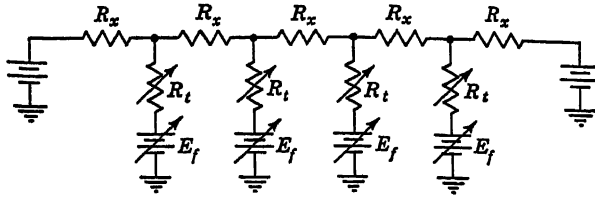
Fig. 10.20

feed-in voltages are then again adjusted, and the process is continued until the potentials corresponding to the desired number of time intervals have been obtained.

An earlier suggestion for the analog simulation of a completely discretized approximation of the diffusion equation is due to Kron.[19] In this case the time derivative is approximated by averaging the forward- and backward-difference terms as in Eq. (10.3). The time domain is viewed just as the space domain, so that a two-dimensional network is employed to simulate a diffusion system in one space dimension. Referring to Fig. 10.21a, the length of the heat-flow path is limited to a distance L. Time is unlimited, and therefore the vertical distance representing t is not bounded. The xt domain is shown overlaid with a rectangular grid having the spacings h along x and j along t. For any interior point, such as 0, the finite difference form of Eq. (10.76) is

$$\frac{\phi_1 - \phi_0}{h^2} + \frac{\phi_3 - \phi_0}{h^2} + \frac{\phi_2 - \phi_0}{2ja} - \frac{\phi_4 - \phi_0}{2ja} = 0 \qquad (10.86)$$

A typical network point in the equivalent circuit for Eq. (10.86) is shown in Fig. 10.21b, with R_1, R_2, R_3 positive resistances of magnitudes h^2, $2ja$, and h^2, respectively, and R_4 a negative resistance $-2ja$. Alternative circuit arrangements making use of inductance and capacitance are shown in Fig. 10.21c and d. A portion of the complete equivalent circuit, stretching over several nodes, is shown in (e). Because of the negative coupling elements required between rows of nodes, the typical elements shown in (c) and (d) alternate from row to row.
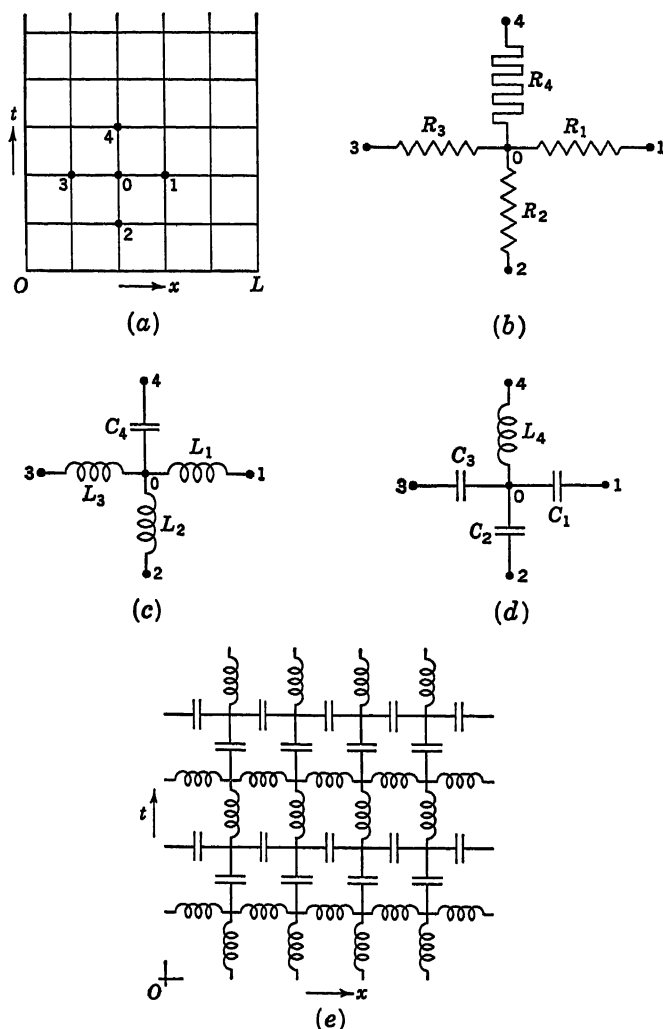
Fig. 10.21

10.8. The Wave Equation.
In setting up dynamical analogies for distributed systems in Chap. 9, the one-dimensional wave equation $c^2 \, \partial^2 \theta / \partial x^2 = \partial^2 \theta / \partial t^2$ was found to govern compressional and torsional waves in bars, transverse waves in strings, and acoustical waves in pipes. More generally, the wave equation is written

$$\nabla^2 \phi = \frac{1}{c^2} \frac{\partial^2 \phi}{\partial t^2} \tag{10.87}$$

where $\nabla^2 \phi$ is the Laplacian of ϕ. Thus the one-dimensional equation is

extended to two dimensions (*e.g.*, membranes) and to three dimensions (*e.g.*, acoustic fields).

When steady-state sinusoidal vibrations of circular frequency ω are involved, the acceleration term is related to the displacement by the
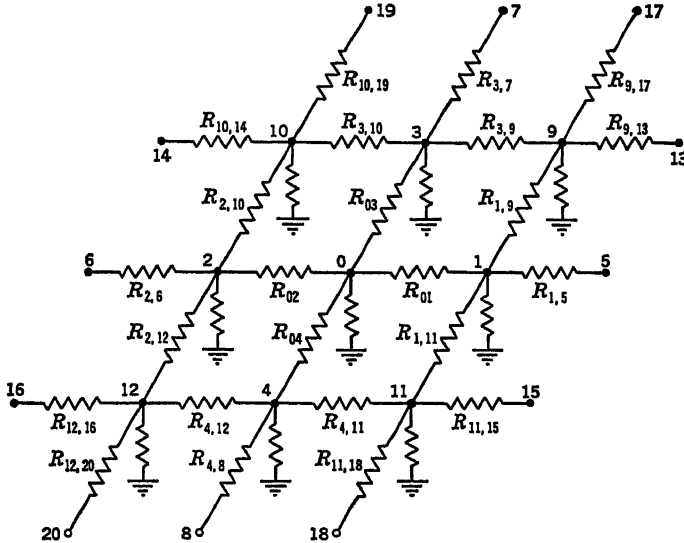
Fig. 10.22

equation

$$\frac{\partial^2 \phi}{\partial t^2} = -\omega^2 \phi \qquad (10.88)$$

Equation (10.87) becomes, therefore,

$$\nabla^2 \phi + \frac{\omega^2}{c^2} \phi = 0 \qquad (10.89)$$

A finite-difference network can be set up rather simply for this equation since it does not involve the open boundary in time, which a transient state requires.

For a two-dimensional membrane in cartesian coordinates, Eq. (10.89) in finite-difference form is

$$\frac{\phi_1 + \phi_0}{h^2} + \frac{\phi_2 - \phi_0}{h^2} + \frac{\phi_3 - \phi_0}{h^2} + \frac{\phi_4 - \phi_0}{h^2} + \frac{\omega^2}{c^2} \phi_0 = 0 \quad (10.90)$$

The electrical network representing Eq. (10.90), using direct current, is shown in Fig. 10.22 if the grid resistances are made equal to h^2, while the resistances to ground are negative and of magnitude ω^2/c^2. The significance of the subscripts of the grid resistors is indicated in Sec. 10.9.

If alternating current is used to excite the network, inductors and capacitors may be used to represent the positive and negative impedances required.

Since Eq. (10.89) represents free vibrations, ω must be a natural frequency, which is not known except when a solution is obtained. In a free undamped vibration, no forces are required to maintain the motion. Swenson and Higgins[20] use this fact to establish the correct values of ω in a d-c network solution of membrane vibration. If a value is assumed for ω and the negative resistances adjusted in accordance with ω^2/c^2, an external d-c voltage applied to a node will fix the displacement amplitude (ϕ) at that location on the membrane, and the current flowing into the battery will be a measure of the force required to maintain this amplitude of motion at this point. Voltages measured at the other nodal points give the shape of the membrane when excited by this force at this frequency.

If ω is now changed and the negative resistances readjusted to their new values, a different current will flow through the battery in order to maintain the same displacement amplitude as before. This current is plotted against assumed values of frequency, and the correct natural frequency is determined from the point on the curve at which the current is zero.

Fields governed by the wave equation can also be simulated by a dynamic analogy[21-23] similar in concept to the RC analog for diffusion fields. The one-, two-, or three-dimensional field is represented by a rectangular array of circuit elements, and capacitors are connected from each network node to ground. In this case, however, the series elements are inductors rather than resistors. In cartesian coordinates, the finite-difference approximation of Eq. (10.87) in one and two space dimensions is

(a) $$\frac{\phi_1 - \phi_0}{h^2} + \frac{\phi_2 - \phi_0}{h^2} = \frac{1}{c^2}\frac{d^2\phi_0}{dt^2}$$

(b) $$\frac{\phi_1 - \phi_0}{h^2} + \frac{\phi_2 - \phi_0}{h^2} + \frac{\phi_3 - \phi_0}{h^2} + \frac{\phi_4 - \phi_0}{h^2} = \frac{1}{c^2}\frac{d^2\phi_0}{dt^2}$$

(10.91)

Consider now an electrical network having nodes of the type shown in Fig. 10.23a and b. In accordance with Kirchhoff's law, the node equations for the typical nodes are, for one- and two-dimensions respectively,

(a) $$\frac{1}{L}\int_0^t (V_1 - V_0)\,dt + \frac{1}{L}\int_0^t (V_2 - V_0)\,dt = C\frac{dV_0}{dt}$$

(b) $$\frac{1}{L}\int_0^t (V_1 - V_0)\,dt + \frac{1}{L}\int_0^t (V_2 - V_0)\,dt$$
$$+ \frac{1}{L}\int_0^t (V_3 - V_0)\,dt + \frac{1}{L}\int_0^t (V_4 - V_0)\,dt = C\frac{dV_0}{dt}$$

(10.92)

or differentiating with respect to time,

(a) $$\frac{V_1 - V_0}{L} + \frac{V_2 - V_0}{L} = C\frac{d^2V_0}{dt^2}$$

(10.93)

(b) $$\frac{V_1 - V_0}{L} + \frac{V_2 - V_0}{L} + \frac{V_3 - V_0}{L} + \frac{V_4 - V_0}{L} = C\frac{d^2V_0}{dt^2}$$

To complete the analogy between Eqs. (10.91) and (10.93), the product of the magnitudes of the inductors L and the magnitude of the capacitor C must be made equal to $1/c^2$. The LC networks then constitute analogs
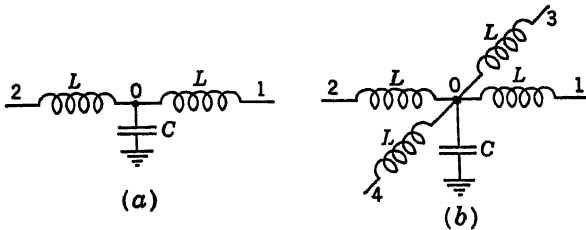
Fig. 10.23

of the fields described by the wave equation. Such network analogs can be employed to solve transient as well as steady-state problems.

10.9. Nonlinear Partial Differential Equations. Following the pattern for the three simultaneous ordinary differential equations, the network may be extended to nonlinear partial differential equations in two independent variables, generalizing somewhat on the discussion already made in connection with the Laplace and Poisson equations. The network for the Poisson type of equation may easily accommodate a nonlinear term which depends on ϕ but not its derivatives by admitting currents to the nodes as in Sec. 10.5. The partial differential equation may be extended to include first derivatives or mixed derivatives. The network spacings in the directions of the two independent variables may be different.

A rather general equation of this type is one discussed by Johnson and Alley:[4]

$$\frac{\partial^2\phi}{\partial x^2} + f(x)\frac{\partial\phi}{\partial x} + A\frac{\partial^2\phi}{\partial y^2} + g(y)\frac{\partial\phi}{\partial y} - k\phi + F(x,y,\phi) = 0 \quad (10.94)$$

where $f(x)$ and $g(y)$ are prescribed functions of x alone and y alone, respectively. The network spacing h will be taken in the x direction and the spacing j in the y direction, as shown in Fig. 10.24a. Writing the

derivatives in the usual finite-difference forms, Eq. (10.94) becomes

$$\left(\frac{1}{h^2} + \frac{f_0}{2h}\right)(\phi_1 - \phi_0) + \left(\frac{1}{h^2} - \frac{f_0}{2h}\right)(\phi_2 - \phi_0) + \left(\frac{1}{j^2} + \frac{g_0}{2j}\right)(\phi_3 - \phi_0)$$

$$+ \left(\frac{1}{j^2} - \frac{g_0}{2j}\right)(\phi_4 - \phi_0) - k\phi_0 + F(x_0, y_0, \phi_0) = 0 \quad (10.95)$$

The corresponding typical node of the electrical circuit for representing Eq. (10.95) is shown in Fig. 10.24b. Again, unilateral conductances are apparent in both the x and the y directions. These may be converted to bilateral conductances by the multiplication procedures already discussed. Since mixed derivatives are not involved, the multiplication
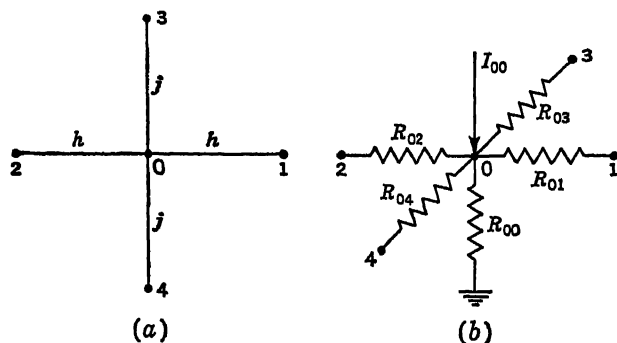
Fig. 10.24

factors connected with nodes along the x direction (spaced h apart) are independent of those along the y direction (spaced j apart). Thus all conductances may be made bilateral in this network by using both factors in each nodal equation.

In Fig. 10.24b, the value of R_{01} will depend on whether 0 or 1 is the node for which the summation of currents is taken. Similarly, the values of R_{02}, R_{03}, or R_{04} will depend upon which end of the resistance is being considered as the node at the moment. The point 0 is shown in Fig. 10.22 as part of a more extended network. The connecting resistances are identified by subscripts consisting of the numbers of the two nodes they connect. Since the node 0 occupies an arbitrary position in the network, a pair of multiplying factors would be associated with it. Suppose these factors to be K_0, related to the x position, and J_0, related to the y position. Then Eq. (10.95) will be

$$K_0 J_0 \left(\frac{1}{h^2} + \frac{f_0}{2h}\right)(\phi_1 - \phi_0) + K_0 J_0 \left(\frac{1}{h^2} - \frac{f_0}{2h}\right)(\phi_2 - \phi_0)$$

$$+ K_0 J_0 \left(\frac{1}{j^2} + \frac{g_0}{2j}\right)(\phi_3 - \phi_0) + K_0 J_0 \left(\frac{1}{j^2} - \frac{g_0}{2j}\right)(\phi_4 - \phi_0)$$

$$- K_0 J_0 k \phi_0 + K_0 J_0 F(x_0, y_0, \phi_0) = 0 \quad (10.96)$$

Each conductance attached at 0 is thus increased by the same factor K_0J_0. Since the entering current is likewise increased by the same factor, there is no change in the voltage distribution between 0 and its neighboring points.

If position 1 is now considered as a node, the only resistance common to nodes 0 and 1 is R_{01} and the multiplying factor need be changed only the amount necessary to make this resistance bilateral. Being a change only in the x direction, just the K_0 factor is changed to K_1. The equation for the node at position 1 is, therefore,

$$K_1J_0\left(\frac{1}{h_2} + \frac{f_1}{2h}\right)(\phi_5 - \phi_1) + K_1J_0\left(\frac{1}{h^2} - \frac{f_1}{2h}\right)(\phi_0 - \phi_1)$$

$$+ K_1J_0\left(\frac{1}{j^2} + \frac{g_0}{2j}\right)(\phi_9 - \phi_1) + K_1J_0\left(\frac{1}{j^2} - \frac{g_0}{2j}\right)(\phi_{11} - \phi_1)$$

$$- K_1J_0k\phi_1 + K_1J_0F(x_1,y_0,\phi_1) = 0 \quad (10.97)$$

Since $g(y)$ depends only on y and y has not been affected in going to position 1, the value g_0 is the same as g_1 and is thus used in Eq. (10.97). By choosing K_1 in accordance with

$$\frac{K_1}{K_0} = \frac{(1/h^2) + (f_0/2h)}{(1/h^2) - (f_1/2h)} \quad (10.98)$$

the resistance R_{01} will be bilateral. The factor K_0 applies to nodes 8, 4, 0, 3, 7 and any others along this line. The factor K_1 applies to nodes 18, 11, 1, 9, 17 and any others in line with them.

If we now go on to position 9 as a node, the finite-difference equation for this point will be

$$K_1J_3\left(\frac{1}{h^2} + \frac{f_1}{2h}\right)(\phi_{13} - \phi_9) + K_1J_3\left(\frac{1}{h^2} - \frac{f_1}{2h}\right)(\phi_3 - \phi_9)$$

$$+ K_1J_3\left(\frac{1}{j^2} + \frac{g_3}{2j}\right)(\phi_{17} - \phi_9) + K_1J_3\left(\frac{1}{j^2} - \frac{g_3}{2j}\right)(\phi_1 - \phi_9)$$

$$- K_1J_3k\phi_9 + K_1J_3F(x_9,y_9,\phi_9) = 0 \quad (10.99)$$

Since points 14, 10, 3, 9, and 13 are all at the same value of y, the same J factor will apply to the finite-difference equations written for all of these points. In this case the J factor has been labeled J_3 and appears as such in Eq. (10.99). Since x has not changed in going from (1) to (9), the factor K_1 applies to Eq. (10.99) as well as to Eq. (10.97). Thus, to make $R_{1,9}$ bilateral, J_3 is chosen so that

$$\frac{J_3}{J_0} = \frac{(1/j^2) + (g_0/2j)}{(1/j^2) - (g_3/2j)} \quad (10.100)$$

By proceeding over a given finite-difference net in this manner, the multiplying factors for each line of nodes in the x and y directions may be deter-

mined to ensure bilateral conductances throughout the network representing Eq. (10.94).

A three-dimensional network may be developed by stacking layers of the type in Fig. 10.22. The equation for this case would be

$$\frac{\partial^2 \phi}{\partial x^2} + f(x)\frac{\partial \phi}{\partial x} + A\frac{\partial^2 \phi}{\partial y^2} + g(y)\frac{\partial \phi}{\partial y} + B\frac{\partial^2 \phi}{\partial z^2} + p(z)\frac{\partial \phi}{\partial z}$$
$$- k\phi + F(x,y,z,\phi) = 0 \quad (10.101)$$

10.10. Partial Differential Equations with Mixed Derivatives. A typical second-order partial differential equation in two independent
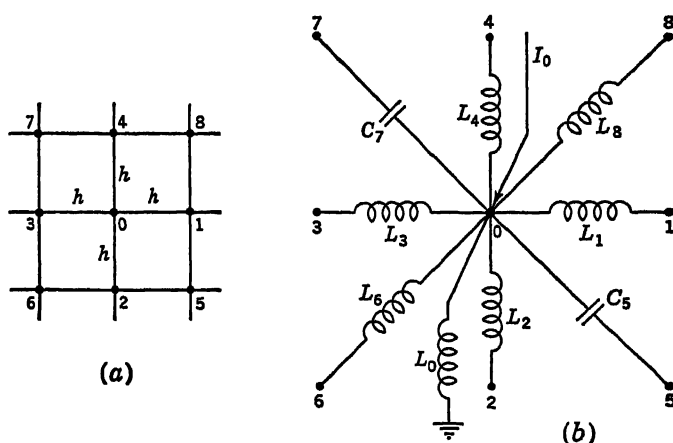
Fig. 10.25

variables and with a mixed derivative is

$$\frac{\partial^2 \phi}{\partial x^2} + A\frac{\partial^2 \phi}{\partial y^2} + B\frac{\partial^2 \phi}{\partial x \, \partial y} - k\phi + F(x,y,\phi) = 0 \quad (10.102)$$

In developing a network for this equation, a typical node 0 with its surrounding eight points, shown in Fig. 10.25a, is used. Assuming equal spacing h in both directions, the second derivatives at 0 are obtained in the usual manner. The mixed derivative at 0 may be obtained in either one of two ways. On the one hand, the first derivatives with respect to x may be taken at points 2 and 4 and then the derivative with respect to y taken between these points. On the other hand, the first derivatives with respect to y may be taken at points 3 and 1 and then the derivative with respect to x taken between these points. In either case the same expression results, as it should, since the values of mixed derivatives are independent of the order of differentiation.

Following the first procedure,

$$\left(\frac{\partial \phi}{\partial x}\right)_2 = \frac{\phi_5 - \phi_6}{2h} \qquad \left(\frac{\partial \phi}{\partial x}\right)_4 = \frac{\phi_8 - \phi_7}{2h} \qquad (10.103)$$

$$\left(\frac{\partial^2 \phi}{\partial y\,\partial x}\right)_0 = \frac{(\partial\phi/\partial x)_4 - (\partial\phi/\partial x)_2}{2h} = \frac{\phi_8 - \phi_7}{4h^2} - \frac{\phi_5 - \phi_6}{4h^2}$$

$$= \frac{(\phi_8 - \phi_0) + (\phi_6 - \phi_0) - (\phi_7 - \phi_0) - (\phi_5 - \phi_0)}{4h^2} \qquad (10.104)$$

Equation (10.102) in finite-difference form is, therefore,

$$\frac{\phi_1 - \phi_0}{h^2} + \frac{\phi_3 - \phi_0}{h^2} + A\,\frac{\phi_2 - \phi_0}{h^2} + A\,\frac{\phi_4 - \phi_0}{h^2} + B\,\frac{\phi_8 - \phi_0}{4h^2}$$

$$+ B\,\frac{\phi_6 - \phi_0}{4h^2} - B\,\frac{\phi_7 - \phi_0}{4h^2} - B\,\frac{\phi_5 - \phi_0}{4h^2} - k\phi_0$$

$$+ F(x_0, y_0, \phi_0) = 0 \qquad (10.105)$$

The corresponding network for the typical node is shown in Fig. 10.25b. Since negative admittances are required on some of the diagonals, inductors and capacitors are shown for the circuit elements and the circuit is operated with alternating current. Direct-current operation is possible if negative resistance circuits are used. In Fig. 10.25b,

$$\omega L_1 = \omega L_3 = h^2 \qquad \omega L_2 = \omega L_4 = \frac{h^2}{A} \qquad \omega C_5 = \omega C_6 = \frac{B}{4h^2}$$

$$\omega L_6 = \omega L_8 = \frac{4h^2}{B} \qquad \omega L_0 = \frac{1}{k} \qquad I_0 = F(x_0, y_0, \phi_0) \qquad (10.106)$$

where ω is the constant exciting frequency.

10.11. Analogy for Beams. In the preceding chapter equivalent lumped systems to represent beams were developed by means of influence numbers. From the standpoint of setting up a dynamical analogy suitable for transient analysis, this lumped model had the serious drawback of requiring some negative springs. If the analogy is developed through the finite-difference approach, a different circuit is obtained, which requires transformers but not negative springs.[24,25]

The basis for this approach is the following set of equations derived from Fig. 9.26:

$$\theta = \frac{\partial y}{\partial x} \qquad -M = EI\,\frac{\partial \theta}{\partial x} \qquad S = \frac{\partial M}{\partial x} \qquad (10.107)$$

$$-\frac{\partial S}{\partial x} + m\,\frac{\partial^2 y}{\partial t^2} = 0 \qquad (10.108)$$

where θ is the slope of the beam at any position x and the other symbols are defined in Sec. 9.9.

Suppose that one's attention is directed to n points equally spaced along the beam from one end to the other. These points are the mid-points of n equal sections x of the beam. In Fig. 10.26a the kth point and its neighbors are shown. If the beam deflections at these points are labeled y_{k-1}, y_k, y_{k+1}, etc., the slope of the beam at the mid-point position between y_k and y_{k+1} (that is, at $y_{k+\frac{1}{2}}$) may be taken approximately as the
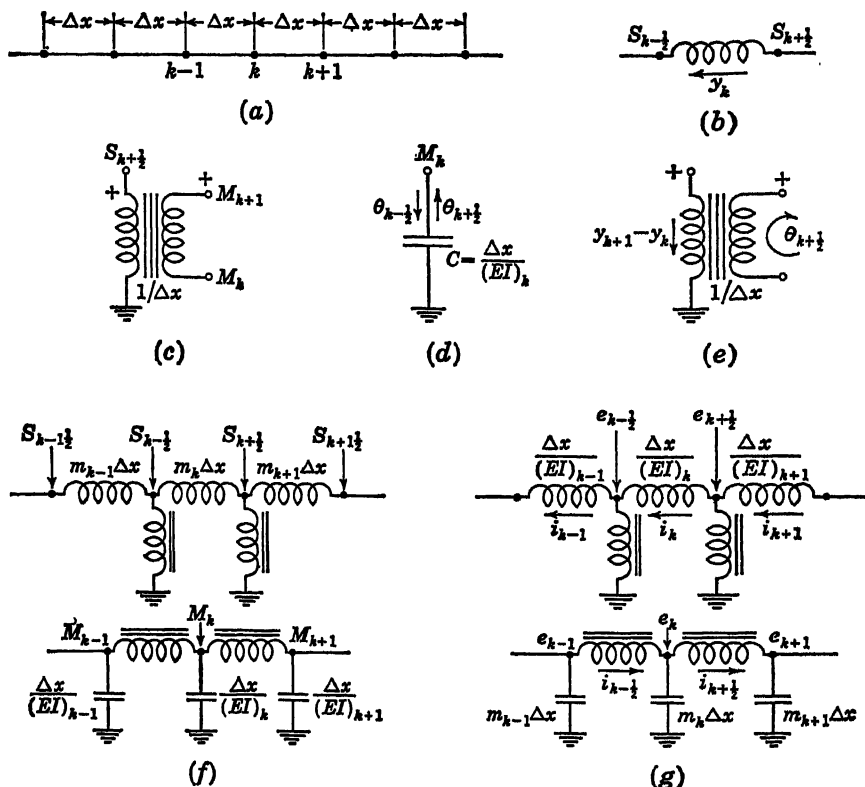
Fig. 10.26

slope of the chord connecting y_k to y_{k+1}. Thus the first of Eqs. (10.107) may be written

$$\theta_{k+\frac{1}{2}} = \frac{y_{k+1} - y_k}{\Delta x} \tag{10.109}$$

Similarly, the remaining equations become

$$-M_k = (EI)_k \frac{\theta_{k+\frac{1}{2}} - \theta_{k-\frac{1}{2}}}{\Delta x} \tag{10.110}$$

$$S_{k+\frac{1}{2}} = \frac{M_{k+1} - M_k}{\Delta x} \tag{10.111}$$

Finally, Eq. (10.108) becomes

$$-\frac{S_{k+\frac{1}{2}} - S_{k-\frac{1}{2}}}{\Delta x} + m_k \frac{d^2 y_k}{dt^2} = 0$$

or

$$S_{k+\frac{1}{2}} - S_{k-\frac{1}{2}} = m_k \, \Delta x \, \frac{d^2 y_k}{dt^2} \tag{10.112}$$

where m_k is the mass per unit length of beam at the kth location.

In the mass-inductance analogy, forces are simulated by voltages and displacements by circulating charges. Thus, if a voltage difference $S_{k+\frac{1}{2}} - S_{k-\frac{1}{2}}$ is impressed across a coil having a self-inductance $L_k = m_k \, \Delta x$, a charge $q_k = y_k$ will flow through the coil and the corresponding current will be $i_k = dy_k/dt$. This situation is illustrated in Fig. 10.26b. Equation (10.112) is thus satisfied.

Equation (10.111) shows that the voltage $S_{k+\frac{1}{2}}$ is related to a voltage difference $M_{k+1} - M_k$ by a constant ratio $1/\Delta x$. A transformer enforcing this relationship is shown in (c). Since M_k and M_{k+1} are forces (moments), the analogy between force and voltage still holds.

In Eq. (10.110), the angular displacements (slopes) $\theta_{k+\frac{1}{2}}$ and $\theta_{k-\frac{1}{2}}$ are to be represented by electric charges. The equation indicates that the voltage M_k is proportional to the difference in electric charges. This situation arises if a capacitor is used as an element in the common branch of two adjacent circuits. Thus in (d) a capacitor of capacitance $C_k = \Delta x/(EI)_k$ is used, and Eq. (10.110) is satisfied.

From Eq. (10.109) it is clear that the charge $\theta_{k+\frac{1}{2}}$ is related to the difference in charges $y_{k+1} - y_k$ by the ratio $1/\Delta x$. This relationship calls for a transformer, as indicated in (e).

If all the individual parts of the analogy indicated in (b) to (e) are now connected to each other at the points they have in common, a circuit will result which satisfies all the relations common to point k and its neighbors as expressed by Eqs. (10.109) to (10.112). The two transformers in (c) and (e) are actually one and the same transformer; the charge transformation ratio is the reciprocal of the voltage-transformation ratio, so that both Eqs. (10.109) and (10.111) are satisfied in the one transformer. Adjacent cells of the same construction are then connected to the pairs of terminals $S_{k-\frac{1}{2}}$, M_k and $S_{k+\frac{1}{2}}$, M_{k+1}. The complete mass-inductance analogy for a cantilever beam of five sections is shown in Fig. 10.27. In (a), the nodal points 0 to 5 are shown on the beam. In (b) the analog circuit is developed. The mass assumed to be concentrated at 0 and 5 is $\frac{1}{2}m \, \Delta x$, and at 1 to 4 it is $m \, \Delta x$, where m is the mass per unit of length of the beam. Since y_0 and θ_0 are both zero, there should be no current circulating in the left-hand cell. Consequently, the terminals at these ends are left disconnected. The initial coil representing $\frac{1}{2}m \, \Delta x$ is left

out, since it is concentrated at the support and thus does not enter into the vibration problem. At the free end of the cantilever, the shear and moment are both zero, so that the terminals at this end of the circuit are shown grounded. The capacitance from M_5 to ground is left out since it would be grounded on both sides anyway.

It can be shown that Fig. 10.26*f* also represents the mass-capacitance analogy for the beam section if the inductance is assigned the value $\Delta x/(EI)_k$, the capacitance the value $m_k \Delta x$, and if slopes and deflections

(a)

(b)
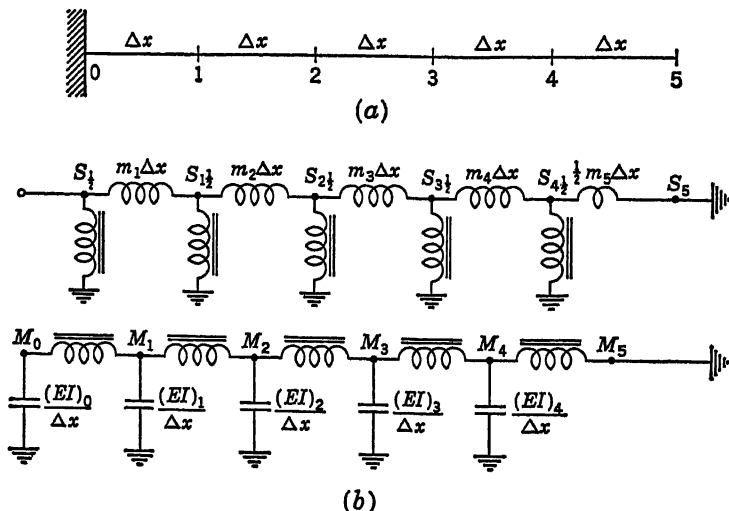
Fig. 10.27

are represented by voltages at network nodes, while forces and moments are represented by rates of change of current in network loops.

Referring to Fig. 10.26*g*, the following relations are seen to hold between electrical quantities:

$$e_{k+\frac{1}{2}} - e_{k-\frac{1}{2}} = \frac{\Delta x}{(EI)_k}\frac{di_k}{dt} \qquad (10.113)$$

$$\frac{i_{k+1} - i_k}{\Delta x} = i_{k+\frac{1}{2}} \quad \text{or} \quad \frac{(di_{k+1}/dt) - (di_k/dt)}{\Delta x} = \frac{di_{k+\frac{1}{2}}}{dt} \quad (10.114)$$

$$e_{k+\frac{1}{2}} = \frac{e_{k+1} - e_k}{\Delta x} \qquad (10.115)$$

$$\frac{i_{k-\frac{1}{2}} - i_{k+\frac{1}{2}}}{m\,\Delta x} = \frac{de_k}{dt} \quad \text{or} \quad \frac{di_{k-\frac{1}{2}}}{dt} - \frac{di_{k+\frac{1}{2}}}{dt} = m\,\Delta x\,\frac{d^2 e_k}{dt^2} \quad (10.116)$$

Replacing voltages and current rates by their analogous quantities, Eqs. (10.113) to (10.116) become

$$\theta_{k+\frac{1}{2}} - \theta_{k-\frac{1}{2}} = \frac{\Delta x}{(EI)_k} M_k \tag{10.117}$$

$$\frac{M_{k+1} - M_k}{\Delta x} = S_{k+\frac{1}{2}} \tag{10.118}$$

$$\theta_{k+\frac{1}{2}} = \frac{y_{k+1} - y_k}{\Delta x} \tag{10.119}$$

$$S_{k-\frac{1}{2}} - S_{k+\frac{1}{2}} = m_k \, \Delta x \, \frac{d^2 y_k}{dt^2} \tag{10.120}$$

These equations are the beam equations in finite-difference form if the beam convention is taken as in Fig. 10.28. The differential equations based on this figure are

$$-\frac{\partial S}{\partial x} = m \frac{\partial^2 y}{\partial t^2} \tag{10.121}$$

$$S = \frac{\partial M}{\partial x} \tag{10.122}$$

$$\theta = \frac{\partial y}{\partial x} \tag{10.123}$$

$$M = EI \frac{\partial^2 y}{\partial x^2} = EI \frac{\partial \theta}{\partial x} \tag{10.124}$$

The agreement between the above three sets of equations is clear.
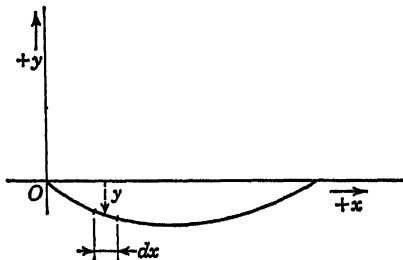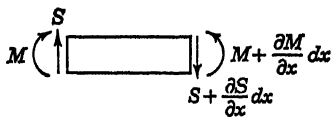
Axial tension may be included in the beam analogy.[26] The restoring force due to axial tension is found from Fig. 10.29 and is included in the equation of motion of the beam section [either Eq. (10.108) or Eq. (10.121)]. For vertical motion, the vertical components of T are needed.

(a)

(b)
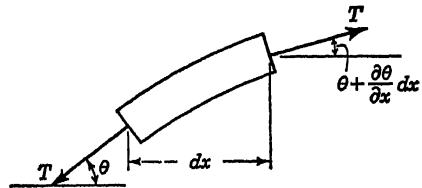
Fig. 10.28

Fig. 10.29

The resultant upward force is (for small angles, such that $\sin \theta = \theta$)

$$T \frac{\partial \theta}{\partial x} dx$$

Substituting into Eq. (10.108), we have

$$-\frac{\partial S}{\partial x} - T\frac{\partial \theta}{\partial x} + m\frac{\partial^2 y}{\partial t^2} = 0 \qquad (10.125)$$

In finite differences,

$$-\frac{S_{k+\frac{1}{2}} - S_{k-\frac{1}{2}}}{\Delta x} - T\frac{\theta_{k+\frac{1}{2}} - \theta_{k-\frac{1}{2}}}{\Delta x} + m_k\frac{\partial^2 y_k}{\partial t^2} = 0$$

Using Eq. (10.109) and multiplying through by Δx,

$$-(S_{k+\frac{1}{2}} - S_{k-\frac{1}{2}}) = \frac{T}{\Delta x}(y_{k+1} - 2y_k + y_{k-1}) + m_k\Delta x\frac{\partial^2 y_k}{\partial t^2} = 0 \quad (10.126)$$

Figure 10.30 shows two cells of Fig. 10.26f with capacitors of capacitance $\Delta x/T$ inserted in the input leads of the transformer primaries. The
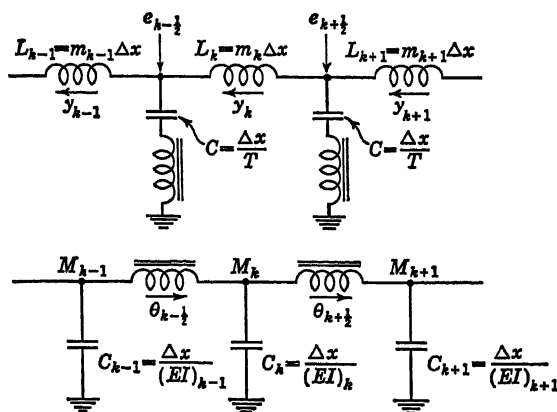
Fig. 10.30

voltages into the transformer primaries are the shears $S_{k+\frac{1}{2}}$ and $S_{k-\frac{1}{2}}$, as before. The voltage across the inductance $m_k\,\Delta x$ is now altered by the presence of the capacitors. The voltages $e_{k+\frac{1}{2}}$ and $e_{k-\frac{1}{2}}$ are given by

$$e_{k+\frac{1}{2}} = S_{k+\frac{1}{2}} + \frac{y_{k+1} - y_k}{\Delta x/T} \qquad e_{k-\frac{1}{2}} = S_{k-\frac{1}{2}} + \frac{y_k - y_{k-1}}{\Delta x/T}$$

whence

$$e_{k+\frac{1}{2}} - e_{k-\frac{1}{2}} = S_{k+\frac{1}{2}} - S_{k-\frac{1}{2}} + \frac{T}{\Delta x}(y_{k+1} - 2y_k + y_{k-1}) = m_k\Delta x\frac{\partial^2 y_k}{\partial t^2}$$

$$(10.127)$$

Thus, the electrical circuit shown satisfies Eq. (10.126) and represents the bending vibration of a beam subjected to axial tension.

The mass-capacitance circuit including axial tension is shown in Fig. 10.31. Two cells of the kind shown in Fig. 10.26g are used, with the addition of inductances $\Delta x/T$ shunting the secondaries of the transformers.

Equation (10.121), including axial tension, is

$$-\frac{\partial S}{\partial x} + T\frac{\partial \theta}{\partial x} = m\frac{\partial^2 y}{\partial t^2} \tag{10.128}$$

In finite difference form this is Eq. (10.126) with the sign reversed on the tension and acceleration terms.
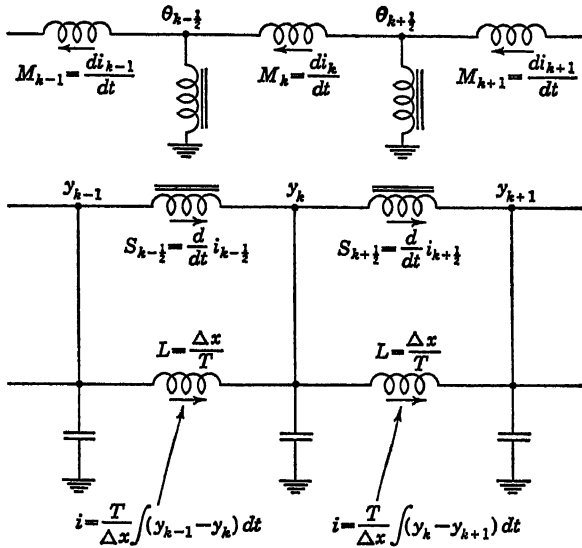
Fig. 10.31

In Fig. 10.31, the current approaching the node y_k is

$$i_{k-\frac{1}{2}} + \frac{T}{\Delta x}\int_0^t (y_{k-1} - y_k)\, dt$$

That leaving the node is

$$i_{k+\frac{1}{2}} + \frac{T}{\Delta x}\int_0^t (y_k - y_{k+1})\, dt$$

The difference in these currents serves to charge the capacitor at the rate $m_k\, \Delta x\, dy_k/dt$. Thus

$$i_{k-\frac{1}{2}} - i_{k+\frac{1}{2}} + \frac{T}{\Delta x}\int_0^t (y_{k-1} - 2y_k + y_{k+1})\, dt = m_k\, \Delta x\, \frac{dy_k}{dt} \tag{10.129}$$

Since forces are represented as derivatives of currents in this analogy,

Eq. (10.129) becomes, on differentiation (and upon substitution of $S_{k-\frac{1}{2}} = di_{k-\frac{1}{2}}/dt$ and $S_{k+\frac{1}{2}} = di_{k+\frac{1}{2}}/dt$):

$$S_{k-\frac{1}{2}} - S_{k+\frac{1}{2}} + \frac{T}{\Delta x}(y_{k-1} - 2y_k + y_{k+1}) = m_k \Delta x \frac{d^2 y_k}{dt^2} \quad (10.130)$$

Comparing with the finite difference form of Eq. (10.128), it is clear that the analogy shown in Fig. 10.31 also represents the vibration of a beam in bending with axial tension.

Deflections due to shear[26,27] and effects of rotatory inertia[26] of the beam sections may be included in the equivalent circuits if desired.

The circuits described for vibration could be used for static loads on beams as well. Alternating current must be used to represent static loads because of the transformers. Inertia effects, represented by the inductance (or capacitance), are eliminated by removing the corresponding elements from the circuit.

10.12. The Lattice Analogy for Plane Stress Systems. The basis for the numerical and electrical networks discussed so far in this chapter has been the replacement of a continuum by a latticework of discrete points whose interactions through appropriate connecting links satisfied approximately the partial differential equations applying to the continuum. Such a procedure has almost limitless possibilities for physical representation. Thus it seems conceivable that a continuous elastic body subjected to prescribed external loads may be replaced by an equivalent framework of pinned elastic members of such proportions and properties that the deflections of a typical elementary frame of this framework are directly related to the deflections in a corresponding element of volume of the elastic continuum. Just such an approach is credited to R. W. Carlson,[28] and its application to various types of stress distribution problems has been described by McHenry[28] and Hrennikoff.[29]

Consider in Fig. 10.32a a finite square element h by h, which is part of an elastic lamina of thickness t, subjected to forces producing plane stress. If normal stresses σ_x and σ_y alone act on this element, the strains produced in the x and y directions are

$$\epsilon_x = \frac{\sigma_x}{E} - \mu \frac{\sigma_y}{E} \qquad \epsilon_y = -\mu \frac{\sigma_x}{E} + \frac{\sigma_y}{E} \quad (10.131)$$

where μ is the Poisson ratio for the material.

The corresponding elongations of the square element in the x and y directions are

$$e_x = h\epsilon_x \qquad e_y = h\epsilon_y \quad (10.132)$$

A pin-jointed frame may be constructed as in Fig. 10.32c, so that when loads are applied at the joints corresponding to $\sigma_x h t$ and $\sigma_y h t$, the changes

in dimensions of the frame in the x and y directions will correspond to the elongations e_x and e_y of the original continuous elastic element. So far as the over-all effects are concerned, the pin-jointed frame is the finite-difference analog of the continuous element. A continuous body which consists of a number of adjoining continuous square elements may be represented by a corresponding number of adjoining frames forming a latticework.
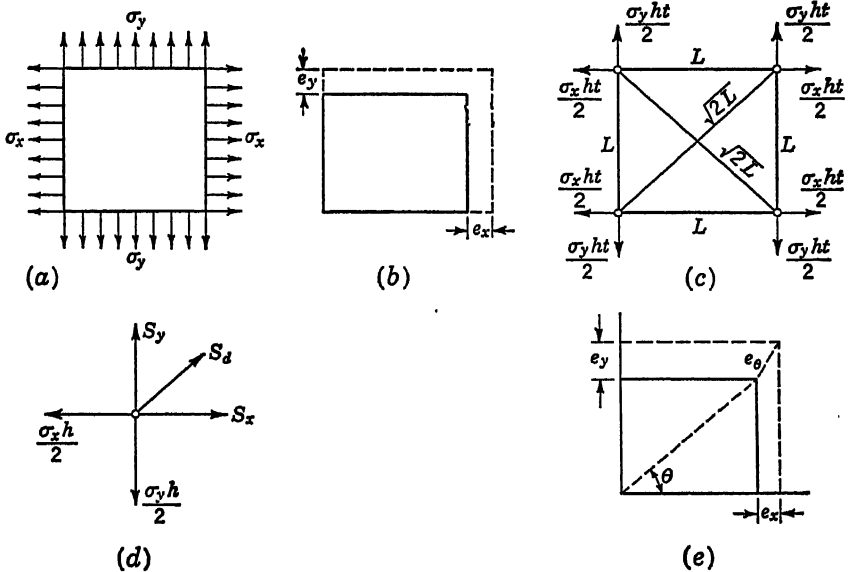
Fig. 10.32

Referring to the lattice element in Fig. 10.32c, the loads in the members are in static equilibrium with the applied loads at each joint. Representing in (d) the force system acting at one joint, S_x, S_y, and S_d are the loads in the horizontal, vertical, and diagonal members, respectively, in the frame. The equations of equilibrium are

$$\frac{\sigma_x ht}{2} = S_x + \frac{S_d}{\sqrt{2}} \qquad \frac{\sigma_y ht}{2} = S_y + \frac{S_d}{\sqrt{2}} \qquad (10.133)$$

The elongations of the horizontal and vertical members are given by Eq. (10.132). The elongation of a member of length L, cross-sectional area A_1, made of a material having a Young's modulus E_1, and subjected to an axial load S is

$$e = \frac{SL}{A_1 E_1} \qquad (10.134)$$

Thus, using Eqs. (10.134) and (10.131) in (10.132),

$$\frac{h\sigma_x}{E} - \mu \frac{h\sigma_y}{E} = \frac{S_x L}{A_1 E_1} \qquad -\mu \frac{h\sigma_x}{E} + \frac{h\sigma_y}{E} = \frac{S_y L}{A_1 E_1} \qquad (10.135)$$

Substituting Eqs. (10.133) into (10.135), and eliminating S_d between them, we obtain

$$\frac{2}{E} \frac{(1 + \mu)}{t} S_x - \frac{2}{E} \frac{(1 + \mu)}{t} S_y = \frac{S_x L}{A_1 E_1} - \frac{S_y L}{A_1 E_1}$$

$$\frac{2}{E} \frac{(1 + \mu)}{t} (S_x - S_y) = \frac{L}{A_1 E_1} (S_x - S_y) \qquad (10.136)$$

whence the cross-sectional area and the material of the framing lattice members should be such that

$$A_1 E_1 = \frac{ELt}{2(1 + \mu)} \qquad (10.137)$$

for the specified conditions.

Equations (10.131) provide the strains along the x and y directions. The strains in other directions are related to these as follows:[30]

$$\epsilon_\theta = \epsilon_x \cos^2 \theta + \epsilon_y \sin^2 \theta \qquad (10.138)$$

where θ is the angle between the x axis and the direction in which the strain is desired (Fig. 10.32e).

In the analogy being developed, the strains along the diagonal of the square element and of the analogous frame are desired. Thus, $\theta = 45°$, and we have

$$\epsilon_d = \frac{\epsilon_x + \epsilon_y}{2} \qquad (10.139)$$

The elongation e_d along the diagonal of the square element, and along the diagonal of the frame, is

$$e_d = h \sqrt{2} \, \epsilon_d = \frac{S_d L \sqrt{2}}{A_d E_d} \qquad (10.140)$$

Substituting from Eq. (10.139),

$$\frac{h\epsilon_x}{2} + \frac{h\epsilon_y}{2} = \frac{S_d L}{A_d E_d} \qquad (10.141)$$

From Eqs. (10.131)

$$\epsilon_x + \epsilon_y = \frac{1 - \mu}{E} (\sigma_x + \sigma_y) \qquad (10.142)$$

and from Eqs. (10.133)

$$\frac{h\sigma_x}{2} + \frac{h\sigma_y}{2} = \frac{S_x + S_y}{t} + \sqrt{2} \frac{S_d}{t} \qquad (10.143)$$

Thus, Eq. (10.141) becomes

$$(S_x + S_y) + \sqrt{2}\, S_d = \frac{S_d L t E}{(1 - \mu) A_d E_d} \qquad (10.144)$$

From Eqs. (10.135) and (10.141),

$$(S_x + S_y) \frac{L}{A_1 E_1} = h\epsilon_x + h\epsilon_y = \frac{2 S_d L}{A_d E_d} \qquad (10.145)$$

Substituting into Eq. (10.144), we will obtain

$$A_d E_d = \frac{L' E}{(1 - \mu)\sqrt{2}} - \sqrt{2}\, A_1 E_1 \qquad (10.146)$$

or, making use of Eq. (10.137),

$$A_d E_d = \frac{\sqrt{2}\, \mu L t E}{1 - \mu^2} \qquad (10.147)$$

The diagonal members may thus be of different material and of different area from the framing members, but must satisfy Eq. (10.147).

If shear loads alone are now applied to the element of continuum and corresponding loads applied to the elementary frame, the elongations
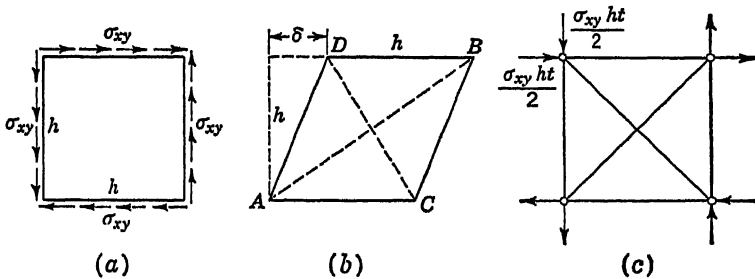
Fig. 10.33

and contractions in the diagonals of the continuous element and of the frame must be the same for the sizes given by Eqs. (10.137) and (10.147) if the lattice analogy is to be suitable for any arbitrary loading conditions.

Referring to Fig. 10.33a, the continuous square element is shown with a shear stress σ_{xy} acting along its four edges. The element deflects as shown in (b). For small angles, the sides do not change in length for all practical purposes, but the diagonals do. The corresponding loading on the lattice element is shown in (c). Equal loads act in the directions shown at all four corners of the frame.

The shear strain in (b) is defined by the ratio δ/h and is symbolized by γ_{xy}. It is related to shear stress through the expression

$$\frac{\delta}{h} = \gamma_{xy} = \frac{\sigma_{xy}}{G} \qquad (10.148)$$

where G is the shear modulus (modulus of rigidity) of the material. G is related to the Young's modulus E as follows:

$$E = 2(1 + \mu)G \qquad (10.149)$$

The longitudinal strain along a line making an angle θ with respect to the x axis in Fig. 10.33b is given by[30]

$$\epsilon_\theta = \gamma_{xy} \sin \theta \cos \theta \qquad (10.150)$$

In this case $\theta = 45°$, so that the strain along the diagonal AB is

$$\epsilon_d = \frac{\sigma_{xy}}{2G} \qquad (10.151)$$

For the diagonal CD, $\theta = 135°$, so that the strain is of opposite sign, although of equal magnitude.

The elongation of the diagonal AB is

$$e_d = \epsilon_d h \sqrt{2} \qquad (10.152)$$

This must equal the elongation of the same diagonal in the frame in Fig. 10.33c. In this frame, the applied loads are in equilibrium with induced loads in the diagonal members and there are no loads in the framing members. Consequently, Eq. (10.137) holds regardless of the type of loading to which the element is subjected. The load in the diagonal AB is, therefore,

$$S_d = \frac{\sigma_{xy} h t}{\sqrt{2}} \qquad (10.153)$$

The elongation of the diagonal is

$$e_d = \frac{\sigma_{xy} h t L}{A_d E_d} \qquad (10.154)$$

Equating Eqs. (10.154) and (10.152) and making use of the Eqs. (10.149) and (10.151), we find

$$A_d E_d = \frac{LtE}{\sqrt{2}(1 + \mu)} \qquad (10.155)$$

Thus, for the analogy to be completely applicable, Eqs. (10.155) and (10.147) should be the same. That is,

$$\frac{\sqrt{2}\,\mu LtE}{1 - \mu^2} = \frac{LtE}{\sqrt{2}(1 + \mu)} \qquad (10.156)$$

For this to be the case, it is clear that μ must equal $\frac{1}{3}$. Obviously, the analogy holds strictly only for an apparently restricted group of materials having a Poisson ratio of $1:3$. Fortunately, many common engineering materials, including steels, aluminum alloys, copper, brass, and mag-

nesium alloys, have Poisson ratios rather close to this value. The analogy may therefore be employed with reasonable success in the stress analysis of parts made from these materials.

Hrennikoff[29] shows that values of μ between $\frac{1}{3}$ and $\frac{1}{2}$ may be simulated by pinning horizontal and vertical auxiliary members of area A_2 to the quarter points of the diagonals, as illustrated in Fig. 10.34. For $A_2 = 0$, $\mu = \frac{1}{3}$. For $A_2 = \infty$, $\mu = \frac{1}{2}$. To obtain a μ less than $\frac{1}{3}$, A_2 must be negative. Although the physical construction of a lattice involving members with negative areas is not possible, the use of analog computers or of equivalent electrical circuits does permit negative areas.

Assuming that $\mu = \frac{1}{3}$, the area-modulus requirements of the frame to simulate the continuous element are

$$A_1 E_1 = \frac{3LtE}{8} \qquad A_d E_d = \frac{3LtE}{4\sqrt{2}} \qquad (10.157)$$

The procedure in applying the lattice analogy to a specific problem consists of replacing the actual continuous lamina by means of a pin-jointed framework consisting of elementary frames of the type in Fig. 10.32c. The actual load distribution at the boundaries is represented by concentrated loads applied at the boundary joints of the lattice, as in Figs. 10.32c and 10.33c. Numerical procedures[31] may then be used to evaluate the loads in the various members of the lattice and the deflections of the joints without actually resorting to the construction of the physical lattice.
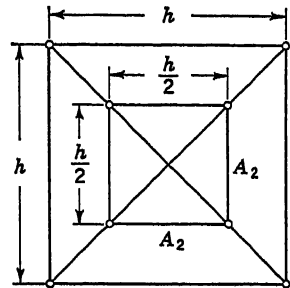
Fig. 10.34

Mechanically, this may be accomplished by building a pinned lattice of elastic members with frictionless joints. The members should be able to take compressive, as well as tensile, loading. This condition can be obtained with rubber bands if in the initial setting all rubber bands are stretched in tension an amount equal to or greater than the maximum expected compressive load. The initially stretched condition of the rubber-band lattice will then correspond to the unstressed state of the specimen. The tensile loadings on the prototype are simulated by increasing the tensile loads on the model at the appropriate joints, while compressive loads on the prototype are simulated by decreasing the tensile loads on the model at the corresponding joints. The joints are simulated by means of thumbtacks pressed through the crossovers of the rubber bands in the initially stretched condition. In the latticework, adjacent pairs of cells always have one side in common.

Gravitational, centrifugal, or other body forces may be included in the lattice analogy by providing at each joint a force component representing one-fourth of the body force acting on the enclosed element of the body.

The parallelism existing between the law of static equilibrium for forces at a joint and Kirchhoff's law for the sum of currents at a node and that existing between Hooke's law relating force to deflection and Ohm's law relating current to voltage points to a method for solving pin-jointed structural problems by means of electrical circuits. Thus, instead of constructing a mechanical or rubber-band model, as suggested above, an electrical circuit may be set up to provide the same information in a much more convenient and rapid manner. Bush[32] describes the application of such an analogy to determinate and indeterminate pin-jointed structures and also to rigid-jointed structures.
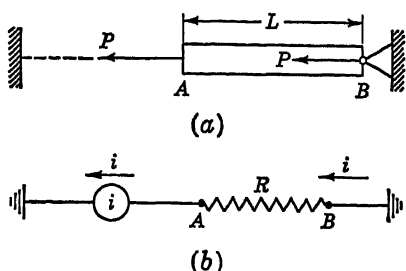
(a)

(b)

Fig. 10.35

In the two-dimensional problem with which we are concerned, two equations of equilibrium must be satisfied at each joint [see Eqs. (10.133)]. Consequently, in the equivalent electrical circuit there must be two nodes for each joint. Consider, first, the trivial case of a single bar subjected to an axial load, as shown in Fig. 10.35a. In this case only one equation of equilibrium exists for each joint (end) of the bar. The corresponding electrical circuit will consist of one node for each joint and is shown in (b). If the current flow at end A be given the same direction as the applied force at that end, the direction of current flow at the other end will correspond to the direction of the force exerted by the bar on its support.

The elongation of the bar as a result of the load P will be

$$e_{AB} = \frac{PL}{AE} \qquad (10.158)$$

This is a statement of Hooke's law.

In the electrical circuit, Ohm's law gives

$$E_{AB} = iR \qquad (10.159)$$

where E_{AB} is the voltage drop across R. Thus, with i analogous to P, R is analogous to L/AE, and E_{AB} is analogous to e_{AB}.

A more complex, but still determinate, structure is shown in Fig. 10.36a. Force components P_1 and P_2 are applied at joint A. Joint C takes only a vertical ground reaction, while joint D takes both a horizontal and a vertical ground reaction.

For the four joints, eight equations of equilibrium must be written and the corresponding electrical circuit will have eight nodes. The joints

and corresponding forces are shown in Fig. 10.36b. The equations of force equilibrium are

	Horizontal	*Vertical*	
Joint A	$P_2 - S_{AB} + S_{AC} \cos \theta_2 = 0$	$-P_1 + S_{AC} \sin \theta_2 = 0$	(10.160)
Joint B	$S_{AB} - S_{DB} \cos \theta_1 = 0$	$S_{BC} - S_{DB} \sin \theta_1 = 0$	(10.161)
Joint C	$S_{DC} - S_{AC} \cos \theta_2 = 0$	$-S_{BC} + R_1 - S_{AC} \sin \theta_2 = 0$	(10.162)
Joint D	$-R_3 - S_{DC} + S_{DB} \cos \theta_1 = 0$	$-R_2 + S_{DB} \sin \theta_1 = 0$	(10.163)

The four nodes of the network arranged to satisfy the four equations for horizontal force equilibrium are shown in (c). The expressions for

(a)

(b)

(c)

(d)
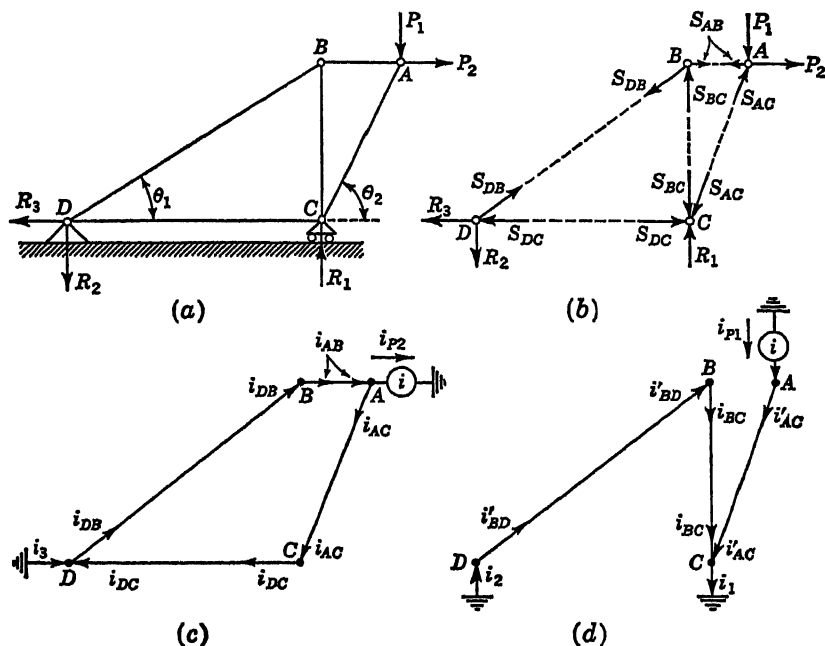
Fig. 10.36

the current sum at each node are

Node A	$i_{P2} - i_{AB} + i_{AC} = 0$	(10.164)
Node B	$i_{AB} - i_{DB} = 0$	(10.165)
Node C	$i_{DC} - i_{AC} = 0$	(10.166)
Node D	$i_{DB} - i_3 - i_{DC} = 0$	(10.167)

The wires AB, AC, DC, and BD must have resistances in accordance with Eq. (10.158) in order that the voltage drops between nodes represent the *horizontal* components of elongation in each member.

The four nodes of the network arranged to satisfy the four equations for vertical force equilibrium are shown in (d). The current sums at the

nodes are

Node A	$-i_{P1} + i'_{AC} = 0$	(10.168)
Node B	$i_{BC} - i'_{BD} = 0$	(10.169)
Node C	$-i_{BC} + i_1 - i'_{AC} = 0$	(10.170)
Node D	$-i_2 + i'_{BD} = 0$	(10.171)

Here, again, the resistances of the wires between nodes must have values in accordance with Eq. (10.158) in order that the voltage drops between nodes represent the *vertical* components of elongation in each member.
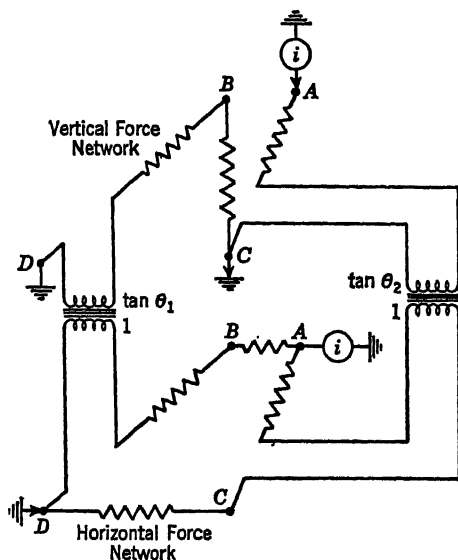
Fig. 10.37

In Eqs. (10.164) to (10.171), i_{AC} represents $S_{AC} \cos \theta_2$, while i'_{AC} represents $S_{AC} \sin \theta_2$. Thus

$$\frac{i'_{AC}}{i_{AC}} = \frac{S_{AC} \cos \theta_2}{S_{AC} \sin \theta_2} = \tan \theta_2 \qquad (10.172)$$

The ratios of the currents in the wires AC of the two networks are the slope of the member AC in the frame. Similarly,

$$\frac{i'_{DB}}{i_{DB}} = \frac{S_{DB} \cos \theta_1}{S_{DB} \sin \theta_1} = \tan \theta_1 \qquad (10.173)$$

These relationships between currents may be enforced by means of current transformers having turns ratios equal to the slopes of the diagonal members. Thus, the complete circuit for the frame in Fig. 10.36a is shown in Fig. 10.37.

The elementary lattice of Figs. 10.32c and 10.33c is shown under com-

bined normal and shear loadings in Fig. 10.38a and its equivalent circuit in (b). In this case 1:1 current transformers are used because the diagonals are all at 45°. The currents shown entering and leaving the nodes in (b) are due to additional cells of the network attached at those points, there being as many elements (b) in the network as there are elementary frames of the type (a) in the lattice analogy. If body forces are involved, then additional currents would be provided at each node from external sources to account for these forces.

The preceding discussion was limited to the simple, but practically important, case of plane stress. Equivalent circuits can also be devel-

(a)   (b)
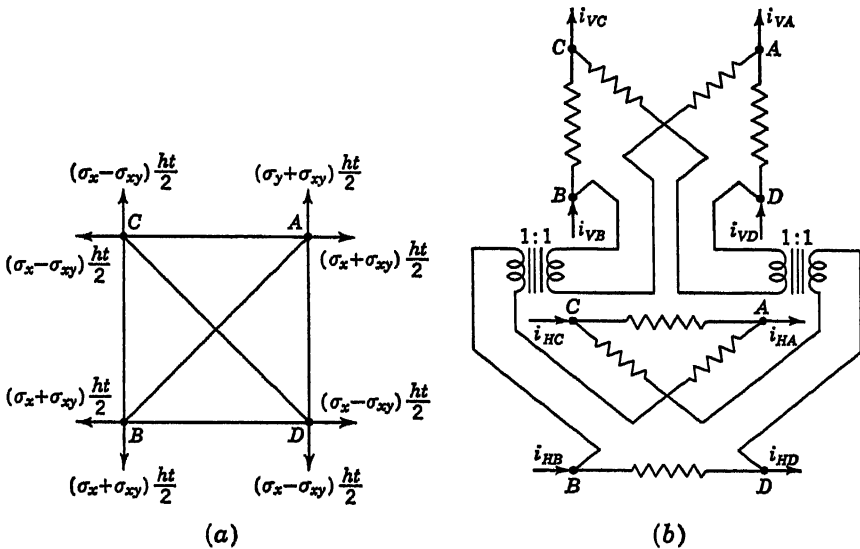
Fig. 10.38

oped for the general three-dimensional problems of the theory of elasticity[33,34] in terms of cartesian, cylindrical, spherical, or other coordinate systems. Most of these analog systems are so complex as to be of questionable value in the analysis of physical problems.

10.13. Utilization of Electronic Analog Computers. While networks of passive electrical elements constitute the most important engineering tools for the solution of finite-difference approximations, there exist numerous applications in this area for electronic differential analyzers. Electronic analog computers are employed to:

1. Generate nonlinear and time-varying boundary excitations
2. Generate feed-in currents in Poisson-type equations and in nonlinear problems
3. Form circuit elements having negative magnitudes
4. Solve directly the finite-difference equations at each node

The generation by electronic circuits of voltages which are nonlinear functions of time or are functions of the dependent variable is described in some detail in Chap. 4. These function generators can be connected directly to the boundary nodes of one-, two-, or three-dimensional network analogs to conform to specified boundary conditions. For the generation of the feed-in currents required for problems of the Poisson type or problems in which nonlinear terms are to be simulated by feed-in currents, current generators rather than voltage generators are required. The voltage generators described in Chap. 4 can be adapted for the generation of current functions by connecting a resistor R_L to the network node or other points in the circuit where a feed-in current is required. As shown in Fig. 10.39, the input terminal of a voltage function generator is connected to the network node having a voltage V_0. In order that the specified current i_0 flow into node 0,
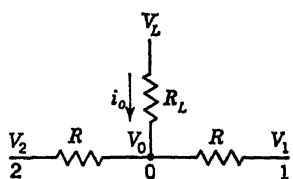
$$i_0 = \frac{V_L - V_0}{R_L} \qquad (10.174)$$

Fig. 10.39

Equation (10.174) can be employed to specify the relationship between the input voltage V_0 and the input voltage V_L of the function generator. For example, consider the simulation of the nonlinear equation[35]

$$\frac{d^2\phi}{dx^2} = K\phi^{-\frac{3}{2}} \qquad (10.175)$$

In finite-difference form, this equation becomes

$$\frac{\phi_1 - \phi_0}{\Delta x^2} + \frac{\phi_2 - \phi_0}{\Delta x^2} = K\phi_0^{-\frac{3}{2}} \qquad (10.176)$$

The terms on the left side of Eq. (10.176) are simulated by a one-dimensional resistance network so that each term corresponds to a current flowing into node 0. Dividing both sides of Eq. (10.176) by R,

$$\frac{\phi_1 - \phi_0}{R} + \frac{\phi_2 - \phi_0}{R} = \frac{K \Delta x^2}{R} \phi_0^{-\frac{3}{2}} \qquad (10.177)$$

To facilitate the simulation of the nonlinear term, Eq. (10.177) can be rewritten as

$$\frac{\phi_1 - \phi_0}{R} + \frac{\phi_2 - \phi_0}{R} + \frac{(\phi_0 - K \Delta x^2 \phi_0^{-\frac{3}{2}}) - \phi_0}{R} = 0 \qquad (10.178)$$

According to Eq. (10.178), a typical node of potential ϕ_0 should be connected to three nodes with potentials of ϕ_1, ϕ_2, and $(\phi_0 - K \Delta x^2 \phi_0^{-\frac{3}{2}})$, respectively, through three equal resistors R. The problem can be

solved, therefore, by attaching to each node of a one-dimensional resistance network a resistor R in magnitude and by applying a voltage $(\phi_0 - K \Delta x^2 \phi_0^{-\frac{1}{2}})$ to its free end. This is illustrated in Fig. 10.40a, where the rectangles represent computer units supplying these voltages. The circuit refers to a system governed by Eq. (10.175) with boundary conditions 0 at $x = 0$ and E at $x = 5\Delta x$. A function-generating circuit,

(a)

(b)
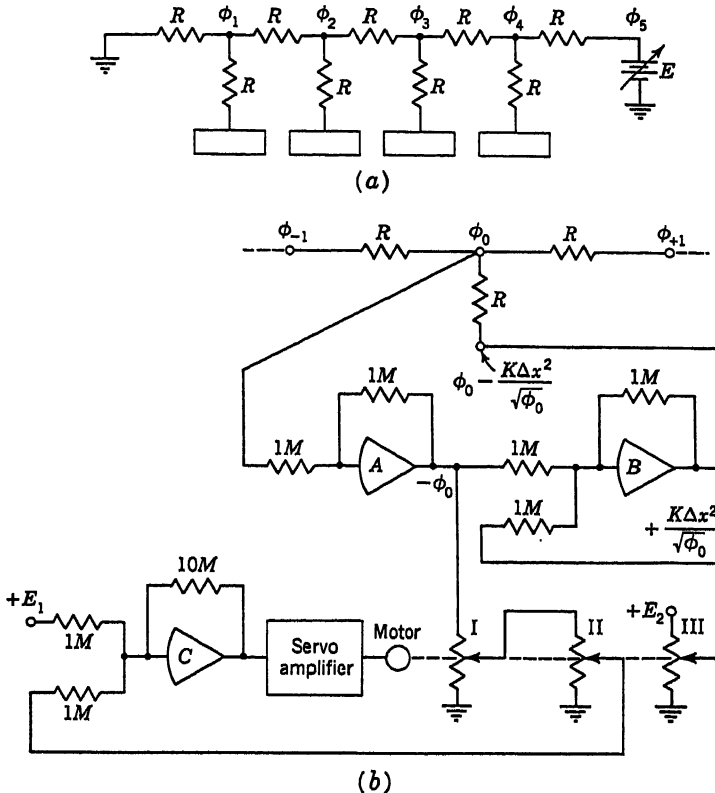
Fig. 10.40

employing servo multipliers to generate the required nonlinear function, is shown in Fig. 10.40b. E_1 and E_2 are fixed voltages determined by K. Such a unit must be used at each node of the resistance network.

Negative resistance and negative reactance elements are required for the simulation of many types of nonlinear ordinary and partial differential equations.

In discussing the nature of negative resistors, it has long been recognized that the mere specification of the magnitude of such a resistor is insufficient to permit a general analysis of its behavior. While, in the case of a positive resistor, the resistance magnitude uniquely determines

the ratio of its excitation to its response, the same is not true for a negative resistor. Negative resistors are variously classified as voltage-controlled and current-controlled or open-circuit stable and short-circuit stable.[36] The current through an open-circuit stable negative resistor R_n approaches infinity if a positive resistor R_p is connected across its terminals and if $R_p < R_n$. The short-circuit stable negative resistor, on the other hand, exhibits such instability if $R_p > R_n$. Analog-computer units for the realization of these two types of elements are shown in Figs. 10.41 and 10.42.

The analysis of the short-circuit stable negative resistor of Fig. 10.41 proceeds as follows: An input voltage e_1, with respect to ground, is applied to terminal 1. A voltage $-e_1$ in magnitude then exists at the
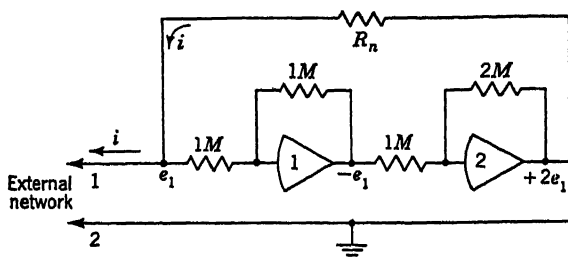
Fig. 10.41

output of amplifier 1, and a voltage $+2e_1$ appears at the output of amplifier 2. The potential difference across resistor R_n is therefore $(2e_1 - e_1)$, and a current $i = e_1 R_n$ flows *into* the junction at terminal 1. Provided the input resistor to amplifier 1 (generally one or more megohms) is large compared with the external impedance connected to terminal 1-2, this entire current flows into the external network. The more positive terminal 1, the larger the current flowing out of this terminal. A resistor $-R_n$ in magnitude has therefore been realized.

A loop containing two operational amplifiers is stable only if the loop gain is less than unity when the phase shift is 360°. The gain from the input of amplifier 1 to the output of amplifier 2 is $2\angle 360°$, and the voltage fed back to the input is $z_{ext}/(R_n + z_{ext})$ times the output of amplifier 2. If at some frequency the external impedance z_{ext} has a zero phase angle and a magnitude larger than R_n, the circuit is unstable. This is evidently the case if terminals 1-2 are left open. The element $-R_n$ is of the voltage-controlled type, because the current i is determined by the voltage e_1. The voltage difference between terminals 1-2 resulting from an input current cannot be derived or specified in a clear and direct manner, however. For this type of element, $i = e/R_n$ but $e \neq iR_n$.

In the open-circuit stable negative resistor shown in Fig. 10.42, a current excitation i flows into terminal 2 and produces a voltage $e_1 = iR_n$

at the input of amplifier 1 (provided $R_n \ll 1M$). The output voltage of amplifier 2 is therefore $2iR_n$ and a voltage difference $(2iR_n - iR_n) = iR_n$ results across terminals 1–2. The terminal *into* which the current flows has the more negative polarity. In this case, the output voltage is governed by the input current, so that this type of element is a negative resistor of the current-controlled type. Here, instability occurs if the
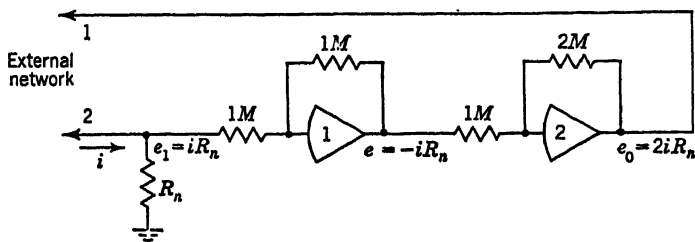
Fig. 10.42
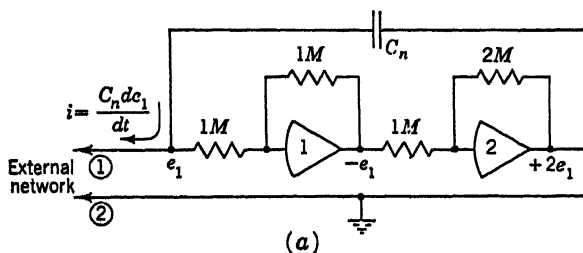
(a)
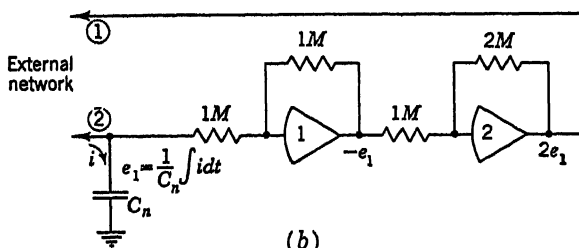
(b)

Fig. 10.43

external impedance has a phase angle of zero and a magnitude smaller than R_n. Short-circuiting terminals 1–2 therefore results in instability.

The same approach is employed to obtain negative reactors. Figure 10.43a shows how a short-circuit stable negative capacitor can be obtained. A potential difference equal to e_1 appears across C_n so that a current $i = C\, de/dt$ flows *out* of terminal 1 into the external network. The open-circuit stable capacitor is obtained by connecting the capacitor C_n from the input terminal to ground as shown in Fig. 10.43b.

Electronic analog-computer units can be applied directly to the solu-

tion of partial differential equations by performing the mathematical operations specified by the finite approximation at each junction of the finite-difference net and by interconnecting in a suitable manner the computer units associated with each node. Rogers[37] and Howe[38,39] have used this method to treat the diffusion, wave, and biharmonic equations.

As an illustration of the basic method, consider the one-dimensional Laplace equation

$$\frac{\partial^2 \phi}{\partial x^2} = 0 \qquad (10.179)$$

whose finite-difference approximation is

$$\frac{\phi_1 + \phi_2 - 2\phi_0}{\Delta x^2} = 0 \qquad (10.180)$$

or

$$\phi_0 = \tfrac{1}{2}(\phi_1 + \phi_2) \qquad (10.181)$$

According to Eq. (10.181), the voltage at each node is equal to one-half the sum of the voltages at adjacent nodes. The circuit, therefore,
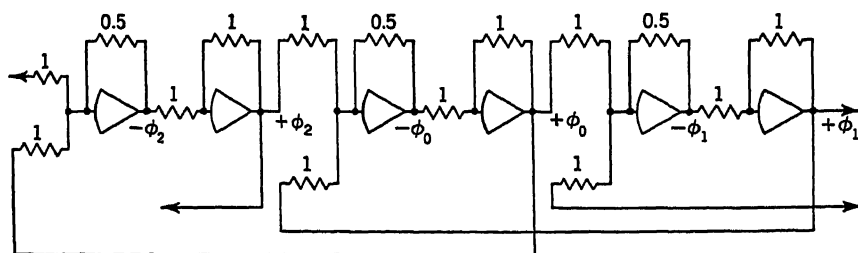
(a)
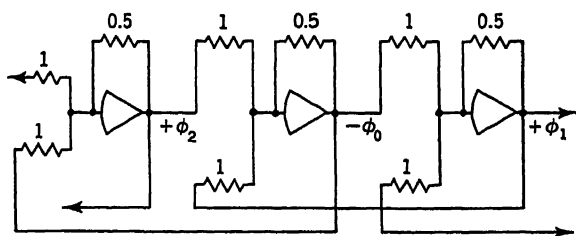
(b)

Fig. 10.44

requires a summer at each node as well as a sign changer to counteract the sign change inherent in each summing operation. The appropriate circuit is shown in Fig. 10.44a. The sign changers can be dispensed with and a considerable saving in equipment can be effected if potentials which alternate in polarity at successive nodes are accepted as solutions. As shown in Fig. 10.44b, the network makes available $+\phi_1$ and $+\phi_2$ but only $-\phi_0$.

The diffusion equation, Eq. (10.76), is approximated in one, two, and three dimensions as

$$\frac{\phi_1 - \phi_0}{h^2} + \frac{\phi_2 - \phi_0}{h^2} = \frac{1}{\alpha}\frac{d\phi_0}{dt}$$

$$\frac{\phi_1 + \phi_0}{h^2} + \frac{\phi_2 - \phi_0}{h^2} + \frac{\phi_3 - \phi_0}{h^2} + \frac{\phi_4 - \phi_0}{h^2} = \frac{1}{\alpha}\frac{d\phi_0}{dt}$$

$$\frac{\phi_1 - \phi_0}{h^2} + \frac{\phi_2 - \phi_0}{h^2} + \frac{\phi_3 - \phi_0}{h^2} + \frac{\phi_4 - \phi_0}{h^2} \tag{10.182}$$

$$+ \frac{\phi_5 - \phi_0}{h^2} + \frac{\phi_6 - \phi_0}{h^2} = \frac{1}{\alpha}\frac{d\phi_0}{dt}$$

where $\Delta x^2 = \Delta y^2 = \Delta z^2 = h^2$, which can be reformulated as

$$\phi_0 = \frac{\alpha}{h^2}\int_0^t (\phi_1 + \phi_2 - 2\phi_0)\, dt$$

$$\phi_0 = \frac{\alpha}{h^2}\int_0^t (\phi_1 + \phi_2 + \phi_3 + \phi_4 - 4\phi_0)\, dt \tag{10.183}$$

$$\phi_0 = \frac{\alpha}{h^2}\int_0^t (\phi_1 + \phi_2 + \phi_3 + \phi_4 + \phi_5 + \phi_6 - 6\phi_0)\, dt$$

A typical node of the electronic analog network therefore consists of an integrator with inputs from two, four, and six nodes, respectively. Node
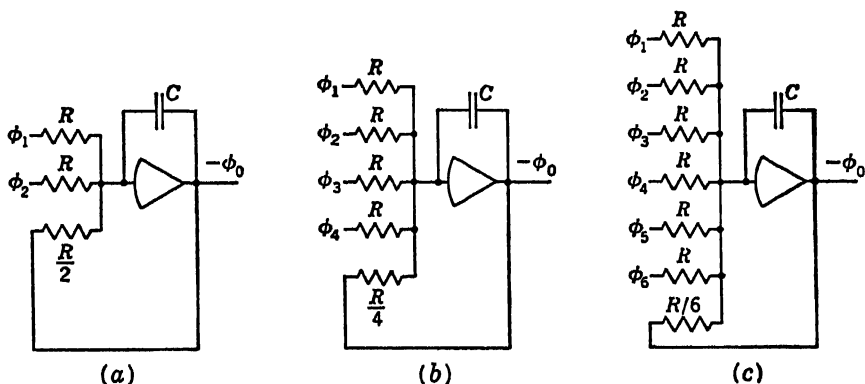
Fig. 10.45

circuits for one-, two-, and three-dimensional systems are shown in Fig. 10.45a, b, and c.

The wave equation, Eq. (10.87), can likewise be treated in this manner. In three dimensions, the finite-difference approximation, Eq. (10.90) can be rewritten as

$$\frac{c^2}{h^2}(\phi_1 + \phi_2 + \phi_3 + \phi_4 + \phi_5 + \phi_6 - 6\phi_0) = \frac{d^2\phi_0}{dt^2} \tag{10.184}$$

The summation and two integrations indicated by this equation may be performed in the circuit shown in Fig. 10.46a, requiring three amplifiers per node.

Rogers[37] shows the scheme in Fig. 10.46b for reducing the number of amplifiers required, by using appropriate transfer impedances in the input and feedback loops of the amplifiers. As described in Sec. 2.13, in operational from, the input transfer function is $2R_1(T_1s + 1)$, the
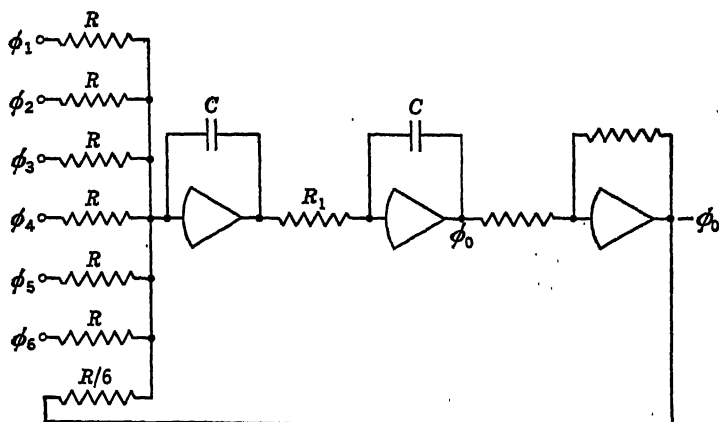
(a)
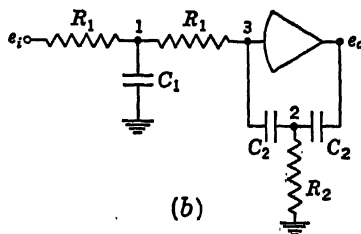
(b)

Fig. 10.46

feedback-loop transfer function is $2(T_2s + 1)/C_2T_2s^2$, and the over-all amplifier transfer function is $(T_2s + 1)/[(T_1s + 1)R_1C_2T_2s^2]$, where $T_1 = \frac{1}{2}R_1C_1$ and $T_2 = 2R_2C_2$. If $T_1 = T_2$ and $R_1{}^2C_1C_2 = 2$, the transfer function becomes $1/s^2$. In other words, a double integration is performed with one amplifier. In the actual problem, we should have $R_1{}^2C_1C_2 = 2h^2/c^2$.

For readers not familiar with operational methods, the validity of the circuit may be shown by applying Kirchhoff's law to nodes 1, 2, and 3. Bearing in mind that node 3 is essentially at ground potential, the current sums at the nodes are given by the equations

$$\frac{e_i - e_1}{R_1} - C_1 \frac{de_1}{dt} - \frac{e_1}{R_1} = 0$$

$$\frac{e_1}{R_1} = -C_2 \frac{de_2}{dt} \qquad (10.185)$$

$$-C_2 \frac{de_2}{dt} = \frac{e_2}{R_2} + C_2 \left(\frac{de_2}{dt} - \frac{de_0}{dt} \right)$$

Solving these equations simultaneously to eliminate e_1, e_2, and their derivatives (differentiating where necessary), the resulting equation is (upon making the substitution $R_1 C_1 = 4 R_2 C_2$)

$$e_i = -\frac{R_1{}^2 C_1 C_2}{2} \frac{d^2 e_o}{dt^2}$$

or

$$e_o = -\frac{2}{R_1{}^2 C_1 C_2} \iint e_i \, dt \, dt \qquad (10.186)$$

The input voltage e actually consists of a sum of seven voltages, as in Fig. 10.46a. Each of the first six input circuits ($\phi_1 - \phi_6$) consists of the input arrangement shown in (b). The output voltage $e_o = -\phi_0$ is fed back to the input as the seventh required voltage through the same type of input circuit, which has different values for the two Rs and the C to account for the numerical multiplier 6. Calling these R_3 and C_3, their values are $R_3 = R_1/6$, $C_3 = 6C_1$.

Equations involving higher derivatives than the second are often difficult to set up in passive equivalent circuits without the use of isolating transformers. An example of an equation with a fourth derivative is the beam-vibration problem discussed in Sec. 10.11. Electronic analog-computer circuits of the type discussed in this section handle these higher derivatives as easily as the lower ones, merely at the expense of more inputs per amplifier.

Consider, for example, the equation

$$\frac{d^4 \phi}{dx^4} + A \frac{d^3 \phi}{dx^3} + B \frac{d^2 \phi}{dx^2} + C \frac{d\phi}{dx} + D\phi = 0 \qquad (10.187)$$

A typical set of nodes is shown in Fig. 10.47a, with Eq. (10.187) to be satisfied at each node. Taking point 0 as the node, two adjacent points on each side of 0 are required to develop $d^4\phi/dx^4$ and $d^3\phi/dx^3$. The development proceeds as follows: the fourth derivative at 0 is the difference of third derivatives at A and B divided by h; the third derivative at A is the difference of second derivatives at 1 and 0 divided by h; the third derivative at B is similarly found; the third derivative at 0 is the difference of second derivatives at A and B divided by h; the second derivative at 1 is the difference of first derivatives at C and A divided

by h; the second derivatives at A, 0, B, and 2 are similarly found; the first derivative at C is $(\phi_3 - \phi_1)/h$; the first derivative at 1 is $\frac{1}{2}(\phi_3 - \phi_0)/h$; the required first derivatives at all the other points are similarly determined, bearing in mind that one may use only the values of ϕ at the
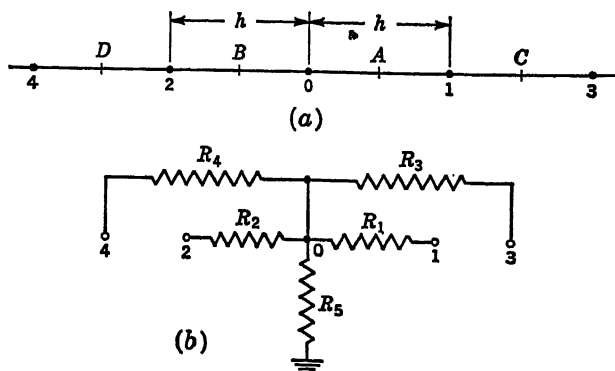
Fig. 10.47

network points 0-4, and not at in-between points A-D. Upon setting up all the finite–difference equivalents, the following relations result:

$$\left(\frac{d^4\phi}{dx^4}\right)_0 \approx \frac{1}{h^4}\,(\phi_3 - 4\phi_1 + 6\phi_0 - 4\phi_2 + \phi_4)$$

$$\left(\frac{d^3\phi}{dx^3}\right)_0 \approx \frac{1}{2h^3}\,(\phi_3 - 2\phi_1 + 2\phi_2 - \phi_4)$$

$$\left(\frac{d^2\phi}{dx^2}\right)_0 \approx \frac{1}{h^2}\,(\phi_1 - 2\phi_0 + \phi_2)$$

$$\left(\frac{d\phi}{dx}\right)_0 \approx \frac{1}{2h}\,(\phi_1 - \phi_2)$$

(10.188)

If an equivalent circuit based on the sum of currents at a node is to be set up for Eqs. (10.188), expressions must be set up in terms of differences with respect to the node. Thus, Eqs. (10.188) become

$$\left(\frac{d^4\phi}{dx^4}\right)_0 \approx \frac{\phi_3 - \phi_0}{h^4} - \frac{\phi_1 - \phi_0}{h^4/4} - \frac{\phi_2 - \phi_0}{h^4/4} + \frac{\phi_4 - \phi_0}{h^4}$$

$$\left(\frac{d^3\phi}{dx^3}\right)_0 \approx \frac{\phi_3 - \phi_0}{2h^3} - \frac{\phi_1 - \phi_0}{h^3} + \frac{\phi_2 - \phi_0}{h^3} - \frac{\phi_4 - \phi_0}{2h^3}$$

$$\left(\frac{d^2\phi}{dx^2}\right)_0 \approx \frac{\phi_1 - \phi_0}{h^2} + \frac{\phi_2 - \phi_0}{h^2}$$

$$\left(\frac{d\phi}{dx}\right)_0 \approx \frac{\phi_1 - \phi_0}{2h} - \frac{\phi_2 - \phi_0}{2h}$$

(10.189)

Combining Eqs. (10.189) in Eq. (10.187), the Kirchhoff equation for the

current sum at node 0 becomes

$$\left(\frac{1}{h^4} + \frac{A}{2h^3}\right)(\phi_3 - \phi_0) + \left(-\frac{4}{h^4} - \frac{A}{h^3} + \frac{B}{h^2} + \frac{C}{2h}\right)(\phi_1 - \phi_0)$$

$$+ \left(-\frac{4}{h^4} + \frac{A}{h^3} + \frac{B}{h^2} - \frac{C}{2h}\right)(\phi_2 - \phi_0) + \left(\frac{1}{h^4} - \frac{A}{2h^3}\right)(\phi_4 - \phi_0)$$

$$+ D\phi_0 = 0 \quad (10.190)$$

The circuit shown in Fig. 10.46b satisfies Eq. (10.190) if

$$\frac{1}{R_1} = -\frac{4}{h^4} - \frac{A}{h^3} + \frac{B}{h^2} + \frac{C}{2h}$$

$$\frac{1}{R_2} = -\frac{4}{h^4} + \frac{A}{h^3} + \frac{B}{h^2} - \frac{C}{2h}$$

$$\frac{1}{R_3} = \frac{1}{h^4} + \frac{A}{2h^3} \quad (10.191)$$

$$\frac{1}{R_4} = \frac{1}{h^4} - \frac{A}{2h^3}$$

$$\frac{1}{R_5} = -D$$

A difficulty arises when the circuit for node 0 is to be connected into similar circuits for nodes 1 and 2, and 3 and 4. Unilateral impedance elements are required between 0 and 4, 0 and 3, and 1 and 2.

Substitution of Eqs. (10.188) into Eq. (10.187) points out the electronic analog computer circuit necessary to represent node 0. The resulting equation is

$$\phi_0 = \frac{1}{M}\left[\left(-\frac{4}{h^4} - \frac{A}{h^3} + \frac{B}{h^2} + \frac{C}{2h}\right)\phi_1 + \left(-\frac{4}{h^4} + \frac{A}{h^3} + \frac{C}{h^2} - \frac{D}{2h}\right)\phi_2\right.$$

$$\left. + \left(\frac{1}{h^4} + \frac{A}{2h^3}\right)\phi_3 + \left(\frac{1}{h^4} - \frac{A}{2h^3}\right)\phi_4\right] \quad (10.192)$$

where $M = -(6/h^4) + (2B/h^2) - D$.

REFERENCES

1. Southwell, R. V.: "Relaxation Methods in Engineering Science," Oxford University Press, New York, 1940.
2. Southwell, R. V.: "Relaxation Methods in Theoretical Physics," Oxford University Press, New York, 1946.
3. Karplus, W. J.: "Analog Simulation: Solution of Field Problems," McGraw-Hill Book Company, Inc., New York, 1958.
4. Johnson, W. C., and R. E. Alley, Jr.: "An Electrical Method for the Solution of Differential Equations," Report 3, ONR Contract N6or-105, Task Order VI, Princeton University, Princeton, N. J., June, 1948.
5. Liebmann, H.: Die angenaherte Ermittelung harmonischer Functionen und konformer Abbildungen, *Sitzber. math.-naturw. Abt. bayer. Akad. Wiss. München*, 1918, p. 385.

6. Shortley, G. H., and R. Weller: The Numerical Solution of Laplace's Equation, *J. Appl. Phys.*, **9**:334–348 (1938).
7. Emmons, W. H.: The Numerical Solution of Heat-conduction Problems, *Trans. ASME*, **65**:607–615 (1943).
8. Hogan, T. K.: A General Experimental Solution of Poisson's Equation for Two Independent Variables, *J. Inst. Engrs. Australia*, **15**:89–92 (1943).
9. Liebmann, G.: Solution of Partial Differential Equations with a Resistance Network Analogue, *Brit. J. Appl. Phys.*, **1**:92–103 (1950).
10. Fox, L.: Some Improvements in the Use of Relaxation Methods for the Solution of Ordinary and Partial Differential Equations, *Proc. Roy. Soc. (London)*, (A)**190**: 31–59 (1947).
11. Richardson, L. F.: How to Solve Differential Equations Approximately by Arithmetic, *Math. Gaz.*, **12**:415–421 (1924–1925).
12. Slater, J. C., and N. H. Frank: "Introduction to Theoretical Physics," p. 201, McGraw-Hill Book Company, Inc., New York, 1933.
13. Paschkis, V., and H. D. Baker: A Method for Determining Unsteady-state Heat Transfer by Means of an Electrical Analogy, *Trans. ASME*, **64**:105–112 (1942).
14. Paschkis, V.: Comparison of Long-time and Short-time Analog Computers, *Trans. AIEE*, **68**:70–73 (1949).
15. Bruce, W. A.: An Electrical Device for Analyzing Oil-reservoir Behavior, *Trans. AIMME* (Petroleum Division), **151**:112–124 (1943).
16. Neel, C. B., Jr.: An Investigation Utilizing an Electrical Analogue of Cyclic De-icing of a Hollow Steel Propeller with an External Blade Shoe, *NACA TN* 2852, December, 1952.
17. Liebmann, G.: A New Electrical Method for the Solution of Transient Heat Conduction Problems, *Trans. ASME*, **78**:655–665 (1956).
18. Liebmann, G.: Solution of Transient Heat-transfer Problems by the Resistance Network Analog Method, *Trans. ASME*, **78**:1267–1272 (1956).
19. Kron, G.: Numerical Solutions of Ordinary and Partial Differential Equations by Means of Equivalent Circuits, *J. Appl. Phys.*, **16**:172–186 (1945).
20. Swenson, G. W., Jr., and T. J. Higgins: A Direct-current Network Analyzer for Solving Wave-equation Boundary-value Problems, *J. Appl. Phys.*, **23**:126–131 (1952).
21. Spangenberg, K., G. Walters, and F. Schott: Electrical Network Analyzers for the Solution of Electromagnetic Field Problems, Part I, Theory, Design and Construction, *Proc. IRE*, **37**:724–729 (1949).
22. Kron, G.: Equivalent Circuits to Represent the Electromagnetic Field Equations, *Phys. Rev.*, **64**:126–128 (1943).
23. Whinnery, J. R., and S. Ramo: A New Approach to the Solution of High Frequency Field Problems, *Proc. IRE*, **32**:284–288 (1944).
24. McCann, G. D., and R. H. MacNeal: Beam-vibration Analysis with the Electric-analog Computer, *J. Appl. Mechanics*, **17**:13–26 (1950).
25. MacNeal, R. H.: The Solution of Elastic Plate Problems by Electrical Analogies, *J. Appl. Mechanics*, **18**:59–67 (1951).
26. Benscoter, S. U., and R. H. MacNeal: Introduction to Electrical-circuit Analogies for Beam Analysis, *NACA TN* 2785, September, 1952.
27. Trent, H. M.: An Equivalent Circuit for a Vibrating Beam Which Includes Shear Motions, *J. Acoust. Soc. Am.*, **22**:355–357 (1950).
28. McHenry, D.: A Lattice Analogy for the Solution of Stress Problems, *J. Inst. Civil Engrs. (London)*, **21**:59–82 (1943–1944).
29. Hrennikoff, A.: Solutions of Problems of Elasticity by the Framework Method, *J. Appl. Mechanics*, **8**:169–175 (1941).

30. Murphy, G.: "Advanced Mechanics of Materials," p. 41, McGraw-Hill Book Company, Inc., New York, 1946.

31. Southwell, R. V.: Relaxation Methods as Applied to Structures, *Structural Eng.*, **26**:463–506 (1948).

32. Bush, V.: Structural Analysis by Electric Circuit Analogies, *J. Franklin Inst.*, **217**:289–329 (1934).

33. Kron, G.: Equivalent Circuits for the Elastic Field, *J. Appl. Mechanics*, **11**:149–161 (1944).

34. Gross, W. A.: "Adaptation of Electrical Network Methods to the Solution of Problems in the Theory of Elasticity," Ph.D. Thesis, University of California, Berkeley, Calif., August, 1951.

35. Karplus, W. J.: The Use of Electronic Analogue Computers with Resistance Network Analogues, *Brit. J. Appl. Phys.*, **6**:356–357 (1955).

36. Karplus, W. J.: Synthesis of Non—P.R. Driving Point Impedance Functions Using Analog Computer Units, *IRE Trans. on Circuit Theory*, **4**:170–172 (1957).

37. Rogers, T. A.: "Electronic Analog Computers and Partial Differential Equation Solutions," Memorandum to Department of Engineering, University of California, Los Angeles, 1952, 12 pages.

38. Howe, R. M., and V. S. Haneman: The Solution of Partial Differential Equations by Difference Methods Using the Electronic Differential Analyzer, *Proc. IRE*, **41**:1497–1508 (1953).

39. Howe, C. E., and R. M. Howe: Application of the Electronic Differential Analyzer to the Oscillation of Beams, Including Shear and Rotary Inertia, *J. Appl. Mechanics*, **22**:13–19 (1955).

11

CONTINUOUS FIELD ANALOGS

In Chap. 10, the partial differential equations characterizing field problems are approximated by finite-difference expressions. That procedure is useful because it permits the simulation of continuous fields by means of lumped electrical elements. An alternative approach is to represent the original system, which is continuous in nature, by an analog model which is also continuous. As before, the objective is to construct an experimental system, linked to the prototype system by a direct analogy, on which measurements can be taken more conveniently or more economically than on the original system. Only two types of direct continuous analogs have assumed an important role in analog simulations. These are the stretched membrane models, which are particularly useful in structural analysis, and the electrically conductive sheet systems, which have been employed to study potential fields in many areas of physics. A number of other continuous analogs employing fluid-flow fields, magnetic fields, optical fields, and even thermal fields have been used in special applications from time to time. Nearly all continuous field analogs are limited in their applicability to the study of fields governed by Laplace's and Poisson's equations, and few can be adapted to the simulation of three-dimensional systems.

11.1. The Stretched Membrane. Suppose a thin sheet of rubber to be stretched uniformly in all directions and clamped in a flat frame. We assume that a uniform tension T exists throughout the sheet within this boundary. If the frame is now distorted out of plane in an arbitrary manner, the membrane surface will acquire double curvature, the elevation of the surface varying smoothly from point to point to meet the distorted boundary. Each small element of area of the distorted film is in static equilibrium under the action of the tensile forces acting at its edges. If the boundary elevations do not vary too abruptly, the tension T is not appreciably affected by the distortion and may be considered to be unaltered. Under these conditions we may proceed to set up the equations of equilibrium for an elementary area $dx\,dy$ of the membrane.

Figure 11.1*a* shows such a membrane with boundary elevations varying from point to point in a predetermined manner. Figure 11.1*b* shows the element $dx\ dy$ edge on. The slope of this element at x is $\partial z/\partial x$; at $x + dx$ it is $\partial z/\partial x + (\partial^2 z/\partial x^2)\ dx$. The downward component of the tension at x is $T(\partial z/\partial x)$ if the slope is gentle enough so that the sine and the tangent of the angle of slope are not significantly different. The upward component of the tension at $x + dx$ is $T[\partial z/\partial x + (\partial^2 z/\partial x^2)\ dx]$. Multiplying by the length dy, the net upward pull on the element due to the change in slope in the x direction is $T(\partial^2 z/\partial x^2)\ dx\ dy$. A similar expression is
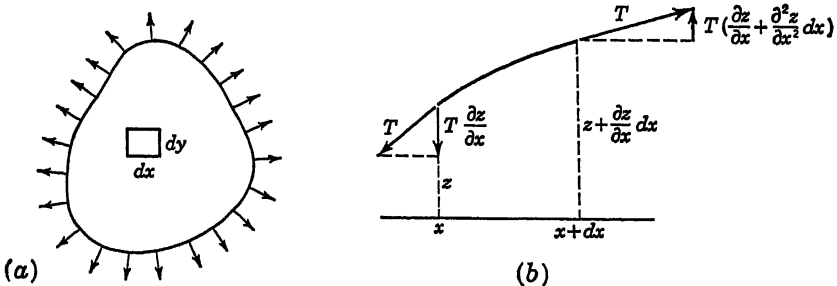
Fig. 11.1

obtained if the variation of slope in the y direction is considered. Since the element is in static equilibrium, the sum of the forces acting on it must equal zero. Thus, adding and dividing by $dx\ dy$, the equilibrium equation becomes

$$\frac{\partial^2 z}{\partial x^2} + \frac{\partial^2 z}{\partial y^2} = 0 \qquad (11.1)$$

The membrane may be used, therefore, to simulate any problem for which the Laplace equation (11.1) applies and for which boundary conditions may be set up as elevations. Such problems include steady-state heat conduction in a two-dimensional medium of constant conductivity. The edges of the membrane are built up in proportion to the boundary temperatures, whereupon lines of constant elevation in the membrane will represent lines of constant temperature in the conducting medium. If points inside the boundary are maintained at constant temperature by some external means, the membrane would be maintained at those points at the appropriate elevations by means of frictionless pegs. The rate of heat flow in any given direction is proportional to the temperature gradient in that direction, which in the case of the membrane would be represented by the slope. Points of steepest slope will represent positions of greatest heat transfer (and therefore of greatest thermal stress), while points of minimum slope may indicate hot spots. The total heat

flow across a boundary would be obtained by integrating the membrane slope (normal to the boundary) with respect to distance along the boundary. The contour lines and the lines of steepest descent on the membrane form an orthogonal system. If the spacing were made small enough in both directions, a system of curvilinear squares would result. The heat-flow path is confined between lines of steepest descent, which thus form tubes of heat flow. The feasibility of using the membrane for heat-conduction studies has been demonstrated.[1]

The same problem arises in electrostatic fields (vacuum-tube[2] or capacitor design). The voltage distribution in a two-dimensional field must satisfy the Laplace equation. By elevating a stretched membrane at all points corresponding to known electrode voltages, elevations at other points in the membrane would correspond to voltages existing at those points in the given electrostatic field. Electron velocities and trajectories in such a field will depend on the voltage gradient and electron mass. By using a rolling ball to simulate an electron, the ball trajectory on the rubber sheet will simulate the electron path. Thus, by introducing balls at different initial velocities and directions, electron paths may be easily observed and recorded for different electrode arrangements. Electron multiplier tubes have been designed with the aid of such a gravitational model.[3] If an electrode voltage is oscillatory, it may be simulated by moving the corresponding peg of the stretched rubber sheet up and down in the same fashion (but at a much lower frequency, of course). Such a method has been used in the study of cathode-ray tubes with alternating fields[4] and in the design of the input space of the Resnatron.[5] Certain errors are involved in simulating electrostatic fields by rubber models. An analysis of such errors has been made by Walker.[6]

In the field of elasticity, the stretched elastic membrane has found more than one application. The experimental techniques of photoelasticity have been ably supplemented with the membrane analogy. A photoelastic test yields values of principal stress difference $(P - Q)$ throughout a loaded model. Generally, it is desirable to find the principal stresses P and Q separately. At unloaded boundary points, one of the principal stresses is zero, so that the principal stress difference and the principal stress sum have the same values. It can be shown from the theory of elasticity that the sum of the principal stresses throughout the body obeys Laplace's equation. Consequently, knowing what the boundary values are (from photoelastic tests), a stretched membrane with appropriate boundary elevations will provide the stress sum at all other points in the model. This sum, combined with the difference from photoelastic tests, will yield the individual values of P and Q. A rubber membrane was used in this manner to supplement photoelastic tests on a tension

specimen with a central hole.[7]   In another analysis, a soap film was used instead of rubber sheet to supplement photoelastic tests on cantilever-beam models.[8]

The use of a soap film as a membrane has certain advantages.   Made of a solution of potassium or sodium oleate, glycerin, and distilled water, soap films capable of lasting for 24 hr have been constructed.[8]   A board dipped into such a solution and then drawn over an opening in a piece of sheet metal will leave a thin film clinging to the edges of the hole and stretched across the opening.   The surface tension of the film provides the required uniform tension in all directions without the need for special stretching apparatus.   The main disadvantages of such a film are the care which must be taken to avoid pricking it and the tendency of the solution to drain to low points and thus weight the film or make measurements more difficult.   If, however, in a problem such as the heat-conduction problem mentioned above there is an insulated area within the boundaries, *i.e.*, a hole in the conducting sheet, no heat would flow across this boundary and the temperature gradient normal to the boundary would be zero.   In a membrane representation of this problem, the heat-conducting region would be represented by an open hole in a piece of sheet metal, the edges of the hole being deformed to give the proper elevations.   The inside nonconducting area would be represented by another boundary to which the membrane must cling with zero slope. While this might be done with a rubber membrane by varying the elevations around the inner boundary until zero slope were obtained, the soap film would automatically assume this position if the inner boundary is in the shape of a wall along which the edge of the soap film may creep until it finds its position of equilibrium.   At this position of equilibrium surface tension is normal to the wall; hence the slope of the film is zero.

Such a film may thus be used to simulate the two-dimensional flow of an ideal fluid around obstacles.   The elevations of the film would represent the velocity potential.   Since no flow takes place through the surface of an obstacle, the gradient of velocity potential normal to the surface of the obstacle must be zero.   A soap film constructed as in the previous paragraph satisfies this condition.

In the analysis of the membrane (or soap film) equation up to this point, the assumption was made that the slope of the membrane was small, so that the sine and tangent of the slope angle were substantially equal.   If this restriction is removed, the equation of equilibrium for the soap film becomes[9]

$$\frac{\partial^2 z}{\partial x^2}\left[1 + \left(\frac{\partial z}{\partial y}\right)^2\right] + \frac{\partial^2 z}{\partial y^2}\left[1 + \left(\frac{\partial z}{\partial x}\right)^2\right] - 2\frac{\partial^2 z}{\partial x\, \partial y}\frac{\partial z}{\partial x}\frac{\partial z}{\partial y} = 0 \quad (11.2)$$

Bateman[10] shows that for the irrotational compressible flow of fluid,

$$\left[c^2 - \left(\frac{\partial \phi}{\partial x}\right)^2\right]\frac{\partial^2 \phi}{\partial x^2} + \left[c^2 - \left(\frac{\partial \phi}{\partial y}\right)^2\right]\frac{\partial^2 \phi}{\partial y^2} - 2\frac{\partial \phi}{\partial x}\frac{\partial \phi}{\partial y}\frac{\partial^2 \phi}{\partial x\, \partial y} = 0 \quad (11.3)$$

where $c^2 = dp/d\rho$ is the local velocity of sound, $\partial \phi/\partial x = u$ and $\partial \phi/\partial y = v$, the x and y components of the local fluid velocity $q = [(u^2 + v^2)^{\frac{1}{2}}]$. If the pressure-density relation of the fluid is of the Earnshaw-Chaplygin type[11]

$$p = A - \frac{B}{\rho} \quad (11.4)$$

then

$$b^2 = c^2 - q^2 \quad (11.5)$$

where b is a constant. Thus we may substitute $b^2 + q^2$ in place of c^2 in Eq. (11.3), which results in

$$\left[b^2 + \left(\frac{\partial \phi}{\partial y}\right)^2\right]\frac{\partial^2 \phi}{\partial x^2} + \left[b^2 + \left(\frac{\partial \phi}{\partial x}\right)^2\right]\frac{\partial^2 \phi}{\partial y^2} - 2\frac{\partial \phi}{\partial x}\frac{\partial \phi}{\partial y}\frac{\partial^2 \phi}{\partial x\, \partial y} = 0 \quad (11.6)$$

Equations (11.6) and (11.2) are exactly alike if the constant b^2 is equal to unity. For the compressible flow of this type of fluid, the elevations of the open soap bubble give the potential function ϕ. Bateman suggested the soap-film analogy for this case.[10]

11.2. The Transversely Loaded Membrane. When a stretched membrane is subjected to transverse loads, the equation of equilibrium for small slopes becomes the Poisson equation

$$\frac{\partial^2 z}{\partial x^2} + \frac{\partial^2 z}{\partial y^2} = -\frac{P}{T} \quad (11.7)$$

where P is the transverse load per unit area applied in the positive z direction.

One of the simplest loads which can be applied is a uniformly distributed pressure on one side of the membrane. This may be done either with air pressure or hydrostatic head. Prandtl[12] proposed in 1903 the use of a membrane under uniformly distributed pressure as a means for determining stress distributions in a prismatic bar subjected to torsion.

It can be shown by means of the theory of elasticity that the shear stress distribution over the cross section of a straight bar subjected to torques at its ends may be expressed in terms of the gradient of a stress function in much the same manner as velocities in potential flow are expressed in terms of a potential function gradient. Thus, referring to Fig. 11.2, which shows a cross section of a straight bar, at a point x,y on

the surface, the shear stresses in the x and y directions may be written as

$$\sigma_{zx} = \frac{\partial \phi}{\partial y} \qquad \sigma_{zy} = -\frac{\partial \phi}{\partial x} \qquad (11.8)$$

If G is the modulus of rigidity of the bar material and θ the angle of twist in radians per unit of length of the bar, the theory of elasticity shows that

$$\frac{\partial^2 \phi}{\partial x^2} + \frac{\partial^2 \phi}{\partial y^2} = -2G\theta \qquad (11.9)$$

Fig. 11.2

At any point on the boundary, e.g., point B in Fig. 11.2, the shear stress on the cross section must be tangent to the boundary. If it were not, then there would be a stress component normal to the boundary, which is not possible at an unloaded surface. The line CD is drawn perpendicular to the boundary. The projections of the component stresses σ_{zyb} and σ_{zxb} on CD must be equal and opposite. Thus,

$$\sigma_{zyb} \sin \alpha = \sigma_{zxb} \sin \beta \qquad (11.10)$$

Since $\sin \alpha = dx/ds$ and $\sin \beta = dy/ds$, and by means of Eqs. (11.8), this equation becomes

$$-\frac{\partial \phi_b}{\partial x}\frac{dx}{ds} = \frac{\partial \phi_b}{\partial y}\frac{dy}{ds} \qquad (11.11)$$

or

$$\frac{\partial \phi_b}{\partial x} dx + \frac{\partial \phi_b}{\partial y} dy = 0 \qquad (11.12)$$

which means that the stress function ϕ_b along the boundary is constant. For solid bars, this constant is arbitrary and may be taken equal to zero. For bars with one or more hollows, the stress function is a constant along each inner boundary, but it is a different constant for each such boundary.

In the application of the membrane to torsional problems, the boundary of the membrane has the same contour as the cross section of the bar. The boundary is everywhere at zero elevation and the membrane is bowed out by a uniformly distributed pressure. The contour lines (lines of equal elevation) of the membrane are the constant-ϕ lines of the cross section. The resultant shear stress at each point is tangent to such a contour. The slope of the membrane provides the shear stress in accordance with Eqs. (11.8). The slope at right angles to any contour line (including the boundary contours) is a measure of the resultant shear stress at that point.
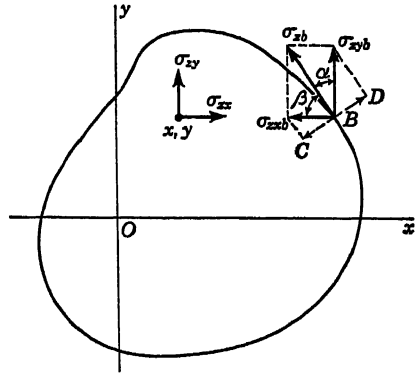
The soap film as a membrane for torsional problems has been widely used.   Griffith and Taylor[13-15] had developed soap-film techniques for such problems in detail many years ago.   Since then there have been frequent disclosures of the theory and application of the method to various torsion problems.[16-18]

In Griffith and Taylor's work the films were formed on holes cut to the required shapes in flat plates.   It was found necessary to chamfer the edges of the holes to an angle of about 45° in order to establish definitely the edge of the film.   Various materials were tried for the plate, the most satisfactory one being 18-gauge bare aluminum.   The plate was used in a horizontal position since it was determined that the effect of the weight of the film was negligible.   In a vertical position excessive drainage occurs, leading to a short life.   Weibel[8] found that sag was inappreciable for unsupported spans of 1-in. but amounted to about 0.006 in. in the middle of 3-in. spans.

In order to make direct use of data provided by a soap film for evaluating torsional stresses, it is necessary to know the value of film tension and the pressure.   A simpler approach not requiring these measurements consists of using the same film and pressure for a circular hole representing a circular shaft for which an exact solution is known.   With a circular shaft as reference, the measured slopes of the soap film under test may be compared with measured slopes on the circular soap film and thus corresponding shear stresses are compared for two bars, one of them circular, made of the same material and subjected to the same twist per unit length (not to the same torque).   Both holes are placed in the same sheet, have the same soap solution spread over them, and are subjected to the same pressure beneath the films.

Measurements may be made either by measuring contours of equal elevation from which the slope of the film may be determined by graphic methods, or a collimator may be used for direct measurement of slopes by means of a light beam reflected from the surface of the film.

The former method appears to be preferred by workers in the field.   A common method of determining contour lines is to mount a micrometer head on a sheet of plate glass which is guided to slide always parallel to the plate providing the fixed boundary for the soap film.   The elevation of a steel needle point projecting through the glass is accurately adjustable by means of the micrometer screw.   Setting the needle point for a given elevation (a given contour), one may slide the glass plate around the film locating these points at which a slight distortion of the reflected image of the point in the soap film indicates contact between the two and, therefore, a point on the contour line.   Readings of elevation by means of the needle-point method may be made to an accuracy of ±0.001 in.   A hinged cover on the box containing the soap film when brought down

against the micrometer head is pricked by a sharp point on the head, thereby locating on a sheet of recording paper on the cover the position of the point found.

Drainage of the film occurs during its existence, causing in time the appearance of a black spot at the high point of the film, which gradually spreads down the sides of the film. The film may be renewed by placing a drop of soap solution on the needle point and allowing it to contact the high point of the film.

This problem of drainage is one of the drawbacks of the method, since the liquid collects around the edge of the film, forming a bead or fillet which makes direct measurement of slopes at the boundary difficult.

The appearance of the black spot on the film after about 15 min provides a convenient means for direct observation of contour lines since it has been found that the advancing edge of the black area is a line of constant elevation. Thus successive photographs looking down on the film will provide in a few hours a record of the contour shapes. For quantitative analysis, of course, the horizontal and vertical displacements of the edge would be required. These are not so conveniently determined; hence the black-area method is useful mainly in providing a qualitative picture of the contour distribution over the film.

Tests by Griffith and Taylor on sections which could also be calculated indicate that minimum deviation of measured contour shapes from calculated shapes occurs when the mean inclination of the film around the boundary is 20°. This situation arises because the analogy between the torsion function ϕ and the elevation z of the soap film holds strictly only when the slopes are small enough so that the sine and the tangent are equal.

Where a check by direct calculation could be made, Griffith and Taylor found that the soap-film method gave results agreeing to within 1 or 2 per cent with theory.

The utility of the method resides in its application to bars having cross sections not capable of analytical solution. Roark[19] lists expressions for maximum shear stress in structural sections and in other sections which have been solved by the membrane analogy. He suggests that these values are perhaps accurate to ± 10 per cent.

When the section is such as to have one or two axes of symmetry, only one-half or one-fourth of the cross section need be represented by the hole in the plate. Thus the scale of the model may be increased with improved precision in the test data. The axes of symmetry are represented by septa, or diaphragms, which extend upward perpendicular to the test plate. It is advisable to extend the septa downward also, so that they project about $\frac{1}{8}$ in. below the bottom surface of the test plate to permit free drainage of solution.

. Another development in soap-film measurement and analysis techniques is due to A. D. Moore.[20]   In this method a camera lens is pointed downward at a soap film through an aperture in a ceiling.   Circles drawn concentrically on the ceiling about the camera lens, and radial lines on the ceiling drawn from the lens as center are reflected from the soap film into the lens as distorted curves due to the curvature of the film.   A single photograph thus serves to record the effect of the soap-bubble form, from which contour lines may be determined by analysis at leisure.

Moore has also developed the "sandbed mapper" in which the streamlines of a thin layer of fluid in viscous flow are shown to correspond to the lines of steepest descent in a soap film.   In this technique a constant-thickness permeable bed (consisting of a "sand" of nickel or copper shot about 0.02 in. in diameter) serves as a uniformly distributed source or sink of the same shape as the cross section of the bar under torsion.   A glass plate spaced slightly above the bed provides a thin two-dimensional horizontal layer through which laminar flow of water may take place. With the sandbed used as a sink, water is drawn in around the edges of the submerged sandbed, flows over the sandbed surface under the glass plate, and sinks into the sandbed at a substantially uniformly distributed rate on the assumption that the entire pressure drop occurs through the sandbed and only a negligible drop in the space between the glass and the bed.   Dye crystals at the edges of the bed produce streaks in the flowing water, which may be photographed through the glass plate and analyzed in terms of lines of steepest descent in a soap film.

In another approach to the problem of torsion, Drucker and Frocht[21] have shown that the fringe patterns, obtained by observing the scattered light leaving the end of a bar of photoelastic material exposed to a sheet of polarized light perpendicular to axis of the bar, are the same as the membrane contours.

While the discussion of the pressurized membrane has so far been devoted to an analysis of torsion, other applications of the analogy may be made.   One such application has been made in determining pressure distributions in oil and gas fields.[22]   The fluids in such fields are compressible.   The effective velocity of flow q of such a fluid is given by D'Arcy's law:

$$q = -\frac{k}{\mu}\frac{dp}{ds} \qquad (11.13)$$

where k is the permeability of the consolidated sand of the field, μ the viscosity of the fluid, and dp/ds the pressure gradient in the direction of q.   The density of the fluid is taken as an exponential function of the pressure, namely,

$$w = w_0 e^{\alpha p} \qquad (11.14)$$

where w_0 is the density at $p = 0$ and α is the compressibility of the fluid. On the basis of these equations and the equation of continuity for compressible flow, the differential equation for the density distribution in the field is

$$\frac{\partial^2 w}{\partial x^2} + \frac{\partial^2 w}{\partial y^2} = \frac{\mu \alpha f}{k} \frac{\partial w}{\partial t} \tag{11.15}$$

where f is the porosity of the sand. For a field producing at a constant rate, $\partial w / \partial t$ is approximately a constant (negative). Thus a membrane under constant pressure may be used to evaluate the fluid-density distribution in the reservoir and from this the pressure distribution. Geometrical similarity between the shape of the hole in the plate and the plan form of the reservoir should be reasonably well maintained. The elevation of the edge of the hole corresponds to the fluid density at the boundaries of the field. At points in the soap film corresponding to well locations, the film is depressed to elevations corresponding to the fluid densities at the well bottom holes. Thin hollow tubes used for this purpose also provide a means for removing drainage collecting in the depressions in the film.

The constant-pressure membrane analogy may be used for other problems in which there is a continuous distribution of constant-strength sources or sinks leading to a Poisson equation of the type given by Eq. (11.7). Such problems might arise in dielectric or high-frequency heating of lamina and in soil aeration.[23]

It is not feasible to vary the pressure from point to point on a soap film. A rubber membrane is somewhat more versatile in this respect in that loads might be applied by means of different dead weights to different points of the membrane. A rubber membrane might also be used to give a permanent record if a wet plaster mix is used to provide hydrostatic pressure. When the plaster is hard, the block may be stripped from the mold and measurements made at leisure.

11.3. Multiply Connected Regions. Mention already has been made in Sec. 11.1 of the use of soap films for multiply connected regions. The torsion of hollow bars is another, but fundamentally different, example of such an application.

When the torsion function ϕ is to be determined for a hollow section, ϕ has, of course, a constant value for each boundary, but a different value for the different boundaries. Restricting attention to a bar with a single hollow (Fig. 11.3), the shear stress direction at the inner and outer boundaries is tangent to the boundary at the point in question.

In applying the soap-film analogy to such a bar, it is easy to see that the shape of the hole in the test plate should be geometrically similar to the solid portion of the shaft. This means that a sheet of metal shaped

like the cross section of the hollow in the bar must be held in proper horizontal relation to the edge representing the outer boundary of the bar. A less evident situation is the level at which this loose plate should be held vertically relative to the outer boundary plate. This level cannot be set arbitrarily since the film slope will be markedly affected by variations in level. A method of determining the proper level is indicated below.

Around each contour of the stress function ϕ of a bar in torsion the following relation must be satisfied:[24]

$$\int_c \sigma_{bt} \, ds = 2G\theta A_b \qquad (11.16)$$

where σ_{bt} is the shear stress at the boundary and A_b the total area inside the boundary.

Fig. 11.3

If the soap film truly represents the stress function ϕ, then

$$\sigma_{bt} = \left(\frac{dz}{dn}\right)_b$$

where $(dz/dn)_b$ is the slope of the film normal to the boundary. Thus

$$\int_c \left(\frac{dz}{dn}\right)_b \, ds = 2G\theta A_b \qquad (11.17)$$

Since $2G\theta = P/T$, Eq. (11.17) may be written also as

$$\int_c T \left(\frac{dz}{dn}\right)_b \, ds = PA_b \qquad (11.18)$$

From Fig. 11.4 it is evident that $T(dz/dn)_b$ is the vertical component of the film tension at the boundary and that this integrated around the boundary exactly balances the pressure acting on the plate A_b. Thus if the plate were guided by means of frictionless guides so that it always occupied the proper position relative to the outer edge of the

Fig. 11.4

hole, and if it were possible to balance the plate accurately so that it could be considered weightless in so far as the soap film is concerned, then the plate would automatically assume its proper elevation and provide an experimental solution of the hollow-bar torsion problem. Griffith and Taylor attempted this method but found that the pressures and surface tensions were so slight that the method proved impractical.

A practical method for determining the proper height of one boundary
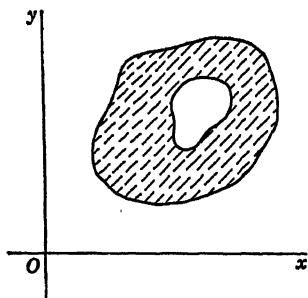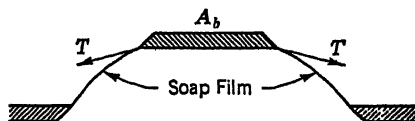
relative to the other is to run two tests with arbitrary positions of the inner boundary and then linearly combining these positions in proper proportion so the relation [Eq. (11.17)] is satisfied. This method stems from the fact that if ϕ_1 and ϕ_2 are the stress functions corresponding to the two arbitrary positions of the inner boundary, then the true stress function ϕ is given by

$$\phi = m_1\phi_1 + m_2\phi_2 \tag{11.19}$$

where

$$m_1 + m_2 = 1$$

This can be shown by substitution into Eq. (11.9). Thus, putting ϕ_1 into the equation

$$\frac{\partial^2\phi_1}{\partial x^2} + \frac{\partial^2\phi_1}{\partial y^2} = -2G\theta \tag{11.20}$$

and with ϕ_2 substituted into it

$$\frac{\partial^2\phi_2}{\partial x^2} + \frac{\partial^2\phi_2}{\partial y^2} = -2G\theta \tag{11.21}$$

Multiplying these equations respectively by m_1 and m_2 and adding, the result is

$$m_1\left(\frac{\partial^2\phi_1}{\partial x^2} + \frac{\partial^2\phi_1}{\partial y^2}\right) + m_2\left(\frac{\partial^2\phi_2}{\partial x^2} + \frac{\partial^2\phi_2}{\partial y^2}\right) = -2G\theta(m_1 + m_2) \tag{11.22}$$

If $m_1 + m_2 = 1$, then

$$m_1\left(\frac{\partial^2\phi_1}{\partial x^2} + \frac{\partial^2\phi_1}{\partial y^2}\right) + m_2\left(\frac{\partial^2\phi_2}{\partial x^2} + \frac{\partial^2\phi_2}{\partial y^2}\right) = \frac{\partial^2\phi}{\partial x^2} + \frac{\partial^2\phi}{\partial y^2} = -2G\theta \tag{11.23}$$

In the first test, the boundary is set at a level z_{bi_1} and the soap film is established. Measurements of slope are made at points on the inner boundary. By means of graphical integration the following integral is evaluated:

$$\int_c \left(\frac{dz}{dn}\right)_{bi_1} ds \tag{11.24}$$

For the second test, the boundary is reset to a different level, z_{bi_2}, and the integral evaluated

$$\int_c \left(\frac{dz}{dn}\right)_{bi_2} ds \tag{11.25}$$

Equation (11.17) is then satisfied by

$$m_1 \int_c \left(\frac{dz}{dn}\right)_{bi_1} ds + m_2 \int_c \left(\frac{dz}{dn}\right)_{bi_2} ds = 2G\theta A_b \tag{11.26}$$

Equation (11.26) and the relation $m_1 + m_2 = 1$ are used to evaluate m_1

and m_2, whence

$$z_{bi} = m_1 z_{bi_1} + m_2 z_{bi_2} \tag{11.27}$$

Equation (11.27) gives the correct level for the inner boundary. A third test with this correct level will evaluate the stress distribution over the area of the hollow bar.

If the bar contains additional hollows, the procedure is as outlined above, except that arbitrary positions are set for the plates representing the hollows and as many additional tests are run as there are additional hollows. Equation (11.26) is written for each internal boundary, so that in the event that there are k hollows this equation becomes

$$m_1 \int_{c_1} \left(\frac{dz}{dn}\right)_{b_1 i_1} ds_1 + m_2 \int_{c_1} \left(\frac{dz}{dn}\right)_{b_1 i_2} ds_1 \cdots + m_k \int_{c_1} \left(\frac{dz}{dn}\right)_{b_1 i_k} ds_1$$
$$+ m_{k+1} \int_{c_1} \left(\frac{dz}{dn}\right)_{b_1 i_{k+1}} ds_1 = 2G\theta A_1 \tag{11.28}$$

Similar equations are written for each of the other boundaries, so that, in all, k equations of this type will have been determined for the k internal boundaries of the soap film. The $(k + 1)$th equation is that connecting the ms alone, namely,

$$m_1 + m_2 + \cdots + m_k + m_{k+1} = 1$$

Thus, after $k + 1$ tests with arbitrary settings of the boundaries, a final correct setting of the boundaries can be accomplished, and a final test run made to determine the shear stress distribution in this bar under torsion.

11.4. Transformations to the Laplace Equation. The ever-present danger of rupturing the film under pressure and the necessity for accurately adjusting the pressure to the same value for each test in order to ensure satisfying the relation (11.26) led to the development of a zero-pressure soap film.

Suppose in the Poisson equation for the torsion stress function ϕ one were to introduce a change of variable governed by the transformation[15]

$$\phi = \psi - G\theta \frac{Ax^2 + 2Hxy + By^2 + Gx + Fy + D}{A + B} \tag{11.29}$$

where A, B, D, F, G, H are arbitrary constants. The Poisson equation in ϕ then reduces to the Laplace equation in ψ, namely,

$$\frac{\partial^2 \psi}{\partial x^2} + \frac{\partial^2 \psi}{\partial y^2} = 0 \tag{11.30}$$

Since $\phi_b = $ const around each boundary, the boundary values for ψ_b must be

$$\psi_b = \phi_b + G\theta \frac{Ax^2 + 2Hxy + By^2 + Gx + Fy + D}{A + B} \tag{11.31}$$

Considering first a solid bar in torsion, a hole is cut in a sheet-metal plate, as for the pressure-film analogy, of a shape geometrically similar to that of the cross section of the bar. This sheet instead of remaining flat, as had been the case previously, is now deformed so that the edge of the opening, representing the outer boundary of the cross section, is elevated various amounts along its length above a reference horizontal plane in accordance with

$$z_b = G\theta \frac{Ax^2 + 2Hxy + By^2 + Gx + Fy + D}{A + B} \tag{11.32}$$

A soap film drawn over this deformed edge will now provide the function z analogous to the transformed stress function ψ for the particular bar being subjected to torsion. The deformation of the plate must not be great enough to alter the geometrical similarity between the plan form of the distorted opening and the shape of the bar itself.

The constants A through H in the boundary condition are arbitrary, for Laplace's equation will be satisfied in any case. The choice of values should be governed by the criterion of keeping the film as flat as possible. However, in the interest of simplicity, the constants are frequently so chosen that

$$z_b = \frac{G\theta}{2}(x^2 + y^2) \tag{11.33}$$

for which $A = B = \frac{1}{3}$ and $D = F = G = H = 0$.

In applying the zero-pressure film to the torsion of hollow sections, refer again to Eq. (11.18). Note that when P goes to zero, this equation becomes

$$\int_c T\left(\frac{dz}{dn}\right)_b ds = 0 \tag{11.34}$$

which means that the net vertical pull exerted by the soap film on the deformed edge representing any one of the boundaries of a bar in torsion must equal zero.

Considering in detail the case of a bar with a single hollow, the solid area of the bar is represented by a geometrically similar annular hole cut in sheet metal. The outer plate, containing the edge representing the outer boundary of the cross section, is deformed in accordance with Eq. (11.33), or the more general expression. The inner plate, which represents the hollow, is also deformed so that its edge obeys the same equation. Now, however, the inner plate must also be raised in level with respect to the outer plate by a constant additional amount since it must satisfy the boundary condition

$$z_{bi} = K + \frac{G\theta}{2}(x^2 + y^2) \tag{11.35}$$

where K is a constant to be determined.

The deformed inner boundary is arbitrarily displaced an amount K_1 with respect to the deformed outer boundary, the soap film is applied, and the expression Eq. (11.34), not equal to zero except for the correct K, is evaluated. It is again evaluated in a second test with a second arbitrary setting K_2. Note that since T is a constant, it may be divided out of Eq. (11.34) and the equation evaluated without it.

$$\int_c \left(\frac{dz}{dn}\right)_{bi} ds = 0 = m_1 \int_c \left(\frac{dz}{dn}\right)_{bi_1} ds + m_2 \int_c \left(\frac{dz}{dn}\right)_{bi_2} ds \quad (11.36)$$
$$m_1 + m_2 = 1$$

from which m_1 and m_2 may be evaluated. Then

$$K = m_1 K_1 + m_2 K_2 \quad (11.37)$$

A third test in which the inner boundary is elevated the amount K determined from Eq. (11.37) now supplies values of z which correspond directly to the values of ψ for the hollow bar in torsion.

The extension to bars with more than one hollow is obvious on the basis of the presentation for the pressure film.

Transformations of a more general type of Poisson's equation into Laplace's equation may be made. In the equation

$$\frac{\partial^2 \phi}{\partial x^2} + \frac{\partial^2 \phi}{\partial y^2} = f(x,y) \quad (11.38)$$

the variable ϕ may be replaced by a variable ψ defined by

$$\phi = \psi + F(x,y) \quad (11.39)$$

If it is possible to choose $F(x,y)$ such that

$$\frac{\partial^2 F}{\partial x^2} + \frac{\partial^2 F}{\partial y^2} = f(x,y) \quad (11.40)$$

then the substitution of Eq. (11.39) into Eq. (11.38) will lead to the Laplace equation in ψ. This can always be done if $f(x,y)$ is a polynomial containing arbitrary powers of x and y individually, but all product terms will either contain x to the first power only with y raised to any power or contain y to the first power only with x raised to any power. Both types of product terms cannot be present simultaneously.

As an example, suppose

$$f(x,y) = Ax^5 + By^3 + Cyx^7 + Dyx^3 + E \quad (11.41)$$

If all the terms containing x are integrated twice with respect to x, the terms containing y alone are integrated twice with respect to y, and the constant term is integrated twice with respect to either x or y (or both integrals may be used in appropriate proportions), the resulting integral

will satisfy Eq. (11.40). To this equation may be added such terms as Gx, Hy, and Kxy. Thus Eq. (11.41) leads to

$$F(x,y) = \frac{A}{42} x^7 + \frac{B}{20} y^5 + \frac{C}{72} yx^9 + \frac{D}{20} yx^5 + \frac{E}{2} \left(\frac{Mx^2 + Ny^2}{M + N} \right)$$
$$+ Gx + Hy + Kxy \quad (11.42)$$

Equation (11.42) may be further modified and still satisfy Eq. (11.40) by multiplying by y all terms in the variable x alone and by multiplying by x all terms in the variable y alone. It is evident that considerable latitude is allowed in the transformation function to reduce Eq. (11.38) to Eq. (11.30).

11.5. Membrane Analogy for Shear Stress in Beams. The shear stresses in a beam subjected to bending may be determined by means of a membrane.[15] Figure 11.5 shows a beam subjected to bending in one of its principal planes. Axis Ox is a principal axis of the cross section. If the load W passes through the shear center of the cross section, the bar will bend without twisting.
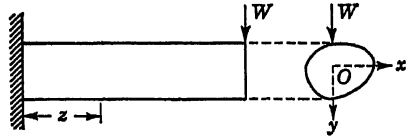
Fig. 11.5

Otherwise, the bar will be subjected not only to bending but also to torsion. Shear stresses may exist on the cross section of the bar for both reasons. In addition, a normal stress will exist due to the bending moment. Thus, with the bending stress σ_z given by

$$\sigma_z = - \frac{W(L - z)}{I} y \quad (11.43)$$

the compatibility relations for an element of cross section become

$$\frac{\partial^2 \sigma_{zx}}{\partial x^2} + \frac{\partial^2 \sigma_{zx}}{\partial y^2} = 0 \quad (11.44)$$

$$\frac{\partial^2 \sigma_{zy}}{\partial x^2} + \frac{\partial^2 \sigma_{zy}}{\partial y^2} = - \frac{W}{I(1 + \mu)} \quad (11.45)$$

Taking
$$\sigma_{zz} = - \frac{\partial \phi}{\partial y} \quad (11.46)$$

and
$$\sigma_{yz} = \frac{\partial \phi}{\partial x} - \frac{Wy^2}{2I} + \left[\frac{\mu}{2(1 + \mu)} \right] \frac{Wx^2}{I} \quad (11.47)$$

the equations of equilibrium are satisfied, and Eqs. (11.44) and (11.45) become

$$\frac{\partial}{\partial y} \left(\frac{\partial^2 \phi}{\partial x^2} + \frac{\partial^2 \phi}{\partial y^2} \right) = 0 \quad (11.48)$$

$$\frac{\partial}{\partial x} \left(\frac{\partial^2 \phi}{\partial x^2} + \frac{\partial^2 \phi}{\partial y^2} \right) = 0 \quad (11.49)$$

Equations (11.48) and (11.49) are satisfied simultaneously only if

$$\frac{\partial^2 \phi}{\partial x^2} + \frac{\partial^2 \phi}{\partial y^2} = K \qquad (11.50)$$

The constant K represents the twist in the bar due to the load being offset from the shear center. Considering the load applied at the shear center, $K = 0$, and the stress function for shear stress due to bending satisfies the Laplace equation

$$\frac{\partial^2 \phi}{\partial x^2} + \frac{\partial^2 \phi}{\partial y^2} = 0 \qquad (11.51)$$

At the boundary there are no stresses normal to the boundary in the plane of the cross section. Consequently, Eq. (11.10) applies. In terms of the stress function ϕ,

$$\left[\frac{\partial \phi}{\partial x} - \frac{Wy^2}{2I} + \frac{\mu}{2(1+\mu)} \frac{Wx^2}{I} \right] \frac{dx}{ds} = -\frac{\partial \phi}{\partial y} \frac{dy}{ds} \qquad (11.52)$$

Thus
$$\frac{\partial \phi_b}{\partial x} \frac{dx}{ds} + \frac{\partial \phi_b}{\partial y} \frac{dy}{ds} = \frac{W}{2I} \left(y^2 - \frac{\mu}{1+\mu} x^2 \right) \frac{dx}{ds} \qquad (11.53)$$

or
$$d\phi_b = \frac{W}{2I} \left(y^2 - \frac{\mu}{1+\mu} x^2 \right) dx \qquad (11.54)$$

This equation may be integrated to provide the value of ϕ_b around the periphery of the cross section. Thus

$$\phi_b = \frac{W}{I} \left[\int_c \frac{y^2}{2} dx - \int_c \frac{\mu}{2(1+\mu)} x^2 dx \right] \qquad (11.55)$$

The first term in Eq. (11.55) represents the summation of moments of areas, such as the one shown crosshatched in Fig. 11.6, about the x axis. Since the x axis is a principal axis of the section, it passes through the center of gravity. Consequently, the summation of the area moments must be zero. The second term yields
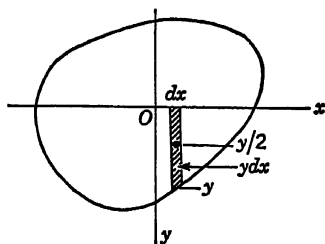
Fig. 11.6

$$\phi_b = -\frac{W\mu x^3}{I6(1+\mu)} \qquad (11.56)$$

Thus, to use a zero-pressure membrane to determine the stress function for shear due to bending, it would appear that the edges of the membrane should be elevated to positions in accordance with Eq. (11.56). However, Prof. S. C. Redshaw points out that Eq. (11.56) is derived by discarding the first term of Eq. (11.55). This first term vanishes only when taken around the entire boundary; it must not be ignored when calculating individual boundary values.

Although the development just described infers that the shear load is applied through the shear center of the cross section, the position of the shear center along the x axis does not enter into the analysis explicitly and hence need not be known to determine the shear stresses. However, this method does provide a means for determining the shear center location, because the resultant of the distributed shear stresses over the cross section must pass through the shear center when there is no twist to the bar.

11.6. Scale Factors for the Membrane Analogy. Referring to Eq. (11.38), if the load distribution $P(x,y)$ and tension T of the membrane are so adjusted that $P(x,y)/T = f(x,y)$, then the values of z measured on the membrane are directly equal to the values of ϕ in the problem being simulated. If it is not practical to do this, it is necessary to apply a scale factor S_1 such that $S_1 f(x,y)$ equals $P(x,y)/T$. Equation (11.38) then becomes

$$\frac{\partial^2(S_1\phi)}{\partial x^2} + \frac{\partial^2(S_1\phi)}{\partial y^2} = S_1 f(x,y) \tag{11.57}$$

Elevations of the membrane now represent the function $S_1\phi$.

It has been assumed so far that in setting up a membrane for Eq. (11.57) the membrane dimensions are identical with the actual area over which ϕ is to be determined. This is rarely likely to be the case. The membrane dimensions are likely to be quite different in magnitude from the area dimensions. Scale factors are necessary here also. Since geometrical similarity is to be maintained, the same scale factor must apply to both x and y. Suppose that the problem dimensions x, y are related to the hole dimensions X, Y by the equations

$$x = S_2 X \qquad y = S_2 Y \tag{11.58}$$

These values may be substituted into Eq. (11.57), yielding

$$\frac{\partial^2(S_1\phi)}{\partial(S_2 X)^2} + \frac{\partial^2(S_1\phi)}{\partial(S_2 Y)^2} = S_1 f(x,y) \tag{11.59}$$

$$\frac{\partial^2 z}{\partial X^2} + \frac{\partial^2 z}{\partial Y^2} = S_1 S_2{}^2 f(x,y) \tag{11.60}$$

where z replaces $S_1\phi$. If $P(x,y)/T$ be made equal to $S_1 S_2{}^2 f(x,y)$, then values of z measured at X, Y correspond to values of $S_1\phi$ at x, y in the actual problem.

11.7. Elastoplastic Torsion and the Membrane Analogy. For bars with a pronounced yield point in shear, the progress of yield over the cross section may be studied by the membrane analogy.[25] If the bar material has a stress-strain diagram which may be approximated by the idealized "curve" of Fig. 11.7, it is clear that at any point in a purely

plastic region the shear-stress components must always have a resultant given by

$$(\sigma_{zx}{}^2 + \sigma_{zy}{}^2)^{\frac{1}{2}} = S_y \qquad (11.61)$$

where S_y is the yield-point stress in shear.

Expressing the shear stresses in terms of the stress function ϕ [Eqs. (11.8)],

$$\left[\left(\frac{\partial\phi}{\partial x}\right)^2 + \left(\frac{\partial\phi}{\partial y}\right)^2\right]^{\frac{1}{2}} = S_y = \left(\frac{\partial\phi}{\partial n}\right)_{\max} \qquad (11.62)$$

This is the equation for the maximum slope of the ϕ surface. As a bar is subjected to increasing angular twist, the slope of the ϕ surface increases at each point until it reaches the value S_y. This value will be reached at different angles of twist for the different points. However, for each point at which the slope S_y is reached, further twisting of the bar does not change its slope but merely serves to bring other points in the bar to this value. The condition of constant maximum slope in a membrane may be obtained by building up from the membrane boundary a rigid wall (or roof) of slope S_y normal to the boundary. The membrane is subjected to air pressure as usual to simulate the angle of twist. For angles of twist not producing plastic flow anywhere in the bar, the membrane will not touch the walls sloping up over it. At any point where plastic flow occurs (yield point is reached), the membrane will touch the wall and its slope will be fixed to that of the wall. As the twist of the bar is increased (increased air pressure under the membrane), increasing areas of contact between the membrane and the rigid wall will become evident (increasing regions of plasticity). Using glass or a clear plastic for the walls and a rubber membrane, the contact areas would be directly visible. A soap film would not be suitable for obvious reasons.
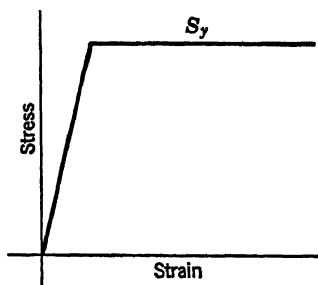
The formation of the surface of constant maximum slope is fairly simple when the boundary of the bar cross section consists of straight lines and arcs of circles, for then these surfaces are planes and cones which meet along predetermined lines of intersection. For other boundaries the construction is not so easy,[26] but being ruled surfaces (developable), they may be constructed. Nadai[25] has shown that such surfaces may be built up by means of the sand-heap analogy. By sprinkling dry sand on a horizontal plate cut to the shape of the given solid cross section, until the angle of repose of the sand heap is attained over the entire plate, the surfaces of the heap of sand are the surfaces of constant slope representing

maximum shear stress. Coker and Dadswell found that dry plaster of paris was a most suitable powder for the same purpose. The sand-heap analogy has been used for visualizing torsional stress distributions in the completely plastic state for solid bars[27] and for bars with hollows.[28]

11.8. Analogy of the Electrically Conducting Sheet. In Fig. 11.8a a sheet of conducting material (either solid or liquid) is shown. Its boundary is subjected to a given voltage distribution V_b, and a distributed current i per unit area is supplied over its surface. Considering an infinitesimal element $dx\,dy$ of the sheet, the current leaving across its

(a)   (b)
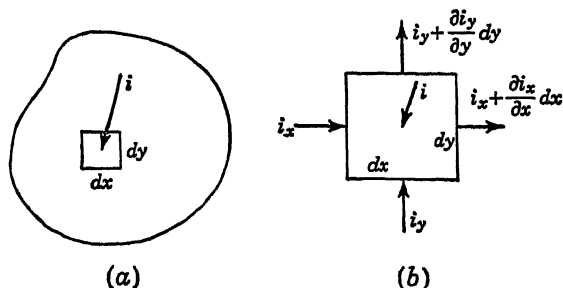
Fig. 11.8

boundaries must equal the current entering across its other boundaries and through its surface. The current flow across each boundary is pro-. portional to the voltage gradient at that boundary. Thus, the current balance equation (equation of continuity) is

$$\left(i_x + \frac{\partial i_x}{\partial x}\,dx\right) dy - i_x\,dy + \left(i_y + \frac{\partial i_y}{\partial y}\,dy\right) dx - i_y\,dx - i\,dx\,dy = 0$$

$$(11.63)$$

or

$$\frac{\partial i_x}{\partial x} + \frac{\partial i_y}{\partial y} = i \qquad (11.64)$$

where i_x and i_y are the current flows per unit length of boundary. In terms of voltage gradients,

$$i_x = -\frac{1}{R}\frac{\partial V}{\partial x} \qquad i_y = -\frac{1}{R}\frac{\partial V}{\partial y} \qquad (11.65)$$

where R is the resistivity of the sheet (resistance between two parallel edges of a square—independent of the size of the square). Equation (11.64) therefore becomes

$$\frac{\partial^2 V}{\partial x^2} + \frac{\partial^2 V}{\partial y^2} = -Ri \qquad (11.66)$$

This is the equation of the stretched membrane if V is associated with z, i with the transverse load P, and R with $1/T$. Thus, in any problem for

which an edge-supported membrane (without a "roof") may be used, a conducting sheet may also be used. In fact, problems of a more general character may be solved by the conducting sheet because the current input and the thickness of the sheet, that is, R, may be varied from point to point. If R is made variable, then the substitution of Eqs. (11.65) into (11.64) yields the relation

$$\frac{\partial}{\partial x}\left(\frac{1}{R}\frac{\partial V}{\partial x}\right) + \frac{\partial}{\partial y}\left(\frac{1}{R}\frac{\partial V}{\partial y}\right) = -i \qquad (11.67)$$

For a conducting sheet made of material having uniform properties, the resistivity referred to a unit square is given by

$$R = \frac{\rho}{h} \qquad (11.68)$$

where ρ is the resistivity of the material per unit cube and h is the thickness of the sheet in the same units. Thus, using Eq. (11.68) in Eq. (11.67),

$$\frac{\partial}{\partial x}\left(h\frac{\partial V}{\partial x}\right) + \frac{\partial}{\partial y}\left(h\frac{\partial V}{\partial y}\right) = -\rho i \qquad (11.69)$$

In the application of the conducting-sheet analogy, it is not practical to supply a distributed current over the entire surface of the sheet. Such a distribution is approximated by subdividing the given sheet into finite elements of area α, and the total current $i\alpha$ to be distributed over each area element is fed as a concentrated current I_α into the center of the area element. The magnitude of α may differ from point to point along the sheet, particularly near curved or irregular boundaries. It is convenient to rule, or otherwise locate, a grid of squares over the conducting sheet to form the elements α. With the required concentrated currents fed into the centers of these area elements, voltages measured at the grid intersection points provide the solution of the partial differential equation.

Although as many current electrodes may be used simultaneously as there are area elements α, this may not always be the most desirable procedure because of possible interactions in the current supply network, leading to difficulties in adjusting all current probes to the necessary values. For linear differential equations [e.g., Eqs. (11.66) and (11.69)], the complete solution may be built up by a superposition of particular solutions, each particular solution corresponding to one (or more) current probes in operation. Thus, suppose the given area to be divided into n elements of small area $\alpha_1, \alpha_2, \ldots, \alpha_n$. Using only a single current probe, the current $i\alpha_1$ is fed into the center of area α_1 and the voltages $V_{11}, V_{21}, \ldots, V_{m1}$ read at the m intersection points of the grid. The current probe is then shifted to the center of α_2, the current $i\alpha_2$ is pro-

vided, and the voltages V_{12}, V_{22}, . . . , V_{m2} are read at the same intersection points. The procedure is repeated for each α. The final solution, corresponding to the condition of all αs being fed current simultaneously, is

$$V_1 = \sum_{j=1}^{n} V_{1j} \qquad V_2 = \sum_{j=1}^{n} V_{2j} \qquad \cdots \qquad V_m = \sum_{j=1}^{n} V_{mj} \quad (11.70)$$

It is evident that such problems as film slope, solution drainage, uniform tension, and membrane sag do not arise when a conducting sheet is used. The scale factors may be made large and accuracy correspondingly increased. The problem of life of the model is a minor one, for the conducting sheet is not fragile—it may be steel, metallized paper, paper impregnated with a conducting material (*e.g.*, Teledeltos facsimile paper), conducting plastic,[28a] or simply tap water.

If tap water or other electrolyte is used as the conducting medium, three-dimensional problems, which are governed by the Laplace equation may be solved. Electrodes and models may be submerged in such a medium and measurements made with an exploring probe insulated from the electrolyte except for its tip.

11.9. Applications of the Conducting-sheet Analogy. The use of an electrically conducting medium to simulate heat-conduction problems has a long history. One of the earliest applications of the method was in the determination of shape factors for heat conduction through corners.[29] Later applications included further studies of shape effect[30] and of effect of embedded metals.[31–33]

Assuming that appropriate boundary voltages have been applied around a conducting-sheet model of a two-dimensional heat-conduction problem, the constant voltage contours in the electrical sheet will correspond to the isothermals in the prototype. Local heat-flow rates for irregular configurations are most conveniently determined from measurements of voltage gradients across the corresponding boundaries of the model. Total heat-flow rates would be determined by measuring the total current leaving the voltage supply used for setting boundary voltages.

In many applications not only are the heat-flow rates important, but also the steady-state temperatures at critical surfaces. Such, for example, are cases where the junction between an insulating blanket and a supporting surface must be kept below the damage point for the supporting medium. Also, outside walls of refrigerated rooms must be maintained at temperatures above the dew point of the ambient air to avoid condensation damage. Since practical structures are usually of complex form, the electrically conducting sheet may well serve as a con-

venient means for determining heat-flow rates and interfacial or surface temperatures.

Kayan studied the problem of heat flow in composite walls and floor slabs by means of full-scale two-dimensional models cut from metallized paper.[34-36] Concrete walls and floors overlaid with thermal insulation were represented by a conducting sheet of constant thickness. The difference in conductivity of the two materials was simulated by perforating the metallized paper with closely spaced square holes over the region representing the insulation, thereby reducing its average electrical conductivity the required amount. The resistance to heat flow through
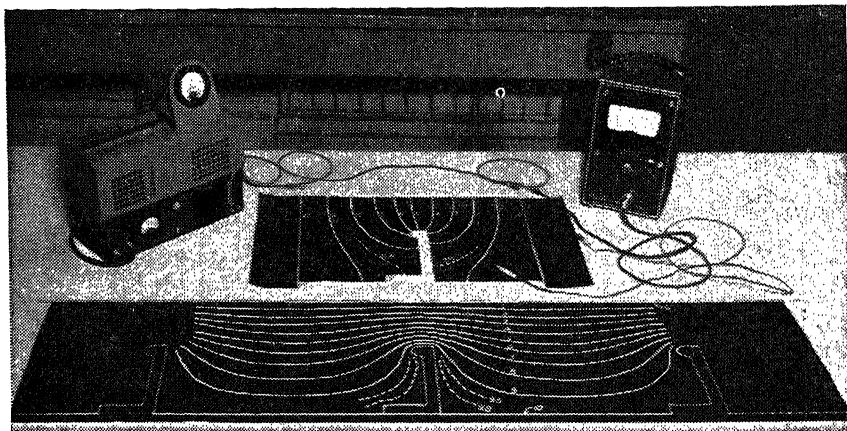
Fig. 11.9

the surface film of air was simulated by an additional width of unperforated conducting sheet.

As in the stretched membrane, there are two families of orthogonal curves which may be traced on the conducting sheet. One family consists of the equipotential lines; the other consists of the current flow lines (streamlines). If one family of lines has been obtained experimentally for equal increments in voltage, the other family may be drawn in by the method of curvilinear squares. It is often more convenient, however, to produce the second family of curves experimentally also, after sketching in, if necessary, the two boundary curves of the second family. Thus, referring to Fig. 11.9, there is shown a family of equipotential lines obtained at 10 per cent intervals on a conducting sheet between an irregular edge kept at one voltage and a straight edge kept at another voltage. The sheet is Teledeltos facsimile paper[37] with silver paint (DuPont No. 4817) used for the boundary electrodes. A copper wire was bent to the form of the boundaries and was cemented at intervals to the painted boundary with a blob of silver paint. The wire was a pre-

cautionary measure to ensure a constant voltage along an entire length of silver boundary irrespective of loading. The equipotential lines were obtained very simply by applying 5 volts across the silver boundaries and using a probe and a high input impedance d-c vacuum-tube voltmeter to trace the equipotentials at $\frac{1}{2}$-volt increments. A silver blueprint marking pencil spotted the probe positions and produced the white lines shown. As can be seen from the figure, a minimum of apparatus is required. A d-c power supply is shown, although a storage battery would have served the purpose equally well.

After drawing the first set of equipotentials (lower part of photograph), two orthogonal curves are sketched in at the boundaries between which flow lines are desired. These curves are not shown in the lower part of the photograph, but they are shown as boundary lines on the sheet in the upper part. This new sheet now has insulated edges where the first sheet had conducting edges and has conducting edges where the first sheet had insulated edges. A voltage difference of 5 volts applied between the conducting edges of the new sheet permitted sketching the orthogonal set of equipotentials shown. In this set, the same amount of current flows through each passage, or "tube," defined by two adjacent solid lines. The concentrating effect of the irregular projections is quite evident. Where the 10 per cent equipotentials were far apart, intermediate dotted lines were plotted.

The similarity between electric and magnetic fields led to the use of a conducting sheet to determine the reluctance of magnetic fields and the shapes of the magnetic lines of force.[38] Metal sheets simulated the magnetic fields in various parts of electric machinery.

Conducting-sheet applications to both inviscid and viscous incompressible flow have been made. To obtain lines of constant velocity potential for flow about an obstacle, the constant potential lines for the upstream and downstream edges of the flow field are represented as highly conducting edges of the conducting sheet (Fig. 11.10a). If tap water is used for the sheet, these edges would be obtained by inserting copper sheets across the tank at the ends. The tank walls and bottom are necessarily nonconducting. In such a liquid tank the model would also be of nonconducting material. If a solid conducting sheet is used to represent the flow field, e.g., Teledeltos paper, heavy copper electrodes may be pressed against the sheet at the edges, or in the case of the paper, silver paint applied along these edges would provide the necessary equipotentials. The model would be represented by a hole of the proper shape cut out of the sheet.

It should be mentioned that while direct current may be used with solid conducting sheets, alternating current is necessary with electrolytic tanks because with direct current electrolysis and polarization seriously

affect potentials in the liquid near the electrodes. These effects do not have time to occur when alternating current is used. With 1,000-cycle alternating current or some other frequency in the audio range, earphones may be used for detecting points along the equipotential line corresponding to the setting of the voltage divider.

The streamlines about the obstacle may be obtained either by sketching in the orthogonal family of curves in Fig. 11.10a or by placing the highly conducting electrodes along the other edges of the tank[39] and making the

(a)   (b)
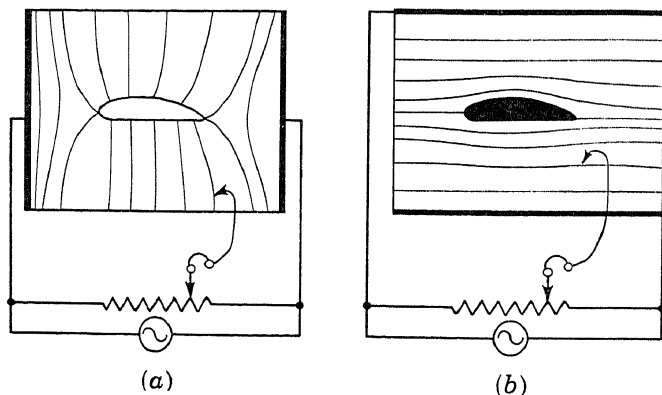
Fig. 11.10

model itself highly conducting (a metal model in tap water, or a silver-paint model on Teledeltos paper). This case is shown in Fig. 11.10b.

In this figure the airfoil is shown at zero angle of attack. If the airfoil were tilted, the flow would attempt to pass around the sharp trailing edge and in potential flow acquire a theoretically infinite velocity. In actual practice a circulation of strength Γ is developed around the airfoil such that for any angle of attack the vector sum of the circulation and the potential flow result in a finite velocity at the trailing edge. The streamlines due to circulation are circles far from the airfoil, while at the airfoil the streamline follows the surface of the airfoil.

In an actual electrical model of a flow field with circulation, to determine the circulatory component of the flow the outer boundary of the flow field is maintained at a constant potential (streamline). The model is maintained at another constant potential such that the amount of current proportional to the required Γ of the flow field flows between them. The value of Γ must be adjusted to maintain tangency of the flow off the trailing edge of the airfoil section.

Electrolytic tank models have been used to study the flow about turbine and pump blades.[40] Various applications to aerodynamical problems are described by Malavard.[41]

Viscous-flow representation by means of a membrane has been discussed in connection with the study of oil flow in underground reservoirs. The conducting-sheet representation of this problem brings in some new features not possible with the membrane. For incompressible flow, D'Arcy's law [Eq. (11.13)] in a two-dimensional domain yields the equation

$$\frac{\partial^2 p}{\partial x^2} + \frac{\partial^2 p}{\partial y^2} = 0 \qquad (11.71)$$

This equation may be represented by a membrane, a conducting sheet, a fluid mapper,[42,43] or any other technique whereby the Laplace equation may be solved. However, important phases of the oil-field problem include the encroachment of edge water into an oil horizon, the fingering" which takes place toward wells near the edge, and the progress of the water front in artificial flooding operations. An electrolytic conducting sheet provides a means for visual observation of these phenomena. This technique was used by Wyckoff, Botset, and Muskat[44] to trace the flow of ions in electrolytic models of oil fields. The electrolyte was held in a thin layer of gelatin to reduce ion velocities. Since the average velocity of ions in an electrolyte is proportional to the voltage gradient, just as the average velocity of molecules in consolidated sand is proportional to the pressure gradient (D'Arcy's law), the ions may be used to represent water molecules; and if a means could be provided for tagging the ions so that they could be visible en masse, the progress of the water front through an oil field could be directly observed in this model. In the reference apparatus, hollow glass electrodes also containing the gelatinized electrolyte represented the input and output wells. Under the influence of a d-c potential between wells, or between the edge of the electrolyte and the wells, OH ions diffused toward the positive electrodes. A phenolphthalein indicator in the electrolyte indicated the progress of the OH ions toward the output wells by turning pink. Photographs taken at successive intervals of time served to map the progressive spread of the pink area representing the penetration of water toward the producing wells.

Swearinger[45] studied the problem of predicting recovery of condensate from a producing horizon, where the residue gas is returned through another well. The injected dry gas displaces the wet gas. A gelatin sheet was also used. However, the injection "wells" were provided with deep-blue copper ammonium ions and the producing "wells" with colorless zinc ammonium ions. Under a d-c potential across electrodes, the blue ions diffused from the input wells toward the output wells and the progress of the "dry gas" front was observed as a spreading blue area.

Using the same type of electrolytic model, Botset[46] studied various flood patterns and edge-water encroachment. Provision was made for

20 wells. By varying the input rates and well configurations a rapid and inexpensive qualitative study may be made of recoveries obtainable under various operating conditions.

A problem similar to the oil-field problem is that of seepage of water through and underneath dams and the drainage fields through sand, gravel, and drain tile. The water-seepage problem has considerable practical significance in the determination of internal pressures built up within the dam and the uplift forces acting on it.[47,48]

In contrast to the oil-field problem, however, where the differences in elevation in the oil-producing sand layer did not have any appreciable effect on the pressure distribution in the field, in the seepage problem the flow pattern is due to a hydrostatic pressure, which varies from zero at a free water surface to wh at the depth h below the water surface.

In seepage problems the components of flow velocity through an element of volume of porous medium are

$$v_x = - \frac{k}{\mu} \frac{\partial p}{\partial x} \qquad v_y = - \frac{k}{\mu} \left(\frac{\partial p}{\partial y} + \rho g \right) \qquad (11.72)$$

If the velocity components are expressed in terms of the velocity-potential function

$$\phi = \frac{k}{\mu} (p + wy) \qquad (11.73)$$

the equation of equilibrium of inflow and outflow for water considered as incompressible becomes

$$\frac{\partial^2 \phi}{\partial x^2} + \frac{\partial^2 \phi}{\partial y^2} = 0 \qquad (11.74)$$

In this case ϕ is not simply the pressure, as in Eq. (11.71), but is the *total head*, which includes both pressure and elevation.

The flow of ground water through strata of various permeabilities and out through buried drain tile has been studied by this method, making use of Teledeltos paper. The differences in permeability between various layers were simulated in a single sheet of paper by cutting rectangular holes in the paper to reduce its average conductivity in accordance with the reduced permeability of the corresponding stratum. A voltage applied to a line of silver paint across the top of the sheet simulated the total head at the ground-water surface. Zero potential at the silver dot representing the drain tile simulated zero head at the tile location. Equipotentials and flow lines were obtained by usual methods.

Childs[49] studied the drainage problem with the aid of sheets of paper soaked in a solution containing graphite, pressed together, and dried to form a conducting medium.

Three-dimensional models were similarly constructed by Reltov[50] for

seepage studies under dams. He also found the best material for his models to be graphite. The graphite is mixed with talcum, powdered marble, or fine quartz sand and compacted with distilled water to give a mass that would stick together. The conductivities at different sections of the model may be made different by varying the proportions of non-conducting material with respect to the graphite.

In studying seepage under dams, the dam is considered impervious in comparison with the soil underneath it. In the electrical analogy, the dam model is of nonconducting material (*e.g.*, a hole of the proper shape cut in Teledeltos paper). The headwater and tail-water total heads with respect to a common reference are represented by horizontal equipotential lines (*e.g.*, silver paint) at the underwater ground levels on both sides of the dam. By including a large enough section of earth around the dam, the exact shape of the three other boundaries of the conducting sheet is not of great importance and would have little effect on the pressures developed at the dam. In a model[51] using a 5 per cent salt solution, the tank was of rectangular form, with the exception of the edge which contained two copper electrodes and a nonconducting model of the dam cross section. The other edges were nonconducting.

At the other extreme is the case of seepage through a dam which is placed on an impervious foundation. While this is not likely to be a real situation, it does illustrate techniques which are applicable to actual dam designs. This type of problem appears to have been first treated by Wyckoff and Reed[52] by means of a conducting-sheet analogy. It is interesting to note that here again graphite has been used to produce a conducting sheet by spraying 12 to 20 coats of Aquadag (graphite colloid), diluted with water, on Bristol board.

Figure 11.11a shows a permeable dam on an impervious foundation. Excluding capillary effects, a particle of water penetrating into the dam at B will not move directly to C, but will follow a gradually descending path such as BD in accordance with D'Arcy's law under the gravitational head. BD thus forms the top flow line, the dam model being dry above BD and wet below it. Assuming atmospheric pressure within the dry portion of the dam, the line BD represents a falling off of potential head in accordance with the vertical distance from EA to points on DB. A particle of water reaching D arrives there with a total head corresponding to the vertical distance from EA to D. Thereupon, the particle is free to slide without restraint to the bottom of the dam.

Since, in the conducting-sheet model, voltages represent total head, the edge AB of the model must be an equipotential line because all particles of water in contact with the surface AB of the dam have the same total head (pressure plus elevation). On the other hand, particles of water reaching the face EC of the dam have no pressure head (atmospheric

pressure taken as reference zero), but only potential head (elevation). Consequently, this edge of the conducting model should be subjected to a voltage distribution which varies linearly from a maximum at C (corresponding to the voltage impressed on AB) to zero at E. There are several ways in which this could be done. Wyckoff and Reed clamped a resistance strip along this edge of the conducting sheet, making the strip of relatively low resistance to avoid loading effects.

The conducting-sheet model is shown in Fig. 11.11b. Strictly speaking, since the curve BD is the topmost streamline, there should be no conducting sheet above BD. Unfortunately, the location of BD is unknown

(a)

(b)
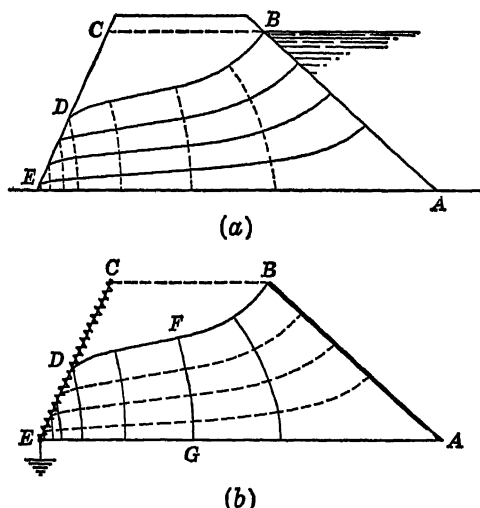
Fig. 11.11

until the problem is solved. Wyckoff and Reed obtained BD by a method of successive trials in which the edge of the conducting sheet was gradually trimmed away, the voltage distribution along the cut edge being checked meanwhile, until the voltages along the cut edge became proportional to the distances of the edge above EA. Once this edge has been established, the equipotential lines (shown full) may be plotted by measurement and the flow lines (shown dotted) may be drawn in perpendicularly to the equipotentials.

11.10. Applications of Conducting Sheets of Variable Thickness. Equation (11.69) represents the voltage distribution in a conducting sheet of variable thickness. Such a sheet is often necessary in the study of field problems involving varying properties of the medium, compressibility, or axial symmetry. A method of achieving these effects with a sheet of uniform thickness was mentioned in Sec. 11.9. It involves punching holes in the conducting sheet to reduce its conductivity in

selected regions. Actually, such a procedure takes us back to the finite-difference procedures and the resistance networks of Chap. 10.

An example of variable properties is one involving heat conduction. The thermal conductivity of a material often depends upon its temperature in a significant manner. The steady-state equation of continuity for such a material in a two-dimensional region is

$$\frac{\partial}{\partial x}\left(k\frac{\partial T}{\partial x}\right) + \frac{\partial}{\partial y}\left(k\frac{\partial T}{\partial y}\right) = 0 \qquad (11.75)$$

If the variation in k from point to point were known at the start, it would be a relatively simple matter to adjust the thickness of the electrically conducting sheet to correspond, and a single test would provide the steady-state temperature distribution.

Since k and T are, in general, interdependent quantities, a solution to the problem must be known before the analogy could be set up. This means the use of a method of successive approximations wherein an assumed solution is corrected in successive stages until no further corrections are needed. The first test may be run with a sheet of uniform thickness (constant k). The temperature distribution so obtained may now be used to readjust the sheet thickness to match. A second test provides a more accurate temperature distribution and permits a further readjustment of the sheet thickness. These stages of testing and readjustment may be carried on as long as they lead to significant improvements in accuracy.

With a solid conducting sheet (e.g., metal or plastic) such adjustments in thickness are not practical. With a liquid sheet, the bottom of the tank holding the layer of liquid may be provided with a thick layer of wax which may be easily carved to provide the necessary variation in depth of electrolyte. Even more conveniently, the tank may be provided with a flexible rubber bottom which may be adjusted by piling sand underneath it to give the required variation in depth of electrolyte.

Another problem requiring a sheet of variable thickness is that of compressible flow. A tank with a 2-in.-thick wax bottom and containing copper sulfate solution was used by Taylor and Sharman[53] to study the problem of compressible flow past a circular cylinder. The equation of continuity for this case is

$$\frac{\partial}{\partial x}\left(\rho u\right) + \frac{\partial}{\partial y}\left(\rho v\right) = 0 \qquad (11.76)$$

where u and v are the component velocities and ρ the local density of the fluid. Expressing u and v in terms of a velocity potential,

$$u = \frac{\partial \phi}{\partial x} \qquad v = \frac{\partial \phi}{\partial y} \qquad (11.77)$$

the equation of continuity becomes

$$\frac{\partial}{\partial x}\left(\rho\,\frac{\partial \phi}{\partial x}\right) + \frac{\partial}{\partial y}\left(\rho\,\frac{\partial \phi}{\partial y}\right) = 0 \tag{11.78}$$

The thickness of the conducting sheet must be proportional to the density of the fluid at the corresponding point. The density, however, is dependent on the resulting velocity and on the thermodynamic law of the fluid. The velocity-density relation is expressed in the Bernoulli equation:

$$\int \frac{dp}{\rho} + \frac{1}{2}\left(u^2 + v^2\right) = K_1 \tag{11.79}$$

where p is the local pressure and K_1 is a constant determined from known boundary or initial conditions. The adiabatic pressure-density relation for an ideal gas is

$$p\rho^{-\gamma} = K_2 \tag{11.80}$$

where $\gamma = c_p/c_v$, the ratio of the specific heats, and K_2 is another constant also determined by boundary or initial conditions.

If V_0 is the velocity of a uniform stream far from the obstacle, $c_0 \ (= dp/d\rho)$ the corresponding acoustic velocity, and ρ_0 the density there, then the above relations yield

$$\frac{\rho}{\rho_0} = \left(1 - \frac{\gamma - 1}{2}\frac{q^2 - V_0{}^2}{c_0{}^2}\right)^{1/(\gamma-1)} \tag{11.81}$$

where $q^2 = u^2 + v^2$.

In applying the electrolytic tank to this problem, a uniform depth of electrolyte is first provided. The velocity distribution q is determined from the voltage contours and is used to calculate the density distribution from Eq. (11.81). This then provides a basis for carving the wax bottom to a variable depth for the next determination of the q distribution. The process is repeated as needed to obtain the required degree of accuracy. Taylor and Sharman found that if a speed in excess of the local speed of sound is attained anywhere in the flow field around the cylinder, the process does not converge and no solution on this basis is obtainable.

The electrolytic tank of variable thickness has also been used to solve problems in the theory of fluid-film lubrication.[54] The differential equation governing the pressure distribution in bearings under fluid-film conditions was originally developed by Reynolds.[55] The equation was based on the assumption of a thin film (pressure constant across its thickness) and a constant oil viscosity. Subsequently, variable viscosity was included. Lamb[56] shows that the oil pressure in the film must satisfy the equation

$$\frac{\partial}{\partial x}\left(\frac{\delta^3}{12\mu}\frac{\partial p}{\partial x}\right) + \frac{\partial}{\partial y}\left(\frac{\delta^3}{12\mu}\frac{\partial p}{\partial y}\right) = \frac{\partial}{\partial x}\left(\frac{\delta U}{2}\right) + \frac{\partial}{\partial y}\left(\frac{\delta V}{2}\right) \tag{11.82}$$

where δ = local oil-film thickness

μ = local oil viscosity

p = local oil pressure

x, y = coordinates of given point in plane of developed oil film

U = bearing surface local velocity in x direction

V = bearing surface local velocity in y direction

The physical significance of the terms in Eq. (11.82) may better be appreciated by considering their derivation from the fundamental relations of viscous flow. In Fig. 11.12, the oil particle shown is in equilibrium under the action of the shear forces and normal pressures. For equilibrium in the x direction,

$$\left(\sigma_{zx} + \frac{\partial \sigma_{zx}}{\partial z}\,dz\right) dx\,dy - \sigma_{zx}\,dx\,dy = -p\,dy\,dz$$
$$+ \left(p + \frac{\partial p}{\partial x}\,dx\right) dy\,dz \quad (11.83)$$

or
$$\frac{\partial \sigma_{zx}}{\partial z} = \frac{\partial p}{\partial x} \quad (11.84)$$

Similarly, equilibrium in the y direction yields

$$\frac{\partial \sigma_{zy}}{\partial z} = \frac{\partial p}{\partial y} \quad (11.85)$$

The shear stresses are proportional to velocity gradients. Thus

$$\sigma_{zx} = \mu\,\frac{\partial u}{\partial z} \qquad \sigma_{zy} = \mu\,\frac{\partial v}{\partial z} \quad (11.86)$$

and

$$\mu\,\frac{\partial^2 u}{\partial z^2} = \frac{\partial p}{\partial x} \qquad \mu\,\frac{\partial^2 v}{\partial z^2} = \frac{\partial p}{\partial y} \quad (11.87)$$

Because of the thinness of the film, the velocity w in the z direction is assumed to be zero and the pressure across the thickness of the oil film is assumed to be constant. Figure 11.12 has been drawn on this basis.

Fig. 11.12

Velocity gradients in the plane of the film are considered negligible in comparison with those across the thickness of the film. Thus, Eqs. (11.87) may be integrated across the film thickness for the velocities, yielding

$$u = \frac{z^2}{2\mu}\,\frac{\partial p}{\partial x} + C_1 z + C_2 \quad (11.88)$$

$$v = \frac{z^2}{2\mu}\,\frac{\partial p}{\partial y} + C_3 z + C_4 \quad (11.89)$$
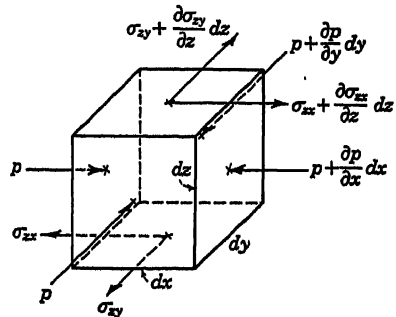
The constants of integration are determined from the known boundary values of u and v. These are

At $z = 0$ $u = v = 0$ (11.90)
At $z = \delta$ $u = U$ $v = V$

Consequently,

$$C_2 = C_4 = 0 \tag{11.91}$$

$$C_1 = \frac{U}{\delta} - \frac{1}{2\mu}\left(\frac{\partial p}{\partial x}\right)\delta \tag{11.92}$$

$$C_2 = \frac{V}{\delta} - \frac{1}{2\mu}\left(\frac{\partial p}{\partial y}\right)\delta \tag{11.93}$$

The velocity distribution across the thickness h of the oil film becomes, therefore,

$$u = \frac{1}{2\mu}z(z - \delta)\frac{\partial p}{\partial x} + \frac{Uz}{\delta} \tag{11.94}$$

$$v = \frac{1}{2\mu}z(z - \delta)\frac{\partial p}{\partial y} + \frac{Vz}{\delta} \tag{11.95}$$

The oil flow rates across vertical sections of the oil film of height δ and of unit width are

$$Q_x = \int_0^\delta \left[\frac{1}{2\mu}z(z - \delta)\frac{\partial p}{\partial x} + \frac{Uz}{\delta}\right]dz \tag{11.96}$$

$$Q_y = \int_0^\delta \left[\frac{1}{2\mu}z(z - \delta)\frac{\partial p}{\partial y} + \frac{Vz}{\delta}\right]dz \tag{11.97}$$

$$Q_x = -\frac{\delta^3}{12\mu}\frac{\partial p}{\partial x} + \frac{U\delta}{2} \tag{11.98}$$

$$Q_y = -\frac{\delta^3}{12\mu}\frac{\partial p}{\partial y} + \frac{V\delta}{2} \tag{11.99}$$

Considering an element of volume $dx\,dy\,\delta$ in the oil film, the flow entering the element in the x direction is $Q_x\,dy$ and that leaving the volume in the same direction is $Q_x\,dy + (\partial Q_x/\partial x)\,dx\,dy$. The excess leaving is $(\partial Q_x/\partial x)\,dx\,dy$. Similarly, the excess leaving the element of volume in the y direction is $(\partial Q_y/\partial y)\,dx\,dy$. For incompressible flow, the equation of continuity is

$$\frac{\partial Q_x}{\partial x} + \frac{\partial Q_y}{\partial y} = 0 \tag{11.100}$$

Substituting Eqs. (11.98) and (11.99) into (11.100), Eq. (11.82) will result. Thus, Eq. (11.82) represents the balance between incoming and outgoing fluid at any point due to pressure gradients and velocity drag. If oil were introduced through oilholes in the journal bearing, another term would be added to Eq. (11.82) to include this quantity.

Equation (11.82) may be represented by the electrically conducting sheet.[57] From Eq. (11.69) it is seen that

$$h = \frac{\delta^3}{12\mu} \tag{11.101}$$

$$-\rho i = \frac{\partial}{\partial x}\left(\frac{\delta U}{2}\right) + \frac{\partial}{\partial y}\left(\frac{\delta V}{2}\right) \tag{11.102}$$

The conducting sheet should have the same plan form as that of the developed oil film, its thickness varying from point to point in accordance

(a)

(b)

(c)
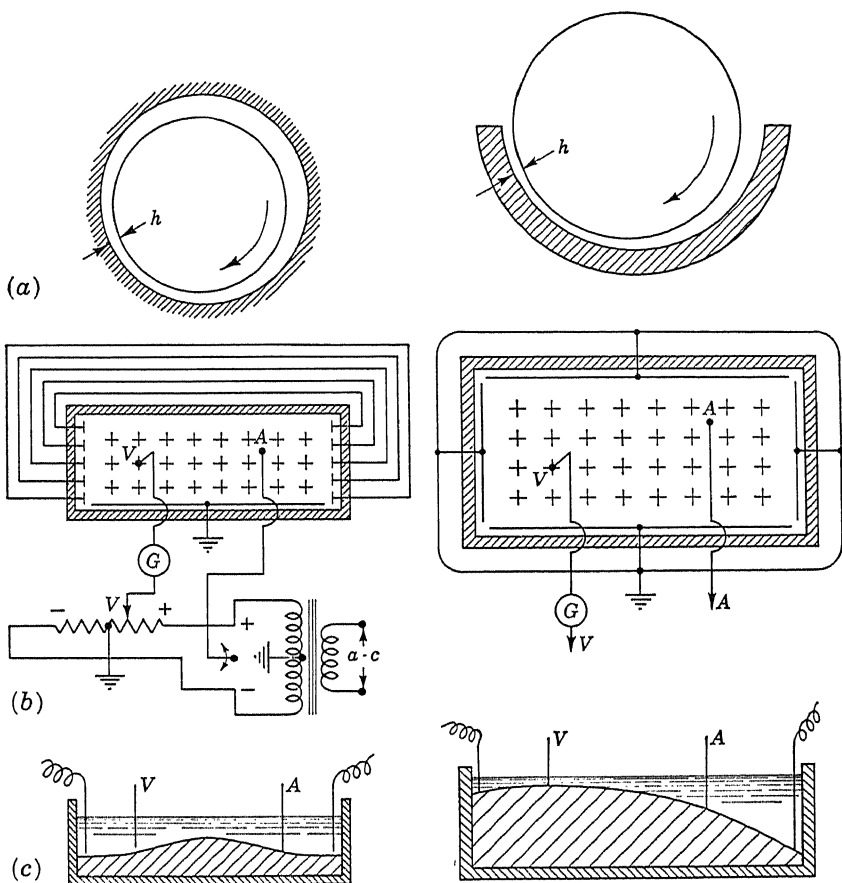
Fig. 11.13   Fig. 11.14

with Eq. (11.101) and a distributed current fed into its surface in accordance with Eq. (11.102). Boundary voltages around the edge of the sheet should correspond to the pressures existing at the edges of the oil film. If oil is supplied at a predetermined quantity rate at any particular posi-

tion in the bearing through an oilhole, a corresponding current input should be provided at the same position in the conducting sheet model. If, on the other hand, a constant oil pressure is maintained at an oil inlet, then a constant voltage would be maintained at the corresponding position in the conducting sheet model.

Typical arrangements for electrolytic models of bearings are shown in Figs. 11.13 and 11.14, the former applying to a full journal bearing, the latter to a partial journal bearing. In these tanks the plan form of the oil film may be represented to a convenient scale. The film thickness is invariably represented to a different and considerably enlarged scale in order to permit accurate carving of the tank bottom.
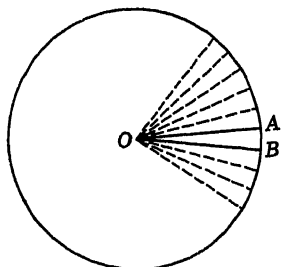
The exposed edges of the oil film are subjected to atmospheric pressure (zero gauge pressure). Consequently, the corresponding edges of the electrolytic tank are maintained at zero voltage. If the bearing is symmetrical in all respects about its centerplane, then only one half of it need be represented by the tank, the plane of symmetry being represented by an insulated wall of the tank. The insulating wall serves to mirror the voltage distribution, thus giving the effect of the full bearing length with only a half model.

Fig. 11.15

The full journal bearing has only two edges exposed to atmospheric pressure, so that in the corresponding half model one edge is kept at zero voltage and one edge is insulated. The other two edges represent the same section of the oil film where the complete ring was cut and then ·spread into a flat sheet. Consequently, these two edges in the model must have exactly the same voltage distributions point by point. This is accomplished by using a row of narrow metal electrodes at each end and interconnecting corresponding pairs of electrodes with wires.

Figures 11.13 and 11.14 show in the plan views networks of squares with a current electrode A at the center of a square in each to provide the concentrated equivalent of the distributed current over the square area. A voltage probe V is shown at intersection points of the grid.

Electrically conducting sheets of variable thickness may be used to solve certain three-dimensional problems involving axial symmetry. Referring to the circular cross section in Fig. 11.15 for such a problem, a conducting sheet whose thickness varies linearly as does the wedge OAB would simulate the problem. This can be seen from the fact that in the tank the upper surface, seen edge on as the line OA, and the lower surface, seen edge on as the line OB, are insulated surfaces, so that the image of the section OAB appears adjacent to it, above and below. These are

imaged successively around the circle, so that phenomena occurring in the wedge-shaped tank OAB are analogous to the axially symmetrical phenomena occurring throughout the axially symmetrical body.

Wedge-shaped conducting sheets are easily obtained by tilting an electrolytic tank so that the bottom of the tank and the surface of the liquid intersect at the axis of symmetry. Such a tilted tank is shown in Fig. 11.16 to study the potential distribution about a cigar-shaped model. The model in such a tank may tend to be rather small, so that frequently a deep tank is used and one-quarter[58] or one-half[59] the model submerged
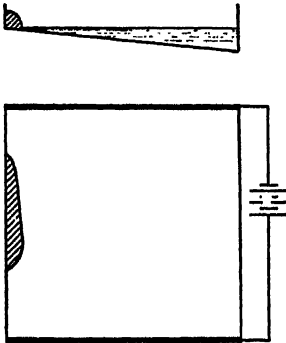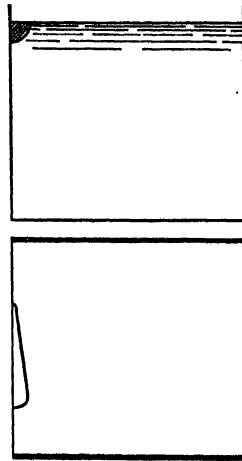
Fig. 11.16   Fig. 11.17

in it. Figure 11.17 shows the same problem as that in Fig. 11.15, but using a model representing one-quarter of the axially symmetric body. The voltage exploring probe need trace out equipotentials only on the surface of the electrolyte.

The electrolytic tank may be required to simulate composite media, as, for example, the axially symmetrical heat-conduction problem through concentric layers of different material. If layers of electrolyte having different compositions are to represent such a composite structure, the separating surface must provide continuity in voltage in going from one layer into the next. Rice[58] suggested the use of insulating diaphragms with metal pins through a diaphragm connecting the adjacent electrolytes electrically point for point. Other suggestions include the construction of the diaphragm by alternate metallic and insulating strips.

Jacobsen[60] developed a conducting-sheet analogy for the torsion of non-uniform shafts of circular cross section. Stepped or filleted shafts and shafts with circumferential grooves have been investigated in this manner. Figure 11.18 shows a section of such a shaft, the ends of which are suffi-

ciently removed from the fillet so that the shear stress distribution across each end is essentially that of a uniform shaft of that diameter subjected to the given twisting couple. In analyzing the problem of shear stress distribution through the filleted region, it is assumed that any given point in the bar is displaced only in the circumferential direction. Consequently, the only stresses present on a cross section are $\sigma_{\theta r}$ and $\sigma_{\theta z}$. The equation of equilibrium to be satisfied is (see Sec. 11.15)

$$\frac{\partial \sigma_{\theta r}}{\partial r} + \frac{\partial \sigma_{\theta z}}{\partial z} + \frac{2\sigma_{\theta r}}{r} = 0 \qquad (11.103)$$

The shear strains are

$$\gamma_{\theta r} = \frac{\partial v}{\partial r} - \frac{v}{r} = \frac{\sigma_{\theta r}}{G} \qquad \gamma_{\theta z} = \frac{\partial v}{\partial z} = \frac{\sigma_{\theta z}}{G} \qquad (11.104)$$

Following the usual procedures where components of an undetermined dependent variable are involved, these equations may be reduced to a single equation in terms of only one dependent variable (the stress function) by an appropriate choice of the transformation functions. In the present case the transformation functions are
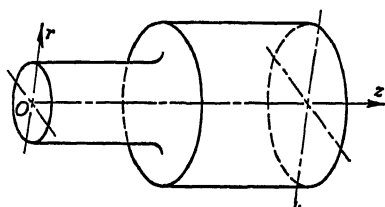
$$\sigma_{\theta r} = -\frac{1}{r^2}\frac{\partial \phi}{\partial z} \qquad \sigma_{\theta z} = \frac{1}{r^2}\frac{\partial \phi}{\partial r} \qquad (11.105)$$

A substitution into Eq. (11.103) shows it to be satisfied by the relations of Eqs. (11.105). A substitution into Eqs. (11.104) yields

$$-\frac{1}{r^2}\frac{\partial \phi}{\partial z} = G\left(\frac{\partial v}{\partial r} - \frac{v}{r}\right) = Gr\frac{\partial}{\partial r}\left(\frac{v}{r}\right) \qquad (11.106)$$

$$\frac{1}{r^2}\frac{\partial \phi}{\partial r} = G\frac{\partial v}{\partial z} = Gr\frac{\partial}{\partial z}\left(\frac{v}{r}\right) \qquad (11.107)$$

Differentiating the first equation with respect to z and the second with respect to r and subtracting the first from the second, we obtain

$$\frac{\partial}{\partial r}\left(\frac{1}{r^2}\frac{\partial \phi}{\partial r}\right) + \frac{\partial}{\partial z}\left(\frac{1}{r^2}\frac{\partial \phi}{\partial z}\right) - G\frac{\partial}{\partial z}\left(\frac{v}{r}\right) = 0 \qquad (11.108)$$

Replacing the last term by its equivalent in terms of ϕ from Eq. (11.107), Eq. (11.108) becomes, after performing the indicated differentiations,

$$\frac{\partial^2 \phi}{\partial r^2} - \frac{3}{r}\frac{\partial \phi}{\partial r} + \frac{\partial^2 \phi}{\partial z^2} = 0 \qquad (11.109)$$

The resultant shear stress at an unloaded boundary on the cross section

must be tangent to the boundary. Thus

$$\frac{\partial \phi}{\partial z} dz + \frac{\partial \phi}{\partial r} dr = 0 \tag{11.110}$$

This means, then, that ϕ_b is constant on the surface of the shaft. If the shaft were hollow, ϕ_{bi} would also be constant over the inner surface, although of a different value.

The surfaces of constant ϕ are thus surfaces of revolution, the inner and outer surfaces being the actual inner and outer surfaces of the shaft, while the intermediate surfaces assume shapes giving a gradual transition from the shape of the inner surface to that of the outer surface. For a solid shaft, the inner surface would be the center line of the shaft. Figure 11.19 shows in its upper half the traces of these surfaces on a longitudinal section taken through the axis of Fig. 11.18.
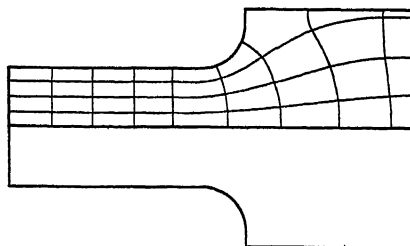
Because of axial symmetry, all points on a ring of radius r at a position z along the axis behave identically. Such a ring will be rotated through an angle ψ by the applied torque. In terms of the linear displacement v along the arc of radius r,

Fig. 11.19

$$\psi = \frac{v}{r} \tag{11.111}$$

From Eqs. (11.105), (11.107), and (11.111), we have

$$-\frac{1}{r^2} \frac{\partial \phi}{\partial z} = Gr \frac{\partial \psi}{\partial r} \qquad \frac{1}{r^2} \frac{\partial \phi}{\partial r} = Gr \frac{\partial \psi}{\partial z} \tag{11.112}$$

Making the substitution into Eq. (11.109), the equation for the angular displacement ψ is found to be

$$\frac{\partial^2 \psi}{\partial r^2} + \frac{3}{r} \frac{\partial \psi}{\partial r} + \frac{\partial^2 \psi}{\partial z^2} = 0 \tag{11.113}$$

The surfaces of constant ψ are surfaces in which every point has the same angular displacement. They are surfaces orthogonal to the surfaces of constant ϕ. In the case of uniform circular shaft they would be the cross-sectional planes. In the case of the filleted shaft, they would be as shown in Fig. 11.19, distorted out of plane in the vicinity of the fillet, but plane at the ends far enough away from the fillet. Two surfaces of constant ψ spaced apart a small distance ds along a surface of constant ϕ will

be displaced relative to each other by a small angle $d\psi$. Considering the
ϕ surface a distance r from the axis, the relative motions of the adjacent ψ
surfaces at that radius causes a shear strain $r \, d\psi/ds$ at that position. The
initially square element in the ϕ surface at that point becomes distorted,
as shown by the dotted rhombus in Fig. 11.20. Consequently, the shear
stress developed at that point is
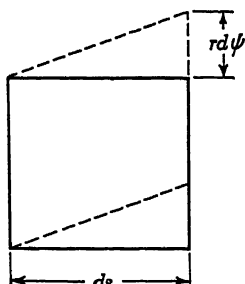
Fig. 11.20

$$\sigma_{\psi\phi} = G \frac{r \, d\psi}{ds} \qquad (11.114)$$

The same situation holds for the outer surface of
the shaft, which is also a surface of constant ϕ.

If the surface of constant ψ may be determined,
the shear stress distribution in the shaft would
follow. Jacobsen showed that if a conducting
sheet having the same plan form in the yx plane
as one of the symmetrical halves of a longitudinal
section of the shaft in the rz plane be constructed so that its thickness
varied with the cube of the y dimension, but remained uniform in the x
direction, the equation for the voltage distribution in such a "razor-blade"
conducting sheet is the same as the equation for ψ. This conducting
sheet may then be used to determine the family of lines of constant ψ.

Substituting into Eq. (11.69) the relation

$$h = cy^3 \qquad (11.115)$$

where c is a constant of proportionality, and letting $i = 0$, we obtain

$$\frac{\partial^2 V}{\partial x^2} + \frac{3}{y} \frac{\partial V}{\partial y} + \frac{\partial^2 V}{\partial y^2} = 0 \quad (11.116)$$

At $x = 0$ and $x = L$ (the two ends
of the conducting sheet), the equi-
potentials are straight lines corre-
sponding to the traces of the surfaces
of constant ψ ("equiangular" surfaces)
at the ends in Fig. 11.19. These con-

Fig. 11.21

ditions may be enforced by placing electrodes across the ends of an
electrolytic tank properly shaped for form and thickness. Jacobsen
used a steel conductor with heavy copper electrodes soldered to its ends.
The conducting sheet for the shaft of Fig. 11.18 is shown sketched in
Fig. 11.21. End views show how the sheet thickness changes as the cube
of the distance from the sharp edge.
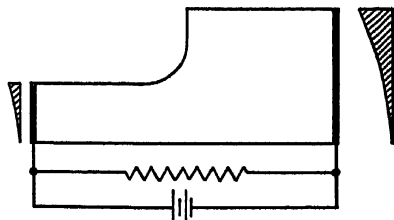
According to Eq. (11.114), the shear stress will be proportional to the
radius and the voltage gradient along a surface of constant ϕ in the elec-
trical model. The outer surface is the most critical one, so that measure-

ments of voltage gradient may be made along the outer edge of the model, with two closely spaced probes. These may be compared with a similar measurement made close to the left end of the model in order to evaluate the stress concentrating effect of the fillet. The stress concentration K may then be determined from

$$K = \frac{r_s \, \Delta V_s}{r_0 \, \Delta V_0} \tag{11.117}$$

where ΔV_s and ΔV_0 are the voltage differences measured by two probes at a test location s on the rim of the model and at the reference location 0 at the left end, assuming the same spacing along the surface was used between the probes at both locations. The corresponding radii at these points are r_s and r_0.

11.11. Miscellaneous Applications of Analogies to Field Problems. The electrolytic bath and other conducting-sheet analogies described in the preceding sections require the use of a probe for measuring and plotting voltage distributions. A pantograph is often used to record probe positions on a separate sheet of paper where it is not possible (*e.g.*, liquid bath) or it is undesirable to record directly on the conducting sheet. While the probe is usually manually positioned, automatic methods[61,62] have also been developed for tracing all the required equipotentials.

An interesting application of the conducting-sheet method in which the electrolytic bath produces its own equipotentials was described many years ago by Guébhard.[63,64] Making use of an electrolyte consisting of a mixture of acetates of copper and lead, with traces of potassium acetate to reduce polarization effects at the electrodes, Guébhard showed that the passage of current between electrodes resulted in multicolored lead oxide deposits on a metal plate covering the bottom of the bath and that the isochromatic lines in the oxide deposits coincided with the equipotentials in the electrolyte.

The electrolytic bath has been used to determine the increase in pressure occurring on the face of a dam as a result of earthquake motion.[65] Assuming the dam to be rigid and to move as a unit with the ground, the equations of motion of a particle of water as a result of earthquake hydrodynamic pressures P are (in two dimensions)

$$\frac{\partial P}{\partial x} = \rho \frac{\partial^2 v_x}{\partial t^2} \qquad \frac{\partial P}{\partial y} = \rho \frac{\partial^2 v_y}{\partial t^2} \tag{11.118}$$

Considering water to be incompressible, the equation of continuity is

$$\frac{\partial v_x}{\partial x} + \frac{\partial v_y}{\partial y} = 0 \tag{11.119}$$

whereupon Eq. (11.118) becomes the Laplace equation

$$\frac{\partial^2 P}{\partial x^2} + \frac{\partial^2 P}{\partial y^2} = 0 \qquad (11.120)$$

The set of streamlines is orthogonal to the constant-pressure lines given by Eq. (11.120). Actually, the boundary conditions on the streamlines are known, rather than those on pressure. Because of the dam's horizontal motion, the same quantity of water must flow through each equal increment of depth at the face of the dam. This is simulated in the electrolytic tank by applying a uniformly varying potential along the face of the dam model, as shown in Fig. 11.22. A uniformly wound resistance AB constitutes this end of the tank. The zero streamline is the bottom of the reservoir. The water surface AD and the other end of the reservoir CD are insulated edges. CD is considered far enough away to have little influence on earthquake pressures developed on the face AB.
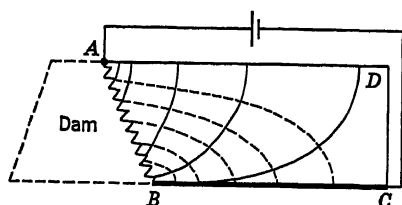
Fig. 11.22

The streamlines are obtained from the conducting-sheet test, and the earthquake pressures are obtained by drawing in an orthogonal family of curves.

Considerable use is made of the electrolytic bath as an aid in the design of electron guns and high vacuum tubes.[66,67] The model is built on a large scale, the electrodes are readily available for shaping and rearranging spatially, and many mathematically unmanageable design conditions are rapidly investigated.

A technique similar to that of photoelasticity has been used for field mapping, making use of the fact that most liquids become doubly refracting when exposed to an electric field.[68] Certain colloidal solutions of bentonite were found to be particularly active in this respect. Using polarized light, two orthogonal families of curves are obtained, the isoclinics giving field direction, the isochromatics field intensity.

REFERENCES

1. Wilson, L. H., and A. J. Miles: Application of the Membrane Analogy to the Solution of Heat-conduction Problems, *J. Appl. Phys.*, **21**:532–535 (1950).
2. Fremlin, J. H., and J. Walker: The Stretched Rubber Sheet, *J. Sci. Instr.*, **24**:50–51 (1947).
3. Zworykin, V. K., G. A. Morton, E. G. Ramberg, J. Hillier, and A. W. Vance: "Electron Optics and the Electron Microscope," p. 418, John Wiley & Sons, Inc., New York, 1945.
4. Hollmann, H. E.: Theoretical and Experimental Investigations of Electron

Motions in Alternating Fields with the Aid of Ballistic Models, *Proc. IRE*, **29**: 70–79 (1941).

5. Clark, J. W., and R. E. Neuber: A Dynamic Electron Trajectory Tracer, *Proc. IRE*, **38**:521–524 (1950).

6. Walker, G. B.: Factors Influencing the Design of a Rubber Model, *Proc. Inst. Elec. Engrs. (London)*, part II, **96**:319–324 (1949).

7. McGivern, J. G., and H. L. Supper: A Membrane Analogy Supplementing Photoelasticity, *Trans. ASME*, **56**:601–605 (1934). [Also *J. Franklin Inst.*, **217**:491–504, (1934).]

8. Weibel, E. E.: Studies in Photoelastic Stress Determination, *Trans. ASME*, **56**:637–649 (1934).

9. Szebehely, V. G.: An Analogy between Open Soap Bubble and Compressible Flow, Readers' Forum, *J. Aeronaut. Sci.*, **17**:809 (1950).

10. Bateman, H.: Notes on a Differential Equation Which Occurs in the Two-dimensional Motion of a Compressible Fluid and the Associated Variational Problems, *Proc. Roy. Soc. (London)*, (A)**125**:598–618 (1929).

11. Truesdell, C.: The Analogy between Irrotational Gas Flow and Minimal Surfaces, Readers' Forum, *J. Aeronaut. Sci.*, **18**:502 (1951).

12. Prandtl, L.: Zur Torsion von prismatischen Staben, *Physik. Z.*, **4**:758–759 (1903).

13. Griffith, A. A., and G. I. Taylor: The Use of Soap Films in Solving Torsion Problems, *Proc. Inst. Mech. Engrs. (London)*, pp. 755–809, 1917. (Also in British Air Ministry R. and M. 333, June, 1917.)

14. Griffith, A. A.: The Use of Soap Films in Solving Stress Problems, pp. 39–42, *Proc. 1st Intern. Congr. Appl. Mechanics*, Delft, 1924.

15. Griffith, A. A., and G. I. Taylor: "The Application of Soap Films to the Determination of the Torsion and Flexure of Hollow Shafts," Technical Report of the Advisory Committee for Aeronautics for 1917–1918 (British), vol. III, pp. 938–949. (Also in British Air Ministry R. and M. 392, January, 1918.)

16. Trayer, G. W., and H. March: Torsion of Members Having Sections Common in Aircraft Construction, *NACA TR* 334, 1930.

17. Marin, J.: Evaluating Torsional Stresses by Membrane Analogy, *Machine Design*, **15**(6):118–123, 198, 200, 202 (June, 1943).

18. Neubauer, E. T. B., and O. Boston: Torsional Analysis of Twist-drill Sections by Membrane Analogy, *Trans. ASME*, **69**:897–902 (1947).

19. Roark, R. J.: "Formulas for Stress and Strain," p. 168, McGraw-Hill Book Company, Inc., New York, 1943.

20. Moore, A. D.: Soap Film and Sand Bed Mapper Techniques, *J. Appl. Mechanics*, **17**:291–298 (1950).

21. Drucker, D. C., and M. M. Frocht: Equivalence of Photoelastic Scattering Patterns and Membrane Contours for Torsion, *Proc. SESA*, **5**(2):34–41 (1948).

22. Miles, A. J., and E. A. Stephenson: Pressure Distribution in Oil and Gas Reservoirs by Membrane Analogy, *Trans. AIMME* (Petroleum Division), **127**:135–145 (1938).

23. van Bavel, C. H. M.: A Soil Aeration Theory Based on Diffusion, *Soil Sci.*, **72**: 33–46 (1951).

24. Timoshenko, S., and J. N. Goodier: "Theory of Elasticity," 2d ed., chap. 11, McGraw-Hill Book Company, Inc., New York, 1951.

25. The Prandtl-Nadai Torsion Theories and Their Applications, *Engineering*, **123**: 771 (1927).

26. Schilling, F.: Uber die Boschungsflachen mit Kegelschnitten als Basiskurven, *Z. angew. Math. u. Mech.*, **3**:197–217 (1923).

27. Nadai, A.: Plastic Torsion, *Trans. ASME*, **53**:29–48 (1931).

28. Sadowsky, M. A.: An Extension of the Sand-heap Analogy in Plastic Torsion Applicable to Cross Sections Having One or More Holes, *J. Appl. Mechanics*, **8**:166–168 (1941).

28a. Coler, M. A.: Plastics Can Be Electrical Conductors, *Elec. Mfg.*, **44**(5):60–63 (November, 1949).

29. Langmuir, I., E. Q. Adams, and G. S. Mickle: Flow of Heat through Furnace Walls: The Shape Factor, *Trans. Am. Electrochem. Soc.*, **24**:53–84 (1913).

30. Awberry, J. H., and F. H. Schofield: Effect of Shape on Heat-loss through Insulation, *Proc. 5th Intern. Congr. Refrig.*, **3**:591–610 (1928).

31. Schofield, F. H.: The Heat-loss from a Plate Embedded in an Insulating Wall, *Phil. Mag.*, **10**(7):480–500 (1930).

32. Schofield, F. H.: The Heat-loss from a Cylinder Embedded in an Insulating Wall, *Phil. Mag.*, **12**(7):329–349 (1931).

33. Kayan, C. F.: Temperature Patterns and Heat Transfer for a Wall Containing a Submerged Metal Member, *Refrig. Eng.*, **51**:533–537 (1946).

34. Kayan, C. F.: An Electrical Geometrical Analogue for Complex Heat Flow, *Trans. ASME*, **67**:713–718 (1945).

35. Kayan, C. F.: Temperature Distribution in Complex Wall Structures by Geometrical Electrical Analogue, *Refrig. Eng.*, **49**:113–117 (1945).

36. Kayan, C. F.: Effect of Floor Slab on Building Structure Temperatures and Heat Flow, *Heating, Piping, Air Conditioning*, **19**(6):103–111 (June, 1947).

37. Hotchkiss, G.: Electrosensitive Recording Paper for Facsimile Telegraph Apparatus and Graphic Chart Instruments, *Western Union Tech. Rev.*, **2**:176–187 (1948).

38. Douglas, J. F. H.: The Reluctance of Some Irregular Magnetic Fields, *Trans. AIEE*, **34**:1067–1134 (1915).

39. Relf, E. F.: An Electrical Method of Tracing Stream Lines for the Two-dimensional Motion of a Perfect Fluid, British Air Ministry R. and M. 905, April, 1924.

40. Hahn, E. P.: Experimental Solution of Hydrodynamic Equations, *Engineering*, **123**:178–180 (1927).

41. Malavard, L.: The Use of Rheo-electrical Analogies in Certain Aerodynamical Problems, *J. Roy. Aeronaut. Soc.*, **51**:739–756 (1947).

42. Moore, A. D.: Fields from Fluid Flow Mappers, *J. Appl. Phys.*, **20**:790–804 (1949).

43. Moore, A. D.: The Further Development of Fluid Mappers, *Trans. AIEE*, **69**:1615–1624 (1950).

44. Wyckoff, R. D., H. G. Botset, and M. Muskat: The Mechanics of Porous Flow Applied to Water-flooding Problems, *Trans. AIMME* (Petroleum Division), **103**:219–249 (1933).

45. Swearinger, J. S.: Predicting Wet Gas Recovery in Recycling Operations, *Oil Weekly*, **96**(3):30, 32–33, 36, 38 (Dec. 25, 1939).

46. Botset, H. G.: The Electrolytic Model and Its Application to the Study of Recovery Problems, *Trans. AIMME* (Petroleum Division), **165**:15–25 (1946).

47. Harza, L. F.: Uplift and Seepage under Dams on Sand, *Trans. ASCE*, **100**:1352–1385 (1935).

48. Casagrande, A.: Seepage through Dams, *J. New Engl. Water Works Assoc.*, **51**(6):131–172 (June, 1937).

49. Childs, E. C.: The Water Table, Equipotentials and Streamlines in Drained Land, *Soil Sci.*, **56**:317–330 (1943).

50. Reltov, B. F.: Electrical Analogy Applied to Three-dimensional Study of Percolation under Dams Built on Pervious Heterogeneous Foundations, *Trans. 2d Congr. on Large Dams*, Washington, D.C., **5**:73–85 (1936).

51. Lane, E. W., F. B. Campbell, and W. H. Price: The Flow Net and the Electric Analogy, *Civil Eng.*, **4**:510–514 (1934).
52. Wyckoff, R. D., and D. W. Reed: Electrical Conduction Models for the Solution of Water Seepage Problems, *Physics*, **6**:385–401 (1935).
53. Taylor, G. I., and E. F. Sharman: A Mechanical Method for Solving Problems of Flow in Compressible Fluids, *Proc. Roy. Soc. (London)*, (A)**159**:194–217 (1937).
54. Needs, S. J.: Effects of Side-leakage in 120-degree Centrally-supported Journal Bearings, *Trans. ASME*, **56**:721–732 (1934).
55. Reynolds, O.: On the Theory of Lubrication and Its Application to Mr. Beauchamp Tower's Experiments, Including an Experimental Determination of the Viscosity of Olive Oil, *Trans. Roy. Soc. (London)*, part I, **117**:157–234 (1886).
56. Lamb, H.: "Hydrodynamics," 6th ed., p. 584, Cambridge University Press, New York, 1932.
57. Kingsbury, A.: On Problems in the Theory of Fluid-film Lubrication, with an Experimental Method of Solution, *Trans. ASME*, **53**:59–75 (1931). (Paper No. APM-53-5.)
58. Rice, C. W.: An Experimental Method of Obtaining the Solution of Electrostatic Problems with Notes on High-voltage Bushing Design, *Trans. AIEE*, **36**:905–1072 (1917).
59. Hepp, G.: Measurements of Potential by Means of the Electrolytic Tank, *Philips Tech. Rev.*, **4**:223–230 (1939).
60. Jacobsen, L. S.: Torsional Stress Concentrations in Shafts of Circular Cross Section and Variable Diameter, *Trans. ASME*, **47**:619–641 (1925).
61. Green, P. E., Jr.: Automatic Plotting of Electrostatic Fields, *Rev. Sci. Instr.*, **19**:646–653 (1948).
62. Mickelsen, J. K.: Automatic Equipment and Techniques for Field Mapping, *Gen. Elec. Rev.*, **52**(11):19–23 (November, 1949).
63. Guébhard, A.: Figuration électrochimique des lignes équipotentielles sur des portions quelconques du plan, *J. phys. radium*, **1**(2):205–222 (1882).
64. Guébhard, A.: Sur la figuration électrochimique des systèmes équipotentiels, *J. phys. radium*, **1**(2):483–492 (1882).
65. Zangar, C. N.: Hydrodynamic Pressures on Dams Due to Horizontal Earthquakes, *Proc. SESA*, **10**(2):93–102 (1953).
66. Samuel, A. L.: Some Notes on the Design of Electron Guns, *Proc. Natl. Electronics Conf.*, **1**:48–61 (1944).
67. Jacobs, J. E., and J. A. M. Lyon: Electrolytic Tank Studies in Designing High Vacuum Tubes, *Proc. Natl. Electronics Conf.*, **6**:136–144 (1950).
68. Mueller, H.: Electro-optical Field Mapping, *J. Opt. Soc. Am.*, **31**:286–291 (1941)

APPENDIX

Appendix 1

TABLE A1.1. TABLE OF TRANSFER IMPEDANCES*
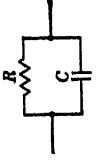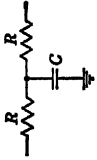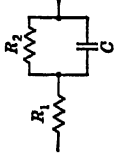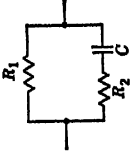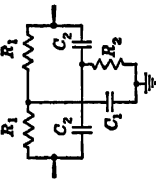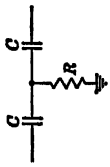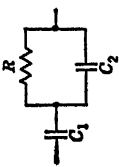
Transfer impedance	Network	Relations	Inverse relations
A		$A = R$	$R = A$
$\dfrac{A}{1+sT}$		$A = R$ $T = RC$	$R = A$ $C = \dfrac{T}{A}$
$A(1+sT)$		$A = 2R$ $T = \dfrac{RC}{2}$	$R = \dfrac{A}{2}$ $C = \dfrac{4T}{A}$
$A\left(\dfrac{1+s\theta T}{1+sT}\right)$ $\theta < 1$		$A = R_1 + R_2$ $T = R_2 C$ $\theta = \dfrac{R_1}{R_1 + R_2}$	$R_1 = A\theta$ $R_2 = A(1-\theta)$ $C = \dfrac{T}{A(1-\theta)}$
		$A = R_1$ $T = (R_1 + R_2)C$ $\theta = \dfrac{R_2}{R_1 + R_2}$	$R_1 = A$ $R_2 = \dfrac{A\theta}{1-\theta}$ $C = \dfrac{T(1-\theta)}{A}$

TABLE A1.1. TABLE OF TRANSFER IMPEDANCES* (Continued)

Transfer impedance	Network	Relations	Inverse relations
$A \dfrac{1 + sT_1}{1 + s^2 T_1 T_2}$		$A = 2R_1$ $T_1 = \dfrac{R_1 C_1}{2} = 2R_2 C_2$ $T_2 = R_1 C_2$ $R_1 C_1 = 4R_2 C_2$	$R_1 = \dfrac{A}{2}$ $R_2 = \dfrac{AT_1}{4T_2}$ $C_1 = \dfrac{4T_1}{A}$ $C_2 = \dfrac{2T_2}{A}$
$\dfrac{1}{sB}$		$B = C$	$C = B$
$\dfrac{1}{sB}(1 + sT)$		$B = C$ $T = RC$	$R = \dfrac{T}{B}$ $C = B$
$\dfrac{1}{sB}\dfrac{1 + sT}{sT}$		$B = \dfrac{C}{2}$ $T = 2RC$	$R = \dfrac{T}{4B}$ $C = 2B$
$\dfrac{1}{sB}\dfrac{1 + sT}{1 + s\theta T}$ $\theta < 1$		$B = C_1$ $T = R(C_1 + C_2)$ $\theta = \dfrac{C_2}{C_1 + C_2}$	$R = \dfrac{T(1 - \theta)}{B}$ $C_1 = B$ $C_2 = \dfrac{B\theta}{1 - \theta}$
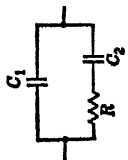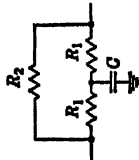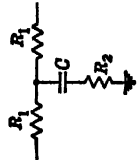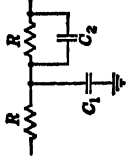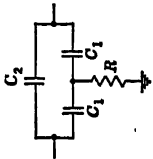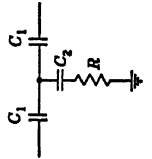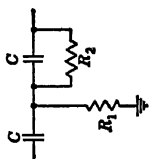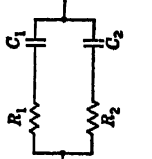
Transfer function	Circuit	Relations	Inverse relations
$\dfrac{1}{sB}\dfrac{1+sT}{1+s\theta T}$, $\theta < 1$		$B = C_1 + C_2$ $T = RC_2$ $\theta = \dfrac{C_1}{C_1 + C_2}$	$R = \dfrac{T}{B(1-\theta)}$ $C_1 = B\theta$ $C_2 = B(1-\theta)$
		$A = \dfrac{2R_1R_2}{2R_1 + R_2}$ $T = \dfrac{R_1C}{2}$ $\theta = \dfrac{2R_1}{2R_1 + R_2}$	$R_1 = \dfrac{A}{2(1-\theta)}$ $R_2 = \dfrac{A}{\theta}$ $C = \dfrac{4T(1-\theta)}{A}$
$A\dfrac{1+sT}{1+s\theta T}$, $\theta < 1$		$A = 2R_1$ $T = \left(R_2 + \dfrac{R_1}{2}\right)C$ $\theta = \dfrac{2R_2}{2R_2 + R_1}$	$R_1 = \dfrac{A}{2}$ $R_2 = \dfrac{A\theta}{4(1-\theta)}$ $C = \dfrac{4T(1-\theta)}{A}$
		$A = 2R$ $T = \dfrac{R}{2}(C_1 + C_2)$ $\theta = \dfrac{2C_2}{C_1 + C_2}$	$R = \dfrac{A}{2}$ $C_1 = \dfrac{2T(2-\theta)}{A}$ $C_2 = \dfrac{2T\theta}{A}$

TABLE A1.1. TABLE OF TRANSFER IMPEDANCES* (Continued)

Transfer impedance	Network	Relations	Inverse relations
$\dfrac{1}{sB}\dfrac{1+s\theta T}{1+sT}$ $\theta < 1$		$B = C_2$ $T = RC_1 \dfrac{2C_2 + C_1}{C_2}$ $\theta = \dfrac{2C_2}{2C_2 + C_1}$	$R = \dfrac{T\theta^2}{4B(1 - \theta)}$ $C_1 = \dfrac{2B(1 - \theta)}{\theta}$ $C_2 = B$
		$B = \dfrac{C_1^2}{2C_1 + C_2}$ $T = RC_2$ $\theta = \dfrac{2C_1}{2C_1 + C_2}$	$R = \dfrac{T\theta^2}{4B(1 - \theta)}$ $C_1 = \dfrac{2B}{\theta}$ $C_2 = \dfrac{4B(1 - \theta)}{\theta^2}$
		$B = \dfrac{R_1}{R_1 + R_2} C$ $T = R_2 C$ $\theta = \dfrac{2R_1}{R_1 + R_2}$	$R_1 = \dfrac{T\theta^2}{2B(2 - \theta)}$ $R_2 = \dfrac{T\theta}{2B}$ $C = \dfrac{2B}{\theta}$
$\dfrac{1}{sB}\dfrac{(1 + sT_1)(1 + sT_2)}{1 + sT_3}$ $T_1 < T_2 < T_3$		$B = C_1 + C_2$ $T_1 = R_1C_1$ $T_2 = (R_1 + R_2)\dfrac{C_1C_2}{C_1 + C_2}$ $T_3 = R_2C_2$	$R_1 = \dfrac{T_1(T_3 - T_1)}{B(T_2 - T_1)}$ $R_2 = \dfrac{T_3(T_3 - T_1)}{B(T_3 - T_2)}$ $C_1 = \dfrac{T_3 - T_1}{B(T_2 - T_1)}$ $C_2 = \dfrac{B(T_3 - T_2)}{T_3 - T_1}$
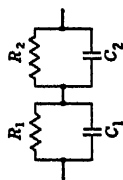
Circuit	Relationships	Solved for
	$A = R_1 + R_2$ $T_1 = R_1C_1$ $T_2 = \dfrac{R_1R_2}{R_2}(C_1+C_2)$ $T_3 = R_2C_2$	$R_1 = \dfrac{A(T_2-T_1)}{T_3-T_1}$ $R_2 = \dfrac{A(T_3-T_2)}{T_3-T_1}$ $C_1 = \dfrac{T_1(T_3-T_1)}{A(T_2-T_1)}$ $C_2 = \dfrac{T_3(T_3-T_1)}{A(T_3-T_2)}$
	$A = R_2$ $T_2 = R_1C_1$ $T_1T_3 = R_1R_2C_1C_2$ $T_1 + T_3 = R_1C_1 + R_2C_2 + R_2C_1$	$R_1 = \dfrac{AT_2^2}{(T_3-T_2)(T_2-T_1)}$ $R_2 = A$ $C_1 = \dfrac{(T_3-T_2)(T_2-T_1)}{AT_2}$ $C_2 = \dfrac{T_1T_3}{AT_2}$
	$A = R_1 + R_2$ $T_2 = \dfrac{R_1R_2}{R_1+R_2}C_2$ $T_1T_3 = R_1R_2C_1C_2$ $T_1 + T_3 = R_1C_1 + R_2C_2 + R_2C_1$	$R_1 = \dfrac{AT_2^2}{T_1T_2 + T_2T_3 - T_1T_3}$ $R_2 = \dfrac{A(T_3-T_2)(T_2-T_1)}{T_1T_2 + T_2T_3 - T_1T_3}$ $C_1 = \dfrac{T_1T_3}{AT_2}$ $C_2 = \dfrac{(T_1T_2 + T_2T_3 - T_1T_3)^2}{AT_2(T_3-T_2)(T_2-T_1)}$
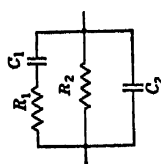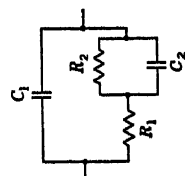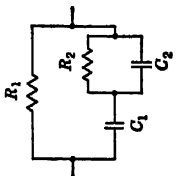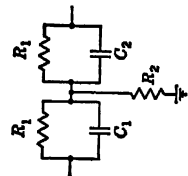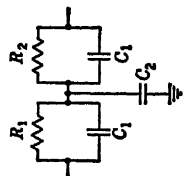
$$A\frac{1+sT_2}{(1+sT_1)(1+sT_3)}$$
$$T_1 < T_2 < T_3$$

TABLE A1.1. TABLE OF TRANSFER IMPEDANCES* (Continued)

Transfer impedance	Network	Relations	Inverse relations
$A\dfrac{1+sT_2}{(1+sT_1)(1+sT_3)}$ $T_1 < T_2 < T_3$		$A = R_1$ $T_2 = R_2(C_1 + C_2)$ $T_1T_3 = R_1R_2C_1C_2$ $T_1 + T_3 = R_1C_1 + R_2C_2 + R_2C_1$	$R_1 = A$ $R_2 = \dfrac{A(T_3 - T_2)(T_2 - T_1)}{(T_1 + T_3 - T_2)^2}$ $C_1 = \dfrac{T_1 + T_3 - T_2}{A}$ $C_2 = \dfrac{T_1T_3(T_1 + T_3 - T_2)}{A(T_3 - T_2)(T_2 - T_1)}$
$A\dfrac{1+sT_2}{(1+sT_1)(1+sT_3)}$ $T_2 \le T_1 \le T_3$		$A = 2R_1 + \dfrac{R_1^2}{R_2}$ $T_1 = R_1C_1$ $T_2 = \dfrac{R_1R_2}{R_1 + 2R_2}(C_1 + C_2)$ $T_3 = R_1C_2$	$R_1 = \dfrac{AT_2}{T_1 + T_3}$ $R_2 = \dfrac{AT_2^2}{(T_1 + T_3)(T_1 + T_3 - 2T_2)}$ $C_1 = \dfrac{T_1(T_1 + T_3)}{AT_2}$ $C_2 = \dfrac{T_3(T_1 + T_3)}{AT_2}$
$A\dfrac{1+sT_2}{(1+sT_1)(1+sT_3)}$ $T_1 \le T_3 \le T_2$		$A = R_1 + R_2$ $T_1 = R_1C_1$ $T_2 = \dfrac{R_1R_2}{R_1 + R_2}(2C_1 + C_2)$ $T_3 = R_2C_1$	$R_1 = \dfrac{AT_1}{T_1 + T_3}$ $R_2 = \dfrac{AT_3}{T_1 + T_3}$ $C_1 = \dfrac{T_1 + T_3}{A}$ $C_2 = \dfrac{T_1 + T_3}{A}\left(\dfrac{T_2}{T_3} + \dfrac{T_2}{T_1} - 2\right)$

438
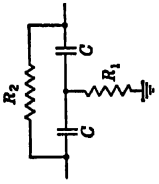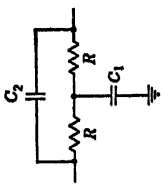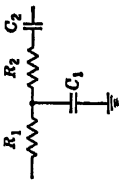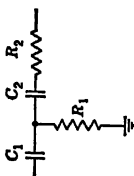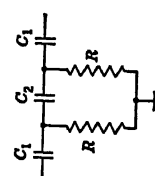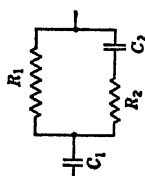
Transfer function	Circuit	Relations	Solution
$A\dfrac{1+sT_1}{1+sT_1+s^2T_1T_2}$		$A = R_2$ $T_1 = 2R_1C$ $T_2 = \dfrac{R_2C}{2}$	$R_1 = \dfrac{AT_1}{4T_2}$ $R_2 = A$ $C = \dfrac{2T_2}{A}$
$A\dfrac{1+sT_2}{1+sT_1+s^2T_1T_2}$		$A = 2R$ $T_1 = 2RC_2$ $T_2 = \dfrac{RC_1}{2}$	$R = \dfrac{A}{2}$ $C_1 = \dfrac{4T_2}{A}$ $C_2 = \dfrac{T_1}{A}$
$\dfrac{1}{sB}(1+sT_1)(1+sT_2)$ $T_1 \neq T_2$		$R = C_2$ $T_1T_2 = R_1R_2C_1C_2$ $T_1 + T_2 = R_1C_1 + R_2C_2 + R_1C_2$	$R_1 = \dfrac{(\sqrt{T_1} - \sqrt{T_2})^2}{B}$ $R_2 = \dfrac{\sqrt{T_1T_2}}{B}$ $C_1 = \dfrac{B\sqrt{T_1T_2}}{(\sqrt{T_1} - \sqrt{T_2})^2}$ $C_2 = B$

TABLE A1.1. TABLE OF TRANSFER IMPEDANCES* (Continued)

Transfer impedance	Network	Relations	Inverse relations
$\dfrac{1}{sB}\dfrac{(1+sT_1)(1+sT_2)}{s\sqrt{T_1T_2}}$ $T_1 \neq T_2$		$R = C_2$ $T_1T_2 = R_1R_2C_1C_2$ $T_1+T_2 = R_1C_1 + R_2C_2 + R_1C_2$	$R_1 = \dfrac{(\sqrt{T_1} - \sqrt{T_2})^2}{B}$ $R_2 = \dfrac{\sqrt{T_1T_2}}{B}$ $C_1 = \dfrac{B\sqrt{T_1T_2}}{(\sqrt{T_1} - \sqrt{T_2})^2}$ $C_2 = B$
$\dfrac{1}{sB}\dfrac{(1+sT_1)(1+sT_2)}{s^2T_1T_2}$ $T_1 < T_2$		$B = \dfrac{C_1C_2}{C_1+2C_2}$ $T_1 = RC_1$ $T_2 = R(C_1+2C_2)$	$R = \dfrac{T_1(T_2 - T_1)}{2BT_2}$ $C_1 = \dfrac{2BT_2}{T_2 - T_1}$ $C_2 = \dfrac{BT_2}{T_1}$
$\dfrac{1}{sB}\dfrac{(1+sT_1)(1+sT_3)}{1+sT_2}$ $T_1 < T_2 < T_3$		$B = C_1$ $T_2 = (R_1+R_2)C_2$ $T_1T_3 = R_1R_2C_1C_2$ $T_1+T_3 = R_1C_1 + R_2C_2 + R_1C_2$	$R_1 = \dfrac{T_1+T_3-T_2}{B}$ $R_2 = \dfrac{T_1T_3(T_1+T_3-T_2)}{B(T_3-T_2)(T_2-T_1)}$ $C_1 = B$ $C_2 = \dfrac{B(T_3-T_2)(T_2-T_1)}{(T_1+T_3-T_2)^2}$

$$\frac{1}{sB}\frac{(1+sT_1)(1+sT_2)}{1+sT_2}$$
$$T_1 < T_2 < T_3$$
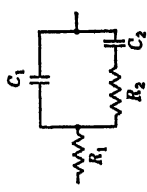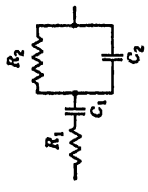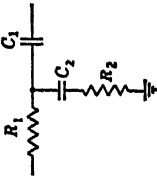
Circuit	Relations	Element values
C_1 — R_2, C_2 — R_1	$B = C_1 + C_2$ $T_2 R_2 = \dfrac{C_1 C_2}{C_1 + C_2}$ $T_1 T_3 = R_1 R_2 C_1 C_2$ $T_1 + T_3 = R_1 C_1 + R_2 C_2 + R_1 C_2$	$R_1 = \dfrac{T_1 T_3}{B T_2}$ $R_2 = \dfrac{(T_1 T_2 + T_2 T_3 - T_1 T_3)(T_2 - T_1)}{B T_2^2}$ $C_1 = \dfrac{T_1 T_2 + T_2 T_3 - T_1 T_3}{B T_2^2}$ $C_2 = \dfrac{B(T_3 - T_2)(T_2 - T_1)}{T_1 T_2 + T_2 T_3 - T_1 T_3}$
R_2, C_2 — R_1, C_1	$B = C_1$ $T_2 = R_2 C_2$ $T_1 T_3 = R_1 R_2 C_1 C_2$ $T_1 + T_3 = R_1 C_1 + R_2 C_2 + R_2 C_1$	$R_1 = \dfrac{T_1 T_3}{B T_2}$ $R_2 = \dfrac{(T_3 - T_2)(T_2 - T_1)}{B T_2}$ $C_1 = B$ $C_2 = \dfrac{B T_2^2}{(T_3 - T_2)(T_2 - T_1)}$
C_1 — R_1, C_2 — R_2	$B = C_1$ $T_2 = R_2 C_2$ $T_1 T_3 = R_1 R_2 C_1 C_2$ $T_1 + T_3 = R_1 C_1 + R_2 C_2 + R_1 C_2$	$R_1 = \dfrac{T_1 T_3}{B T_2}$ $R_2 = \dfrac{T_1 T_2 T_3}{B(T_3 - T_1)(T_3 - T_2)}$ $C_1 = B$ $C_2 = \dfrac{B(T_3 - T_1)(T_3 - T_2)}{T_1 T_3}$

441

TABLE A1.1. TABLE OF TRANSFER IMPEDANCES* (Continued)

Transfer impedance	Network	Relations	Inverse relations
$A\dfrac{1 + sT_3}{1 + sT_1 + s^2 T_1 T_2}\dbinom{\text{complex}}{\text{roots}}$ $T_2 > \dfrac{T_1}{4}$ $T_3 > T_2$		$A = \dfrac{2R_1 R_2}{2R_1 + R_2}$ $T_1 = \dfrac{R_1(R_1 C_1 + 2R_2 C_2)}{2R_1 + R_2}$ $T_2 = \dfrac{R_1 R_2 C_1 C_2}{R_1 C_1 + 2R_2 C_2}$ $T_3 = \dfrac{R_1 C_1}{2}$	$R_1 = \dfrac{AT_3{}^2}{2[T_3{}^2 - T_1(T_3 - T_2)]}$ $R_2 = \dfrac{AT_3{}^2}{T_1(T_3 - T_2)}$ $C_1 = \dfrac{4[T_3{}^2 - T_1(T_3 - T_2)]}{AT_3}$ $C_2 = \dfrac{T_1 T_2}{AT_3}$
		$A = 2R_1$ $T_1 = R_2 C_1 + 2R_1 C_2$ $T_2 = \dfrac{R_1(R_1 + 2R_2)C_1 C_2}{R_2 C_1 + 2R_1 C_2}$ $T_3 = \left(R_2 + \dfrac{R_1}{2}\right) C_1$	$R_1 = \dfrac{A}{2}$ $R_2 = \dfrac{AT_1(T_3 - T_2)}{4[T_3{}^2 - T_1(T_3 - T_2)]}$ $C_1 = \dfrac{4[T_3{}^2 - T_1(T_3 - T_2)]}{AT_3}$ $C_2 = \dfrac{T_1 T_2}{AT_3}$
		$A = 2R$ $T_1 = R(C_2 + 2C_3)$ $T_2 = \dfrac{RC_3(C_1 + C_2)}{C_2 + 2C_3}$ $T_3 = \dfrac{R}{2}(C_1 + C_2)$	$R = \dfrac{A}{2}$ $C_1 = \dfrac{2[2T_3{}^2 - T_1(T_3 - T_2)]}{AT_3}$ $C_2 = \dfrac{2T_1(T_3 - T_2)}{AT_3}$ $C_3 = \dfrac{T_1 T_2}{AT_3}$

$$A\, \frac{1 + sT_3}{1 + sT_1 + s^2T_1T_2} \quad \begin{pmatrix} \text{complex} \\ \text{roots} \end{pmatrix}$$

$$T_2 > \frac{T_1}{4}$$
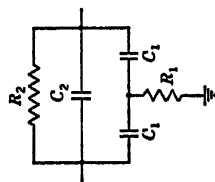
$$T_3 < T_1$$

$A = R_2$

$T_1 = 2R_1C_1 + R_2C_2$

$T_2 = \dfrac{R_1R_2C_1(C_1 + 2C_2)}{2R_1C_1 + R_2C_2}$

$T_3 = 2R_1C_1$

$R_1 = \dfrac{AT_3^2}{4[T_1T_2 - T_3(T_1 - T_3)]}$

$R_2 = A$

$C_1 = \dfrac{2[T_1T_2 - T_3(T_1 - T_3)]}{AT_3}$

$C_2 = \dfrac{T_1 - T_3}{A}$
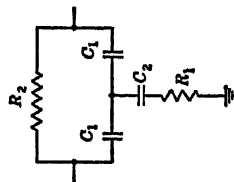
$A = R_2$

$T_1 = \dfrac{C_1(2R_1C_2 + R_2C_1)}{2C_1 + C_2}$

$T_2 = \dfrac{R_1C_2R_1C_2}{2R_1C_2 + R_2C_1}$

$T_3 = \dfrac{2R_1C_1C_2}{2C_1 + C_2}$
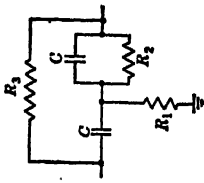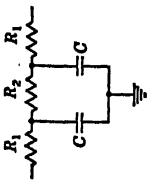
$R_1 = \dfrac{AT_3^2}{4[T_1T_2 - T_3(T_1 - T_3)]}$

$R_2 = A$

$C_1 = \dfrac{2T_1T_2}{AT_3}$

$C_2 = \dfrac{4T_1T_2[T_1T_2 - T_3(T_1 - T_3)]}{AT_3^2(T_1 - T_3)}$

Transfer impedance	Network	Relations	Inverse relations
$A \dfrac{1 + sT_3}{1 + sT_1 + s^2 T_1 T_2}$ $T_2 > \dfrac{T_1}{4} \left(\text{complex} \atop \text{roots} \right)$ $T_3 < T_1$		$A = R_3$ $T_1 = \dfrac{R_1(2R_3 + R_2)C}{R_1 + R_2}$ $T_2 = \dfrac{R_2 R_3 C}{R_1 + R_2}$ $T_3 = \dfrac{2R_1 R_2 C}{R_1 + R_2}$	$R_1 = \dfrac{AT_3^2}{2[2T_1 T_2 - T_3(T_1 - T_2)]}$ $R_2 = \dfrac{AT_3}{2(T_1 - T_2)}$ $R_3 = A$ $C = \dfrac{2T_1 T_2}{AT_3}$
$A(1 + sT_1)(1 + sT_2)$ $T_1 < T_2$		$A = 2R_1 + R_2$ $T_1 = \dfrac{R_1 R_2}{2R_1 + R_2}C$ $T_2 = R_1 C$	$R_1 = \dfrac{A\, T_2 - T_1}{2T_2}$ $R_2 = \dfrac{A\, T_1}{T_2}$ $C = \dfrac{2T_2^2}{A(T_2 - T_1)}$

*F. R. Bradley and R. McCoy, Driftless D-C Amplifier, *Electronics*, **25**:144–148 (April, 1952).

444.

TABLE A1.2. VOLTAGE TRANSFER FUNCTIONS FOR VARIOUS COMBINATIONS OF RESISTORS AND CAPACITORS OF:*
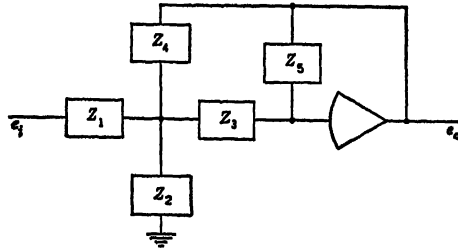
Capacitors	Resistors	Voltage transfer function: $-e_o/e_i$
Z_1, Z_2	Z_3, Z_4, Z_5	$\dfrac{sC_1R_4R_5}{sR_3R_4(C_1+C_2)+(R_3+R_4+R_5)}$
Z_1, Z_3	Z_2, Z_4, Z_5	$\dfrac{s^2C_1C_3R_2R_4R_5}{s[R_2R_4(C_1+C_3)+R_2R_5C_3]+(R_2+R_4)}$
Z_1, Z_4	Z_2, Z_3, Z_5	$\dfrac{sC_1R_2R_5}{s[R_2R_3(C_1+C_4)+R_2R_5C_4]+(R_2+R_3)}$
Z_1, Z_5	Z_2, Z_3, Z_4	$\dfrac{sC_1R_4}{s^2R_3R_4C_1C_5+sC_5(R_3+R_4+R_3R_4/R_2)+1}$
Z_2, Z_3	Z_1, Z_4, Z_5	$\dfrac{sC_3R_4R_5}{s[R_1R_4(C_2+C_3)+R_1R_5C_3]+(R_1+R_4)}$
Z_2, Z_4	Z_1, Z_3, Z_5	$\dfrac{R_5}{s[R_1R_3(C_2+C_4)+R_1R_5C_4]+(R_1+R_3)}$
Z_2, Z_5	Z_1, Z_3, Z_4	$\dfrac{R_4}{s^2R_1R_3R_4C_2C_5+sC_5(R_3R_4+R_1R_3+R_1R_4)+R_1}$
Z_3, Z_4	Z_1, Z_2, Z_5	$\dfrac{sC_3R_2R_5}{s^2R_1R_2R_5C_3C_4+sR_1R_2(C_3+C_4)+(R_1+R_2)}$
Z_3, Z_5	Z_1, Z_2, Z_4	$\dfrac{C_3R_2R_4}{sC_3C_5R_1R_2R_4+[R_1R_2(C_3+C_5)+R_1R_4C_5+R_2R_4C_5]}$
Z_4, Z_5	Z_1, Z_2, Z_3	$\dfrac{R_2}{s^2R_1R_2R_3C_4C_5+s[C_5(R_1R_2+R_1R_3+R_2R_3)+C_4R_1R_2]}$
Z_1, Z_2, Z_3	Z_4, Z_5	$\dfrac{s^2C_1C_3R_4R_5}{s[R_4(C_1+C_2+C_3)+R_5C_3]+1}$
Z_1, Z_2, Z_4	Z_3, Z_5	$\dfrac{sC_1R_5}{s[R_3(C_1+C_2+C_4)+R_5C_4]+1}$
Z_1, Z_2, Z_5	Z_3, Z_4	$\dfrac{sC_1R_4}{s^2R_3R_4C_5(C_1+C_2)+sC_5(R_3+R_4)+1}$
Z_1, Z_3, Z_4	Z_2, Z_5	$\dfrac{s^2C_1C_3R_2R_5}{s^2R_2R_5C_3C_4+sR_3(C_1+C_3+C_4)+1}$
Z_1, Z_3, Z_5	Z_2, Z_4	$\dfrac{sC_1C_3R_2R_4}{sR_2R_4(C_1C_5+C_3C_5)+R_2(C_3+C_5)+R_4C_5}$

TABLE A1.2. VOLTAGE TRANSFER FUNCTIONS FOR VARIOUS COMBINATIONS OF RESISTORS AND CAPACITORS* (*Continued*)

Capacitors	Resistors	Voltage transfer function: $-e_o/e_i$
Z_1, Z_4, Z_5	Z_2, Z_3	$\dfrac{R_2 C_1}{s R_2 R_3 C_5 (C_1 + C_4) + R_2 (C_4 + C_5) + R_3 C_5}$
Z_2, Z_3, Z_4	Z_1, Z_5	$\dfrac{s C_3 R_5}{s^2 R_1 R_5 C_3 C_4 + s R_1 (C_2 + C_3 + C_4) + 1}$
Z_2, Z_3, Z_5	Z_1, Z_4	$\dfrac{R_4 C_3}{s R_1 R_4 C_5 (C_2 + C_3) + R_1 (C_3 + C_5) + R_4 C_5}$
Z_2, Z_4, Z_5	Z_1, Z_3	$\dfrac{1}{s^2 R_1 R_3 C_5 (C_2 + C_4) + s[R_1(C_4 + C_5) + R_3 C_5]}$
Z_3, Z_4, Z_5	Z_1, Z_2	$\dfrac{R_2 C_3}{s R_1 R_2 (C_3 C_4 + C_2 C_5 + C_4 C_5) + C_5 (R_1 + R_2)}$

* A. Bridgman and R. Brennan, "Simulation of Transfer Functions Using Only One Amplifier," 1957 WESCON Convention Record, part 4, pp. 273–278, San Francisco, August, 1957.

Appendix 2
PROBLEMS

CHAPTER 2

1. Calculate the ratio of the output to the input voltage in the circuit shown below for $R = 0.33K$, $R = 0.50K$, and $R = 0.66K$. Determine for each case the actual voltage error and the percentage error.
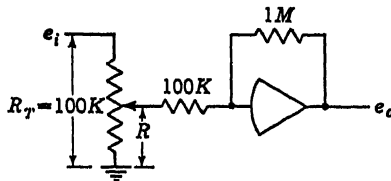
Fig. P.1

2. Three potentiometers of equal resistances are cascaded in a computer. All are grounded at one end, and all sliders are set at mid-position. What is the error in the voltage at the last slider as compared with the voltage to be inferred from the geometrical settings (i.e., error due to loading)? Consider the last slider to feed into an infinite load resistance. What is the voltage error if the first potentiometer is set at 0.6 of full scale and the second potentiometer is set at 0.4 of full scale?

3. A 100-kilohm potentiometer is loaded by a 500-kilohm resistor. The potentiometer has a center-tap to permit loading-error compensation. What should be the magnitude of the compensation resistor for maximum effectiveness, and how should it be connected? What is the maximum voltage error and percentage error of the compensated potentiometer? At what positions of the slider do these maxima occur?

4. If two taps, located at $R/R_T = 0.33$ and $R/R_T = 0.66$, respectively, are available on the potentiometer described in Prob. 3, what compensating resistors should be added to the circuit to minimize loading errors? What would be the maximum voltage and percentage errors in this case?

5. Using a minimum number of operational amplifiers design suitable circuits for performing the following operations:

a. $e_o = -(0.1e_1 + 2e_2 + 1.5e_3)$ *b.* $e_o = -\int_0^t (10e_1 + 3e_2 + 2e_3 + e_4)\, dt$

c. $e_o = e_1 + e_2 + 3e_3$ *d.* $e_o = e_1 - 2e_2 - 3e_3 + 0.5e_4$

e. $e_o = e_1 - 2\int_0^t e_2\, dt - 6e_3 + 0.5\int_0^t e_4\, dt$

f. $e_1 = 2e_1 + 3\int_0^t (e_2 - 3e_3)\, dt - \int_0^t (e_1 + e_3)\, dt$

447

6. Using the transfer functions listed in Table A1.1, design electronic circuits for the generation of the following functions. All capacitators should fall within the range from 0.5 to 10 μf, and all resistors should fall within the range of 20 kilohms to 5 megohms.

a. $e_o = -\dfrac{4s^2 + 5s + 4}{s^2 + 4s + 3}$

b. $e_o = \dfrac{s^2 + s + 2}{5s^2 + 3s + 4}$

c. $e_o = -\dfrac{s^3 + s^2 + s}{s^4 + s^3 + 5s^2 + s + 4}$

d. $e_o = \dfrac{(6s^2 + 1)(s + 3)}{(12s^2 + 5)(s + 1)}$

e. $e_o = -\dfrac{s^3 + 6s^2 + 3s + 2}{s^2 + s + 1}$

f. $e_o = \dfrac{(s^2 + s + 1)(s^2 + s + 4)}{(s^2 + s + 2)(s^2 + s + 3)}$

7. What is the transfer function e_o/e_i of each of the following circuits (resistors in megohms, capacitators in microfarads)?
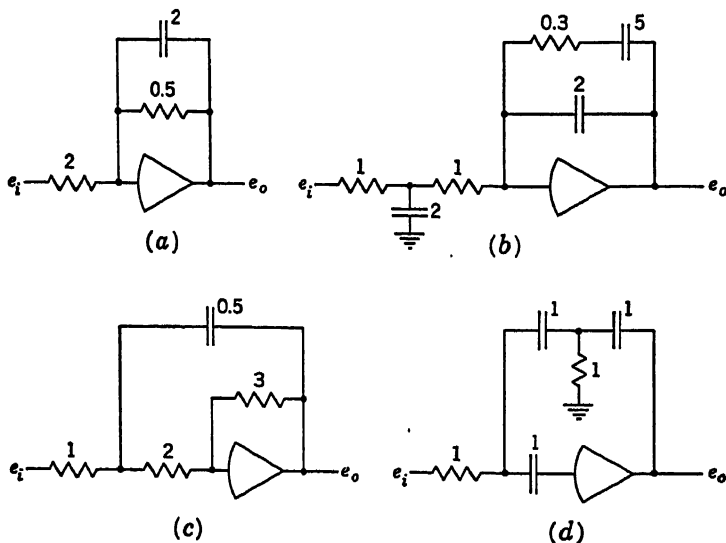
Fig. P.7

8. What are the transfer functions of the following circuits? Why are such circuits never used in general-purpose analog computation?
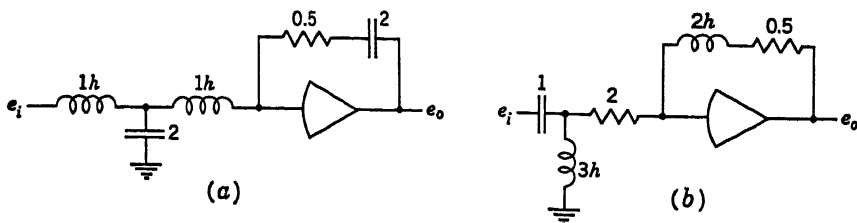
Fig. P.8

9. Using the transfer impedances in Appendix 1, design operational circuits having the same transfer functions as each of the circuits of Prob. 8.

10. Find e_o/e_i of the circuit shown. For what value of K does the circuit act as a differentiator?
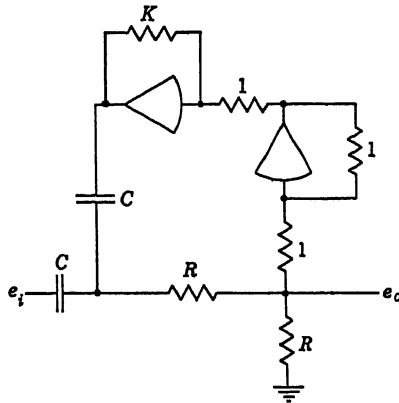
Fig. P.10

11. Draw the circuit diagram for each of the expressions in Prob. 5 using the alternative notation described in Sec. 2.15.

12. Find e_o/e_i for the circuit shown.
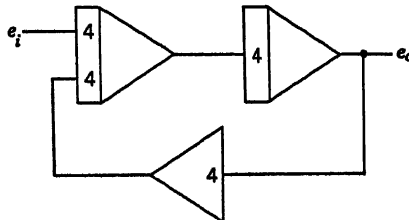
Fig. P.12

CHAPTER 3

13. With reference to the circuit of Fig. 3.1, assume that the input resistors of the operational amplifier are each 1 megohm and that potentiometer II is loaded by a resistance of 500 kilohms. Assume that both potentiometers I and II have resistances of 100 kilohms and that both e_1 and e_2 vary from 0 to $+100$ volts. What is the maximum possible voltage error due to potentiometer loading?

14. With reference to the circuit of Fig. 3.1, assume that all conditions are the same as those specified in Prob. 13 except that the load resistor on potentiometer II is increased to 1 megohm. What is the maximum angular position error (the extent to which X differs from e_1/E)?

15. It is desired to mechanize the following equation using a multiplier for producing both the product and the quotient. The range of the variable z is known to be from -50 to $+50$. The variable y is known to vary from -10 to -100 volts.

$$zy + \frac{z}{y} = 0$$

16. It is desired to approximate a square-law curve (parabola) using the method described in Sec. 3.3. Four diodes and four bias batteries are available. Specify the magnitudes of the bias voltages and the associated resistors in order that the desired curve be approximated with a minimum voltage error.

17. Prepare a table listing the various methods for function multiplication discussed in Chap. 3, including columns listing the basic operating principle of each method, their relative advantages and disadvantages, and any special equipment which is required.

18. The circuit shown in Fig. 3.19 acts as a dividing circuit if the amplifier is perfect. What is the relationship between the output voltage e_o and the input voltages e_1 and e_2 if the amplifier contains appreciable shunt capacitance, so that a small capacitor C may be considered to be placed from the output to the summing point (grid of first amplifier stage) of the amplifier?

19. With reference to the circuit of Fig. 3.12a, find the magnitudes of G_0, G_1, G_2, G_3, and G_4, as well as the magnitudes of the bias voltages E_1, E_2, E_3, E_4 in order that the logarithmic curve shown in Fig. 3.12b is generated.

CHAPTER 4

20. Plot e_o versus e_i for each of the circuits shown.
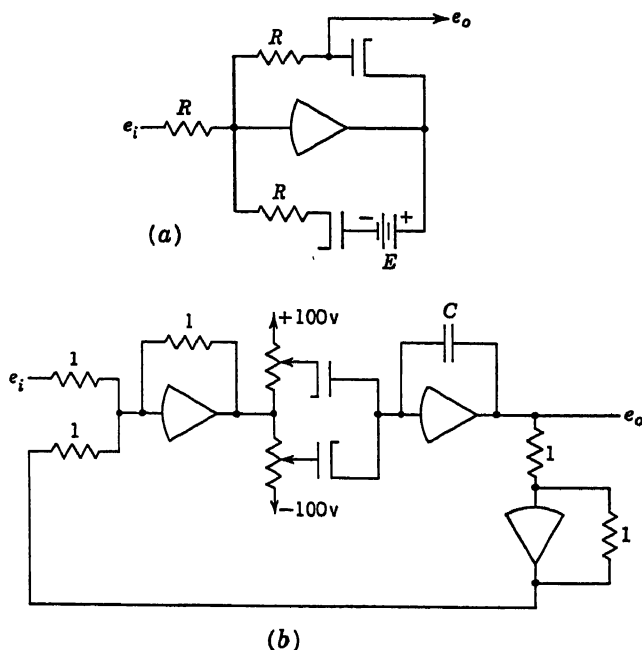
Fig. P.20

21. Discuss the performance of the circuit shown, where e_1 and e_2 are positive voltages.
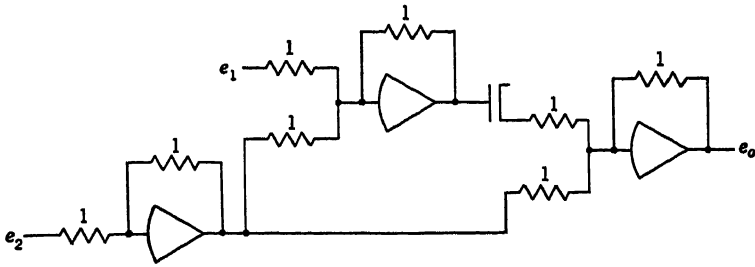
Fig. P.21

22. Design circuits having the transfer functions shown.

(a)   (b)
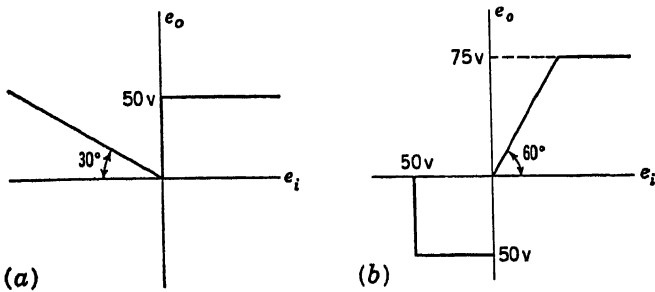
Fig. P.22

23. Sketch the approximate wave shape of the voltages at points A, B, C, D, and E in the circuit shown.
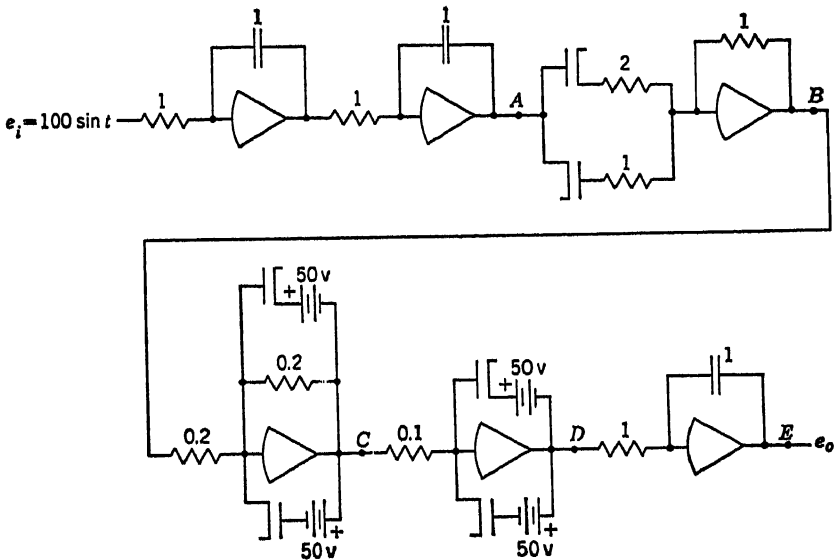
Fig. P.23

24. Sketch e_o versus e_i in the accompanying circuit for:

a. $R_A = R_B = 0.1R_f$
    $R_1 = 0$
    $R_C = R_D = 0.2R_f$

b. $R_1 = 10R_C = 10R_D$
    $R_A = R_B = 0$
    $R_f = \infty$
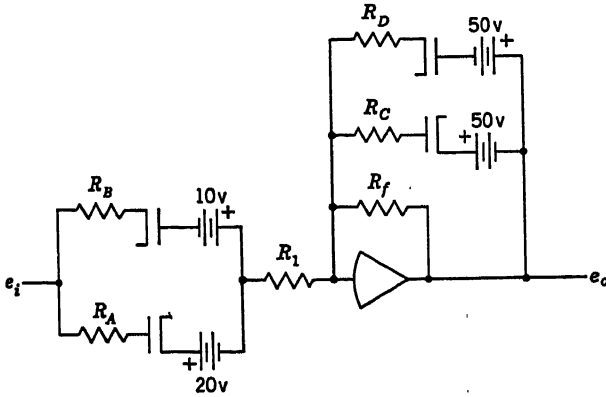
Fig. P.24

25. A function generator is to be used to linearize the output of a temperature-measuring device in order to enable it to operate a linear controller, as shown in the figure. Assume that the transducer output is a d-c voltage in range from 0 to $+100$ volts and that the desired relationship is $y' = 16x$.

a. Show in block-diagram form the relation of the system, measuring device, and function generator.
b. Design a function generator to obtain the desired linear output. Assume the transducer characteristic to be a cubic, $y = x^3$.
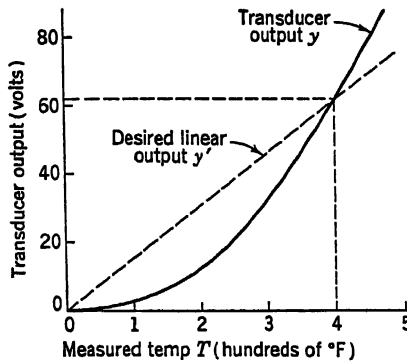
Fig. P.25

26. Design servo function generators capable of generating the following functions:

    a. $z = \dfrac{2x^3}{y^2}$ $-100 < x < 0$ $10 < y < 100$

    b. $z = \dfrac{2x^2}{y^3}$ $-100 < x < +100$ $-100 < y < -10$

27. Design a computer circuit capable of generating the following functions:

    a. $y = e^t \cos\left(5t - \dfrac{\pi}{2}\right)$; use no multipliers.

    b. $y = e^{-x}$ where $x = 3t^2 - 10t$; use only amplifiers and one multiplier.

28. Using the functional relationships in Table 4.2, design servo-multiplier circuits for generating the following functions:

    a. $y = \tan x$
    b. $y = e^x$
    c. $y = \sin h^{-1} x$

29. The function $f(\tau) = \dfrac{1}{T} \displaystyle\int_0^T F(t)F(t - \tau)\, d\tau$ is known as the autocorrelation function of $F(t)$ and is of considerable importance in the study systems affected by noise.

    a. Assuming τ to be held fixed, show a computer schematic for obtaining $f(\tau)$. Assume T to be a large constant.
    b. Discuss reasons for using the nonlinear components involved in your circuit and their limitations in handling this problem (*e.g.*, why use one type of multiplier instead of another, etc.).
    c. Suggest a possible way of generating $f(\tau)$ as a continuous function of τ.

CHAPTER 5

30. Devise circuits containing mechanical computing elements to perform each of the operations specified in Prob. 5.

31. Compare the capabilities and limitations of the mechanical computing elements discussed in Chap. 5 with those of the electronic computing elements discussed in Chaps. 2 and 3 for the performance of each of the following operations:

    a. Combined addition and integration.
    b. Multiplication of two dependent variables.
    c. Generation of time function expressed as the ratio of two polynomials in s.
    d. Differentiation of a dependent variable with respect to time.

CHAPTER 6

32. Determine the values of the resistors R_1, R_2, R_3, R_4, and R_5 of the circuit shown in order to solve the equation

$$\frac{d^2x}{dt^2} + 2.5\frac{dx}{dt} + 10x = 0$$

at $t = 0$ $x = 100$ $\dfrac{dx}{dt} = 0$

Both feedback capacitors are 1 µf in magnitude.
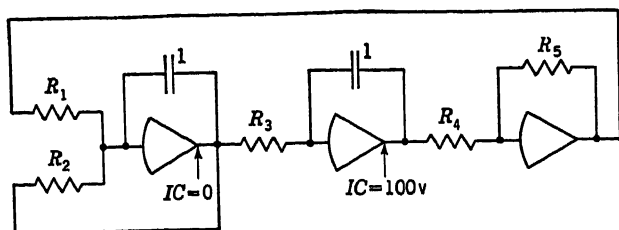
Fig. P.32

33. Draw the circuit diagram for the electronic differential analyzer solution of the following differential equation. Your diagram should include element values for all resistors and capacitors. Label the output of each amplifier to indicate what quantity is simulated by the voltage at that point, and show all initial condition settings.

$$2\frac{d^4x}{dt^4} + 3\frac{d^2x}{dt^2} - 2\frac{dx}{dt} - 2x = 0$$

at $t = 0$
$$\frac{d^4x}{dt^4} = 0 \qquad \frac{dx}{dt} = 0$$
$$\frac{d^3x}{dt^3} = 6 \qquad x = 3$$
$$\frac{d^2x}{dt^2} = 0$$

34. Given the computer diagram shown, determine the machine equation being solved.
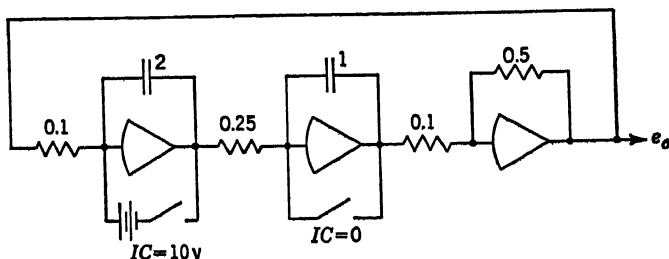
Fig. P.34

35. Given the equation

$$\frac{dx}{dt} + 2x = 2\frac{dy}{dt} + y$$

at $t = 0$
$$x = 0 \qquad y = 0$$
$$\frac{dx}{dt} = 0 \qquad \frac{dy}{dt} = 0$$

draw a circuit diagram for the electronic differential analyzer solution. Assume that $y = y(t)$ is an available function.

36. For each of the following equations make the necessary substitution of variable to

a. Speed up the solution by a factor 4.
b. Slow down the solution by a factor 6.

$$2\frac{d^3y}{dt^2} + \frac{d^2y}{dt^2} + 3\frac{dy}{dt} + \frac{1}{5}y = 0$$

$$\frac{d^4y}{dt^4} + t\frac{dy}{dt} + 3y = \cos 3t$$

37. Given the equation

$$\frac{d^2y}{dt^2} + 0.005\frac{dy}{dt} + 25y = 0$$

approximately what is the natural frequency of the system? Make a suitable change of variable to make the natural frequency approximately equal to $\frac{1}{2}$ cps.

38. Legendre's equation

$$(1 - t^2)\frac{d^2y}{dt^2} - 2t\frac{dy}{dt} + n(n+1)y = 0$$

where n is a constant, is to be solved on an electronic analog computer with a change of time scale such that $t = 10\tau$, where τ is computer time. What is the equation to be instrumented on the computer?

39. For each of the following equations, determine the approximate maximum magnitudes of the dependent variable and its derivatives. Draw a computer schematic including appropriate scale factors for an electronic differential analyzer whose amplifiers have a range -100 to $+100$ volts. No change in time scale is required.

a. $3\dfrac{d^2y}{dt^2} + \dfrac{dy}{dt} + 9y = 0$

At $t = 0$ $\qquad\qquad y = 0 \qquad \dfrac{dy}{dt} = 10$

b. $10\dfrac{d^2y}{dt^2} + 0.1\dfrac{dy}{dt} + 0.5y = 0$

At $t = 0$ $\qquad\qquad y = 5 \qquad \dfrac{dy}{dt} = 0$

40. The curve shown was generated by an electronic differential analyzer as the solution of a damped vibrating system governed by a linear second-order differential equation. The machine variable was $X = 5x$, where x is the problem variable. The machine time variable was $\tau = 10t$, where t is problem time. Determine the solution of the problem; i.e., find $x(t)$. What are the coefficients of the equation governing the system? Assume that at time $t = 0$, the velocity $dx/dt = 0$.
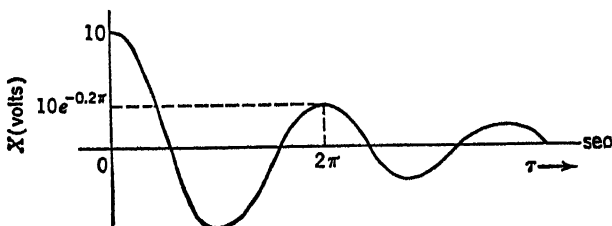
Fig. P.40

41. Draw the computer schematic for the solution of the following sets of simultaneous equations. All initial conditions are zero.

$a.$ $\dfrac{d^2x}{dt^2} - \dfrac{dy}{dt} - \dfrac{z}{2} = f(t)$ $\qquad$ $b.$ $\dfrac{d^3x}{dt^3} + x + 3\dfrac{dy}{dt} = 0$

$\dfrac{1}{3}\dfrac{d^2y}{dt^2} - \dfrac{dz}{dt} - x = 0$ $\qquad\qquad$ $\dfrac{d^2y}{dt^2} + 2y + z = 0$

$\dfrac{d^2z}{dt^2} - \dfrac{dx}{dt} - y = 0$ $\qquad\qquad$ $\dfrac{dz}{dt} + \dfrac{1}{2}z = f(t)$

42. Attempts to set up an electrical analog to simulate the set of differential equations

$$-A\frac{d^2x}{dt^2} + B\frac{dy}{dt} = 0$$

$$A\frac{d^2y}{dt^2} + B\frac{dx}{dt} = 0$$

were not successful. However, it was observed d^2y/dt^2 could be eliminated from the second equation by differentiating the first equation with respect to time and by subtracting it from the second equation. There results an equation for a system with a single degree of freedom. Set up a circuit for the resulting equation.

43. For the block diagram shown

$a.$ Draw the electronic analog computer circuit with positive output, using a minimum number of operational amplifiers.

$b.$ Express the parameters K_1, K_2, T_1, T_2, T_3, T_4, and T_5 in terms of the circuit constants (resistance and capacitor magnitudes).

$c.$ Specify practical values for all resistors and capacitors. (Resistors range from 10 K to 10 megohms; capacitors range from 0.1 to 10.0μf.)
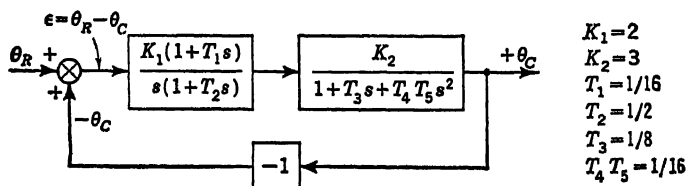
Fig. P.43

44. The block diagram illustrates a servomechanism having position feedback and velocity feedback. Prepare an electronic analog-computer circuit diagram using a minimum number of operational amplifiers.
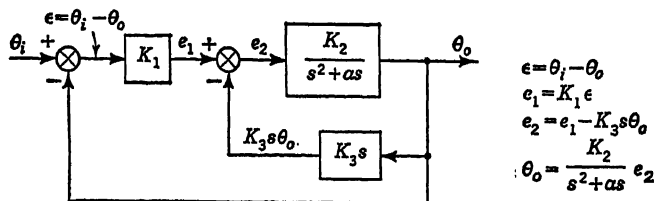
Fig. P.44

45. From the circuit diagram shown, determine the nonlinear differential equation being solved.
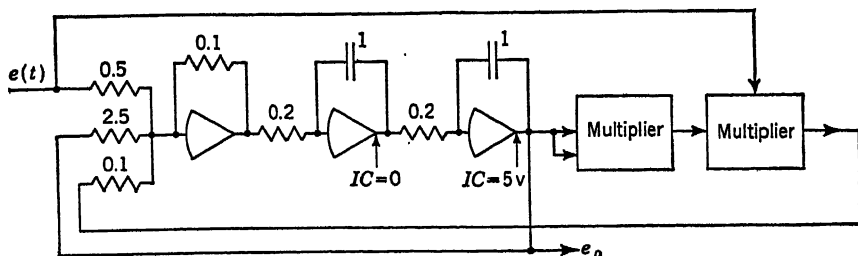
Fig. P.45

46. The block diagram of a control system with backlash is shown. Draw an electronic analog-computer diagram that will simulate this system.
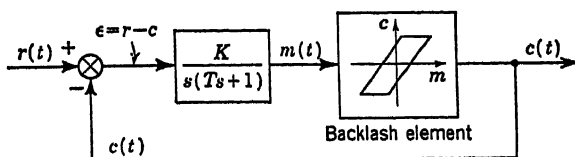
Fig. P.46

47. Set up a circuit for the solution of the following equation on the electronic analog computer. Use only multipliers and amplifiers.

$$\frac{d^2x}{dt^2} - 50 \sin \frac{dx}{dt} + x = 0$$

at $t = 0$ $$x = 10 \qquad \frac{dx}{dt} = 0$$

48. Consider the following spring-mass-dashpot system where the spring characteristic and the dash characteristic are both nonlinear as shown. The system equa-
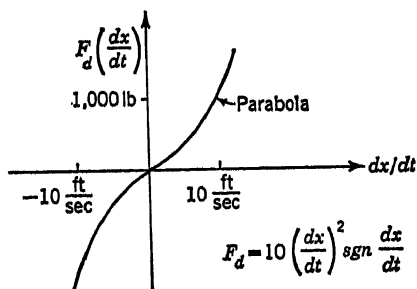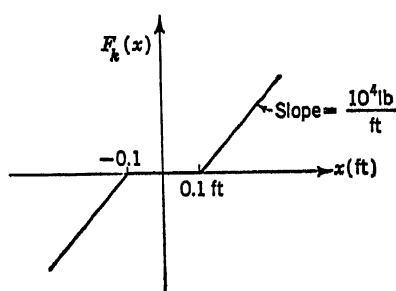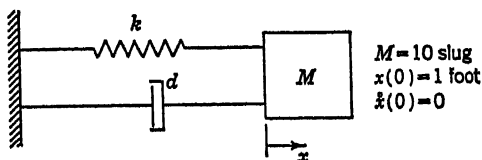
Fig. P.48

tion is

$$M \frac{d^2x}{dt^2} + F_d \frac{dx}{dt} + F_k x = 0$$

The natural frequency of the system will decrease as the oscillation damps out, since the effective spring constant will decrease with decreasing amplitude. The damping will likewise decrease with the amplitude due to the nonlinear dashpot characteristic. At the start, the natural frequency will be nearly

$$\omega_0 = \left(\frac{9,000}{M}\right)^{\frac{1}{2}} = 9.5 \text{ rad/sec}$$

so that a time scale change to slow down the solution by a factor of 10 is recommended. Perform this time scale change, and design an electronic analog-computer circuit using a servo multiplier to solve the governing equation.

49. A circuit for the solution of Mathieu's equation

$$\frac{d^2y}{dt^2} + \frac{\omega^2}{\beta^2}\left(a - 2q \cos 2\frac{\omega t}{\beta}\right)y = 0$$

where a and q are constant, is presented in Appendix 3 (Experiment 6). Suppose that the given information includes values for y at $t = 0$ and $t = 60$ sec. Describe how you would use the circuit under these conditions.

50. Draw a computer schematic for representation of the servo system shown. Note that one of the blocks includes a transport lag.
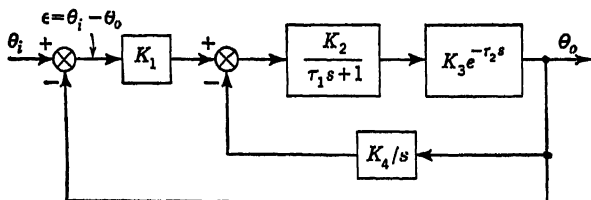
Fig. P.50

51. A first-order system characterized by the transfer function

$$\frac{e_o}{e_i} = \frac{1}{1 + \tau s}$$

has an initial, but unknown, output voltage $e_o(0)$ at time $t = 0$, when it is subjected to a step input voltage $e_i = 100$ volts. As a result of its initial condition and of the step input voltage, the output voltage at time $t = T$ is measured to be some value $e_o(T)$. It is desired to determine the voltage $e_o(0)$ with an analog computer by running the problem *backward*, starting with the known conditions at time T. Draw the computer schematic showing initial conditions, input voltage, and pot settings.

52. Draw a *mechanical* differential analyzer diagram for the solution of the equation

$$\frac{d^2y}{dx^2} + \sin\left(\frac{dy}{dx}\right) + \frac{1}{y} = 0$$

Use no more than six integrators.

53. Prepare a *mechanical* differential analyzer diagram for the solution of the equation

$$\left(\frac{d^2y}{dx^2}\right)^{\frac{1}{2}}\left[1 + \left(\frac{d^2y}{dx^2}\right)\right] + y \log_e x = C$$

Avoid input tables if possible, and use one output table to give y versus x.

CHAPTER 7

54. The pair of equations

$$4x_1 + 5x_2 = 20$$
$$3x_1 + 9x_2 = 4.5$$

are to be solved on a potentiometric unit by manual iteration.

    a. What settings should be made on the potentiometers?
    b. Would there be any difficulties in obtaining convergence during the first trials? If so, what would be the difficulties and how could they be corrected?

55. Consider the system of equations

$$5x + 5y + 2z = 28$$
$$15x - 2y + 2z = 19$$
$$5x + 4y - 5z = 31$$

    a. Reduce the system to proper form for analog-computer solution.
    b. Draw the electronic amplifier diagram and insert numerical values for all circuit constants.

56. The equation

$$(A + iB)x + (C + iD)y = G$$

where $i = (-1)^{\frac{1}{2}}$, is to be solved on an electric analog computer. Show how this can be done, making use of passive elements only.

57. Given the simultaneous homogeneous set of equations

$$(m_1\lambda^2 + n)x_1 - px_2 = 0$$
$$-px_1 + (m_2\lambda^2 + g\lambda n)x_2 = 0$$

where λ is complex, show how these could be solved by electric analog methods.

CHAPTER 8

58. Given the equation

$$(a + ib)x^3 + (c + id)x^2 + (e + if)x + (g + ih) = 0$$

where $i = (-1)^{\frac{1}{2}}$, show how this equation might be solved on an analog computer.

59. Sketch an electronic analog-computer circuit that will yield the simultaneous solutions of the polynomials $f(x)$ and $g(x)$ where

$$x^3 - 3x^2 + 10x - 10 = f(x)$$
$$3x^3 + 7x^2 - x + 15 = g(x)$$

60. Devise an electronic analog circuit that will determine the real roots of the polynomial

$$x^4 - 3x^3 + 7x^2 - 12x + 10 = 0$$

by first factoring the polynomial in the following manner:

$$x\{x[x(x - 3) + 7] - 12\} + 10 = 0$$

The circuit for one solution of the problem has three multipliers, one integrator, and three adders. Neglect scale factors and multiplier constants.

61. The polynomial

$$z^2 + 2z + 10 = f(z)$$

can be solved for complex roots by assuming a solution of the form $z = x + iy = A(\cos\theta + i\sin\theta)$. The sine and cosine terms can be obtained from a sine wave generator.

Develop an electronic analog-computer circuit that will generate $R(A,\theta)$ and $I(A,\theta)$ where

$$f(z) = R(A,\theta) + iI(A,\theta)$$

and where R is the real part and I is the imaginary part. (Multipliers will have to be used.) The function $f(A,\theta)$ could be displayed on a scope; if this were done, how would one determine the roots of the polynomial from the scope pattern?

CHAPTER 9

62. For each of the mechanical circuits shown, draw an electric analog circuit based on the mass-capacitance analogy and another circuit based on the mass-inductance analogy.

(a) (b)

(c)

(d)

(e)
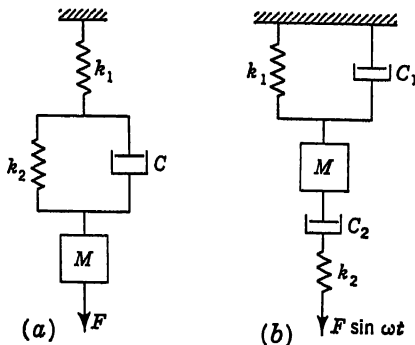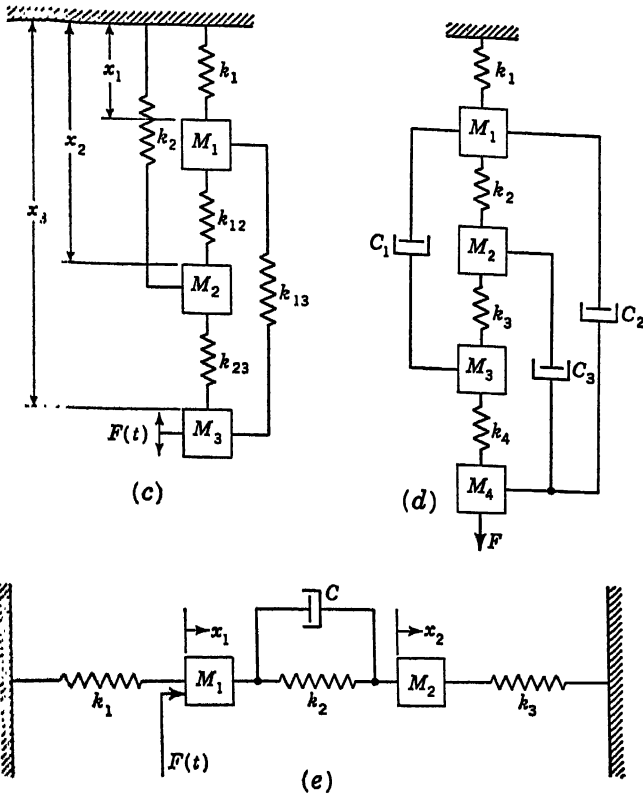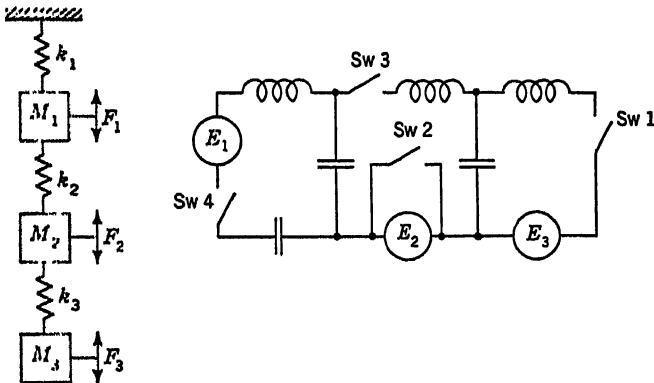
Fig. P.62

Fig. P.63

63. The electric circuit shown is the mass-inductance analog of the mechanical system. What would be analogous in the mechanical system to:

> *a.* Opening only switch 3 of the electrical system (switch 2 remains open; switches 1 and 4 remain closed)?

b. Opening only switch 1 (switch 2 remains open; switches 3 and 4 remain closed)?

c. Closing switch 2 (switches 3, 4, and 1 remain closed)?

d. Opening only switch 4 (switch 2 remains open; switches 1 and 3 remain closed)?

64. A mass-capacitance analog of the spring mass system shown is required. Measurements: the mass is 1 slug, the spring constant is $K = 100$ lb/ft, and the damping coefficient has a value $B = 1$ lb-sec/ft. Assume a current source $i(t) = I_0 \sin \omega_e t$ with $I_0 = 5$ amp, assume that the mass is analogous to a 1-μf capacitor, and further assume that electrical time is 1,000 times faster than mechanical time, that is, $t_e = 0.001 t_m$. Draw the electrical analog (mass capacitance). What is the value of the inductance and of the resistance? How would a displacement of the mass of 1 ft be represented in the analog?
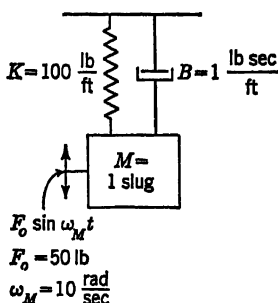
Fig. P.64
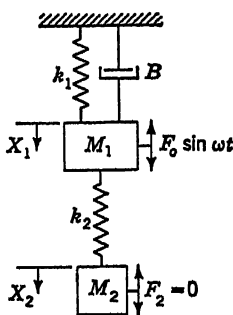
Fig. P.65

65. The following numerical values are given for the vibration absorber system shown in the figure:

$$gM_1 = 38.6 \text{ lb} \qquad K_1 = 20 \text{ lb/in.}$$
$$gM_2 = 1.93 \text{ lb} \qquad K_2 = 5 \text{ lb/in.}$$
$$B = 0.25 \text{ lb-sec/in.} \qquad \omega_m = 25 \text{ rad/sec}$$
$$F_0 = 50 \text{ lb}$$

Determine the numerical values for the electrical elements of a mass-inductance analog for the given system.

Assume that M_1 is represented by a 1-henry coil and the voltage available is $E = 100 \sin pt$, where $p = 1,000$ rad/sec. Indicate how you would measure X_1 and X_2 on the analog.

66. The mass M_1 is suspended from a movable support by the spring with constant K_1, as shown. Attached to M_1 is a vibration damper consisting of a dashpot, spring, and mass. The plunger which carries the piston is rigidly attached to M_1. The chamber of M_2 is attached to and supported by the spring K_2. The lower end of K_2 is attached to the piston. The friction at B is viscous. The motion is translational. Assume that the movable support is given an up-and-down sinusoidal motion by $f(t)$.

a. Write the differential equation of the system (mechanical).

b. Sketch the analogous electrical network for the mass-capacitance analogy.

c. Sketch the electrical network for the mass-inductance analogy.
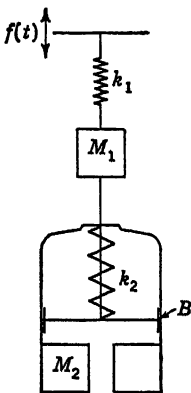
Fig. P.66
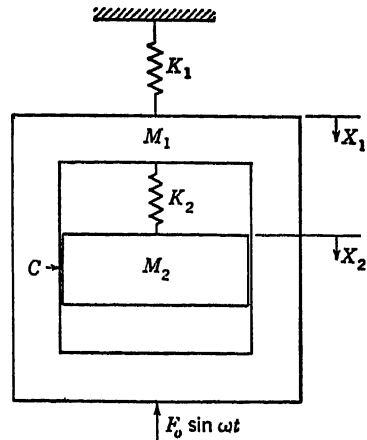
Fig. P.67

67. The following numerical values are given for the system shown in the figure:

$K_1 = 1,000$ lb/in. $F_0 = 10$ lb

$K_2 = 100$ lb/in. $W = 20$ rad/sec

$W_1 = 100$ lb $C = 5$ lb-sec/in.

$W_2 = 10$ lb

Determine the numerical values of the electrical elements to be used in the mass-inductance analog of the given system. Assume that a 60-cycle voltage source is available, also a 1-henry coil and a 0.1-henry coil. Sketch the mechanical network and the electrical network based on a mass-inductance analogy. Indicate what measurements you would make on the electrical circuit to determine the displacements X_1 and X_2.

68. Construct the mass-capacitance analog and the mass-inductance analog for the undamped mechanical systems shown in the figure.
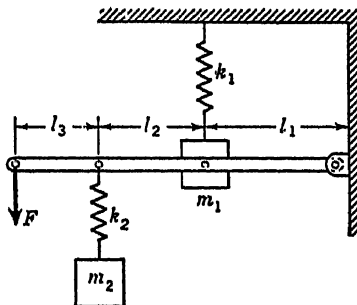
Fig. P.68

CHAPTER 10

69. Given the ordinary differential equation

$$\frac{d^3\phi}{dx^3} + A\frac{d^2\phi}{dx^2} - K\phi^2 = 0$$

where $\phi = C_1$, $d\phi/dx = C_2$, and $d^2\phi/dx^2 = C_3$ at $x = 0$:

    a. Set up a typical node for an electrical network which can be used to solve the finite-difference form of this equation.

    b. Show enough nodes near $x = 0$ to demonstrate how the boundary conditions are applied.

    c. Are the impedances bilateral? If not, can they be made so?

70. The following nonlinear ordinary differential equation is to be solved by a resistance network over an interval x_1 to x_2:

$$\frac{d^2\phi}{dx^2} + \phi\frac{d\phi}{dx} + \phi x - x^2 = 0$$

The conditions to be satisfied at the two ends of the interval are

$$\phi = C_1 \qquad \text{at } x = x_1$$
$$\phi = C_2 \qquad \text{at } x = x_2$$

Develop the resistance network applicable. All resistors are to be bilateral. Discuss the method of using this analog.

71. Given the differential equation

$$\frac{\partial^2\phi}{\partial x^2} + \frac{\partial^2\phi}{\partial x \partial y} = x^3 y^2 \phi$$

which holds over a given surface. The boundary conditions call for $\phi = A$, a constant value, at all boundary points.

An electrical network consisting entirely of passive elements (no electronic devices) is to be used to solve this equation. The network points are equally spaced in both directions, having the spacing h.

Show a typical node with attached electrical elements, indicating clearly the value to be specified for each element.

Show how four such typical nodes, in a square array, are interconnected.

72. Given the equation

$$\frac{\partial^2\phi}{\partial x^2} + \frac{\partial^3\phi}{\partial x^2 \partial y} = A \qquad \text{where } A = \text{const}$$

Express the equation in finite difference form.

Show a typical node (using inductances for positive impedances and capacitors for negative impedances).

Show, in a separate diagram, the elements connected into the node just to the right and into the node just above the typical node.

73. The diffusion of heat through a copper plate is described by the following equation:

$$\nabla^2 T = \frac{1}{\alpha}\frac{\partial T}{\partial t}$$

The copper plate is square and has the following dimensions:

$$\text{Side length} = 18 \text{ in.}$$
$$\text{Thickness} = \tfrac{1}{2} \text{ in.}$$

The method of difference equations is to be used to build an electrical analog which should include passive elements only (no electronic amplifiers). The plate is con-

sidered ideally divided in 2- by 2-in. elementary squares, and the temperature at the center of the plate is suddenly raised to 100°C while the edges are kept at 0°C.

  a. Write the finite-difference equation for one elementary square.
  b. Show how you would construct the electrical analog circuit.
  c. Determine the values of the necessary circuit constants.

Data: $\alpha = \dfrac{K}{\rho C p}$

where K = thermal conductivity of copper: 218 Btu/(hr)(ft²)(°F/ft)
      ρ = density of copper: 558 lb/ft³
      C_p = heat capacity of copper: 0.0918 Btu/(lb)(°F)

74. Analyze the analog simulation network shown.

  a. Construct the finite-difference equation.
  b. Develop the partial differential equations being simulated.
  c. What boundary and initial conditions are required?
  d. What is the significance of the ratio L/R?
  e. What would be a possible application of this circuit?
  f. Why is this type of circuit not widely used?
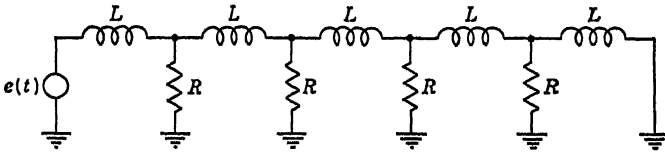
Fig. P.74

75. The pressure distribution p in a flat lubricating film is given by the equation

$$\frac{\partial}{\partial x} B \left(\frac{\partial p}{\partial x} \right) + \frac{\partial}{\partial y} B \left(\frac{\partial p}{\partial y} \right) = \frac{\partial G}{\partial x} + \frac{\partial H}{\partial y}$$

where x, y = coordinates of any point in the film
  $B = \dfrac{d^3}{12u}$
  $G = \dfrac{Ud}{2}$
  $H = \dfrac{Vd}{2}$
  u = viscosity of oil at given point (known, but variable from point to point)
  d = film thickness at given point (known, but variable from point to point)
  U = relative velocity of bearing surfaces in x direction at given point (known, but variable from point to point)
  V = relative velocity of bearing surfaces in y direction (known, but variable from point to point)

  a. Develop a finite-difference equation, using the spacing h in both directions.
  b. Set up a typical node for a resistance network to solve the finite-difference equation, showing resistance values to be used and current sources, if any, required.

CHAPTER 11

76. The following equation is to be solved by using the largest possible soap film (not to exceed 1-in. unsupported span). The area over which the equation applies is elliptical, having major and minor axes of 6 and 3 in., respectively. The origin of the coordinate system is taken at the center of gravity of the ellipse.

$$\frac{\partial^2\phi}{\partial x^2} + A^2\frac{\partial^2\phi}{\partial y^2} = Bxy + Cx^3 + D$$

At the boundary the function ϕ has the values given by $\phi_b = Ex_b + Fy_b^2$. Making use of the *zero pressure* film, sketch the plan form and two elevations of the built-up edge over which the film is to be drawn. Show clearly how the elevations of the edge were determined and how the plan form of the film compares with the given elliptical area.

Suppose that at one point on the film the elevation is found to be 0.100 in. How is this related to the value of ϕ at the corresponding point in the given area?

77. The following equations are to be solved by means of a membrane or soap film. The origin of coordinates is taken at the center of gravity of the area in question.

$$\frac{\partial q}{\partial x} + \frac{\partial r}{\partial y} + ax + by = 0$$

$$\frac{\partial^2 q}{\partial x^2} + \frac{\partial^2 q}{\partial y^2} = -a$$

$$\frac{\partial^2 r}{\partial x^2} + \frac{\partial^2 r}{\partial y^2} = -b$$

At the boundary $ql = rm = 0$, where l and m are the direction cosines of the normal to the boundary. a and b are constants.

Show how these equations can be developed into the equation for the membrane.

78. Sketch and describe the setup necessary to obtain with a soap film or membrane the streamlines about an elliptical cylinder in potential flow. What changes would be necessary in order to obtain the velocity potentials by measurement? Would it be feasible to use either a soap film or a rubber membrane for these models?

79. Given a 2- by 2-in. area over which the following equation must be satisfied:

$$\frac{\partial^2\phi}{\partial x^2} + \frac{\partial^2\phi}{\partial y^2} = x^3y + xy^5$$

subject to the boundary condition $\phi_b = 0$. This equation is to be solved by means of a sheet of conducting paper without current input to the surface of the sheet. Suppose a roll of paper of 30 in. width is available. Sketch and dimension the model you would cut from it to represent the required solution to the largest possible scale. Show the boundary potential distribution you would use.

Appendix 3

LABORATORY EXPERIMENTS

Experiment 1.   Electronic Computing Elements

The following exercises are to be wired on a problem board, then checked by the instructor.   After being checked they can be placed in the computer for verification of the mathematical operation.

Exercise 1.   Summation: $10 + 20 = 30$

Wire an operational amplifier as an adder as shown in Fig. A3.1.   The voltage sources $e_1 = 10$ volts and $e_2 = 20$ volts are applied to the amplifier through a relay which is open before the "operate" switch is thrown.   Measure e_o with a voltmeter V to verify the addition.   Note the sign change.   Let $R_1 = R_2 = R_f = 1$ megohm.

Exercise 2.   Multiplication by a Constant

  a. Change R_1 of Fig. A3.1 to 0.5 megohm and R_2 to 3 megohms.   Use the applied voltages e_1 and e_2 of Exercise 1.   What is the voltage e_o when the "operate" switch is thrown?
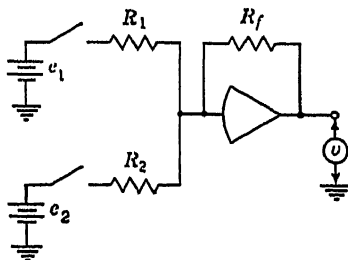
Fig. A3.1

  b. Replace the 0.5- and 3-megohm resistors by decade potentiometers.   With $e_1 = 10$ volts, $e_2 = 20$ volts,

  i. $R_1 = 500$ kilohms; $R_2 = 400$ kilohms.
  ii. $R_1 = 250$ kilohms; $R_2 = 300$ kilohms.

What computation is performed in each case?

Exercise 3.   Differentiation

Wire an operational amplifier as shown in Fig. A3.2.   Let e_i be the output of a sine-wave generator, $R_f = 1$ megohm, $C_i = 1$ or 0.1 μf.   Verify the equation

$$e_o = -RC \frac{de_i}{dt}$$

What is e_o when e_i is a triangular wave?   A square wave?
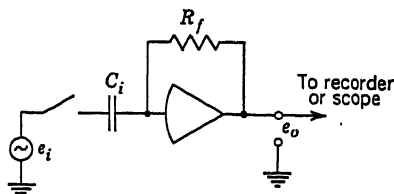
Fig. A3.2

Exercise 4.   Integration

a. Connect an amplifier as shown in Fig. A3.3.   Let $R_i = 1$ megohm, $C_f = 1$ μf.   Make the input voltage $e_i = 10$ volts.   Measure the output voltage e_o with a voltmeter.   Note that the capacitor is shorted before the operate switch is thrown.   What equation is the circuit solving?   Change C to 0.1 μf or R to 100 kilohms.   What effect has this on the voltage e_o?
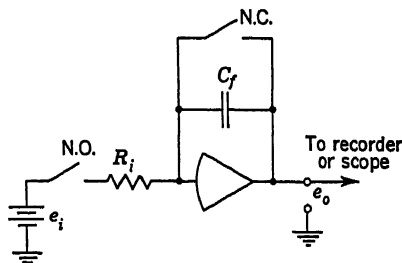
Fig. A3.3

b. Connect two amplifiers as integrators, as shown in Fig. A3.4, with $R_1 = R_2 = 1$ megohm, $C_1 = C_2 = 1$ μf, $e_i = 10$ volts; I.C. $= -5$ volts.   What equation is being solved?   What should be the value of the voltage e_o after 2 sec?   Make a plot of the output voltage $e_o(t)$ on the recorder.
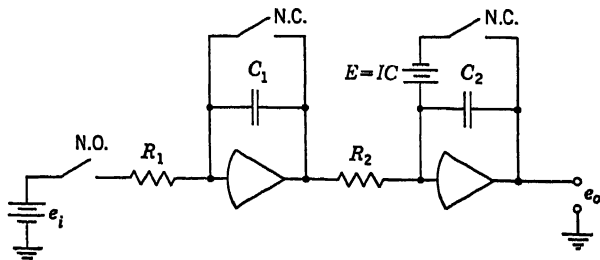
Fig. A3.4

Exercise 5.   Use of Complex Transfer Impedances

a. Connect an amplifier as shown in Fig. A3.5. Let $R_1 = R_2 = 1$ megohm, $C_f = 1\ \mu f$. Obtain a plot of the output voltage. What equation is being solved?
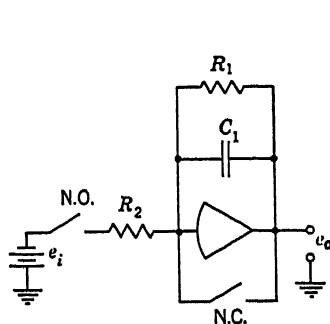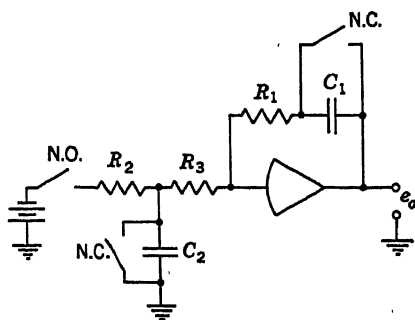
Fig. A3.5   Fig. A3.6

b. Repeat for the circuit shown in Fig. A3.6. Let $R_1 = R_2 = R_3 = 1$ megohm, $C_1 = 1\ \mu f$, $C_2 = 2\ \mu f$. Use the table of transfer impedances in Appendix 1.

Experiment 2.   Solution of a Linear Second-order Differential Equation

The free vibrations of the spring mass system of Fig. A3.7 are damped by the viscous damping mechanism. The constant c depends on the properties of the fluid in the damper.
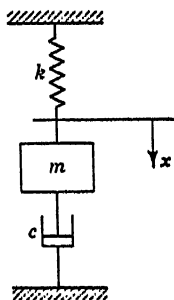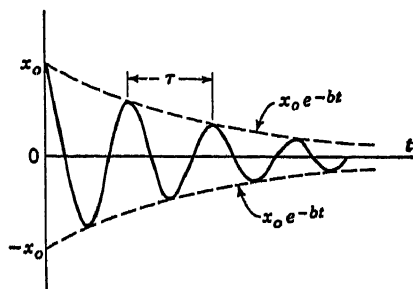
Fig. A3.7   Fig. A3.8

The equation of motion (Newton's law) is

$$\ddot{x} + \frac{c}{m}\dot{x} + \frac{k}{m}x = 0$$

The solution of this equation for damped free vibrations is

$$x = x_0 e^{-bt}\cos \omega t$$

where
$$b = \frac{c}{2m} \qquad \omega = \sqrt{\frac{k}{m} - \left(\frac{c}{2m}\right)^2}$$

when the mass m is released a distance x_0 from the equilibrium position. The solution is plotted in Fig. A3.8

with
$$\tau = \frac{2\pi}{\omega}$$

The damping constant c can be determined from an experimental record of the vibrations by measuring two successive amplitudes at times t_1 and $t_2 = t_1 + \tau$. These amplitudes are $x_1 = x_0 e^{-bt_1}$ and $x_2 = x_0 e^{-b(t_1+\tau)}$. Their ratio

$$\frac{x_1}{x_2} = e^{b\tau} \quad \text{or} \quad \log \frac{x_1}{x_2} = b\tau \quad \text{(logarithmic decrement)}$$

Measurement of x_1, x_2, and τ permits the determination of the constant b and thus c. If $(c/2m)^2 > k/m$, the motion is nonvibratory and represents the case where damping is so severe that the body never crosses the equilibrium position when released from some initial displacement. If $(c/2m)^2 = K/m$, the motion is said to be critically damped and represents the transition condition between a damped vibration and an over damped nonvibratory motion.

Computer Solution of Damped Free Vibrations

  a. Solve the differential equation on the electronic analog computer. Assume $K = 1,000$ lb/ft, $m = 10$ lb-sec²/ft. Use a damping coefficient c of such magnitude that the vibration damps out in 20 to 30 cycles.
  b. From the oscillograph record of this motion find the logarithmic decrement and check the value of c.
  c. Determine the value of c that produces the condition of "critical damping" by adjusting the coefficient of the damping term on the computer solution.
  Check the computer's value of c with the equation $(c/2m)^2 = K/m$ for critical damping.

Experiment 3. Solution of Simultaneous Differential Equations

Two pendulums are coupled by a weak spring as shown in Fig. A3.9. This system, having two degrees of freedom, has two natural modes of oscillation. These correspond to oscillation in unison and in opposition. A third type of oscillation, which
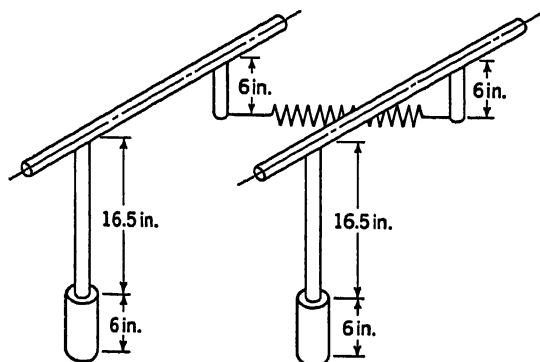
Fig. A3.9

is not a true mode but a superposition of the two natural modes, also exists. This mode is characterized by a continual transfer of energy from one pendulum to the other.

A mechanical analysis of the system permits the determination of the moment of inertia I, the damping constant D, and the distance b of the center of gravity from one end of the rods. The differential equations for the two-pendulum system can then

be written as

$$I\ddot{\theta}_1 + D\dot{\theta}_1 + mgb\theta_1 + Ka^2(\theta_1 - \theta_2) = 0$$
$$I\ddot{\theta}_2 + D\dot{\theta}_2 + mgb\theta_2 + Ka^2(\theta_2 - \theta_1) = 0$$

where K is the spring constant of the spring, a is a length, and m is mass. θ_1 and θ_2 refer to the angular deflection of the two pendulums, respectively.

Substituting numerical values specified for the coupled compound pendulums under study, the above two equations reduce to

$$\ddot{\theta}_1 = -0.044\dot{\theta}_1 - 22.9\theta_1 - 1.58(\theta_1 - \theta_2)$$
$$\ddot{\theta}_2 = -0.044\dot{\theta}_2 - 22.9\theta_2 - 1.58(\theta_2 - \theta_1)$$

Construct an electronic analog-computer system for the solution of these equations and obtain simultaneous plots of θ_1 and θ_2 as a function of time for

a. Both pendulums initially deflected equally in the same direction.
b. Both pendulums initially deflected equally in opposite directions.
c. One pendulum initially deflected, while the other has zero initial deflection.

Experiment 4. Solution of Van der Pol's Equation

The solution of the Van der Pol equation

$$\ddot{y} + \mu(y^2 - 1)\dot{y} + y = 0$$
$$\ddot{y} = \frac{d^2y}{dt^2} \qquad \dot{y} = \frac{dy}{dt}$$

where μ is a constant parameter, can be used to describe the build-up of oscillations in certain nonlinear electrical circuits and furnishes an interesting example of the d-c analog-computer solution of a nonlinear differential equation. The Van der Pol equation is seen to resemble the performance equations of a damped harmonic oscillator.

$$\ddot{x} + r\dot{x} + x = 0$$

but has a nonlinear damping term which will tend to build up the amplitude of oscillations for small values of y (i.e., y less than unity) and to decrease the amplitude for large values of y. If an oscillator described by the Van der Pol equation is given a small initial displacement y_0, periodic oscillations of constant amplitude will result after an initial transient. The duration of this transient will vary in an inverse manner with the parameter μ, and the wave form of $y(t)$ in the steady state will depend upon μ. If, for example, $\mu \gg 1$, it is seen that the build-up of oscillations will require a very long time and also that the oscillations will be very nearly sinusoidal. It is easy to show, however, that the steady-state amplitude of oscillations is independent of μ (at least for small μ.)

For small μ, the solution of the equation is

$$y(t) = A \sin (t + \phi)$$

where ϕ may be taken as zero with no loss of generality in the following argument. In a steady state, the energy dissipation over a complete cycle must be zero. The energy loss per cycle is given by the integral over a cycle of the instantaneous power dissipation:

$$E = \int_0^{2\pi/\omega} (r\dot{x})(\dot{x}) \, dt$$

Applying this to the Van der Pol equation yields

$$E = 0 = \int_0^{2\pi} \mu(y^2 - 1)(\dot{y})^2 \, dt$$

$$0 = \mu \int_0^{2\pi} (A^2 \sin^2 t - 1)(A^2 \cos^2 t) \, dt$$

$$0 = A^2\mu \int_0^{2\pi} (A^2 \sin^2 t \cos^2 t - \cos^2 t) \, dt$$

$$0 = A^2\mu\pi \left(\frac{A^2}{4} - 1\right)$$

$$\therefore A = 2$$

Hence the steady-state peak amplitude is 2. This value remains quite constant even for large μ.

For large μ, the wave form becomes somewhat square rather than sinusoidal. The transition is interesting to observe on a phase plane plot, in which velocity is plotted vs. displacement.

A suggested circuit diagram for the electronic analog solution of Van der Pol's equation is shown in Fig. A3.10. Study this diagram and determine the correct magnitude of R_1 and the significance of the potentiometer settings. For initial conditions $y(0) = \dot{y}(0) = 5$ and $\mu = 0.1, 0.4, 0.7,$ and 1.0, obtain plots of

  a. y versus time
  b. $\dot{y}$ versus time
  c. y versus $\dot{y}$

Fig. A3.10

Experiment 5.   Solution of Duffing's Equation

A vibrating system consisting of a mass and a nonlinear spring is governed by the equation

$$m\ddot{x} + c(x + u^2x^3) = P \cos \Omega t$$

where c is the spring constant, m is the mass, u is a coefficient with the units L^{-2}, and the term on the right-hand side is a driving force. This equation can be put in

dimensionless form by letting

$$q = \sqrt{\frac{3}{4}}\, ux \qquad K^2 = \frac{c}{m} \quad \text{and} \quad s = \frac{p}{K^2} \qquad p = \frac{P}{m}$$

then

$$\frac{\ddot{q}}{K^2} + q + \frac{4}{3} q^3 = s \cos \Omega t$$

which is known as Duffing's equation.

A suggested circuit for the solution of this equation is shown in Fig. A3.11. Study this circuit to determine the function of each component. Calculate the values of all resistors and capacitors. Instrument this circuit on the computer and obtain the system response by determining q as a function of time for values of Ω ranging from 0.1 to 3.0. Let $s = K = 1.0$. Prepare a plot of the peak amplitude of q versus Ω.
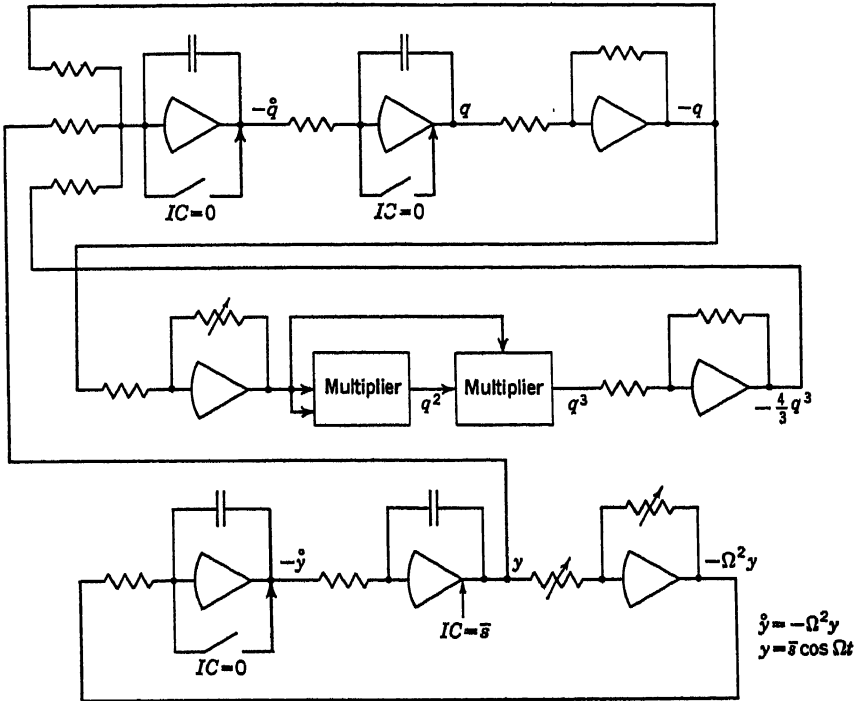
Fig. A3.11

Experiment 6.   Solution of Mathieu's Equation

Mathieu's equation, when expressed as

$$\ddot{y} + \frac{\omega^2}{\beta^2} \left(a - 2q \cos \frac{2\omega}{\beta} t \right) y = 0$$

may be considered as being characteristic of a mass-spring system in which the spring constant varies periodically. Figure A3.12 is a circuit suggested for the solution of this equation. Study this circuit carefully, and determine the significance of all com-

ponents. Obtain plots of y versus time for various combinations of parameter values and initial conditions in the following ranges:

$$2 < y(0) < 4 \text{ volts}$$
$$0 < a < 25$$
$$0 < q < 10$$

Let $\dot{y}(0) = 0$, $\omega = \beta = 1$. Determine the regions of stable, unstable, and periodic response within these ranges.
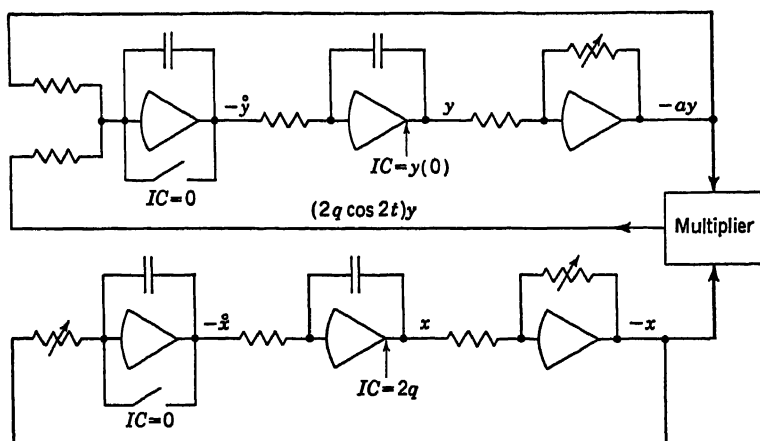
Fig. A3.12

Experiment 7. Solution for Roots of Polynomials

Given the quartic equation

$$x^4 - 2x^3 - x^2 + 2x = 0$$

whose roots are $-1, 0, 1, 2$. Solve for positive roots by integrating the fourth derivative four times. Use the method described in Sec. 8.2, but employ an electronic rather than a mechanical differential analyzer.

Experiment 8. Solution of the Diffusion Equation by RC Analog

A cylindrical copper bar is thermally insulated along its entire outside surface. One end of the bar terminates in an ice bath (32°F), while the other end is attached to a periodically varying heat source. The characteristics of this heat source are illustrated in Fig. A3.13, while the copper bar is shown in Fig. A3.14. The temperature
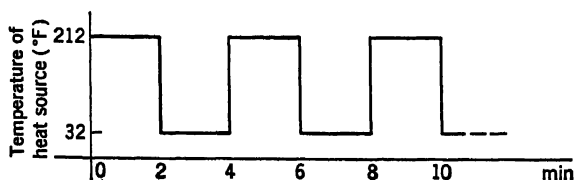
Fig. A3.13
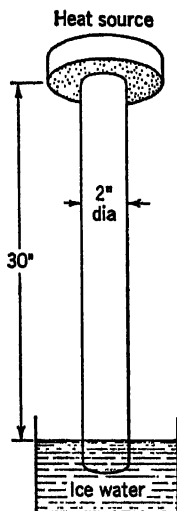
Fig. A3.14

distribution within the bar is governed by the one-dimensional diffusion equation:

$$\frac{\partial^2 T}{\partial x^2} = \frac{1}{a}\frac{\partial T}{\partial t}$$

where T = temperature, °F
  x = distance, ft
  t = time, hr
  a = thermal diffusivity, ft²/hr
  $a = k/\lambda C_p$
  k = thermal conductivity, Btu/(hr)(ft²)(°F/ft)
  λ = weight density, lb/ft³
  C_p = unit heat capacity, Btu/(lb)(°F)

The following specifications apply to the copper bar:

Length = 30 in.
Diameter = 2 in.
  k = 218 Btu/(hr)(ft²)(°F/ft)
  γ = 558 lb/ft³
  C_p = 0.0918 Btu/(lb)(°F)

The bar is initially at 32°F. It is desired to determine the temperature as a function of time at six points, located at $2\frac{1}{2}$, $7\frac{1}{2}$, $12\frac{1}{2}$, $17\frac{1}{2}$, $22\frac{1}{2}$, and $27\frac{1}{2}$ in., respectively, from one end of the bar.

Construct a passive electrical analog of the heat-conduction system. Use resistors and capacitors as shown in Fig. A3.15. The source e may be a square-wave generator, or the required excitation may be generated by manually opening and closing a switch to a dry cell at appropriate intervals of time.
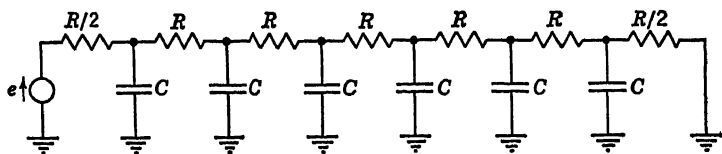
Fig. A3.15

Experiment 9. Solution of the Diffusion Equation by Resistance Network Analog

Repeat Experiment 8, but employ an analog model consisting only of fixed and variable resistors as shown in Fig. A3.16. Use the method described in Sec. 10.7 to determine the resistance magnitudes, and use sufficiently small increments of time (Δt) to obtain solutions which are substantially similar to those obtained in Experiment 8.
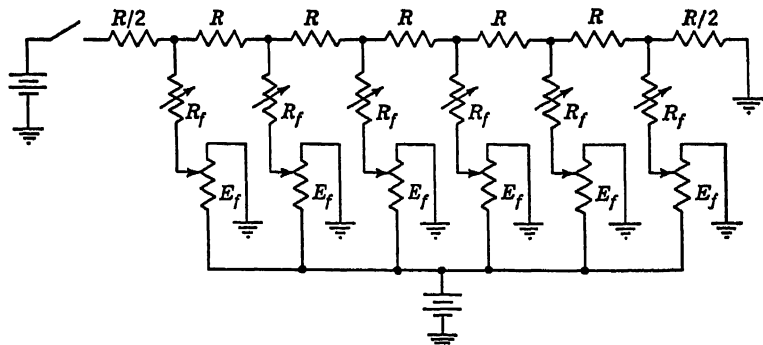
Fig. A3.16

Experiment 10. Solution of the Diffusion Equation by Electronic Analog

Repeat Experiment 8, but employ an electronic analog model as shown in Fig. A3.17.

Fig. A3.17

INDEX